

Dissertation zur Erlangung des Doktorgrades
der Fakultät für Chemie und Pharmazie
der Ludwig-Maximilians-Universität München

STUDIES TOWARD THE
TOTAL SYNTHESIS OF STEPHADIAMINE
AND
DEVELOPMENT OF PHOTOCHROMIC
GALACTOCEREBROSIDES

Nina Vrielink
aus Nordhorn, Deutschland

2017

Erklärung

Diese Dissertation wurde im Sinne von § 7 der Promotionsordnung vom 28. November 2011 von Herrn Prof. Dr. Dirk Trauner betreut.

Eidesstattliche Versicherung

Diese Dissertation wurde eigenständig und ohne unerlaubte Hilfe erarbeitet.

München, den 06. Juni 2017

(Nina Vrielink)

Dissertation eingereicht am: 06. Juni 2017

1. Gutachter: Prof. Dr. Dirk Trauner

2. Gutachter: Prof. Dr. Anja Hoffmann-Röder

Mündliche Prüfung am: 12. Juli 2017

TO MY FAMILY AND FELIX

Parts of this work have been published in peer-reviewed journals:

- “*Synthetic Approaches towards Alkaloids Bearing α -Tertiary Amines*” – A. Hager,[‡] N. Vrieling,[‡] D. Hager, J. Lefranc, D. Trauner*, *Nat. Prod. Rep.* **2016**, *33*, 491–522. (‡ = authors contributed equally)

Parts of this work have been presented on scientific conferences:

- “*Studies Toward the Asymmetric Synthesis of the Norhasubanan Alkaloid (+)-Stephadiamine*” N. Vrieling, B. M. Stoltz, D. Trauner. **ORCHEM 2016**, Weimar, Germany, September 2016.
- “*Towards the Asymmetric Synthesis of (+)-Stephadiamine*” N. Vrieling, B. M. Stoltz, D. Trauner. **Gordon research conference „Stereochemistry“**, Newport, USA, August 2016.
- “*Studies Toward the Asymmetric synthesis of the Norhasubanan Alkaloid (+)-Stephadiamine*” N. Vrieling, B. M. Stoltz, D. Trauner. **17th Tetrahedron Symposium**, Sitges, Spain, June 2016.
- „*Synthetic Studies toward (+)-Stephadiamine*“ N. Vrieling, A. Hager, D. Hager, B. M. Stoltz, D. Trauner. **Tokyo LMU Symposium**, Munich, Germany, October 2015.
- “*Assembly of the Heteropropellane Core of the Norhasubanan Alkaloid (+) Stephadiamine enabled by a Cascade Reaction*“ N. Vrieling, A. Hager, D. Hager, B. M. Stoltz, D. Trauner. **24th International Symposium Synthesis in Organic Chemistry**, Cambridge, UK, July 2015.
- “*Assembly of the Heteropropellane Core of the Norhasubanan Alkaloid (+) Stephadiamine enabled by a Cascade Reaction*“ N. Vrieling, A. Hager, D. Hager, B. M. Stoltz, D. Trauner. **16th Tetrahedron Symposium**, Berlin, Germany, June 2015.
- “*Synthetic Studies toward (+)-Stephadiamine*“ N. Vrieling, A. Hager, D. Hager, B. M. Stoltz, D. Trauner. **27. Irseer Naturstofftage**, Irsee, Germany, February 2015.
- “*Synthetic Studies toward (+)-Stephadiamine*“ N. Vrieling, A. Hager, D. Hager, B. M. Stoltz, D. Trauner. **50thth anniversary of the Heinrich Wieland Prize**, Munich, Germany, October 2014.

Parts of this work are currently prepared for publication:

- “*Total Synthesis of Stephadiamine enabled by a Unique Cascade Reaction*” – N. Vrieling, B. M. Stoltz, D. Trauner*, *manuscript in preparation*.

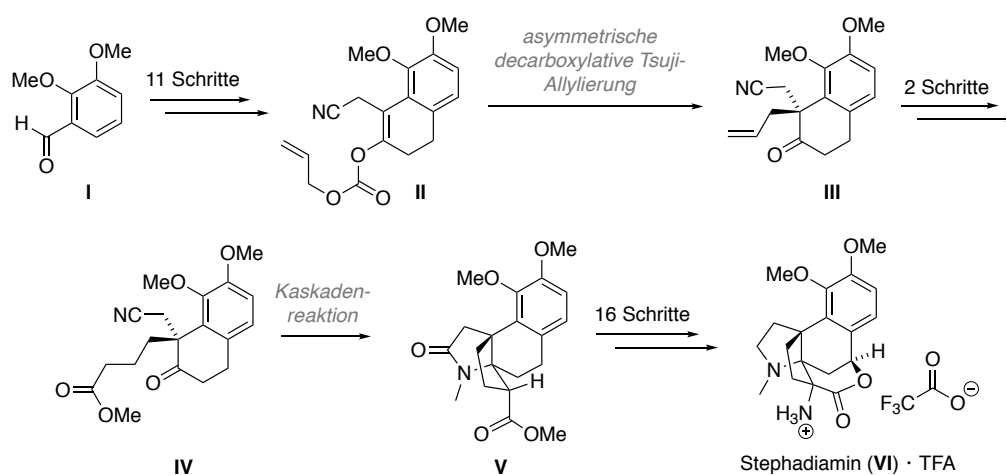
Submitted publications, which are not discussed in this thesis:

- “*Light control of L-type Ca^{2+} channels using a diltiazem photoswitch*” – T. Fehrentz,[‡] F. M. E. Huber,[‡] N. Vrieling, T. Bruegmann, J. A. Frank, N. H. F. Fine, D. Malan, J. G. Danzl, D. B. Tikhonov, S. Hell, P. Sasse, D. J. Hodson, B. S. Zhorov, N. Klöcker, D. Trauner, **2017**, “*Nature Chemical Biology*” – under revision. (‡ = authors contributed equally)

Abstract (German)

KAPITEL 1: STUDIEN ZUR TOTALSYNTHESE VON STEPHADIAMIN

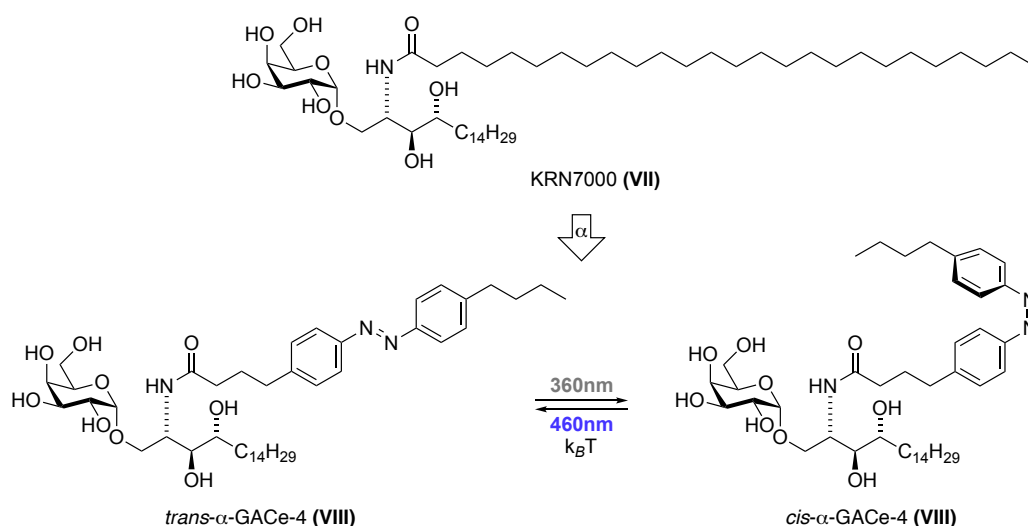
Diese Dissertation beschreibt unsere Studien zur Synthese des Naturstoffs (+)-Stephadiamin (**VI**), welcher in geringen Mengen 1984 aus *Stephania japonica* isoliert wurde und das erste Beispiel eines Norhasubanan-Alkaloids darstellt. (+)-Stephadiamin (**VI**) besitzt ein einzigartiges pentazyklisches Gerüst mit insgesamt vier stereogenen Zentren, darunter zwei benachbarte α -tertiäre Amine (ATAs) sowie ein benzylisches, quartäres Stereozentrum. Das benzyliche Stereozentrum wurde erfolgreich mithilfe einer decarboxylativen Tsuji-Allylierung ausgehend von Enolcarbonat **II** installiert (elf Schritte von kommerziell erhältlichem Aldehyd **I**). Dieses Stereozentrum wurde anschließend verwendet, um die Einführung aller weiteren Stereozentren des Naturstoffs zu dirigieren. Eine neue Kaskadenreaktion wurde entwickelt, um in einem Schritt zwei Fünfringe mit zwei Stereozentren, eines davon ein ATA, des pentazyklischen Skeletts von Stephadiamin aufzubauen. Die Einführung des dritten benachbarten quartären Stereozentrums stellte sich aufgrund des sterischen Anspruchs als sehr schwierig heraus. Dieses Problem wurde letztendlich mit einer Tollens-Reaktion gelöst und das entstandene Stereozentrum wurde mit einer Curtius-Umlagerung in das zweite ATA umgewandelt. Weitere chemische Transformationen führten zu der Synthese des TFA-Salzes von Stephadiamin (**VI**).



KAPITEL II: SYNTHESE VON PHOTOCHROMEN

GALACTOCEREBROSIDEN

Das zweite Kapitel dieser Dissertation beschreibt die Synthese von photoschaltbaren Derivaten der Galactocerebroside α - und β -Galactosylceramid (GalCer). KRN7000 (α -GalCer, **VII**) ist ein Wirkstoff aus dem Bereich der Immuntherapie und wird für die Anwendung in der Krebstherapie untersucht. In Verbindung mit dem Glykoprotein CD1d aktiviert KRN7000 (**VII**) natürliche Killer-T-Zellen (NKT-Zellen) was zu einer Produktion von unterschiedlichen Zytokinen führt, die entweder eine T_H1 - oder T_H2 -Immunantwort hervorrufen. Basierend auf Struktur-Wirkungsbeziehungen haben wir photoschaltbare Analoga (z.B. α -GACe-4, **VIII**) synthetisiert, um die bevorzugte Produktion von entzündungshemmenden Zytokinen (T_H1 -Zytokine) zu stimulieren. Diese funktionalisierten Azobenzole könnten in Zukunft zu einem besseren Verständnis der T_H1 - versus T_H2 -Zytokinproduktion führen und möglicherweise sogar zur Beeinflussung der T_H1/T_H2 -Immunantwort mithilfe von Licht verwendet werden.

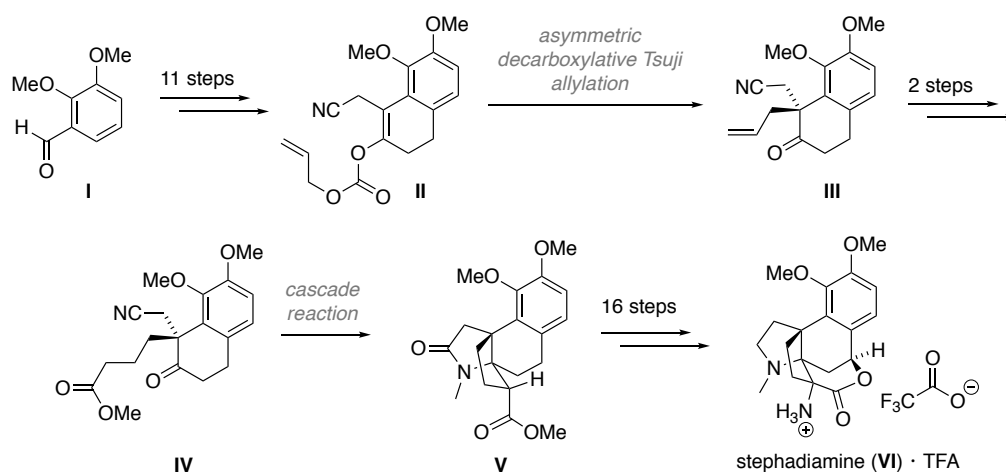


Zusätzlich haben wir ein photoschaltbares Derivat von β -GalCer, einem Glykosphingolipid (GSL), das zum Beispiel in Membranzellen der Schleimhaut vorgefunden wird, hergestellt. In Kooperation mit der Schwille-Gruppe haben wir photoschaltbares β -GACe-4 und α -GACe-4 (**VIII**) in eine *lipid raft*-imitierende unterstützte Lipiddoppelschicht eingebracht. Mithilfe von atomarer Kraftmikroskopie (AFM) haben wir ihr Verhalten bei der Bestrahlung mit Licht untersucht. Diese Derivate könnten in der Zukunft von Nutzen sein, um die Interaktionen von Proteinen und GSL zu untersuchen, beispielsweise der Bindung des rekombinanten HIV-1 Oberflächenproteins gp120 (rpg120) zu β -GACe-4.

Abstract (English)

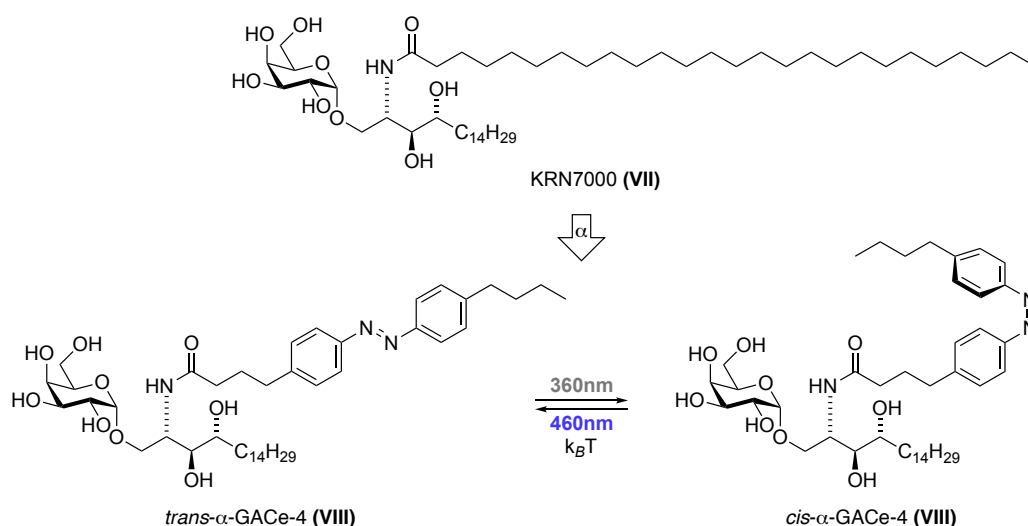
CHAPTER 1: STUDIES TOWARD THE TOTAL SYNTHESIS OF STEPHADIAMINE

This thesis describes our synthetic efforts toward the synthesis of (+)-stephadiamine (**VI**), which was isolated as a minor component of *Stephania japonica* in 1984 and represents the first example of a norhasubanan alkaloid. (+)-Stephadiamine (**VI**) features a unique pentacyclic skeleton bearing a total of four stereogenic centers, including two adjacent α -tertiary amines (ATA) and a benzylic quaternary stereocenter. This benzylic stereocenter was successfully set using a decarboxylative Tsuji allylation starting from stabilized enol carbonate **II** (11 steps from aldehyde **I**). This stereocenter was then used to direct the formation of all other stereocenters of the natural product. A new cascade reaction was developed to assemble the complex pentacyclic core of (+)-stephadiamine (**VI**), constructing two five-membered rings and two stereocenters (including one ATA) in a single step (**IV** \rightarrow **V**). Installation of the third adjacent stereocenter proved to be highly challenging due to the steric hindrance associated with this position. We were able to overcome this by the use of a Tollens reaction to install a quaternary stereocenter, which was later converted to the second ATA of stephadiamine *via* a Curtius reaction. Additional transformations subsequently provided the TFA salt of stephadiamine (**VI**).



CHAPTER II: SYNTHESIS OF PHOTOCROMIC GALACTOCEREBROSIDES

Chapter two of this thesis describes the synthesis of azo-derivatives of galactocerebrosides, namely α - and β -galactosylceramides (GalCer). KRN7000 (α -GalCer, **VII**) is an immunotherapy drug under investigation for use as a potential treatment for cancer. Associated with the glycoprotein CD1d, KRN7000 (**VII**) activates natural killer T (NKT) cells, leading to the production of different cytokines modulating a T_H1/T_H2 immune response. Based on structure-relationship studies, we designed photoswitchable analogs (*e.g.*, α -GACe-4, **VIII**) to mainly activate the production of pro-inflammatory cytokines (T_H1 -type cytokines). These functionalized azobenzenes may help to improve our understanding of T_H1 versus T_H2 -type cytokine production and we hope that they could be used to modulate a T_H1/T_H2 immune response.



In addition, we prepared photoswitchable analogs of β -GalCer, a common glycosphingolipid that is for example expressed on mucosal membrane cells. In collaboration with the Schwille laboratory, we incorporated photoswitchable β -GACe-4 and α -GACe-4 (**VIII**) into a lipid raft-mimicking supported lipid bilayer. Using atomic force microscopy (AFM), we characterized their behaviour on irradiation with light. Ultimately, these tools could be of use to study binding of proteins to the glycosphingolipids (GSLs), for example the interaction of recombinant HIV-1 surface glycoprotein gp120 (rgp120).

Acknowledgements

First and foremost, I want to thank Prof. Dirk Trauner for the opportunity to pursue my Ph.D. work under his guidance and letting me work on very challenging projects. I'm very grateful to Prof. Dr. Trauner for giving me the freedom to follow my own ideas and helping me to become a more independent scientist. Prof. Trauner's passion and enthusiasm for alkaloid synthesis and chemical biology never failed to motivate and inspire me.

I'm also very thankful to Prof. Dr. Anja Hoffmann-Röder, who is not only my second examiner, but also my mentor in the LMU Mentoring program and collaboration partner in the galactocerebroside project. I would like to thank Prof. Hoffmann-Röder for her marvelous support in all of these functions throughout the last years.

In addition, I would like to thank Dr. Thomas Magauer, Prof. Dr. Manfred Heuschmann, Prof. Dr. Konstantin Karaghiosoff and Prof. Dr. Franz Bracher for being on my defence committee.

I would like to thank my collaborators for very fruitful and productive collaborations. I'm especially grateful to Prof. Brian M. Stoltz, who hosted me at CalTech. I benefited enormously from my time in his laboratory and gained valuable insight in methodology research. In addition, I would also like to thank Dr. Scott Virgil, Prof. Dr. Benjamin List, Gabriele Pupo (asymmetric catalysis project), Prof. Dr. Anja Hoffmann-Röder, Prof. Dr. Petra Schwillle and Prof. Dr. Moriya Tsuji, Andreas Baumann, Dr. Henri Franquelim, Samuel Leitao, Dr. James Frank, Dr. Henry Toombs Ruane (photoswitchable galactocerebroside), Dr. Timm Fehrentz, Dr. Florian Huber and everyone who was involved in the biological evaluation of FHU-779 (photoswitchable Ca²⁺-channel blockers), Dr. Johannes Broichhagen, Dr. Timm Fehrentz, Dr. David J. Hodson and Philipp Leippe (photoswitchable cAMP/cGMP).

For funding, I would like to thank the SFB749, the Deutsche Telekom Stiftung, the Otto-Bayer-Foundation and the LMUMentoring program. These programs allowed me to spend a time abroad (Otto-Bayer scholarship) and attend multiple conferences and workshops (Deutsche Telekom Stiftung and LMU Mentoring program). I am especially grateful to my mentors Edelgard Bulmahn, Prof. Dr. Anja Hoffmann-Röder and Dr. Christian Bruckmeier for consultation and advice on career choices. In addition, I would like to thank Christiane Frense-Heck, who is responsible for the Ph.D. program of the Deutsche Telekom Stiftung – this program means a lot to me and I greatly benefited from the associated prospects and the financial support.

A very special thanks goes to Dr. Julius Reyes, Felix Hartrampf, Antonio Rizzo, Daniel Terwilliger, Dr. James Frank, Andreas Baumann, Dr. Bryan Matsuura, Dr. Henri Franquelim, Nils Winter and Benjamin Williams, who spent considerable time and effort to proof-read parts of this thesis.

I would like to acknowledge my talented and very motivated students Julian Feilner, Pascal Schäfer, Stefania Sassnink, Lars Grunenberg, Igor Martin, Philip Watson and Fabio Raith for their hard work in the lab.

My time in the lab would not have been as enjoyable without my colleagues in the Trauner lab. I would like to thank especially Dr. Hong-Dong Hao, Dr. Julius Reyes, Katharina Hüll and Felix Hartrampf, who have tremendously supported me during the last months of my Ph.D. – I would not have been able to accomplish my results without you. In addition, I would like to thank Dr. Ahmed Ali, Dr. Nicolas Armanino, Dr. David Barber, Dr. James Frank, David Konrad, Philipp Leippe, Dr. Robin Meier, Antonio Rizzo, Daniel Terwilliger, Dr. Henry Toombs-Ruane, Nynke Veprek, Dr. Giulio Volpin, Benjamin Williams and Nils Winter for being the best colleagues one could ask for. I would like to thank Dr. Johannes Broichhagen, Dr. Arunas Damijonaitis, Dr. Nicolas Guimond, Dr. Anastasia Hager, Dr. Dominik Hager, Dr. Daniel Hog, Dr. Guillaume Journot, Dr. Julien Lefranc, Dr. Florian Löbermann, Dr. Martin Olbrich, Dr. Desiree Strych and Dr. Sebastian Strych for creating a great and welcoming group atmosphere during my Master's thesis and the beginning of my Ph.D. In addition I would like to thank the whole Magauer group for an amazing time – especially Dr. Klaus Speck, Dr. Cedric Hugelshofer, Sofia Torres and Lara Weisheit.

In addition, I would like to thank the permanent staff of the Trauner laboratories, Alexandra Grilc, Luis de la Osa de la Rosa, Mariia Palchyk and Dr. Martin Sumser for organizing everyday lab life. A special thanks goes to Carrie Louis for her assistance with HPLC/NMR and keeping my spirits up with thoughtful little presents. I am especially grateful to Heike Traub for endless support, organizing all the paperwork and making the impossible possible.

All the experimental work could not have been performed without the analytical department (Dr. Spahl, S. Kosak, Dr. Stevenson, C. Dubler). I am especially grateful to Dr. Peter Mayer for his amazing work in single crystal X-ray crystallography.

Last but not least, I would like to thank my family and friends for their support. In particular, I owe my thanks to my parents and my brother Markus, who always believed in me – I am very grateful for everything you have done for me. In addition, I like to thank Felix' family for the support they gave me in the last years. My biggest thanks I would like to express to Felix, who always encouraged and motivated me. I am very grateful for the time we spent together and I'm looking forward to everything that may come in the future.

List of abbreviations

Å	Ångstrom
°C	degrees Celsius
δ	chemical shift in ppm downfield relative to a standard
→	followed by
μw	microwave
Ac	acetyl
acac	acetylacetonate
ACe	photoswitchable <i>D-erythro</i> -ceramide
ACDC	asymmetric counteranion-directed catalysis
ACHN	1,1'-azobis(cyclohexanecarbonitrile)
AFM	atomic force microscopy
AIBN	1,1'-azobis(isobutyronitrile)
ANDEN	(+)-(11 <i>S</i> ,12 <i>S</i>)bis[2'-(diphenylphosphino)benzamido]-9,10-dihydro-9,10-ethanoanthracene
ATA	α-tertiary amine
DOPE	1,2-dioleoyl- <i>sn</i> -glycero-3-phosphoethanolamine
AZADO	2-azaadamantane- <i>N</i> -oxyl
AzCa	azo-capsaicin derivative
BAIB	(diacetoxyiodo)benzene
BINAP	2,2'-Bis(diphenylphosphino)-1,1'-binaphthyl
Bn	benzyl
Boc	<i>tert</i> -Butyloxycarbonyl
BQ	benzoquinone
Bu	butyl
Bz	benzoyl
C18-SM	<i>N</i> -stearoyl- <i>D-erythro</i> -sphingosylphosphorylcholine
calcd	calculated
CAM	ceric ammonium molybdate(IV)
CAN	ceric ammonium nitrate
cat.	catalytic

CBS	Corey-Bakshi-Shibata
Cbz	carboxybenzyl
CD1d	member of the CD1 (cluster of differentiation 1) family of glycoproteins
CD4	cluster of differentiation 4
<i>cf.</i>	<i>confer</i> (compare)
CFL	compact fluorescence bulb
Chol	cholesterol
CoA	coenzyme A
COSY	correlation spectroscopy
CSA	camphorsulfonic acid
CSF	colony-stimulating factors
cod	1,5-cyclooctadiene
Cy	cyclohexyl
DABCO	(1,4-diazabicyclo[2.2.2]octane)
DACH	1,2-diaminocyclohexane- <i>N,N'</i> -bis(2-diphenylphosphinobenzoyl)
dba	dibenzylideneacetone
DBAD	dibenzyl diazodicarboxylate
DBU	1,8-diazabicyclo[5.4.0]undec-7-ene
DCM	dichloromethane
DDQ	2,3-dichloro-5,6-dicyano-1,4-benzoquinone
DEAD	diethyl azodicarboxylate
DIBAL-H	diisobutylaluminium hydride
DIPEA	<i>N,N</i> -diisopropylethylamine (Hünig's base)
DKR	dynamic kinetic resolution
DMA	<i>N,N</i> -Dimethylacetamide
DMAP	4-dimethylaminopyridine
DME	1,2-dimethoxyethane
DMF	dimethyl formamide
DMSO	dimethyl sulfoxide
DNA	deoxyribonucleic acid
DOPC	1,2-dioleoyl- <i>sn</i> -glycero-3-phosphocholine
DOR	δ -opioid receptor
dpm	2,2,6,6-tetramethyl-3,5-heptanedionato
DPPA	diphenylphosphoryl azide
dppf	1,1-bis(diphenylphosphino)ferrocene
<i>d.r.</i>	diastereomeric ratio

dtbppy	bis-(<i>tert</i> -butyl)-2,2'-bipyridine
DyKAT	dynamic kinetic asymmetric transformations
E	electrophilicity value
EDCI	1-ethyl-3-(3-dimethylaminopropyl)carbodiimide
EDTA	ethylenediaminetetraacetic acid
<i>ee</i>	enantiomeric excess
EI	electron ionization
eq.	equivalent(s)
ER	endoplasmatic reticulum
Et	ethyl
EtOAc	ethyl acetate
ESI	electrospray ionization
<i>e.g.</i>	<i>exempli gratia</i> (for example)
FAAzo	photoswitchable fatty acid
g	gram
G	Grubbs catalyst
GACe	galactosyl azo ceramide
GalCer	galactosyl ceramide
GalCerS	galactosylceramide synthase
GCS	glucosylceramide synthase
gp120	virus-glycoprotein 120
GPCR	G-protein coupled receptor
GRACe	red-shifted galactosyl ceramide (galactosyl <u>r</u> ed-shifted <u>a</u> zo <u>c</u> eramide)
GSL	glycosphingolipid
h	hour(s)
HBTU	(2-(1 <i>H</i> -benzotriazol-1-yl)-1,1,3,3-tetramethyluronium-hexafluorophosphat)
HG	Hoveyda-Grubbs catalyst
Hex	hexanes
HFIP	hexafluoroisopropanol
HIV	human immunodeficiency virus
HMBC	heteronuclear multiple bond correlation
HMDS	hexamethyldisilazide

HMPA	hexamethylphosphoramide
HPLC	high performance liquid chromatography
HRMS	high resolution mass spectrometry
HSQC	heteronuclear single quantum correlation
MTBE	methyl- <i>tert</i> -butylether
HTX	histrionicotoxin
Hz	Hertz
<i>i</i> -	<i>iso</i>
IC ₅₀	half maximal inhibitory concentration
IFN	interferon
IL	interleukins
IR	infrared spectroscopy
IUPAC	International Union of Pure and Applied Chemistry
<i>J</i>	coupling constant
L ₀	liquid-ordered
L _d	liquid-disordered
LCMS	liquid chromatography-mass spectrometry
LDA	lithium diisopropylamide
LiAlH ₃	lithium aluminum hydride
m	mass
Me	methyl
min	minutes
mL	milliliter
MOM	methoxymethyl
MS	molecular sieves
MVK	methyl vinyl ketone
N	nucleophilicity value
NADPH	nicotinamide adenine dinucleotide phosphate (reduced form)
NBS	<i>N</i> -bromosuccinimide
NCS	<i>N</i> -chlorosuccinimide
NHC	<i>N</i> -heterocyclic carbene
NIS	<i>N</i> -iodosuccinimide

NK	natural killer cells
NKT	natural killer T cells
NMM	<i>N</i> -methylmorpholine
NMO	<i>N</i> -methylmorpholine- <i>N</i> -oxide
NMR	nuclear magnetic resonance
NOESY	nuclear Overhauser effect spectroscopy
<i>o</i>	<i>ortho</i>
OMe	methoxy
<i>p</i>	<i>para</i>
PACe	photoswitchable pythoceramide
PCC	pyridinium chlorochromate
PCL	photochromic ligand
PDC	pyridinium dichromate
Pd/C	palladium on charcoal
PE	petroleum ether
PG	protecting group
pH	potential of hydrogen
Ph	phenyl
Ph.D.	Doctor of Philosophy
PHOX	phosphinooxazoline
Piv	pivaloyl
PIFA	[bis(trifluoroacetoxy)iodo]benzene
ppm	parts per million
PPTS	pyridinium <i>p</i> -toluenesulfonate
ppy	2-(2-pyridinyl)phenyl
Pr	propyl
py	pyridine
PTL	photoswitchable tethered ligand
<i>p</i> -TSA	<i>p</i> -toluenesulfonic acid
quant.	quantitative
QUINAP	1-(2-diphenylphosphino-1-naphthyl)isoquinoline
R_f	retardation factor (TLC)
rgp120	recombinant HIV-1 surface glycoprotein gp120

RNA	ribonucleic acid
r.t.	room temperature
sat.	saturated
<i>S. japonica</i>	<i>Stephania japonica</i>
SLB	supported lipid bilayers
s.m.	starting material
S _N	nucleophilic substitution
s _N	nucleophile-specific sensitivity parameter
T	temperature
t	time
<i>t</i> -	<i>tert</i>
TBAT	tetrabutylammonium difluorotriphenylsilicate
TBD	1,5,7-triazabicyclo[4.4.0]dec-5-ene
TBDPS	<i>tert</i> -butyldiphenylsilyl
TBHP	<i>tert</i> -butyl hydroperoxide
TBS	<i>tert</i> -butyldimethylsilyl
TCM	Traditional Chinese Medicine
TEMPO	2,2,6,6-tetramethylpiperidinyloxy
TES	triethylsilyl
TFA	trifluoroacetic acid
TFAA	trifluoroacetic anhydride
TfO	trifluoromethanesulfonate
T _H	T helper
THF	tetrahydrofuran
TIPS	triisopropylsilyl
TIRF	total internal reflection fluorescence spectroscopy
TIS	triisopropylsilane
TLC	thin layer chromatography
TMDS	1,1,3,3-tetramethyldisiloxane
TMEDA	tetramethylenediamine
TMS	tetramethylsilane
TNF	tumour necrosis factors
TPAP	tetrapropylammonium perruthenate
TPP	tetraphenylporphyrin
TRIP	3,3'-bis(2,4,6-triisopropylphenyl)-2,2'-binaphtholate

TRPV	vanilloid receptor
Ts	4-methylphenylsulfonyl
Tr	trityl
TTX	tetrodotoxin
UHPLC	ultra-high performance liquid chromatography
UV	ultraviolet
XPhos	2-dicyclohexylphosphino-2',4',6'-triisopropylbiphenyl

Table of contents

Abstract (German).....	IV
Abstract (English)	VI
Acknowledgements	VIII
List of abbreviations	X
Table of contents.....	XVII

CHAPTER I: STUDIES TOWARD THE TOTAL SYNTHESIS OF STEPHADIAMINE

1 Introduction	3
1.1 α-Tertiary amines as a retron in alkaloid synthesis.....	3
1.1.1 Alkaloids bearing α -tertiary amines (ATAs).....	3
1.1.2 Classification and selected examples of synthetic strategies	5
1.1.2.1 Installation of ATAs <i>via</i> C-C bond formation.....	6
1.1.2.2 Installation of the ATA <i>via</i> C-N bond formation.....	17
1.1.2.3 Cascade reactions for the implementation of α -tertiary amines	24
1.1.3 Installation of ATAs in hasubanan alkaloid synthesis	30
1.2 Hasubanan alkaloids isolated from <i>japonica</i> species.....	33
1.2.1 <i>Stephania japonica</i> and its application in Traditional Chinese Medicine (TCM).....	33
1.2.2 Isolation and structure of (+)-stephadiamine.....	34
1.2.3 Proposed biosynthesis of (+)-stephadiamine.....	35
2 Project outline	37
2.1 Aims and significance of the project.....	37
2.2 Initial work	38
2.2.1 Retrosynthesis	38
2.2.2 Initial experimental work.....	38
3 Results and discussion	41
3.1 Implementation of the quaternary benzylic stereocenter	41
3.1.1 The Tsuji allylation	41
3.1.2 Screening of the decarboxylative Tsuji allylation.....	43
3.1.3 Direct allylation of the tetralone.....	52
3.1.4 Enantiomeric enrichment and determination of the absolute stereochemistry.....	55

3.1.5	List's organocatalytic version of the direct Tsuji allylation	56
3.2	Metathesis and cascade reaction	57
3.2.1	Ester approach.....	57
3.2.2	Aldehyde approach.....	68
3.3	Implementation of the second ATA.....	78
3.4	Installation of the lactone.....	82
3.5	Completion of the synthesis	93
4	Summary and outlook	98

CHAPTER II: SYNTHESIS OF PHOTOCROMIC GALACTOCEREBROSIDES

5	Introduction.....	103
5.1	Sphingolipids, ceramides and cerebroside.....	103
5.1.1	General classification and biological relevance.....	103
5.1.2	The synthetic α -galactosylceramide KRN7000	104
5.1.3	β -Galactosylceramide in HIV research	105
5.2	Photopharmacology	106
5.3	Photoswitchable lipids and ceramides.....	108
5.4	Aims and significance of the project.....	109
6	Photoswitchable derivatives of Galactosylceramides	111
6.1	Development of photochromic derivatives of α-galactosylceramide	111
6.1.1	Design and retrosynthesis of the photochromic ligands.....	111
6.1.2	Synthesis of α -galactosylceramide derivatives.....	113
6.2	Development of photochromic derivatives of β-galactosylceramide	117
6.2.1	Design of the photochromic ligand.....	117
6.2.2	Synthesis of a β -galactosylceramide derivative.....	118
6.3	Biophysical characterization of α-GACe and β-GACe	120
7	Summary and outlook	123

CHAPTER III: EXPERIMENTAL PROCEDURES AND ANALYTICAL DATA

8	Experimental	127
8.1	Methods and equipment	129
8.2	Experimental data of chapter I	131

8.3	Experimental data of chapter II.....	185
9	Appendix	225
9.1	Single-crystal X-ray analysis.....	225
9.2	NMR spectra of chapter I	268
9.3	NMR spectra of chapter II.....	316
9.4	Chiral HPLC data.....	369
10	Literature.....	373

CHAPTER I

STUDIES TOWARD THE TOTAL SYNTHESIS OF STEPHADIAMINE

1 Introduction

1.1 α -Tertiary amines as a retron in alkaloid synthesis*

1.1.1 Alkaloids bearing α -tertiary amines (ATAs)

Alkaloids account for some of the most structurally complex and biologically active natural products – to date more than 50.000 natural products are known and over 12.000 of these are alkaloids.^[1] They are famous for their toxic and sometimes psychomimetic, euphoria inducing, hallucinogenic and even addictive properties.^[2] Consequently, they have been used as both poison and medicine and have played an important role in the development of synthetic organic chemistry, pharmacology and medicine.

Alkaloids are produced by practically all phyla of marine and terrestrial organisms at any evolutionary level.^[3] One of their main functions in plants is for chemical defense against herbivores. As such, they benefit their producers in various ways, *e.g.*, as antimicrobials, antifungals, antivirals and herbicides.^[3-4] Most alkaloids fall into the class of specific modulators and have been shaped during evolution so that they can interfere with critical targets within potential enemies by mimicking endogenous ligands, hormones or substrates.^[3] As a consequence of their structural diversity and relatively weak basicity, they interact with a large variety of biological targets, such as neuroreceptors, ion channels, DNA/RNA, the cytoskeleton, enzymes involved in ribosomal protein biosynthesis and are able to modulate membrane permeability. However, alkaloids do not only act as toxic agents. When administered at lower dosages, they sometimes show useful pharmacological activities.^[5-6] Alkaloid natural products and synthetic analogs have found wide medical application, *e.g.*, in relieving pain and spasms, stimulating circulation and respiration, reducing blood pressure and killing tumor cells.^[3]

In general, alkaloids can be defined as naturally produced organic nitrogen-containing secondary metabolites. Although only a small number of amino acids are involved in their biosynthesis, alkaloids encompass enormous structural diversity.^[7] By incorporating polyketide and terpenoid elements and additional late-stage redox transformations, this structural complexity is increased even further.

Alkaloids are usually classified along biosynthetic criteria, however they can also be categorized according to certain structural motifs, *e.g.*, their nitrogen-containing structure (quinolone, isoquinoline, piperidine, pyridine, etc.) or the nature of the amine incorporated into the alkaloid. In

* This chapter has been adapted from the review “*Synthetic Approaches towards Alkaloids Bearing α -Tertiary Amines*” – A.

general, there are three different classes of amines (Figure I.1A): primary (one C–N bond), secondary (two C–N bonds) and tertiary amines (three C–N bonds). Furthermore, the carbon that is bound to the nitrogen, the α -carbon (Figure I.1B), can be classified as α -primary (one additional C–C bond), α -secondary (two additional C–C bonds) or α -tertiary (three additional C–C bonds). All combinations of these structural motifs, ranging from primary α -primary amines to tertiary α -tertiary amines, can be found in nature.

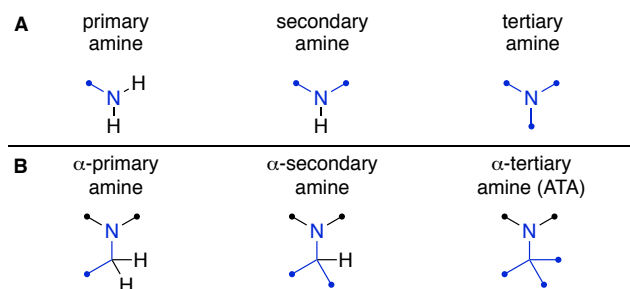


Figure I.1 Classification of amines.

Amongst these motifs, the α -tertiary amine (ATA), *i.e.* a tetrasubstituted carbon atom surrounded by three carbons and one nitrogen, stands out among the structural features frequently found in alkaloids.^[8–11] An ATA is defined as a nitrogen atom bound to an sp^3 -hybridized carbon that bears three additional C–C bonds, which renders this α -carbon stereogenic and its installation synthetically challenging in most alkaloids. In most cases, the nitrogen is sp^3 -hybridized. However, broadening the definition of an ATA, the nitrogen can also be sp^2 - or sp -hybridized, *e.g.*, an amide or isonitrile. This definition highlights the particular C–N bond of a fully substituted carbon, and thereby obviates the confusion that is often evoked by the term ‘quaternary stereocenter’, which, strictly speaking, corresponds only to a carbon bound to four additional carbon atoms.

Figure I.2 presents some alkaloids that illustrate this definition and emphasizes that the nitrogen in ATAs (highlighted in blue) can show various degrees of substitution. Stephadamine (**I.1**) and huperzine A (**I.2**) contain primary ATAs, whereas tetrodotoxin (**I.3**), histrionicotoxin 283A (HTX 283A, **I.4**), amathaspiramide F (**I.5**) and *N*-methyl-euphococcinine (**I.6**) contain secondary ATAs. Halichlorine (**I.7**), himgaline (**I.8**), stephadiamine (**I.1**) and porantherine (**I.9**) contain sterically demanding tertiary ATAs. In addition, porantherine (**I.9**) is an example for an alkaloid featuring a twofold ATA. Stephadamine (**I.1**) contains two adjacent ATAs, wherein the primary ATA additionally contributes to an α -amino acid motif. The dimeric indole alkaloid stephacidin B (**I.10**) contains four ATAs in total, which are incorporated in two bridged diketopiperazine moieties.

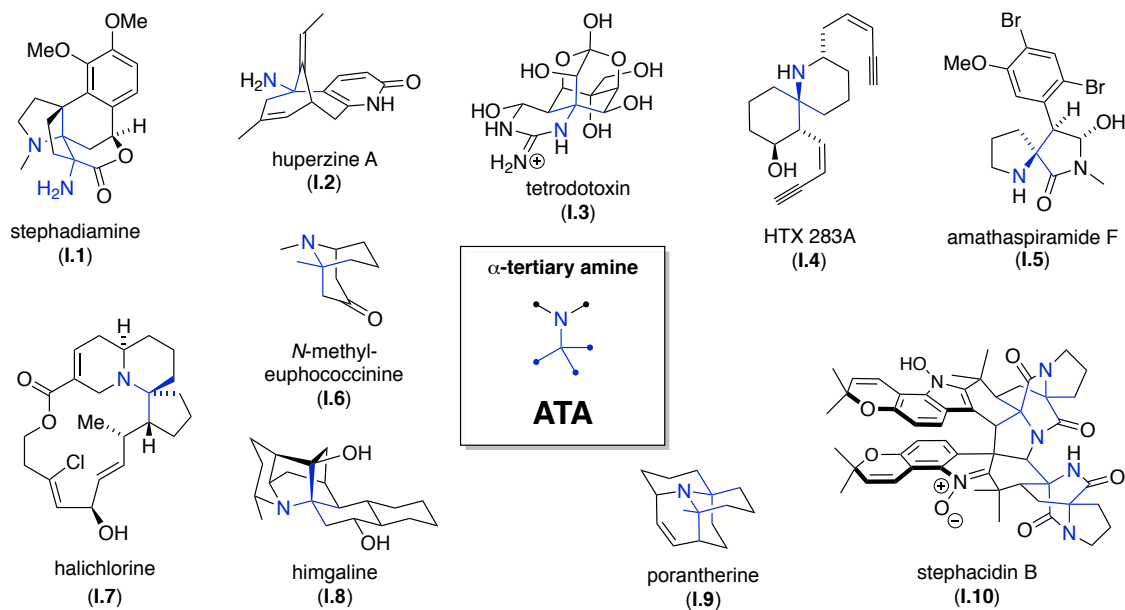


Figure I.2 Structurally diverse alkaloids that contain the ATA motif.

Although several methods have been reported for the synthesis of ATAs, only few are commonly used in total synthesis. The following chapters therefore provide a brief summary of these synthetic methods and discuss their application in total synthesis.

1.1.2 Classification and selected examples of synthetic strategies

Many approaches have been reported for the synthesis of ATAs, but only a few methods are commonly applied in the total synthesis of alkaloids. In this chapter, an overview of these methods accompanied by selected examples of applications in natural product synthesis is provided. Whenever possible, these methods are classified according to the bond that is formed as well as the electronic nature of the transformation (Figure I.3). It should be noted that this “simplified” categorization cannot be applied to all methods used in ATA synthesis.

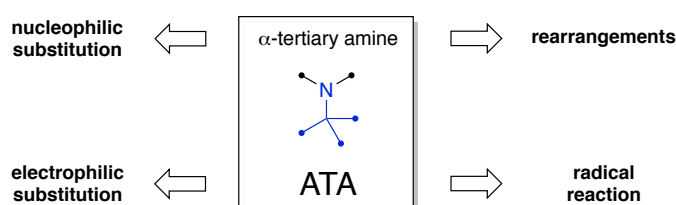
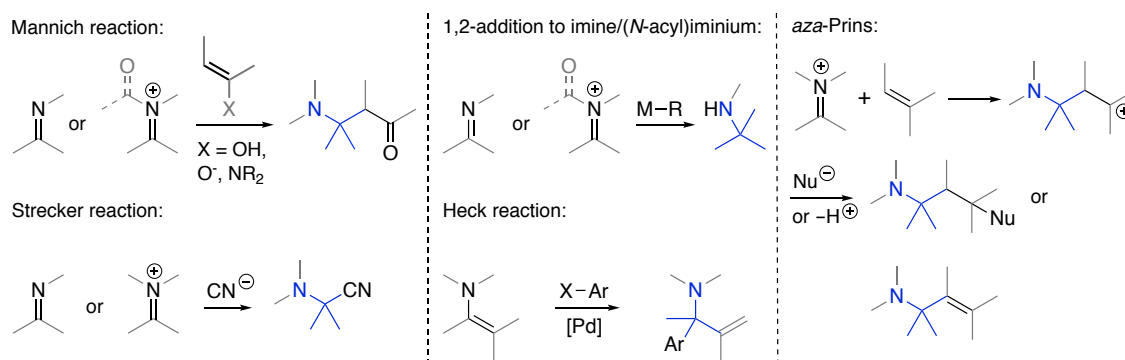


Figure I.3 Classification of methods for the construction of ATAs.

In recent years, new methods to create ATAs have been developed, such as C–H bond azidations^[12] and hydroaminations.^[13] As they have not yet been employed in the total synthesis of alkaloids, they are not featured in this introduction.

1.1.2.1 Installation of ATAs *via* C–C bond formation

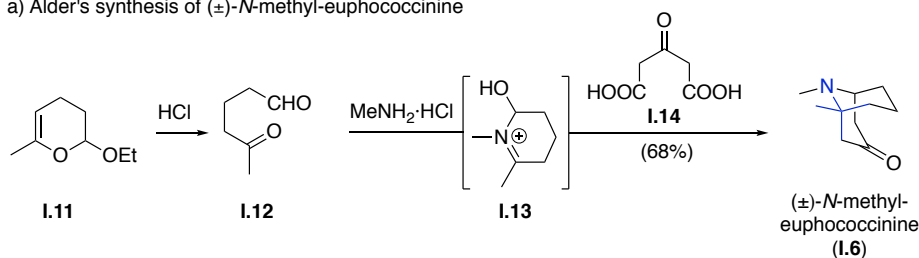
ATAs can either be introduced by a reaction in which a C–C bond or a C–N bond is formed. In the case of C–C bond formation, the addition of carbon nucleophiles to electrophilic α -carbons, as in activated imines and iminium ions, represents one of the most popular methods to install ATAs (Scheme I.1). This class of methods includes Mannich, Strecker and aza-Prins reactions as well as 1,2-additions of nucleophilic reagents (often organometallic) to C–N double bonds. *N*-acyliminium ions are particularly powerful electrophiles in reactions of this type. Heck reactions involving enamines also fall into this category.



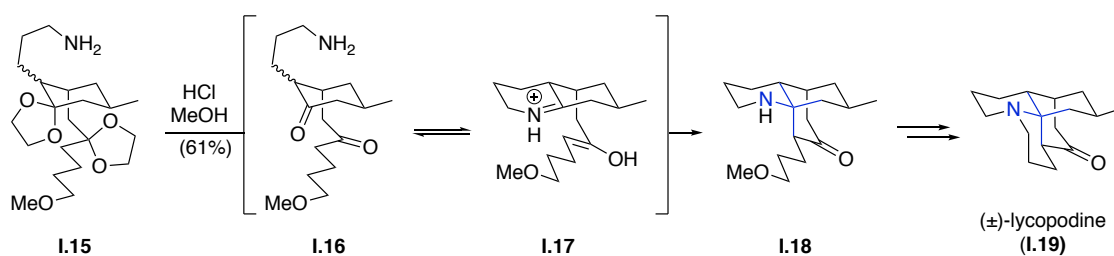
Scheme I.1 C–C bond formation involving electrophilic α -carbons.

There are numerous examples of Mannich reactions for the construction of ATAs. Already in 1959, Alder synthesized *N*-methyl-euphococcinine (**I.6**) using a Mannich reaction analogous to the famous tropinone syntheses of Robinson^[14–15] and Schöpf^[16] (Scheme I.2a).^[17] Starting from dihydropyran **I.11**, ketoaldehyde **I.12** was formed under acidic conditions. Ketoaldehyde **I.12** was then transformed into iminium ion **I.13**, and addition of 1,3-acetonedicarboxylic acid (**I.14**) led to the formation of *N*-methyl-euphococcinine (**I.6**) in a one-pot process.^[18–19] This biomimetic Mannich strategy was often adopted in other syntheses of euphococcinine and adaline.^[20–22] A very similar, albeit asymmetric, strategy was used by Davis in 2012 to synthesize structurally related azabicyclononane natural products (not shown).^[23]

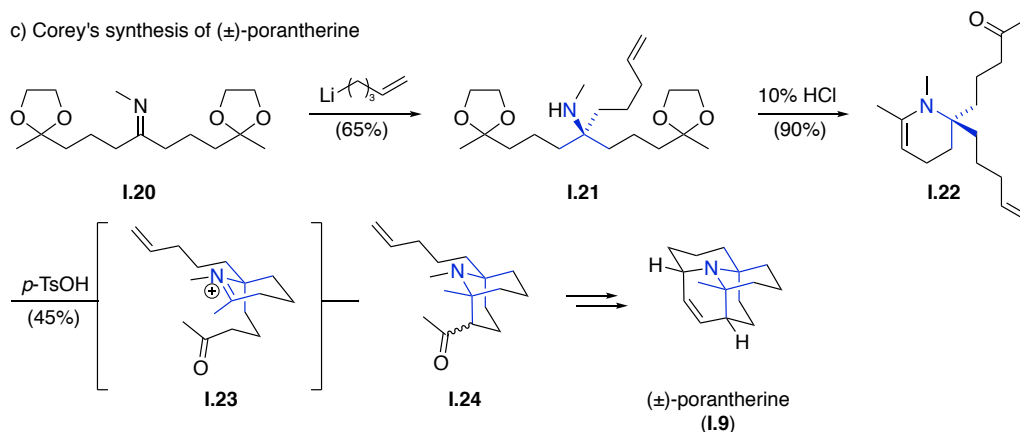
The construction of ATAs *via* Mannich reaction is very popular and has found use toward structurally very different alkaloids such as asparagine A (**I.148**),^[24] FR901483,^[25–26] and gracilamine.^[27] Also, Mannich reactions have been the predominant strategy in *Lycopodium* alkaloid synthesis.

a) Alder's synthesis of (±)-*N*-methyl-euphoccocinine

b) Heathcock's synthesis of (±)-lycopodine



c) Corey's synthesis of (±)-porantherine



Scheme I.2 Homotropane alkaloid synthesis by Alder (1959), lycopodine synthesis by Heathcock (1982) and porantherine synthesis by Corey (1974).

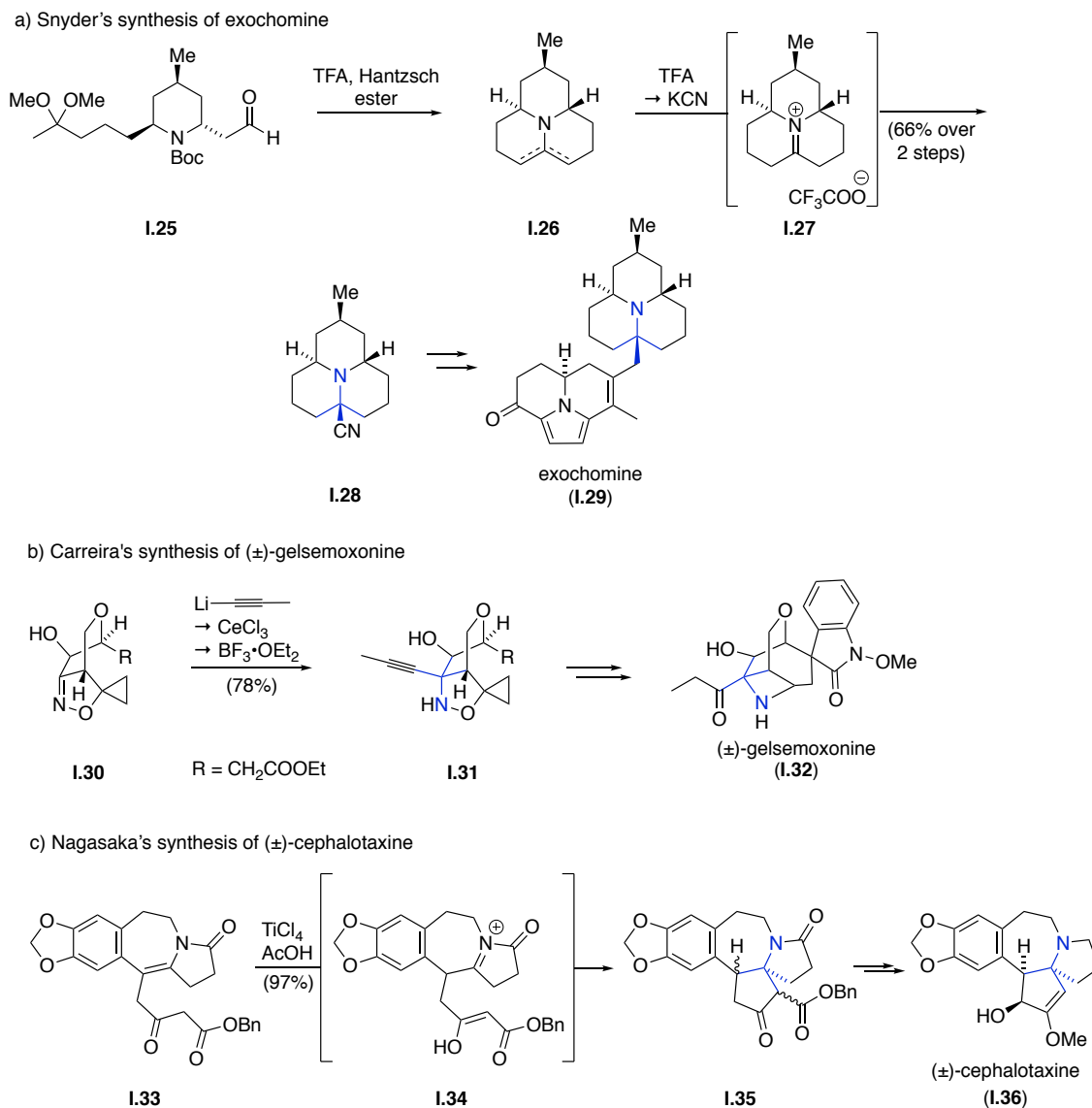
In 1982, Heathcock established one of the most elegant and groundbreaking routes to lycopodine (I.19), which has been adapted multiple times throughout the years towards other *Lycopodium* alkaloids (Scheme I.2b).^[28–30] Starting from amino bisacetal I.15, both ketones underwent deprotection to give reactive monocyclic intermediate I.16. Condensation of the amino group gave iminium ion I.17 which underwent an intramolecular Mannich reaction to furnish tricyclic secondary ATA I.18. The formation of two rings and the installation of the ATA thus occurred in a one-pot procedure, which mimics the proposed biosynthesis of lycopodine (I.19). Further optimization by Heathcock and co-workers resulted in an eight step synthesis – the shortest synthesis of this popular synthetic target to date.^[30] Using this strategy, lycodine (I.43) and lycodoline were also prepared by Heathcock.^[30] Synthetic campaigns involving a biomimetic Mannich reaction have been used by Evans toward clavolonine (2005)^[31] and Fujioka toward other *Lycopodium* alkaloids (2011).^[32] Although the Mannich approach is very elegant, a major disadvantage can be long reaction times (up to 18 days as for lycopodine (I.19)), due to the

necessary simultaneous formation of an iminium ion and an enol as depicted in intermediate **I.17**.^[30] A solution to this problem was recently offered by Carter, who was able to prepare and isolate an imine-containing TBS-enol ether, which formed the respective ATA after treatment with zinc triflate (not shown).^[33–34]

In addition to these historically important and famous examples, Mannich reactions have also been investigated for structurally different *Lycopodium* alkaloids. Schumann (1982)^[35–37] utilized this classic Mannich strategy to access racemic lycodine (**I.43**), α -obscurine and *N*-acetylflabellidine (not shown).^[35–37] In 2010, Sarpong used the same cascade as an opening sequence towards an asymmetric synthesis of (+)-complanadine A, a lycodine dimer.^[38] In the same year, Shair published an approach towards the *Lycopodium* alkaloid fastigiatine using a transannular Mannich reaction^[39–40] and in 2014 Takayama achieved a very short synthesis of (–)-lycodine (**I.43**) and (+)-flabellidine using a similar Mannich strategy as the key step (see chapter 1.1.2.3).^[41]

Porantherine (**I.9**), which is structurally related to the *Lycopodium* alkaloids, but not a member of the family, possess a twofold ATA and only two total syntheses have been reported to date, both of which rely on a Mannich reaction to install the ATA motif (Scheme I.2c).^[42–43] In 1974, Corey published the first synthesis of porantherine (**I.9**), and the installation of both ATAs involved electrophilic α -carbons. The first ATA present in **I.9** was set by the addition of an alkyl organolithium species to imine **I.20**, which was then treated with acid to give enamine **I.22** (*via* secondary amine **I.21**). The second ATA was subsequently formed by an acid-catalyzed Mannich reaction *via* iminium ion **I.23**, yielding bicycle **I.24** possessing the twofold ATA. In summary, the Mannich reaction and variants thereof constitute one of the most popular strategies in alkaloid synthesis to install ATAs.

The other strategies depicted in Scheme I.1 were not used as exhaustively as the Mannich reaction, however there are a few examples of their application in alkaloid total synthesis. The Strecker reaction, for example, has been used in Shibasaki's synthesis of lactacystin (**I.51**),^[44–45] Ohfuné's synthesis of manzacidins A (**I.100**) and C^[46] and Myers' synthesis of avrainvillamide (**I.55**) and stephacidin B (**I.10**, not shown).^[47] A nice example of the Strecker reaction in ATA synthesis is the recent synthesis of exochomine (**I.29**) by Snyder (Scheme I.3a).^[48] They were able to form iminium ion **I.27** by treatment of *in situ* generated enamine **I.26** with TFA (starting from Boc-protected piperidine **I.25**). They then tested the reactivity of the iminium ion **I.27** towards different nucleophiles, however “*virtually every nucleophile probed, such as tributylvinyl tin, allyltrimethylsilane (under Sakurai conditions), Grignard reagents, vinyl boronic acids (under Petasis-type conditions), or enolates (prepared both in situ and pre-formed), failed to deliver any coupling adduct.*”^[48] Radical addition to iminium ion **I.27** failed as well. Addition of KCN was singularly effectiveable to yield ATA **I.28**. Additional transformations finally led to exochomine (**I.29**).



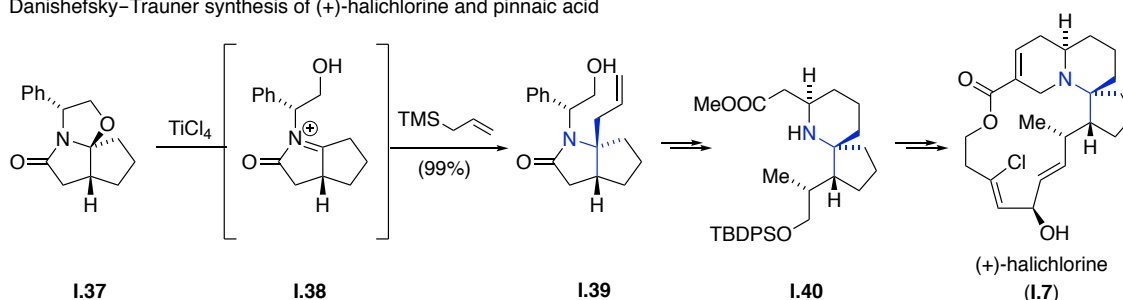
Scheme I.3 Synthesis of exochomine by Snyder (2016), gelsemoxonine by Carreira (2013) and cephalotaxine by Nagasaka (2002).

1,2-Addition of nucleophilic reagents to C–N double bonds was already discussed in Corey's synthesis of porantherine (**I.9**, Scheme I.2c).^[42–43] Furthermore, this general transformation has been applied in Ayer's synthesis of lycopodine (**I.19**),^[49–50] Qin's synthesis of lundurine A,^[51] Carreira's synthesis of gelsemoxonine (**I.32**)^[52] and Nagasaka's synthesis of cephalotaxine (**I.36**),^[53] amongst others. Carreira set the ATA present in **I.31** *via* a diastereoselective propynyllithium addition to isoxazoline **I.30** (Scheme I.3b). By contrast, Nagasaka made use of a powerful *N*-acyliminium ion cyclization in his synthesis of cephalotaxine (**I.36**, Scheme I.3c).^[54] Lactam **I.33** was treated with TiCl₄ and AcOH to form an *N*-acyliminium ion **I.34**, which was trapped in an intramolecular fashion by a β -ketoester to provide ATA **I.35** as a mixture of diastereomers (1:4.3, *cis/trans*). Intermediate **I.35** was then further transformed to cephalotaxine (**I.36**).

Another reaction in this category is the aza-Sakurai reaction that has been used for example in the Danishefsky–Trauner synthesis of halichlorine (**I.7**) in 1999 (Scheme I.4),^[55] which was followed by a synthesis of pinnaic acid in 2001 (not shown).^[56–57] They made use of Meyers' lactam **I.37** as a chiral precursor, which was transformed into the ATA-containing bicycle **I.39** using TiCl_4 and allyltrimethylsilane in an aza-Sakurai reaction (*via* *N*-acyliminium ion **I.38**). Intermediate **I.40** could be diversified to reach both halichlorine (**I.7**) and pinnaic acid.

The Pictet–Spengler reaction, which has been applied in Stork's synthesis of lycopodine (**I.19**),^[58] Inubishi's synthesis of (\pm)-3-demethoxyerythratidinone^[59] and several *Erythrina* alkaloid syntheses,^[60–62] also falls into this category.

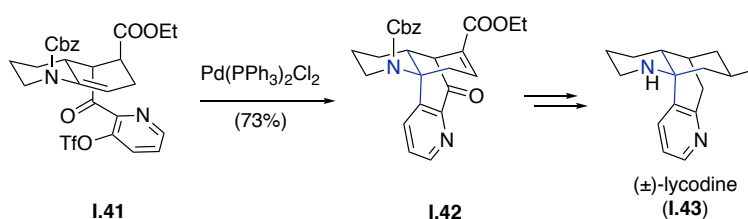
Danishefsky–Trauner synthesis of (+)-halichlorine and pinnaic acid



Scheme I.4 Synthesis of halichlorine by Danishefsky and Trauner (1999).

The application of a Heck reaction to set an ATA is rather unusual in alkaloid synthesis, but a few examples of this elegant approach have been reported. Tsukano and Hiramata used an intramolecular Heck reaction of a pyridyl triflate and an ene-carbamate **I.41** to furnish the ATA-containing pentacyclic core **I.42** of lycodine (**I.43**, Scheme I.5).^[63] Sun and Lin furnished the ATA in huperzine A (**I.2**) using an intramolecular Heck reaction of an enamine (not shown).^[64]

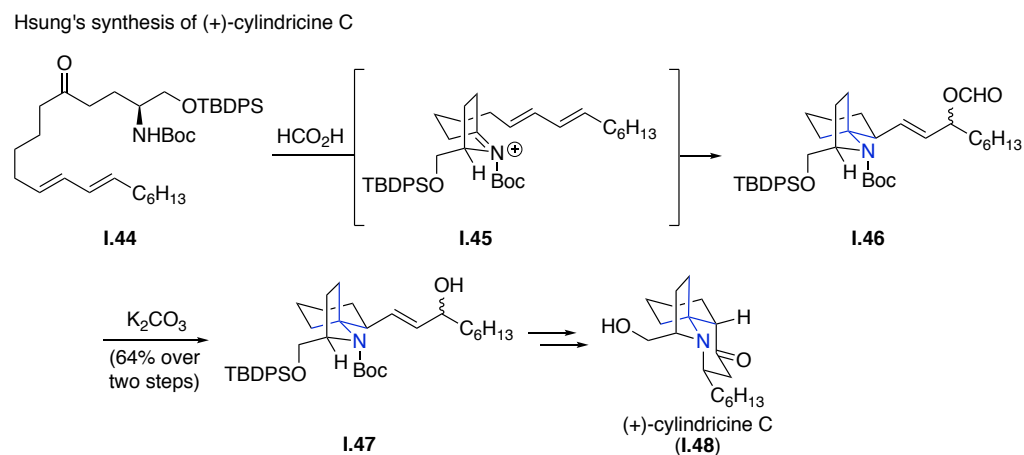
Tsukano's and Hiramata's synthesis of (\pm)-lycodine



Scheme I.5 Synthesis of lycodine by Tsukano and Hiramata (2010).

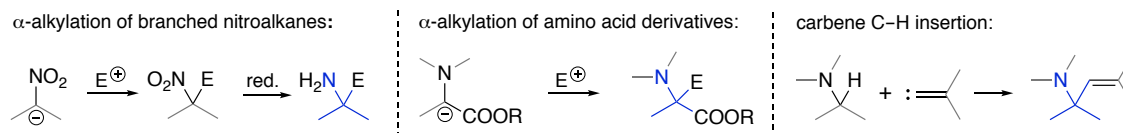
The last reaction in this category is the aza-Prins reaction, which has been used several times in the synthesis of ATAs. The Hsung group synthesized cylindricine C (**I.48**) from the linear precursor **I.44**. Intramolecular condensation to the *N*-acyliminium ion **I.45** set the stage for the nucleophilic

attack of a diene to furnish bicyclic ATA **I.46** (Scheme I.6).^[65–66] Hydrolysis of the formyl group then gave allylic alcohol **I.47** in 64% yield over two steps.



Scheme I.6 Synthesis of cylindricine C by Hsung (2004).

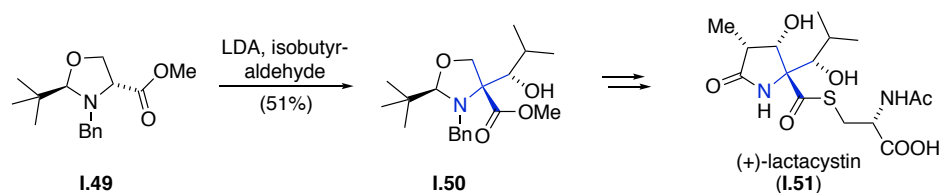
By contrast to the previous examples, the α -carbon can also serve as a carbon nucleophile (Scheme I.7). However, these reactions are less commonly employed. The alkylation of branched nitroalkanes or deprotonated amino acid derivatives falls into this category. In addition, insertions into nucleophilic C–H bonds adjacent to a C–N bond can be used for ATA installation.



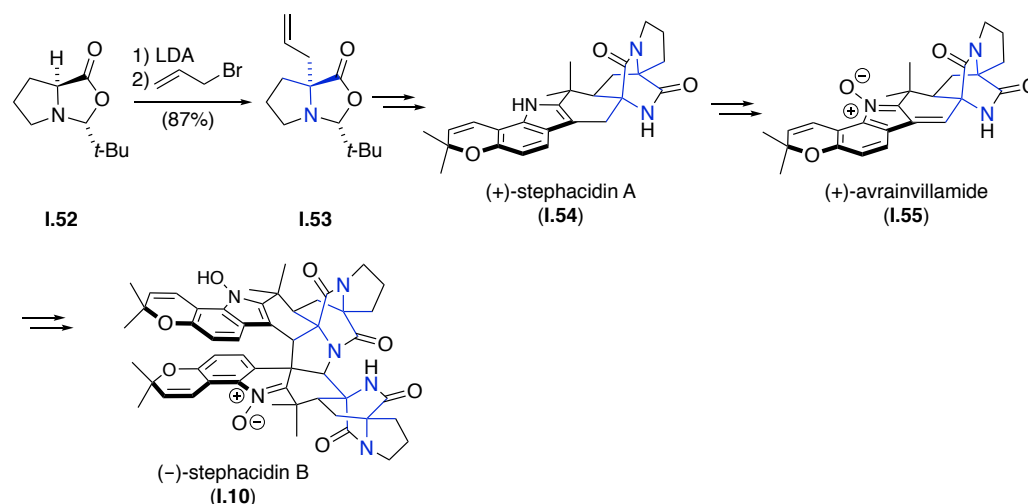
Scheme I.7 C–C bond formation involving nucleophilic α -carbons.

The α -alkylation of amino acid derivatives has been used in Corey's first synthesis of lactacystin (**I.51**) (Scheme I.8a).^[67] Starting from *cis*-oxazolidine derivative **I.49**, an aldol reaction with isobutyraldehyde set the ATA to furnish lactacystin precursor **I.50**. α -Alkylation has been a popular strategy to set the ATA in lactacystin (**I.51**) and salinosporamides and most syntheses reported to date involve an alkylation or aldol reaction of an α -amino acid derivative.^[67–75] More recently, Baran used Seebach's method for chirality transfer^[76] in the α -alkylation of proline derivative **I.52** to provide **I.53**, forging the first ATA of stephacidin A (**I.54**) in a diastereoselective manner (Scheme I.8b).^[77] Stephacidin A (**I.54**) could be further transformed into avrainvillamide (**I.55**) and stephacidin B (**I.10**).

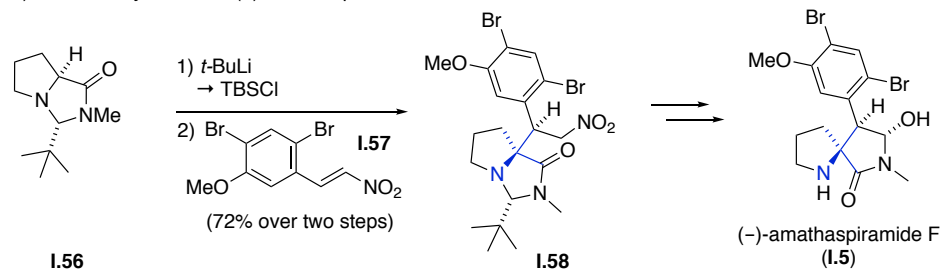
a) Corey's synthesis of (+)-lactacystin



b) Baran's synthesis of (+)-stephacidin A, (+)-avrainvillamide and (-)-stephacidin B



c) Trauner's synthesis of (-)-amathaspiramide F

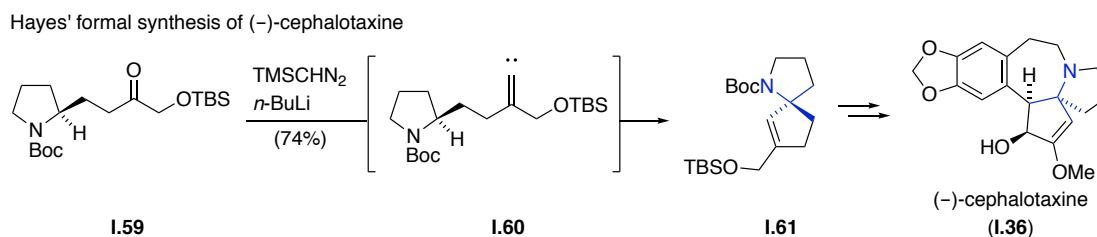


Scheme 1.8 Syntheses of lactacystin by Corey (1992), synthesis of prenylated indole alkaloids by Baran (2005) and synthesis of amathaspiramide F by Trauner (2002).

A third example of an α -alkylation of amino acid derivatives in alkaloid total synthesis is Trauner's synthesis of amathaspiramide F (**1.5**), which was reported in 2002 (Scheme 1.8c).^[78] Amino acid **1.56** was converted to the corresponding silyl ketene acetal, which then underwent Michael addition to the nitro styrene **1.57**, installing the ATA of **1.58** in a diastereoselective manner. Additional transformations led to the first synthesis of amathaspiramide F (**1.5**).

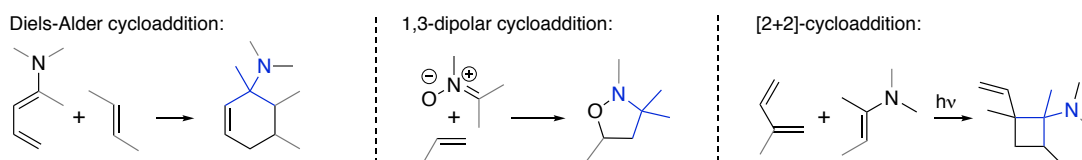
Carbene insertions are still relatively rare in ATA synthesis, however two examples have been reported by Hayes and co-workers. In their synthesis of cephalotaxine (**1.36**) they applied an vinylidene C–H insertion reaction. Derived from ketone **1.59**, vinylidene **1.60** can insert into the C–H bond adjacent to the carbamate to furnish spiro[4.4]azanone **1.61**, which could be further

transformed into cephalotaxine (**I.36**) (Scheme I.9).^[79] Another carbene insertion was reported by the same group in their synthesis of lactacystin (**I.51**).^[80]



Scheme I.9 Synthesis of cephalotaxine by Hayes (2008).

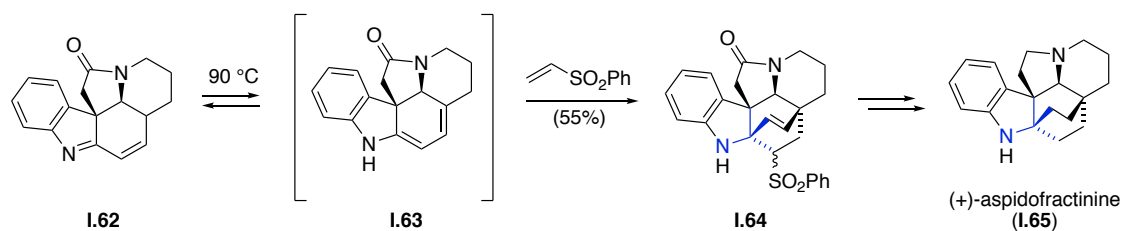
Pericyclic reactions have occasionally been employed to form the C–C bond of an ATA (Scheme I.10). This includes Diels–Alder cycloadditions of 1-aminodienes, 2-azadienes, and certain aminodienophiles, 1,3-dipolar cycloadditions of nitrones or azomethine ylids as well as [2+2]-cycloadditions.



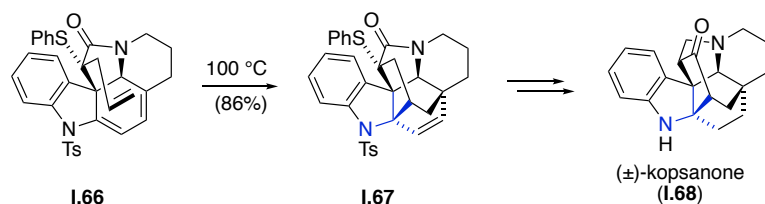
Scheme I.10 C–C bond formation involving pericyclic reactions.

Pericyclic reactions are particularly powerful as they build up a high degree of structural complexity in a single transformation. Therefore, pericyclic reactions constitute an effective strategy for the construction of sterically demanding ATAs. The Diels–Alder reaction has proven to be very effective for the synthesis of *Kopsia* alkaloids, a family which possesses an ATA incorporated into a bicyclo[2.2.2]octane system.^[81–89] The Diels–Alder approaches can be categorized as either intermolecular^[90–93] or intramolecular.^[94–98] In 1990, Spino used the intermolecular variant to set the ATA in aspidofractinine (**I.65**) using phenyl vinyl sulfone as a dienophile (Scheme I.11a).^[93] Highly reactive aminodiene **I.63** was formed from compound **I.62** by thermal isomerization and subsequently underwent cycloaddition with phenyl vinyl sulfone from the sterically more accessible convex side to give sulfone **I.64**, containing the complete carbon skeleton of aspidofractinine (**I.65**).

a) Spino's synthesis of (+)-aspidofractinine



b) Magnus' synthesis of (±)-kopsanone



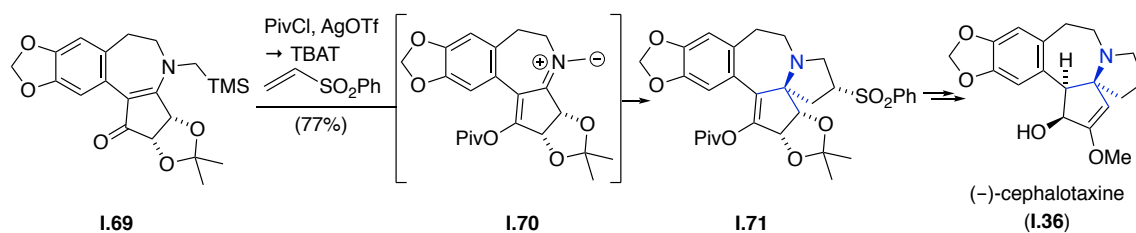
Scheme 1.11 *Kopsia* alkaloid syntheses by Spino (2009) and Magnus (1983).

By contrast, an intramolecular Diels–Alder approach was chosen by Magnus to construct the ATA in both kopsanone (**1.68**) and 10,22-dioxokopsane (Scheme I.11b).^[94–95] A strategically placed sulfide **1.66** forced the dienophile into close proximity with the diene. The intramolecular cycloaddition reaction proceeded at 100 °C and gave kopsanone precursor **1.67**, which could subsequently be transformed into the natural product **1.68**. This approach was also applied to the closely related alkaloids kopsijasmine, kopsine, (–)-kopsinilam and (–)-kopsinine (**1.87**).^[96–98] In addition, Fuchs applied an intramolecular nitroso-Diels–Alder cycloaddition to assemble the carbon skeleton of cephalotaxine (**1.36**) in 1988^[99] and an intramolecular Diels–Alder approach was used in Williams' synthesis of stephacidin A (**1.54**) and notoamide B in 2007 (not shown).^[100]

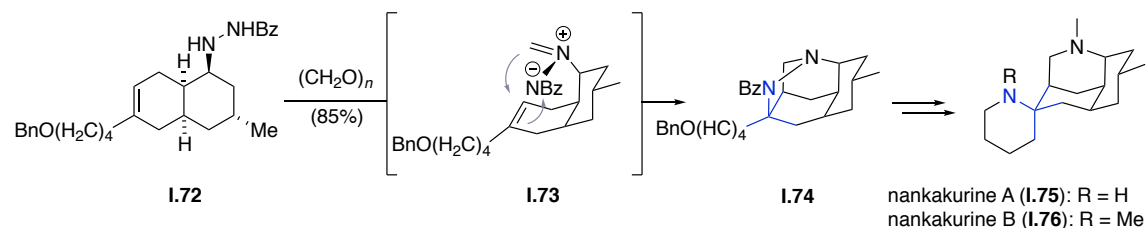
1,3-Dipolar cycloadditions have been used even more extensively than Diels–Alder reactions to implement ATAs. In 2006, Gin applied an intermolecular 1,3-dipolar cycloaddition in his synthesis of cephalotaxine (**1.36**) making use of phenyl vinyl sulfone as the dipolarophile, which had already been utilized as a potent dienophile in Spino's synthesis of aspidofractinine (**1.65**) (see Scheme I.11a).^[101–102] Gin transformed vinylogous amide **1.69** into azomethine ylide **1.70**, which then participated in a 1,3-dipolar cycloaddition to yield cephalotaxine precursor **1.71** (Scheme I.12a).^[101–102] The rather unexpected stereochemical outcome of this cycloaddition was confirmed by X-ray analysis.

An intramolecular 1,3-dipolar cycloaddition was applied in Overman's synthesis of nankakurine A (**1.75**) and nankakurine B (**1.76**) (Scheme I.12b).^[103] Condensation of benzoyl hydrazine **1.72** with formaldehyde furnished azomethine imine **1.73** *in situ*, which then underwent 1,3-dipolar cycloaddition to form tetracyclic pyrazolidine **1.74**. Following N–N bond cleavage with SmI₂, pyrazolidine **1.74** could be transformed into both nankakurines.^[103]

a) Gin's synthesis of (-)-cephalotaxine



b) Overman's synthesis of (+)-nankakurines A and B

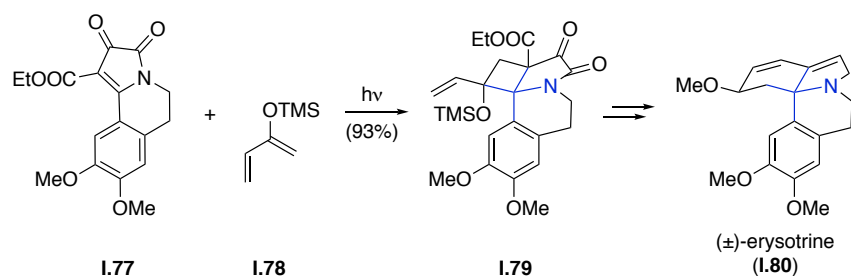


Scheme I.12 Synthesis of cephalotaxine by Gin (2006) and synthesis of nankakurines A and B by Overman (2010).

In addition to these examples, 1,3-dipolar cycloadditions have also found application in the syntheses of *Stemona* alkaloids,^[104] manzacidines^[105–106] and homotropane alkaloids (not shown).^[107]

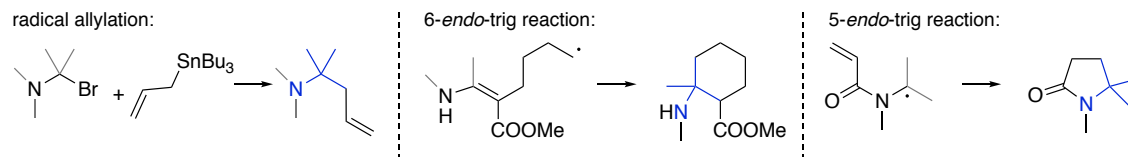
[2+2]-Cyclizations are much less encountered than [4+2]-cyclizations or 1,3-dipolar cycloadditions and have only been applied a few times in ATA synthesis.^[108–114] One example by Tsuda features an intermolecular photochemical [2+2]-cycloaddition of tricycle **I.77** and 2-siloxydiene **I.78** in case of the synthesis of erysotrine (**I.80**) (Scheme I.13).^[113] The resulting cyclobutane **I.79** subsequently expanded into the six-membered ring of erysotrine (**I.80**).

Tsuda's synthesis of (±)-erysotrine



Scheme I.13 Synthesis of erysotrine by Tsuda (1992).

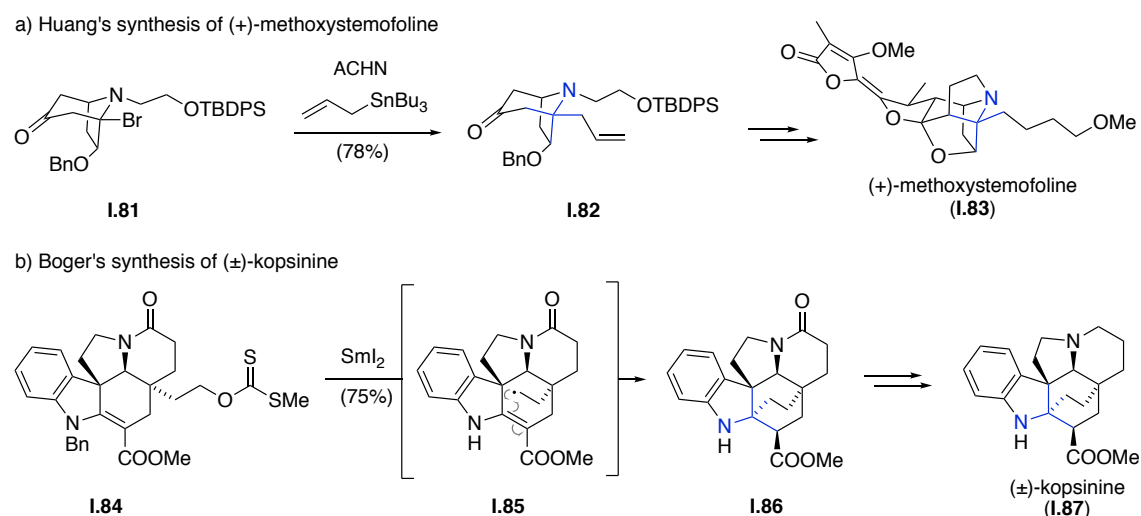
The last subclass of reactions to form the final C–C bond in an ATA is radical reactions, which are relatively rare, but not unprecedented (Scheme I.14). 5-*endo*-trig and 6-*endo*-trig cyclizations and radical transfer allylations fall into this category.



Scheme I.14 C–C bond formation involving radical reactions.

A radical bridgehead allylation was applied by Huang to construct the ATA of methoxystemofoline (**I.83**) (Scheme I.15a).^[115] Starting from bromide **I.81** a Keck allylation using 1,1'-azobis(cyclohexanecarbonitrile) (ACHN) as a radical initiator and allyltributylstannane provided ATA-containing bicycle **I.82** at an early stage of the total synthesis.

With respect to radical cyclizations to construct ATAs, a transannular 6-*endo*-trig cyclization was applied in Boger's synthesis of kopsinine (**I.87**, Scheme I.15b).^[116] Xanthate **I.84** was treated with SmI_2 to form primary radical **I.85**, which then undergoes 6-*endo*-trig cyclization followed by reduction and diastereoselective protonation of the ester enolate to install the ATA of **I.86** as a single diastereomer. A 5-*endo*-trig radical cyclization as part of a domino sequence will be discussed in detail for Inubushi's synthesis of stemonamide (**I.162**) and isostemonamide in section 1.1.2.3 regarding cascade reactions.^[117–118]

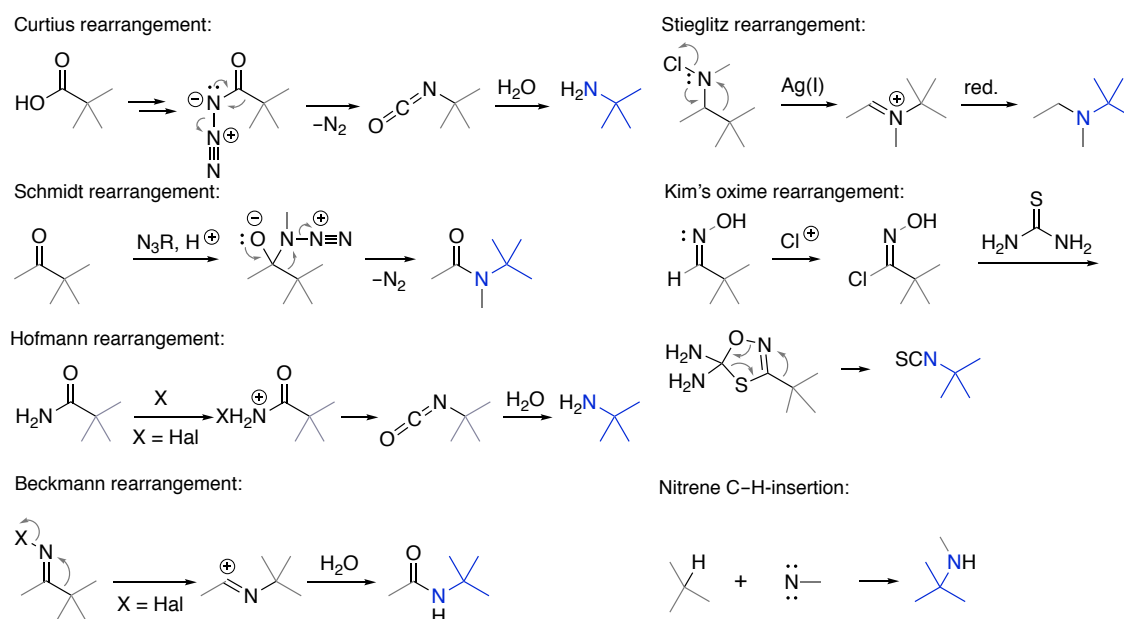


Scheme I.15 Synthesis of methoxystemofoline by Huang (2015) and synthesis of kopsinine by Boger (2013).

In summary, a large variety of methods have been developed to furnish the C–C bond of an ATA. The most popular reaction in this class of transformations is the Mannich reaction, which has been used multiple times in total synthesis. It should be noted that most Mannich reactions were applied in an intramolecular fashion to circumvent the steric hindrance associated with an ATA.

1.1.2.2 Installation of the ATA *via* C–N bond formation

In case of the C–N bond formation, intramolecular rearrangements that involve an electrophilic nitrogen are often used for the installation of ATAs (Scheme I.16). Prominent strategies include Curtius, Schmidt, Hofmann, Beckmann, Stieglitz^[8] and Kim's oxime rearrangement.^[119–121] In most cases, these reactions can be classified as 1,2-sigmatropic rearrangements. In addition, related nucleophilic substitutions using *N*-haloamines have been applied in the synthesis of ATAs. Apart from these rearrangements, an electrophilic nitrogen also occurs in the insertion of nitrenes into C–H bonds.

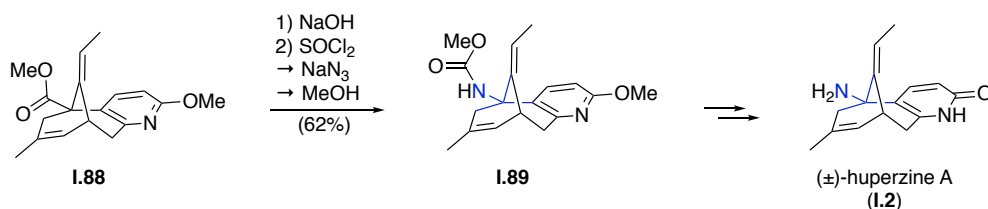


Scheme I.16 C–N bond formation involving electrophilic nitrogens.

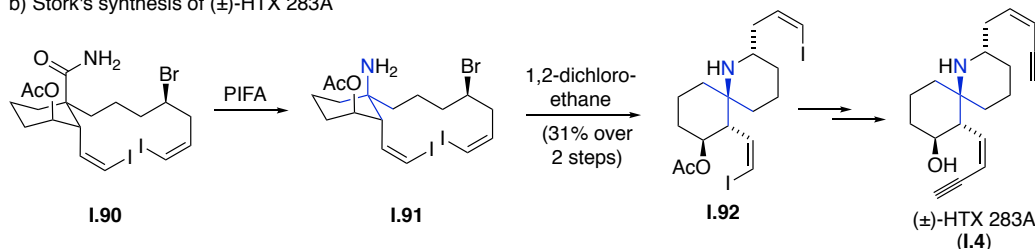
The Curtius rearrangement and variants thereof are probably the most popular choice for the formation of primary ATAs. As a demonstrative example, it has been applied numerous times in syntheses of huperzine A (**I.2**). The first synthesis of this popular synthetic target was published in 1989 by Kozikowski (Scheme I.17a).^[122] In their synthesis, methyl ester **I.88** was hydrolyzed to the carboxylic acid, which was transformed into the acyl azide *via* the acyl chloride. This acyl azide subsequently underwent a Curtius rearrangement to the isocyanate, which was trapped by methanol to provide methyl carbamate **I.89**. Double deprotection of intermediate **I.89** gave huperzine A (**I.2**). Many huperzine A syntheses and several semi-syntheses were published in the following years and most of them feature a racemic or enantiomerically pure carboxylic acid derivative of precursor **I.88**, retaining the Curtius rearrangement as the key step for the ATA formation.^[122–132] Curtius rearrangements have also been used for the synthesis of other ATA-containing alkaloids, such as histrionicotoxins,^[133–134] lundurines^[135] and amathaspiramides.^[136]

An example for a Schmidt reaction as part of a cascade can be found in Zhang's synthesis of stemonamide (**I.162**),^[137] which is described in detail in chapter 1.1.2.3. The closely related Hofmann rearrangement was applied in Stork's synthesis of HTX 283A (**I.4**) to set the ATA (Scheme I.17b).^[138] Primary amide **I.90** was oxidized with [bis(trifluoroacetoxy)iodo]benzene (PIFA) leading to alkyl migration and decarboxylation to give ATA **I.91**. One of the most famous applications of the Beckmann rearrangement in alkaloid synthesis appears in the synthesis of tetrodotoxin (TTX, **I.3**) by Kishi in 1972 (Scheme I.17c).^[139–142] Mesylated oxime **I.93** was converted to ATA **I.94** in a Beckmann rearrangement at an early stage of the synthesis. Additional transformations involving a series of stereoselective redox transformations, ring cleavage and installation of the cyclic guanidine led to the first synthesis of TTX (**I.3**).

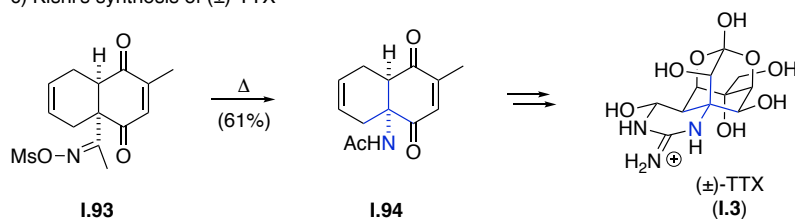
a) Kozikowski's synthesis of (±)-huperzine A



b) Stork's synthesis of (±)-HTX 283A



c) Kishi's synthesis of (±)-TTX



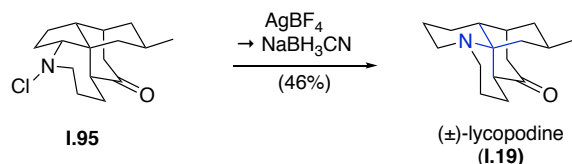
Scheme I.17 Kozikowski's synthesis of huperzine A (1989), Stork's synthesis of HTX 283A (1990) and Kishi's synthesis of TTX (1972).

An unusual albeit elegant method for the synthesis of ATAs is the Stieglitz rearrangement. In 1998, Grieco made use of this transformation for the synthesis of lycopodine (**I.19**) (Scheme I.18a).^[143] *N*-chloro amine **I.95** was treated with silver tetrafluoroborate, and following rearrangement the resulting imine was reduced with sodium cyanoborohydride to yield lycopodine (**I.19**).

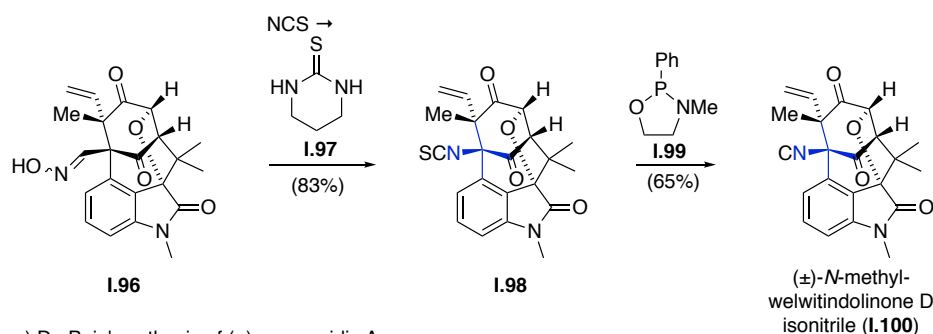
Another unusual approach for the implementation of an ATA was reported in the first total synthesis of *N*-methylwelwitindolinone D isonitrile (**I.100**) by Rawal in 2011 (Scheme I.18b).^[144–146] Starting from aldoxime **I.96**, isothiocyanate **I.98** was formed by a rearrangement found by

Huisgen.^[120–121] This rearrangement proceeds through the intermediacy of a nitrile oxide. Desulfuration using Mukaiyama's oxazaphospholidine **I.99** then provided the natural product *N*-methylwelwitindolinone D isonitrile (**I.100**).

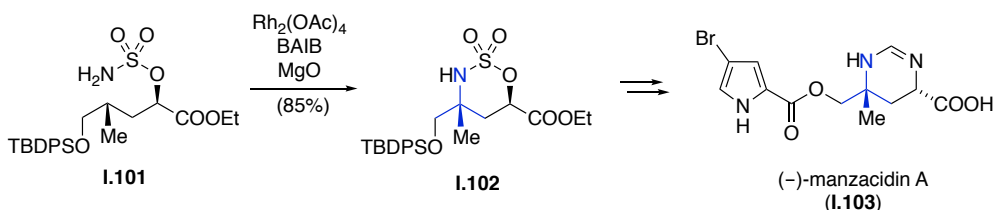
a) Grieco's synthesis of (±)-lycopodine



b) Rawal's synthesis of (±)-*N*-methylwelwitindolinone D isonitrile



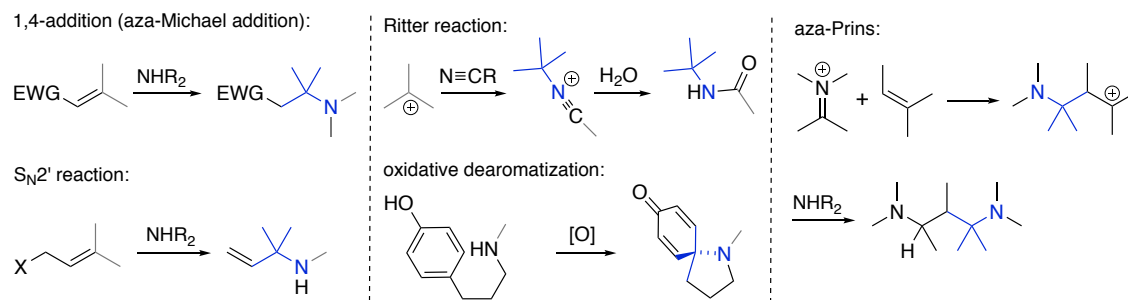
c) Du Bois' synthesis of (-)-manzacidin A



Scheme I.18 Grieco's synthesis of lycopodine (1998), Rawal's synthesis of *N*-methylwelwitindolinone D isonitrile (2011) and Du Bois' synthesis of manzacidin A (2002).

For several years, Du Bois has been developing and applying his signature nitrene insertion for the introduction of ATAs, and in 2002, manzacidin A (**I.103**) and C were prepared using an elegant oxidative Rh-catalyzed nitrene insertion starting from sulfamate ester **I.101** to yield cyclic sulfamate **I.102** (Scheme I.18c).^[147] Only one year later, Du Bois used a similar strategy to set the ATA in tetrodotoxin (TTX, **I.3**).^[148]

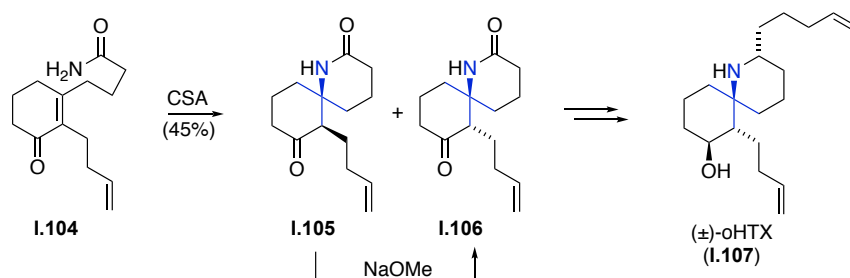
Nucleophilic addition or substitution involving a nucleophilic nitrogen is a common strategy for ATA synthesis as well (Scheme I.19). Aza-Michael additions, S_N2 and S_N2' reactions and haloaminations belong to this category. Carbocations may also be trapped by a nucleophilic nitrogen in the aza-Prins and Ritter reactions. In addition, oxidative dearomatizations have been used to establish ATAs.



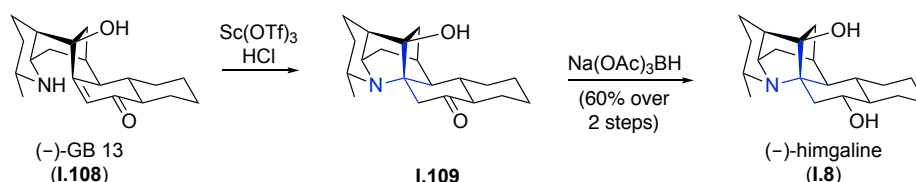
Scheme I.19 C–N bond formation involving nucleophilic nitrogens. EWG = electron-withdrawing group.

The aza-Michael addition is one of the most popular reactions in ATA formation and has been applied to many different classes of alkaloids, such as homotropane alkaloids,^[149–150] histrionicotoxins,^[151–153] hasubanan alkaloids,^[154–159] indole alkaloids,^[160–162] cephalotaxins,^[163–164] erythrina alkaloids,^[165] amathaspiramides,^[78] and indolizidine and quinolizidine alkaloids.^[166–170]

a) Kishi's synthesis of (±)-octahydrohistrionicotoxin



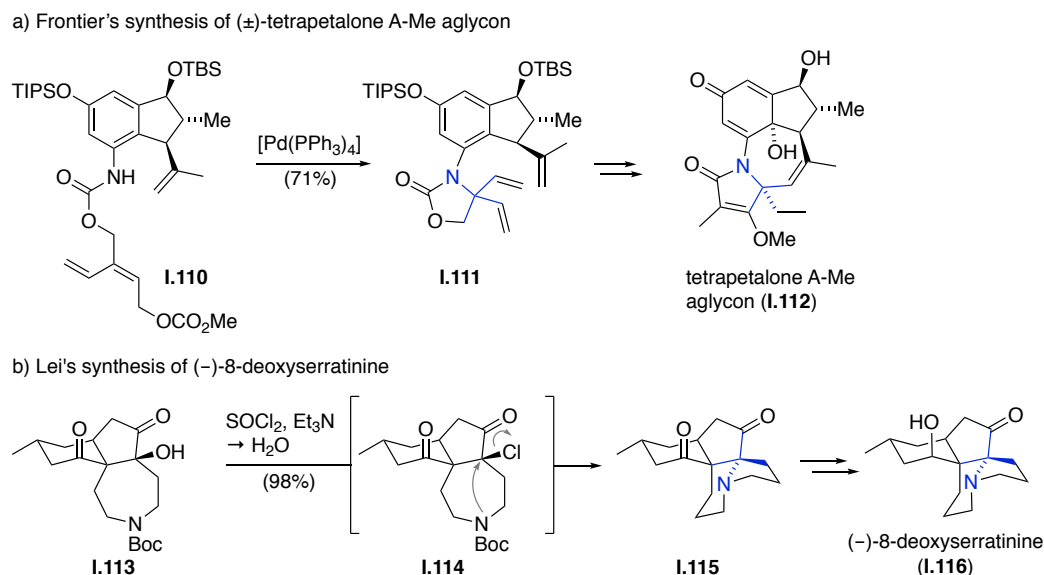
b) Chackalamannil's synthesis of (-)-himgaline



Scheme I.20 Synthesis of oHTX by Kishi (1975) and synthesis of himgaline by Chackalamannil (2009).

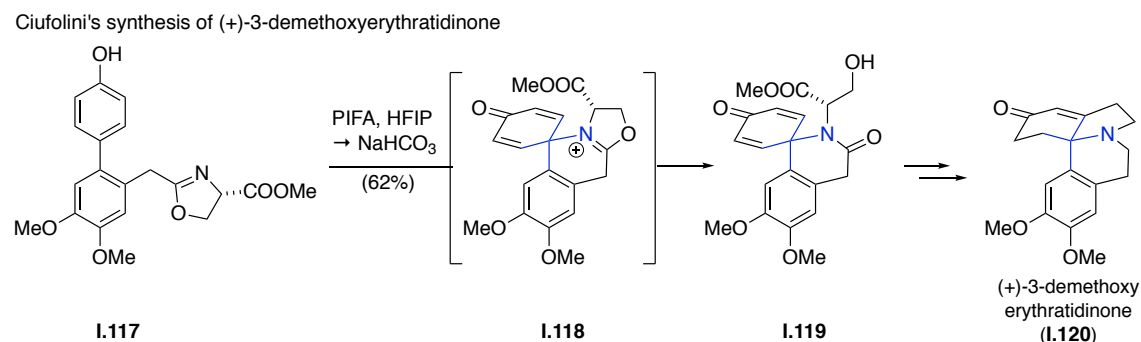
An example of an aza-Michael addition in alkaloid synthesis is shown in Scheme I.20a – as part of Kishi's synthesis of octahydrohistrionicotoxin (oHTX, **I.107**) (Scheme I.20a).^[151–153] The ATA is set by an intramolecular acid-catalyzed addition starting from primary amide **I.104**. The Michael addition yielded a 2:1 mixture of epimeric spiro lactams **I.105** and **I.106**. The undesired diastereomer **I.105** could be epimerized to **I.106** on treatment with NaOMe. Further transformations yielded oHTX (**I.107**). Another application of such a 1,4-addition is Chackalamannil's elegant and biomimetic conversion of GB 13 (**I.108**) into himgaline (**I.8**) *via* ketone **I.109** under Lewis and Brønsted acidic conditions (Scheme I.20b).^[171]

Another class of reactions that has been used for the installation of ATAs is nucleophilic substitution. Recently, Frontier published a synthesis of tetrapetalone A-Me aglycon (**I.112**) using a palladium-catalyzed Tsuji allylation starting from carbamate **I.110** (Scheme I.21a).



Scheme I.21 Synthesis of tetrapetalone A-Me aglycon by Fronier (2014) and synthesis of 8-deoxyserratinine by Lei (2014).

The nitrogen of the carbamate trapped the resulting Pd-allyl species and thereby formed the ATA **I.111** present in tetrapetalone A-Me aglycon (**I.112**).^[172] One of the very rare examples of a S_N2 reaction in ATA formation is Lei's synthesis of (-)-8-deoxyserratinine (**I.116**) (Scheme I.21b).^[173] Tertiary alcohol **I.113** was transformed into chloride **I.114**, which was subsequently displaced by the free secondary amine to give tertiary amine **I.115**, which could be further transformed into (-)-8-deoxyserratinine (**I.116**).

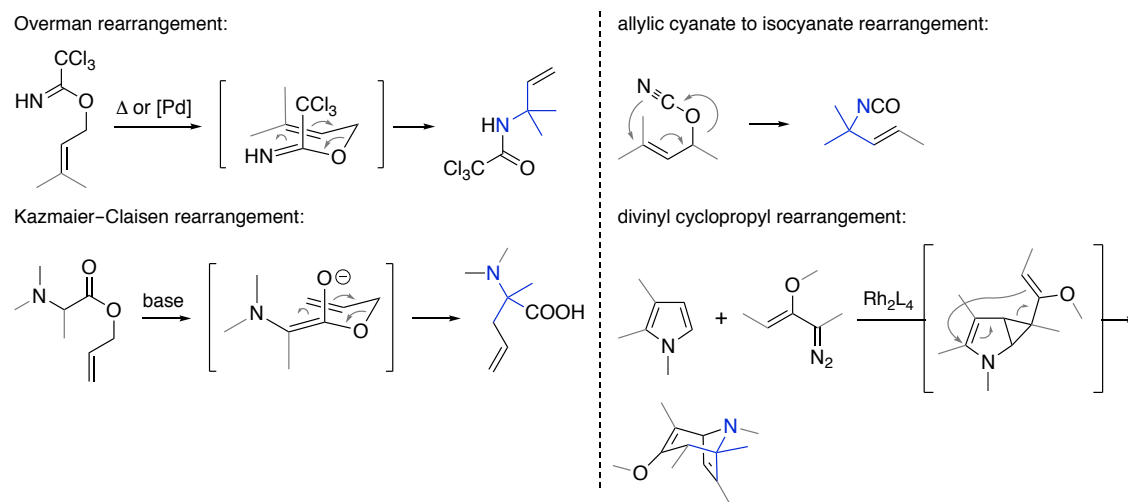


Scheme I.22 Synthesis of 3-demethoxyerythratidinone by Ciufolini (2015).

An additional method capable of installing ATAs is the oxidative dearomatization of phenols. This reaction has found application in Ciufolini's 3-demethoxyerythratidinone (**I.120**) synthesis where

oxazoline **I.117** was oxidized with PIFA to give spiroperidine **I.119**. This transformation presumably proceeds *via* intermediate **I.118** with subsequent hydrolysis (Scheme I.22).^[174–175]

Pericyclic reactions may also be used to install ATAs (Scheme I.23). In this class of reactions a C–N bond is formed employing methods such as the Overman, the Kazmaier–Claisen, the 3,3-sigmatropic rearrangements of allylic cyanates and divinyl cyclopropane rearrangements.^[8]

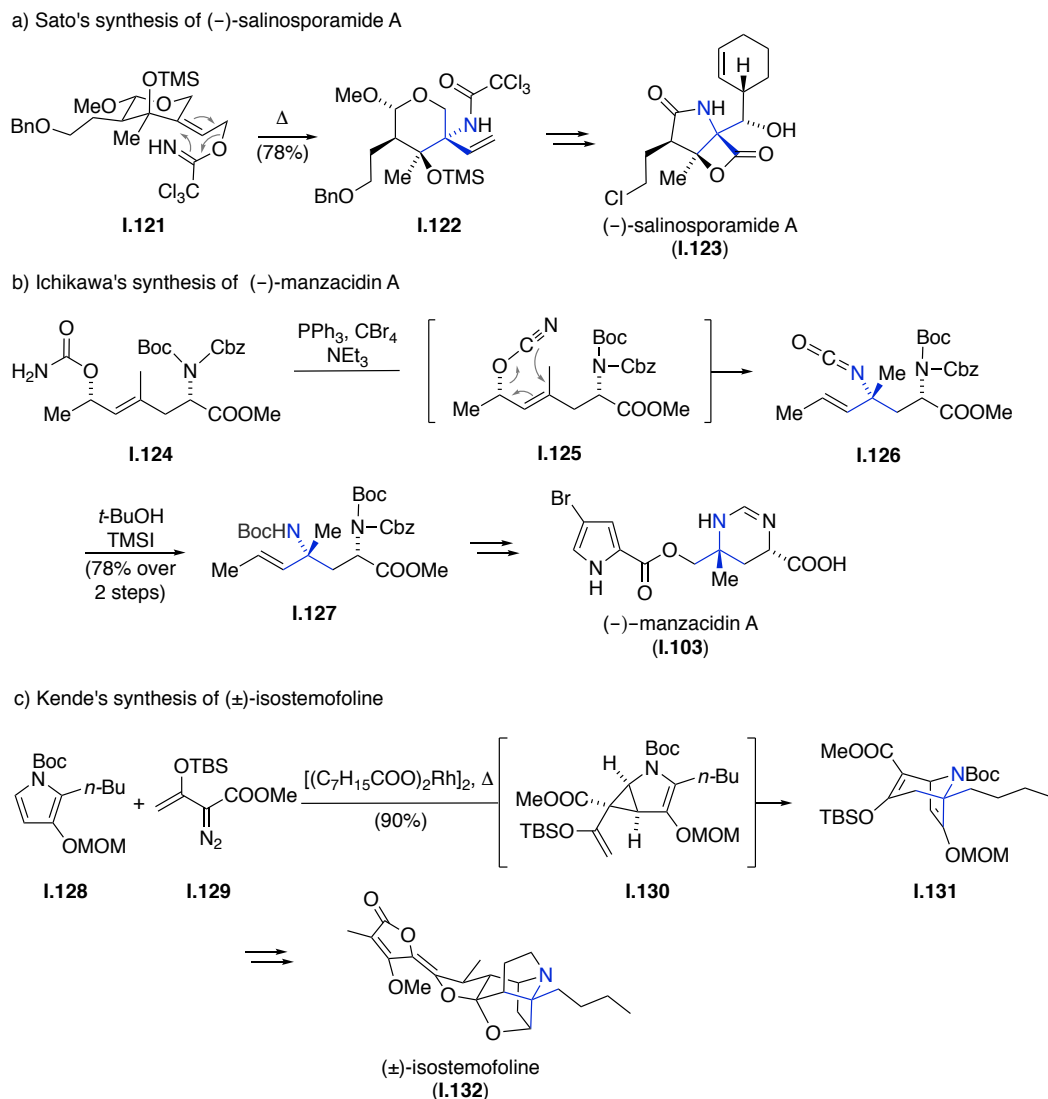


Scheme I.23 C–N bond formation using pericyclic reactions.

Overman rearrangements are frequently used to establish ATAs. Sato and Chida's synthesis of salinosporamide A (**I.123**) utilizes such a stereoselective rearrangement (Scheme I.24a).^[176] For this purpose, trichloroacetimidate **I.121** was heated to induce 3,3-sigmatropic rearrangement to provide trichloroacetamide **I.122**, as a key intermediate in the synthesis of salinosporamide A (**I.123**).

Other pericyclic reactions to form a C–N bond are relatively rare. In Ichikawa's synthesis of manzacidin A (**I.103**), a rare allyl cyanate to isocyanate rearrangement is applied as the key step (Scheme I.24b).^[177] For this purpose, carbamate **I.124** was converted to allyl cyanate **I.125** by dehydration, which subsequently underwent rearrangement with [1,3]-chirality transfer. Thus obtained isocyanate **I.126** was then transformed to manzacidin A (**I.100**) (*via* amine **I.127**).^[176]

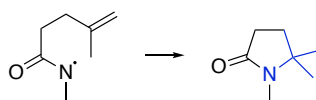
Another unusual approach for ATA installation is the use of a divinyl cyclopropane rearrangement. In 1999 Kende published the first synthesis of a *Stemona* alkaloid by employing this transformation (Scheme I.24c).^[178] The ATA was formed in an elegant process using a Rh-catalyzed cyclopropanation of pyrrole **I.128** using vinyl diazoester **I.129**, yielding divinyl cyclopropane **I.130**. Subsequent Cope-like rearrangement afforded bicycle **I.131**. The natural product isostemofoline (**I.132**) was assembled in several additional steps.



Scheme I.24 Synthesis of salinosporamide A by Sato (2011), synthesis of manzacidin A by Ichikawa (2012) and synthesis of isostemofoline by Kende (1999).

The use of radical reactions to form the C–N bond in an ATA is extremely rare (Scheme I.25). However one example including a radical 5-*exo*-trig cyclization of a nitrogen-centered amidyl radical as part of a cascade sequence is described in detail in chapter 1.1.2.3 (Scheme I.34).

5-*exo*-trig cyclization:



Scheme I.25 C–N bond formation involving radical reactions.

In conclusion, Curtius rearrangements and Michael additions are by far the most popular strategies to install the C–N bond as the last step in an ATA synthesis. As mentioned previously in the last

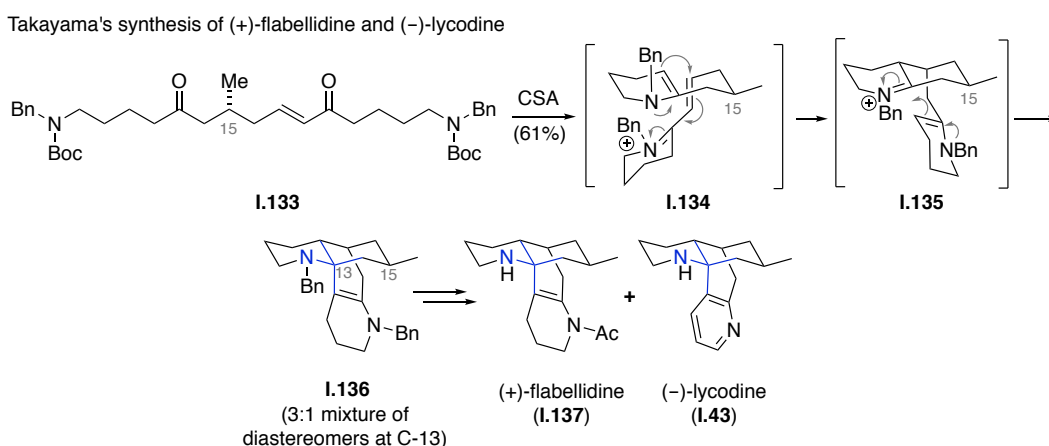
chapter, intramolecular transformations are applied to avoid issues of sterical hindrance associated with an ATA.

1.1.2.3 Cascade reactions for the implementation of α -tertiary amines

The development of cascade reactions has been a fascinating and expanding branch of organic chemistry and has attracted considerable attention from the synthetic community.^[179–187] This class of reactions is defined as chemical reactions that consist of at least two consecutive transformations where the isolation of intermediates is not required or, in some cases, possible.^[186] Strictly speaking, in cascade reactions no reagents are added after the initial step and the reaction conditions do not change throughout the whole sequence, thus distinguishing them from one-pot reactions.

The advantages of cascade reactions in synthesis include improved step economy as well as economies of time, labor, resource management, and waste generation.^[179] Cascade reactions can therefore be considered under the term “green chemistry“, as they minimize the amount of chemical resources, *e.g.*, solvents, chemicals, etc., required for the generation of a product that would otherwise have to be made in several individual steps. The development of cascade reactions “to provide specific targeted molecules of considerable structural and stereochemical complexity poses a significant intellectual challenge and can be one of the most impressive activities in natural product synthesis.”^[179]

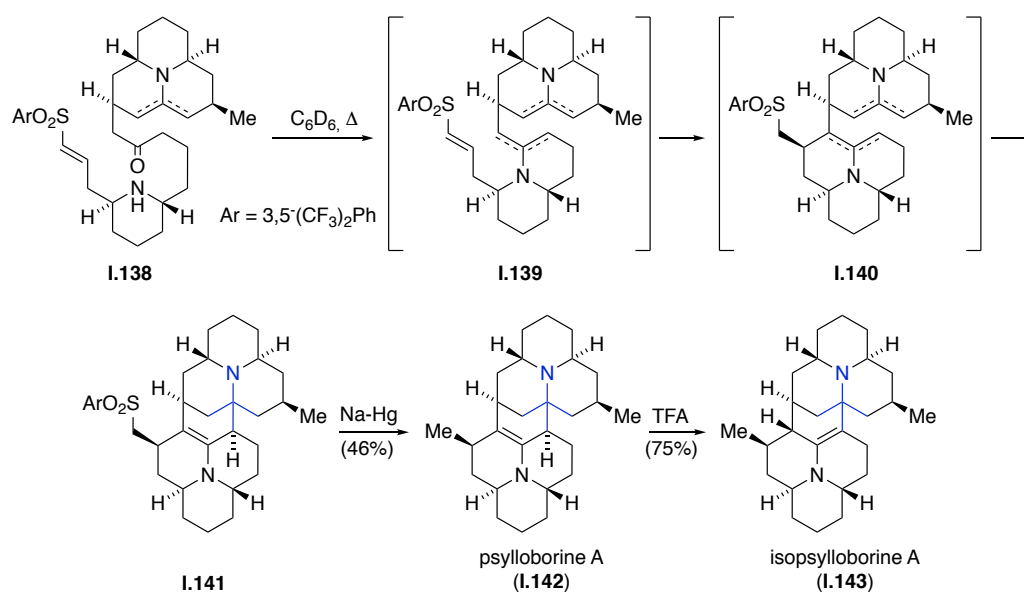
In a few cases, cascade reactions have also been developed for the preparation of α -tertiary amines toward alkaloid total syntheses. In these cases, the cascade reactions very often occur in an intramolecular fashion to circumvent the problem of steric hindrance associated with an ATA. For organizational purposes, the examples in this chapter are classified by the last bond that is formed and the nature of the transformation that occurs.



Scheme I.26 Synthesis of flabellidine and lycodine by Takayama (2014).

There are several impressive examples for cascade reactions in which the C–C bond is formed at an electrophilic α -carbon. Most of them involve Mannich reactions, therefore three examples showcasing a Mannich cascade are included in this chapter. In 2014, Takayama published a short synthesis of (–)-lycodine (**I.43**) and the first asymmetric synthesis of (+)-flabellidine (**I.137**) inspired by the biosynthetic proposal for *Lycopodium* alkaloids (Scheme I.26).^[41] Based on a suggested biosynthesis by the Spenser group,^[188–192] they envisaged that the stereochemistry of the methyl group at C-15 would control the stereochemistry of an enamine conjugate addition (indicated in **I.134**) and a subsequent Mannich reaction (as in **I.135**). Linear precursor **I.133**, featuring a single stereocenter, was prepared in eight linear steps. When this precursor was subjected to acidic conditions, double Boc-deprotection and double intramolecular condensation occurred to give iminium ion **I.134**. Intramolecular conjugate addition of the enamine to the α,β -unsaturated iminium ion gave second iminium ion **I.135**, which resembles the presumed precursor to most lycopodium alkaloids, phlegmarine. Iminium ion **I.135** finally underwent a Mannich reaction to yield tetracyclic skeleton **I.136** with a diastereomeric ratio of 3:1 at C-13 and a yield of 61%. They were then able to transform this intermediate into (+)-flabellidine (**I.137**) (11 steps and 21% overall yield) and (–)-lycodine (**I.43**) (in 11 steps and 15% overall yield).

Snyder's synthesis of the coccinellid alkaloids psyllorborine A and isopsyllorborine A



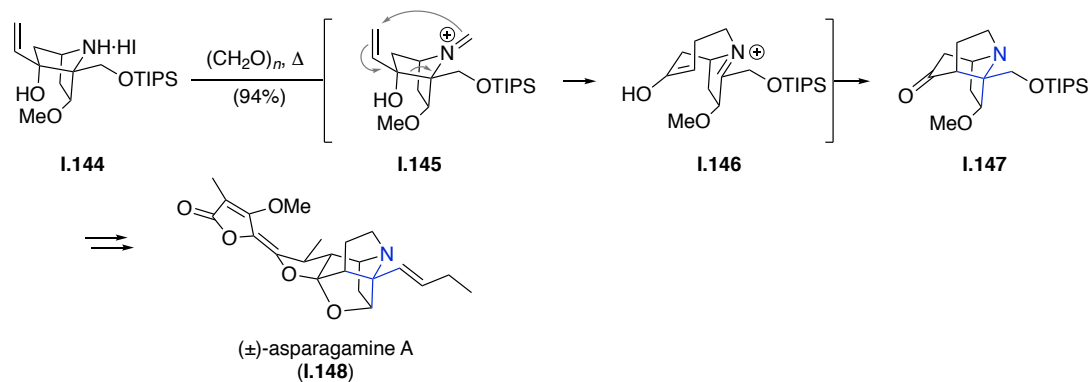
Scheme I.27 Synthesis of psyllorborine A and isopsyllorborina A by Snyder (2016).

A second application of Mannich cascades in ATA synthesis is Snyder's recently published synthesis of psyllorborine A (**I.142**) and isopsyllorborine A (**I.143**) (Scheme I.27).^[193] In his Michael–Mannich cascade, three rings and three stereocenters, including the ATA, are set in one transformation. Upon heating to 65 °C in deuterated benzene, secondary amine **I.138** was

condensed with the ketone to give enamine **I.139**, which then added to the Michael system and furnished hexacyclic **I.140**, containing two enamines in a yield of 15% over three steps (previous cascade reaction and Boc-deprotection not shown). Subsequent Mannich reaction then furnished heptacyclic ATA **I.141**. Reduction of the aryl sulfone with Na–Hg amalgam completed the synthesis of psylloborine A (**I.142**) that could be isomerized to isopsylloborine A (**I.143**) under acidic conditions.

Another example of a cascade reaction that includes a Mannich reaction is Overman's famous synthesis of asparagamine A (**I.148**) (Scheme I.28).^[24] He applied his signature reaction, the aza-Cope–Mannich cascade, to construct the scaffold of the stemonamide class of alkaloids. Ammonium iodide **I.144** was treated with paraformaldehyde to give iminium ion **I.145**, which subsequently underwent a (reversible) charge-accelerated 3,3-sigmatropic rearrangement (aza-Cope reaction) to yield iminium ion **I.146** that now reacted in an irreversible intramolecular Mannich reaction to afford the ATA present in asparagamine A (**I.148**) in 94% yield. This cascade has been proven to be highly applicable to other molecules with ATAs, such as FR901483.^[26, 194] Overman himself showcased this methodology in a variety of structurally demanding molecules, such as strychnine^[195] and 16-methoxytabersonine (not shown).^[196]

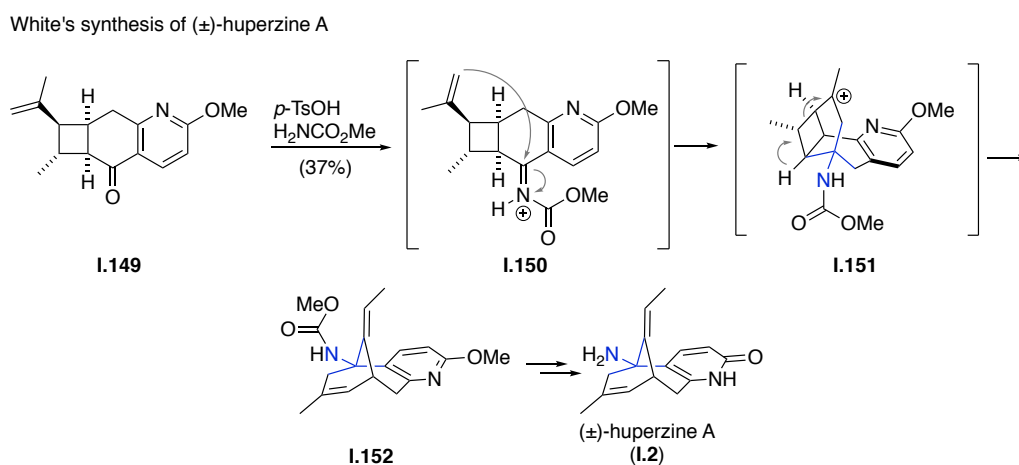
Overman's synthesis of (±)-asparagamine A



Scheme I.28 Synthesis of asparagamine A by Overman (2003).

A cascade reaction in which an ATA C–C bond is formed by addition to an electrophilic α -carbon is showcased in White's synthesis of the acetylcholinesterase inhibitor huperzine A (**I.2**) (Scheme I.29).^[197] As stated before, the ATA in huperzine A (**I.2**) has been set *via* 1,2-sigmatropic rearrangements in almost all other synthetic attempts (see chapter 1.1.2.2). In contrast, White applied an elegant and highly efficient aza-Prins cyclization/cyclobutane fragmentation for the construction of the ATA in the aminobicyclo[3.3.1]nonene scaffold. Ketone **I.149** was condensed with methyl carbamate to give *N*-acyliminium ion **I.150** that was trapped by an *endo*-oriented isopropenyl group in an aza-Prins reaction. The obtained cyclobutylcarbiny cation **I.151** is highly

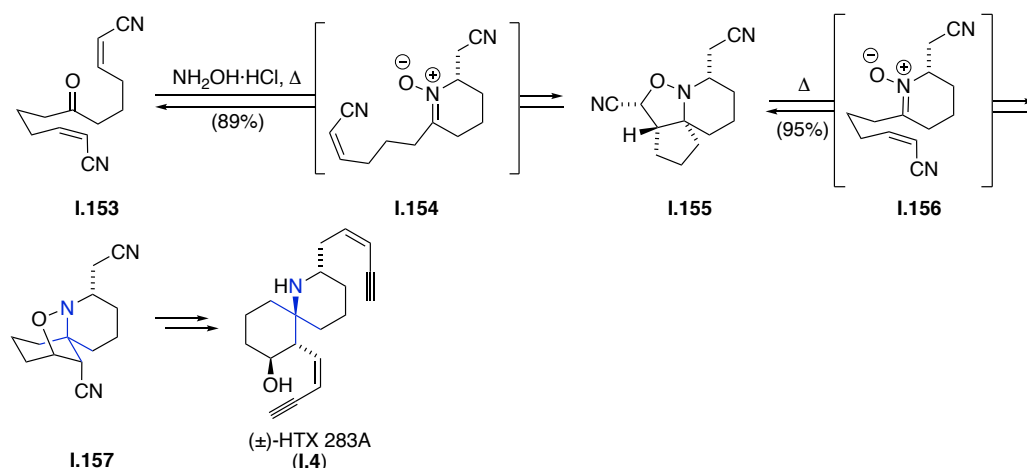
strained and therefore undergoes a fragmentation to the aminobicyclo[3.3.1]nonene skeleton **I.152**, which could be transformed into huperzine A (**I.2**) using Kozikowski's protocol.^[122]



Scheme I.29 Synthesis of huperzine A by White (2013).

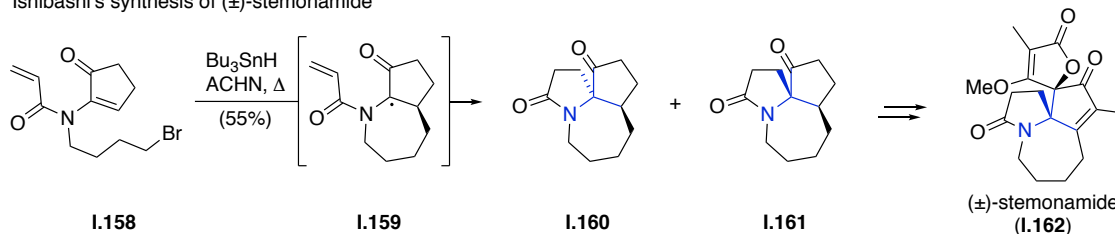
ATAs have not only been constructed by additions to electrophilic α -carbons but also by pericyclic reactions. A cycloaddition cascade was used in Stockmann and Fuchs' short racemic synthesis of HTX 283A (**I.4**), a noncompetitive inhibitor of nicotinic acetylcholine receptors (Scheme I.30).^[198] C_2 -symmetric ketodinitrile **I.153** was prepared in three steps, which included the use of a challenging cross-metathesis reaction, and was then allowed to condense with hydroxylamine. Subsequent intramolecular aza-Michael addition of the oxime gave nitrone **I.154**, which underwent intramolecular 1,3-dipolar cycloaddition to give isoxazolidine **I.155**, albeit as the wrong regioisomer. Tricyclic ATA **I.155** underwent retro-[3+2] cycloaddition upon heating, allowing equilibration to the more stable conformer **I.156** and the so-called 'Holmes dinitrile' (**I.157**) after another [3+2] cycloaddition. This intermediate had been previously converted into HTX 283A (**I.4**) by Holmes in four steps.^[199–200] However, Stockman and Fuchs optimized the last steps of the synthesis and were able to synthesize HTX 283A (**I.4**) in 9 steps and 17% overall yield. Another example of a pericyclic cascade reaction to set an ATA is Nicolaou's synthesis of the veterinary antibiotic thiostrepton involving an aza-Diels–Alder dimerization of two identical thiazolidine fragments as the first step of their complex cascade sequence (not shown).^[201–205]

Stockman and Fuchs' synthesis of (±)-HTX 283A

**Scheme I.30** Synthesis of HTX 283A by Stockman and Fuchs (2006).

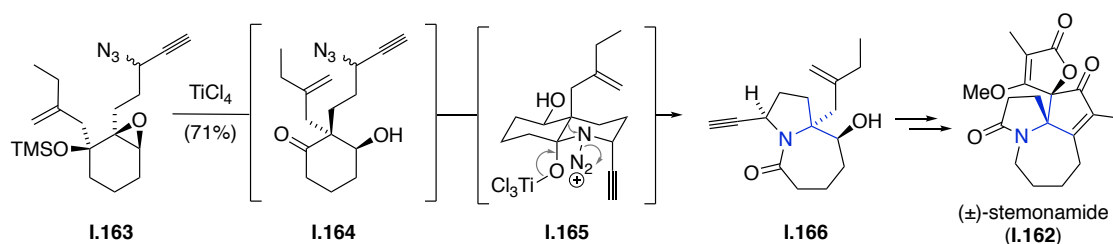
An example of a free radical cascade reaction to set an ATA can be found in Inubushi's racemic syntheses of stemonamide (**I.162**), isostemonamide and their reduced derivatives stemonamine and isostemonamine (Scheme I.31).^[117–118] Reaction of bromide **I.158** with tributyltin hydride and ACHN effected an initial 7-*endo-trig* cyclization to give intermediate radical **I.159**. This radical subsequently underwent a 5-*endo-trig* cyclization to yield a mixture **I.160** and **I.161**. Additional transformations of both compounds furnished stemonamide (**I.162**), alongside some of its congeners.

Ishibashi's synthesis of (±)-stemonamide

**Scheme I.31** Synthesis of stemonamide by Ishibashi (2008).

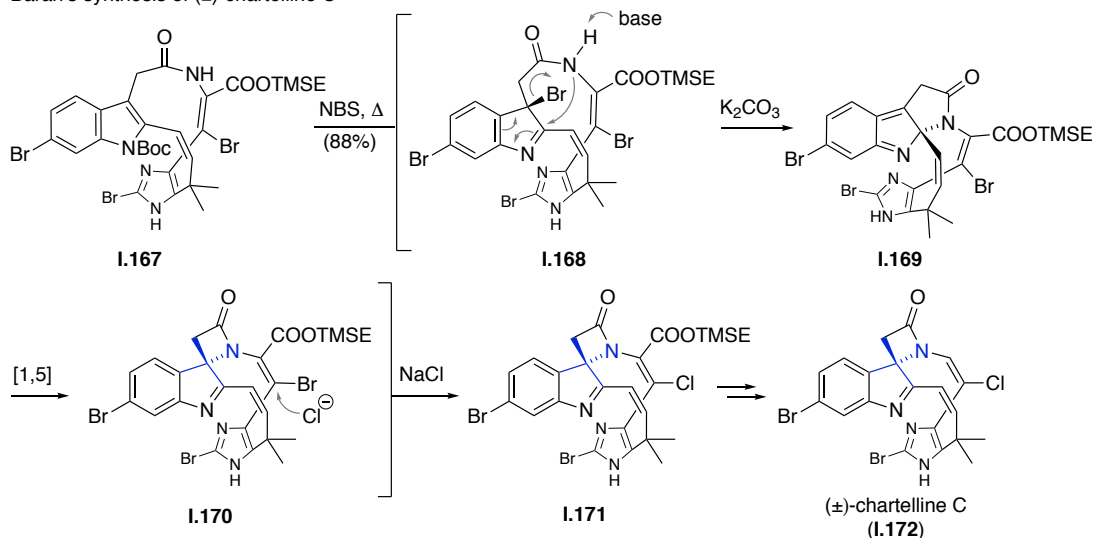
The second class of cascade reactions involves C–N bond formation as the last step to install the ATA. In Zhang's synthesis of stemonamide (**I.162**) and related *Stemona* alkaloids, a reaction sequence that involves an electrophilic nitrogen was applied (Scheme I.32).^[137] Starting from α -hydroxy epoxide **I.163** the cascade was initiated by a TiCl_4 -mediated semipinacol rearrangement to give intermediate ketone **I.164**, which then formed the ATA in an Aubé–Schmidt reaction to yield lactam **I.166** as a 5:1 mixture of diastereomers (*via* transition state **I.165**). Using this strategy, Zhang was able to synthesize stemonamide (**I.162**) and three additional *Stemona* alkaloids.^[137, 206–207]

Zhang's synthesis of (±)-stemonamide

**Scheme I.32** Synthesis of stemonamide by Zhang (2011).

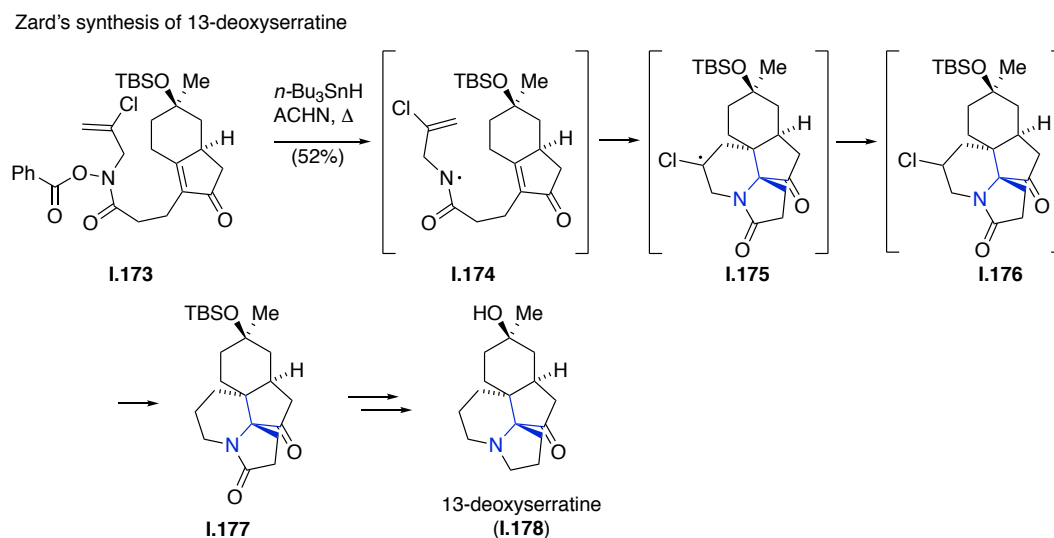
An impressive cascade reaction was implemented in the synthesis of chartelline C (**I.172**) by Baran and co-workers in 2005 (Scheme I.33).^[208–209] In their synthesis, indole **I.167** was brominated with *N*-bromosuccinimide (NBS) at 185 °C to form tetrabromide **I.168**. On addition of 18-crown-6 and base, γ -lactam **I.169** was formed and ATA formation was then the result of a 1,5-shift to give ring-contracted spiro- β -lactam **I.170**. Work-up with aqueous sodium chloride solution led to efficient halogen exchange at the vinylogous bromoformate to afford desired lactam **I.171**, which could be converted into chartelline C (**I.172**).

Baran's synthesis of (±)-chartelline C

**Scheme I.33** Synthesis of chartelline C by Baran (2005).

A very rare ATA formation involving a nitrogen-centered radical can be found in Zard's synthesis of 13-deoxyserratine (**I.178**) (Scheme I.34).^[210] His synthesis commences with *O*-benzoyl hydroxamic acid derivative **I.173**, which forms a nitrogen-centered amidyl radical **I.174** on treatment with *n*-Bu₃SnH and ACN. The radical then participated in sequential 5-*exo*-trig and 6-*endo*-trig cyclizations to furnish α -chlorocarbonyl radical **I.175**. Hydrogen abstraction from *n*-Bu₃SnH gave intermediate **I.176**, which was further reduced to 13-desoxyserattine precursor

I.177 by *in situ* dechlorination. The yield of 52% for this cascade reaction is impressive as an ATA and an adjacent quaternary stereocenter are formed in a single transformation.

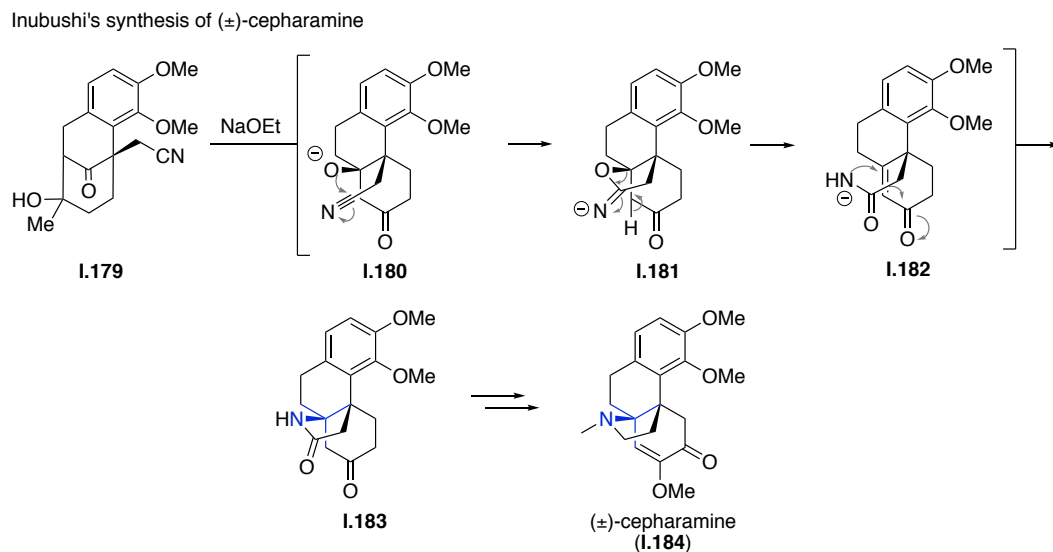


Scheme I.34 Synthesis of 13-deoxyserratine by Zard (2002).

In conclusion, a variety of cascade reactions have been applied in ATA synthesis. However, as already elaborated in the preceding chapters, the ATA is mainly set by Mannich or Michael additions. This observation not only illustrates the popularity but also the robustness of these reactions.

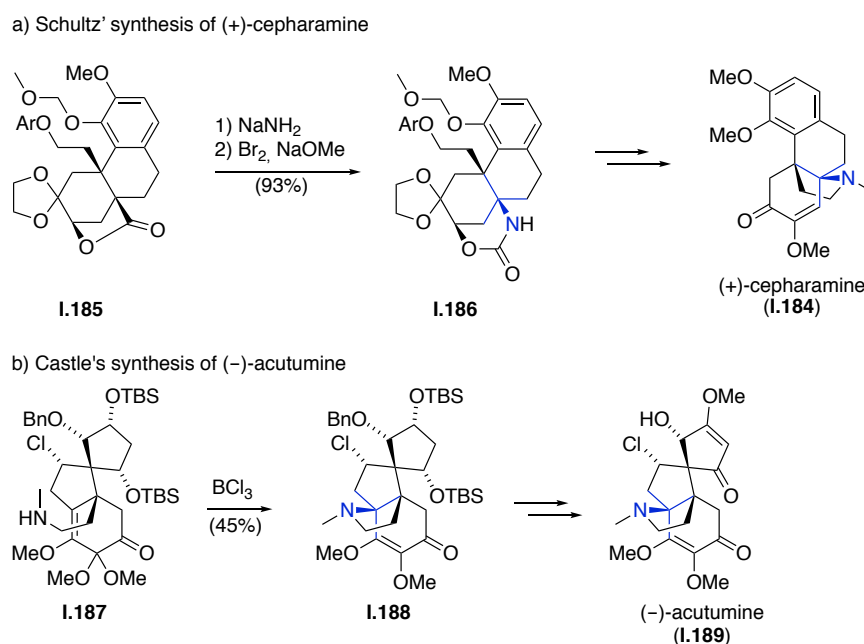
1.1.3 Installation of ATAs in hasubanan alkaloid synthesis

Due to their beautiful structures and unusual [4.4.3]-propellane core, hasubanan alkaloids have received significant attention from the synthetic community and several total syntheses have been reported to date.^[154–159, 211–219] The first syntheses of hasubanan alkaloids date back to the 1960s and 1970s, when Inubushi synthesized (\pm)-cepharamine (**I.184**),^[154–155] (\pm)-hasubanonine (**I.198**),^[156–157] (\pm)-aknadilactam^[156] and (\pm)-metaphanine (**I.214**)^[158–159] (Scheme I.35). These syntheses all commence from precursor **I.179**, which upon subjection to basic conditions undergoes a cascade reaction involving a retro-Michael/aza-Michael addition (**I.180** \rightarrow **I.181**) to furnish common tetracyclic precursor **I.183** (no yield reported).^[220]



Scheme I.35 Synthesis of Cepharamine by Inubushi (1969).

Almost 30 years later, Schultz reported the synthesis of the unnatural enantiomer (+)-cepharamine (**I.184**) using a Hofmann rearrangement to introduce the ATA. Starting from lactone **I.185** (Scheme I.36a),^[212] aminolysis followed by 1,2-rearrangement led to 1,3-oxazinan-2-one **I.186** that was further derivatized to obtain (+)-cepharamine (**I.184**).



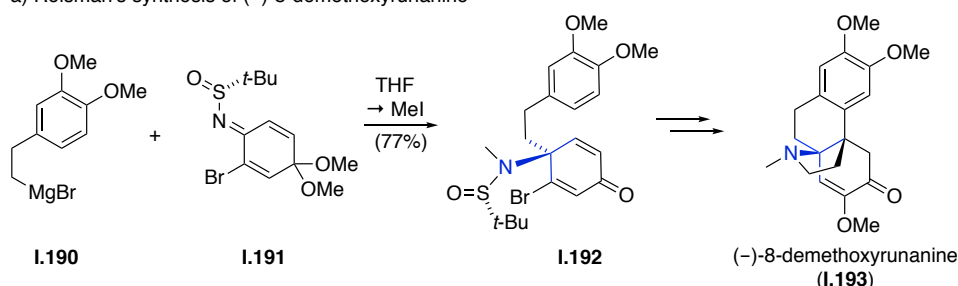
Scheme I.36 Synthesis of hasubanan alkaloids Schultz (1998) and Castle (2009).

In 2006, Castle and co-workers published their approach to the *rac*-hasubanonine core, which included an acid-catalyzed conjugate addition as the key step.^[221–222] Later, they extended their strategy to provide enantiopure (-)-acutumine (**I.189**) in which the ATA was set in a formal $\text{S}_{\text{N}}2'$ -

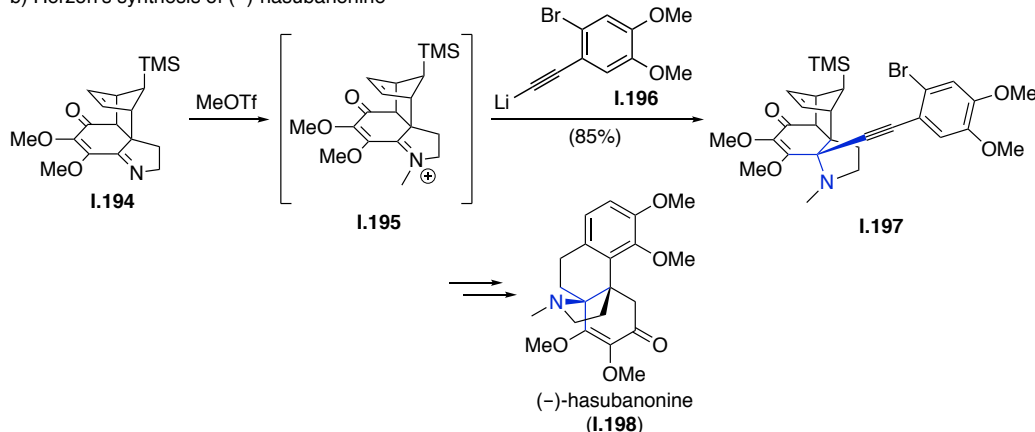
reaction (Scheme I.36a).^[215] From **I.187**, an allylic cation was generated under Lewis-acidic conditions and subsequently intercepted by the secondary amine. Resulting ATA-containing pyrrolidine **I.188** was then converted into acutumine (**I.189**).

In contrast to all other hasubanan syntheses, Reisman installed the ATA in (-)-8-demethoxyrunanine (**I.193**) at the very beginning of her synthesis (Scheme I.37a).^[217] Diastereoselective addition of Grignard reagent **I.190** into chiral *N*-*tert*-butanesulfinimine **I.191** gave sulfonamide **I.192**, which was subsequently converted into (-)-8-demethoxyrunanine (**I.193**) and a number of related alkaloids.

a) Reisman's synthesis of (-)-8-demethoxyrunanine



b) Herzon's synthesis of (-)-hasubanonine



Scheme I.37 Synthesis of hasubanan alkaloids by Reisman (2011) and Herzon (2011).

In the same year, Herzon published the first enantioselective synthesis of hasubanonine (**I.198**) (Scheme I.37b).^[216] Iminoquinone Diels–Alder adduct **I.194** was methylated to give iminium ion **I.195** that was immediately reacted with alkynyllithium **I.196**, providing ATA **I.197**. This strategy proved to be versatile, as not only (-)-hasubanonine (**I.198**), but also many other hasubanan alkaloids such as (-)-runanine, (-)-delavayine, (+)-periglucine B and (-)-acutumine (**I.189**) could be prepared with modifications of this strategy.^[216, 218–219]

In summary, a variety of different methods have been applied to install the ATA in hasubanan alkaloids. As in most other alkaloid syntheses, the installation of this structural motif always constitutes a key step and requires careful planning when designing a retrosynthesis.

1.2 Hasubanan alkaloids isolated from *japonica* species

1.2.1 *Stephania japonica* and its application in Traditional Chinese Medicine (TCM)

The genus *Stephania* belongs to the *Menispermaceae* family, which is native to warmer parts of the world. Plants of the genus *Stephania* are generally slender climbers with peltate and membranous leaves.^[223] *Stephania japonica*, a plant belonging to this genus, is native to village margins and open forests across Southeast Asia and the Pacific region. The first specimen was discovered in Japan, hence the name *Stephania japonica*.

It is widely used in traditional Chinese and Taiwanese medicine, where it is known as *qian jin teng* or snakevine.^[223–226] The root and stem leaves of the snakevine are believed to have a detoxicating effect and remove “heat, wind and dampness”.^[227] Extracts of the plant have been used for example for the treatment of malaria, dysentery and rheumatic arthralgia.^[227] To date, more than 50 alkaloids have been found in *S. japonica*,^[228] spanning four different natural product classes: dibenzylisoquinolines, hasubananes, aporphines and protoberberines.^[229] Some of these natural products were identified as biologically active (Figure I.4): the bisbenzylisoquinoline isotrilobine (**I.199**) was found to increase the efficiency of doxorubicin in resistant breast cancer cells, and cepharanthine (**I.200**) is already a registered drug for the treatment of pulmonary fibrosis.^[230–231]

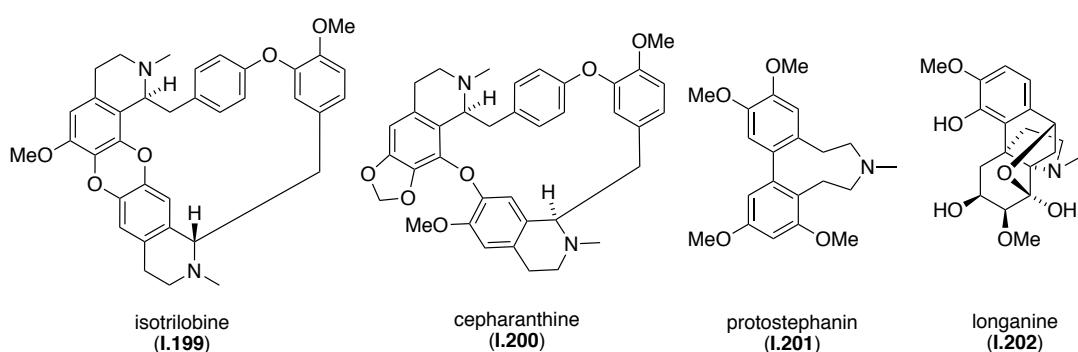


Figure I.4 The biologically active alkaloids isotrilobine, cepharanthine, protostephanin and longanine isolated from *Stephania japonica*.

Protostephanin (**I.201**), which belongs to the family of morphinan alkaloids, is an antihypertensive agent^[232] and a few members of the hasubanan family bind to the human δ -opioid receptor (DOR).^[233] In general, activation of opioid receptors results in euphoria, analgesia and decreased respiration. The most potent ligand for the δ -opioid receptor from the hasubanan family is

longanine (**I.202**) with a half maximal inhibitory concentration (IC_{50}) value of 700 nM. The hasubanan alkaloids tested showed similar binding affinity for both the μ - and δ -opioid receptors, with IC_{50} values ranging from 0.7 to 46 μ M, but low affinity for the κ -opioid receptor. However, when compared to morphinan opioid ligands, the binding of hasubanan alkaloids is relatively weak, probably due to the opposite absolute configuration at the benzylic quaternary stereocenter.^[234]

1.2.2 Isolation and structure of (+)-stephadiamine

The norhasubanan alkaloid (+)-stephadiamine (**I.1**) was isolated in 1984 by Taga *et al.* from the alcoholic extracts of the common scrambler *Stephania japonica* and represents a new class of alkaloids that is closely related to the hasubanan and morphinan alkaloids.^[224] (+)-Stephadiamine (**I.1**) was isolated “with difficulty in $4 \times 10^{-6}\%$ yield from the mother liquor after removal of metaphanine,”^[224] and thus biological evaluation has not been possible to date. Nevertheless, Taga *et al.* assigned the structure of the novel alkaloid by 1H NMR analysis, mass spectrometry and IR spectroscopy. Moreover, it was possible to obtain an X-ray structure of (+)-stephadiamine (**I.1**) (Figure I.5) and its absolute stereochemistry was assigned by the X-ray structure of *N*-(*p*-bromobenzoyl)-stephadiamine (not shown). From a structural point of view, pentacyclic (+)-stephadiamine (**I.1**) has a unique [3.3.4]-propellane core structure that consists of a tetrahydronaphthalene system fused to a cyclopentane and a pyrrolidine.^[235] The aza-propellane motif is characteristic for hasubanan alkaloids; however, as opposed to the hasubanan alkaloids, the cyclohexenone is contracted to a cyclopentane in (+)-stephadiamine (**I.1**).

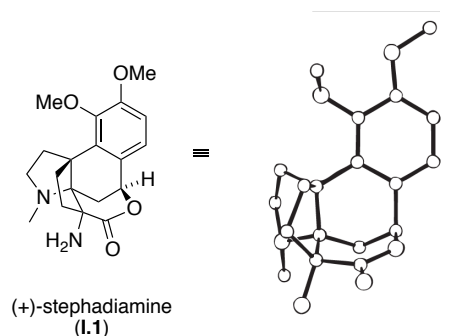


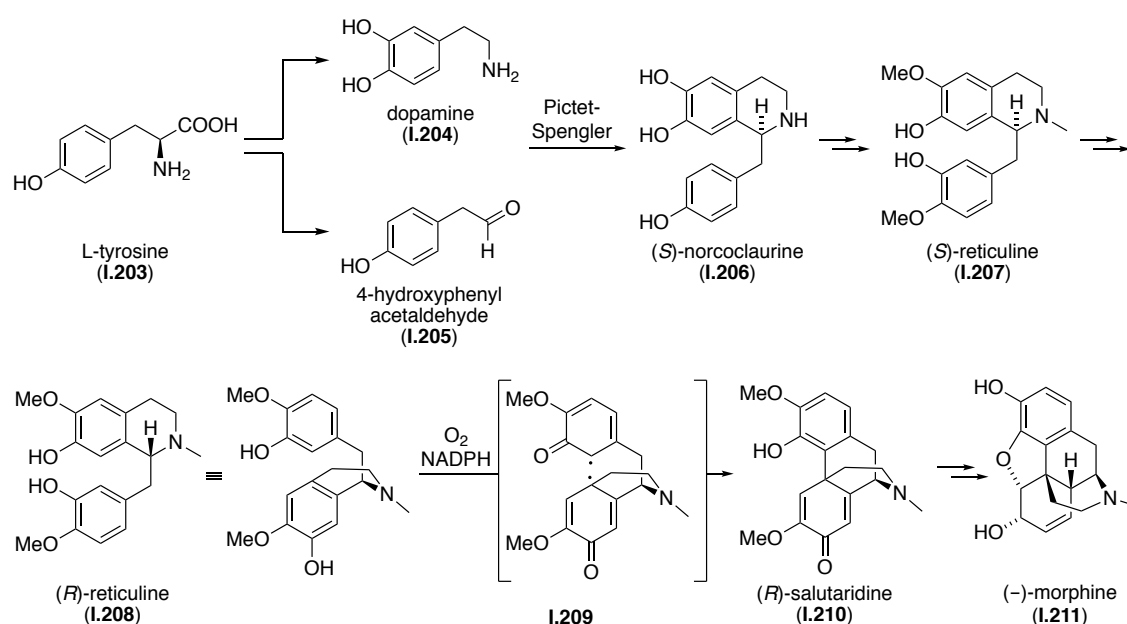
Figure I.5 Molecular and X-ray structure of the isolated norhasubanan (+)-stephadiamine (**I.1**).

In addition, the cyclopentane and tetrahydronaphthalene systems in (+)-stephadiamine (**I.1**) are further connected by a bridging δ -lactone, which is unique in the hasubanan family of alkaloids. Stephadiamine (**I.1**) features a total of four stereocenters, including two adjacent ATAs and a benzylic quaternary center, which are responsible for its cage-like structure. In addition, both ATAs are part of a 1,2-*cis* diamine motif, one of them being primary and the other tertiary. In general, 1,2-

diamines constitute an unusual structural motif and, to the best of our knowledge, no other alkaloid contains two adjacent 1,2-*cis* ATAs.

1.2.3 Proposed biosynthesis of (+)-stephadiamine

Morphinan, hasubanan and norhasubanan alkaloids bear a structural similarity that suggests a related biosynthetic pathway. The biosynthesis of (–)-morphine (**I.211**) has been studied in detail and is relatively well understood. Dopamine (**I.204**) and 4-hydroxyphenylacetaldehyde (**I.205**) are formed biosynthetically from the amino acid L-tyrosine (**I.203**) (Scheme I.38).^[236] These building blocks then most likely participate in a Pictet–Spengler reaction to furnish (*S*)-norcoclaurine (**I.206**), which is then oxidized and methylated to (*S*)-reticuline (**I.207**). Inversion of the benzylic stereocenter transforms (*S*)-reticuline (**I.207**) into (*R*)-reticuline (**I.208**), which is a key intermediate in all morphinan biosyntheses. Subsequent intramolecular *o,p*-phenol oxidative coupling gives (*R*)-salutaridine (**I.210**) *via* biradical intermediate **I.209**, and additional enzyme-catalyzed transformations furnish (–)-morphine (**I.211**).^[236]

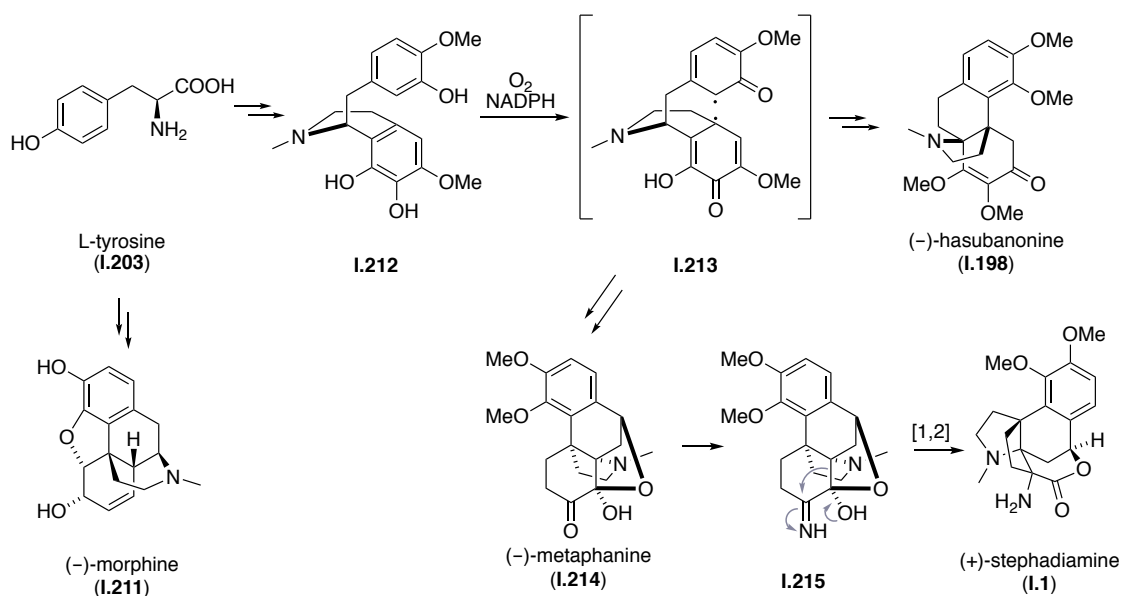


Scheme I.38 Proposed biosynthesis of (–)-morphine (**I.211**).

The biosynthesis of the hasubanan alkaloids has not yet been fully elucidated. However, the structural resemblance to the morphinan alkaloids suggests a shared biochemical pathway. Battersby therefore proposes a biosynthesis that involves oxidized isoquinoline frameworks similar to (*S*)-reticuline (**I.207**). This proposal was confirmed through feeding experiments of ¹⁴C-enriched

isoquinolines to *S. japonica*, the source of (-)-hasubanone (**I.198**) (Scheme I.39).^[237–240] The detected isoquinoline **I.212** resembles (*R*)-reticuline (**I.208**) and therefore Battersby and co-workers proposed a similar biosynthetic pathway for hasubanone (**I.198**) as for morphine (**I.211**).

Even less is known about the biogenesis of the target compound (+)-stephadiamine (**I.1**). However, due to its strong resemblance to morphinans and hasubanans, it was suggested by Hager *et al.* that L-tyrosine (**I.203**) is most likely the precursor for (+)-stephadiamine (**I.1**).^[241–242] In this case, the skeleton of the natural product would arise from an identical or similar Pictet–Spengler reaction and a phenolic coupling. In contrast to the hasubanan alkaloids, a series of ring contractions or rearrangements would have to occur to furnish the unique propellane core and δ -lactone of this norhasubanan alkaloid.^[241–242] A possible biosynthesis could proceed through (-)-metaphanine (**I.214**), another hasubanan alkaloid co-isolated with stephadiamine (**I.1**) from *S. japonica*.^[243] Elaborating on this hypothesis, condensation of NH₃ with **I.214** to putative key intermediate imine **I.215** could then be converted to (+)-stephadiamine (**I.1**) by [1,2]-semipinacol-type rearrangement.[†]



Scheme I.39 Proposed mechanism for the biosynthesis of (+)-stephadiamine.

[†] This biosynthetic proposal has been developed in cooperation with Prof. Dr. W. Steglich.

2 Project outline

2.1 Aims and significance of the project

Due to their structural complexity and associated synthetic challenges, members of the morphinan and hasubanan families have been popular targets for alkaloid total synthesis. However, as stated in the previous chapter, no synthetic efforts have been published for the structurally unique norhasubanan alkaloid (+)-stephadiamine (**I.1**), which was isolated more than ten years ago.^[244] Stephadiamine (**I.1**) possesses three contiguous fully substituted carbons: two α -tertiary amines (ATAs) and a benzylic quaternary carbon. Moreover, the two amines, a primary and a tertiary ATA, form a 1,2-*cis*-diamine, an extremely rare structural motif in nature. As such, stephadiamine (**I.1**) constitutes a significant synthetic challenge with which to apply and develop new synthetic methods for the construction of sterically encumbered ATAs. It was therefore the goal of this Ph.D. thesis to develop a concise and practical synthetic route to stephadiamine (**I.1**). In addition, only trace amounts of stephadiamine (**I.1**) were isolated by Taga *et al.*, and therefore investigation of its biological activity was not possible. Synthetic stephadiamine (**I.1**) would allow for its biological assessment. From a synthetic point of view, a main task of a synthesis of stephadiamine (**I.1**) is the construction of the highly congested propellane. Synthetic planning was thus guided by this challenge.

In earlier studies by Dominik Hager and Anastasia Hager and those described in the Master's thesis of the author, a route towards the popular hasubanan and morphinan β -tetralone building block was optimized and used as a starting point for all synthetic considerations. In all synthetic plans, it was envisaged to construct the aza-propellane core *via* functionalization of the acidic α -position of the β -tetralone. It was the first goal of this Ph.D. thesis to develop a strategy for the construction of the propellane core of stephadiamine (**I.1**). At an early point of this project, a cascade reaction was developed and optimized, which then became the foundation of all subsequent synthetic planning.

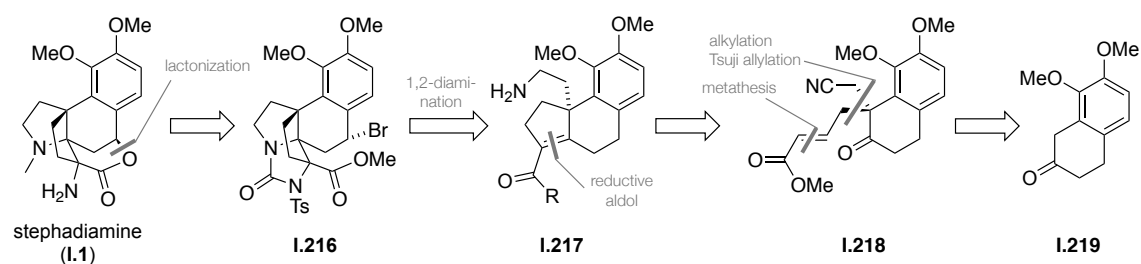
In this route, the benzylic stereocenter was set using a decarboxylative Tsuji allylation starting from a stabilized enol-carbonate. These substrates represent a remaining challenge in asymmetric Pd-catalyzed allylations. In collaboration with Prof. Brian M. Stoltz of the California Institute of Technology we opted to address this challenge and expand the scope of this transformation to enable an asymmetric total synthesis of (+)-stephadiamine (**I.1**).

2.2 Initial work

2.2.1 Retrosynthesis

Prior to this Ph.D. thesis, the total synthesis of stephadiamine (**I.1**) was already investigated as part of the Ph.D. theses of Dominik Hager and Anastasia Hager and the Master's thesis of the author. The most challenging task in a synthesis of stephadiamine (**I.1**) is the installation of the two ATAs, which are located next to a benzylic quaternary stereocenter. As outlined in chapter 1.1, numerous methods for the installation of ATAs have been published in the literature, however for our retrosynthesis we envisaged to develop novel 1,2-diamination chemistry.

For the synthesis of stephadiamine **I.1**, we envisaged to install the lactone in the last step of the synthesis starting from amino acid derivative **I.216** (Scheme I.40). This pentacyclic ATA-containing precursor **I.216** in turn could be accessed from primary amine **I.217** *via* 1,2-diamination. This intermediate could in turn be obtained from Michael system **I.218** by reduction and reductive aldol reaction. The quaternary benzylic stereocenter present in this structure could then be installed in an alkylation/Tsuji allylation sequence starting from literature-known β -tetralone **I.219**. Based on a procedure by Yu and co-workers, tetralone **I.219** could be prepared by Fujiwara–Moritani reaction (palladium-catalyzed aryl C–H olefination) and subsequent Dieckmann cyclization from commercially available, albeit very expensive, 2,3-dimethoxyphenylacetic acid (**I.223**).^[245] During this Ph.D. thesis, the starting material was prepared from aldehyde **I.220** following a literature procedure from Detterbeck and Hesse.^[246]



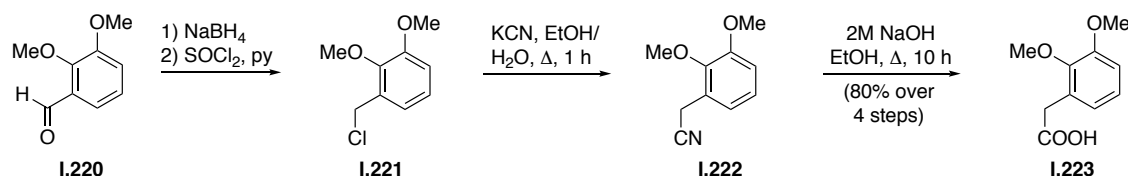
Scheme I.40 Previous retrosynthetic analysis for the synthesis of stephadiamine.

In our retrosynthetic planning, we envisaged that the Tsuji allylation^[247–249] would present a handle to render the synthesis asymmetric and that this resulting chirality would allow for the diastereoselective installation of all other stereocenters.

2.2.2 Initial experimental work

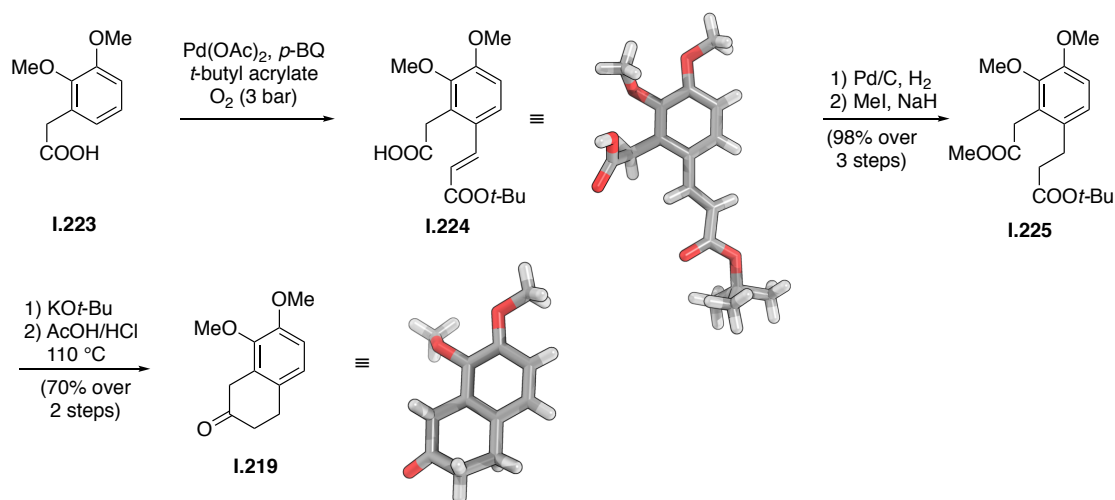
Prior to the contributions described in this Ph.D. thesis, optimization and characterization of Yu's β -tetralone-synthesis starting from the commercially available acid **I.223** were carried out in

collaboration with Anastasia Hager and Dominik Hager, two former Ph.D. students in the Trauner group. Thus a detailed discussion of this synthesis can be found in their Ph.D. theses.^[241–242] The following experiments in Scheme I.43 were first carried out by the author during her Master's thesis in the Trauner laboratories. Yields and procedures described in this chapter are optimized conditions.



Scheme I.41 Synthesis of the commercially available acid **I.223** from inexpensive starting material **I.220**.

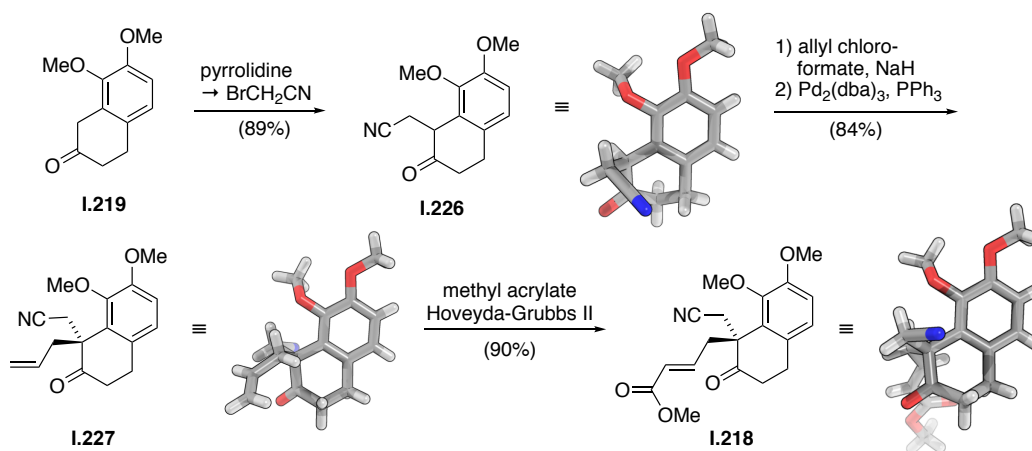
Following our retrosynthetic strategy, the first goal was the synthesis of commercially available, yet prohibitively expensive 2,3-dimethoxyphenylacetic acid (**I.223**). We therefore followed a short synthesis by Detterbeck and Hesse (Scheme I.41).^[246] The synthesis started with commercially available and inexpensive 2,3-dimethoxybenzaldehyde (**I.220**). In a four step sequence, the aldehyde was reduced with NaBH₄ and transformed into chloride **I.221** using thionyl chloride. S_N2 reaction of chloride **I.221** with KCN gave nitrile **I.222** in good yield. Finally, the desired carboxylic acid **I.223** was formed by a base-mediated hydrolysis. No chromatographic purification was necessary, allowing for the rapid synthesis of large amounts of acid **I.223** with a yield of 80% over four steps on 50 g scale.



Scheme I.42 Optimized procedure for the synthesis of β-tetralone **I.219**.

Prior to this Ph.D work, the large-scale synthesis of dimethoxy β-tetralone **I.219** was already established in the Trauner group. β-Tetralones themselves are popular intermediates in the synthesis of hasubanan and morphinan alkaloids,^[250–254] but most reported preparations suffer from either low-yielding steps or expensive catalysts and starting materials.^[255–259] Therefore, a recently

published synthesis^[245] of β -tetralone **I.219** starting from commercially available 2,3-dimethoxyphenylacetic acid (**I.223**) was optimized by Anastasia Hager and Dominik Hager, two former Ph.D. students in the Trauner group.^[241–242] The sequence commenced with a Fujiwara–Moritani reaction^[260–262] under conditions published by Yu and co-workers.^[245] Thus obtained enoate **I.224** was then hydrogenated and the free carboxylic acid was methylated to give diester **I.225** in 98% over three steps. Dieckmann condensation followed by subsequent decarboxylation then furnished β -tetralone **I.219**. Using this optimized route, literature-known intermediate was synthesized on multi-gram scale in nine steps involving only two chromatographic separations in an overall yield of 55% (Scheme I.42).



Scheme I.43 Installation of the benzylic quaternary stereocenter.

Next, the β -tetralone **I.219** was alkylated with bromoacetonitrile under Stork's conditions^[263] in 78% yield (Scheme I.43). We then investigated the decarboxylative Tsuji allylation starting from nitrile **I.226**. Exposure of ketone **I.226** to NaH generated the thermodynamic enolate, which was trapped by allyl chloroformate to furnish the corresponding enol carbonate. In the next step, the enol carbonate smoothly underwent the desired allylation in the presence of $\text{Pd}_2(\text{dba})_3$ and PPh_3 , giving α -allylcyclohexanone **I.227** in an excellent yield of 84% over two steps. A cross metathesis then furnished conjugated ester **I.228**. Initial attempts to cyclize reductive aldol precursor **I.218** were not successful. Where applicable, further discussion of these results can be found in later chapters (*e.g.*, asymmetric decarboxylative Tsuji allylation).

3 Results and discussion

3.1 Implementation of the quaternary benzylic stereocenter

3.1.1 The Tsuji allylation

The implementation of quaternary stereogenic centers remains a challenging task due to the steric hindrance associated with such a substituted carboatom.^[264–272] To transform racemic compounds, such as nitrile **I.226** into a single enantioenriched product, the racemate has to undergo a stereoconvergent transformation.^[273] This class of reaction can be categorized into three subclasses:

1. Stereoablative transformations
2. Dynamic kinetic resolutions (DKRs)
3. Dynamic kinetic asymmetric transformations (DyKATs)

It was shown in previous studies that benzylic quaternary centers could be set *via* decarboxylative Tsuji allylations in an elegant fashion,^[248, 274–277] and we already demonstrated that the racemic version of this reaction works well to furnish α -allylcyclohexanone **I.227** (Chapter 2.2.2). The decarboxylative Tsuji allylation belongs to the subclass of stereoablative reactions. Stereoablative processes are characterized by the formation of an intermediate that is formed by the irreversible deletion of stereoinformation to form a prochiral species (see Figure I.6). This process involves an identical or similar reaction rate ($k_{\text{racR}} = k_{\text{racS}}$) for the formation of the prochiral species.

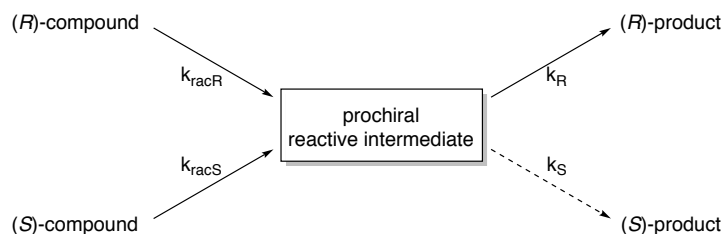


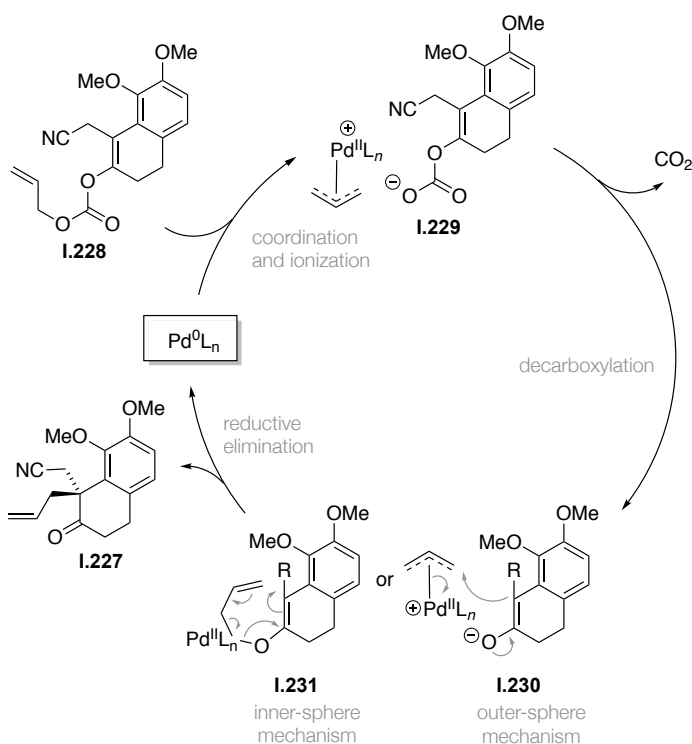
Figure I.6 Principle of a stereoablative enantioconvergent process.

The prochiral reactive intermediate then interacts with a chiral catalyst to give preferably one of the enantiomeric products, due to the different rates of product formation ($k_R \gg k_S$). In contrast to dynamic kinetic resolutions or dynamic kinetic asymmetric transformations, the stereoablative process relies on the formation of a prochiral intermediate followed by the irreversible formation – rather than by a reversible process – of an enantioenriched product.

Historically, the Tsuji allylation reaction was discovered as part of a series of palladium-catalyzed reactions “*in which unstabilized enolates or enol equivalents were transformed into the corresponding allylated ketones under essentially neutral reaction conditions*” by Tsuji and co-workers in the 1980s.^[276] Almost 20 years later, Stoltz and co-workers developed an asymmetric version of one of these reactions, the

so-called decarboxylative Tsuji allylation. By refining the original procedure and utilizing chiral phosphine-based ligands (*P,N*-ligands, PHOX-ligands), they were able to achieve excellent enantioselectivities for unstabilized enol carbonates (for structures of ligands see Figure I.7). Only one year later the group of Trost demonstrated that their DACH ligands (*P,P*-ligand) and several other C_2 -symmetric ligands are able to transfer chiral information for more electron-rich enol carbonates. The application of these ligands has been further extended to additional highly enantioselective variants, which also proceed under mild reaction conditions. The groups of Tsuji, Trost, and Stoltz, among others, have studied the mechanism of the decarboxylative Tsuji allylation extensively.^[247,276,278-279] The proposed

catalytic cycle for the decarboxylative Tsuji allylation is depicted in Scheme I.44. Catalytically active Pd(0) coordinates to the double bond of allyl carbonate **I.228** to form a η^2 π -allyl complex (not shown).^[280] On oxidative addition, an η^3 π -allyl complex **I.229** is formed. Following CO_2 release and ligand exchange, the resultant nucleophilic enolate may either be a stabilized enolate ion-paired with the dissociated π -allyl palladium complex (outer sphere mechanism *via* **I.230** followed by reductive elimination) or bound covalently to the allylpalladium(II)

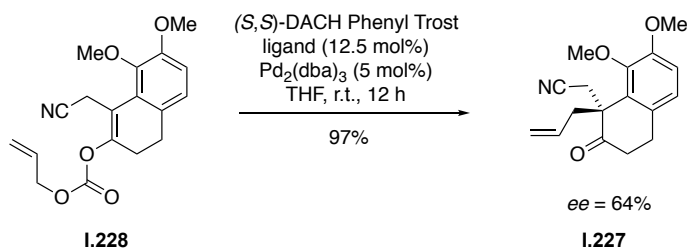


Scheme I.44 Proposed catalytic cycle of the Tsuji allylation.

species (inner sphere mechanism *via* 7-membered cyclic transition state **I.231**). In the last step, reductive elimination provides α -allylcyclohexanone **I.227** with concomitant regeneration of catalytically active Pd(0).^[277] For the enantiodetermining allylation step, several mechanistic studies by the groups of Stoltz and Trost have been published over the years. These studies suggest that Trost ligands might favor an outer sphere mechanism,^[275] whereas an inner sphere process might be preferred by PHOX ligands,^[279,281] although both pathways are feasible.^[277] For both mechanisms, nonpolar aprotic solvents are preferred as they stabilize the inner sphere complex and outer sphere complex by promoting tighter ion-pairing, which ultimately leads to higher enantiomeric excess (*ee*).^[277]

Today the Tsuji allylation serves as a powerful tool for the installation of quaternary stereocenters, and the methodology has been extended to complex molecules such as intermediates in the

synthesis of natural products.^[282–285] However, the asymmetric introduction of quaternary stereocenters starting from enolate-stabilized enolcarbonates is a challenging problem for this methodology.^[286] Initial experiments conducted during the Master's thesis of the author proved that this strategy could be suitable for an asymmetric total synthesis of **(I.1)**.^[287] To this end, reaction of **I.228** with Trost's commercially available (*S,S*)-DACH Phenyl ligand (**I.235**) provided α -allylcyclohexanone **I.227** in near quantitative yield with 64% enantiomeric excess (*ee*) as determined by chiral HPLC. Although the absolute stereochemistry was not determined at this stage, Trost's model for the prediction of the stereochemical outcome suggests that this ligand should lead to desired (*R*)-**I.227** (model will be discussed in chapter 3.1.2).



Scheme I.45 First conditions tested for an asymmetric Tsuji allylation.

To further improve the enantioselectivity of this reaction, a screening of ligands and reaction conditions was carried out in collaboration with the Stoltz laboratories in Pasadena at the California Institute of Technology. In addition, we also set out to determine the absolute stereochemistry of the obtained product.

3.1.2 Screening of the decarboxylative Tsuji allylation[‡]

Regarding the Tsuji allylation, several ligands have proven to successfully transfer chiral information, such as the *P,N*-coordinating PHOX-ligands (*S*)-*t*-Bu-PHOX (**I.232**) and (*S*)-CF₃-*t*-Bu-PHOX (**I.233**), the *P,N*-coordinating QUINAP ligand (**I.234**) and *P,P*-C₂-symmetric-coordinating DACH-ligands such as (*R,R*)-DACH-Phenyl Trost ligand (**I.235**), (*R,R*)-DACH-Naphthyl Trost ligand (**I.236**) and (*R,R*)-ANDEN-Phenyl Trost ligand (**I.237**, Figure I.7). In initial experiments, these ligands were screened at a concentration of 0.030 M and 5 mol% catalyst loading in several nonpolar aprotic solvents (see Experimental section, Procedure A, Chapter 8.2). The reactions were carried out at 25 °C for 20 h to ensure complete conversion. We do not expect erosion of *ee* after completion of the reaction, as C–C bond formation is most likely irreversible.

[‡] All experiments were carried out by the author in the laboratories of Prof. Brian M. Stoltz at the California Institute of Technology in Pasadena, CA, USA.

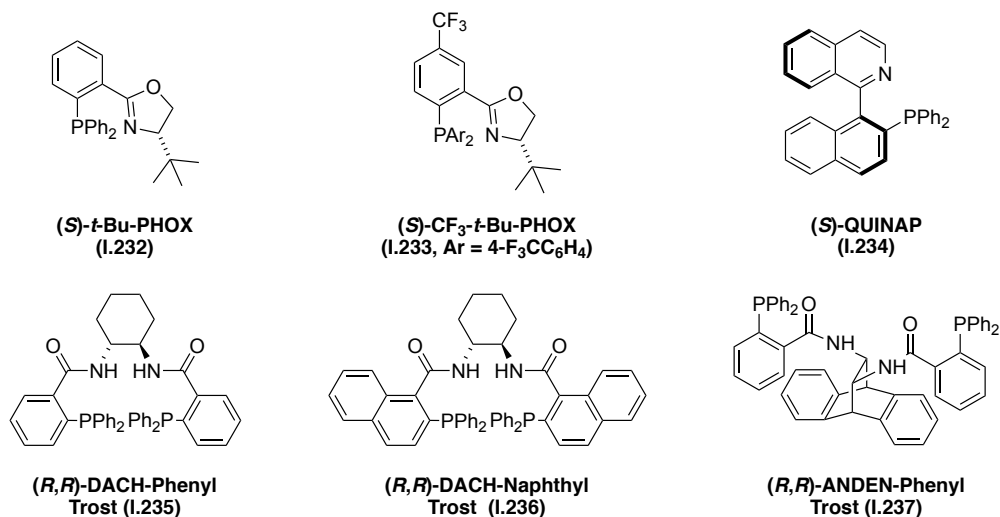
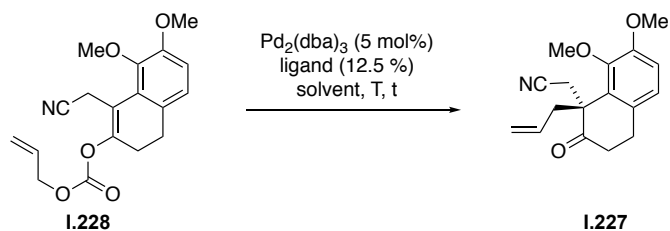


Figure I.7 Ligands used for the optimization of the asymmetric Tsuji allylation.

As determined by chiral HPLC, all reactions went to completion within this time period. The *ee* was calculated based on the HPLC traces of crude reaction mixtures.

Table I.1 Initial ligand screen for the asymmetric decarboxylative Tsuji allylation.

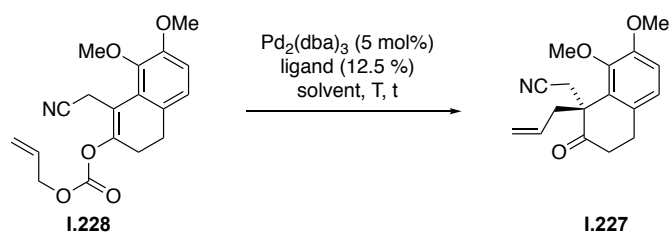


Entry	Ligand	Solvent	T (°C)	t (h)	% <i>ee</i>
1	(<i>S</i>)- <i>t</i> -Bu-PHOX (I.232)	THF	25	20	3
2	(<i>S</i>)- <i>t</i> -Bu-PHOX (I.232)	toluene	25	20	1
3	(<i>S</i>)- <i>t</i> -Bu-PHOX (I.232)	2:1 hexane/toluene	25	20	6
4	(<i>S</i>)-CF ₃ - <i>t</i> -Bu-PHOX (I.233)	THF	25	20	10
5	(<i>S</i>)-CF ₃ - <i>t</i> -Bu-PHOX (I.233)	toluene	25	20	26
6	(<i>S</i>)-CF ₃ - <i>t</i> -Bu-PHOX (I.233)	2:1 hexane/toluene	25	20	38
7	(<i>R,R</i>)-ANDEN-Phenyl Trost (I.237)	THF	25	20	22
8	(<i>R,R</i>)-ANDEN-Phenyl Trost (I.237)	toluene	25	20	13
9	(<i>R,R</i>)-ANDEN-Phenyl Trost (I.237)	2:1 hexane/toluene	25	20	25
10	(<i>S</i>)-QUINAP (I.234)	THF	25	20	14
11	(<i>S</i>)-QUINAP (I.234)	toluene	25	20	3
12	(<i>S</i>)-QUINAP (I.234)	2:1 hexane/toluene	25	20	11

The most popular and commercially available (*S*)-*t*-Bu-PHOX ligand (**I.232**) gave negligible *ee* values (1 to 6%) (Table I.1, entries 1–3) and thereby proved to be an ineffective catalytic system for substrate **I.228**. We then tested the more electron-deficient (*S*)-CF₃-*t*-Bu-PHOX ligand (**I.233**), which gave a higher *ee* as to be expected for an enol-stabilized enolcarbonate.^[288] In THF, the *ee* for the transformation was 10% (entry 4), but when conducted in the less polar solvent toluene, an *ee* of 26% was obtained (entry 5). The least polar solvent mixture that still gave a homogeneous solution of catalyst, 2:1 hexane/toluene, provided an *ee* of 38% (entry 6). In addition to these two PHOX ligands, we also evaluated (*R,R*)-ANDEN-Phenyl Trost ligand (**I.237**), which is generally the best Trost ligand for this transformation due to its large bite angle. However, this highly engineered ligand only gave an *ee* of 13–25% (entries 7–9), which is worse than our preliminary results with the (*S,S*)-DACH-Phenyl Trost ligand (**I.235**).^[287] Unfortunately (*S*)-QUINAP ligand (**I.234**) did not provide higher *ee* values (entries 10–12).

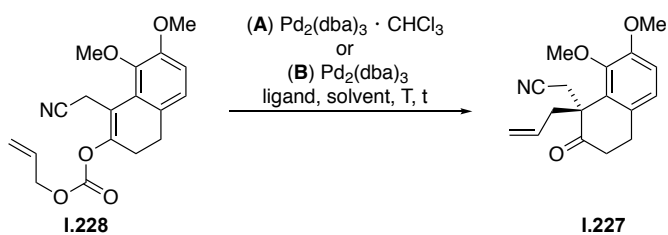
In addition to these experiments, we also investigated different reaction temperatures for the (*S*)-CF₃-*t*-Bu-PHOX ligand (**I.232**) (Table I.2, entries 1–4). We noticed that temperature had little to no influence on the enantioselectivity.

Table I.2 Temperature screen for the (*S*)-CF₃-*t*-Bu-PHOX ligand.



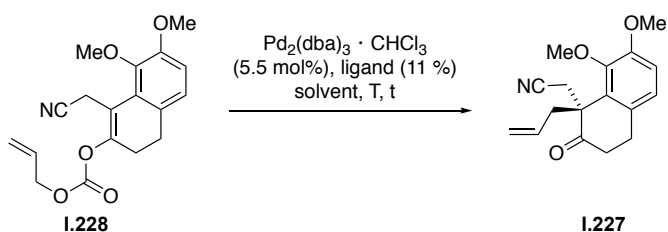
Entry	Ligand	Solvent	T (°C)	t (h)	% <i>ee</i>
1	(<i>S</i>)-CF ₃ - <i>t</i> -Bu-PHOX (I.233)	2:1 hexane/toluene	20	14	39
2	(<i>S</i>)-CF ₃ - <i>t</i> -Bu-PHOX (I.233)	2:1 hexane/toluene	0	14	42
3	(<i>S</i>)-CF ₃ - <i>t</i> -Bu-PHOX (I.233)	2:1 hexane/toluene	-15	14	34
4	(<i>S</i>)-CF ₃ - <i>t</i> -Bu-PHOX (I.233)	2:1 hexane/toluene	-60	14	37

In parallel, we also further investigated the (*R,R*)-ANDEN-Phenyl Trost ligand (**I.235**), as this ligand very often gives the best results in Tsuji allylations. As for the Trost ligands, two different Pd sources are commonly used for decarboxylative Tsuji allylations – Pd₂(dba)₃ and its chloroform adduct. We observed that the palladium source does not have a significant impact on *ee*: in THF, the chloroform adduct is 3% better than Pd₂(dba)₃ (Table I.3, entries 1 and 4), in toluene the *ee* was identical (entry 2 and 5), and in a mixture of toluene and hexane the chloroform adduct gave a slightly higher *ee* than Pd₂(dba)₃ (entries 3 and 6).

Table I.3 Screen for Pd sources and solvents.

Entry	Ligand	Pd source	solvent	T (°C)	t (h)	%ee
1	(<i>R,R</i>)-ANDEN-Phenyl Trost (I.237) (12.5 mol%)	B (5.0 mol%)	THF	25	20	22
2	(<i>R,R</i>)-ANDEN-Phenyl Trost (I.237) (12.5 mol%)	B (5.0 mol%)	toluene	25	20	13
3	(<i>R,R</i>)-ANDEN-Phenyl Trost (I.237) (12.5 mol%)	B (5.0 mol%)	2:1 hexane/toluene	25	20	25
4	(<i>R,R</i>)-ANDEN-Phenyl Trost (I.237) (11.0 mol%)	A (5.5 mol%)	THF	25	12	25
5	(<i>R,R</i>)-ANDEN-Phenyl Trost (I.237) (11.0 mol%)	A (5.5 mol%)	toluene	25	12	13
6	(<i>R,R</i>)-ANDEN-Phenyl Trost (I.237) (11.0 mol%)	A (5.5 mol%)	2:1 hexane/toluene	25	12	27

Since the chloroform adduct appeared slightly better, we used it as the palladium source. We next screened three different commercially available Trost ligands, DACH-Phenyl (**I.235**), DACH-Naphthyl (**I.236**) and ANDEN-Phenyl (**I.237**). Each one was tested with five different solvents or solvent mixtures (DME, MTBE, THF, toluene and hexane/toluene). We found that the DACH-Phenyl Trost ligand (**I.235**) gave similar *ee*'s in all five solvent systems (Table I.4, entries 1–5). The highest *ee*'s (52% and 53%) were obtained in toluene and hexane/toluene (entries 4 and 5). The DACH-Naphthyl Trost ligand (**I.236**) yielded worse *ee*'s overall, however the general trend was the same: the ligand works better in apolar solvents than in polar, coordinating solvents (entries 6–10). The ANDEN-Phenyl Trost ligand (**I.237**) gave the lowest *ee*'s of the three Trost ligands (entries 11–15).

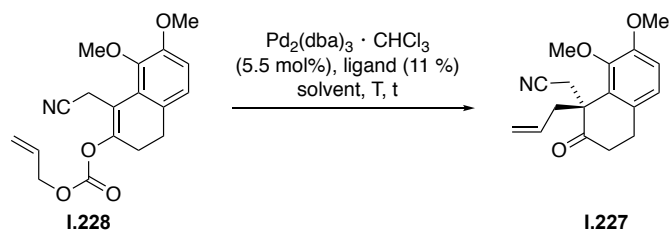
Table I.4 Second screen for Trost ligands and solvents.

Entry	Ligand	Solvent	T (°C)	t (h)	%ee
1	(<i>R,R</i>)-DACH-Phenyl Trost (I.235)	DME	25	12	51
2	(<i>R,R</i>)-DACH-Phenyl Trost (I.235)	MTBE	25	12	46
3	(<i>R,R</i>)-DACH-Phenyl Trost (I.235)	THF	25	12	47

Entry	Ligand	Solvent	T (°C)	t (h)	%ee
4	(<i>R,R</i>)-DACH-Phenyl Trost (I.235)	toluene	25	12	52
5	(<i>R,R</i>)-DACH-Phenyl Trost (I.235)	2:1 hexane/toluene	25	12	53
6	(<i>R,R</i>)-DACH-Naphthyl Trost (I.236)	DME	25	12	22
7	(<i>R,R</i>)-DACH-Naphthyl Trost (I.236)	MTBE	25	12	24
8	(<i>R,R</i>)-DACH-Naphthyl Trost (I.236)	THF	25	12	24
9	(<i>R,R</i>)-DACH-Naphthyl Trost (I.236)	toluene	25	12	26
10	(<i>R,R</i>)-DACH-Naphthyl Trost (I.236)	2:1 hexane/toluene	25	12	29
11	(<i>R,R</i>)-ANDEN-Phenyl Trost (I.237)	DME	25	12	6
12	(<i>R,R</i>)-ANDEN-Phenyl Trost (I.237)	MTBE	25	12	24
13	(<i>R,R</i>)-ANDEN-Phenyl Trost (I.237)	THF	25	12	25
14	(<i>R,R</i>)-ANDEN-Phenyl Trost (I.237)	toluene	25	12	13
15	(<i>R,R</i>)-ANDEN-Phenyl Trost (I.237)	2:1 hexane/toluene	25	12	27

As the most basic DACH-Phenyl Trost ligand (**I.235**) performs best for enol carbonate **I.228**, we focused on this ligand in all further experiments. We reasoned that by lowering the temperature, we would potentially slow down the speed of the reaction, thereby favoring one of the diastereomeric transition states.

Table I.5 Temperature screening for (*R,R*)-DACH-Phenyl Trost (**I.235**).

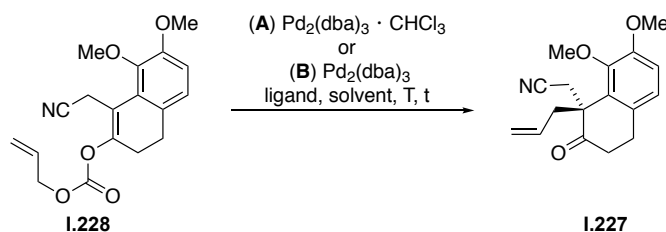


Entry	Ligand	Solvent	T (°C)	t (h)	%ee
1	(<i>R,R</i>)-DACH-Phenyl Trost (I.235)	THF	-15	24	48
2	(<i>R,R</i>)-DACH-Phenyl Trost (I.235)	2:1 hexane/toluene	-15	24	66
3	(<i>R,R</i>)-DACH-Phenyl Trost (I.235)	THF	-60	24	46
4	(<i>R,R</i>)-DACH-Phenyl Trost (I.235)	2:1 hexane/toluene	-60	24	55
5	(<i>R,R</i>)-DACH-Phenyl Trost (I.235)	THF	-78	24	54
6	(<i>R,R</i>)-DACH-Phenyl Trost (I.235)	2:1 hexane/toluene	-78	24	54

Therefore, we investigated different reaction temperatures the $\text{Pd}_2(\text{dba})_3 \cdot \text{CHCl}_3$ in two different solvent systems (Table I.5). At -15°C , 2:1 hexane/toluene gave a significantly higher *ee* than in THF (entries 1 and 2). At -60°C the difference was diminished (entries 3 and 4) and at -78°C the *ee* was identical for both solvents (entries 5 and 6). The observation that the *ee* for reactions in THF did not change significantly at decreased temperatures whereas those in toluene and hexane decreased is probably due to the decreased solubility of the catalyst in the nonpolar solvent mixture.

When comparing these results with our initial results from the author's Master's thesis (Scheme I.45),^[287] we obtained lower *ee* values than originally observed. We reasoned, that there might be a purity issue with the palladium source or ligand. And indeed, when we submitted a sample of DACH-Phenyl Trost ligand (**I.235**) to UHPLC, we observed two masses belonging to the ligand and its oxidized version. We therefore recrystallized the ligand in the glovebox and confirmed the purity by UHPLC. As we also wanted to ensure, that the palladium source is not responsible for the drop in *ee*, we again tested $\text{Pd}_2(\text{dba})_3$ and its chloroform adduct. Before adding the preformed catalyst to the substrate, the solution containing the catalyst was filtered through a plug of glass filter paper. Using this procedure, we were able to obtain *ee*'s of $>60\%$ again when running the reaction at -10°C for both palladium sources (Table I.6, entries 1–4).

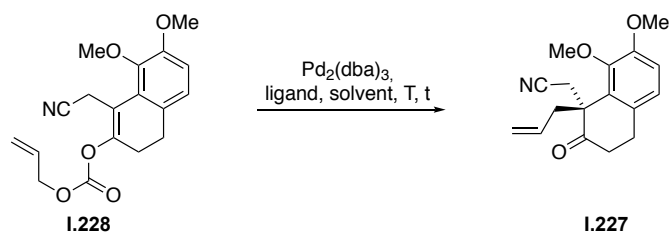
Table I.6 Second screen for solvents and different palladium sources.



Entry	Ligand	Pd source	Solvent	T (°C)	t (h)	% ee
1 ^{a)}	(<i>R,R</i>)-DACH-Phenyl Trost (I.235)	A	toluene	-10	2	60
2 ^{a)}	(<i>R,R</i>)-DACH-Phenyl Trost (I.235)	A	2:1 hexane/toluene	-10	2	66
3 ^{a)}	(<i>R,R</i>)-DACH-Phenyl Trost (I.235)	B	toluene	-10	2	64
4 ^{a)}	(<i>R,R</i>)-DACH-Phenyl Trost (I.235)	B	2:1 hexane/toluene	-10	2	59

a) Tsuji allylation after passage of the preformed catalyst through a plug of glass filter paper; recrystallized ligand used.

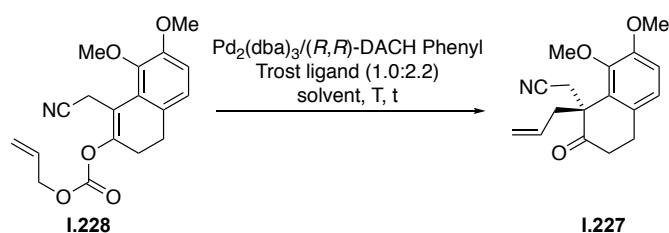
However, the *ee*'s were still not stable and varied slightly when running the same reaction twice. We therefore became interested if the exact ligand to metal ratio would influence the outcome of the reaction (Table I.7). When comparing ratios of 1:2, 1:2.2 and 1:4.4 of $\text{Pd}_2(\text{dba})_3$ to ligand, we observed that ratios of 1:2 and 1:2.2 gave *ee*'s of 64% (entries 1 and 2), but that a ratio of 1:4.4 led to a substantial decrease (17% *ee*, entry 3). We reasoned that excess ligand may possibly be changing the coordination at palladium and by some mechanism lower the observed *ee*.

Table I.7 Screening for different Pd₂(dba)₃ to ligand ratios.

Entry	Ligand	Pd ₂ (dba) ₃ to ligand ratio	Solvent	T (°C)	t (h)	%ee
1 ^{a)}	(<i>R,R</i>)-DACH-Phenyl Trost (I.235)	1.0 : 2.0	toluene	-10	2	64
2 ^{a)}	(<i>R,R</i>)-DACH-Phenyl Trost (I.235)	1.0 : 2.2	toluene	-10	2	64
3 ^{a)}	(<i>R,R</i>)-DACH-Phenyl Trost (I.235)	1.0 : 4.4	toluene	-10	2	17

a) Tsuji allylation after passage of the preformed catalyst through a plug of glass filter paper; recrystallized ligand used.

To ensure that Pd₂(dba)₃ itself is not catalytically active, a control experiment was run without ligand. Only starting material was recovered, which suggests that no side reactions due to excess Pd₂(dba)₃ are to be expected. As the ratio of Pd₂(dba)₃ must be kept close to 1:2.2, we decided to investigate the influence of reaction concentration as well as catalyst (Table I.8). We started off with a concentration of 0.03 M and 5 mol% catalyst loading in toluene and a 2:1 hexane/toluene mixture and observed an *ee* of 64% in toluene and an *ee* of 59% in the hexane/toluene mixture (entries 1 and 2).

Table I.8 Screening conditions for different concentrations and catalyst loadings.

Entry	Conc. (M)	Pd ₂ (dba) ₃	Solvent	T (°C)	t (h)	%ee
1 ^{a)}	0.03	5 mol%	toluene	-10	2	64
2 ^{a)}	0.03	5 mol%	2:1 hexane/toluene	-10	2	59
3 ^{a)}	0.01	5 mol%	toluene	-10	2	66
4 ^{a)}	0.01	5 mol%	2:1 hexane/toluene	-10	2	58
5 ^{a)}	0.001	5 mol%	toluene	-10	2	66
6 ^{a)}	0.001	5 mol%	2:1 hexane/toluene	-10	2	62
7 ^{a)}	0.03	1 mol%	toluene	-10	2	60
8 ^{a)}	0.03	1 mol%	2:1 hexane/toluene	-10	2	66

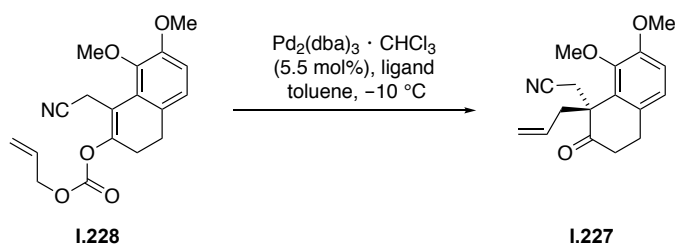
a) Tsuji allylation after passage of the preformed catalyst through a plug of glass filter paper; recrystallized ligand used.

At a concentration of 0.01 and 0.001 M and 5 mol% catalyst loading the *ee* increased slightly to 66% in toluene. Further dilution proved to be fruitless (entries 3 and 5). In the hexane/toluene mixture, we observed the same trend albeit with slightly worse results (entries 4 and 6). Using a substrate concentration of 0.03 M with 1% catalyst loading, we observed comparable results (entries 7 and 8).

After this extensive screening of solvents, temperatures, ligands, palladium sources and reaction concentrations, we were interested in the reaction time and the effect of the ligand on the reaction time. We therefore set up a kinetic experiment with triphenylphosphine (PPh₃) and DACH-Phenyl Trost ligand (**I.235**): both reactions were conducted at -10 °C, and progress was monitored by HPLC every 5 minutes (Table I.9). To our surprise, the reaction with the DACH-Phenyl Trost ligand (**I.235**) was completed within 5 min. As we observed an immediate color change upon addition of the substrate, we reasoned that the reaction may even be finished within seconds or faster. Using triphenylphosphine as ligand, we observed slow but continuous progress of the reaction, and after 12 h the starting material had been completely consumed.

These experiments demonstrate that the nature of the ligand may have a large influence on the reaction rate and that the Tsuji allylation of this substrate can be extraordinarily fast. In most reported cases, this reaction is performed at room temperature or elevated temperatures.

Table I.9 Time dependence of the reaction using different ligands.



Entry	Ligand	Solvent	T (°C)	t (h)
1 ^{a)}	(<i>R,R</i>)-DACH-Phenyl Trost (I.235) (11 mol%)	toluene	-10	<5 min
2	PPh ₃ (22 mol%)	toluene	-10	12 h

a) Tsuji allylation after passage of the preformed catalyst through a plug of glass filter paper; recrystallized ligand used.

Taking all results into account, we were wondering if the C–C bond-forming step, at which the stereochemical information is transferred, acts as the rate-determining step. Also, if the rate of the reaction is close to a diffusion-controlled process, we were curious if this could explain the low *ee* of the reaction, considering it could not be influenced significantly by solvent, temperature or concentration.^[289] In Mayr's database, phenyl-substituted allyl-Pd complexes have an electrophilicity value of $E = -10$ and the anion of phenylpropan-2-one has a nucleophilicity value of $N = 25$ ^[290] and a S_N parameter of $S_N = 0.60$ (in DMSO).^[291] By combining these values in Mayr's equation [$\log k_{20^\circ\text{C}} = S_N(N+E)$], reaction constants of $k = 10^9 \text{ L mol}^{-1} \text{ s}^{-2}$ are obtained, which are close to the

diffusion barrier. However, if we now take into account, that substrate **I.228** should be more reactive than phenylpropan-2-one, we reason, that our reaction could indeed proceed without energy barriers and thus lead to relatively low *ee* values. In most cases (but not always), reactions, “which proceed with such high rates do not have activation energies, [and] the corresponding regioselectivities (as well as stereoselectivities) cannot be derived from transition-state models”,^[289, 292–293]

At this stage, we set out to determine the absolute stereochemistry of the decarboxylative Tsuji allylation using Trost’s model.^[294] In this model, the DACH ligand (in the depicted case, the (*R*)-enantiomer) is presented according to the groundstate structure of the ligand-palladium- π -allyl complex based on molecular modeling structures. Obtaining a crystal structure of compound **I.238** was not possible due to its instability. In Trost’s model (Figure I.8), the walls represent the “chiral space created by the propeller-like array of the phenyl rings; the raised flaps represent the phenyls, which lie in a plane approximately parallel to the allyl, while the lowered flaps represent phenyls which are somewhat perpendicular to the allyl. [...] If one considers palladium(0) as the nucleophile in the ionization and palladium(II) the leaving group in the alkylation reaction, then both ionization and nucleophilic attack should occur at an angle that closely approaches 180° relative to palladium in the π -allyl.”^[294] Due to these reasons, they propose that the favored trajectory for the ionization and the following nucleophilic attack would occur *via* an *exo* rather than an *endo* mode with respect to the allyl fragment.

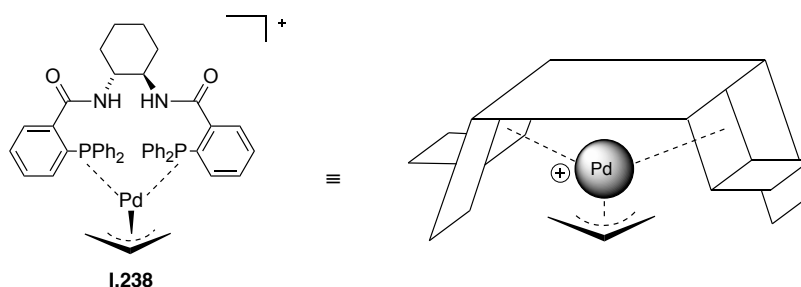
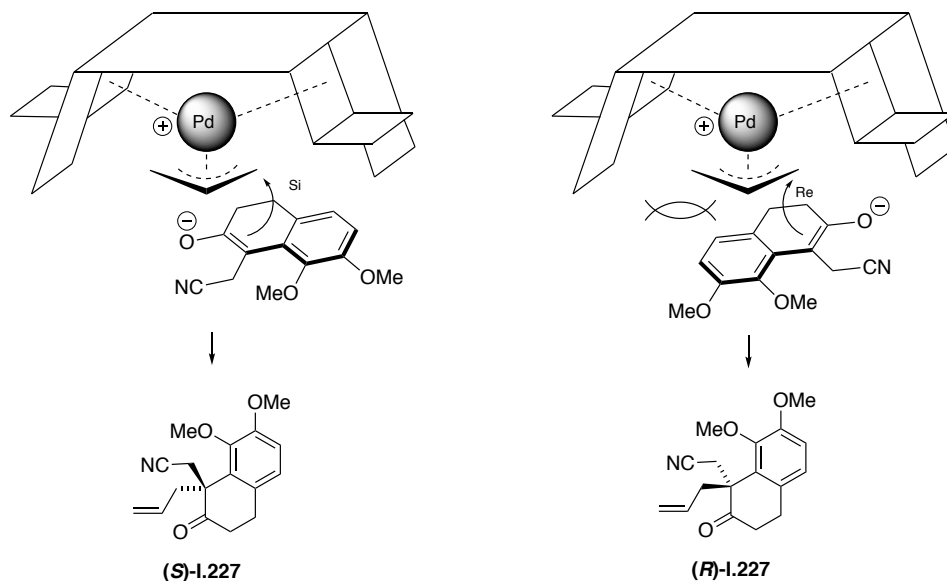


Figure I.8 Trost’s model for the stereochemical outcome of the asymmetric Tsuji allylation.

Using this model, we propose two different orientations of the tetralone enolate, one leading to the (*S*)-stereoisomer and one leading to the (*R*)-stereoisomer of α -cyclohexanone **I.227** (Scheme I.46). In the first and favored case, the catalyst approaches the molecule from the *Si*-face and repulsive interactions are minimized. This transition-state would lead to the (*S*)-stereoisomer when using the (*R,R*)-catalyst. This absolute stereochemistry proved to be correct (see chapter 3.1.4).



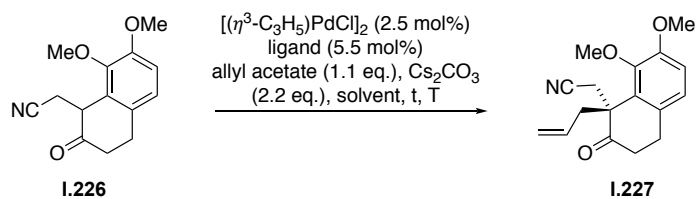
Scheme I.46 Model for the determination of the absolute stereochemistry using (*R,R*)-DACH Phenyl Trost.

In summary, using the decarboxylative Tsuji allylation, we were able to achieve *ee*'s up to 66% with full conversion of the starting enol carbonate. As we were not able to further improve these results, we then investigated other methodologies for the installation of the quaternary stereocenter.

3.1.3 Direct allylation of the tetralone[§]

We next investigated direct allylation methodologies related to the decarboxylative Tsuji allylation. Trost reported conditions for a direct allylation using allyl palladium(II) chloride dimer ($[(\eta^3\text{-C}_3\text{H}_5)\text{PdCl}]_2$), a Trost ligand, allyl acetate as allyl source and Cs_2CO_3 as base (Table I.10).

Table I.10 Conditions tested for the direct Tsuji allylation starting from ketone **1.226**.

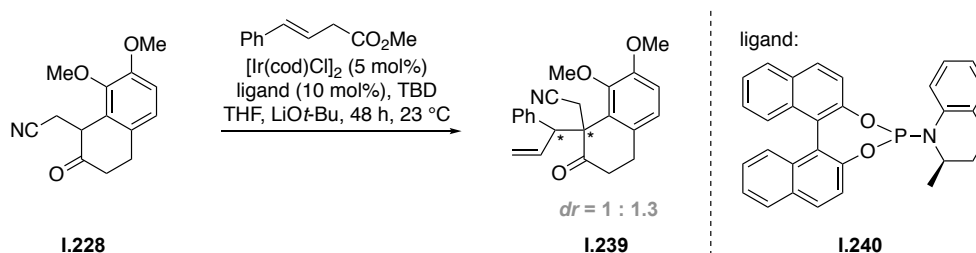


Entry	Ligand	Solvent	T (°C)	t (h)	% <i>ee</i>
1	(<i>R,R</i>)-DACH-Phenyl Trost (1.235)	DME	0	12	7
2	(<i>R,R</i>)-DACH-Naphthyl Trost (1.236)	DME	0	12	5
3	(<i>R,R</i>)-ANDEN-Phenyl Trost (1.237)	DME	0	12	2

[§] All experiments were carried out by the author in the laboratories of Prof. Brian Stoltz at the California Institute of Technology in Pasadena, CA, USA.

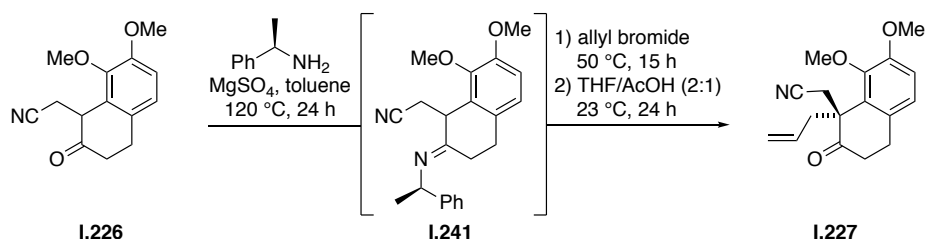
We tested all three commercially available Trost ligands – DACH-Phenyl (**I.235**), DACH-Naphthyl (**I.236**) and ANDEN-Phenyl (**I.237**). Although all three gave full conversion, poor enantiomeric excess was observed (entries 1–3).

We thus changed the system completely and envisaged an Ir-catalyzed allylation. Recently, Stoltz and co-workers reported an asymmetric allylation of acyclic β -ketoesters.^[295] Due to the acidity of the α -carbon in tetralone **I.228**, we believed that this methodology could also be applicable for our substrate. At this point, it was important to take into consideration that Ir-catalyzed allylations usually lead to branched products. Aware of this, we initially wanted to investigate the general applicability of this methodology. The test reaction was carried out using $[\text{Ir}(\text{cod})\text{Cl}]_2$ (5 mol%), ligand **I.230** (10 mol%), and 1,5,7-triazabicyclo[4.4.0]dec-5-ene (TBD) in degassed THF. After 10 minutes, the preformed catalyst was added to a solution of LiOt-Bu and ketone **I.228** followed by the addition of cinnamyl carbonate. The reaction stirred at 25 °C for 48 h. After this time, the reaction was filtered and analysis *via* chiral HPLC and NMR suggested that a *dr* of 1:1.3 at the benzylic quaternary stereocenter of **I.239** was obtained. As these results were not very promising, we did not investigate this strategy further.



Scheme I.47 Direct Iridium-catalyzed Tsuji allylation.

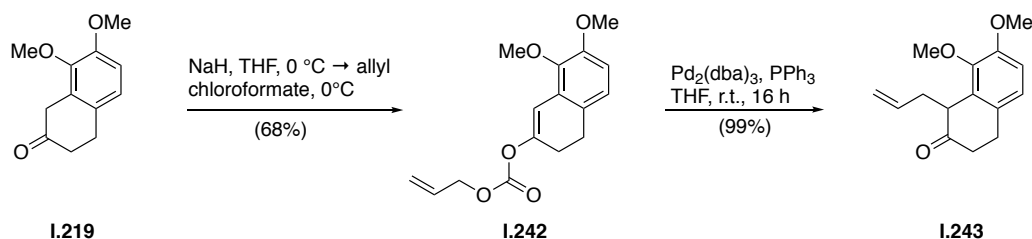
Next we explored the use of an alkylation published by Pfau and D'Angelo, who reported an enantioselective synthesis of quaternary carbon centers through alkylation of chiral imines.^[296] This method was applied in Corey's synthesis of a benzenoid analogue of glycinoeclepin A.^[297] Pfau and D'Angelo reported their method for additions to Michael systems but we reasoned that using our acidic tetralone, α -allylations could be facilitated as well.



Scheme I.48 Pfau and D'Angelo's chiral alkylation method.

Following Corey's procedure, tetralone **I.226**, (*R*)- α -methylbenzylamine and MgSO₄ were heated in toluene to 120 °C for 24 h, then allyl bromide was added and the reaction was stirred at 50 °C for 15 h. Then, THF and acetic acid were added. Unfortunately, only starting material was observed.

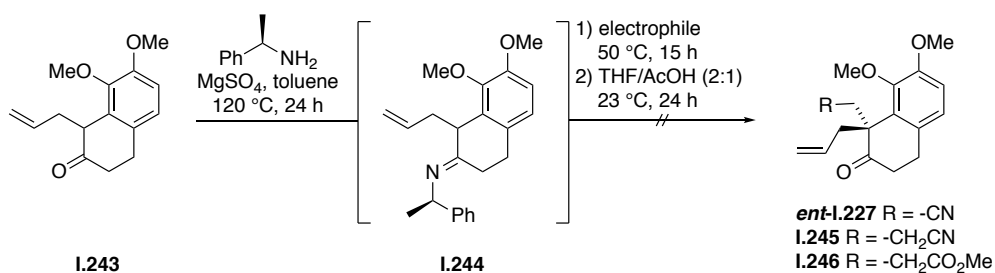
As this reaction did not work, we changed the substrate for the alkylation and attempted the use of allylated β -tetralone **I.219**. Ketone **I.243** was prepared in two steps in high yields from tetralone **I.219** using a racemic decarboxylative Tsuji allylation (Scheme I.49 *via* enol carbonate **I.242**).



Scheme I.49 Synthesis of allylcyclohexanone **I.243**.

With allylcyclohexanone **I.243** in hand, we investigated the previously introduced alkylation method *via* imine **I.244** using the electronically different electrophiles bromoacetonitrile, acrylonitrile and methylacrylate (Table I.11, entries 1–3). However, only starting material was recovered under all reaction conditions.

Table I.11 Conditions tested for the alkylation of tetralone **I.243**.



Entry	Electrophile	Expected product	Observation
1	bromoacetonitrile	I.227	no reaction
2	acrylonitrile	I.245	no reaction
3	methylacrylate	I.246	no reaction

Given that the best results were obtained with the decarboxylative Tsuji allylation, we decided to investigate enantiomeric enrichment of the compound, as the yield of the allylation was almost quantitative and the product was highly crystalline. Enantiomeric enrichment and separation of the enantiomers would also possibly allow for the determination of absolute stereochemistry.

3.1.4 Enantiomeric enrichment and determination of the absolute stereochemistry

Modern organic synthesis focuses on the development of asymmetric methodology for the synthesis of chiral compounds, however, as demonstrated in the previous chapters, not all reactions can be optimized to provide good enantioselectivities. Also, scale up of an asymmetric methodology is not always possible and therefore several methods for the separation of enantiomers have been developed. Chiral column chromatography and chiral HPLC are popular methods for the separation of enantiomers.^[298] We separated the two enantiomers of **I.227** by chiral HPLC, isolating approximately 150 mg of each enantiomer. Both samples were then crystallized individually from chloroform at 0 °C. The absolute stereochemistry, which was previously anticipated using Trost's model, was confirmed by X-ray crystallography.** Although no heavy atom was present in the molecule and MoK α radiation was used, stereochemistry could be determined due to high-resolution data up to 0.6 Å with a Flack parameter of $x = -0.1(2)$ for the (*R*)-enantiomer and $x = -0.09(2)$ for the (*S*)-enantiomer.

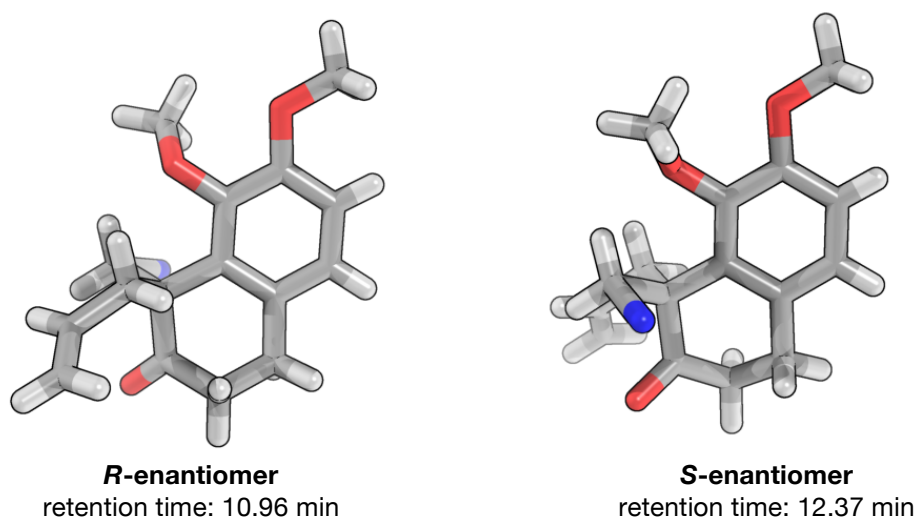


Figure I.9 Determination of the absolute stereochemistry of **I.227** by chiral HPLC and X-ray analysis.^{††}

These findings are in agreement with the structural assignment based on Trost's model for the stereochemical outcome of Tsuji allylations with (*R,R*)-DACH phenyl Trost ligand (**I.235**) giving mainly (*S*)-**I.227** and (*S,S*)-DACH phenyl preferentially forming (*R*)-**I.227**. As the (*R*)-enantiomer is the desired stereoisomer for (+)-stephadiamine (**I.1**), we carried out the asymmetric decarboxylative Tsuji allylation using (*S,S*)-DACH phenyl Trost ligand and then investigated the crystallization of the resulting (*R*)-enantiomer.

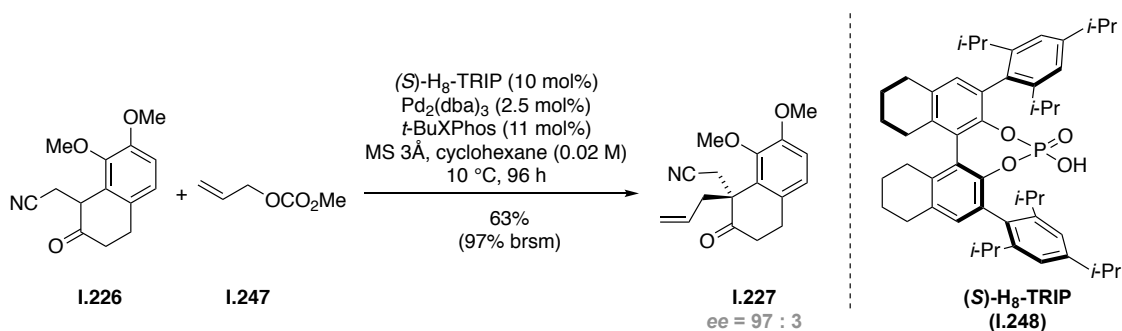
** X-Ray analysis was carried out by Dr. Peter Mayer at LMU Munich using MoK α -radiation. If the Flack parameter, which is based on the anomalous dispersion effect, is found to be near 0, the absolute structure, which is determined by structure refinement, is probably correct. If the value is close to 1, the opposite structure would be correct. If a value of $x = 0.5$ is obtained, the crystal could be either racemic or twinned.

†† Retention time was determined on a DAICEL CHIRALPAK® IB column (see chapter 8.2).

For synthetic purposes, it would be advantageous to separate the enantiomers *via* crystallization rather than by chiral HPLC, so as to obtain large amounts of the desired enantiomer. After some experimentation with various solvent mixtures, it was found that best results were obtained when (R)-**I.227** was recrystallized from a mixture of Et₂O:*n*-heptane (3:10) at 4 °C. Under these conditions, an *ee* of 97% was obtained. HPLC analysis revealed a remaining 1:1 mixture of both enantiomers in the mother liquor. The near quantitatively yielding asymmetric decarboxylative Tsuji allylation in combination with a single recrystallization thus constitutes a viable method for the synthesis of large quantities of either enantiomer, if needed in the future.

3.1.5 List's organocatalytic version of the direct Tsuji allylation

In 2016, an organocatalytic direct allylation method was published by List and co-workers.^[299] Using material that was prepared in our laboratories,[‡] a collaborator from the List group carried out a Pd-catalyzed allylation making use of their powerful asymmetric counteranion-directed catalysis (ACDC) methodology.^[300] Using the chiral phosphoric acid (*S*)-H₈-TRIP (**I.248**) in combination with Pd₂(dba)₃ and *t*-BuXPhos in cyclohexane at 10 °C, they were able to get yields of 63% (97% based on recovered starting material) with a remarkable *ee* of 97:3 after 96 h reaction time.



Scheme I.50 Direct Tsuji allylation of nitrile **I.226**.

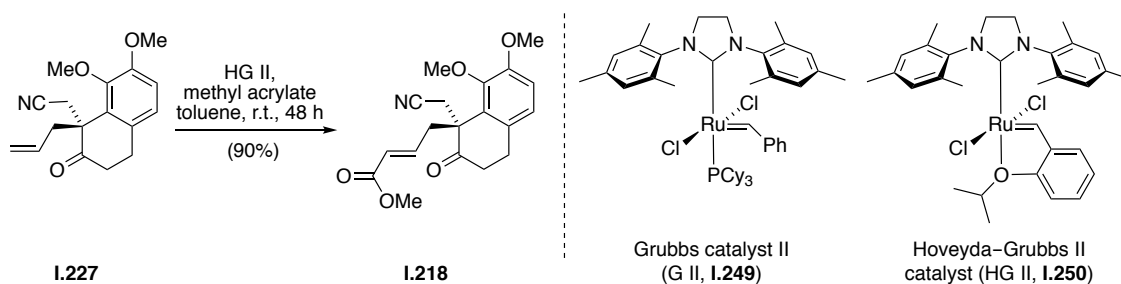
In additional experiments, higher yields with slightly lower *ee*'s were obtained when the reaction was run at a higher concentration. This method would not only shorten the sequence by one step, as compared to the decarboxylative Tsuji allylation, but also furnishes the α -allylcyclohexanone **I.227** with a much higher *ee*.

[‡] All experiments were carried out by Gabriele Pupo in the List laboratories at the Max-Planck-Institute for Kohlenforschung in Mülheim an der Ruhr, GER.

3.2 Metathesis and cascade reaction

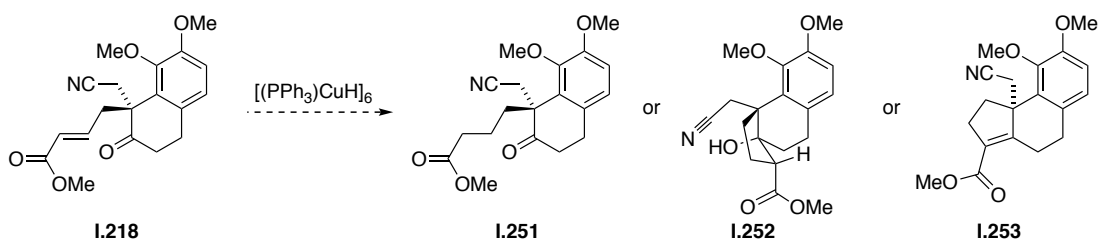
3.2.1 Ester approach

With allylcyclohexanone **I.227** in hand, we investigated the alkene cross metathesis reaction with methyl acrylate. Under optimized conditions, **I.227** underwent metathesis to give unsaturated ester **I.218** in 90% yield using Hoveyda–Grubbs catalyst 2nd generation (GH II, **I.250**) in toluene. It should be noted that the yield of this transformation was significantly lower using Grubbs II catalyst (G II, **I.249**), probably due to side reactions of the catalyst with the acrylate ester. It has been reported that the tricyclohexylphosphine (PCy₃) ligand reacts with acrylates to create a reactive carbanion that engages in multiple pathways, *e.g.*, Rauhut–Currier reaction and catalyst deactivation.^[301]



Scheme I.51 Metathesis of **I.227** with methyl acrylate.

Following our retrosynthetic analysis, we screened conditions for the reductive aldol reaction to furnish tricyclic intermediate **I.252** or the elimination product **I.253** (Scheme I.52). Following conjugate reduction, we anticipated that the resultant ester enolate would engage the more reactive ketone. We expected that ester **I.251** could be a major side product of this reaction.^{§§}



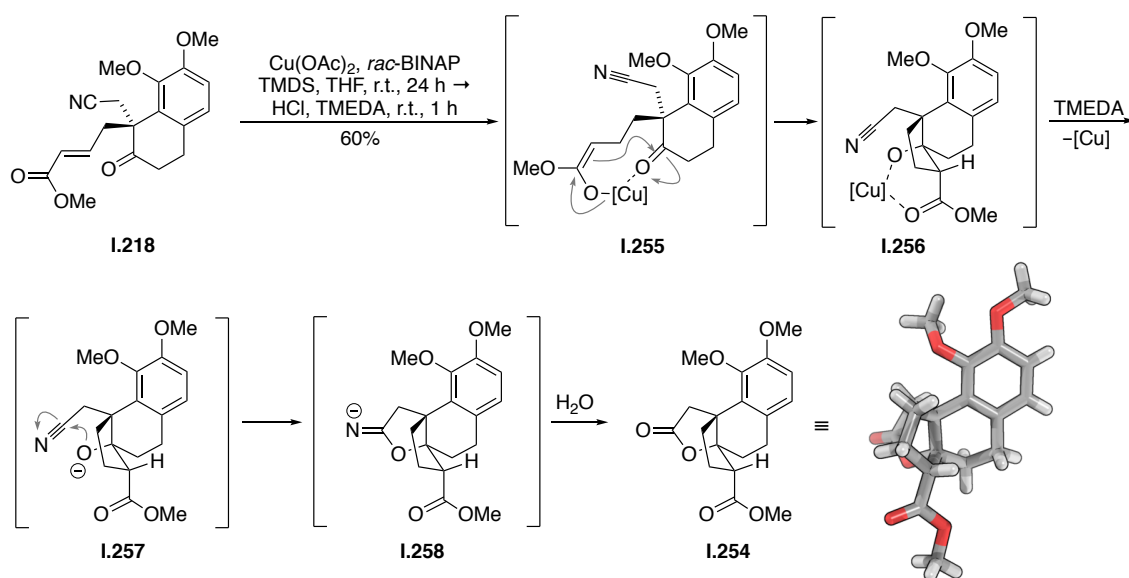
Scheme I.52 Strategy for the construction of tricycle **I.252** or **I.253**.

A variety of hydride sources such as boranes, indium hydrides, rhodium hydrides and copper hydrides are typical conditions for this type of transformation,^[302] with Stryker's reagent

^{§§} An authentic sample of **I.251** was obtained by hydrogenation with Pd/C under hydrogen atmosphere; see Scheme I.55.

for 10 h, tertiary alcohol **I.252** was obtained as the major product (more than 50% by NMR, entry 3). When this sample was dried under reduced pressure, we observed slow transformation to lactone **I.254**, indicating that alcohol **I.252** is an intermediate en route to lactone **I.254**. Using the same conditions at 0 °C, we isolated lactone **I.254** in 38% yield (entry 4) and at room temperature the yield raised to 41% (entry 5). Surprisingly, by prolonging the reaction time from 4 h to 18 h, the yield dropped to 34% (entry 6).

Lactone **I.254** was often isolated as a green solid, indicating the presence of residual copper. Therefore, we changed the work-up procedure to include a tetramethylenediamine (TMEDA) wash. In this way, we were able to improve the yield to 60% (entry 7). When citric acid was used, the yield dropped to 47% (entry 8).



Scheme I.53 Suggested mechanism for the copper-hydride induced reductive aldol cascade reaction.

We then investigated *in situ* formation of copper hydride based on methodology developed by Lam and co-workers (entry 9–12).^[303] Using copper(II) acetate, 1,1'-bis(diphenylphosphino)ferrocene (dppf) and tetramethyldisiloxane (TMDS) in THF, we isolated lactone **I.254** in 30% yield (entry 9). By changing the ligand to racemic 2,2'-bis(diphenylphosphino)-1,1'-binaphthyl (BINAP) and using 0.1 eq. copper (II) acetate, we observed starting material **I.218** and 47% of the desired lactone **I.254** (entry 10). By using 0.5 eq. copper (II) acetate, the yield increased to 60%, and we observed very clean conversion (entry 11).

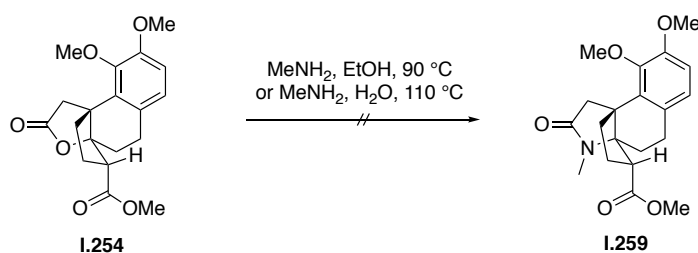
For the formation of propellane product **I.254**, we propose that the addition of a copper hydride, formed *in situ* from $\text{Cu}(\text{OAc})_2$, BINAP and TMDS, provides enolate **I.255** (Scheme I.53), which undergoes an intramolecular aldol reaction to furnish copper-chelate **I.256**. Following a simple aqueous work up, we were able to isolate traces of **I.252**, which supports our mechanistical

hypothesis. Upon addition of TMEDA to the reaction mixture, copper (II) is sequestered, and an intramolecular attack of the alkoxide in **I.257** to the nitrile, likely due to their close proximity, gives imidate **I.258**. Upon aqueous acidic work-up, this imidate is then hydrolyzed to lactone **I.254**.

The crystal structure of lactone **I.254** revealed a perfect antiperiplanar configuration of the α -hydrogen next to the ester and the oxygen of the lactone. We therefore reasoned that addition of base could lead to a retro-oxa-Michael addition and the thus obtained product could be converted to an amide. However, adding sodium hydride (NaH) to the reaction led to a complex reaction mixture, which did not contain lactone **I.254** or the elimination product **I.253** (entry 12). In conclusion, both copper hydride sources, Stryker's reagent and copper (II) acetate in combination with silane, yielded lactone **I.254** in 60% yield. However, *in situ* copper hydride formation proved to be more reliable and gave cleaner conversion to desired product **I.254**.

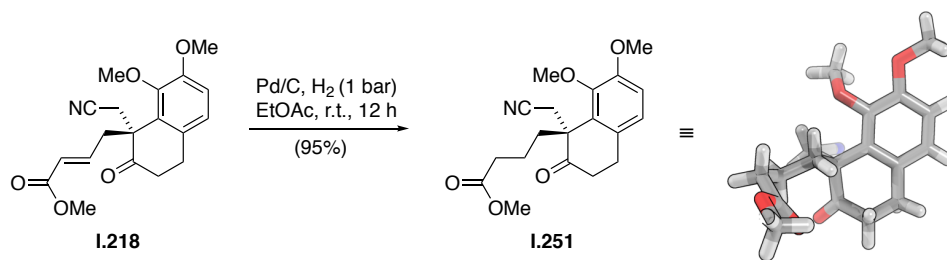
In addition to these copper hydride-mediated reactions, we also investigated the use of L-selectride as a hydride source, however this transformation led to decomposition of the starting material (entry 13).^[304–305] Using Rh(cod)₂OTf, triphenylphosphine and hydrogen, only starting material was isolated (entry 14).^[306]

As these yields could not be improved further, we envisaged to install the lactam present in stephadiamine **I.1** *via* condensation with methylamine as described by Elworthy *et al.*^[307] In our case, however, lactone **I.254** could not be opened using methylamine in ethanol, and only hydrolysis of the methyl ester was observed when the reaction was carried out in H₂O (Scheme I.54). In addition, we also tried to trigger a retro-oxa-Michael addition by the addition of LDA at -78 °C and slowly warming to room temperature, nevertheless no reaction occurred (not shown).



Scheme I.54 Attempted condensation of lactone **I.254** with methylamine.

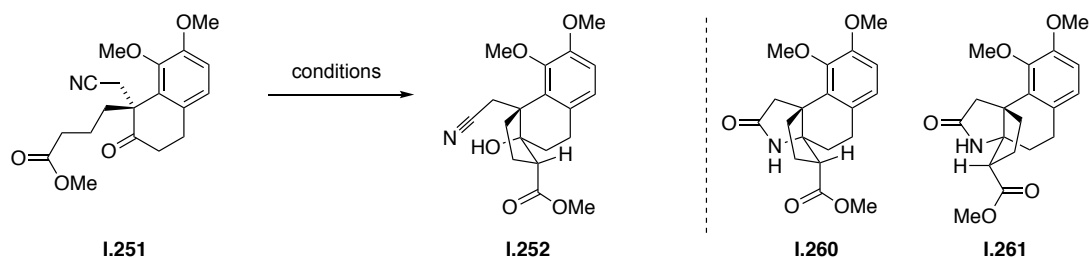
We therefore envisaged to carry out the cascade reaction in a stepwise manner and potentially stop at the stage of tertiary alcohol **I.252** as described by Pinto's synthesis of gibberellin analogs^[308] and Feldman's synthesis of nordiamantane.^[309] Conjugated ester **I.218** was hydrogenated using palladium on charcoal (Pd/C) under hydrogen atmosphere to give ester **I.251** (Scheme I.55).



Scheme I.55 Hydrogenation of unsaturated ester **I.218**.

When ester **I.251** was treated with sodium methoxide (NaOMe, 0.25 eq.) in methanol at moderate temperature, we were able to isolate a mixture of starting material and tertiary alcohol **I.252** (Table I.13, entry 1).^[308] This result was particularly interesting for us as we had observed the formation of exactly the same compound as an intermediate in the reductive aldol cascade reaction. Using 1.2 eq. sodium methoxide in methanol at 75 °C, we isolated two new products, which were identified as **I.260** and its epimer **I.261** (entry 2). As this compound now features the azapropellane core of stephadiamine (**I.1**), which we tried to install in previous attempts (see Scheme I.54), we decided to keep this reaction as the key step of our synthesis. We optimized the reaction conditions and found that the use of freshly prepared NaOMe gave the best results (entries 3–4). Eventually, we were able to obtain lactam **I.260** in a 99% yield.

Table I.13 Conditions tested for the aldol reaction of **I.251**.

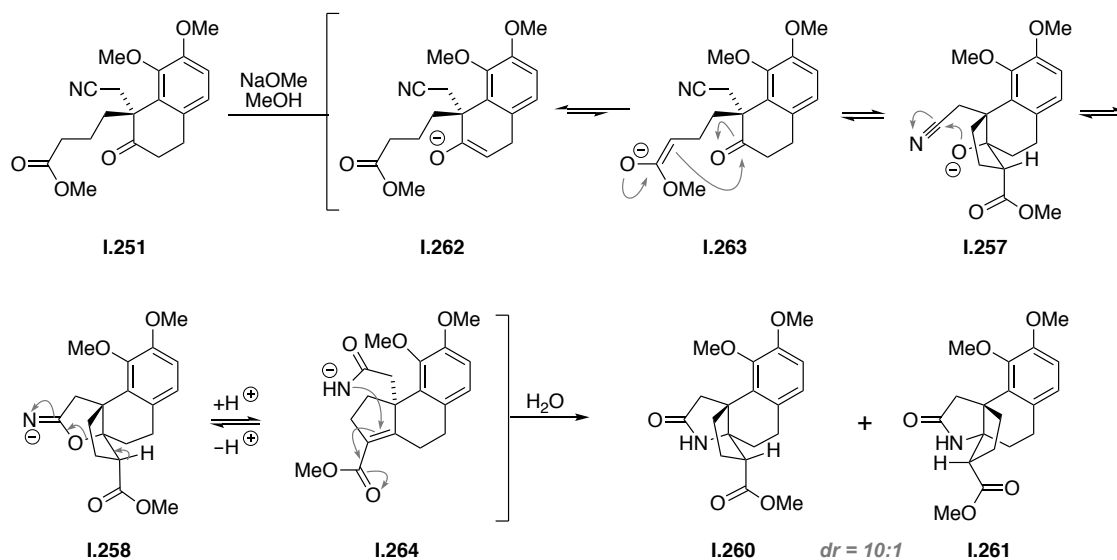


Entry	Scale [mmol]	Conditions	I.251 : I.252 : I.260+I.261 ^{a)}	<i>d.r.</i> of I.260 : I.261
1	0.3	NaOMe (0.25 eq.), MeOH, 20 °C to 70 °C, 12 h	1 : 2 : 0	–
2	0.3	NaOMe (1.2 eq.), MeOH, 75 °C, 26 h	0 : 0 : >99	4:1
3	0.3	Na (1.2 eq.), MeOH, 75 °C, 26 h	0 : 0 : >99	9:1
4	3.2	Na (1.2 eq.), 3 Å MS, MeOH, 75 °C, 16 h	0 : 0 : >99	10:1

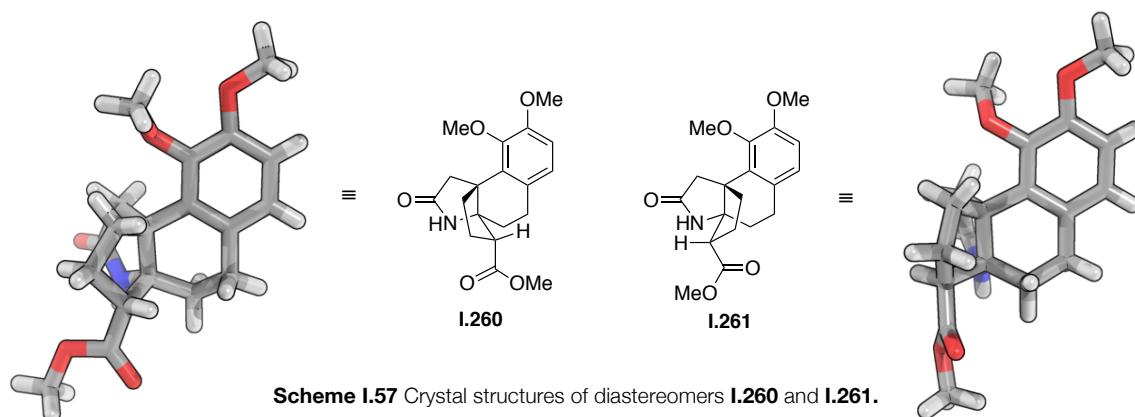
a) Ratio was determined by comparison of the methoxy signals in the ¹H NMR spectrum of the crude reaction mixture.

Our findings resemble the cascade reaction reported by Inubushi and co-workers for their synthesis of cephamine (see chapter 1.1.3),^[154–155] although in our case a [3.3.4]-propellane core with an additional stereocenter is constructed from **I.251**.

Mechanistically, we propose that this remarkably efficient transformation proceeds analogously to Inubushi's cascade reaction and the formation of lactone **I.254**. Initial deprotonation of compound **I.251** would lead to the formation of enolate **I.262**. Intramolecular acylation of this compound, however, would lead to a bridged and relatively strained intermediate. Most probably, a small amount of ester enolate **I.263** is formed, which readily undergoes intramolecular aldol reaction with the ketone to give tertiary alkoxide **I.257**. As described before, this alkoxide subsequently adds into the proximal nitrile. The formed imidate **I.258** then undergoes a retro-oxa Michael reaction under the basic reaction conditions to give tricyclic primary carbamate anion **I.263**. Finally, aza-Michael addition and diastereoselective protonation provides lactams **I.260** and **I.261** in a 10:1 ratio.

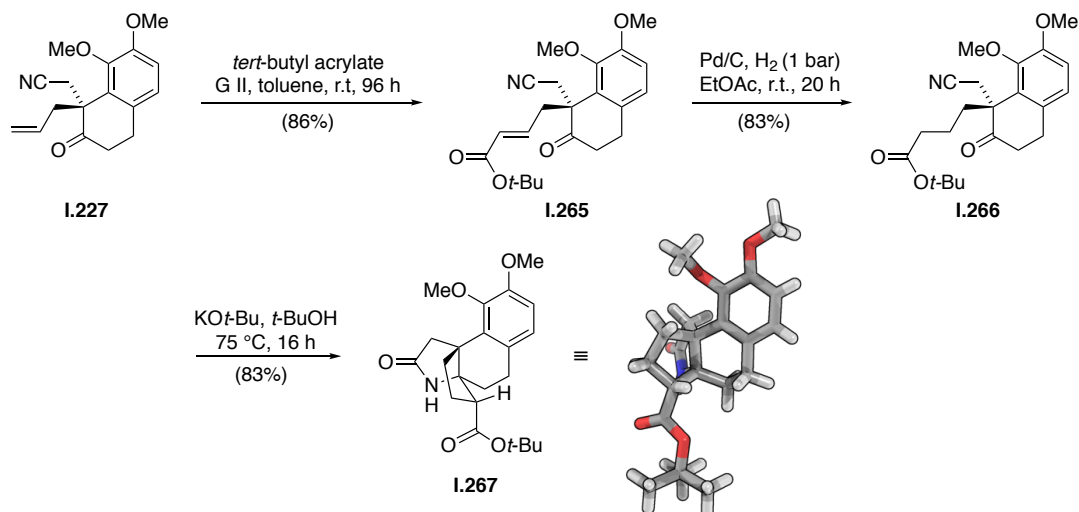


Lactams **I.260** and **I.261** have been separated by column chromatography and have been both fully characterized. In addition, we were able to obtain crystal structures of both diastereomers (see Scheme I.57, Lewis structures are presented according to the crystal structures).



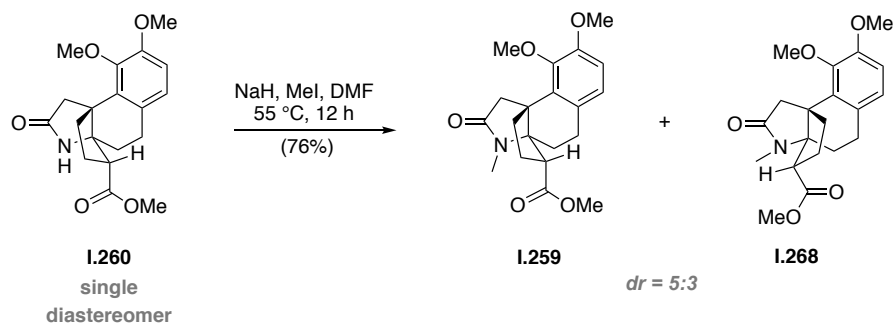
Under all reaction conditions, diastereomer **I.260** was obtained as the major diastereomer. At this point we envisaged that **I.260** could be a precursor for an intramolecular nitrene insertion to install

the second ATA and we therefore considered that a modified substrate could induce the cascade sequence to give **I.261** as the major diastereomer. For example increasing the bulk of the ester could potentially lead to a diastereomeric ratio in favour of **I.261**. With this idea in mind, we carried out a metathesis starting from α -allylcyclohexanone **I.227** using *tert*-butyl acrylate instead of methyl acrylate (Scheme I.58). Unsaturated ester **I.265** was hydrogenated to give cascade precursor **I.266**. Using KO*t*-Bu and the corresponding solvent *tert*-butanol, cascade product **I.267** was readily obtained, but again with the same diastereoselectivity.



Scheme I.58 cascade reaction using *tert*-butyl ester **I.266**.

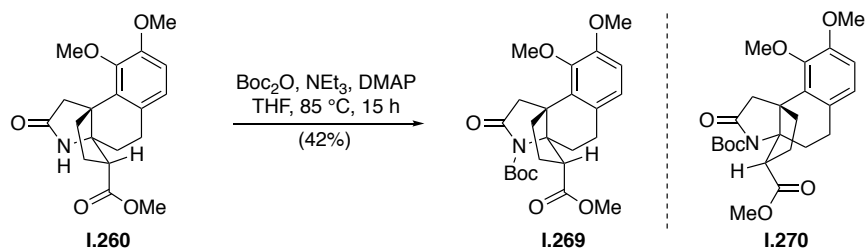
As this approach proved unsuccessful, cascade product **I.260** was *N*-methylated. Under standard conditions, epimerization of the diastereomeric center was observed. When **I.260** alone was used for the *N*-methylation, a 5:3 mixture of *N*-methylated cascade products **I.259** and **I.268** was obtained at 55 °C (Scheme I.59).



Scheme I.59 Equilibration of the diastereomeric center in **I.260** at 55 °C under basic conditions.

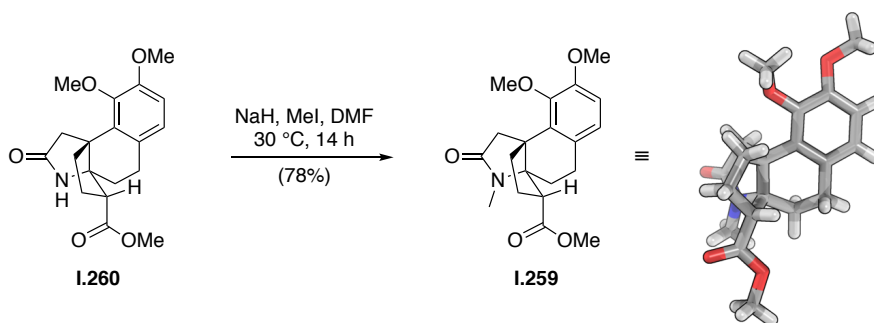
We reasoned that a large *N*-substituent, such as a Boc group, would add significant bulk to this position and result in the preferential formation of one ester diastereomer upon treatment with base. By using standard Boc-protection conditions, however, no reaction occurred. Under forcing

conditions using Boc_2O , NEt_3 and 4-dimethylaminopyridine (DMAP) at $85\text{ }^\circ\text{C}$,^[310] *N*-Boc lactam **I.269** could be obtained in 42% yield. No formation of **I.270** was observed when **I.260** was used as a single diastereomer (Scheme I.60). Additionally, treatment of **I.269** with sodium hydride resulted in no change.



Scheme I.60 Boc protection of lactam **I.260**.

As attempts to equilibrate the ester did not succeed, cascade product **I.260** was *N*-methylated under milder conditions to preserve the diastereomeric ratio of the starting material (Scheme I.61).



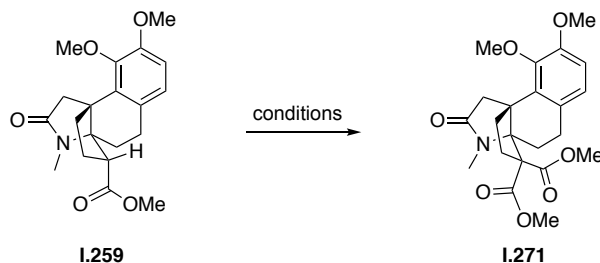
Scheme I.61 Methylation of lactam **I.260**.

At this point, challenging α -carbomethoxylation of ester **I.259** was investigated. Attempted formation of silylketene acetal starting from **I.259** using LDA and TMSCl did not yield any product (not shown). We therefore focused on a direct carboxylation of the α -position using a variety of reagents and bases (Table I.14).

Deprotonation of ester **I.259** with LDA at $-78\text{ }^\circ\text{C}$ followed by addition of Mander's reagent (methyl cyanofornate) did not yield any product (entry 1). Using lithium bis(trimethylsilyl)amide (LiHMDS) and Mander's reagent, clean starting material **I.259** was isolated (entry 2). By contrast, usage of *n*-butyllithium (*n*-BuLi) led to decomposition of the starting material (entry 3). Dimethyl carbonate or methyl chloroformate with NaH as a base, led only to epimerization of the starting material (up to a ratio of 1:1, entries 4 and 5). These results suggest that sodium hydride is able to deprotonate the α -position, but attack into an electrophile seems to be problematic due to the steric hinderance around the propellane core. As a control experiment, we checked if hindered bases such as LDA were able to deprotonate substrate **I.259** at $-78\text{ }^\circ\text{C}$. Therefore CD_3OD was

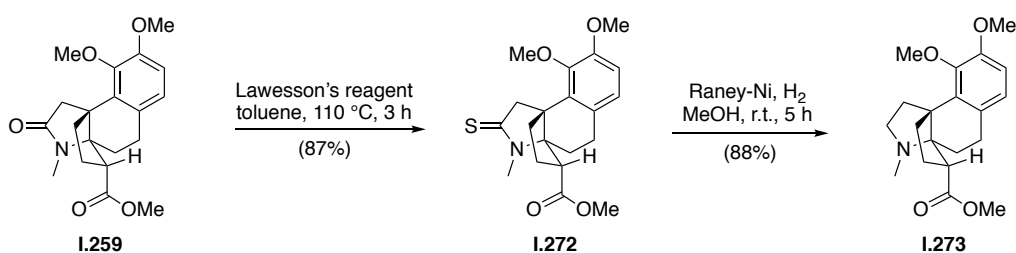
added to deuterate the substrate following addition of LDA. However, the α -proton was still fully visible in the NMR, suggesting that LDA is too sterically demanding for this substrate (entry 6).

Table I.14 Conditions tested for the α -acylation of ester **I.259**.



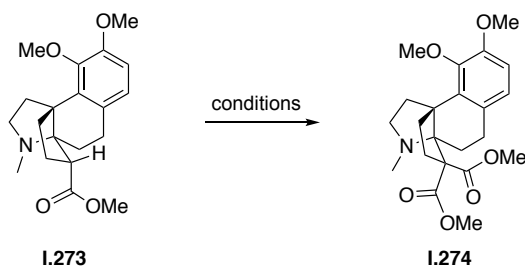
Entry	Conditions ^{a)}	Observation
1	Mander's reagent, LDA, THF, -78 °C to 20 °C, 32 h	starting material reisolated
2	Mander's reagent, LiHMDS, THF, -78 °C to 20 °C, 32 h	starting material reisolated
3	Mander's reagent, <i>n</i> -BuLi, THF, -78 °C to 20 °C, 32 h	decomposition
4	dimethyl carbonate, NaH, THF, 50 °C, 24 h	epimerized starting material
5	methyl chloroformate, NaH, THF, 50 °C to 70 °C, 24 h	epimerized starting material
6	LDA, THF, -78 °C to CD ₃ OD	no incorporation of deuterium

In addition, we attempted to reduce lactam **I.259** chemoselectively to the tertiary amine **I.273** in the presence of the ester and then investigate the α -carboxylation. Beller's procedure ($\text{Zn}(\text{OAc})_2$, $(\text{EtO})_3\text{SiH}$, THF, r.t.)^[311] gave no reaction, $\text{Ru}_3(\text{CO})_{12}$ and TMDS led to decomposition of the starting material.^[312]



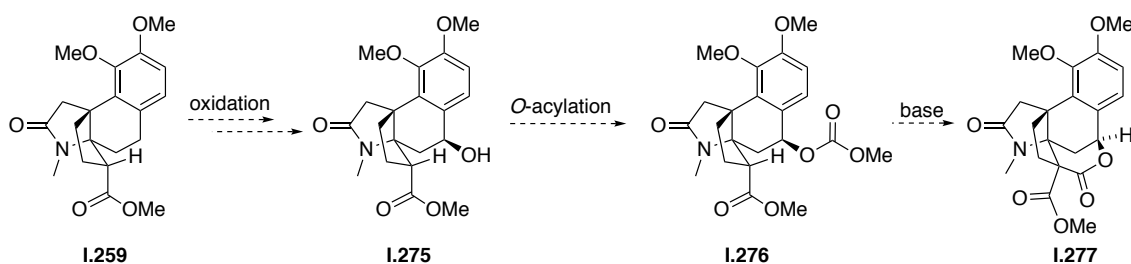
Scheme I.62 Reduction of the lactam to the corresponding tertiary amine **I.259**.

As direct reduction was not applicable, the lactam was transformed into thionolactam **I.272** using Lawesson's reagent (Scheme I.62). This was then cleanly reduced to the tertiary amine with Raney-Ni and hydrogen using a protocol that was applied in Boger's synthesis of vindoline,^[313] however, subsequent α -carboxylation of ester **I.273** proved unsuccessful as well (Table I.15).

Table I.15 Conditions tested for the α -carboxylation of ester **I.273**.

Entry	Conditions ^{a)}	Observation
1	Mander's reagent, NaH, THF, 0 °C to 20 °C, 48 h	no reaction
2	dimethyl carbonate, NaH, THF, 0 °C to 20 °C, 48 h	epimerization at α -carbon of I.273
3	dimethyl carbonate, NaH, toluene, 80 °C, 48 h	no reaction
4	dimethyl carbonate (neat), NaH, 80 °C, 48 h	no reaction
5	dimethyl carbonate, NaOMe, MeOH, 75 °C, 17 h	decomposition
6	methyl chloroformate, NaH, THF, 0 °C to 20 °C, 48 h	no reaction

Turning to a different approach, we investigated the possibility to install the lactone following benzylic oxidation by an intramolecular carboxylation *via* intermediate **I.276** to circumvent issues associated with steric hindrance around the ester moiety. We envisaged a benzylic oxidation to access secondary alcohol **I.275**. *O*-Acylation to install carbonate **I.276** followed by base-mediated lactone formation could then furnish compound **I.277**.

**Scheme I.63** Alternative strategy lactone construction.

For this purpose, a set of oxidations was investigated that could potentially lead to oxidation products **I.275**, **I.278** and **I.279** (Table I.16). Oxidation with Jones reagent in acetone at 0 °C led to decomposition of the starting material (entry 1).^[158–159] By contrast, no reaction occurred using potassium permanganate and copper(II) sulfate or Pearlman's catalyst (Pd(OH)₂/C) in combination with *tert*-butyl hydroperoxide (TBHP) (entries 2 and 3). Excess ceric ammonium nitrate (CAN) in a 1:20 mixture of H₂O and acetonitrile led to decomposition (entry 4). By contrast, lowering the amount of CAN to 2 equivalents and changing the solvent ratio to 1:1, we isolated trace amounts

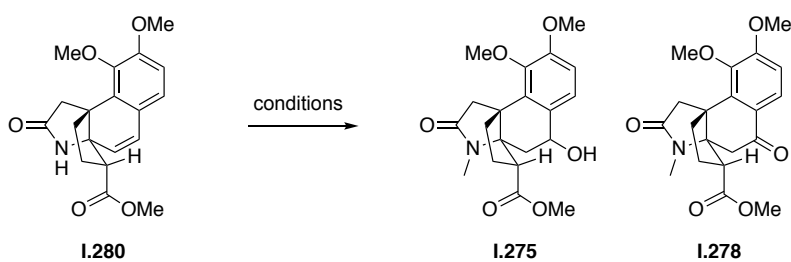
of a compound that was identified as ketone **I.278** (by ^1H NMR and HRMS, entry 5).^{***} Unfortunately, we were never able to improve the yield to synthetically useful levels. We therefore continued testing other methods for the benzylic oxidation (entries 6–8) and eventually found that heating **I.259** in a mixture of excess DDQ and acetic acid in DCE^[314] afforded styrene derivative **I.280** in 50% yield (entry 8).

Table I.16 Conditions tested for the benzylic oxidation of propellane **I.259**.

Entry	Conditions	Observation
1	Jones reagent, acetone, 0 °C	decomposition
2	KMnO ₄ /CuSO ₄ , DCM, 50 °C	no reaction
3	Pd(OH) ₂ /C, TBHP, K ₂ CO ₃ , DCM, 4 °C to r.t.	no reaction
4	CAN, 20:1 MeCN/ H ₂ O, r.t.	decomposition
5	CAN, 1:1 MeCN/ H ₂ O, r.t.	mainly starting material I.259 and traces of ketone I.278
6	TBHP, Co(acac) ₂ , acetone, r.t., 48 h	no reaction
7	DDQ, 1:1 dioxane/acetone, r.t.	no reaction
8	DDQ/AcOH,DCE, 4Å MS, 75 °C, 5 h	elimination product I.280 (50% yield)

We envisaged that styrene **I.280** could serve as a handle for a Wacker oxidation or a Mukaiyama hydration.^[315] For the Mukaiyama hydration, Mn(dpm)₃, oxygen and PhSiH₃ in methanol did not lead to any conversion (Table I.17, entry 1)^[316] whereas the use of Co(acac)₂ led to a complex mixture of compounds (entry 2).^[317] Wacker conditions using palladium(II)acetate, *para*-benzoquinone (*p*-BQ), and fluoroboric acid (HBF₄) in a mixture of *N,N*-dimethylacetamide (DMA), acetonitrile and H₂O also failed to provide any conversion (entry 3).^[318]

^{***} The experiments with CAN as oxidant were carried out by Dr. Hongdong Hao.

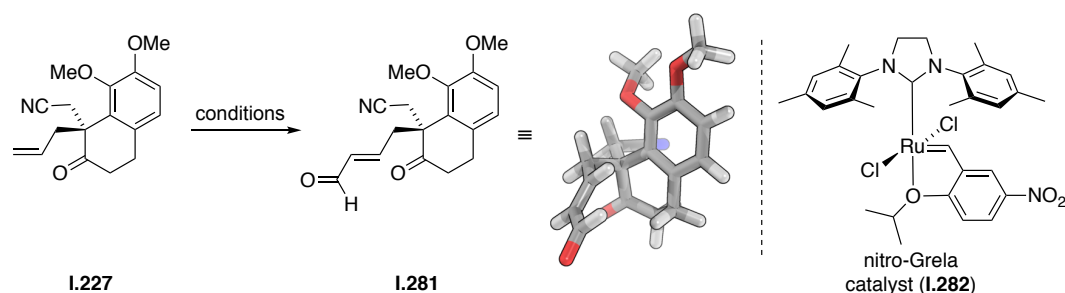
Table I.17 Conditions tested for the benzylic oxidation of styrene **I.280**.

Entry	Conditions	Observation
1	Mn(dpm) ₃ , PhSiH ₃ , O ₂ , MeOH, r.t.	no reaction
2	Co(acac) ₂ , PhSiH ₃ , O ₂ , THF, r.t.	complex mixture
3	Pd(OAc) ₂ , <i>p</i> -BQ, DMA, MeCN, H ₂ O, aq. HBF ₄ , r.t.	no reaction

As it was not possible to install the quaternary stereo center next to the ester functionality, we turned our attention to a different approach.

3.2.2 Aldehyde approach

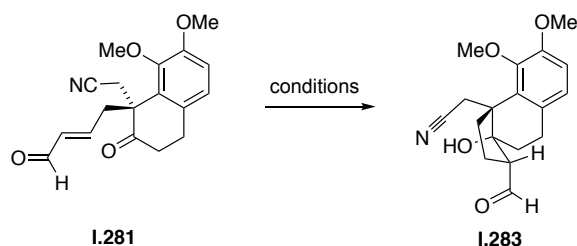
In parallel to the previous approach, the same reactions were investigated with the corresponding aldehyde instead of an ester. However, metathesis of substrate **I.227** with crotonaldehyde proved to be more challenging than the previous metathesis reaction using methyl acrylate (see chapter 3.2.1). Using Grubbs II catalyst (**I.249**) and excess croton aldehyde in toluene at 20 °C, the reaction was relatively slow and 49% of **I.281** was isolated after 40 h reaction time (Table I.18, entry 1). Using 10 mol% grubbs II catalyst (**I.249**) and 10 eq. crotonaldehyde in DCM, the reaction stalled after 12 h and a yield of 53% was obtained (entry 2). Elevating the temperature to 50 °C did not increase the yield of the reaction (entry 3). By changing to Hoveyda–Grubbs II catalyst (**I.250**) in DCM, the yield increased to 75% after 12 h reaction time at room temperature. When the reaction was heated to 50 °C, the yield decreased to 69% (entry 5). In addition to Grubbs II (**I.249**) and Hoveyda–Grubbs II catalyst (**I.250**), we investigated the use of nitro-Grela catalyst (**I.282**), which gave a significantly lower yield (entry 6).

Table I.18 Conditions screened for the synthesis of aldehyde **I.281**.

Entry	Conditions ^{a)}	T	t	Observation
1	Grubbs II (5 mol%), crotonaldehyde (17 eq.), toluene	20 °C	40 h	49% I.281
2	Grubbs II (10 mol%), crotonaldehyde (10 eq.), DCM	20 °C	12 h	53% I.281
3	Grubbs II (10 mol%), crotonaldehyde (10 eq.), DCM	50 °C	12 h	52% I.281
4	Hoveyda–Grubbs II (10 mol%), crotonaldehyde (10 eq.), DCM	20 °C	12 h	75% I.281
5	Hoveyda–Grubbs II (10 mol%), crotonaldehyde (10 eq.), DCM	50 °C	12 h	69% I.281
6	nitro-Grela (10 mol%), crotonaldehyde (10 eq.), DCM	20 °C	12 h	42% I.281

^{a)} Crotonaldehyde was freshly distilled and solvents were degassed prior to usage

Having secured significant quantities of enal **I.281**, we then investigated the reductive aldol reaction on this substrate. When Stryker's reagent was used at $-40\text{ }^{\circ}\text{C}$, decomposition of the starting material was observed under acidic and basic work-up conditions (Table I.19, entry 1 and 2). Krische's procedure using $\text{Rh}(\text{cod})_2\text{OTf}$ and hydrogen led to a complex reaction mixture, which did not contain any of the desired products.^[319]

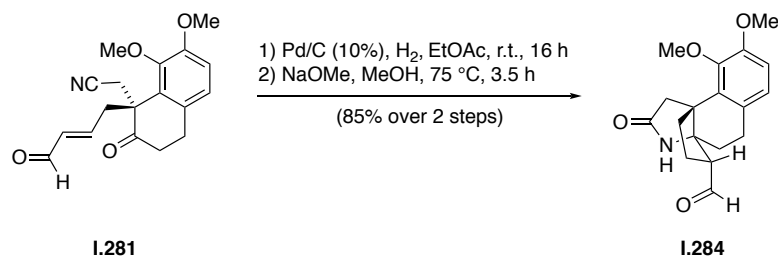
Table I.19 Conditions tested for the reductive aldol reaction of aldehyde **I.281**.

Entry	Conditions ^{a)}	Observation
1	Stryker's reagent, toluene, $-40\text{ }^{\circ}\text{C}$, 4 h \rightarrow HCl, TMEDA	decomposition
2	Stryker's reagent, toluene, $-40\text{ }^{\circ}\text{C}$, 4 h \rightarrow NaOMe, TMEDA	decomposition
3	$\text{Rh}(\text{cod})_2\text{OTf}$, PPh_3 , H_2 (1 atm), K_2CO_3 , THF, $40\text{ }^{\circ}\text{C}$, 4 h	complex mixture

^{a)} All solvents were degassed using standard freeze-pump-thaw techniques (minimum of three cycles)

At this point we attempted the same hydrogenation/cyclization sequence for substrate **I.281** (see chapter 3.2.1). As the cascade reaction occurred with methyl ester **I.251** and *tert*-butyl ester **I.266**

under basic conditions in protic solvent, it was expected that the cascade would also occur with an aldehyde instead of an ester. Reduction of the double bond yielded an unstable saturated aldehyde (not shown), that was subjected to cascade conditions. The reaction proceeded either at room temperature overnight or at 75 °C in 3.5 h and gave 85% conversion to the cascade product **I.284**.

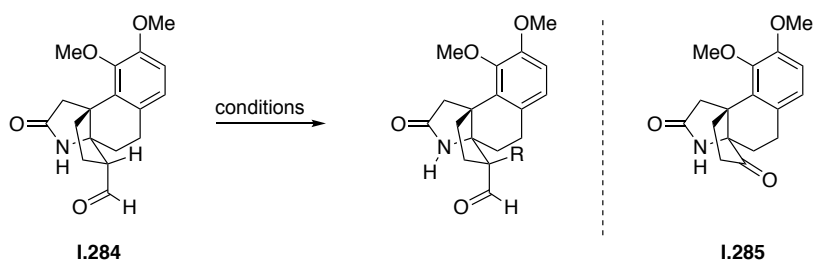


Scheme I.64 Synthesis of cascade product **I.284**.

Using cascade product **I.284**, we tried the direct amination of the acidic α -position of the aldehyde using dibenzylidiazodicarboxylate (DBAD) and proline as an organocatalyst. This method has been described for the α -amination of aldehydes and was successfully used for the implementation of ATAs in the past.^[320–322] However, when applying these conditions to our substrate, only starting material **I.284** was obtained (Table I.20, entry 1). Diethyl azodicarboxylate (DEAD) proved ineffective as well (entry 2).

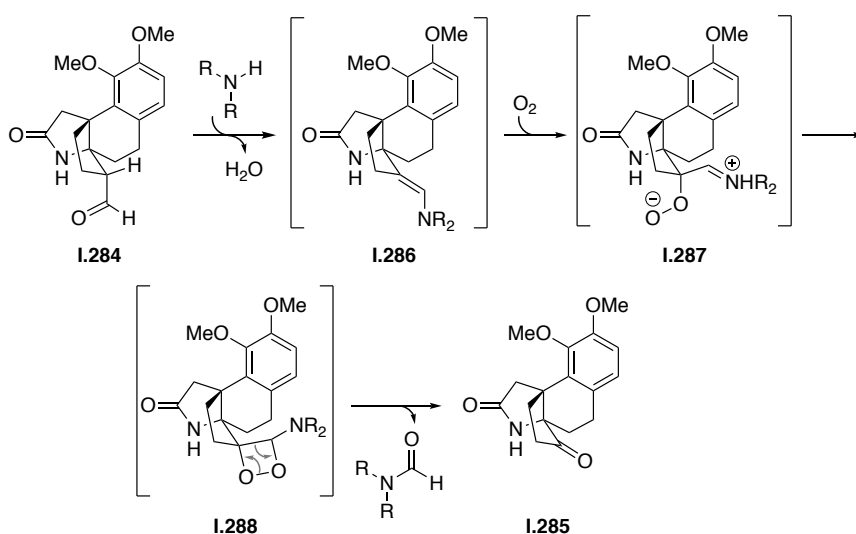
We then turned our attention to α -carboxylations rather than α -aminations of aldehyde **I.284**. Using proline and MgSO₄ followed by methylchloroformate, a very slow conversion to a new product was observed. After 48 h the reaction was stopped and the compound was identified as ketone **I.285**.

Table I.20 Conditions tested for the α -functionalization of aldehyde **I.284**.



Entry	Conditions ^{a)}	Observation
1	proline, DBAD, MeCN, 20 °C, 48 h	no reaction
2	proline, DEAD, MgSO ₄ , THF, 20 °C, 48 h	no reaction
3	pyrrolidine, THF, MgSO ₄ → methyl chloroformate in THF, 48 h	formation of ketone I.285

We were interested in an explanation for the unexpected formation of ketone **I.285** *via* deformylation, as the product could be used for the installation of the ATA (see chapter 1.1.2.1). In most examples in the literature, deformylation reactions are mediated by metals.^[323] However few examples using metal-free deformylations have been reported, such as Yamamoto's nitrosobenzene-mediated C–C bond cleavage^[324] and Johnson's Lewis acid-promoted C–C bond cleavage of aziridines.^[325] In addition, Chi and co-workers reported a metal-free oxidative C–C bond cleavage using amines and oxygen.^[326] Adapting their mechanistic proposal, we suggest the following mechanism for the observed oxidation (Scheme I.65): the respective amine and aldehyde **I.284** condense to form enamine **I.286**, which engages oxygen to form peroxide anion **I.287**. Dioxetane formation to **I.288** followed by retro-[2+2] cycloaddition would then give ketone **I.285**.



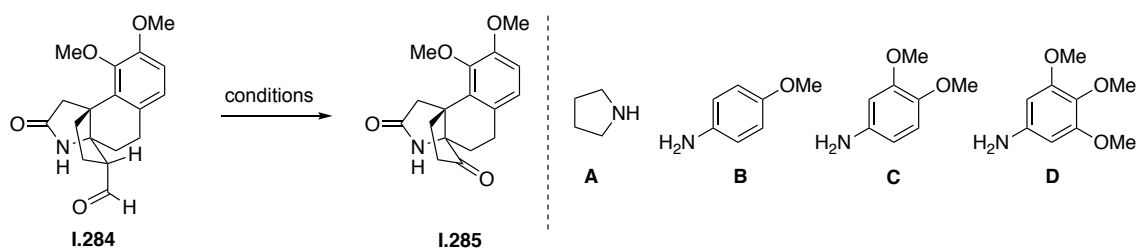
Scheme I.65 Plausible mechanism for the deformylation of aldehyde **I.284**.

We realized that ketone **I.285** could serve as a substrate for a Strecker or Bucherer–Bergs reaction to install the second ATA. Prior to additional experiments, we investigated enamine formation in deuterated chloroform and deuterated toluene. In both solvents full conversion to the enamine was observed after 1 h reaction time.

To obtain ketone **I.285** on a preparative scale, we investigated the use of pyrrolidine (amine A), as this amine initially led to the discovery of the reaction product. By applying oxygen (5 bar) in toluene to the reaction mixture, we obtained traces of product, which were accompanied by an inseparable side product - most likely the formylated amine (Table I.21, entry 1). We envisaged that by addition of $MgSO_4$ we would facilitate elimination of H_2O , however no product was observed in this case (entry 2). Next we turned our attention to *p*-anisidine (amine B), an amine also used in Chi's methodology.^[326] However, no formation of the desired product was observed (entries 3 and 4). We next screened for more electron-rich anilines such as 3,4-dimethoxyaniline (amine C) and

3,4,5-trimethoxyaniline (amine D) (entries 5–12), which more readily form the enamine and oxidize more quickly. Although 3,4-dimethoxyaniline was ineffective (entry 5), we observed formation of significant amounts of desired ketone **I.285** with 3,4,5-trimethoxyaniline: a mixture of starting material **I.284** and product **I.285** was obtained (entry 7) in CHCl_3 . Finally, by switching to toluene as a solvent, we observed complete conversion to the product by ^1H NMR.

Table I.21 Conditions tested for the synthesis of ketone **I.284**.



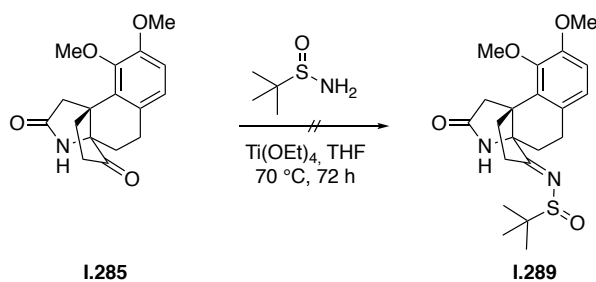
Entry	Conditions ^{a)}	Observation
1	amine A , toluene, r.t., 1 h \rightarrow O_2 (5 bar), 33 h	I.285 and inseparable byproduct
2	amine A , toluene, MgSO_4 , r.t., 1 h \rightarrow O_2 (5 bar), 33 h	starting material I.284
3	amine B , toluene, r.t., 1 h \rightarrow O_2 (5 bar), 20.5 h \rightarrow MeOH, HCl	complex reaction mixture
4	amine B , toluene, r.t., 1 h \rightarrow O_2 (5 bar), 20.5 h \rightarrow NH_4Cl	complex reaction mixture
5	amine C , toluene, r.t., 1 h \rightarrow O_2 (5 bar), 20.5 h	complex reaction mixture
6	amine D , CHCl_3 , 4 Å MS, r.t., 1 h \rightarrow O_2 (5 bar), 24 h	mixture of starting material I.284 and I.285
7	amine D , toluene, O_2 , 4 Å MS, r.t., 1 h \rightarrow O_2 (5 bar), 24 h	I.285 and inseparable byproduct
8	amine D , toluene, r.t., 1 h \rightarrow O_2 (5 bar), 20.5 h \rightarrow NaHCO_3 (pH 12)	I.285 and inseparable byproduct
9	amine D , toluene, r.t., 1 h \rightarrow O_2 (5 bar), 20.5 h \rightarrow NH_4Cl	I.285 and inseparable byproduct
10	amine D , toluene, r.t., 1 h \rightarrow O_2 (5 bar), 20.5 h \rightarrow NH_4Cl , dissolved in 1 M HCl	32% I.285
11	amine D , toluene, 4 Å MS, r.t., 1 h \rightarrow O_2 (5 bar), 24 h \rightarrow HCl	41% I.285
12	amine D , r.t., 1 h \rightarrow O_2 (1 bar), TPP, CDCl_3 , reptile lamp, r.t., 20 min	mixture of I.285 and enamine I.286
13	$\text{Cu}(\text{OAc})_2 \cdot \text{H}_2\text{O}$, DBU, DMF, O_2 , 75 °C, 1.5 h	decomposition
14	$\text{Cu}(\text{OAc})_2 \cdot \text{H}_2\text{O}$, DBU, DMF, O_2 (5 bar), r.t., 33 h	decomposition
15	$\text{Cu}(\text{OAc})_2 \cdot \text{H}_2\text{O}$, DABCO, 2,2'-bipyridine, DMF, O_2 , 75 °C, 1.5 h	decomposition

At this point, a set of different work-up conditions was investigated, as we found that ketone **I.285** was always accompanied by a side product, most likely formylated amine D (entries 8–11). Workup with NaHCO_3 or NH_4Cl gave ketone **I.285** accompanied with inseparable side products (entries 8 and 9). By washing the product with ammonium chloride and stirring the crude reaction mixture in

1 M hydrochloric acid followed by column chromatography, we obtained 32% of the clean product **I.285** (entry 10). By adding hydrochloric acid to the reaction mixture and stirring for another 1 h, we obtained a yield of 41% (entry 11). In addition, photocatalytic conditions using the photosensitizer tetraphenylporphyrin (TPP) and a reptile lamp as light source did not yield any product (entry 12).

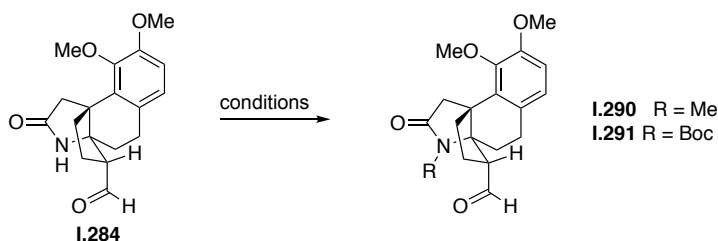
When we were not able to improve the yields further, we investigated Cu-catalyzed conditions (entries 13–15). The earliest report of an aldehyde that was converted to a ketone by oxidative C–C bond cleavage was published in 1969 by van Rheenen using $\text{Cu}(\text{OAc})_2$ and (1,4-diazabicyclo[2.2.2]octane) (DABCO).^[327] Similar to van Rheenen, Nitta *et al.* published a strategy using a different base (1,8-diazabicyclo[5.4.0]undec-7-ene, DBU).^[328] Following their procedures, the reactions were carried out using a copper catalyst and an amine base (DBU or DABCO) at 75 °C or room temperature (entries 13–15). Unfortunately, decomposition of the starting material was observed in all cases.

With small amounts of ketone **I.285** in hand, we tested the transformation of this functional handle. Following a procedure by Reisman and co-workers,^[329] we tried to form the chiral sulfinimine **I.289** using *tert*-butanesulfinamide and titanium (IV) ethoxide, but only starting material was reisolated (Scheme I.66). As ketone **I.285** could not be obtained in good yields and its condensation to the corresponding sulfinimine was not successful, we went back to investigate the α -functionalization of aldehyde **I.284**.



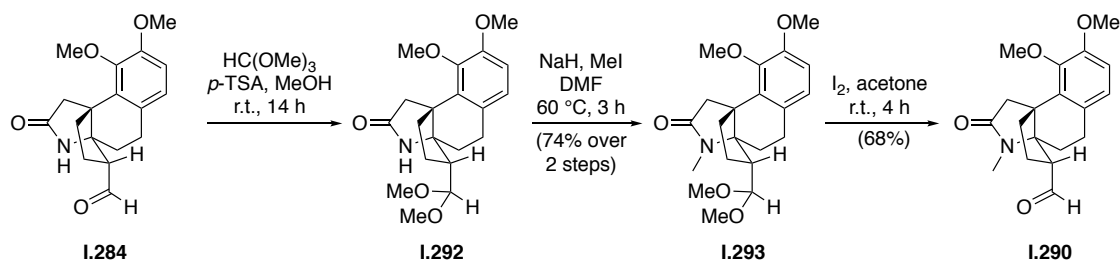
Scheme I.66 Attempted sulfinimine formation of ketone **I.285**.

We assumed that the unprotected lactam could be problematic in the α -functionalization of aldehyde **I.284** and therefore attempted *N*-methylation or Boc-protection of lactam nitrogen. However, using the conditions we had previously established for the derivatization of ester **I.260** (see chapter 3.2.1), no desired product was obtained – probably due to the competing reactivity of the aldehyde (Table I.22, entry 1–3).

Table I.22 Conditions tested for the functionalization of lactam **I.284**.

Entry	Conditions	Observation
1	MeI, NaH, DMF, 0 °C	complex mixture
2	NaH, Boc ₂ O, DMAP, DMF, 50 °C, 12 h	decomposition
3	NEt ₃ , Boc ₂ O, DMAP, DCM, 20 °C, 12 h	decomposition

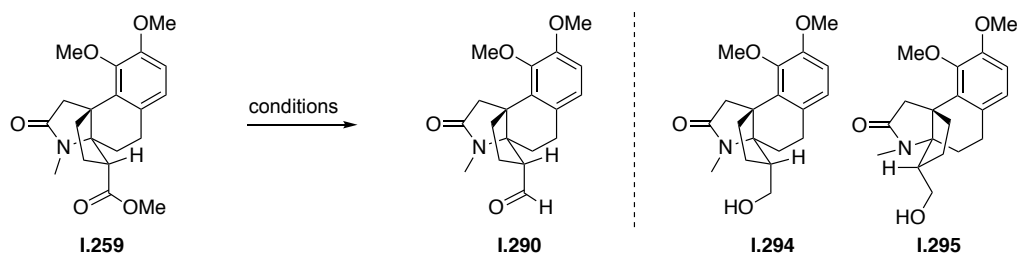
To prevent undesired reactivity from the aldehyde, we protected the aldehyde as dimethoxyacetal **I.292** (Scheme I.67). Subsequent *N*-Methylation then occurred smoothly using iodomethane (MeI) and sodium hydride in DMF at elevated temperatures. For the deprotection of this aldehyde **I.293** a variety of mild methods such as indium(III)triflate in acetone, were applied. Eventually, we found that iodine in acetone gave clean conversion to the aldehyde **I.290** and all impurities could be removed in the work-up process.

**Scheme I.67** Synthesis of *N*-methylated cascade product **I.290**.

As this sequence was rather lengthy and involved several unstable intermediates, we investigated the reduction of ester **I.259** to aldehyde **I.290** using diisobutylaluminium hydride (DIBAL-H, Table I.23). This transformation needed careful optimization, as sometimes overreduction of the ester to the alcohol **I.294** (and its epimer) or the amide to the tertiary amine was observed. It was found that 2.0 to 3.0 equivalents of DIBAL-H were needed for clean conversion to aldehyde **I.290**. We applied two common work-up methods for DIBAL-H – addition of potassium sodium tartrate and the Fieser work-up. Using 2 and 3 equivalents of DIBAL-H in DCM, the reaction was quenched after 4 h at -78 °C by the addition of ethyl acetate followed by Rochelle salt (potassium sodium tartrate) to form an aluminum tartrate complex (entries 1 and 2). Quenching with NaOH (Fieser work-up), led to the formation of unwanted side products (entries 3 and 4). The fully reduced

alcohol **I.294** could be identified in the reaction mixture amongst other unknown species. Hence, the reaction was quenched at -78 °C with ethyl acetate to destroy excess DIBAL-H (entries 5 and 6). Sodium hydroxide solution was subsequently added at this temperature and the reaction was slowly allowed to warm to room temperature. Under these conditions, it was possible to reach yields up to 84% of desired aldehyde **I.290** after flash column chromatography, critically, over DAVISIL[®] (entry 6).

Table I.23 Reduction of ester **I.259** to aldehyde **I.290**.

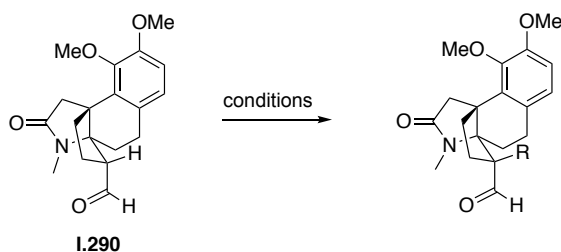


Entry	Conditions ^{a)}	Work-up	Ratio ^{a)} [I.259:I.294:side products]
1	DIBAL-H (2.0 eq.), 4 h	EtOAc / Na,K-tartrate	[23:77:0]
2	DIBAL-H (3.0 eq.), 4 h	EtOAc / Na,K-tartrate	[39:61:0]
3	DIBAL-H (3.0 eq.), 4 h	NaOH	[0:25:75]
4	DIBAL-H (2.0 eq.), 4 h	NaOH	[0:21:79]
5	DIBAL-H (2.5 eq.), 2 h	EtOAc / NaOH	[0:64:36]
6	DIBAL-H (2.5 eq.), 3 h	EtOAc / NaOH	[0:100:0]

84% isolated yield

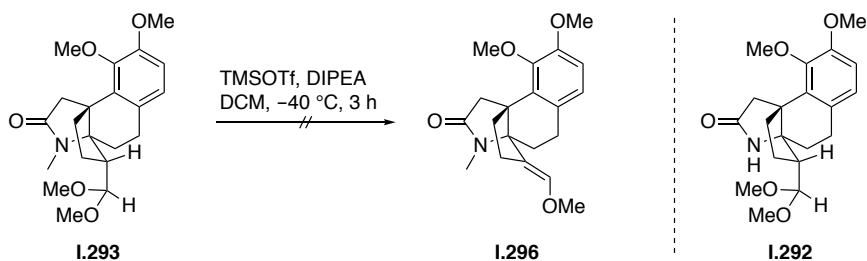
^{a)} The ratio was determined by ¹H NMR by integration of the two methoxy signals of the starting material, the side product and the aldehyde

With clean aldehyde **I.290** in hand, we reinvestigated its carboxymethylation (Table I.24). With dimethyl chloroformate, methyl carbonate or Mander's reagent, only decomposition was observed (entries 1–3). Additionally, when applying the same α -amination conditions as attempted for aldehyde **I.290**, no reaction occurred (entry 4).

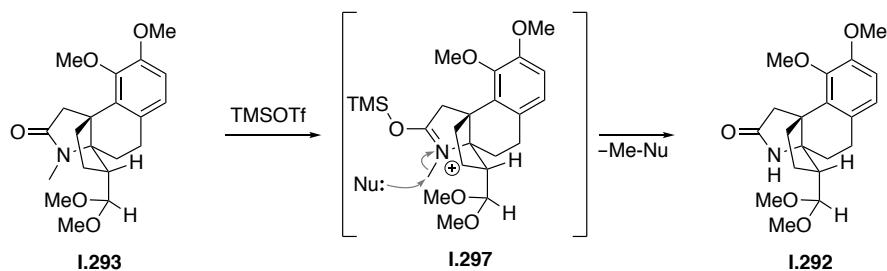
Table I.24 Conditions tested for the functionalization of aldehyde **I.290**.

entry	Conditions ^{a)}	observation
1	dimethyl carbonate, LiHMDS, THF	decomposition
2	methyl chloroformate, LiHMDS, THF, -78 °C	decomposition
3	Mander's reagent, LiHMDS, THF, -78 °C	decomposition
4	pyrrolidine, CDCl ₃ → DBAD, toluene, 20 °C	No reaction

At this juncture, we aspired to make use of previously synthesized dimethyl acetal **I.293** and induce elimination of MeOH to form reactive enol ether **I.296**, which could potentially be α -functionalized. Following a procedure by Garg and co-workers,^[330] substrate **I.293** was treated with *N,N*-diisopropylethylamine (Hünig's base, DIPEA) and TMSOTf and the reaction proceeded to full conversion. (Scheme I.68). Unfortunately, the isolated product was not enol ether **I.296**, but instead demethylated lactam **I.292** with the acetal still intact.

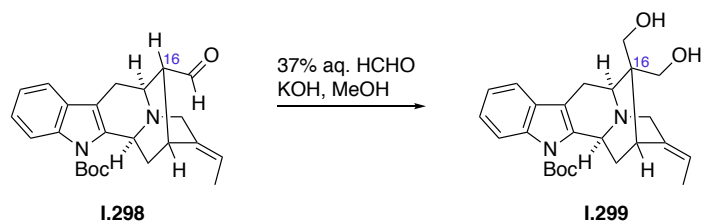
**Scheme I.68** Attempted elimination of methanol from acetal **I.290**.

The demethylation most likely proceeds *via* intermediate **I.297**, which undergoes dealkylation (Scheme I.69). Although this transformation was not of practical use at this stage, it provided insight into the Lewis basicity of this lactam, which we could exploit at a later step in the synthesis to selectively convert it into the tertiary amine found in stephadiamine (**I.1**).



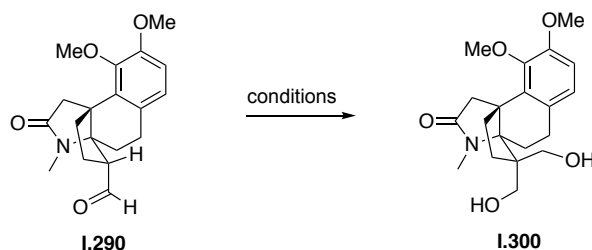
Scheme I.69 Possible mechanism for the demethylation of **I.293**.

At this point, we took a deeper look into the literature and found that Cook *et al.* faced a similar problem toward the synthesis of sarpagine- and ajmaline alkaloids and state that „*numerous efforts (aldolizations, alkylations, and acylations) were originally carried out to construct the quaternary carbon center at C-16, but they were not successful. gratifyingly, it was found that the aldehydic group at C-16 could be converted into diol in 85% yield via the Tollens reaction with 37% aqueous formaldehyde (5 equiv) and KOH (10 equiv) in methanol.*“^[331] We reasoned that this approach makes use of a very small base and a small electrophile, which may be suited for our system.



Scheme I.70 Cook's approach for the installation of a quaternary stereo center.

We thus carried out a Tollens reaction (crossed Cannizzaro reaction) starting from aldehyde **I.290**, and indeed, after 15 h, a new compound was formed. It was identified to be diol **I.300**, wherein the desired prochiral quaternary carbon had been successfully installed. We screened various amounts of base and formaldehyde at different temperatures (Table I.25, entries 1–5). Under optimized conditions, we were able to obtain diol **I.300** with a yield of 73%.

Table I.25 Conditions screened for the Tollens reaction.

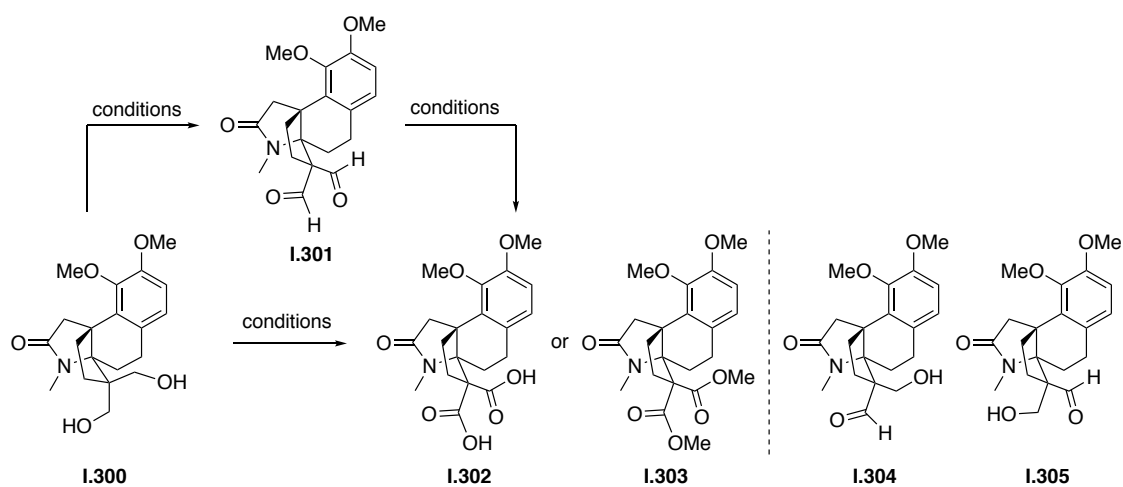
Entry	Conditions	Yield
1	KOH (10 eq.), formaldehyde (25 eq.), r.t., 48 h	46%
2	KOH (10 eq.), formaldehyde (10 eq.), r.t., 48 h	41%
3	KOH (5 eq.), formaldehyde (25 eq.), r.t., 48 h	43%
4	KOH (10 eq.), formaldehyde (25 eq.), 50 °C, 48 h	61%
5	KOH (10 eq.), formaldehyde (10 eq.), 50 °C, 48 h	73%

With prochiral diol **I.300** in hand, we then set out to install the second ATA and the δ -lactone of stephadiamine **I.1**.

3.3 Implementation of the second ATA

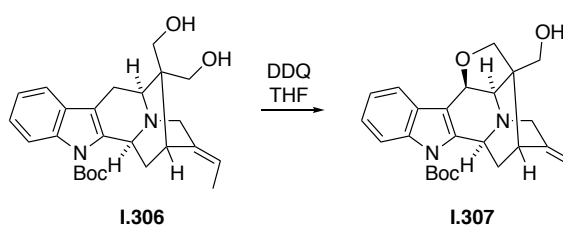
Starting from diol **I.300**, the next goal was the installation of the second ATA. For this purpose, the two hydroxyl groups of **I.300** had to be differentiated. Initially we planned a simultaneous oxidation of both alcohols to furnish either bisaldehyde **I.301** or malonic acid **I.302** (Table I.26). Oxidation of diol **I.300** under Corey–Kim conditions led to decomposition of the starting material (entry 1), whereas Swern oxidation led to a complex reaction mixture (entry 2). Using classical Ley–Griffith conditions or benzeneseleninic acid anhydride [(PhSeO)₂O] in chlorobenzene at 110 °C, we were able to isolate traces of mono-oxidation products **I.304** and **I.305** as a 1:1 mixture, however, no dialdehyde **I.301** could be isolated (entry 3 and 4). These results suggest that the steric environment of the two hydroxyl groups and the potential instability of a dialdehyde **I.301** significantly hampered attempts to isolate the desired product.

In attempts to access malonic acid **I.302**, Jones oxidation, 2,2,6,6-tetramethylpiperidinyloxy (TEMPO)/(diacetoxyiodo)benzene (BAIB, [PhI(OAc)₂]), aqueous Ley–Griffith conditions and Corey–Schmidt oxidations were investigated, but decomposition was observed under all conditions (entries 5–8). Attempted direct oxidation to ester **I.303** using iodine and potassium carbonate in methanol did not occur, and only starting material was isolated (entry 9).

Table I.26 Oxidation of diol **I.300**.

Entry	Oxidation type	Conditions ^{a)}	Expected Product	Observation
1	Corey-Kim	NCS, DMS, Et ₃ N, DCM, -78 °C	I.301	decomposition
2	Swern	DMSO, (COCl) ₂ , Et ₃ N, DCM, -78 °C	I.301	complex mixture
3	Ley-Griffith	TPAP, NMO, DCM, 4 Å MS, r.t., 1 h	I.301	1:1 mixture of I.304 and I.305
4	(PhSeO) ₂ O	(PhSeO) ₂ O (1.0 eq.), chlorobenzene, 110°C, 30 min	I.301	1:1 mixture of I.304 and I.305
5	Jones	CrO ₃ , H ₂ SO ₄ , H ₂ O, acetone, 0 °C	I.302	decomposition
6	TEMPO/BAIB	TEMPO/BAIB, MeCN/H ₂ O	I.302	decomposition
7	Ley-Griffith (aq.)	TPAP, NMO · H ₂ O, DCM, 0 °C	I.302	decarboxylation (by HRMS)
8	Corey-Schmidt	PDC, DMF, r.t.	I.302	decomposition
9	I ₂ /MeOH	I ₂ , MeOH, K ₂ CO ₃ , 70 °C	I.303	no reaction

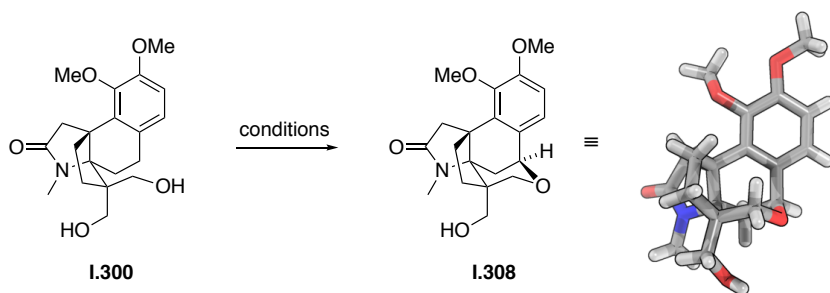
As oxidation of the diol was not feasible, we opted for differentiation of the diol by benzylic etherification as described by Cook (Scheme I.71).^[332]

**Scheme I.71** Cook's differentiation of diol **I.306**.

First, we investigated the use of DDQ in THF at 65 °C and observed traces of benzylic ether **I.308** (entry 1). Using DDQ in a mixture of DMF and THF led to no reaction (entry 2) whereas DDQ in THF with 3Å MS at either room temperature or 65 °C led to decomposition of the starting material

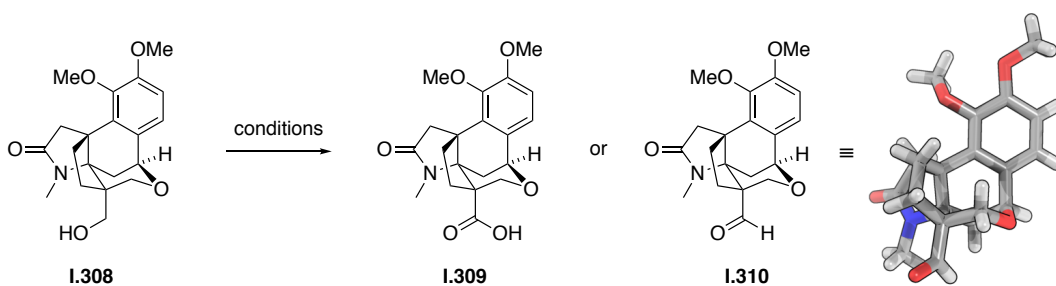
(entries 3 and 4). Performing the reaction under O₂ atmosphere also led to decomposition of the starting material **I.300** (entry 5). We then went back to the reaction conditions that were found for the installation of a benzylic double bond (see chapter 3.2.1, Table I.16), namely DDQ and acetic acid in DCE at 75 °C (entry 6). Under these conditions, desired cyclic ether **I.308** was obtained 71% yield.

Table I.27 Conditions tested for the oxidative functionalization of diol **I.300**.



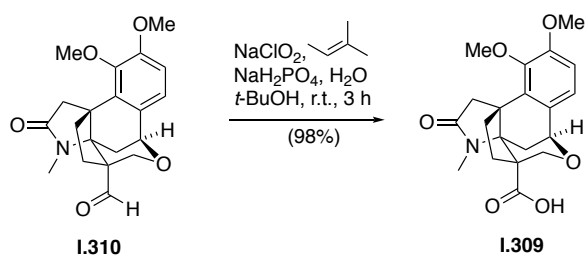
Entry	Conditions	Observation
1	DDQ (5.9 eq.), THF, 65°C, 1 h	traces of cyclic ether I.308
2	DDQ (8.7 eq.), THF/DMF (8:2), 65°C, 2 h	starting material I.300
3	DDQ (5.9 eq.), THF, 3 Å MS, rt, 14 h	decomposition
4	DDQ (5.9 eq.), THF, 3 Å MS, 65°C 4.5 h	decomposition
5	DDQ (5.9 eq.), O ₂ (1 bar), THF, 3 Å MS, rt, 1 h	decomposition
6	DDQ (10 eq.), AcOH (10 eq.), DCE, 3 Å MS, 75 °C, 5 h	cyclic ether I.308 (71%)

Having successfully differentiated the two alcohols, we next had to transform intermediate **I.308** into carboxylic acid **I.309**. At the beginning, conditions for the direct oxidation to the carboxylic acid **I.310** were tested (Table I.28). RuCl₃/NaIO₄ primarily gave aldehyde **I.310** after 1.5 h reaction time and acid **I.309** after 12 h, albeit in low yields (entries 1 and 2). Using tetrapropylammonium perruthenate (TPAP) and *N*-methylmorpholine-*N*-oxide monohydrate (NMO · H₂O), varying mixtures of aldehyde **I.310** and carboxylic acid **I.309** were observed after 1, 5 and 12 h (entries 3–5). Even when H₂O was added and the reaction heated to 40 °C, a mixture of aldehyde **I.309** and carboxylic acid **I.310** was obtained (entries 6 and 7). At this point, we decided to pursue a stepwise oxidation of the primary alcohol **I.308** and application of classic Ley–Griffith conditions, namely catalytic TPAP and NMO in DCM, which provided aldehyde **I.310** (entry 8).

Table I.28 Conditions tested for the oxidation of alcohol **I.308**.

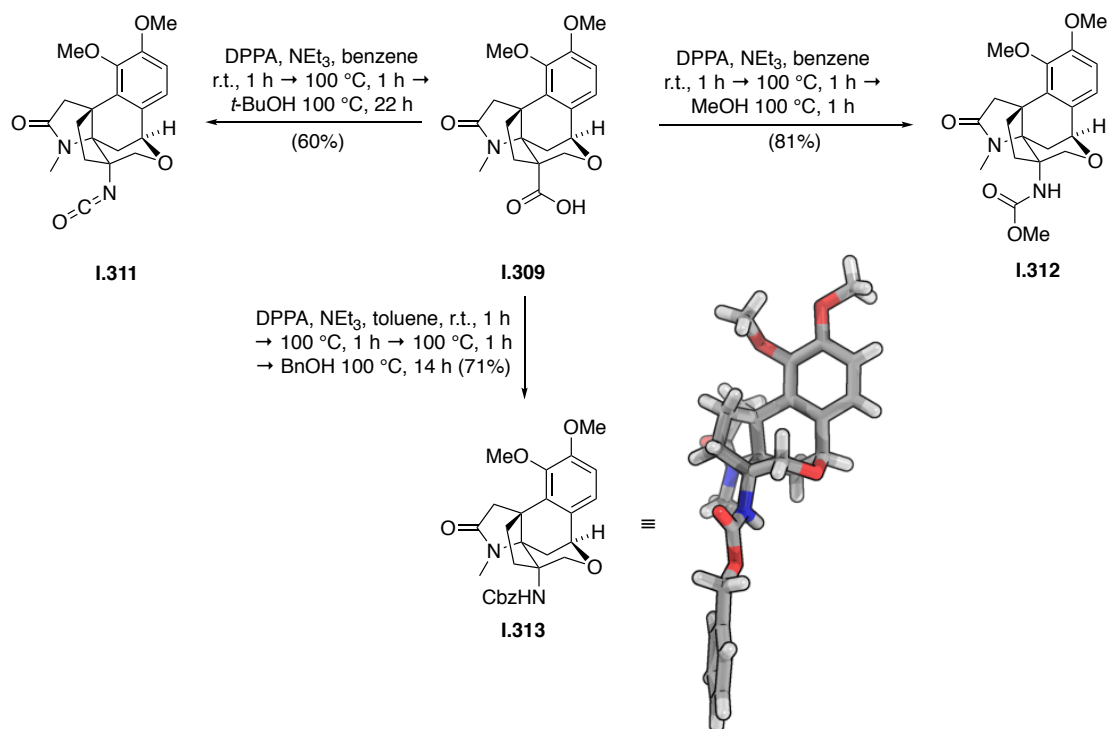
Entry	Conditions	Observation
1	RuCl ₃ , NaIO ₄ , MeCN:CCl ₄ :H ₂ O 2:2:3, r.t., 1.5 h	mainly I.310
2	RuCl ₃ , NaIO ₄ , MeCN:CCl ₄ :H ₂ O 2:2:3, r.t., 12 h	acid I.309 , low yields
3	TPAP, NMO · H ₂ O, MeCN, r.t., 1 h	aldehyde I.310 (traces)
4	TPAP, NMO · H ₂ O, MeCN, r.t., 5 h	mix of I.309 and I.310
5	TPAP, NMO · H ₂ O, MeCN, r.t., 12 h	mix of I.309 and I.310
6	TPAP, NMO · H ₂ O, MeCN/H ₂ O, r.t., 12 h	mix of I.309 and I.310
7	TPAP, NMO · H ₂ O, MeCN/H ₂ O, 40 °C, 12 h	mix of I.309 and I.310
8	TPAP, NMO, DCM, 4Å MS, r.t., 1 h	aldehyde I.310 (70%)

With aldehyde **I.310** in hand, we applied Pinnick–Lindgren conditions with 2-methyl-2-butene as scavenger for hypochlorous acid (HOCl). This transformation again occurred in near quantitative yield and provided carboxylic acid **I.309**, which could be used in the next step without chromatographic purification.

**Scheme I.72** Synthesis of acid **I.309**.

Next, we investigated the Curtius rearrangement for the installation of the second ATA starting from carboxylic acid **I.309** (Scheme I.73). As stated before, 1,2-sigmatropic rearrangements are arguably the most popular choice for the synthesis of primary ATAs in sterically demanding environments (see chapter 1.1.2.2). First, we used diphenylphosphoryl azide (DPPA) and triethylamine in benzene to form the carboxylic azide (for mechanism see Scheme I.16). The reaction was then heated to 100 °C to facilitate rearrangement to the isocyanate. *tert*-Butanol was

added with the intention to obtain the Boc-protected ATA, but only isocyanate **I.311** could be isolated.



Scheme I.73 Installation of the second ATA using a Curtius rearrangement. Cbz = carboxybenzyl.

We reasoned that *tert*-butanol is sterically too demanding for this substrate and therefore added methanol instead. This gave methyl carbamate **I.312** in 81% yield.^[129] Additionally, it was possible to obtain Cbz-protected amine **I.313** using BnOH. With both ATAs of stephadiamine (**I.1**) now installed, we turned our attention to the remaining δ -lactone (see chapter 3.4).

3.4 Installation of the lactone

With ATAs **I.312** and **I.313** in hand, our next goal in the synthesis of stephadiamine (**I.1**) was the installation of the δ -lactone, the final ring of the molecule. Starting from Cbz-protected amine **I.313**, we first envisaged to install the δ -lactone *via* a direct C–H oxidation. Although this transformation requires relatively harsh oxidative conditions, there are several precedents in the literature, *e.g.*, in Thomson's synthesis of maocrystal V (**I.314**),^[333] Zhang's synthesis of jiadifenolide (**I.315**),^[334] Wu's synthesis of artemisinin (**I.316**),^[335] Piva's synthesis of amphisterin B4 (**I.317**) (Figure I.10),^[336] Vanderwal's formal synthesis of 7,20-diisocyanoadociane^[337] and Senter's studies of ring systems similar to ophiobolins and ceroplastins (not shown).^[338]

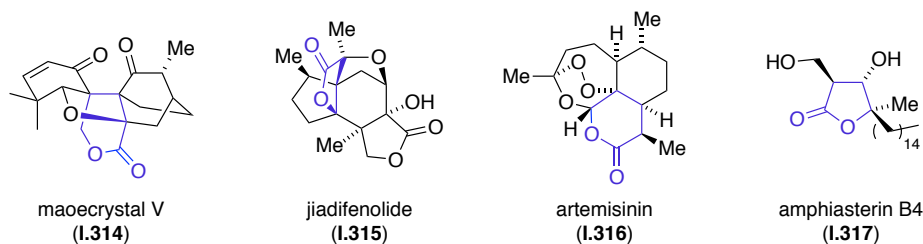
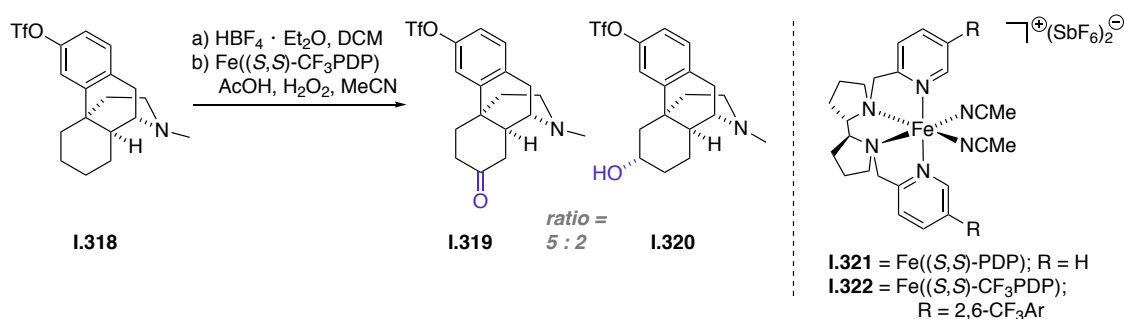


Figure I.10 Natural products with lactones installed *via* late-stage oxidation of a cyclic ether.

Most of these late-stage oxidations have been applied in terpenoid total synthesis and none of the natural products depicted contain either an (electron-rich) aromatic ring or a nitrogen atom. When surveying the literature, numerous reports concerning directed and undirected C–H oxidations can be found over the last few years. Again, however, the number of reports for molecules that contain an aromatic ring and/or nitrogen atoms is very limited. An example of a C–H oxidation of morphine derivative **I.318** in the presence of an electron-poor aromatic ring and a tertiary amine to the respective ketone **I.319** and alcohol **I.320** can be found in Christina White’s remote oxidation of aliphatic C–H Bonds using the White–Chen catalysts **I.321** or **I.322** (Scheme I.74). It comes as no surprise that in order to showcase her oxidative C–H activation methodology on alkaloid-like structures, she exchanged the “natural” methoxy group for a strongly electron-withdrawing triflate to reduce the electron density in the aromatic ring.^[339–340]

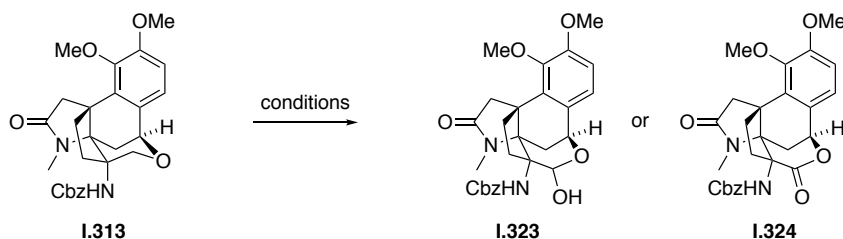


Scheme I.74 White’s C–H oxidation of nitrogen-containing molecules.

We started off with the most commonly employed set of oxidation conditions including ruthenium tetroxide (RuO₄), chromium trioxide (CrO₃) and potassium permanganate (KMnO₄) (Table I.29). With RuCl₃ in combination with NaIO₄ or KMnO₄ only decomposition of the starting material was observed (entries 1 and 2). By contrast, RuCl₃ with BAIB did not lead to any reaction (entry 3). Next, we investigated CrO₃ as an oxidant (entries 4–7). Jones oxidation led to a complex reaction mixture (entry 4), whereas when CrO₃ in combination with 2,4-dimethylpyrazole was used, only starting material was observed (entry 5). The same result was obtained using CrO₃ in combination with acetic acid at 50 °C (entry 6). However, if the temperature was raised to 75 °C, decomposition of the starting material was observed (entry 7). Next, we applied KMnO₄ in combination with

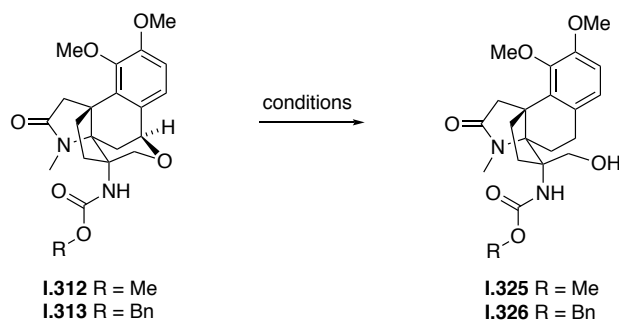
FeCl_3 and $\text{Cu}(\text{OTf})_2$,^[341] but in both cases only decomposition was observed (entries 8 and 9). Finally, we investigated the White–Chen catalyst, which has already seen applications in the oxidative C–H functionalization of alkaloids (entry 10).^[339, 342] Under these conditions, decomposition was observed – probably due to the electron rich nature of the aromatic core.

Table I.29 Conditions tested for the oxidation of cyclic ether **I.313** to lactol **I.323** or lactone **I.324**.



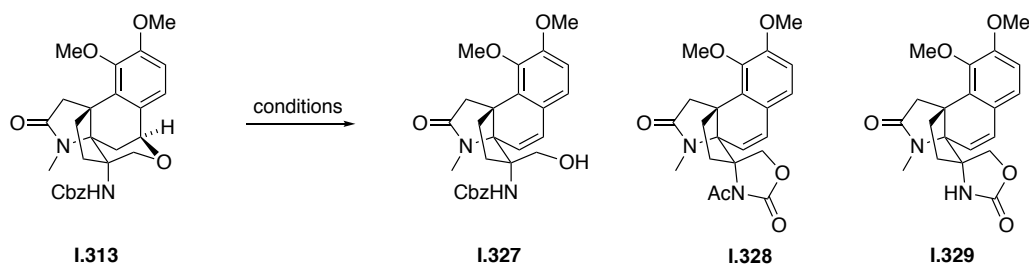
Entry	Conditions	Observation
1	RuCl_3 , NaIO_4 , MeCN, CCl_4 , H_2O	decomposition
2	RuCl_3 , KMnO_4 , MeCN, H_2O , 0 °C to r.t.	decomposition
3	RuCl_3 , $\text{PhI}(\text{OAc})_2$, MeCN, CCl_4 , H_2O , 0 °C to r.t.	starting material
4	Jones reagent, acetone, 0 °C to r.t.	complex mixture
5	CrO_3 , 2,4-dimethylpyrazole, DCM, 0 °C to r.t.	starting material
6	AcOH, CrO_3 , DCM, 50 °C, 12 h	starting material
7	AcOH, CrO_3 , DCE, 75 °C, 12 h	decomposition
8	KMnO_4 , FeCl_3 , acetone, 0 °C to r.t.	decomposition
9	KMnO_4 , $\text{Cu}(\text{OTf})_2$, acetone, 0 °C to r.t.	decomposition
10	White–Chen catalyst, AcOH, H_2O_2 , MeCN, r.t., 25 min	decomposition
11	DMDO, acetone, 0 °C to 20 °C	no reaction

As none of the conditions listed in Table I.29 led to a productive result, we stopped investigating the direct oxidation of the ether to the lactone and decided to cleave and oxidize the C–O bond followed by ring closure. The reductive opening of benzylic ethers is a relatively common transformation that can be achieved *via* hydrogenation or Lewis acid activation.^[343] Initially, we tested PtO_2 and Pd/C in combination with hydrogen (1 bar), but only deprotection of the amine was detected (Table I.30, entries 1 and 2). Then, we applied Et_3SiH in TFA/DCM,^[344–345] TFA and AcOH/DCM at room temperature, but in every case only starting material was recovered (entry 3–6). All three conditions were also investigated at elevated temperature (reaction was slowly warmed to 75 °C) without success.

Table I.30 Conditions tested for the hydrogenation of the benzylic C–O bond.

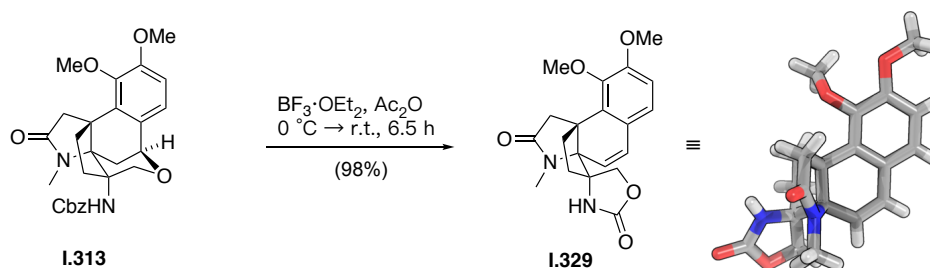
Entry	Starting material	Conditions	Observation
1	I.313	PtO ₂ , H ₂ , AcOH, r.t., 1.5 h	Cbz-deprotection of compound I.313
2	I.313	Pd/C, H ₂ , MeOH, r.t., 15 h	Cbz-deprotection of compound I.313
3	I.312	TFA, Et ₃ SiH, DCM, r.t., 12 h	no reaction
4	I.313	TFA, Et ₃ SiH, DCM, r.t., 12 h	no reaction
5	I.313	TFA, Et ₃ SiH, r.t., 12 h	no reaction
6	I.313	AcOH, Et ₃ SiH, 50 °C, 12 h	no reaction

As this approach proved unsuccessful, different conditions were investigated to enable the elimination of the benzyl ether to give alcohol **I.327** (Table I.31). Heating ether **I.313** under basic or acidic conditions was unproductive (entries 1 and 2), as well as attempted thermal elimination in DMF or toluene at temperatures up to 120 °C (entries 3 and 4). No reaction occurred either with TMSOTf, TBSOTf, TMSCl or BF₃ · OEt₂ from –78 °C to room temperature (entries 5–8). Given these results, we surmised that the elimination was a reversible process and therefore used BF₃ · OEt₂ in combination with either trifluoroacetic anhydride (TFAA, entry 9) or Ac₂O (entry 10) to trap the eliminated alkoxide **I.327**. And indeed, a mixture of elimination products oxazolidinone **I.328** and oxazolidinone **I.329** were obtained (entry 10). Attempts to optimize the formation of oxazolidinone **I.329** by utilizing different polar solvents, such as nitromethane, hexafluoroisopropanol (HFIP) and dioxane, were all met with either decomposition or re-isolation of starting material (entries 11–13).

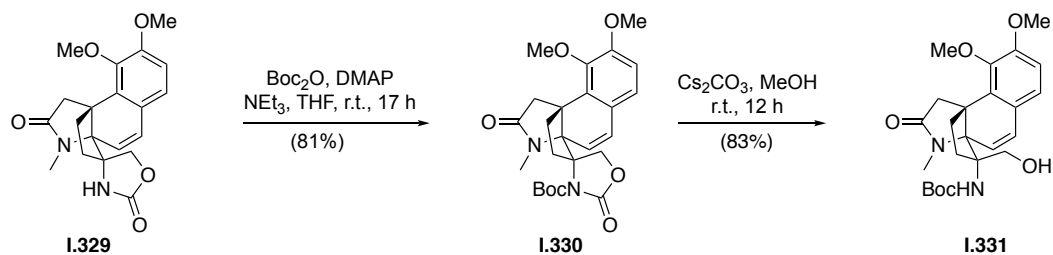
Table I.31 Conditions tested for the Lewis-acid assisted elimination of benzyl ether **I.313**.

Entry	Conditions	Observation
1	NaOH, MeOH, 85 °C, 12 h	no reaction
2	CSA, MeOH, 85 °C, 12 h	no reaction
3	DMF, 120 °C, 24 h	no reaction
4	toluene, 120 °C, 24 h	no reaction
5	TBSOTf ₂ , NEt ₃ , DCM, -78 °C to 20 °C	no reaction
6	TMSOTf ₂ , NEt ₃ , DCM, -78 °C to 20 °C	no reaction
7	TMSCl, NEt ₃ , DCM, -78 °C to 20 °C	no reaction
8	BF ₃ ·OEt ₂ , Et ₃ SiH, DCM, r.t., 12 h	no reaction
9	BF ₃ ·OEt ₂ , TFAA, r.t., 12 h	decomposition
10	BF ₃ ·OEt ₂ , Ac ₂ O, r.t., 24 h	mixture of I.328 and I.329
11	BF ₃ ·OEt ₂ , MeNO ₂ , r.t. to 50 °C, 12 h	no reaction
12	BF ₃ ·OEt ₂ , HFIP, 0 °C to r.t., 12 h	decomposition
13	BF ₃ ·OEt ₂ , dioxane, 0 °C to r.t., 12 h	decomposition

We therefore focused on the optimization of the reaction conditions used in entry 10. It was found that a 3:1 mixture of Ac₂O to BF₃·OEt₂ at 0 °C gave the cleanest conversion to oxazolidinone **I.329** (Scheme I.75). In some cases, acetylated oxazolidinone **I.328** was obtained as a side product. This, however, could be transformed into oxazolidinone **I.329** using In(OTf)₃ and methanol.

**Scheme I.75** Conversion of ether **I.313** to oxazolidinone **I.329** (opposite enantiomer depicted).

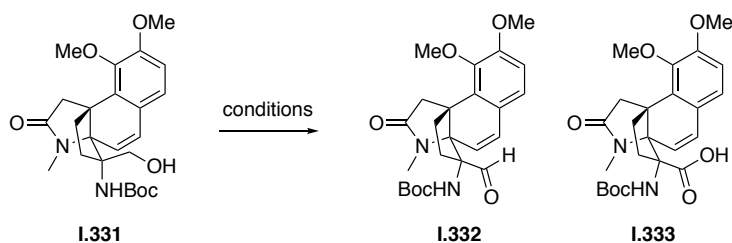
Oxazolidinone **I.329** was then Boc-protected to give compound **I.330** in 81% yield and then hydrolyzed using Cs₂CO₃ in methanol to give alcohol **I.331** in 83% yield (Scheme I.76).



Scheme I.76 Boc-protection and selective oxazolidinone hydrolysis.

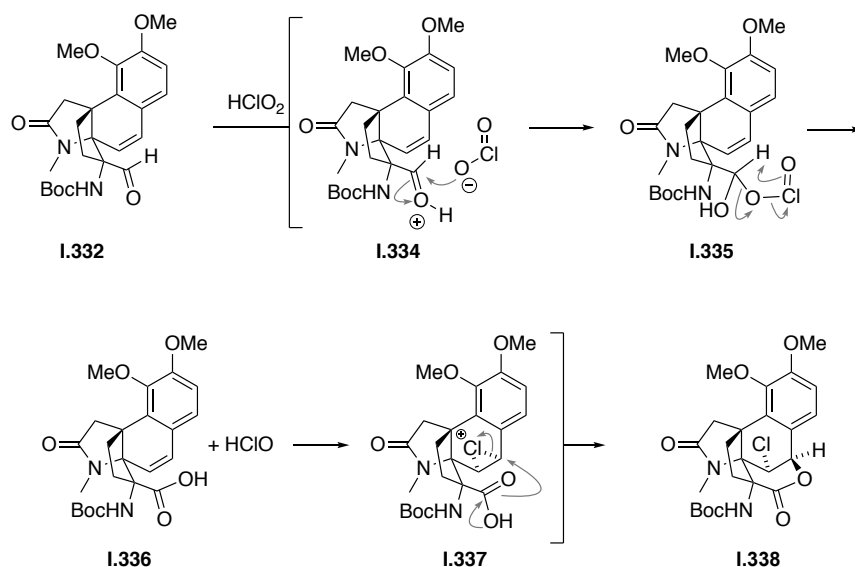
To install the lactone, we needed to oxidize aminoalcohol **I.331** to aldehyde **I.332** or carboxylic acid **I.333**. Direct oxidation to acid **I.333** was investigated first. Using classic Jones oxidation conditions, TEMPO/BAIB or Corey–Schmidt conditions decomposition was observed (Table I.32, entries 1–3). Using aqueous Ley–Griffith conditions, oxidation to aldehyde **I.332** was observed, along with significant decomposition of the material (entry 4). We therefore opted for a stepwise oxidation to the carboxylic acid **I.333** *via* aldehyde **I.332**. Swern oxidation led to a complex reaction mixture (entry 5), but Ley–Griffith oxidation gave clean conversion to the desired aldehyde in near quantitative yield with no chromatographic purification needed (entry 6).

Table I.32 Conditions tested for the oxidation of **I.331**.



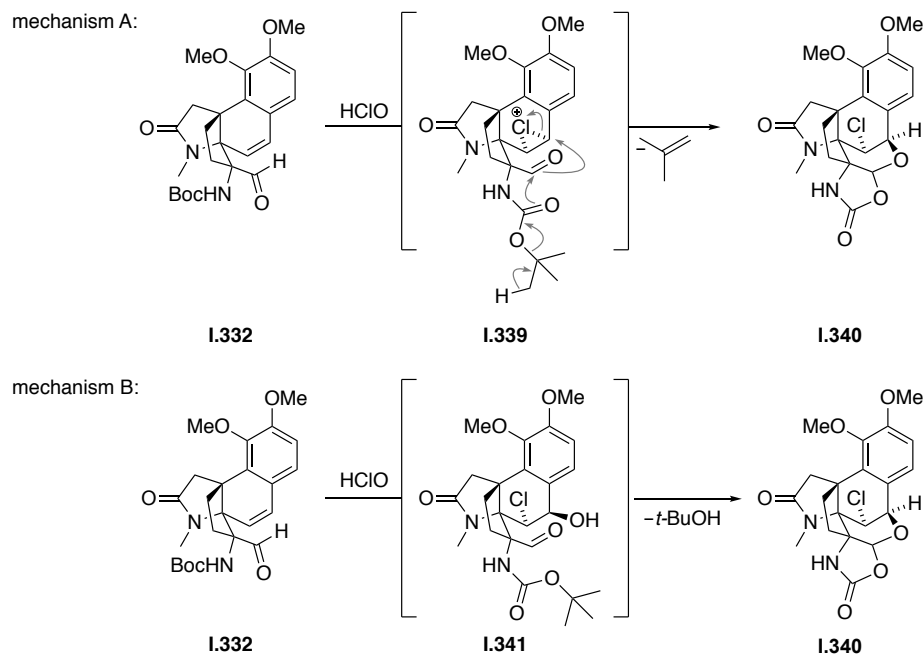
Entry	Oxidation type	Conditions ^{a)}	Expected Product	Observation
1	Jones	CrO ₃ , H ₂ SO ₄ , H ₂ O, acetone, 0 °C	I.333	decomposition
2	TEMPO/BAIB	TEMPO/BAIB, phosphate buffer pH = 6.3, MeCN/H ₂ O	I.333	decomposition
3	Corey–Schmidt	PDC, DMF, r.t.	I.333	decomposition
4	aq. Ley–Griffith	TPAP/NMO, H ₂ O/MeCN/CCl ₄	I.333	oxidation to I.332 , then slow decomposition
5	Swern	DMSO, (COCl) ₂ , Et ₃ N, DCM, -78 °C	I.332	complex mixture
6	Ley–Griffith	TPAP, NMO · H ₂ O, DCM, r.t., 1 h	I.332	clean product, 96%

For the oxidation of aldehyde **I.332** to carboxylic acid **I.333**, we first applied classic Pinnick–Lindgren conditions (Table I.33, entries 1–3). Using sodium chlorite with phosphate buffer in a mixture of *tert*-butanol/H₂O and 2-methyl-2-butene as scavenger, the formation of a side product was observed whose structure could unambiguously be assigned as **I.338** using HRMS and 2D NMR techniques. This same compound was found, when sodium chlorite with phosphate buffer in a mixture of *tert*-butanol/H₂O and hydrogen peroxide as scavenger was used. Reproducing this side reaction proved to be challenging and decomposition was often observed. From a mechanistic standpoint, we expected oxidation of the aldehyde to acid **I.336** would occur with concomitant formation of HOCl, which is usually trapped by the scavenger (Scheme I.77). However, due to the very electron rich nature of the styrene, HOCl reacted, forming chloronium ion **I.337**. This intermediate could then be trapped by the carboxylic acid to form chlorolactone **I.338**.



Scheme I.77 Hypothetical mechanism for the formation of chlorolactone **I.338**.

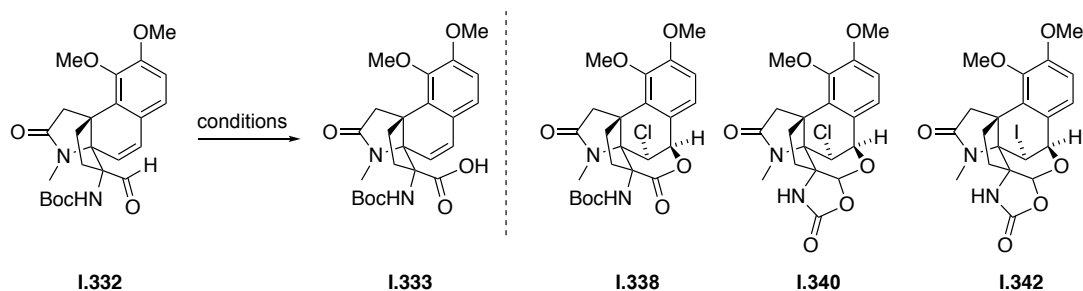
Following this mechanistic hypothesis, we next investigated an oxidation under Pinnick–Lindgren conditions without addition of external scavenger. Under these conditions, we observed traces of the desired chlorolactone **I.338**, but mainly another compound was formed, which was identified as oxazolidinone **I.340** by HRMS and 2D NMR (entry 3). Under these conditions, the formation of chloronium ion **I.339** appears to be faster than the oxidation to acid **I.336**. Intermediate **I.339** is presumably trapped by the aldehyde, which is in turn trapped by the Boc-group to form oxazolidinone **I.340** (mechanism A, Scheme I.78). In an alternative mechanism, a chlorohydrin could be formed directly from styrene **I.332** and the resulting hydroxyl group of **I.341** could add to the aldehyde, which in turn would form oxazolidinone **I.340** following extrusion of *tert*-butanol (mechanism B, Scheme I.78).



Scheme I.78 Possible mechanism for formation of oxazolidinone **I.340**.

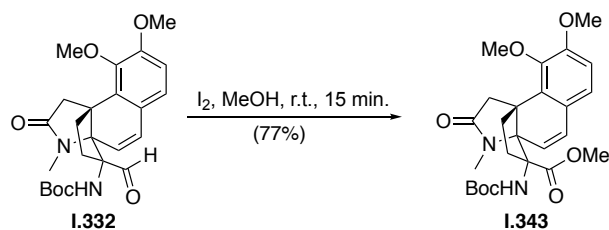
To investigate reactivity further, we subjected aldehyde **I.332** to iodine and potassium hydroxide (KOH) in acetonitrile and H₂O (Table I.33, entry 4). As expected, oxazolidinone **I.342** was formed and, again, the reaction could proceed either *via* mechanism A or B. We then applied less basic conditions by using potassium carbonate in a mixture of *tert*-butanol and H₂O and this time no reaction was observed (entry 5). In the last experiment in this series, we subjected aldehyde **I.332** to iodine in dry acetonitrile and stirred the reaction mixture in the dark at room temperature (entry 6). Although no H₂O or base was added, the reaction went to completion within 24 h and oxazolidinone **I.342** was isolated in 91% yield. This reaction strongly supports that, at least for the iodine-mediated reactions, the mechanism occurs most likely *via* mechanism A. Although these studies gave us valuable insight into the reactivity of styrene **I.332**, oxazolidinone **I.342** did not prove to be a viable intermediate for the synthesis of stephadiamine (**I.1**).

Therefore, we applied a few additional oxidation conditions in attempt to obtain carboxylic acid **I.336**. Pyridinium chlorochromate (PCC) in DMF only led to decomposition of the starting material (entry 7). When Bobbitt's salt [4-(cetylamino)-2,2,6,6-tetramethyl-1-oxo-piperidinium tetrafluoroborate] was used in stoichiometric quantities, complete decomposition of the starting material was observed (entry 8), whereas with catalytic 2-azaadamantane-*N*-oxyl (AZADO) or 1-methyl-2-azaadamantane-*N*-oxyl (Me-AZADO), each with sodium chlorite as the terminal oxidant, no reaction occurred and starting material was reisolated (entries 9 and 10). Silver(II) oxide (Ag₂O) and aqueous NaOH also proved to be ineffective (entry 11).

Table I.33 Oxidation of aldehyde **I.332**.

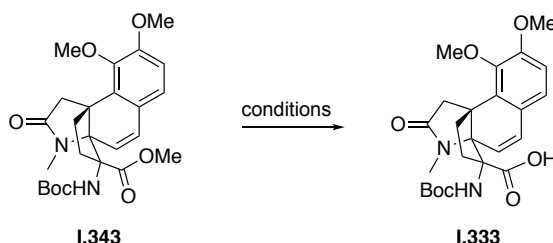
Entry	Conditions ^{a)}	Observation
1	NaClO ₂ , NaH ₂ PO ₄ , 2-methyl-2-butene, <i>t</i> -BuOH, H ₂ O	traces of I.338
2	NaClO ₂ , NaH ₂ PO ₄ , H ₂ O ₂ , <i>t</i> -BuOH, H ₂ O	traces of I.338
3	NaClO ₂ , NaH ₂ PO ₄ , <i>t</i> -BuOH, H ₂ O	I.340 and traces of I.338
4	I ₂ , KOH, MeCN/H ₂ O	I.342
5	I ₂ , K ₂ CO ₃ , H ₂ O, <i>t</i> -BuOH, r.t., 24 h	no reaction
6	I ₂ , MeCN, r.t., 24 h	I.342 (91%)
7	PCC, DMF, r.t., 15 h	decomposition
8	Bobbitt's salt [4-(acetylamino)-2,2,6,6-tetramethyl-1-oxo-piperidinium tetrafluoroborate]	decomposition
9	AZADO, DCM, NaOAc buffer, NaClO ₂ , 15 h	no reaction
10	Me-AZADO, DCM, NaOAc buffer, NaClO ₂ , 15 h	no reaction
11	Ag ₂ O, NaOH, H ₂ O, r.t., 4 h	no reaction

As oxidation of **I.332** to carboxylic acid **I.333** was not possible without ring closure, we opted for an intermediate containing a less electrophilic carbonyl carbon, namely methyl ester **I.343**. Ester **I.343** was easily obtained from aldehyde **I.332** with ten equivalents of iodine in methanol in the dark.^[49, 346] This transformation was clean and starting material was consumed within 15 min at room temperature.

**Scheme I.79** Oxidation to the methyl ester **I.343**.

The ester could not be hydrolyzed under standard conditions, such as sodium hydroxide in aqueous methanol (entry 1, Table I.34). The same lack of reactivity was observed with TMSOK in THF, LiOH in aqueous THF or LiI in pyridine at elevated temperatures (entries 2–4).

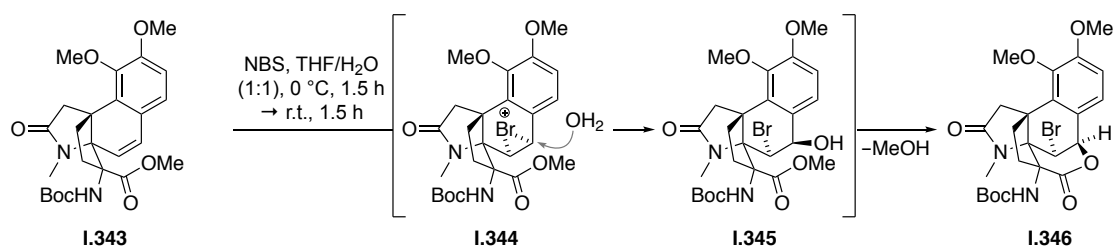
Table I.34 Conditions tested for the hydrolysis of ester **I.343**.



Entry	Conditions ^{a)}	Observation
1	NaOH, MeOH, H ₂ O, 80 °C, 12 h	no reaction
2	TMSOK, THF, 50 °C, 12 h	no reaction
3	LiOH, THF, H ₂ O, r.t. to 50 °C, 15 h	no reaction
4	LiI, pyridine, 130 °C, 2 h	no reaction

As these attempts proved to be ineffective, we next tried to close the lactone directly starting from ester **I.343** (Table I.35). Using triflic acid in deuterated chloroform, a complex reaction mixture was obtained that contained at least three different unidentifiable compounds by ¹H NMR (entry 1). Using *p*-toluenesulfonic acid (*p*-TSA) at elevated temperatures failed to convert any of the starting material (entry 2).

Inspired by our previous results, iodolactonization of ester **I.343** was investigated. This type of reaction is relatively rare, but a few examples and studies have been published over the years. First, we applied standard conditions using iodine in acetonitrile and H₂O at 0 °C with warming, but to no avail (entry 3). Iodine in acetonitrile at room temperature, led only to deprotected starting material **I.349** (entry 4).

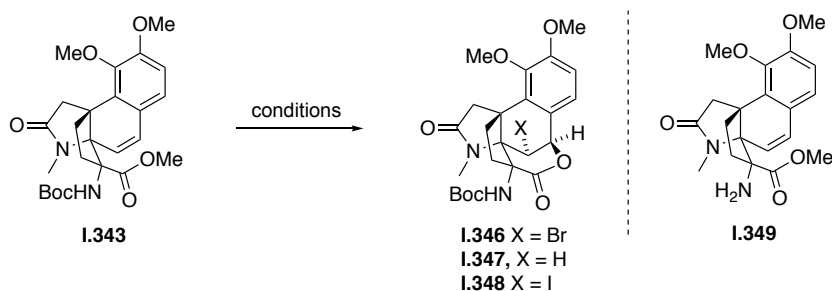


Scheme I.80 Proposed mechanism for the formation of bromolactone **I.346**.

Then, we attempted to close the lactone using a related approach *via* the intermediacy of a halohydrin.^[347] Bromohydrin formation should occur stereoselectively due to facial blocking of the ester of **I.343**. We reasoned that bromonium ion **I.344** could be opened by H₂O from the β -face and that resultant alcohol **I.345** could then directly form δ -lactone **I.346**.

To test this hypothesis, we reacted compound **I.346** with NBS in a mixture of THF and H₂O in the dark (entry 5). After 1.5 hours at this temperature and another 1.5 h at room temperature, starting material had disappeared, and we observed two new compounds by ¹H NMR, one of which showed key signals that were analogous to chlorolactone **I.338**. HRMS (ESI) indicated the formation of bromohydrin **I.345** and bromolactone **I.346**. After stirring this mixture in methanol for 30 min at room temperature, **I.345** was converted into bromolactone **I.346**, suggesting that **I.345** is an intermediate in the formation of **I.346**. This, however, does not exclude the possibility of a direct lactonization of methyl ester **I.343**. Using the same conditions but with *N*-iodosuccinimide (NIS) in place of NBS, no reaction occurred, and starting material was recovered (entry 6).

Table I.35 Conditions tested for the cyclization of ester **I.343** to lactone **I.346**, **I.347** or **I.348**.



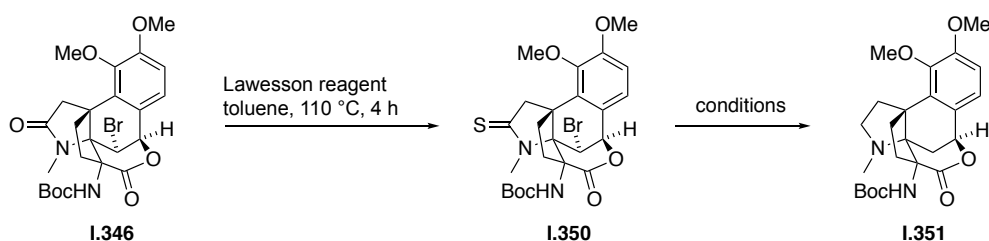
Entry	Conditions ^{a)}	Observation
1	TfOH, CDCl ₃	complex mixture
2	<i>p</i> -TSA, DCE, 50 °C to 80 °C, 24 h	no reaction
3	I ₂ , MeCN, H ₂ O, 0 °C to r.t.	no reaction
4	I ₂ , MeCN, 0 °C to r.t.	formation of I.349 by HRMS
5	NBS, THF:H ₂ O (1:1) <i>then</i> MeOH	I.346 (82%)
6	NIS, THF:H ₂ O (1:1)	no reaction

In summary, the synthesis of the δ -lactone proved to be highly challenging, but bromolactone **I.349** was installed in six steps starting from Curtius product **I.313**.

3.5 Completion of the synthesis

With bromolactone **I.346** in hand, the remaining steps in the synthesis of stephadiamine **I.1** were the reduction of the lactam to a tertiary amine, removal of the secondary bromide and Boc-deprotection. In order to reduce the lactam and the secondary bromide in a single step, we transformed lactam **I.346** into thionolactam **I.350**.^{†††} Then, two Nickel-based reductions were applied: Raney-nickel and nickel(II)chloride/sodium borohydride (Table I.36). Unfortunately, no product could be isolated in both cases, although the mass of the desired amine **I.251** was present by HRMS (ESI). We reasoned that nickel might be strongly coordinated to the 1,2-*cis*-diamine, and thus investigated different work-up protocols. Caddick described for his reduction of nitriles using nickel(II)chloride/sodium borohydride that the introduction of complexing amines during work-up significantly improved the isolation of their Boc protected amine.^[348] We attempted to address this by filtration of the reaction through celite and work-up with ethylenediaminetetraacetic acid (EDTA), however, no product was isolated.

Table I.36 Conditions tested for the reduction on **I.346**.



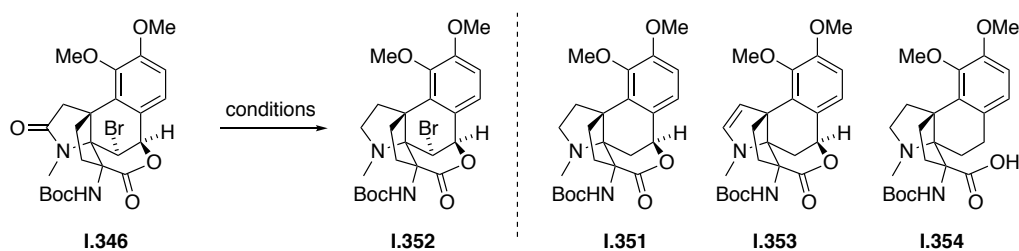
Entry	Conditions	Observation
1	Raney-Nickel, H ₂ , MeOH, r.t., 4 h	decomposition, HRMS indicates presence of I.351
2	NiCl ₂ · 6 H ₂ O, NaBH ₄ , MeOH, 0 °C, 30 min.	decomposition, HRMS indicates presence of I.351

As reduction of the thionolactam did not give us any productive results, we investigated the direct reduction of the lactam to the tertiary amine in the presence of the lactone. The most common method to reduce lactams to tertiary amines is reduction with LiAlH₄, however due to the presence of a lactone and a Boc-group, a different method for chemoselective reduction had to be applied. In most cases, boranes are used for the chemoselective reduction of lactams in the presence of lactones, esters and ketones.^[349–351] We therefore first investigated the use of borane dimethyl sulfide (BH₃ · Me₂S) for the reduction of lactam **I.346**. Using three equivalents of BH₃ · Me₂S in THF at room temperature, clean starting material was recovered (Table I.37, entry 1). When ten equivalents were used, we observed a complex reaction mixture by ¹H NMR and HRMS (ESI), indicating overreduction to amino acid derivative **I.354** (entry 2).

^{†††} Thionolactam **I.350** could not be obtained as a clean compound. Structure was tentatively assigned by ¹H NMR, 2D NMR and HRMS-ESI.

Following this, we attempted the use of Vaska's complex $[\text{Ir}(\text{CO})(\text{PPh}_3)_2\text{Cl}]$, which was recently used by Chida in his synthesis of neostenine^[352] and Dixon's construction of the strychnine core.^[353] In both cases, the chemoselective reduction of the lactam in presence of lactones, esters and ketones was achieved with high selectivities in excellent yield. First, we followed Chida's procedure using $\text{Ir}(\text{CO})(\text{PPh}_3)_2\text{Cl}$, 1,1,3,3-tetramethyldisiloxane (TMDS) in DCM at room temperature.^[352] In principle, after reduction to the hemiaminal, the amine should condense to the iminium ion under acidic conditions and be further reduced *in situ*. Following this procedure, we observed the formation of two new compounds. By HRMS (ESI) these compounds were identified as a mixture of lactam **I.351** and enamine **I.353**. To our surprise, the secondary bromide was reduced during this process. Due to the presence of enamine **I.353**, reasoned that an additional reductant might be needed and thus we attempted Dixon's procedure.^[353] First, the enamine was formed under the same conditions and then methanol followed by NaCNBH_3 and acetic acid was added. After stirring the reaction mixture for 12 h, decomposition of the starting material was observed.

Table I.37 Conditions tested for the reduction of lactam **I.349**.

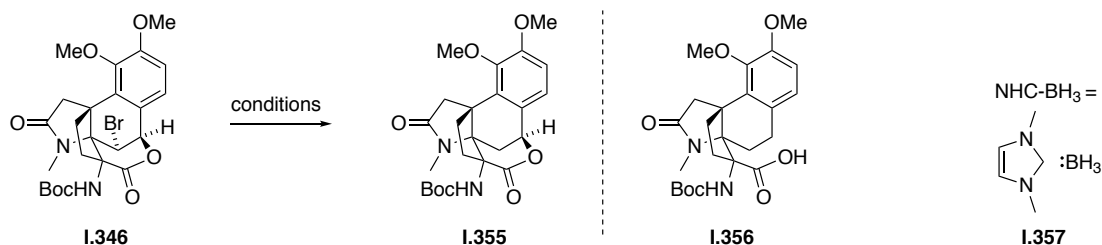


Entry	Conditions	Observation
1	$\text{BH}_3 \cdot \text{Me}_2\text{S}$ (3 eq.), THF, r.t., 24 h	no reaction
2	$\text{BH}_3 \cdot \text{Me}_2\text{S}$ (10 eq.), THF, r.t., 24 h	decomposition, HRMS indicates formation of I.354
3	$\text{Ir}(\text{CO})(\text{PPh}_3)_2\text{Cl}$ (20mol%), TMDS (10 eq), DCM, r.t., 1.5 h \rightarrow TFA, 2 h	I.351 and I.353 , as indicated by HRMS
4	$\text{Ir}(\text{CO})(\text{PPh}_3)_2\text{Cl}_2$ (20mol%), TMDS (10 eq), DCM, r.t., 1 h \rightarrow MeOH, NaBH_3CN , AcOH, 12 h	decomposition

After these initial results, we suspected that the secondary bromide might be causing unwanted side reactions. We therefore decided to first focus on the selective reduction of the secondary bromide (Table I.38). Reductive debromination using Raney-Nickel in methanol under a hydrogen atmosphere led to decomposition of the material (entry 1).^[354] By applying Pd/C in ethyl acetate under H_2 atmosphere, we reisolated starting material (entry 2). Changing the solvent composition from 9:1 ethyl acetate/MeOH to pure methanol resulted in either clean recovery of starting material (10% methanol) or a mixture of two reduction products (100% MeOH) (entries 3 and 4). HRMS indicated the formation of the desired debrominated compound **I.355** and hydrogenolysis

product, acid **I.356**. As all test reactions were carried out on a 1 mg scale, we decided that the reactivity of Pd/C and hydrogen at this scale was not easily controllable, and turned our attention to radical debrominations.

Table I.38 Conditions tested for the dehalogenation of bromolactone **I.349**.



Entry	Conditions	Observation
1	Ra-Ni, H ₂ , MeOH, r.t., 4 h	decomposition
2	Pd/C, H ₂ , EtOAc, r.t., 15 h	no reaction
3	Pd/C, H ₂ , 9:1 EtOAc:MeOH, r.t., 15 h	no reaction
4	Pd/C, H ₂ , MeOH, r.t., 15 h	I.355 and I.356
5 ^{b)}	[Ir(ppy) ₂ (dtbbpy)]PF ₆ , DIPEA, MeCN, CFL, 60 °C, 24 h	inconclusive
6 ^{b)}	Bu ₃ SnH (3 eq), ACHN, toluene, 110 °C, 24 h	no reaction
7 ^{b)}	Bu ₃ SnH (10 eq), AIBN, benzene, 90 °C, 3 h	clean formation of I.355
8 ^{a)b)}	NHC-BH ₃ (10 eq), ACHN, benzene, 90 °C, 3 h	I.355 and side product

a) NHC-BH was prepared by Antonio Rizzo (AK Trauner)

b) Reaction mixture was degassed in three freeze-pump-thaw cycles prior to heating

Using photoredox catalysis (entry 5),^[355] compound **I.346**, [Ir(ppy)₂(dtbbpy)]PF₆ and excess DIPEA in deuterated acetonitrile were heated to 60 °C and illuminated using a compact fluorescence bulb (CFL). After 24 h, all starting material was consumed. A single product was visible by NMR, however the chemical shift of the aromatic and benzylic signals were not consistent with **I.355**, despite confirmation of its mass (HRMS-ESI). Next, we investigated classic radical debromination conditions. With one equivalent tributyltinhydride (Bu₃SnH) and the radical initiator ACHN in toluene at 110 °C, no reaction occurred and starting material was recovered (entry 6).^[356] Using excess Bu₃SnH and azobis(isobutyronitrile) (AIBN) in benzene, we observed full consumption of starting material after 3 h at 90 °C (entry 7). similar observation was made when ten equivalents of 1,3-dimethylimidazol-2-ylidene borane (NHC-BH₃, **I.357**),^[354] was used in combination with AIBN in benzene. Although the reaction using NHC-BH₃ **I.357** is less toxic, we decided to continue exploring the reaction with tributyltinhydride, because the reaction was much cleaner by NMR analysis. Column chromatography using 1:9 K₂CO₃/SiO₂ as stationary phase proved efficient for the removal of tin byproducts and cleanly provided debrominated lactone **I.355**.^[357] The structure of **I.355** was unambiguously confirmed by X-ray crystallography.

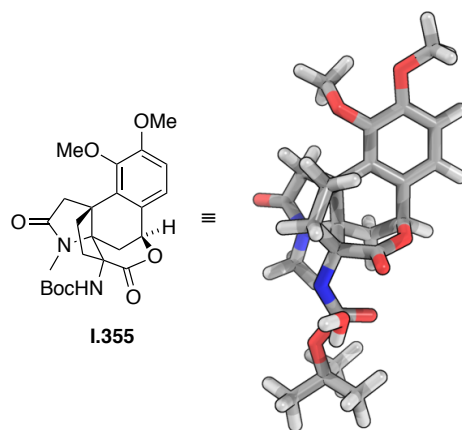
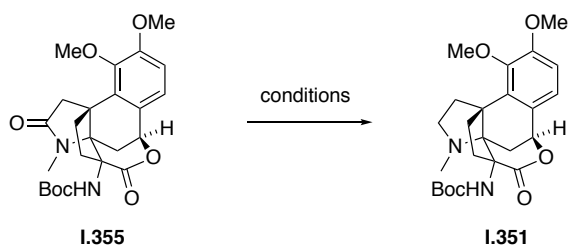


Figure I.11 Crystal structure of lactone **I.355**.

Next, we reinvestigated conditions for the reduction of the *N*-methyl lactam present in **I.355** (Table I.39). Although Ir(CO)(PPh₃)₂Cl appeared promising in experiments with bromolactone **I.346**, no reaction was observed to occur on this debrominated congener (entry 1). Using ten equivalents of BH₃ · Me₂S in THF at room temperature, however, we obtained a ratio ca. 2:1 ratio of starting material **I.355** to desired tertiary ATA **I.351** (entry 2). At elevated temperatures with BH₃ · Me₂S, decomposition of the starting material was observed (entry 3). To our surprise, increasing the loading of BH₃ · Me₂S did not improve conversion of starting lactam (entries 4 and 5). Finally, when BH₃ · Me₂S was used as a co-solvent with THF as a 1:1 solution, decomposition of the starting material was observed (entry 6).^{##}

Table I.39 Conditions tested for the reduction of lactam **I.351**.

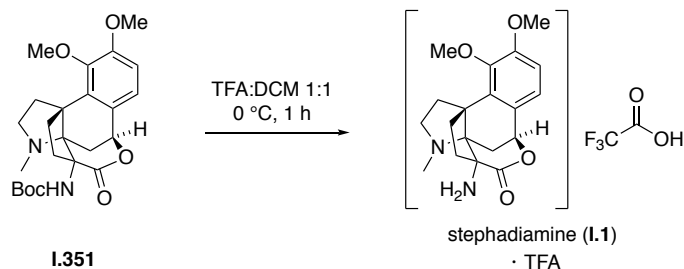


Entry	Conditions	Observation ^{a)}
1	Ir(CO)(PPh ₃) ₂ Cl (20 mol%), TMDS (10 eq.), DCM, r.t., 1.5 h → TFA, 2 h	no reaction
2	BH ₃ · Me ₂ S (10 eq.), THF, r.t., 24 h	68% I.355 : 32% I.351
3	BH ₃ · Me ₂ S (10 eq.), THF, 50 °C., 24 h	decomposition
4	BH ₃ · Me ₂ S (20 eq.), THF, r.t., 24 h	62% I.355 : 38% I.351
5	BH ₃ · Me ₂ S (50 eq.), THF, r.t., 24 h	61% I.355 : 29% I.351
6	1:1 BH ₃ · Me ₂ S/THF, r.t., 24 h	decomposition

a) Ratio of **I.355** to **I.351** was determined by the ratio of the *N*-Me groups in the ¹H NMR spectrum.

^{##} Tertiary amine **I.351** could not be obtained as a clean compound. Structure was tentatively assigned by ¹H NMR and and HRMS-ESI.

With trace quantities of lactone **I.351** in hand, we investigated the final step of the synthesis: Boc-deprotection of the primary ATA. Using a mixture of TFA and DCM at 0 °C, we obtained the TFA salt of stephadiamine (**I.1**), as substantiated by HRMS-ESI (calc: C₁₉H₂₄O₄N₂⁺ : 345.1809 [M+H]⁺; found 345.1811 [M+H]⁺).



Scheme I.81 Final Boc-deprotection to stephadiamine.

The ¹H NMR (CD₃OD) of stephadiamine (**I.1**) · TFA is depicted in Figure I.12. Isolation of stephadiamine (**I.1**) as its free base is currently under investigation.

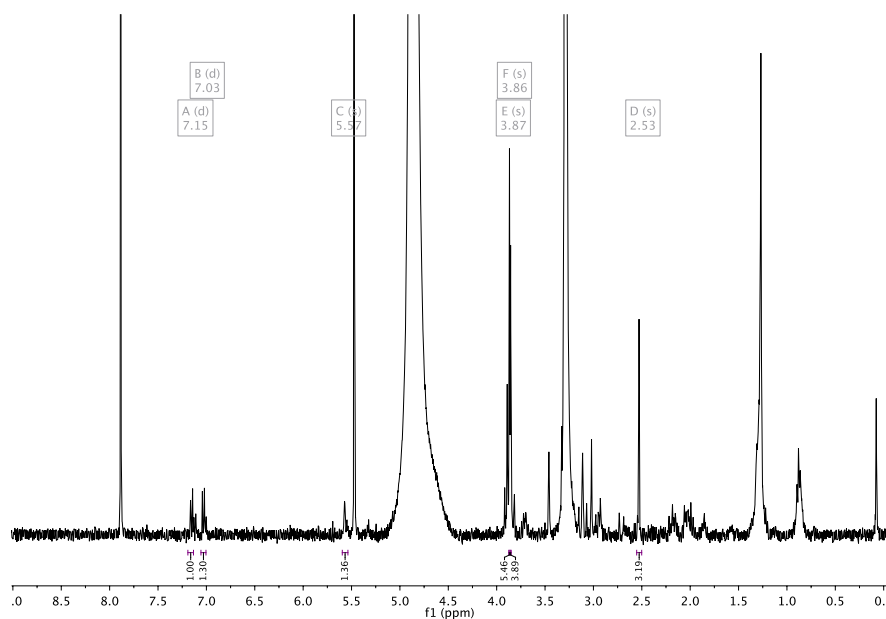
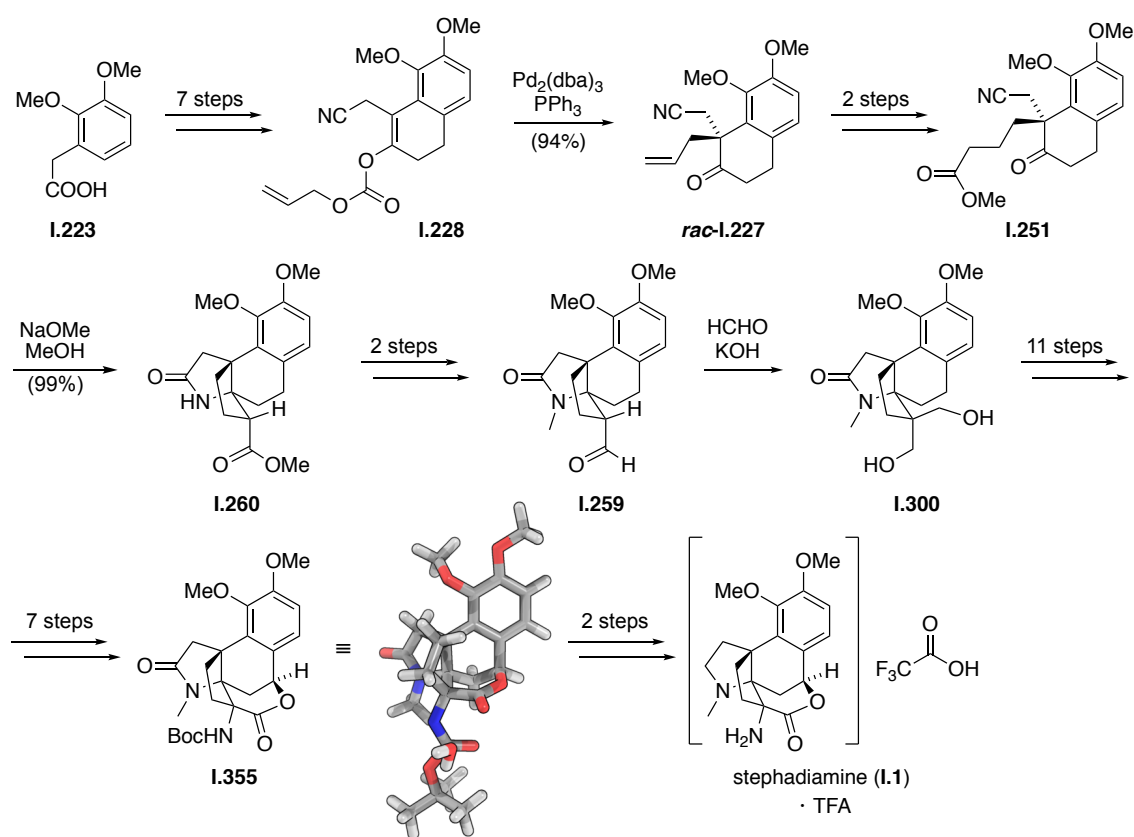


Figure I.12 ¹H NMR of stephadiamine (TFA salt) in CD₃OD. Signals found for stephadiamine (as TFA salt) ¹H NMR (400 MHz, Methanol-d₄) δ = 7.15 (d, J = 8.4 Hz, 1H, Ar-H), 7.03 (d, J = 8.2 Hz, 1H, Ar-H), 5.57 (s, 1H, benzylic H), 3.87 (s, 5H, OMe), 3.86 (s, 4H, OMe), 2.53 (s, 3H, NMe) ppm. Reported signals for stephadiamine (free base): ¹H NMR (CDCl₃) δ = 7.00 (d, J = 8.0 Hz, 1 H, Ar-H), 6.80 (d, J = 8.0 Hz, Ar-H), 5.39 (dd, J = 4.3, 2.0 Hz, 1H, benzylic H), 3.87 (6 H, OMe), 2.54 (s, 3H, N-Me) ppm.

4 Summary and outlook

In summary, progress toward the total synthesis of the hasubanan alkaloid stephadiamine (**I.1**) has been detailed in this thesis. Enol carbonate **I.228** was synthesized in seven steps starting from 2,3-dimethoxyphenylacetic acid (**I.223**) following a literature procedure that we optimized (Scheme I.82). It is worthy to note that this sequence commenced with a carboxylate-directed Fujiwara–Moritani reaction carried out on 10 g scale in near-quantitative yields. Enol carbonate **I.228** served as a substrate for a racemic Tsuji allylation, which set the quaternary position in **I.227** in excellent yield.

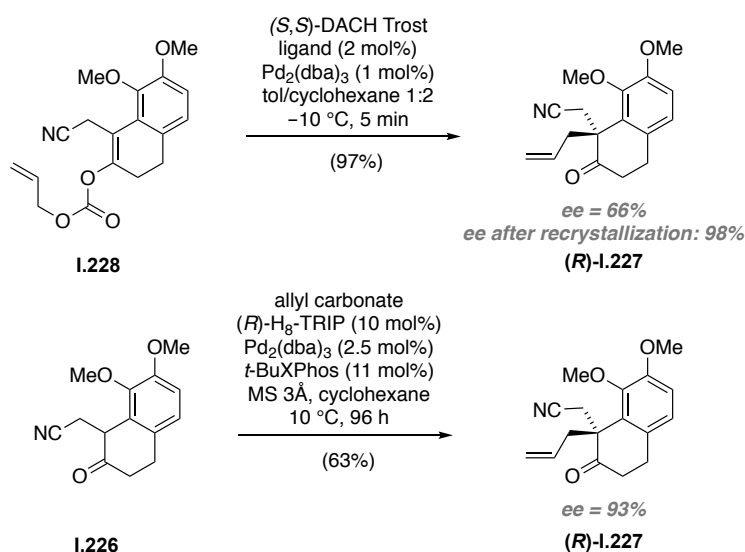


Scheme I.82 Synthesis of stephadiamine (**I.1**) · TFA.

A new cascade reaction was developed to assemble the complex pentacyclic core of (+)-stephadiamine (**I.1**), constructing two five-membered rings and two stereocenters (including one ATA) in a single step (**I.251**→**I.260**). In this high-yielding transformation, the benzylic quaternary stereocenter directed the formation of all other stereocenters of the natural product. Establishment of the third contiguous fully substituted carbon proved highly challenging. Ultimately, a Tollens reaction (crossed Cannizzaro reaction, **I.259**→**I.300**) was used to install a quaternary stereocenter that was later converted to the second ATA of stephadiamine *via* Curtius reaction. In eleven additional steps, ether **I.313** was transformed into lactone **I.355**, whose structure was

unambiguously confirmed by X-ray crystallography. Lactone **I.358** was chemoselectively reduced to the corresponding tertiary ATA and further converted to the TFA salt of stephadiamine (**I.1**). Overall, racemic stephadiamine (**I.1**) • TFA was prepared in 27 steps from commercially available acid **I.223** and isolation of the free base of stephadiamine (**I.1**) is currently under investigation.

With an established route toward the natural product in hand, we sought to render the decarboxylative Tsuji-allylation asymmetric to access (+)-stephadiamine (**I.1**) (Scheme I.83). Although the racemic reaction proceeded in near quantitative yield, this substrate represents a significant challenge for asymmetric Pd-catalyzed allylation reactions.



Scheme I.83 Decarboxylative Tsuji allylations.

We opted to address this challenge and expand the scope of this transformation in collaboration with Prof. Brian M. Stoltz of the California Institute of Technology. After intensive optimization, we obtained allylcyclohexanone **(R)-I.227** with 66% ee and 97% yield. Subsequent recrystallization of enantioenriched material increased the optical purity to 98% ee . Separation of the enantiomers using chiral HPLC allowed for the confirmation of absolute stereochemistry by X-ray analysis. In collaboration with the group of Prof. Benjamin List of Max-Planck-Institute in Mülheim an der Ruhr, we were able to further improve the ee of the reaction by applying their recently reported Pd-catalyzed allylation chemistry using (R) - H_8 -TRIP as chiral ligand.

Future experiments include optimization of the reduction of lactam **I.358** to tertiary amine **I.354** and the development of a protocol to access the free base of stephadiamine (**I.1**). Following these optimizations, the reaction sequence could be carried out with **(R)-I.227** for an asymmetric synthesis of (+)-stephadiamine (**I.1**). The enantiopure material could then be used to investigate the biological activity of this unique norhasubanan alkaloid. In addition, tetralone **I.227** is a common

structural motif in morphinan and hasubanan alkaloids. Ultimately, the developed approach to access either enantiopure (*R*)- or (*S*)-**I.227** could therefore be used in the asymmetric synthesis of related natural products or related drug derivatives.

CHAPTER II

SYNTHESIS OF PHOTOCROMIC GALACTOCEREBROSIDES

5 Introduction

5.1 Sphingolipids, ceramides and cerebroside

5.1.1 General classification and biological relevance

Sphingolipids play an important role in membrane biology as well as signaling and regulation within cells. They are a structurally diverse class of lipids, which are defined by their amino-alcohol backbone that consists of eighteen carbons.^[358] These lipids are most often synthesized in the endoplasmic reticulum (ER) from cytosolic serine and palmitoyl coenzyme A (CoA) and are then further derivatized. Their simplest members, sphingosine (**II.1**) phytosphingosine (**II.2**) and dihydrosphingosine (**II.3**) serve as templates upon which more complexity is generated by derivatization of their alcohol and amine moieties (Figure II.1). Acylation of these backbones with structurally diverse acyl-CoA molecules through the action of distinct ceramide synthases generates molecules defined as ceramide (**II.4**), phytoceramide (**II.5**), or dihydroceramide (**II.6**), respectively.

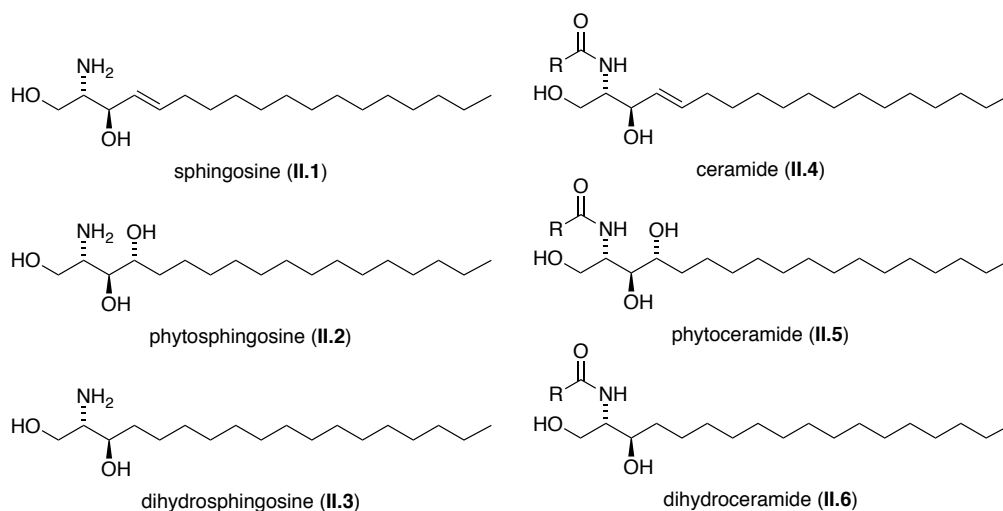


Figure II.1 Structures of sphingosines and ceramides.

In addition, glycosylation of the ceramide with one or more sugar residues produces the large class of glycosphingolipids (GSL), which differ in the type of sphingosine, the sugar moiety and the acyl chain composition. So far, more than 300 different oligosaccharide chains and more than 60 different sphingoid bases have been characterized, creating thousands of different GSL structures.^[359] These microdomains, also called lipid rafts, are composed of specific lipid species and are thought to be a way that cells organize proteins within the plane of the membrane. GSLs can form hydrogen-bond/hydrophobic interactions with sphingomyelin and cholesterol (Chol), which can be observed as segregated microdomains in supported membrane systems.

A subclass of GSLs are the cerebrosides, which are glycosylated with glucose or galactose at the anomeric position.^[360] The glucosphingolipids are generated from the enzyme glucosylceramide synthase (GCS), whereas galactosphingolipids are produced by the evolutionarily dissimilar enzyme galactosylceramide synthase (GalCerS).^[358] Biologically, cerebrosides in cellular membranes can act as surface antigens, and they play an important role in cell signaling, agglutination, communication and development.

However, many details in cerebroside function and signaling are not fully elucidated and “understanding the function of all the existing glycosphingolipids and sphingomyelin species will be a major undertaking in the future since the tools to study and measure these species are only beginning to be developed.”^[358] Such a method to elucidate and manipulate lipid signaling with the spatiotemporal precision of light is photopharmacology.

5.1.2 The synthetic α -galactosylceramide KRN7000

α -Galactosylceramides are a class of molecules that contain acylated sphingosines bound to galactose *via* an α -glycosidic bond. The most prominent member of this class of compounds is the synthetic agelasphin derivative KRN7000 (**II.7**, Figure II.2) – a synthetic cerebroside containing a phytosphingosine backbone. The corresponding structure-activity relationship studies have been carried out with extracts from the Japanese marine sponge *Agelas mauritianus*.^[361]

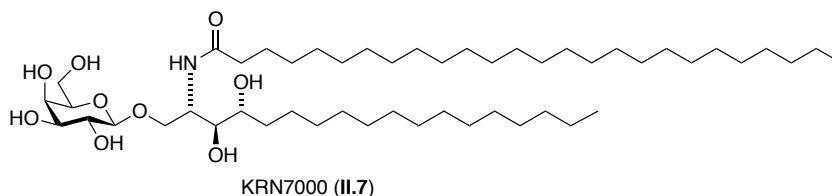


Figure II.2 The synthetic α -galactosylceramide KRN7000 (**II.7**).

KRN7000 (**II.7**) activates natural killer T (NKT) cells, a subpopulation of the T lymphocyte family, when associated with the glycoprotein CD1d and thereby triggers an immune response.^[362] When the binary complex, which consists of KRN7000 bound to CD1d, interacts with the NKT cell receptor (TCR), it forms the active ternary complex. This binding event leads to the production of cytokines, which modulate an immune response. There are many families of cytokines, *e.g.*, chemokines, interferons (IFNs), interleukins (IL), tumour necrosis factors (TNF) and colony-stimulating factors (CSF), which are classified according to their biological activities: A T_{H1} (T helper 1) response is triggered by pro-inflammatory cytokines such as interferon- γ (IFN- γ). The downstream effects associated with these cytokines involve the activation of specific immune cells (NK cells, macrophages and antigen-specific cytotoxic T-lymphocytes, etc.) to antagonize tumors

and infections. By contrast, a T_H2 response is provided by immunomodulatory cytokines such as interleukin 4 (IL-4). These lead to the activation of lymphocytes and the production of antibodies, which are produced for the treatment of autoimmune diseases.^[362] In conclusion, T_H1 - and T_H2 -inducing cytokines are immunomodulatory agents that balance between humoral and cell-based immune responses by orchestrating the maturation, growth, and responsiveness of the cells involved in the immune defense system.

In the case of activation by KRN7000 (**II.7**), T_H1 - and T_H2 -type cytokines can antagonize each other's biological functions, which is called "*cytokine antagonism effect*".^[363–364] Due to this effect, clinical application of KRN7000 (**II.7**) is not possible to date. Therefore, numerous derivatives of KRN7000 (**II.7**), which vary on all positions of the molecule, have been synthesized to map a structure-activity relationship and thereby selectively induce either T_H1 or T_H2 -type cytokine production.^[362] As a summary of these investigations, it was postulated that the T_H1 immune response is favored by a "*a stable glycoside bond, a rigid conformation of the spacer between the D-galactose and ceramide parts, the presence of aromatic rings or long lipid chains, the installation of a small hydrophobic molecule on the C6 sugar position or a carbocyclic ring instead of the D-galactose moiety.*"^[362] For example, Tsuji, Wong and co-workers found that attachment of an aromatic group to *N*-acyl chain greatly enhances IFN- γ /IL-4 secretion, most likely through the alteration of glycolipid/CD1d complex stability.^[365] Moreover, their phenylated derivatives provided very potent NKT cell agonists that exhibit a stronger T_H1 cytokine response than KRN7000 (**II.7**) itself.

While several factors are involved in shifting the cytokine profile, the stability of the binary complex may be an important element. It has been found that after treatment of mice with KRN7000 (**II.7**), the level of IL-4 level is at a maximum after two hours, while the IFN- γ peaks after twelve hours,^[366–367] therefore suggesting that IFN- γ production requires longer TCR stimulation. Therefore a bias towards T_H1 response could be achieved by prolonged stimulation of TCRs on NKT cells through a stabilization of the glycolipid/CD1d complexes.^[365]

We thus envisaged that these binding events could possibly be modulated by photoswitchable derivatives of KRN7000 (**II.7**), which are based on an azo-extension^[368] of the derivatives introduced by Tsuji, Wong and co-workers. Ideally, one isomer would bind stronger to the complex, therefore switching between binding modes with the spatiotemporal precision of light could illuminate the importance of binding strength and times.

5.1.3 β -Galactosylceramide in HIV research

The cluster of differentiation 4 (CD4) is the main cellular host-associated receptor for the human immunodeficiency virus (HIV). However, several CD4-negative cell lines are prone to infection

with certain HIV strains. These results suggest, that there might be alternate modes of viral infection.^[369] The GSL β -GalCer (**II.3**) is expressed on mucosal membrane cells that do not express CD4. Several studies have shown that an alternative pathway of HIV infection occurs in these cells through virus-glycoprotein 120 (gp120) interactions with β -GalCer (**II.3**).^[369–370] Mechanistically, β -GalCer (**II.3**) acts as an anchor and assists in the capture and uptake of the virus but, by contrast to entry receptors, does not enable membrane fusion.^[371]

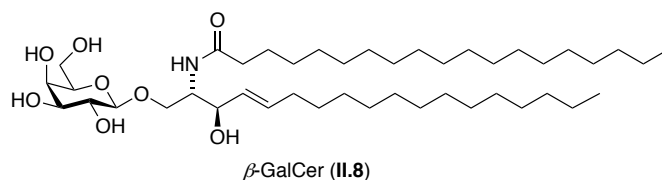


Figure II.3 Structure of β -galactosylceramide.

Using total internal reflection fluorescence (TIRF) spectroscopy, Saavedra *et. al.* found that a carbohydrate on the ceramide is required for recombinant HIV-1 surface glycoprotein gp120 (rgp120) recognition.^[372] At high rgp120 concentrations (25–220 nM), the carbohydrate bound to the ceramide plays a limited role. But at lower concentrations (<20 nM), rgp120 binds to β -GalCer (**II.3**) with an affinity constant of 10^9 M⁻¹. This is a relatively strong interaction in comparison to other protein-receptor interactions at membrane surfaces and resembles the strength of the binding of gp120 to the surface cell receptor CD4,^[373] which is the initial binding event in the primary HIV infection pathway. It was furthermore found, that the selectivity for rgp120 depends on the chemical structure of the sugar group rather than the ceramide moiety.^[372] The region on gp120 that recognizes β -GalCer (**II.3**) is structurally distinct from the binding site for CD4. Therefore it could be addressed by targeted drug delivery, however, “*understanding the molecular events that are responsible for HIV recognition of GalCer is a critical step in developing this dual ligand approach to preventing HIV entry into host cells.*”^[372] For this case, photopharmacology could give insights into the molecular events that are responsible for HIV recognition of β -GalCer (**II.3**).

5.2 Photopharmacology

Photopharmacology is an attempt to control biological function with synthetic photochemical tools that translate a light stimulus into a reversible cellular response.^[368] These light-responsive tools contain an azobenzene photoswitch that allows for reversible control over the molecular configuration. On irradiation with light of a specific wavelength, azobenzenes isomerize from *trans* to *cis*, and *vice versa* (Figure II.4). Due to this change of conformation and polarity, its efficacy at the

target receptor can be fine-tuned using the light stimulus. This enables control over cell signaling with the high spatiotemporal precision of light.

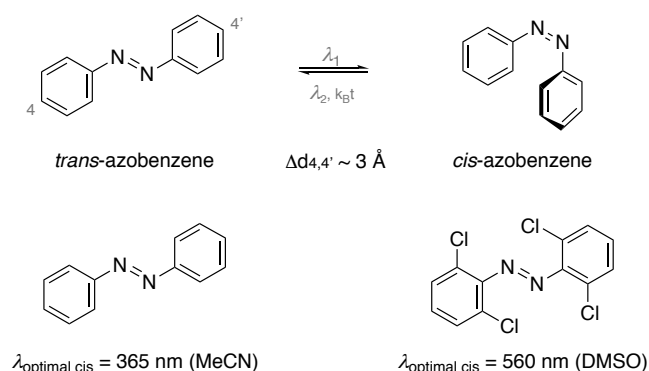


Figure II.4 Conformational change of azobenzene on irradiation with light. $\lambda_{\text{optimal-cis}}$ is the wavelength at which the *cis*-content in the photostationary state is maximized.

Photoswitches can be bound to their target through noncovalent interactions (photochromic ligands, PCLs), or be covalently attached through a linker (photoswitchable tethered ligands, PTLs). Both have been coined photoswitchable ligands or photopharmaceuticals, and have found application in the modulation of various biological targets. These include ion channels, G-protein coupled receptors (GPCRs), transporters, enzymes, and elements of the cytoskeleton.^[374–376]

The properties of azobenzenes are highly tuneable, and can be designed as required for the specific target and biological assay. A standard azobenzene is generally irradiated with 365 nm light, leading to a photostationary stage containing approximately 95% *cis*-isomer. This *cis*-azobenzene is bistable, and spontaneously relaxes back to the *trans*-form thermally ($t_{1/2} = 2$ days), or on irradiation with visible light (e.g., 450 nm).^[368] By contrast, red-shifted tetra-*ortho*-chloro azobenzenes undergo isomerization to the *cis*-configuration at a wavelength of 560 nm (green light).^[377] For the design of azobenzenes, two main approaches are generally employed: azologization and azo-extension (Figure II.5).^[368]

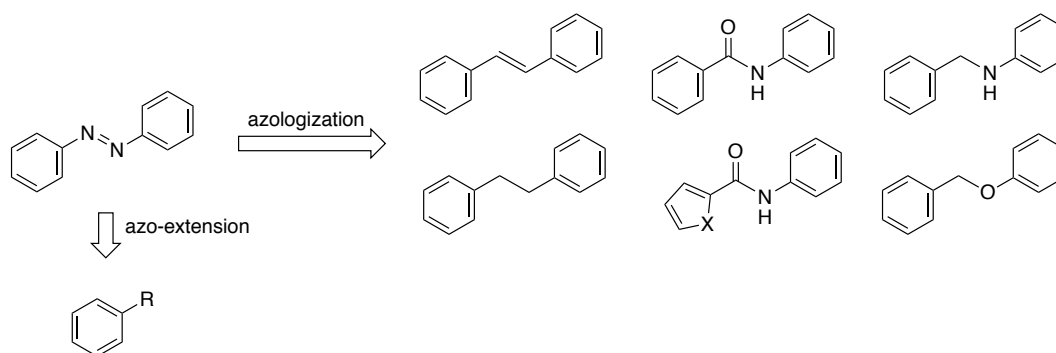


Figure II.5 Strategies for the design of photoswitchable derivatives based on common drug structures.

In the azologization approach, azobenzenes (“azosters”) can mimic structural motifs such as stilbenes, (heterocyclic)*N*-aryl benzamides, benzyl phenyl ethers, benzyl anilines, and 1,2-diaryl ethanes, which are commonly found in drugs or drug candidates. This approach has for example been applied for the azologs of MG-624 (azocholine)^[378] and glimiperide (JB253).^[379] In the second approach, the azo-extension, an azobenzene moiety is extended outside the boundary of the parent drug. This strategy for the synthesis of photoswitchable analogs can easily be applied, knowing the structure-reactivity tables for the given drug. Examples for this approach include azo-propofols^[380] and a photoswitchable version of capsazepine.^[381]

Another strategy to design photoswitchable molecules involves the incorporation of nonpolar azobenzene moieties into lipophilic structures. This approach will be detailed in the following chapter 5.3.

5.3 Photoswitchable lipids and ceramides

In 2015, Trauner and co-workers presented a series of photoswitchable fatty acids (FAAzos) incorporating an azobenzene photoswitch along the fatty acid chain.^[382] They demonstrated that in the *trans*-form the FAAZos resemble long, saturated fatty acids, whereas in their *cis*-form they behave like highly bent fatty acids such as arachidonic acid (**II.9**). For example, photoswitchable analogs of capsaicin (azo-capsaicin derivatives, AzCAs) were prepared, which were able to target the vanilloid receptor 1 (TRPV1), a non-selective cation channel, on irradiation with UV-A light. This publication a seminal report of the fusion of photopharmacology with lipid signalling, and thereby set the groundwork for following studies of photolipids.^[377, 383–384]

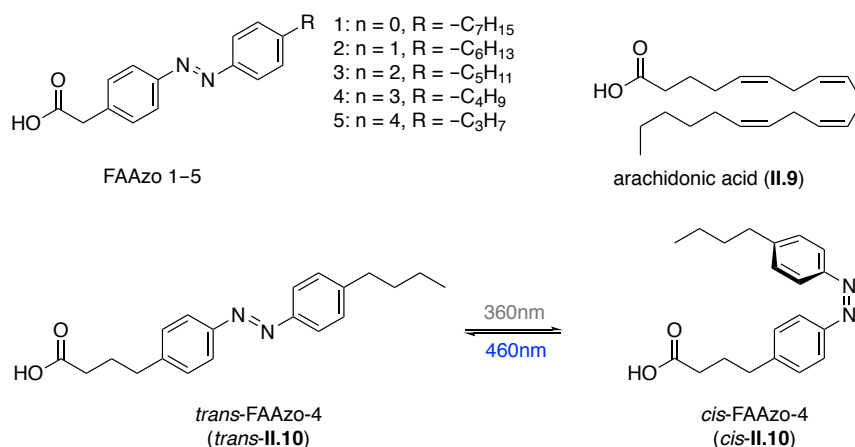


Figure II.6 Photoswitchable fatty acids (FAAZos).

In 2016, the Trauner and Schwille groups, together reported that photoswitchable ceramides enable optical control of lipid rafts within synthetic membranes.^[384] Three different photoswitchable

ceramides (ACes), which varied in the position of the azobenzene in the *N*-acyl chain, were used to manipulate lipid domains in raft-mimicking supported lipid bilayers (SLBs). These effects were visualized by combined atomic force and confocal fluorescence microscopy.

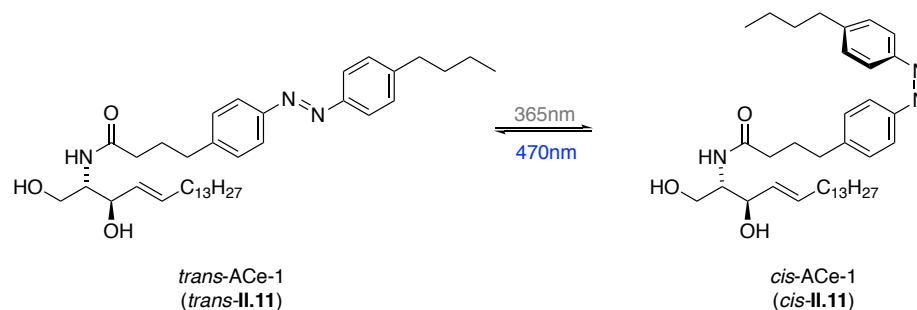


Figure II.7 Photoswitchable ceramide ACE-1.

In their studies, ACes in the *trans*-configuration, such as *trans*-ACE-1 (**II.11**), behaved similar to ceramides in the raft mimicking SLBs, where the azobenzene moiety on the *N*-acyl chain did not influence its interaction with the liquid-ordered (L_0) domains. On irradiation and thus isomerization to *cis*-ACE-1 (*cis*-**II.11**) a conformational change was induced “*in the fatty acid structure from a less bent (similar to saturated C18:0), to more bent acyl chain (similar to unsaturated C18:1), respectively, allowing us to locally and effectively control the degree of lipid saturation within the bilayer.*”^[384]

5.4 Aims and significance of the project

Photoswitchable lipids have already found some application in photopharmacology in the last two years. In first reports, photoswitchable fatty acids (FAAzos) proved that on illumination with light a conformational change is induced, allows fine-tuning of the lipids biophysical properties. As the application for simple fatty acids, ceramides, diacylglycerols and vanilloids has already been showcased, we now wish to broaden the application to glycosphingolipids, namely galactosylceramides, to study their biological and biophysical properties.

α -Galactosylceramides, especially the synthetic derivative KRN7000 (**II.7**), can activate natural killer T (NKT) cells when associated with the glycoprotein CD1d. This effect leads to the production of different cytokines modulating a T_H1/T_H2 immune response. A large number of derivatives have been synthesized to selectively induce either T_H1 or T_H2 -type cytokine production. Based on these studies, we designed a photoswitchable analog of KRN7000 (**II.7**) to activate mainly the production of pro-inflammatory cytokines (T_H1 -type cytokines). These functionalized azobenzenes may help us to manipulate the binding time of the lipid to the receptor, and allow us to control the production of cytokines.

Moreover, we were interested in assessing the biophysical properties of photoswitchable α - and β -galactosylceramides incorporated into lipid raft mimicking SLBs. By using a similar approach as the one described in our joint effort with the Schwille group^[384] based on atomic force (AFM) and fluorescence confocal microscopy, we hope to investigate the behavior of these photoswitchable cerebroside on phase-separated model membranes in comparison with their ceramide counterparts.

Ultimately, photowitchable cerebroside could be of use to study binding of proteins to the GSLs, for example the interaction of recombinant HIV-1 surface glycoprotein gp120 (rgp120) with a photoswitchable analog of β -GalCer (**II.8**).

6 Photoswitchable derivatives of Galactosylceramides

6.1 Development of photochromic derivatives of α -galactosylceramide

6.1.1 Design and retrosynthesis of the photochromic ligands

Based on previous structure-relationship studies on KRN7000 (**II.7**) and related derivatives, we attempted to install the azobenzene moiety in the *N*-acyl chain of the ceramide. Using these tools, we sought to place cytokine production, biased toward T_H1 or T_H2 type, under the control of light. Tsuji, Wong and co-workers observed that derivatives incorporating fatty acids which were truncated and arylated with chain length of $n = 0-4$ were very potent, and also exhibited a stronger T_H1 cytokine response than KRN7000 (**II.7**) itself (Figure II.8).^[365] Modeling studies suggested, that the introduction of a terminal phenyl group promotes additional specific interactions between the phenyl groups and the aromatic amino acids Tyr73 and Trp40 in the CD1d hydrophobic groove, thereby stabilizing the binary complex.

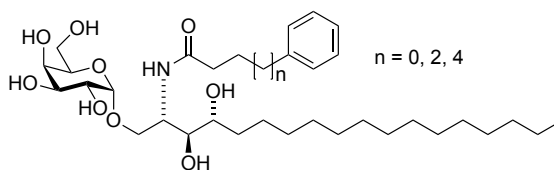


Figure II.8 KRN7000 derivatives, which preferentially induce T_H1 cytokine production.

The most challenging part in the synthesis of galactosylceramides is the formation of a selective α - or β -glycosidic bond. α -Gal linkages can be formed under thermodynamic conditions (anomeric effect), in appropriate solvents (etheral solvent effect), and/or by using a non-participating protecting group at the C2 hydroxyl group.^[385] For the synthesis of α -galactosylceramide derivatives, we followed the synthetic procedure published by M. Tsuji, C.-H. Wong and co-workers.^[365]

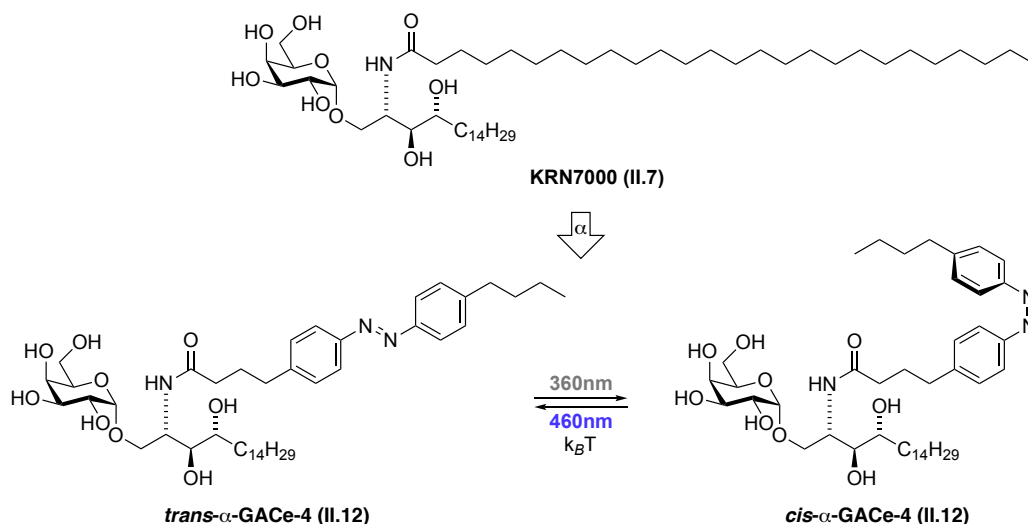
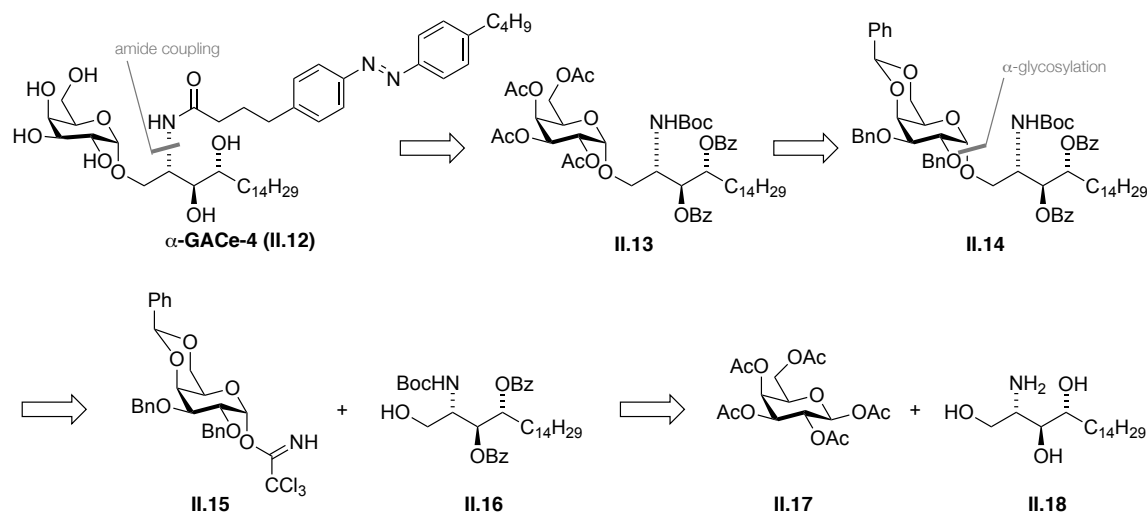


Figure II.9 Incorporation of an azobenzene into KRN7000.

We planned to install the fatty acid azobenzene (FAAzo) in the last steps of the synthesis leading to acetyl protected glycoside **II.13** (Figure II.9), that can be traced back to benzyl- and benzyldiene-protected glycoside **II.14**. This use of protection groups is important for the compatibility with the azobenzene moiety. Typical deprotection conditions for benzyl- and benzyldiene-groups involve hydrogenation conditions (such as Pd/C under H₂ atmosphere), which would lead to concurrent hydrogenation of the azobenzene.



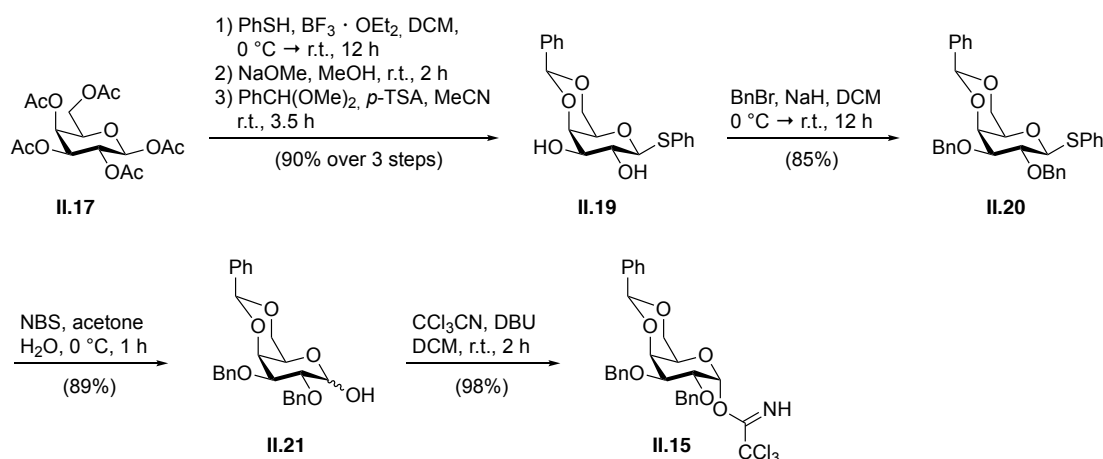
Scheme II.1 Retrosynthesis for photoswitchable α -galactosylceramide derivatives.

Glycoside **II.14** could be obtained from an α -selective glycosylation starting from literature-known protected galactose **II.15**.^[386] In turn, galactose **II.15** can be derived from commercially available β -D-galactose pentaacetate (**II.17**), and protected phytosphingosine **II.16** that can be synthesized from commercially available phytosphingosine (**II.18**).^[387] This strategy has the advantage that it

allows for a late stage introduction of the FAAzOs, allowing us to rapidly synthesize a number of α -galactosyl azo ceramides (GACes) with different photoswitchable chains.

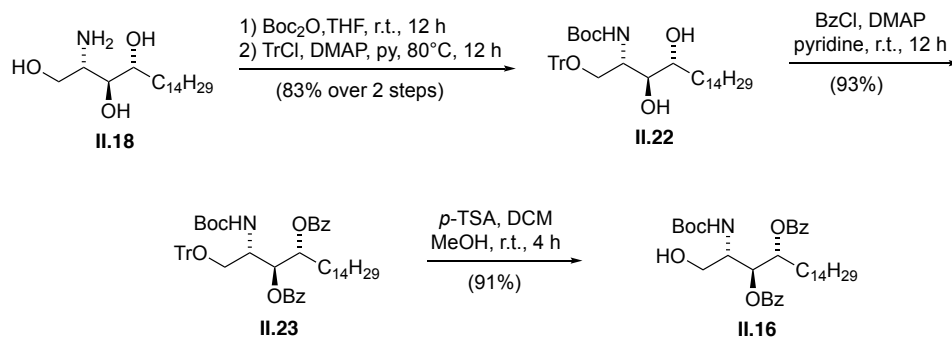
6.1.2 Synthesis of α -galactosylceramide derivatives

Following our retrosynthetic considerations, commercially available β -D-galactose pentaacetate (**II.17**) was thiolated at the anomeric center and fully deprotected under Zemplén conditions.^[388] Protection of the hydroxyl groups at C4 and C5 with a benzylidene protecting group afforded galactose acetal **II.19** in 90% yield over 3 steps. Benzyl protection of the remaining two hydroxyl groups led to fully protected galactose **II.20** in 85% yield. Next, the thioacetal was hydrolysed using NBS in acetone and H₂O, which led to an inseparable mixture of α - and β -galactose derivative **II.21**. The hydroxyl group at C2 was activated as a trichloroacetimidate **II.15** using trichloroacetonitrile and DBU in DCM in an excellent yield of 98%.

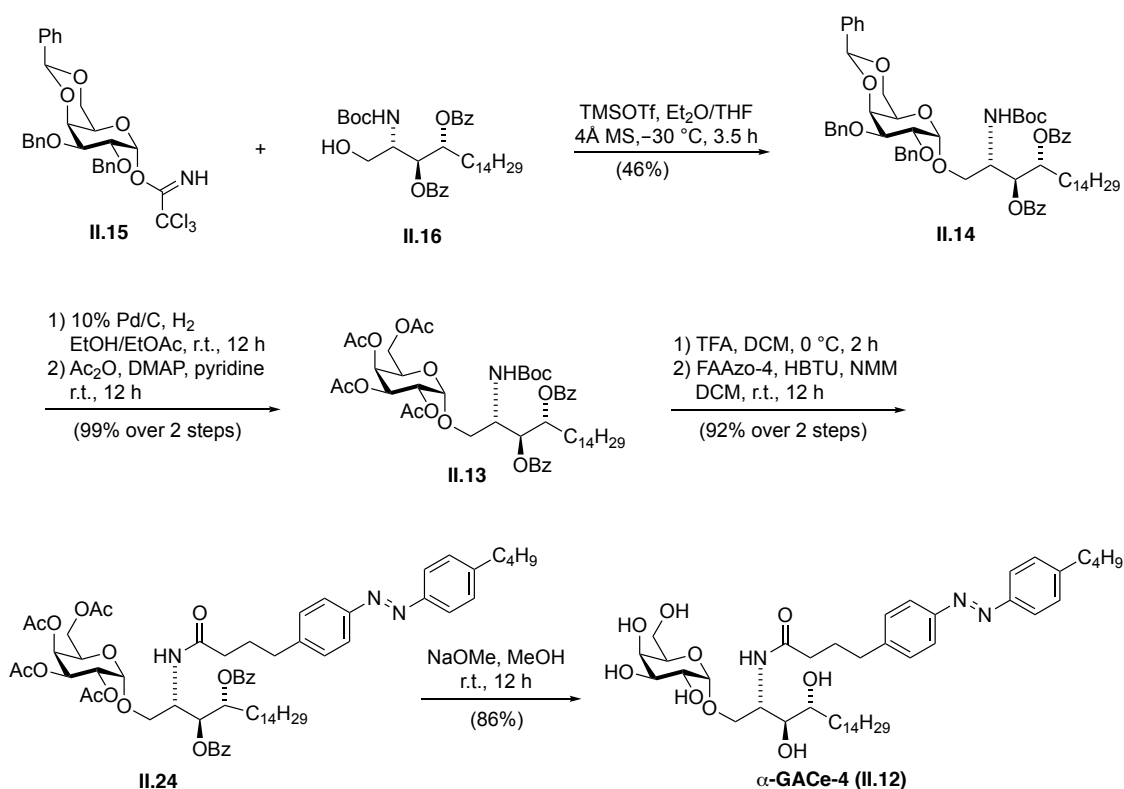


Scheme II.2 Synthesis of protected galactose trichloroacetimidate **II.15**.

For the synthesis of the protected sphingosine building block **II.16**, we commenced our synthesis with commercially available phytosphingosine (**II.18**). This was first Boc-protected and tritylated yielding diol **II.22** in 83% over two steps. The remaining two alcohols were protected with benzoyl chloride leading to fully protected sphingosine **II.23** in 93% yield. Deprotection of the primary alcohol with *p*-TSA furnished the sphingosine building block **II.16** in 91% yield.

Scheme II.3 Synthesis of sphingosine building block **II.16**.

With both building blocks in hand, we set out to investigate glycosylation conditions (Scheme II.4). After some optimization, glycosylation promoted by TMSOTf in a mixture of ethanol and THF led to glycoside **II.14** in 46% yield and an excellent α -selectivity (no β -glycoside was isolated). The α -glycosidic bond was confirmed by a proton–proton coupling of $J = 3.6$ Hz between the equatorial anomeric proton to the adjacent axial proton.

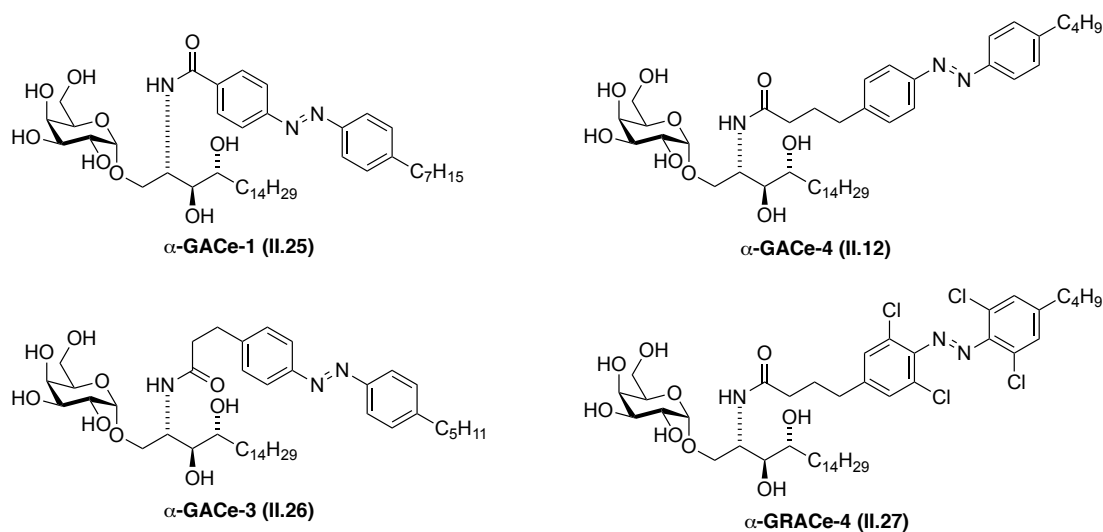


Scheme II.4 Synthesis and derivatization of galactosyl ceramides.

The protected glycoside **II.14** was then hydrogenated using Pd/C in ethanol and EtOAc and re-protected in a mixture of acetic anhydride and catalytic DMAP in pyridine. The obtained acetyl-protected glycoside **II.13** was then Boc-deprotected using TFA and DCM and the FAAzo (*e.g.* FAAzo-4) was attached to the glycoside in an amide coupling using (2-(1*H*-benzotriazol-1-yl)-

1,1,3,3-tetramethyluronium-hexafluorophosphat) (HBTU) and *N*-methylmorpholine (NMM) as coupling agents in 92% over two steps. A final global deprotection of **II.24** yielded α -GalCer-4 (**II.12**) in 86% yield.

Using the same strategy, we were able to synthesize three derivatives, which vary in the position of the azobenzene - α -GACe-1 (**II.25**), α -GACe-3 (**II.26**) and α -GACe-4 (**II.12**, Scheme II.5). In addition, we were able to attach tetrachloro-FAAzo-4 to the glycoside yielding the redshifted α -galactosyl ceramide (GRACe) α -GRACe-4 (**II.27**).

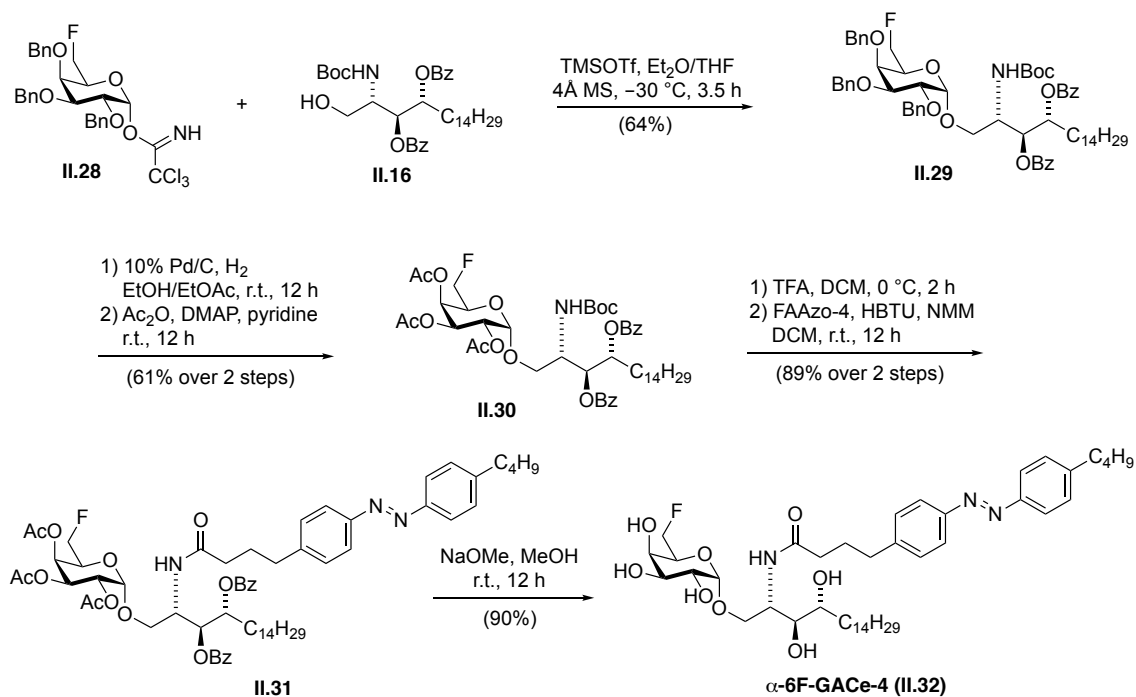


Scheme II.5 Photoswitchable galactosyl ceramide derivatives.

In collaboration with the group of Prof. Dr. Anja Hoffmann-Röder, we synthesized a second set of compounds incorporating a 6-fluoro group into galactose. Tashiro *et al.* reported that a fluorine in the C6-position induced large production of T_H1 -type cytokines such as IFN- γ .^[389] Fluorine is bioisoster albeit more hydrophobic in comparison with a hydroxyl group.^[390–391] It is believed that 6F-galactose derivatives could therefore form a more rigid binary complex with CD1d than KRN7000 (**II.7**), which possesses the hydrophilic 6-hydroxyl group.

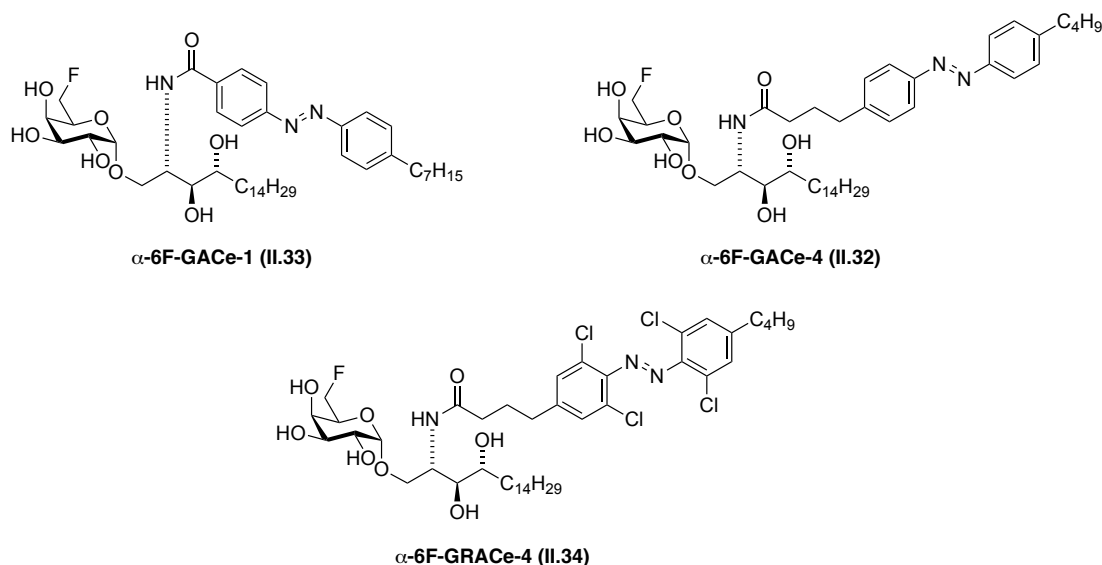
For a second set of compounds, Andreas Baumann (Ph.D. student, Hoffmann-Röder group) repeated the sequence using a 6F-galactose building block **II.28** to synthesize glycoside **II.29** in 64% yield (Scheme II.6).^{§§§} Exchange of the protecting groups *via* hydrogenation and acetylation gave acetylated glycoside **II.30** in 61%. Boc-deprotection and amide coupling using FAAzo-4 yielded fully protected 6F-GACe **II.31** in 89% yield and a global deprotection gave the target compound α -6F-GACe-4 (**II.32**).

^{§§§} 6F-galactose building block **II.28** and glycoside **II.29** were prepared by Andreas Baumann (PhD student in the group of Prof. Dr. Anja Hoffmann-Röder, LMU München, Germany).



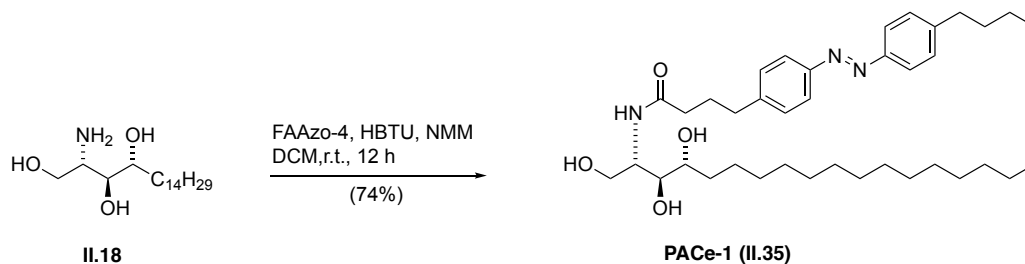
Scheme II.6 Synthesis and derivatization of 6F¹-galactosyl ceramides.

Using this strategy, we were able to synthesize three derivatives in total using different FAAzos for the amide coupling: α -6F-GACe-1 (II.33), α -6F-GACe-4 (II.32) and the red-shifted α -6F-GRACe-4 (II.34, Scheme II.7).



Scheme II.7 Photoswitchable 6F-galactosyl ceramide derivatives.

As a control for biophysical studies in model membranes, we additionally synthesized a photoswitchable phytoceramide derivative (PACe-1, II.35), analogous to the already-published photoswitchable D-*erythro*-ceramide ACe-1 (Scheme II.8).^[384]



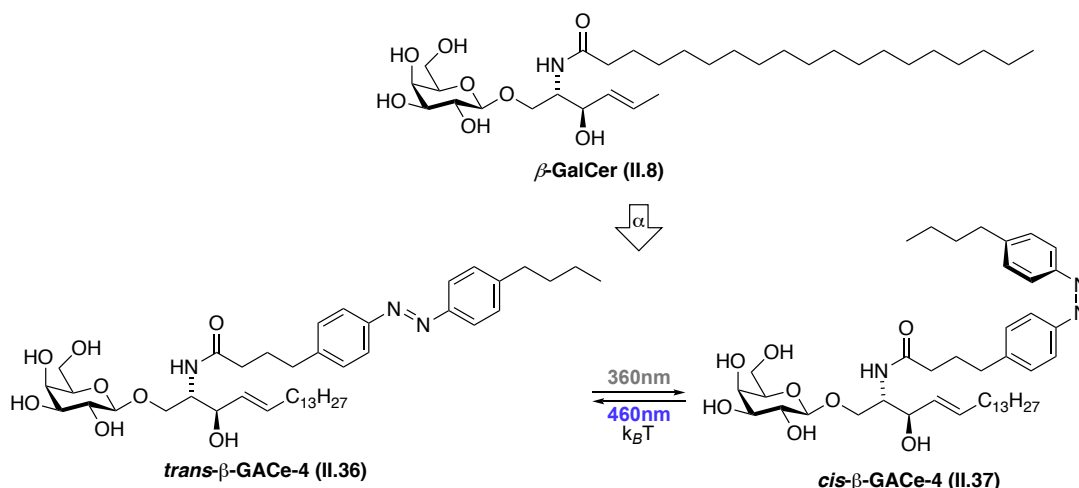
Scheme II.8 Synthesis of PACe-1 (II.35).

In summary, we were able to synthesize seven α -GalCer derivatives of phytoceramide and the photoswitchable phytoceramide PACe-1 (II.35), which can now be used for biophysical characterizations on SLBs and for immunoassays.

6.2 Development of photochromic derivatives of β -galactosylceramide

6.2.1 Design of the photochromic ligand

“Galactosylceramide” (β -GalCer, II.8) generally describes an *N*-acylated *D*-erythro-sphingosine (often simplified as “sphingosine” (II.1)), which is connected to a galactose headgroup *via* a β -glycosidic bond. We therefore planned on building our synthesis on the commercially available building blocks galactose and *D*-erythro-sphingosine (II.1).



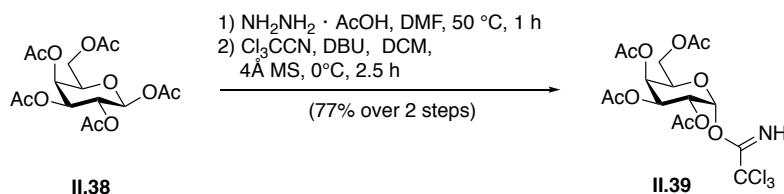
Scheme II.9 Azalozation of β -galactosyl ceramide.

We decided to attach the photoswitchable ceramide ACe-1 to galactose *via* a β -glycosylation to create photoswitchable β -GalCer (II.8, Scheme II.9). By using combined atomic force and confocal fluorescence microscopy, Frank *et al.* have already proven that ACe-1 enables reversible switching of lipid domains in raft-mimicking SLBs.^[384] We hypothesized that this effect would be preserved,

if galactose was attached to ACe-1. For the synthesis of photoswitchable β -GalCer, we envisaged to follow a similar strategy as for α -GalCer derivatives. However, to obtain β -selectivity in the glycosylation step, we exchanged the non-participating protecting groups on the galactose for β -directing acetyl groups. In addition, it has been demonstrated that the nature of the protecting group on the sphingosine (benzoyl, TBS, benzyl) and the choice of the amide precursor (azide, protected alcohol, amide) greatly influences the nucleophilicity of the sphingosine part (acceptor character).^[362] For the synthesis of β -GalCer derivatives, in most cases azide precursors are used.^[392] Azides do not coordinate to the primary alcohol and thereby the nucleophilicity of the sphingosine is greatly enhanced.

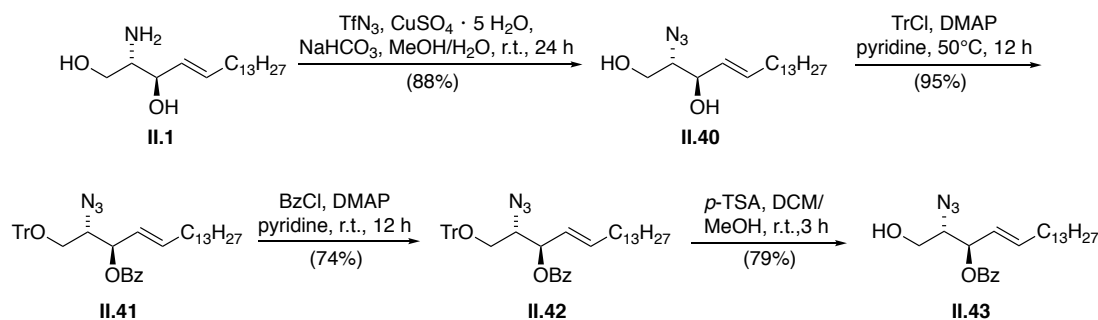
6.2.2 Synthesis of a β -galactosylceramide derivative

Following these retrosynthetic considerations, acetylated galactose **II.38** was deprotected and the thus obtained alcohol was activated as a trichloroacetimidate **II.39** (Scheme II.10).



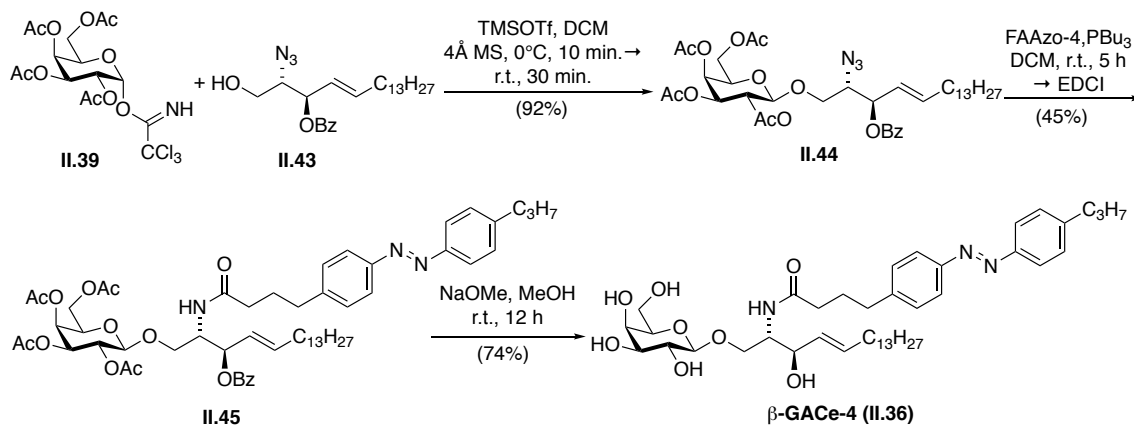
Scheme II.10 Synthesis of acetylated and activated galactose.

For the synthesis of azidosphingosin **II.40**, we started off with *D-erythro*-sphingosine (**II.1**, Scheme II.11). Azidation with freshly prepared triflylazide catalyzed by copper yielded azidosphingosine **II.40**. Protection of the primary alcohol **II.40**, followed by protection of the free secondary alcohol **II.41** and deprotection of the primary alcohol **II.42** afforded the protected sphingosine **II.43** in excellent yield.



Scheme II.11 Synthesis of sphingosine **II.43**.

Glycosylation of azidosphingosine **II.43** with trichloroacetimidate **II.39** yielded protected glycoside **II.44** in 92% yield and excellent β -selectivity (Scheme II.12). Staudinger reduction using PBu_3 and subsequent amide coupling with FAAzo-4 using 1-ethyl-3-(3-dimethylaminopropyl)carbodiimide (EDCI) gave fully protected β -GACe **II.45**. Final deprotection of the benzoyl and acetyl groups furnished β -GalCer-4 (**II.37**) in 74% yield.



Scheme II.12 Synthesis of photoswitchable β -galactosylceramide.

Characterization of β -GalCer-4 (**II.37**) on irradiation revealed that this compound behaved exactly as its FAAzo parent compounds (Figure II.10).

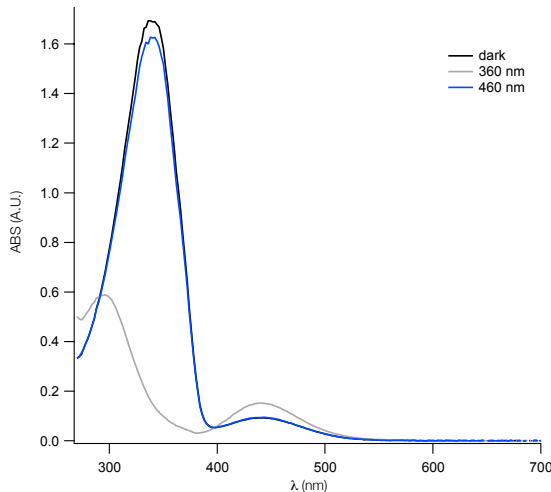


Figure II.10 UV Vis spectrum of β -GalCer-4 (**II.37**).

6.3 Biophysical characterization of α -GACe and β -GACe

The biophysical characterization of α -GACe-4 (II.12), β -GACe-4 (II.37) and respective photoswitchable ceramides PACe-1 (II.35) and ACe-1 (II.11) within raft-mimicking SLBs is being carried out by our collaborators from the group of Prof. Dr. Petra Schwille; more precisely by Dr. Henri G. Franquelim (postdoctoral researcher) and Samuel Leitao (visiting student). As this project is still under progression, for the sake of clarity only the most significant preliminary results will be discussed.

Here, different amounts of photoswitchable cerebroside were incorporated into lipid bilayers composed of 1,2-dioleoyl-*sn*-glycero-3-phosphocholine (DOPC), Chol and *N*-stearoyl-D-*erythro*-sphingosylphosphorylcholine (C18-SM), as previously described.^[384] Analysis of the liquid-disordered (L_d) to liquid-ordered (L_o) phases within these model membranes, deposited on freshly-cleaved mica (muscovite), was carried out using AFM and confocal fluorescence microscopy. First, we observed that the changes induced within the membrane domains on irradiation increased with the amount of photoswitchable cerebroside or ceramide that was incorporated into the SLB (Figure II.11).

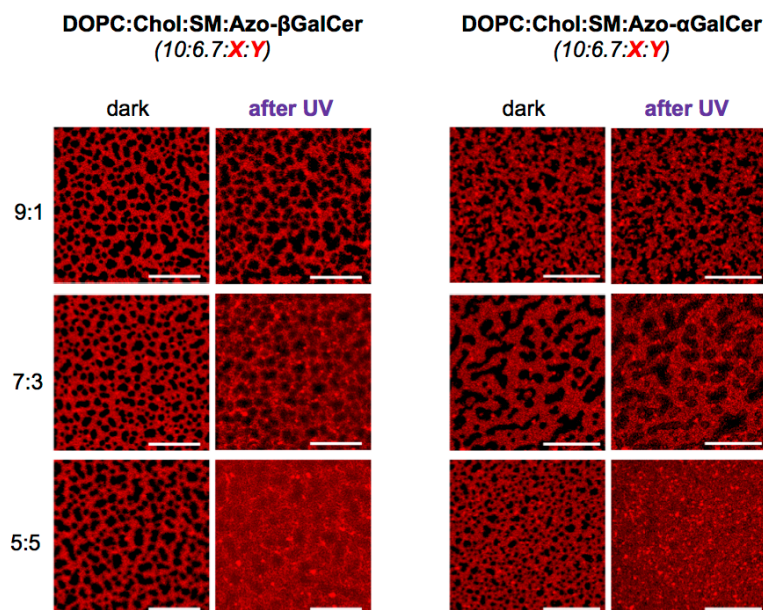


Figure II.11 Transformation of raft-mimicking lipid domains directly after UV-A irradiation. Fluorescence confocal images of SLBs containing DOPC:Chol:SM:Azo- β GalCer and DOPC:Chol:SM:Azo- α GalCer (10:6.7:X:Y, mol. ratios + 0.1 mol.% Atto655-DOPE). Atto655-DOPE (red fluorescence) is marker for liquid-disordered (L_d) domains. Raft-mimicking liquid-ordered (L_o) domains correspond to dark regions on images. Directly after irradiation with $\lambda = 365$ nm, membranes containing higher content of photolipids displayed increased lipid mixing within L_o domains. Scale-bars: 20 μ m.

Using AFM, we could clearly observe that the percentage of L_d to L_o domains could be altered on irradiation of all four compounds, which is in accordance with the already published results for

ACe-1 (**II.11**, Figure II.12).^[384] In both cases, the membranes became more disordered on isomerization to the *cis*-form.

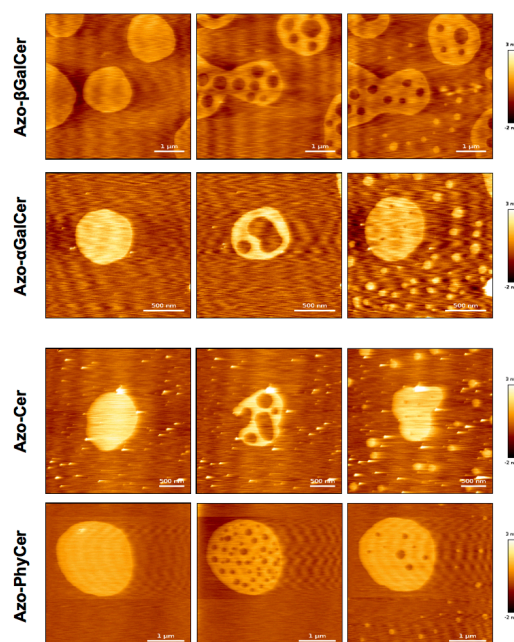


Figure II.12 Proportions of L_d - L_o domains within raft-mimicking SLBs containing photoswitchable ceramides can be altered by light. High-speed AFM images of SLBs containing DOPC:Chol:SM:*photolipid* (10:6.7:5:5, mol. ratios). L_o domains correspond to taller (brighter) regions. Directly after irradiation with $\lambda = 365$ nm, L_o content was reduced, as fluid L_d “lakes” appeared inside L_o domains. In contrast, after irradiation with $\lambda = 470$ nm, L_o content increased and transient L_o islands were observed.

In addition, we were interested if incorporation and photoisomerization of α -GACe-4 (**II.12**) and β -GACe-4 (**II.37**) into the SLBs would affect the properties of the L_o domains. The change in height of the rafts was measured, which directly correlates with the line tension at the lipid phase boundaries.^[393] It was found that switching the cerebroside from *trans*- to *cis*-isomers by irradiation, the difference in height between the L_o - L_d domains increased in a reversible manner (Figure II.13).

C18-SM, which predominantly remains in the L_o domains independently of the light switch, are few picometers larger than their photoswitchable sphingolipid analogues, since they do not have an azobenzene incorporated into their acyl chain. This height change therefore additionally suggests that the photoswitchable derivatives shift into the L_d domains on isomerization to *cis*. On irradiation with blue light, this phenomenon can be reversed. In control experiments, PACe-1 (**II.35**) and ACe-1 (**II.11**) behaved exactly as their glycosylated counterparts. However, as they lack the sugar head group, their overall height was lower.

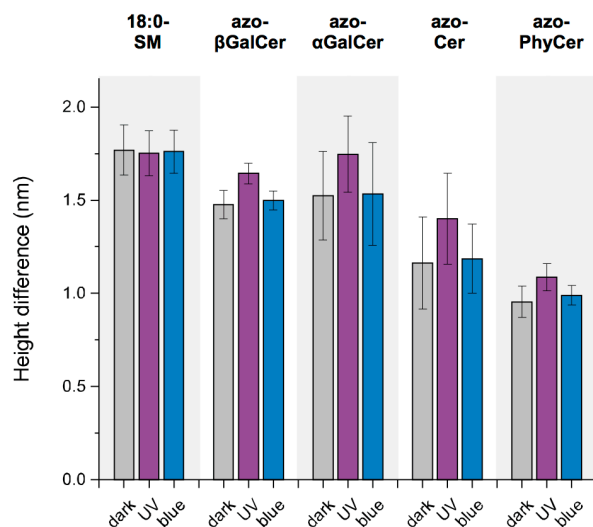
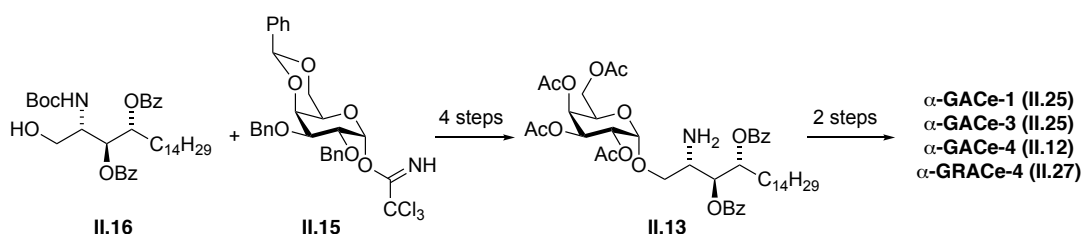


Figure II.13: L_d - L_o height difference within raft-mimicking SLBs containing photoswitchable ceramides can be altered by light. Lipid domain heights of SLBs containing DOPC:Chol:SM:*photolipid* (10:6.7:5:5, mol. ratios) were recovered from AFM images. Directly after irradiation with $\lambda = 365$ nm, the height of the domains increased. In contrast, upon irradiation with $\lambda = 470$ nm, the lipid domains retained their basal height (similar to dark state). In the absence of photolipids (control experiments with lipid bilayers composed of DOPC:Chol:SM (10:6.7:10), left) no significant changes in domain height were observed on irradiation.

With this biophysical characterization of α -GACe-4 (**II.12**) and β -GACe-4 (**II.37**) in hand, we next wanted to investigate the binding of gp120 to β -GACe-4 (**II.37**) incorporated into an SLB displaying a raft-mimicking lipid mixture. Unfortunately, we observed in initial experiments that gp120 creates holes in the SLBs, due to the high affinity of gp120 to the highly-negatively charged mica surface. In the future, we will use a non-supported membrane model system, *e.g.*, β -GACe-4 (**II.37**) incorporated into freestanding giant unilamellar lipid vesicles, as this will remove the artefact caused by the solid support.

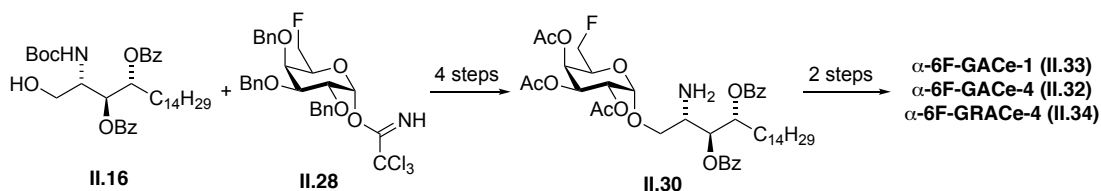
7 Summary and outlook

In summary, we developed a divergent route for the synthesis of photoswitchable α -GalCer derivatives. Starting from commercially available phytoceramide (**II.18**) and β -D-galactose pentaacetate (**II.17**), their protected derivatives **II.16** and **II.15** were prepared in four and six steps (Scheme II.13), respectively. α -Glycosylation under thermodynamic conditions led to the formation of protected glycoside **II.14**, which could be transformed into glycoside **II.13** by exchange of protecting groups and deprotection of the Boc group. Amide coupling to the respective photoswitchable lipid and a global deprotection under Zemplén conditions furnished a total of four photoswitchable α -GalCer derivatives in 15 steps (twelve steps in the longest linear sequence). The late-stage derivatization allowed for the rapid synthesis of multiple derivatives.



Scheme II.13 Synthetic route for six photoswitchable α -GalCer derivatives.

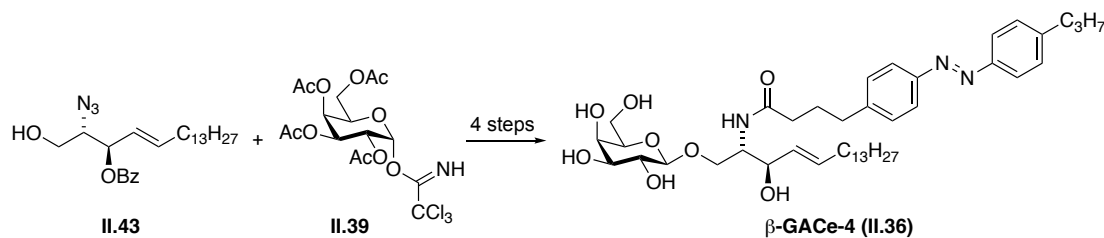
Using a similar approach, three 6F-derivatives were prepared (Scheme II.14). Protected phytoceramide (**II.16**) was glycosylated with protected 6F- β -D-galactose (**II.28**) to yield protected glycoside **II.29**. Three additional steps furnished glycoside **II.30**, which was coupled to the respective photoswitchable lipids. global deprotection under Zemplén conditions^[388] gave three photoswitchable 6F- α -GalCer derivatives. In addition to these cerebrosides, we synthesized the photoswitchable phytoceramide (PACe-1, **II.35**) as a control for the biophysical membrane studies (not shown).



Scheme II.14 Synthetic route for three photoswitchable 6F- α -GalCer derivatives.

For the synthesis of β -GalCer-4 (**II.36**), glycosylation of protected D-*erythro*-sphingosine (**II.1**) with trichloroacetimidate **II.39** yielded protected glycoside **II.44**, which was transformed into β -GalCer-4 (**II.36**) in three additional steps (Scheme II.15). As in the synthesis of α -GalCer derivatives, this

divergent route including a late-stage derivatization would allow for the rapid synthesis of multiple derivatives.



Scheme II.15 Synthesis of the photoswitchable β -GalCer-4 (**II.36**).

All cerebrosides and the photoswitchable ceramide PACe-1 (**II.35**) were characterized using UV-Vis and behave like their FAAzo counterparts.

α -GACe-4 (**II.12**) and β -GACe-4 (**II.36**), alongside the respective photoswitchable ceramides PACe-1 (**II.35**) and ACe-1 (**II.11**) as controls, were characterized in raft-mimicking SLBs using combined atomic force and confocal fluorescence microscopy. However, our ultimate goal was their application as tools for binding studies of proteins to the GSLs, for example the interaction of recombinant HIV-1 surface glycoprotein gp120 (rgp120) with a photoswitchable analog of β -GalCer (**II.8**). To date, these investigations were not successful due to unspecific interactions of gp120 with the mica substrate used in these experiments. In the future, we would like to incorporate β -GalCer-4 (**II.8**) into lipid vesicles to circumvent these surface-induced problems. Using fluorescently-labeled gp120, we could potentially investigate the binding and localization (upon photo-isomerization) of gp120 to such vesicles.

In addition, we would like to continue our protein-binding studies in raft-mimicking SLBs containing photoswitchable GLS. There are several sphingolipid-binding proteins^[394] and bacterial toxins^[395] that enter the cell *via* initial binding to lipid rafts and “*bacteria and toxins are tools of choice to study raft dynamics and lateral sorting of raft-associated proteins as they have been to elucidate other basic intracellular functional pathways. Future challenges include the compositional and functional characterization of different raft sub-classes both at the plasma membrane and intracellularly and their role in infection. The immunological tuning by raft-dependent signaling will also be of great interest.*”^[395] For a number of bacteria, it has been shown that the modification or disruption of lipid rafts, for example by Chol-depleting drugs, inhibits either binding or internalization or both.^[396] Therefore, we would like to study the binding behavior of raft-mimicking SLBs containing photoswitchable GLS to lipid-raft-binding proteins in the liquid-ordered (L_0) or the liquid-disordered (L_d) phase by changing the conformation of photoswitchable β -GalCer (**II.8**) on irradiation with light.

Additionally, we are interested in the application of our photoswitchable KRN7000 derivatives in immunoassays, as we hope that these azobenzenes could be used to modulate a T_H1/T_H2 immune

response. All photoswitchable derivatives are currently under investigation in the laboratory of our collaboration partner Moriya Tsuji, M.D., Ph.D. at Rockefeller University, NY, USA and initial experiments are already underway.

CHAPTER III

EXPERIMENTAL PROCEDURES AND ANALYTICAL DATA

8 Experimental

8.1 Methods and equipment

Unless otherwise noted, all reactions were magnetically stirred and performed under an atmosphere of inert gas (Ar or N₂) using standard Schlenk techniques. The reactions were carried out in oven-dried glassware (200 °C oven temperature). External bath temperatures were used to record all reaction mixture temperatures. Diethyl ether (Et₂O) and tetrahydrofuran (THF) were distilled prior to use under an atmosphere of N₂ from sodium and benzophenone, triethylamine (NEt₃) from calcium hydride. *N,N*-dimethylformamide (DMF), toluene and methanol (MeOH) were purchased from Acros Organics as 'extra dry' reagents under inert gas atmosphere and over molecular sieves. Solvents for flash column chromatography and crystallization experiments were purchased in technical grade and distilled under reduced pressure prior to use. Degassed solvents were degassed under N₂ atmosphere by using either three successive freeze-pump-thaw cycles or by purging the solvent for 30 min with N₂. Petroleum ether (PE) refers to fractions of *iso*-hexanes which boil between 40 and 80 °C. All other reagents were purchased from commercial sources and used without further purification.

Chromatography. Analytical thin-layer chromatography (TLC) was performed on pre-coated glass plates (silica gel 60 F254) from Merck, and visualized by exposure to ultraviolet light (UV, 254 nm) and by staining with aqueous acidic ceric ammonium molybdate(IV) (CAM) solution. Flash column chromatography was performed using Merck silica gel (40–63 μm particle size).

NMR Spectroscopy. Proton nuclear magnetic resonance (¹H NMR) spectra were recorded in 5 mm tubes on a Varian 300, Varian 400, Inova 400 or Varian 600 spectrometer in deuterated solvents at room temperature. Chemical shifts (δ scale) are expressed in parts per million (ppm) and are calibrated using residual protic solvent as an internal reference (CHCl₃: δ = 7.26 ppm).^[397] Data for ¹H NMR spectra are reported as follows: chemical shift (δ ppm) (multiplicity, coupling constants (Hz), integration). Couplings are expressed as: s = singlet, d = doublet, t = triplet, q = quartet, m = multiplet or combinations thereof. Carbon nuclear magnetic resonance (¹³C NMR) spectra were recorded at 75, 100 and 150 MHz, respectively. Carbon chemical shifts (δ scale) are also expressed in parts per million (ppm) and are referenced to the central carbon resonances of the solvents (CDCl₃: δ = 77.16 ppm). In order to assign the ¹H and ¹³C NMR spectra, a range of 2D NMR experiments (COSY, HSQC, HMBC, NOESY) were used as appropriate. The numbering of the proton and carbon atoms does not correspond to the IUPAC nomenclature. Diastereotopic

protons in the ^1H NMR spectra are referenced with a and b, nomenclature is arbitrarily and does not correspond to the spin system.

High performance liquid chromatography (HPLC). HPLC was performed with HPLC grade solvents and deionized H_2O that was purified on a TKA MicroPure H_2O purification system. All solvents were degassed with helium gas prior to use. Unless noticed otherwise, all experiments were carried out at room temperature.

Analytical HPLC spectra were recorded on a ultra-high performance liquid chromatography (UHPLC) system from the Agilent 1260 Infinity series (1260 degasser, 1260 Binary Pump VL, 1260 ALS auto sampler, 1260 TCC thermostated column compartment, 1260 DAD diode array detector), which was computer-controlled through Agilent ChemStation software.

Chiral HPLC spectra were recorded on a high performance liquid chromatography (HPLC) system from the Shimadzu 20A series (DGU-20A3R degasser, LC-20AD Binary Pump VL, SIL-20AHT autosampler, CTO-20A thermostated column compartment, SPD-M20A DAD diode array detector), which was computer controlled through Shimadzu LabSolutions Software (Version 5.42 SP5). Enantiomeric excess (*ee*) was calculated by using the following equation; m_1 refers to the integral of the major peak and m_2 to the integral of the minor peak:

$$ee = \frac{|m_1 - m_2|}{m_1 + m_2} \cdot 100\%$$

High-resolution mass spectrometry (HRMS). A Varian MAT CH7A mass spectrometer was used to obtain high-resolution electron ionization (EI) mass. High-resolution electrospray (ESI) mass spectra were recorded on a Varian MAT 711 MS spectrometer operation in either positive or negative ionization modes.

Infrared spectroscopy (IR). Infrared spectra (IR) were recorded on a Perkin Elmer Spectrum BX II (FTIR System) equipped with an attenuated total reflection (ATR) measuring unit. IR data is reported in frequency of absorption (cm^{-1}). The IR bands are characterized as: w = weak, m = medium, s = strong, br = broad, or combinations thereof.

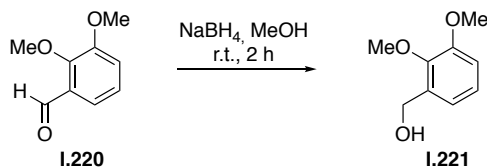
Melting points (mp). Melting points were measured on a Büchi Melting Point B-540 or SRS MPA120 EZ-Melt apparatus and are uncorrected.

Optical rotation. Perkin-Elmer 241 or Krüss P8000-T polarimeter were used to measure optical rotation at the Sodium D-line (589 nm) at the given temperature (T in $^\circ\text{C}$) and concentrations (c in g/100 mL) using spectroscopic grade solvents. The measurements were carried out in a cell with a path length (d) of 0.5 dm. Specific rotations were calculated using the following equation:

$$[\alpha]_D = \frac{\alpha}{c \cdot d} \frac{10^{-1} \cdot \text{deg} \cdot \text{cm}^2}{\text{g}}$$

8.2 Experimental data of chapter I

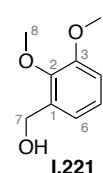
(2,3-Dimethoxyphenyl)methanol (**I.221**)



2,3-Dimethoxybenzaldehyde (**I.220**, 50.0 g, 301 mmol, 1.0 eq.) was dissolved in MeOH (250 mL) and the mixture was cooled to 0 °C. NaBH₄ (6.72 g, 178 mmol, 0.6 eq.) was slowly added and the reaction mixture was allowed to warm to room temperature. After 2 h, the solvent was removed under reduced pressure and the residue was dissolved in H₂O (500 mL). The solution was extracted with DCM (3 × 500 mL) and the combined organic layers were washed with saturated aqueous NaCl solution (750 mL). The organic layer was dried (MgSO₄) and concentrated under reduced pressure to give (2,3-dimethoxyphenyl)methanol (**I.221**) as a yellow oil, which was used in the next step without further purification.

$R_f = 0.54$ [PE/EtOAc, 1:1].

¹H NMR (400 MHz, CDCl₃): $\delta = 7.05$ (dd, $J = 7.9, 7.9$ Hz, 1H, H-5), 6.91 (m, 2H, H-4 and H-6), 4.70 (s, 2H, H-7), 3.89 (s, 3H, H-8), 3.87 (s, 3H, H-9), 2.20 (s, 1H, O-H) ppm.

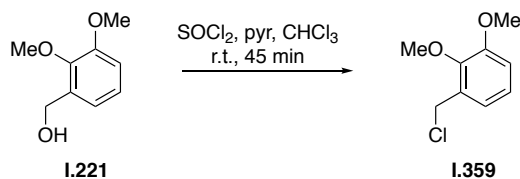


¹³C NMR (101 MHz, CDCl₃): $\delta = 152.5$ (C-3), 147.0 (C-2), 134.6 (C-1), 124.2 (C-5), 120.6 (C-6), 112.2 (C-4), 61.6 (C-7), 60.9 (C-7), 55.8 (C-9) ppm.

IR (ATR): $\tilde{\nu} = 3400$ (m), 2938 (m), 2835 (m), 2360 (vw), 1981 (vw), 1587 (m), 1481 (vs), 1430 (m), 1363 (w), 1272 (s), 1224 (s), 1172 (m), 1082 (s), 1039 (s), 1007 (s), 898 (w), 805 (w), 778 (m), 750 (m), 707 (m) cm⁻¹.

HRMS (EI): calcd. for C₉H₁₂O₃: 168.0786 [M]⁺
 found: 168.0781 [M]⁺.

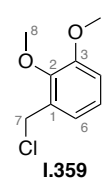
The analytical data matched those previously described in the literature.^[246]

1-(Chloromethyl)-2,3-dimethoxybenzene (I.359)

(2,3-Dimethoxyphenyl)methanol (**I.221**, 50.6 g, 301 mmol, 1.0 eq.) was dissolved in CHCl_3 (300 mL) and pyridine (9.50 mL, 119 mmol, 0.4 eq.) was added. Thionylchloride (40.8 mL, 562 mmol, 1.9 eq.) was slowly added to the reaction mixture and an external ice bath was used to keep the reaction at room temperature. After 45 min., the reaction was cooled to $0\text{ }^\circ\text{C}$ and H_2O (200 mL) was added slowly. The reaction mixture was extracted with DCM ($3 \times 500\text{ mL}$). Afterwards the combined organic layers were washed with H_2O (500 mL) and saturated aqueous NaHCO_3 (500 mL), dried (MgSO_4) and concentrated under reduced pressure to give 1-(chloromethyl)-2,3-dimethoxybenzene (**I.359**) as a yellow oil, which was used in the next step without further purification

$R_f = 0.59$ [PE/EtOAc, 6:1].

$^1\text{H NMR}$ (400 MHz, CDCl_3): $\delta = 7.05$ (dd, $J = 7.9, 7.9$ Hz, 1H, H-5), 6.98 (dd, $J = 7.8, 1.7$ Hz, 1H, H-6), 6.90 (dd, $J = 8.0, 1.6$ Hz, 1H, H-4), 4.65 (s, 2H, H-7), 3.93 (s, 3H, H-8), 3.87 (s, 3H, H-9) ppm.

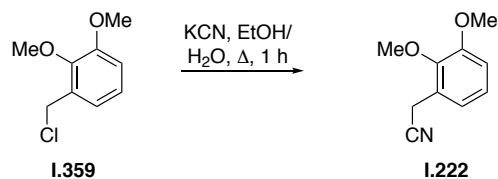


$^{13}\text{C NMR}$ (101 MHz, CDCl_3): $\delta = 152.8$ (C-3), 147.4 (C-2), 131.6 (C-1), 124.2 (C-5), 122.2 (C-6), 113.0 (C-4), 61.2 (C-8), 55.8 (C-9), 41.1 (C-7) ppm.

IR (ATR): $\tilde{\nu} = 3002$ (w), 2967 (w), 2939 (w), 2836 (w), 2360 (w), 2340 (w), 1991 (vw), 1972 (vw), 1916 (vw), 1588 (m), 1483 (s), 1464 (m), 1430 (m), 1310 (m), 1272 (vs), 1228 (m), 1178 (w), 1189 (w), 1151 (w), 1078 (s), 1005 (s), 943 (w), 807 (w), 790 (w), 748 (m), 698 (m), 668 (w) cm^{-1} .

HRMS (EI): calcd. for $\text{C}_9\text{H}_{11}\text{ClO}_2$: 186.0448 $[\text{M}]^+$
 found: 186.0446 $[\text{M}]^+$.

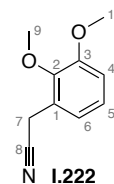
The analytical data matched those previously described in the literature.^[246]

2-(2,3-Dimethoxyphenyl)acetonitrile (**I.222**)

KCN (23.8 g, 366 mmol, 1.2 eq. in H₂O (50 mL)) was heated to 50 °C and 1-(chloromethyl)-2,3-dimethoxybenzene (**I.359**, 56.0 g, 301 mmol, 1.0 eq.) in EtOH (100 mL) was added. The mixture was heated to 90 °C for 1 h. The reaction mixture was then poured into iced-cold H₂O (500 mL) and the aqueous layer was extracted with DCM (3 × 500 mL). The combined organic layers were washed with saturated aqueous NaCl solution (300 mL) and dried (MgSO₄). The organic layer was concentrated under reduced pressure and the crude nitrile **I.222** was used without further purification in the next step.

$R_f = 0.50$ [PE/EtOAc, 3:1].

¹H NMR (400 MHz, CDCl₃): $\delta = 7.06$ (dd, $J = 8.0$ Hz, 8.0 Hz, 1H, H-5), 6.96 (dd, $J = 7.7$, 1.6 Hz, 1H, H-6), 6.91 (dd, $J = 8.2$, 1.5 Hz, 1H, H-4), 3.91 (s, 3H, H-9), 3.88 (s, 3H, H-10), 3.72 (s, 2H, H-7) ppm.

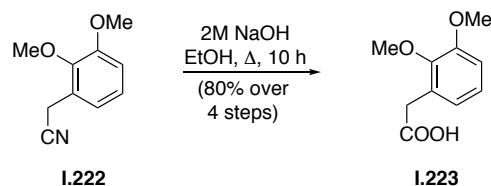


¹³C NMR (101 MHz, CDCl₃) $\delta = 152.7$ (C-3), 146.7 (C-2), 124.3 (C-6), 124.2 (C-1), 121.0 (C-5), 118.2 (C-7), 112.6 (C-4), 60.6 (C-9), 55.8 (C-10), 18.6 (C-7) ppm.

IR (ATR): $\tilde{\nu} = 2940$ (w), 2837 (w), 2361 (m), 2341 (w), 2178 (vw), 2160 (vw), 2098 (vw), 2017 (vw), 1973 (vw), 1726 (vw), 1588 (m), 1485 (vs), 1432 (m), 1275 (s), 1225 (m), 1170 (w), 1074 (s), 1004 (s), 773 (m), 750 (m), 710 (w), 668 (vw) cm⁻¹.

HRMS (EI): calcd. for C₁₀H₁₁NO₂: 177.0790 [M]⁺
 found: 177.0782 [M]⁺.

The analytical data matched those previously described in the literature.^[246]

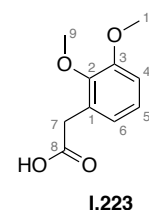
2,3-Dimethoxyphenylacetic acid (I.223)

The crude 2-(2,3-dimethoxyphenyl)acetonitrile **I.222** (53.0 g, 301 mmol, 1 eq.) was suspended in H₂O (220 mL) and 2 N aqueous NaOH (890 mL). The reaction mixture was heated to 100 °C for 10 h. The suspension was washed with Et₂O (500 mL) and the organic layer was discarded. The aqueous layer was acidified with conc. HCl to pH = 1 and extracted with EtOAc (3 × 1000 mL). The combined organic layers were washed with saturated aqueous NaCl solution (1000 mL) and dried (MgSO₄). The concentration of the organic layers under reduced pressure afforded carboxylic acid **I.223** (49.6 g, 253 mmol, 84% over 4 steps) as a white powder.

R_f = 0.17 [PE/EtOAc, 3:1 + 1% AcOH].

mp: 78 – 80 °C

¹H NMR (400 MHz, CDCl₃): δ = 7.02 (dd, *J* = 8.0, 8.0 Hz, 1H, H-5), 6.87 (dd, *J* = 8.3, 1.5 Hz, 1H, H-4), 6.83 (dd, *J* = 7.6, 1.5 Hz, 1H, H-6), 3.86 (s, 6H, H-9, H-10), 3.70 (s, 2H, H-7) ppm.

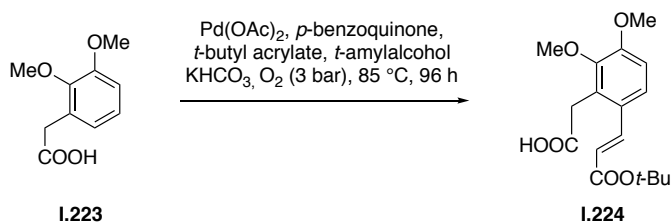


¹³C NMR (101 MHz, CDCl₃): δ = 175.6 (C-8), 152.7 (C-2 or C-3), 147.1 (C-2 or C-3), 127.6 (C-1), 124.1 (C-5), 122.6 (C-6), 112.0 (C-4), 60.6 (C-9 or C-10), 55.7 (C-9 or C-10), 35.6 (C-7) ppm.

IR (ATR): $\tilde{\nu}$ = 2943 (m), 2839 (m), 2362 (m), 2167 (w), 2159 (w), 2047 (w), 2020 (w), 1991 (w), 1972 (w), 1920 (w), 1710 (vs), 1587 (m), 1484 (vs), 1273 (s), 1230 (s), 1170 (m), 1081 (s), 1005 (m), 748 (m), 668 (m) cm⁻¹.

HRMS (EI): calcd. for C₁₀H₁₂O₄: 196.0736 [M]⁺
 found: 196.0730 [M]⁺.

The analytical data matched those previously described in the literature.^[246]

(E)-2-(6-(3-(*tert*-Butoxy)-3-oxoprop-1-en-1-yl)-2,3-dimethoxyphenyl)-acetic acid (I.224)

An autoclave apparatus was charged with a suspension of 2,3-dimethoxyphenylacetic acid (**I.223**, 10.0 g, 51.0 mmol, 1.0 eq.), Pd(OAc)₂ (1.15 g, 5.10 mmol, 10 mol%), *para*-benzoquinone (276 mg, 1.28 mmol, 5 mol%), *tert*-butyl acrylate (22.4 mL, 153 mmol, 3.0 eq.) and dry KHCO₃ (10.2 g, 102 mmol, 2.0 eq.) in dry *tert*-amylalcohol (100 mL). The apparatus was purged with O₂ five times and the reaction mixture stirred under O₂ atmosphere (3 bar) at 85 °C for 96 h. After cooling to room temperature, aqueous HCl (2 M, 150 mL) was added, the aqueous layer was extracted with Et₂O (3 × 200 mL) and the combined organic layers were dried (MgSO₄). All solid material was removed by filtration through a pad of Celite®, which was washed with Et₂O (100 mL). The filtrate was concentrated under reduced pressure and the crude α,β -unsaturated ester **I.224** was used immediately in the next step.

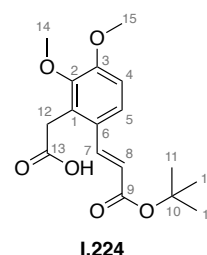
For analytical purposes, a sample of the crude product was purified by flash column chromatography [PE/EtOAc 3:1 + 1% AcOH] to give α,β -unsaturated ester **I.224** as a white solid.

Crystals suitable for single-crystal X-ray analysis (Section 9.1) were obtained from recrystallization [PE/EtOAc 20:1] at 0 °C.

R_f = 0.20 [PE/EtOAc, 3:1 + 1% AcOH].

mp: 115 – 117 °C.

¹H NMR (300 MHz, CDCl₃): δ = 7.73 (d, *J* = 15.7 Hz, 1H, H-7), 7.34 (d, *J* = 8.7 Hz, 1H, H-5), 6.87 (d, *J* = 8.7 Hz, 1H, H-4), 6.20 (d, *J* = 15.6 Hz, 1H, H-8), 3.88 (s, 3H, H-15), 3.87 (s, 2H, H-12), 3.83 (s, 3H, H-14), 1.51 (s, 9H, H-11) ppm.



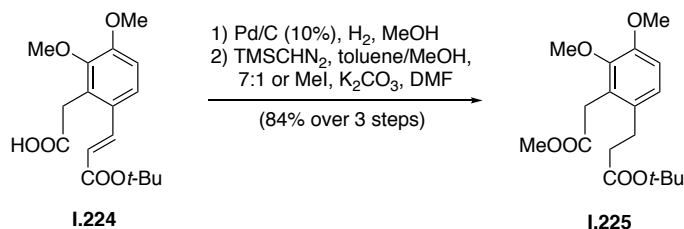
¹³C NMR (75 MHz, CDCl₃): δ = 176.1 (C-13), 166.1 (C-9), 153.4 (C-3), 147.3 (C-2), 139.9 (C-7), 127.4 (C-1), 127.2 (C-6), 122.4 (C-5), 120.5 (C-8), 111.4 (C-4), 80.3 (C-10), 60.4 (C-15), 55.5 (C-14), 31.4 (C-12), 28.0 (C-11) ppm.

IR (ATR): $\tilde{\nu}$ = 2983 (w), 1734 (m), 1700 (s), 1671 (m), 1626 (m), 1594 (m), 1494 (s), 1452 (s), 1255 (m), 1145 (s), 1078 (s), 970 (m) cm⁻¹.

HRMS (EI):	calcd. for C ₁₇ H ₂₂ O ₆ ⁺ :	322.1411 [M] ⁺
	found:	322.1400 [M] ⁺ .

The analytical data matched those previously described in the literature.^[241-242, 245]

***tert*-Butyl 3-(3,4-dimethoxy-2-(2-methoxy-2-oxoethyl)phenyl)propanoate (I.225)**



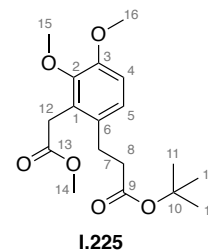
To a solution of α,β -unsaturated ester **I.224** (assumed 51.0 mmol, 1.0 eq) in MeOH (300 mL) was added Pd/C (10% Pd on activated charcoal; 10 wt%, 2.00 g). The flask was purged with H₂ five times and stirred under H₂ atmosphere (1 atm) at room temperature for 16 h. The catalyst was removed by filtration through a pad of Celite[®] which was washed with MeOH (200 mL). Afterwards, the filtrate was concentrated under reduced pressure. For the esterification of the crude product, two different protocols were used (**procedure A** and **procedure B**).

Procedure A: The crude saturated ester was immediately redissolved in toluene/MeOH (7:1, 314 mL). The mixture was cooled to 0 °C and a solution of TMSCHN₂ (2.0 M in hexanes, 30.6 mL, 61.2 mmol, 1.2 eq.) was added dropwise. After stirring for 15 min at 0 °C, the reaction mixture was allowed to warm to room temperature and stirred for additional 40 min. The reaction was quenched with AcOH (15 mL), diluted with saturated aqueous NaHCO₃ (600 mL) and extracted with EtOAc (3 × 400 mL). The combined organic layers were washed with saturated aqueous NaCl solution (500 mL), dried (MgSO₄) and concentrated under reduced pressure. Flash column chromatography [PE/EtOAc, 19:1 to 4:1] afforded methyl ester **I.225** (14.5 g, 42.8 mmol, 84% over 3 steps) as a colorless oil.

Procedure B: The crude saturated ester was immediately redissolved in DMF (250 mL) and K₂CO₃ (21.2 g, 152 mmol, 3 eq.) was added to the stirring solution. The reaction mixture was cooled to 0 °C and MeI (4.13 mL, 66.3 mmol, 1.3 eq.) was added slowly. After 3 h DMF was partially removed under reduced pressure and Et₂O (200 mL) was added. The organic phase was washed with saturated aqueous NH₄Cl solution (200 mL) and extracted with Et₂O (3 × 200 mL). The combined organic layers were washed with saturated aqueous NaCl solution (500 mL), dried (MgSO₄) and concentrated under reduced pressure. Flash column chromatography [PE/EtOAc 19:1 to 4:1] afforded methyl ester **I.225** (16.9 g, 50.0 mmol, 98% over three steps) as a colorless oil.

$R_f = 0.51$ [PE/EtOAc, 3:1].

$^1\text{H NMR}$ (300 MHz, CDCl_3): $\delta = 6.90$ (d, $J = 8.5$ Hz, 1H, H-5), 6.80 (d, $J = 8.5$ Hz, 1H, H-4), 3.84 (s, 3H, H-16), 3.81 (s, 3H, H-15), 3.75 (s, 2H, H-12), 3.69 (s, 3H, H-14), 2.82 (dd, $J = 9.1, 6.8$ Hz, 2H, H-7), 2.49–2.40 (m, 2H, H-8), 1.43 (s, 9H, H-11) ppm.



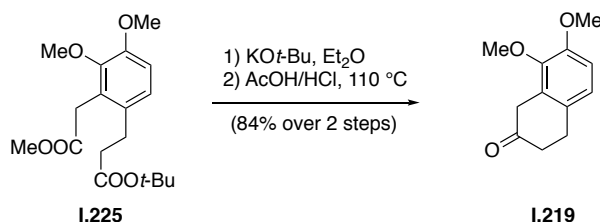
$^{13}\text{C NMR}$ (75 MHz, CDCl_3): $\delta = 172.3$ (2C, C-9, C-13), 151.0 (C-3), 147.6 (C-2), 132.1 (C-6), 127.1 (C-1), 124.1 (C-5), 111.2 (C-4), 80.6 (C-10), 60.5 (C-15), 55.7 (C-16), 51.9 (C-14), 36.3 (C-8), 32.0 (C-12), 28.1 (C-11), 27.4 (C-7) ppm.

IR (ATR): $\tilde{\nu} = 2976$ (w), 2940 (w), 2837 (w), 1726 (s), 1605 (w), 1572 (w), 1492 (s), 1366 (m), 1275 (s), 1227 (m), 1145 (s), 1083 (s), 753 (s) cm^{-1} .

HRMS (ESI): calcd. for $\text{C}_{18}\text{H}_{26}\text{O}_6^+$: 338.1724 $[\text{M}+\text{H}]^+$
found: 338.1718 $[\text{M}+\text{H}]^+$.

The analytical data matched those previously described in the literature.^[241-242, 245]

7,8-Dimethoxy-1,2,3,4-tetrahydronaphthalen-2-one (I.219)



To a solution of diester **I.225** (16.9 g, 50.0 mmol, 1.0 eq.) in Et_2O (750 mL) was added potassium *tert*-butoxide (7.29 g, 65.0 mmol, 1.3 eq.) over a period of 15 min and the resulting mixture was stirred at room temperature for 30 min. The reaction was cooled to 0 °C and aqueous HCl (1 M, 20 mL) was added slowly. The mixture was allowed to warm to room temperature and the aqueous layer was extracted with DCM (3×400 mL). The combined organic layers were washed with saturated aqueous NaCl solution (500 mL), dried (MgSO_4) and concentrated under reduced pressure. The crude product was immediately redissolved in concentrated AcOH (360 mL) and concentrated HCl (90 mL), stirred for 3 h at 110 °C and then cooled to 0 °C. The reaction was neutralized with aqueous 2 M NaOH and the mixture was extracted with Et_2O (3×500 mL) and DCM (2×500 mL). The combined organic layers were dried (MgSO_4) and concentrated under reduced pressure. Flash column chromatography [PE/EtOAc, 9:1 to 3:1] afforded 7,8-dimethoxy-1,2,3,4-tetrahydronaphthalen-2-one (**I.219**, 6.74 g, 32.7 mmol, 65% over 2 steps) as a colorless solid.

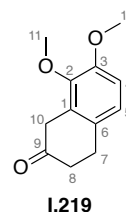
Crystals suitable for single-crystal X-ray analysis (Section 9.1) were obtained from recrystallization [CHCl_3] at 0 °C.

$R_f = 0.43$ [PE/EtOAc, 3:1].

mp: 75 – 76 °C.

$^1\text{H NMR}$ (300 MHz, CDCl_3): $\delta = 6.93$ (d, $J = 8.3$ Hz, 1H, H-5), 6.79 (d, $J = 8.3$ Hz, 1H, H-4), 3.86 (s, 3H, H-12), 3.81 (s, 3H, H-11), 3.60 (s, 2H, H-10), 3.05–2.96 (m, 2H, H-7), 2.59–2.49 (m, 2H, H-8) ppm.

$^{13}\text{C NMR}$ (75 MHz, CDCl_3): $\delta = 210.8$ (C-9), 151.5 (C-3), 146.6 (C-2), 129.8 (C-6), 127.7 (C-1), 123.2 (C-5), 111.1 (C-4), 60.8 (C-11), 56.3 (C-12), 39.1 (C-8), 38.9 (C-10), 28.5 (C-7) ppm.



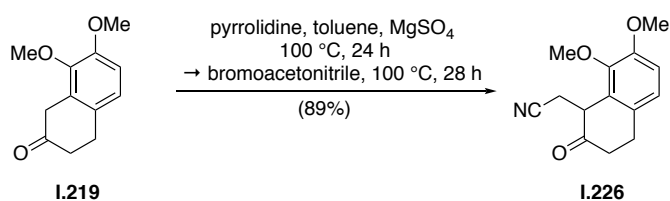
IR (ATR): $\tilde{\nu} = 2998$ (w), 2944 (w), 2836 (w), 1702 (s), 1604 (w), 1582 (w), 1492 (s), 1458 (m), 1428 (m), 1350 (m), 1307 (m), 1273 (s) cm^{-1} .

HRMS (ESI): calcd. for $\text{C}_{12}\text{H}_{14}\text{O}_3^+$: 206.0937 $[\text{M}+\text{H}]^+$

found: 206.0942 $[\text{M}+\text{H}]^+$.

The analytical data matched those previously described in the literature.^[241-242, 245]

2-(7,8-Dimethoxy-2-oxo-1,2,3,4-tetrahydronaphthalen-1-yl)acetonitrile (**1.226**)



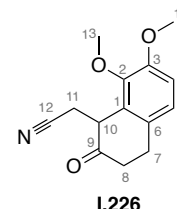
To a solution of β -tetralone **1.219** (10.3 g, 44.2 mmol, 1.0 eq.) and a small amount of dry MgSO_4 in toluene (260 mL) was added pyrrolidine (4.7 mL, 57.4 mmol, 1.3 eq.) and the reaction was stirred at 100 °C for 24 h. The mixture was allowed to cool to room temperature, bromoacetonitrile (4.92 mL, 70.7 mmol, 1.6 eq.) was added and the reaction was stirred at 100 °C for an additional 28 h. The reaction was quenched with H_2O (300 mL) at room temperature, extracted with EtOAc (3×300 mL) and DCM (300 mL) and the combined organic layers were washed with saturated aqueous NaCl solution (400 mL), dried (MgSO_4) and concentrated under reduced pressure. Flash column chromatography [PE/EtOAc, 9:1 to 6:1] afforded 2-(7,8-dimethoxy-2-oxo-1,2,3,4-tetrahydronaphthalen-1-yl)acetonitrile (**1.226**, 9.62 g, 39.2 mmol, 89%) as colorless crystals.

Crystals suitable for single-crystal X-ray analysis (Section 9.1) were obtained from recrystallization [CHCl_3] at 0 °C.

$R_f = 0.25$ [PE/EtOAc, 3:1].

mp: 77–79 °C.

$^1\text{H NMR}$ (300 MHz, CDCl_3): $\delta = 6.94$ (d, $J = 8.3$ Hz, 1H, H-5), 6.88 (d, $J = 8.4$ Hz, 1H, H-4), 3.90 (s, 3H, H-13), 3.88 (s, 3H, H-14), 3.83 (dd, $J = 4.5$, 5.8 Hz, 1H, H-10), 3.34–3.15 (m, 2H, H-7a, H-11a), 2.95–2.89 (m, 2H, H-7b, H-11b), 2.85–2.74 (m, 1H, H-8a), 2.0 (dddd, $J = 15.2$, 13.6, 6.1, 0.5 Hz, 1H, H-8b) ppm.

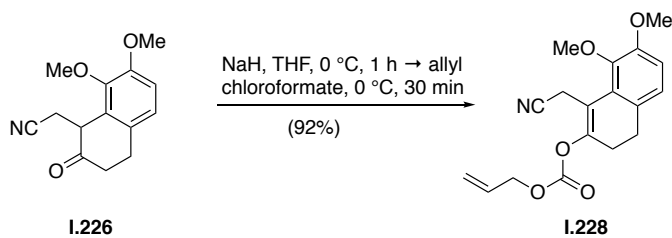


$^{13}\text{C NMR}$ (100 MHz, CDCl_3) $\delta = 209.0$ (C-9), 150.6 (C-3), 146.5 (C-2), 129.5 (C-6), 127.5 (C-1), 123.1 (C-5), 117.7 (C-12), 112.1 (C-4), 60.4 (C-13), 55.5 (C-14), 43.2 (C-10), 39.1 (C-8), 26.9 (C-7), 20.2 (C-11) ppm.

IR (ATR): $\tilde{\nu} = 3006$ (w), 2974 (w), 2940 (w), 2918 (w), 2837 (w), 2244 (m), 1716 (s), 1606 (m), 1581 (m), 1494 (s), 1456 (s), 1421 (s), 1347 (m), 1308 (m), 1279 (s), 1246 (m), 1220 (s), 1156 (m), 1091 (s), 999 (s) cm^{-1} .

HRMS (ESI): calcd. for $\text{C}_{14}\text{H}_{15}\text{O}_3\text{N}^+$: 245.1046 $[\text{M}+\text{H}]^+$
found: 245.1047 $[\text{M}+\text{H}]^+$.

Allyl (1-(cyanomethyl)-7,8-dimethoxy-3,4-dihydronaphthalen-2-yl) carbonate (I.228)

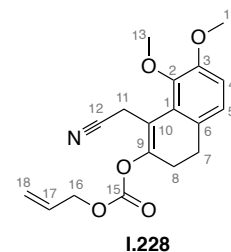


To a solution of nitrile **I.226** (5.00 g, 20.4 mmol, 1.0 eq.) in THF (250 mL) was added sodium hydride (60 wt% in mineral oil, 898 mg, 22.4 mmol, 1.1 eq.) at 0 °C and the mixture was stirred for 1 h. Allyl chloroformate (10 v% in THF, 2.39 mL in 23.9 mL THF, 2.70 g, 22.4 mol, 1.0 eq.) was added and the reaction was stirred at 0 °C for an additional 30 min. The reaction was quenched with H_2O (50 mL) at 0 °C, extracted with EtOAc (3×100 mL) and the combined organic layers were washed with saturated aqueous NaCl solution (100 mL), dried (MgSO_4) and concentrated

under reduced pressure. Flash column chromatography [PE/EtOAc, 8:1] afforded carbonate **I.228** (6.18 g, 18.8 mmol, 92%) as a colorless oil.

$R_f = 0.41$ [PE/EtOAc, 3:1].

$^1\text{H NMR}$ (400 MHz, CDCl_3): $\delta = 6.85$ (d, $J = 8.2$ Hz, 1H, H-5), 6.75 (d, $J = 8.2$ Hz, 1H, H-4), 5.98 (ddt, $J = 17.1, 10.4, 5.9$ Hz, 1H, H-17), 5.43 (dq, 1H, $J = 17.2, 1.5$ Hz, H-18a), 5.34 (dq, $J = 10.4, 1.2$ Hz, H-18b), 4.75–4.71 (m, 2H, H-16), 3.90 (s, 3H, H-13), 3.85 (s, 3H, H-14), 3.70 (s, 2H, H-11), 2.84–2.78 (m, 2H, H-7), 2.54–2.47 (m, 2H, H-8) ppm.

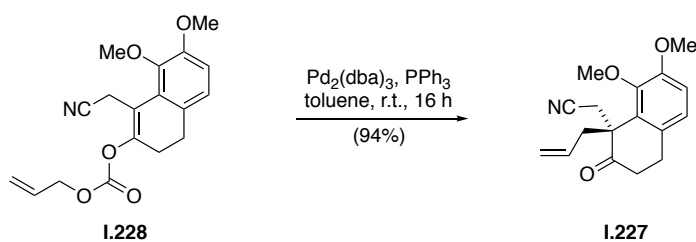


$^{13}\text{C NMR}$ (101 MHz, CDCl_3): $\delta = 151.5$ (C-3), 151.4 (C-15), 151.0 (C-9), 146.3 (C-2), 130.4 (C-17), 128.1 (C-6), 125.2 (C-1), 122.1 (C-5), 119.3 (C-18), 117.6 (C-12), 113.5 (C-10), 111.1 (C-4), 69.1 (C-16), 61.2 (C-13), 55.5 (C-14), 28.2 (C-7), 26.6 (C-8), 16.3 (C-11) ppm.

IR (ATR): $\tilde{\nu} = 3319$ (w), 3197 (w), 2942 (m), 2836 (w), 22.51 (w), 1756 (s), 1661 (m), 1573 (w), 1477 (m), 1418 (m), 1261 (s), 1241 (s), 1206 (s), 1183 (s), 980 (m) cm^{-1} .

HRMS (ESI): calcd. for $\text{C}_{18}\text{H}_{19}\text{O}_5\text{N}^+$: 329.1258 $[\text{M}+\text{H}]^+$
found: 329.1255 $[\text{M}+\text{H}]^+$.

2-(1-Allyl-7,8-dimethoxy-2-oxo-1,2,3,4-tetrahydronaphthalen-1-yl)acetonitrile (**I.227**)



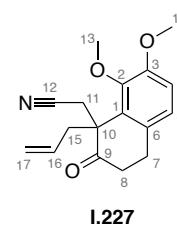
Tris(dibenzylideneacetone)dipalladium(0) (428 mg, 0.468 mmol, 2.5 mol%) and PPh_3 (307 mg, 1.17 mmol, 6.25 mol%) were dissolved in degassed toluene (550 mL) and stirred until the reaction color turned from dark red to orange/yellow (approximately 30 min.). A solution of carbonate **I.228** (6.17 g, 18.7 mmol, 1.0 eq.) dissolved in degassed toluene (50 mL) was added to the preformed catalyst and the reaction was stirred at room temperature for 16 h prior to concentrating the reaction mixture under reduced pressure. Flash column chromatography [PE/EtOAc, 9:1] afforded 2-(1-allyl-7,8-dimethoxy-2-oxo-1,2,3,4-tetrahydronaphthalen-1-yl)acetonitrile (**I.227**, 5.02 g, 17.6 mmol, 94%) as a colorless solid.

Crystals suitable for single-crystal X-ray analysis (Section 9.1) were obtained from recrystallization [CHCl_3] at 20 °C.

$R_f = 0.41$ [PE/EtOAc, 3:1].

mp: 70–71 °C.

$^1\text{H NMR}$ (600 MHz, CDCl_3): $\delta = 6.92\text{--}6.85$ (m, 2H, H-4, H-5), 5.39 (dddd, $J = 17.0, 10.1, 9.0, 5.9$ Hz, 1H, H-16), 5.00–4.94 (m, 2H, H-17), 3.97 (s, 3H, H-13), 3.88 (s, 3H, H-14), 3.29 (d, $J = 16.4$ Hz, 1H, H-11a), 3.13 (d, $J = 16.3$ Hz, 1H, H-11b), 3.05 (dddd, $J = 15.8, 9.7, 6.0, 0.6$ Hz, 1H, H-7a), 3.01–2.94 (m, 1H, H-7b), 2.90 (ddt, $J = 13.7, 5.8, 1.5$ Hz, 1H, H-15a), 2.76–2.64 (m, 2H, H-8), 2.71 (m, 1H, H-15b) ppm.



$^{13}\text{C NMR}$ (150 MHz, CDCl_3): $\delta = 210.3$ (C-9), 151.2 (C-3), 147.5 (C-2), 132.3 (C-16), 129.6 (C-6), 129.1 (C-1), 123.2 (C-5), 118.8 (C-17), 117.6 (C-12), 112.3 (C-4), 60.2 (C-13), 55.5 (C-14), 53.6 (C-10), 42.4 (C-15), 38.8 (C-8), 28.0 (C-7), 24.5 (C-11) ppm.

IR (ATR): $\tilde{\nu} = 2941$ (m), 2839 (w), 1715 (s), 1601 (w), 1576 (w), 1486 (s), 1454 (m), 1415 (w), 1346 (w), 1275 (s) cm^{-1} .

HRMS (ESI): calcd. for $\text{C}_{17}\text{H}_{20}\text{O}_3\text{N}^+$: 286.1438 $[\text{M}+\text{H}]^+$
 found: 286.1435 $[\text{M}+\text{H}]^+$.

To obtain enantiomerically enriched material, experiments with chiral ligands were carried out using **procedures A–E** and using the following HPLC parameters to determine the *ee*:

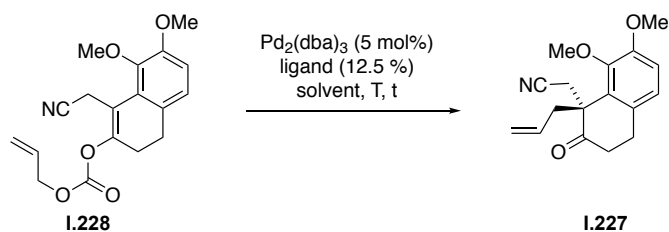
Chiral HPLC: Retention time (*R*)-**1.227**: 10.438 min
 Retention time (*S*)-**1.227**: 12.365 min.

Column: DAICEL CHIRALPAK® IB
 Flow rate: 1 mL/min
 Mobile phase: *n*-hept:*iso*-prop 97.5:2.5 (v/v)
 Temperature: 20 °C
 Wavelength: 198 nm.

(*R*)-**1.227**: $[\alpha]_{\text{D}} = +0.40$ ($c = 1$, DCM).

(*S*)-**1.227**: $[\alpha]_{\text{D}} = -0.38$ ($c = 1$, DMC).

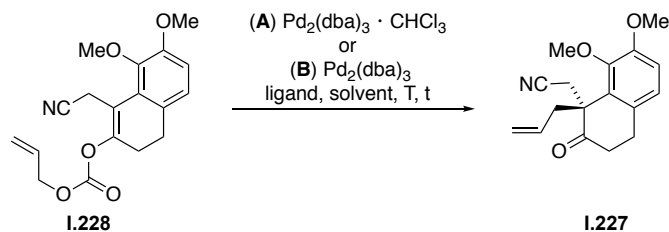
Procedure A: The reaction was carried out at a concentration of 0.030 M in a glovebox under nitrogen atmosphere. Tris(dibenzylideneacetone)dipalladium(0) (1.50 μmol , 5 mol%) and a ligand (3.75 μmol , 12.5 mol%) were dissolved in dry, degassed solvent and the catalyst stirred for 30 min at 25 °C. A solution of carbonate **I.228** (10.0 mg, 30.0 μmol , 1 eq.) in solvent was added to the preformed catalyst and the reaction was stirred at a set temperature T, prior to dilution of the sample with hexanes and ether, filtration over silica and analysis of the %ee by chiral HPLC.



Entry	Ligand	Solvent	T (°C)	t (h)	%ee
1	(S)- <i>t</i> -Bu-PHOX (I.232)	THF	25	20	3
2	(S)- <i>t</i> -Bu-PHOX (I.232)	toluene	25	20	1
3	(S)- <i>t</i> -Bu-PHOX (I.232)	2:1 hexane/toluene	25	20	6
4	(S)-CF ₃ - <i>t</i> -Bu-PHOX (I.233)	THF	25	20	10
5	(S)-CF ₃ - <i>t</i> -Bu-PHOX (I.233)	toluene	25	20	26
6	(S)-CF ₃ - <i>t</i> -Bu-PHOX (I.233)	2:1 hexane/toluene	25	20	38
7	(<i>R,R</i>)-ANDEN-Phenyl Trost (I.237)	THF	25	20	22
8	(<i>R,R</i>)-ANDEN-Phenyl Trost (I.237)	toluene	25	20	13
9	(<i>R,R</i>)-ANDEN-Phenyl Trost (I.237)	2:1 hexane/toluene	25	20	25
10	(S)-QUINAP (I.234)	THF	25	20	14
11	(S)-QUINAP (I.234)	toluene	25	20	3
12	(S)-QUINAP (I.234)	2:1 hexane/toluene	25	20	11
13	(S)-CF ₃ - <i>t</i> -Bu-PHOX (I.233)	2:1 hexane/toluene	20	14	39
14	(S)-CF ₃ - <i>t</i> -Bu-PHOX (I.233)	2:1 hexane/toluene	0	14	42
15	(S)-CF ₃ - <i>t</i> -Bu-PHOX (I.233)	2:1 hexane/toluene	-15	14	34
16	(S)-CF ₃ - <i>t</i> -Bu-PHOX (I.233)	2:1 hexane/toluene	-60	14	37

Procedure B: The reaction was carried out at a concentration of 0.030 M in a glovebox under nitrogen atmosphere. To tris(dibenzylideneacetone)dipalladium(0)-chloroform adduct (1.65 μmol , 5.5 mol%) or tris(dibenzylideneacetone)dipalladium(0) (1.65 μmol , 5.5 mol%) and a ligand (3.30 μmol , 11.0 mol%) a dry, degassed solvent was added and the catalyst stirred for 30 min at 25 °C. A solution of carbonate **I.228** (10.0 mg, 30.0 μmol , 1 eq.) in solvent was added to the

preformed catalyst and the reaction was stirred at the designated temperature for the designated time, prior to dilution of the sample with hexanes and ether and analysis of the %*ee* by chiral HPLC.

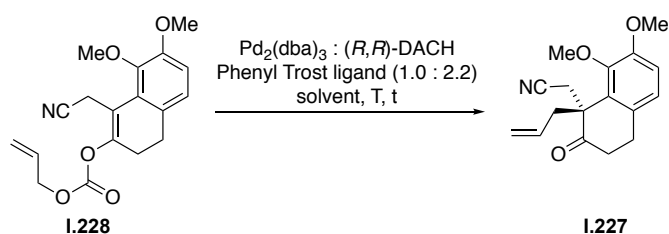


Entry	Ligand	Pd source	Solvent	T (°C)	t (h)	% <i>ee</i>
1	(<i>R,R</i>)-DACH-Phenyl Trost (1.235)	A	DME	25	12	51
2	(<i>R,R</i>)-DACH-Phenyl Trost (1.235)	A	MTBE	25	12	46
3	(<i>R,R</i>)-DACH-Phenyl Trost (1.235)	A	THF	25	12	47
4	(<i>R,R</i>)-DACH-Phenyl Trost (1.235)	A	toluene	25	12	52
5	(<i>R,R</i>)-DACH-Phenyl Trost (1.235)	A	2:1 hexane/toluene	25	12	53
6	(<i>R,R</i>)-DACH-Naphthyl Trost (1.236)	A	DME	25	12	22
7	(<i>R,R</i>)-DACH-Naphthyl Trost (1.236)	A	MTBE	25	12	24
8	(<i>R,R</i>)-DACH-Naphthyl Trost (1.236)	A	THF	25	12	24
9	(<i>R,R</i>)-DACH-Naphthyl Trost (1.236)	A	toluene	25	12	26
10	(<i>R,R</i>)-DACH-Naphthyl Trost (1.236)	A	2:1 hexane/toluene	25	12	29
11	(<i>R,R</i>)-ANDEN-Phenyl Trost (1.237)	A	DME	25	12	6
12	(<i>R,R</i>)-ANDEN-Phenyl Trost (1.237)	A	MTBE	25	12	24
13	(<i>R,R</i>)-ANDEN-Phenyl Trost (1.237)	A	THF	25	12	25
14	(<i>R,R</i>)-ANDEN-Phenyl Trost (1.237)	A	toluene	25	12	13
15	(<i>R,R</i>)-ANDEN-Phenyl Trost (1.237)	A	2:1 hexane/toluene	25	12	27
16	(<i>R,R</i>)-DACH-Phenyl Trost (1.235)	A	THF	-15	24	48
17	(<i>R,R</i>)-DACH-Phenyl Trost (1.235)	A	2:1 hexane/toluene	-15	24	66
18	(<i>R,R</i>)-DACH-Phenyl Trost (1.235)	A	THF	-60	24	46
19	(<i>R,R</i>)-DACH-Phenyl Trost (1.235)	A	2:1 hexane/toluene	-60	24	55
20	(<i>R,R</i>)-DACH-Phenyl Trost (1.235)	A	THF	-78	24	54
21	(<i>R,R</i>)-DACH-Phenyl Trost (1.235)	A	2:1 hexane/toluene	-78	24	54
22 ^{a)}	(<i>R,R</i>)-DACH-Phenyl Trost (1.235)	A	toluene	-10	2	60
23 ^{a)}	(<i>R,R</i>)-DACH-Phenyl Trost (1.235)	A	2:1 hexane/toluene	-10	2	66
24 ^{a)}	(<i>R,R</i>)-DACH-Phenyl Trost (1.235)	B	toluene	-10	2	64
25 ^{a)}	(<i>R,R</i>)-DACH-Phenyl Trost (1.235)	B	2:1 hexane/toluene	-10	2	59

26^{a)b)}	(<i>R,R</i>)-DACH-Phenyl Trost (I.235)	B	toluene	-10	2	64
25^{a)c)}	(<i>R,R</i>)-DACH-Phenyl Trost (I.235)	B	toluene	-10	2	17

a) Tsuji allylation after passage of the preformed catalyst through a plug of glass filter paper; recrystallized ligand used.
 b) Pd₂dba₃ to ligand ratio of 1:2.2
 c) Pd₂dba₃ to ligand ratio of 1:2.2

Procedure C: The reaction was carried out at given concentrations in a glovebox under nitrogen atmosphere. To tris(dibenzylideneacetone)dipalladium(0) and ligand (3.30 μmol, 11.0 mol%) a solvent was added and the catalyst was stirred for 30 min at 25 °C. A solution of carbonate **I.228** (10.0 mg, 0.030 mmol, 1 eq.) in solvent was added to the preformed catalyst and the reaction was stirred at the designated temperature for the designated time, prior to dilution of the sample with hexanes and ether and analysis of the %*ee* by chiral HPLC.

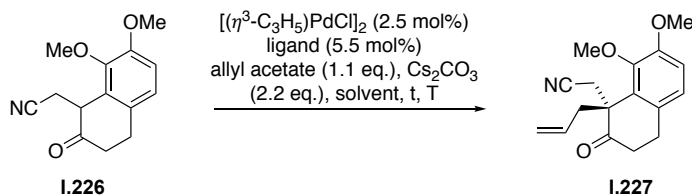


Entry	Conc. (M)	Pd ₂ (dba) ₃	Solvent	T (°C)	t (h)	% <i>ee</i>
1^{a)}	0.03	5 mol%	toluene	-10	2	64
2^{a)}	0.03	5 mol%	2:1 hexane/toluene	-10	2	59
3^{a)}	0.01	5 mol%	toluene	-10	2	66
4^{a)}	0.01	5 mol%	2:1 hexane/toluene	-10	2	58
5^{a)}	0.001	5 mol%	toluene	-10	2	66
6^{a)}	0.001	5 mol%	2:1 hexane/toluene	-10	2	62
7^{a)}	0.03	1 mol%	toluene	-10	2	60
8^{a)}	0.03	1 mol%	2:1 hexane/toluene	-10	2	66
9^{a)}	0.03	5 mol%	toluene	-30	2	50
10^{a)}	0.03	5 mol%	2:1 hexane/toluene	-30	2	64

a) Tsuji allylation after passage of the preformed catalyst through a plug of glass filter paper; recrystallized ligand used.

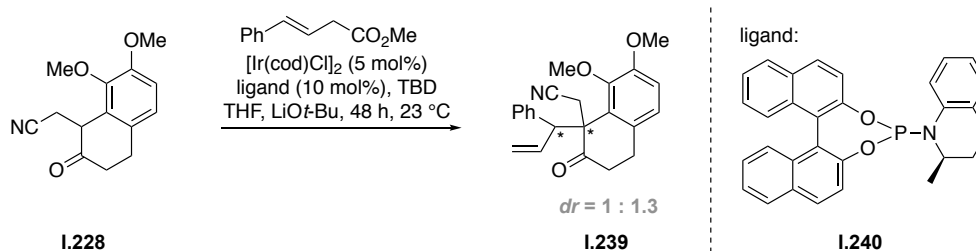
Procedure D: The reaction was carried out at a concentration of 0.18 M in a glovebox under nitrogen atmosphere. Ketone **I.226** (38 mg, 0.16 mmol, 1 eq.) and Cs₂CO₃ (51 mg, 0.16 mmol, 1 eq.) were dissolved in degassed DME (0.5 mL) and stirred at room temperature for 15 min. before being cooled to -78 °C. In a second flask, allylpalladium (II) chloride dimer [(η^3 -C₃H₅)PdCl]₂ (1.4 mg, 3.9 μmol, 2.5 mol%) and ligand (7.8 μmol, 5.0 mol%) were dissolved in

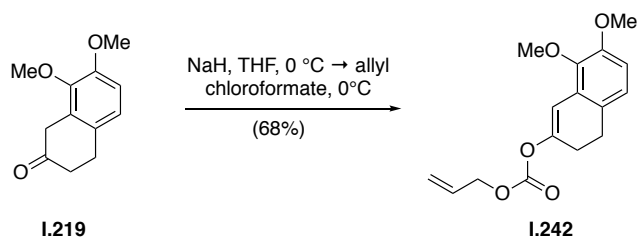
DME (0.4 mL) and stirred at room temperature for 15 min. before allyl acetate (18 μ L, 0.17 μ mol, 1.1 eq.) was added. Stirring was continued for another 5 min., then the preformed catalyst was slowly added *via* syringe into the enolate solution at -78 $^{\circ}$ C. The mixture was slowly allowed to warm to 0 $^{\circ}$ C and stirred at this temperature for 12 h, prior to dilution of the sample with hexanes and ether and analysis of the %*ee* by chiral HPLC.



Entry	Ligand	Solvent	T ($^{\circ}$ C)	t (h)	% <i>ee</i>
1	(<i>R,R</i>)-DACH-Phenyl Trost (I.235)	DME	0	12	7
2	(<i>R,R</i>)-DACH-Naphthyl Trost (I.236)	DME	0	12	5
3	(<i>R,R</i>)-ANDEN-Phenyl Trost (I.237)	DME	0	12	2

Procedure E: The reaction was carried out at a concentration of 0.025 M in a glovebox under nitrogen atmosphere. $[\text{Ir}(\text{cod})\text{Cl}]_2$ (1.0 mg, 1.5 μ mol, 5 mol%), ligand **I.240** (1.4 mg, 3.0 μ mol, 10 mol%), and TBD (0.84 mg, 6.0 μ mol, 20 mol%) were dissolved in degassed THF (0.3 mL) and stirred at 25 $^{\circ}$ C for 10 min, generating an orange solution. In a second vial, $\text{LiO}t\text{-Bu}$ (3.6 mg, 45 μ mol, 1.5 eq.) was dissolved in 0.3 mL of THF, then ketone **I.228** (10 mg, 30 μ mol, 1.0 eq.) was added. After stirring for 10 min, the preformed catalyst solution was transferred to this vial, followed by cinnamyl carbonate (12 mg, 60 μ mol, 2.0 eq.). The vial was sealed and stirred at 25 $^{\circ}$ C for 48 h outside the glovebox prior to dilution of the sample with hexanes and ether and analysis of the %*ee* by chiral HPLC.

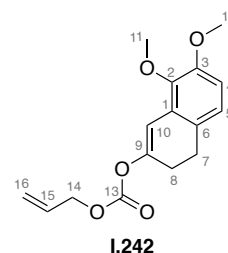


Allyl (7,8-dimethoxy-3,4-dihydronaphthalen-2-yl) carbonate (**I.242**)

To a solution of ketone **I.219** (300 mg, 1.45 mmol, 1.0 eq.) in THF (15 mL) was added sodium hydride (60 wt% in mineral oil, 64.0 mg, 1.60 mmol, 1.1 eq.) at 0 °C and the mixture was stirred for 1 h at this temperature. Allyl chloroformate (10 v% in THF, 175 mg, 1.45 mmol, 1.0 eq.) was added and the reaction was stirred at 0 °C for an additional 30 min. The reaction was quenched with H₂O (100 mL), extracted with EtOAc (3 × 100 mL) and the combined organic layers were washed with saturated aqueous NaCl solution (200 mL), dried (MgSO₄) and concentrated under reduced pressure. Flash column chromatography [PE/EtOAc, 9:1 to 3:1] afforded carbonate **I.242** (286 mg, 0.985 mmol, 68%) as a colorless oil.

$R_f = 0.55$ [PE/EtOAc, 5:1].

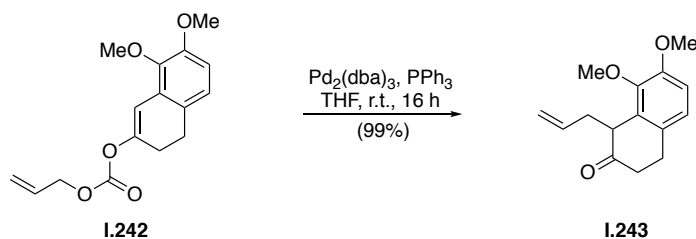
¹H NMR (400 MHz, CDCl₃): $\delta = 6.81$ (d, $J = 8.2$ Hz, 1H, H-5), 6.68 (d, $J = 8.2$ Hz, 1H, H-4), 6.65 (s, 1H, H-10), 5.98 (ddt, $J = 16.5, 10.3, 5.8$ Hz, 1H, H-15), 5.41 (dq, $J = 17.2, 1.4$ Hz, 1H, H-16a), 5.32 (dt, $J = 10.4, 1.2$ Hz, H-16b), 4.70 (dt, $J = 5.9, 1.3$ Hz, 2H, H-14), 3.83 (s, 3H, H-12), 3.79 (s, 3H, H-11), 2.93 (t, $J = 8.2$ Hz, 2H, H-7), 2.53 (t, $J = 8.1$ Hz, 2H, H-8) ppm.



¹³C NMR (101 MHz, CDCl₃): $\delta = 152.7$ (C-13), 151.3 (C-3), 151.3 (C-2), 144.8 (C-15), 131.1 (C-6), 126.8 (C-1), 126.2 (C-9), 122.4 (C-5), 119.3 (C-16), 110.2 (C-4), 109.2 (C-10), 68.9 (C-14), 61.1 (H-11), 55.8 (H-12), 28.1 (C-7), 26.0 (C-8) ppm.

IR (ATR): $\tilde{\nu} = 2940$ (w), 2835 (w), 1754 (s), 1665 (w), 1604 (w), 1577 (w), 1485 (m), 1456 (m), 1422 (m), 1362 (w), 1333 (w), 1313 (w), 1294 (w), 1222 (s), 1159 (m), 1090 (s), 1058 (m), 1032 (m), 978 (m), 940 (m), 872 (m), 802 (m), 778 (m), 752 (m), 679 (m), 668 (m) cm⁻¹.

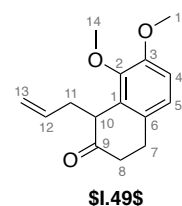
HRMS (ESI): calcd. for C₁₆H₂₂O₄N⁺: 308.1492 [M+NH₄]⁺
 found: 308.1492 [M+NH₄]⁺.

1-Allyl-7,8-dimethoxy-3,4-dihydronaphthalen-2(1H)-one (**I.243**)

Tris(dibenzylideneacetone)dipalladium(0) (7.89 mg, 8.61 μmol , 2.5 mol%) and PPh_3 (5.65 mg, 21.5 μmol , 6.25 mol%) were dissolved in degassed THF (3 mL, 3 \times freeze-pump-thaw) and stirred for 30 min. at room temperature. A solution of carbonate **I.242** (100 mg, 0.344 mmol, 1.0 eq.) dissolved in degassed THF (2 mL, 3 \times freeze-pump-thaw) was added to the preformed catalyst and the reaction was stirred at room temperature for 16 h, prior to concentrating the reaction mixture under reduced pressure. Flash column chromatography [PE/EtOAc, 9:1] afforded allylcyclohexanone **I.243** (84.2 mg, 0.342 mmol, 99%) as a colorless oil.

$R_f = 0.57$ [PE/EtOAc 3:1].

$^1\text{H NMR}$ (400 MHz, CDCl_3): $\delta = 6.90$ (d, $J = 8.3$ Hz, 1H, H-5), 6.79 (d, $J = 8.2$ Hz, 1H, H-4), 5.75–5.63 (m, 1H, H-12), 4.98–4.89 (m, 2H, H-13), 3.86 (s, 3H, H-15), 3.83 (s, 4H, H-10, H-14), 3.13 (ddd, $J = 16.8, 12.3, 5.3$ Hz, 1H, H-7a), 2.86 (ddd, $J = 15.6, 6.5, 3.1$ Hz, 1H, H-7b), 2.73–2.60 (m, 2H, H-8a, H-11b), 2.55 (dt, $J = 14.1, 7.3$ Hz, 1H, H-11a), 2.42 (ddd, $J = 17.0, 12.4, 6.5$ Hz, 1H, H-8b) ppm.

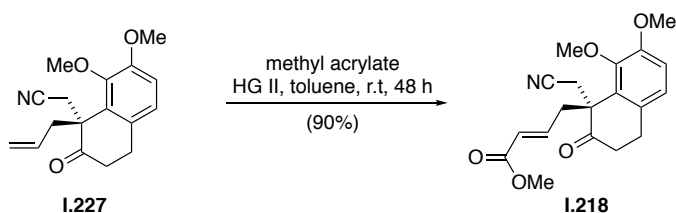


$^{13}\text{C NMR}$ (101 MHz, CDCl_3): $\delta = 212.8$ (C-1), 151.4 (C-3), 146.7 (C-2), 135.0 (C-12), 131.1 (C-1), 129.5 (C-6), 123.1 (C-5), 117.3 (C-11), 111.0 (C-4), 60.9 (C-14), 55.9 (C-15), 48.4 (C-10), 38.4 (C-8), 38.1 (C-11), 27.3 (C-7) ppm.

IR (ATR): 2940 (w), 1709 (s), 1605 (w), 1491 (s), 11456 (m), 1344 (m), 1276 (s), 1221 (m), 1084 (m), 1053 (s), 998 (m), 916 (m), 806 (m) cm^{-1} .

HRMS (ESI): calcd. for $\text{C}_{15}\text{H}_{19}\text{O}_3^+$: 247.1329 [M+H]⁺
 found: 257.1329 [M+H]⁺.

Methyl-4-(1-(cyanomethyl)-7,8-dimethoxy-2-oxo-1,2,3,4-tetra-hydronaphthalen-1-yl)but-2-enoate (I.218)



To a solution of α -allylcyclohexanone **I.227** (500.0 mg, 1.75 mol, 1.0 eq.) and methyl acrylate (2.16 mL, 26.0 mmol, 15 eq.) in toluene (20 mL) was added Hoveyda–Grubbs catalyst 2nd generation (104 mg, 123 μ mol, 7 mol%) and the reaction was stirred for 48 h at room temperature. The reaction was diluted with H₂O (40 mL) and extracted with EtOAc (3 \times 40 mL). The combined organic layers were washed with saturated aqueous NaCl solution (60 mL), dried (MgSO₄) and concentrated under reduced pressure. Flash column chromatography [PE/EtOAc, 6:1] afforded conjugated ester **I.218** (539 mg, 1.57 mmol, 90%) as a colorless solid.

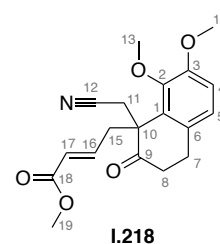
E/Z-ratio: 27:1 (determined by integrals of H-13 in ¹H NMR).

Crystals suitable for single-crystal X-ray analysis (Section 9.1) were obtained from recrystallization [PE/EtOAc, 15:1] at 0 °C.

R_f = 0.24 [PE/EtOAc, 3:1].

mp: 78–81 °C.

¹H NMR (600 MHz, CDCl₃) of the *E*-isomer: δ = 6.93–6.87 (m, 2H, H-4, H-5), 6.46 (ddd, *J* = 15.5, 9.3, 6.2 Hz, 1H, H-16), 5.72 (ddd, *J* = 15.5, 1.6, 1.0 Hz, 1H, H-17), 3.96 (s, 3H, H-13), 3.88 (s, 3H, H-14), 3.65 (s, 3H, H-19), 3.32 (d, *J* = 16.4 Hz, 1H, H-11a), 3.09 (d, *J* = 16.4 Hz, 1H, H-11b), 3.07–3.01 (m, 2H, H-15a, H-7a), 2.92 (ddd, *J* = 15.8, 7.4, 5.5 Hz, 1H, H-7b), 2.82 (ddd, *J* = 0.9, 9.3, 13.8 Hz, 1H, H-15b), 2.73 (ddd, *J* = 13.7, 7.6, 5.2 Hz, 1H, H-8a), 2.63 (ddd, *J* = 13.9, 9.6, 5.5 Hz, 1H, H-8b) ppm.

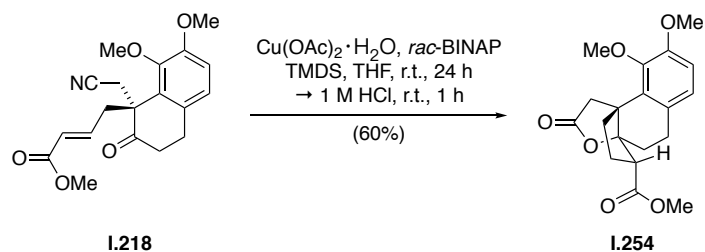


¹³C NMR (150 MHz, CDCl₃) of the *E*-isomer: δ = 210.3 (C-9), 166.1 (C-18), 151.5 (C-3), 147.8 (C-2), 142.5 (C-16), 129.8 (C-6), 128.3 (C-1), 124.6 (C-17), 123.8 (C-5), 117.4 (C-12), 113.0 (C-4), 60.6 (C-13), 55.8 (C-14), 53.4 (C-10), 51.5 (C-19), 40.6 (C-15), 39.2 (C-8), 28.1 (C-7), 25.5 (C-11) ppm.

IR (ATR): $\tilde{\nu}$ = 2948 (w), 1719 (s), 1657 (w), 1488 (m), 1438 (m), 1438 (w), 1347 (w), 1277 (s), 1214 (w), 1171 (m), 1111 (w), 1027 (w), 982 (w), 807 (w) cm⁻¹.

HRMS (EI): calcd. for $C_{19}H_{25}N_2O_5^+$ 361.1758 $[M+NH_4]^+$
 found: 361.1760 $[M+NH_4]^+$.

(3*R*,3*aS*,9*bR*)-Methyl 8,9-dimethoxy-11-oxo-2,3,4,5-tetrahydro-1*H*-3*a*,9*b*-(epoxyethano)-cyclopenta-[*a*]naphthalene-3-carboxylate (I.254)

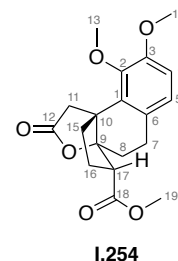


A solution of $Cu(OAc)_2 \cdot H_2O$ (28.9 mg, 146 μ mol, 0.5 eq.) and *rac*-BINAP (90.0 mg, 146 μ mol, 0.5 eq.) in deg. THF (3 mL) was stirred for 15 min. before TMDS (39.1 mg, 291 μ mol, 1 eq.) was added. After additional 15 min. a solution of unsaturated ester **I.218** (100 mg, 291 μ mol, 1 eq.) in deg. THF (1 mL + 0.5 mL rinse) was added rapidly and the reaction stirred for 24 h at room temperature. The reaction was quenched by the addition of aqueous 1 M HCl (2 mL) and the mixture stirred for 1 h before it was diluted by the addition of aqueous saturated NH_4Cl (20 mL) and TMEDA (0.1 mL). The mixture was extracted with EtOAc (3 \times 20 mL) and the combined organic layers were washed with saturated aqueous NaCl solution (40 mL), dried ($MgSO_4$) and concentrated under reduced pressure. Flash column chromatography [pent/ Et_2O , 3:1] afforded tetracyclic lactone **I.254** (60.6 mg, 176 μ mol, 60%) as colorless crystals.

Crystals suitable for single-crystal X-ray analysis (Section 9.1) were obtained from recrystallization [PE/ $EtOAc$, 20:1] at 0 $^{\circ}C$.

$R_f = 0.24$ [PE/ $EtOAc$, 3:1].

1H NMR (400 MHz, $CDCl_3$) $\delta = 6.86$ – 6.76 (m, 2H, H-4, H-5), 3.89 (s, 3H, H-13), 3.85 (s, 3H, H-14), 3.77 (s, 3H, H-19), 3.21 (d, $J = 18.7$ Hz, 1H, H-11a), 2.94 (dd, $J = 6.8, 11.4$ Hz, 1H, H-17), 2.86– 2.77 (m, 2H, H-11b, H-7a), 2.72 (dd, $J = 10.0, 21.8$ Hz, 1H, 8a), 2.60 (dd, $J = 4.4, 13.4$ Hz, 1H, H-7b), 2.52 (ddd, $J = 13.7, 7.5, 1.8$ Hz, 1H, H-8b), 2.30– 2.14 (m, 1H, H-15a), 2.01– 1.87 (m, 2H, H-16), 1.82 (dddd, $J = 13.2, 12.1, 7.3, 0.8$ Hz, 1H, H-16a) ppm.

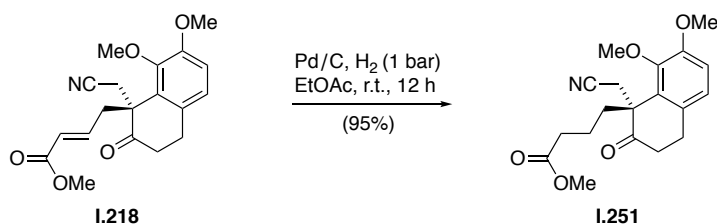


^{13}C NMR (101 MHz, CDCl_3): δ = 177.7 (C-12), 170.7 (C-18), 151.5 (C-2 or C-3), 147.0 (C-2 or C.3), 136.0 (C-1), 126.9 (C-6), 123.2 (C-5), 111.5 (C-4), 95.1 (C-9), 60.5 (C-13), 55.9 (C-14), 52.1 (C-19), 50.6 (C-17), 50.2 (C-10), 44.1 (C-11), 40.3 (C-15), 30.4 (C-7), 26.0 (C-8), 25.4 (C-16) ppm.

IR (ATR): $\tilde{\nu}$ = 2927 (m), 2850 (w), 1772 (s), 1735 (s), 1603 (w), 1489 (s), 1455 (m), 1418 (w), 1355 (w), 1279 (s), 1207 (m), 1192 (m), 1062 (s), 1026 (m) cm^{-1} .

HRMS (EI): calcd. for $\text{C}_{20}\text{H}_{27}\text{NO}_5^+$: 346.1651 $[\text{M}+\text{H}]^+$
found: 346.1649 $[\text{M}+\text{H}]^+$.

Methyl 4-(1-(cyanomethyl)-7,8-dimethoxy-2-oxo-1,2,3,4-tetrahydronaphthalen-1-yl)-butanoate (I.251)



To a solution of crude α,β -unsaturated ester **I.218** (2.00 g, 5.82 mmol, 1.0 eq.) in EtOAc (50 mL), Pd/C (10 wt%, 200 mg) was added. The flask was purged with H_2 five times and stirred under H_2 atmosphere (1 atm) at room temperature for 12 h. The catalyst was removed by filtration through a pad of silica, which was washed with EtOAc (100 mL) to afford saturated ester **I.251** (1.90 g, 5.50 mmol, 95%) as a colorless solid.

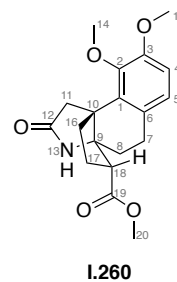
Crystals suitable for single-crystal X-ray analysis (Section 9.1) were obtained from recrystallization [CHCl_3] at 20 $^\circ\text{C}$.

R_f = 0.24 [PE/EtOAc, 3:1].

mp: 85–88 $^\circ\text{C}$.

^1H NMR (400 MHz, CDCl_3): δ = 6.97–6.79 (m, 2H, H-4, H-5), 3.92 (s, 3H, H-13), 3.85 (s, 3H, H-14), 3.58 (s, 3H, H-7), 3.31 (d, J = 16.4 Hz, 1H, H-11a), 3.16–2.91 (m, 3H, H-11b, H-19), 2.75 (t, J = 7.0 Hz, 2H, H-8), 2.17 (dt, J = 7.9, 6.6 Hz, 2H, H-17), 2.05 (dt, J = 11.0, 4.9 Hz, 2H, H-15), 1.43–1.25 (m, 1H, H-16a), 1.28–1.12 (m, 1H, H-16b) ppm.

¹H NMR (400 MHz, CDCl₃) δ = 6.81–6.71 (m, 2H, H-4, H-5), 6.47 (s, 1H, H-13), 3.86 (s, 3H, H-14), 3.82 (s, 3H, H-15), 3.71 (s, 3H, H-20), 2.98 (d, J = 17.7 Hz, 1H, H-11a), 2.87 (dd, J = 11.8, 6.4 Hz, 1H, H-18), 2.74 (dt, J = 16.5, 4.8 Hz, 1H, H-7a), 2.67 (dd, J = 11.8, 4.3 Hz, 1H, H-7b), 2.58 (d, J = 17.7 Hz, 1H, H-11b), 2.49 (dd, J = 12.7, 7.4 Hz, 1H, H-16a), 2.21 (dt, J = 13.6, 4.4 Hz, 1H, H-8a), 2.05 (td, J = 11.2, 10.5, 6.8 Hz, 1H, H-17a), 2.12–1.82 (m, 3H, H-17b, H-16b, H-8b) ppm.



¹³C NMR (101 MHz, CDCl₃): δ = 175.8 (C-12), 173.3 (C-19), 151.5 (C-3), 147.2 (C-2), 137.6 (C-1), 126.7 (C-6), 123.2 (C-5), 111.1 (C-4), 69.2 (C-9), 60.5 (C-14), 55.8 (C-15), 52.0 (C-20), 49.6 (C-18), 49.3 (C-10), 46.5 (C-11), 41.9 (C-16), 31.6 (C-8), 26.9 (C-17), 26.0 (C-7) ppm.

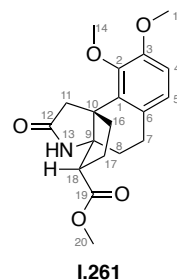
IR (ATR): $\tilde{\nu}$ = 3185 (w), 2952 (m), 2363 (w), 2334 (w), 1734 (m), 1693 (s), 1488 (m), 1416 (m), 1351 (w), 1279 (m), 1214 (m), 1098 (m), 1059 (w), 1023 (w), 984 (w), 797 (w) cm⁻¹.

HRMS (EI): calcd. for C₁₉H₂₃NO₅⁺: 345.1576 [M+H]⁺
 found: 345.1581 [M+H]⁺.

Characterization of the minor diastereomer (**I.261**):

R_f = 0.39 [EtOAc].

¹H NMR (400 MHz, CDCl₃) δ = 6.80–6.72 (m, 2H, H-4, H-5), 6.04 (s, 1H, H-13), 3.92 (s, 3H, H-14), 3.84 (s, 3H, H-15), 3.75 (s, 3H, H-20), 3.13 (dd, J = 11.1, 8.4 Hz, 1H, H-18), 2.93 (d, J = 18.1 Hz, 1H, H-11a), 2.86–2.71 (m, 2H, H-8a, H-11b), 2.58 (dt, J = 16.1, 4.3 Hz, 1H, H-8b), 2.46 (dt, J = 14.0, 9.2 Hz, 1H, H-17a), 2.21–2.10 (m, 1H, H-17b), 2.10–1.95 (m, 2H, H-16), 1.76 (dd, J = 8.4, 4.3 Hz, 2H, H-7) ppm.

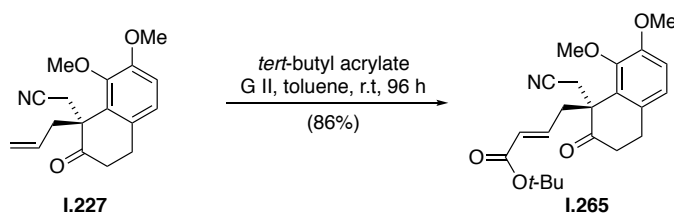


¹³C NMR (101 MHz, CDCl₃): δ = 176.3 (C-12), 172.7 (C-19), 151.4 (C-3), 147.2 (C-2), 136.2 (C-1), 127.4 (C-6), 122.7 (C-5), 111.5 (C-4), 77.0 (C-9), 69.7 (C-14), 60.5 (C-), 55.9 (C-15 or C-18), 55.8 (C-15 or C-18), 51.9 (C-20), 50.6 (C-10), 48.1 (C-11), 39.1 (C-17), 26.2 (C-7), 25.6 (C-16), 24.5 (C-8) ppm.

IR (ATR): $\tilde{\nu}$ = 3210 (w), 2945 (w), 1732 (m), 1693 (s), 1489 (m), 1453 (m), 1437 (w), 1415 (w), 1361 (w), 1280 (m), 1217 (m), 1171 (w), 1102 (w), 1072 (w), 1031 (w), 988 (w), 801 (w), 760 (w) cm⁻¹.

HRMS (EI): calcd. for C₁₉H₂₃NO₅⁺: 345.1576 [M]⁺
 found: 345.1571 [M]⁺.

tert-Butyl (R,E)-4-(1-(cyanomethyl)-7,8-dimethoxy-2-oxo-1,2,3,4-tetrahydronaphthalen-1-yl)but-2-enoate (**I.265**)

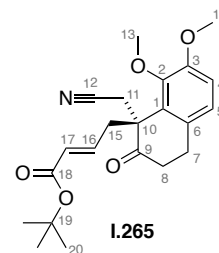


To a solution of α -allylcyclohexanone **I.227** (30.0 mg, 105 μ mol, 1.0 eq.) and *tert*-butyl acrylate (230 μ L, 1.58 mmol, 15 eq.) in toluene (2 mL) was added Grubbs catalyst 2nd generation (6.24 mg, 7.35 μ mol, 7 mol%) and the reaction was stirred for 96 h at room temperature. The reaction mixture was concentrated under reduced pressure. Flash column chromatography [PE/EtOAc, 9:1 to 3:1] afforded conjugated ester **I.265** (34.8 mg, 90.3 μ mol, 86%) as a colorless solid.

E/Z-ratio: 12:1 (determined by integrals of H-13 in ¹H NMR).

R_f = 0.70 [PE/EtOAc, 2:1].

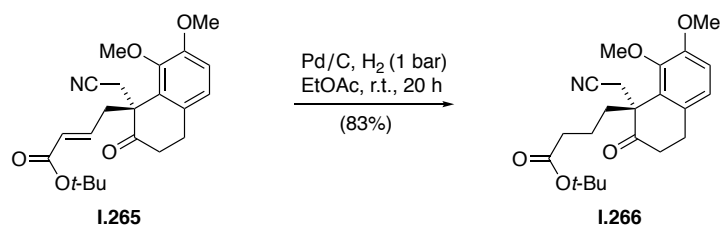
¹H NMR (400 MHz, CDCl₃) of the *E*-isomer: δ = 6.89 (s, 2H, H-4, H-5), 6.34 (ddd, J = 15.3, 9.4, 5.8 Hz, 1H, H-17), 5.69–5.61 (m, 1H, H-16), 3.96 (s, 3H, H-13), 3.88 (s, 3H, H-14), 3.33 (d, J = 16.4 Hz, 1H, H-11a), 3.09 (d, J = 16.4 Hz, 1H, H-11b), 3.05–2.96 (m, 2H, H-7a, H-15a), 2.96–2.88 (m, 1H, H-7b), 2.82–2.74 (m, 1H, H-15b), 2.74–2.59 (m, 2H, H-8), 1.40 (s, 9H, H-20) ppm.



¹³C NMR (101 MHz, CDCl₃) of the *E*-isomer: δ = 210.4 (C-9), 165.0 (C-18), 151.5 (C-3), 147.7 (C-2), 140.9 (C-17), 129.8 (C-6), 128.4 (C-1), 126.6 (C-16), 123.8 (C-5), 117.6 (C-12), 112.9 (C-4), 80.5 (C-19), 77.0 (C-10), 60.6 (C-13), 55.8 (C-14), 53.4 (C-15), 40.5 (C-8), 39.2 (C-7), 28.1 (C-20), 25.4 (C-11) ppm.

IR (ATR): $\tilde{\nu}$ = 2977 (m), 2940 (m), 2841 (w), 1713 (s), 1653 (w), 1602 (w), 1577 (w), 1487 (s), 1455 (m), 1416 (w), 1367 (m), 1346 (m), 1277 (s), 1247 (w), 1232 (s), 1221 (w), 1154 (s), 1110 (m), 1067 (w), 1054 (w), 1024 (w), 983 (m), 928 (w), 872 (w), 850 (w), 830 (w), 808 (m) cm⁻¹.

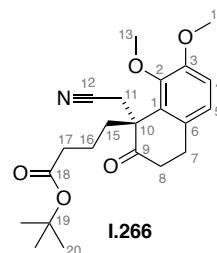
HRMS (EI): calcd. for C₂₂H₂₇NO₅⁺: 385.1884 [M]⁺
 found: 385.1879 [M]⁺.

***tert*-Butyl (R)-4-(1-(cyanomethyl)-7,8-dimethoxy-2-oxo-1,2,3,4-tetrahydronaphthalen-1-yl)butanoate (I.266)**

To a solution of crude α,β -unsaturated ester **I.265** (34.8 mg, 90.3 μmol , 1.0 eq.) in EtOAc (1.2 mL), Pd/C (10 wt%, 3.48 mg) was added. The flask was purged with H₂ five times and stirred under H₂ atmosphere (1 atm) at room temperature for 20 h. The catalyst was removed by filtration through a pad of silica, which was washed with EtOAc (5 mL) to afford saturated ester **I.266** (28.9 mg, 74.6 μmol , 83%) as a colorless oil.

$R_f = 0.69$ [PE/EtOAc, 2:1].

¹H NMR (400 MHz, CDCl₃): $\delta = 6.88$ (s, 2H, H-4, H-5), 3.93 (s, 3H, H-13), 3.87 (s, 3H, H-14), 3.33 (d, $J = 16.4$ Hz, 1H, H-11a), 3.15–2.92 (m, 3H, H-11b, H-7), 2.77 (t, $J = 7.0$ Hz, 2H, H-8), 2.15–1.98 (m, 4H, H-15, H-17), 1.38 (s, 9H, H-20), 1.34–1.23 (m, 1H, H-16a), 1.23–1.08 (m, 1H, H-16b) ppm.

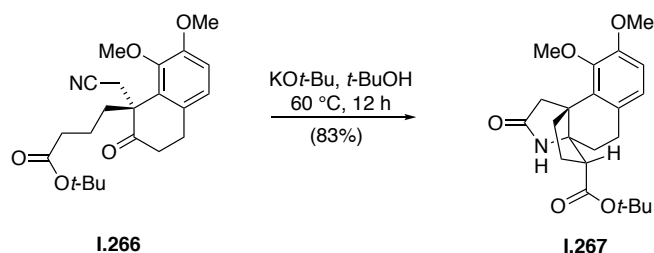


¹³C NMR (101 MHz, CDCl₃): $\delta = 211.4$ (C-9), 172.1 (C-18), 151.5 (C-3), 147.8 (C-2), 129.8 (C-1 or C-6), 129.6 (C-1 or C-6), 123.7 (C-5), 118.0 (C-12), 112.5 (C-4), 80.4 (C-19), 60.5 (C-13), 55.7 (C-14), 53.8 (C-10), 39.2 (C-8), 37.7 (C-15), 35.2 (C-17), 28.4 (C-7), 28.0 (C-20), 25.6 (C-11), 20.8 (C-16) ppm.

IR (ATR): $\tilde{\nu} = 2975$ (m), 2940 (m), 2841 (w), 1717 (s), 1602 (w), 1578 (w), 1487 (s), 1455 (m), 1416 (m), 1392 (w), 1367 (m), 1346 (m), 1274 (s), 1153 (s), 1107 (m), 1051 (m), 984 (w), 925 (w), 874 (w), 946 (w), 808 (w), 756 (w) cm⁻¹.

HRMS (EI): calcd. for C₂₂H₂₇NO₅⁺: 387.2040 [M]⁺
 found: 387.2043 [M]⁺.

tert-Butyl (3*R*,3*aR*,9*bR*)-8,9-dimethoxy-11-oxo-2,3,4,5-tetrahydro-1*H*-3*a*,9*b*-(epiminoethano)cyclo-penta[*a*]naphthalene-3-carboxylate (**I.267**)

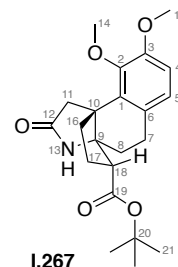


Saturated ester **I.266** (10.0 mg, 25.8 μmol , 1.0 eq.) was dissolved in *t*-BuOH (1 mL) and KO*t*-Bu (3.76 mg, 33.5 μmol , 1.3 eq.) was added. The mixture was heated to 60 °C for 12 h. H₂O (5 mL) was added and the aqueous layer was extracted with EtOAc (3 \times 10 mL). The combined organic layers were washed with saturated aqueous NaCl solution (10 mL), dried (MgSO₄) and concentrated under reduced pressure. Flash column chromatography [PE/EtOAc, 2:1 to 0:1] afforded the lactam **I.267** (8.3 mg, 21.4 μmol , 83%) as a colorless oil.

Crystals suitable for single-crystal X-ray analysis (Section 9.1) were obtained from recrystallization [CHCl₃] at 20 °C.

R_f = 0.41 [EtOAc/PE, 2: 1].

¹H NMR (400 MHz, CDCl₃) δ = 6.84–6.71 (m, 2H, H-5 and H-5), 6.45 (s, 1H, H-13), 3.88 (s, 3H, H-14), 3.84 (s, 3H, H-15), 3.02 (d, J = 17.8 Hz, 1H, H-11a), 2.80 (dt, J = 12.0, 5.8 Hz, 1H, H-18), 2.76–2.67 (m, 1H, H-7), 2.62 (d, J = 17.9 Hz, 1H, H-11b), 2.47 (dd, J = 12.7, 7.4 Hz, 1H, H-16a), 2.25 (dt, J = 13.6, 4.3 Hz, 1H, H-8a), 2.07–1.80 (m, 3H, H-8b, H-16b, H-17), 1.47 (s, 9H, H-21) ppm.

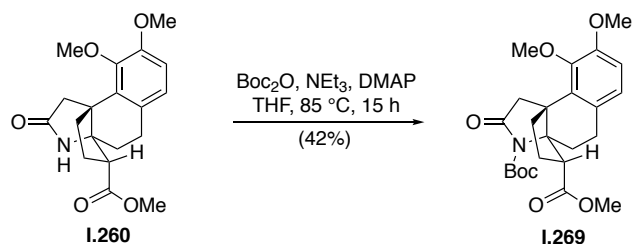


¹³C NMR (101 MHz, CDCl₃): δ = 176.0 (C-19), 172.1 (C-12), 151.4 (C-3), 147.2 (C-2), 137.8 (C-1), 126.7 (C-6), 123.2 (C-5), 111.0 (C-4), 81.5 (C-20), 69.2 (C-9), 60.5 (C-14), 55.8 (C-15), 50.1 (C-18), 49.7 (C-10), 46.3 (C-11), 41.7 (C-16), 31.0 (C-8), 28.2 (C-21), 26.9 (C-17), 26.1 (C-7) ppm.

IR (ATR): $\tilde{\nu}$ = 2974 (w), 2359 (m), 2338 (w), 2180 (w), 1718 (m), 1697 (s), 1654 (m), 1636 (m), 1617 (m), 1576 (w), 1559 (m), 1540 (m), 1522 (w), 1507 (w), 1457 (w), 1489 (m), 1419 (w), 1368 (w), 1280 (w), 1155 (w), 668 (w) cm⁻¹.

HRMS (EI): calcd. for C₂₂H₃₀NO₅⁺: 388.2118 [M+H]⁺
found: 388.2120 [M+H]⁺.

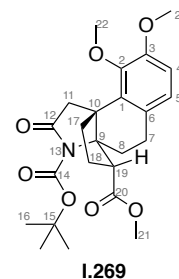
12-(*tert*-Butyl) 3-methyl (3*R*,3*aR*,9*bR*)-8,9-dimethoxy-11-oxo-2,3,4,5-tetrahydro-1*H*-3*a*,9*b*-(epiminoethano)cyclopenta[*a*]naphthalene-3,12-dicarboxylate (**I.269**)



Amide **I.260** (10.4 mg, 30.0 μmol , 1 eq.) was dissolved in THF (1 mL) and NEt_3 (3.64 mg, 5.00 μmol , 1.2 eq.) followed by Boc_2O (7.86 mg, 36.0 μmol , 1.2 eq.) and DMAP (4.40 mg, 36.0 μmol , 1.2 eq.) were added. The reaction mixture was heated to $85\text{ }^\circ\text{C}$ for 15 h. Afterwards the reaction was cooled to room temperature and diluted with EtOAc (50 mL). The organic phase was washed with 1 M aqueous HCl solution ($3 \times 20\text{ mL}$), H_2O ($3 \times 20\text{ mL}$) and saturated aqueous NaCl solution (20 mL), dried (MgSO_4) and concentrated under reduced pressure. Flash column chromatography [PE/EtOAc, 1:3 + 1% NEt_3] afforded Boc-protected amide **I.269** (5.60 mg, 12.6 μmol , 42%) as a yellow oil.

$R_f = 0.77$ [EtOAc/PE, 2:1].

$^1\text{H NMR}$ (400 MHz, CDCl_3) $\delta = 6.80\text{--}6.70$ (m, 2H, H-4, H-5), 3.89 (s, 3H, H-22), 3.83 (s, 3H, H-23), 3.67 (s, 3H, H-21), 3.12 (d, $J = 18.1\text{ Hz}$, 1H, H-11a), 3.02 (t, $J = 8.7\text{ Hz}$, 1H, H-19), 2.70–2.58 (m, 5H, H-11b, H-7, H-8a, H-17a), 2.14 (td, $J = 10.0, 8.8, 6.7\text{ Hz}$, 2H, H-18), 1.98–1.82 (m, 2H, H-8b, H-17b), 1.52 (s, 9H, H-16) ppm.

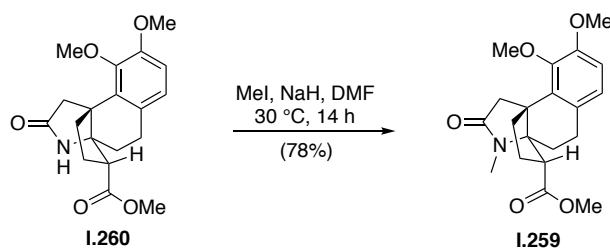


$^{13}\text{C NMR}$ (101 MHz, CDCl_3): $\delta = 174.5$ (C-12), 174.2 (C-20), 151.3 (C-3), 150.6 (C-14), 147.6 (C-2), 135.2 (C-1), 127.9 (C-6), 123.2 (C-5), 111.6 (C-4), 83.1 (C-15), 74.6 (C-9), 60.5 (C-22), 55.9 (C-23), 52.9 (C-19), 52.0 (C-21), 49.5 (C-10), 44.3 (C-11), 36.3 (C-17), 30.9 (C-8), 29.3 (C-18), 28.0 (C-16), 25.6 (C-7) ppm.

IR (ATR): $\tilde{\nu} = 2980$ (w), 2949 (w), 1784 (m), 1730 (s), 1603 (w), 1578 (w), 1489 (m), 1455 (m), 1436 (m), 1416 (w), 1394 (w), 1368 (m), 1301 (s), 1278 (s), 1284 (m), 1216 (w), 1195 (w), 1168 (s), 1100 (m), 1062 (m), 1014 (w), 981 (w), 968 (w), 927 (w), 885 (w), 848 (w), 800 (w), 749 (w), 734 (w) cm^{-1} .

HRMS (ESI): calcd. for $\text{C}_{24}\text{H}_{31}\text{NO}_7\text{Na}^+$: 468.1993 $[\text{M}+\text{Na}]^+$
 found: 468.1997 $[\text{M}+\text{Na}]^+$.

(3*R*,3*aS*,9*bR*)-Methyl 8,9-dimethoxy-12-methyl-11-oxo-2,3,4,5-tetrahydro-1*H*-3*a*,9*b*-(epiminoethano)-cyclopenta[*a*]naphthalene-3-carboxylate (**I.259**)



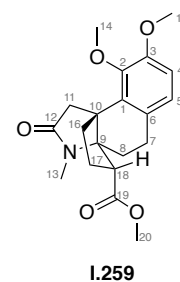
Amide **I.260** (2.71 g, 7.85 mol) was dissolved in DMF (125 mL) and NaH (60 wt% in mineral oil, 377 mg, 9.42 mmol, 1.2 eq.) was added to the stirring solution at 0 °C. The reaction mixture was kept at 0 °C and MeI (586 μ L, 9.42 mmol, 1.2 eq.) was added slowly. The reaction was heated to 30 °C and after 14 h it was stopped by the addition of saturated aqueous NH_4Cl solution (10 mL). A solution of 10% LiCl in H_2O (300 mL) was added and the aqueous layer was extracted with EtOAc (3 \times 500 mL). The combined organic layers were washed with saturated aqueous NaCl solution (500 mL), dried (MgSO_4) and concentrated under reduced pressure. Flash column chromatography [PE/EtOAc, 1:1 to 2:1] afforded *N*-methyl amide **I.259** (2.21 g, 6.15 mmol, 78%) as a bright yellow solid.

Crystals suitable for single-crystal X-ray analysis (Section 9.1) were obtained from recrystallization [CHCl_3] at 0 °C.

Full characterization of the major diastereomer (**I.259**):

$R_f = 0.25$ [EtOAc/PE, 2:1].

$^1\text{H NMR}$ (400 MHz, CDCl_3) $\delta = 6.76$ (s, 2H, H-4, H-5), 3.89 (s, 3H, H-13), 3.84 (s, 3H, H-14), 3.73 (s, 3H, H-19), 3.05 (d, $J = 17.7$ Hz, 1H, H-11a), 2.80 (dd, $J = 11.2, 6.7$ Hz, 1H, H-17), 2.70 (s, 3H, H-20), 2.55 (m, 2H, 11-b,), 2.55 (d, $J = 17.7$ Hz, 1H), 2.30 (ddd, $J = 13.6, 7.7, 4.4$ Hz, 1H), 2.20 – 2.07 (m, 1H), 2.00 (td, $J = 8.6, 4.1$ Hz, 1H), 1.95 – 1.87 (m, 1H), 1.81 (ddd, $J = 13.6, 11.6, 7.4$ Hz, 1H).

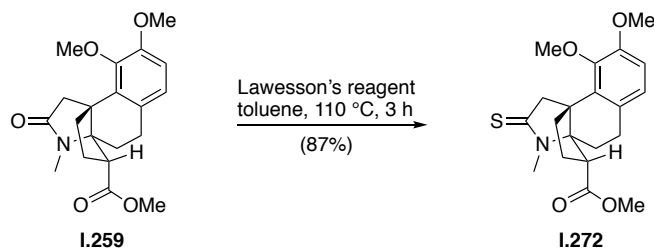


$^{13}\text{C NMR}$ (101 MHz, CDCl_3): $\delta = 176.9$ (C-12), 172.7 (C-18), 151.5 (C-2 or C-3), 147.4 (C-2 or C.3), 137.2 (C-1), 127.2 (C-6), 123.06 (C-5), 111.2 (C-4), 74.9 (C-9), 60.5 (C-13), 55.8 (C-14), 52.0 (C-19), 51.0 (C-17), 49.2 (C-10), 45.8 (C-11), 39.5 (C-15), 29.5 (C-7), 25.9 (C-8), 25.8 (C-16) ppm.

IR (ATR): $\tilde{\nu} = 2949$ (bm), 1733 (m), 1688 (s), 1487 (m), 1452 (w), 1417 (w), 1389 (w), 1279 (m), 1211 (w), 1169 (w), 1099 (1), 1062 (m), 981 (w), 803 (w) cm^{-1} .

HRMS (EI): calcd. for $C_{20}H_{25}NO_5^+$: 359.1727 [M]⁺
 found: 359.1719 [M]⁺.

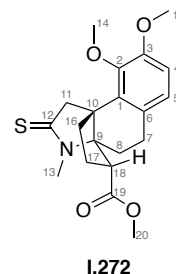
(3R,3a*S*,9bR)-methyl 8,9-dimethoxy-12-methyl-11-thioxo-2,3,4,5-tetrahydro-1*H*-3a,9b-(epi-minoethano)cyclopenta[*a*]naphthalene-3-carboxylate (I.272)



Lactame **I.259** (110 mg, 0.300 mmol, 1 eq) was dissolved in toluene (5 mL) and Lawesson's reagent (121 mg, 0.300 mmol, 1 eq.) was added to the stirring solution. The reaction was heated to 110 °C for 3 h in a pressure tube. The solvent was removed under reduced pressure and purification *via* flash column chromatography [PE/EtOAc, 6:1 to 1:1] afforded thionolactame **I.272** (98.5 mg, 0.262 mmol, 87%) as a bright yellow solid.

$R_f = 0.77$ [EtOAc/PE, 2:1].

¹H NMR (400 MHz, CDCl₃) $\delta = 6.76$ (s, 2H, H-4, H-5), 3.91 (s, 3H, H-14), 3.84 (s, 3H, H-15), 3.75 (s, 3H, H-20), 3.65 (dd, $J = 18.7, 1.2$ Hz, 1H, H-11a), 3.18 (d, $J = 18.7$ Hz, 1H, H-11b), 3.09 (d, $J = 1.1$ Hz, 3H, H-13), 2.85 (dd, $J = 11.2, 6.7$ Hz, 1H, H-18), 2.74 (dd, $J = 8.8, 4.3$ Hz, 1H, H-7a), 2.67 – 2.57 (m, 2H, H-7b, H-16a), 2.36 (ddd, $J = 13.7, 7.6, 4.2$ Hz, 1H, H-8a), 2.13 – 1.99 (m, 2H, H-8b, H-17a), 1.93 (dtd, $J = 13.0, 7.1, 1.9$ Hz, 1H, H-17b), 1.81 (ddd, $J = 13.6, 11.6, 7.4$ Hz, 1H, H-16b) ppm.

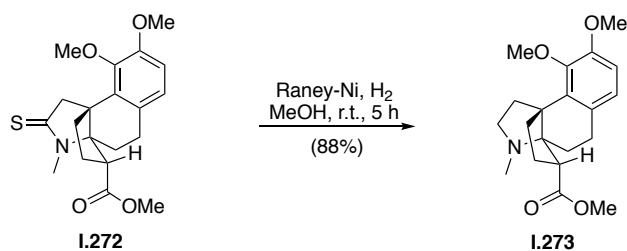


¹³C NMR (101 MHz, CDCl₃): $\delta = 202.4$ (C-12), 172.1 (C-19), 151.6 (C-3), 147.3 (C-2), 136.4 (C-1), 126.7 (C-6), 123.0 (C-5), 111.4 (C-4), 82.9 (C-9), 60.6 (C-14), 58.3 (C-11), 55.9 (C-15), 52.3 (C-20), 51.3 (C-10), 51.0 (C-18), 39.5 (C-16), 32.1 (C-13), 29.3 (C-8), 26.4 (C-17), 25.9 (C-7) ppm.

IR (ATR): $\tilde{\nu} = 2945$ (m), 2838 (w), 1732 (s), 1595 (w), 1488 (s), 1454 (m), 1417 (m), 1393 (m), 1355 (w), 1305 (m), 1278 (s), 1214 (m), 1166 (m), 1097 (m), 1062 (m), 979 (w), 934 (w), 802 (w) cm⁻¹.

HRMS (ESI): calcd. for $C_{20}H_{26}NO_4S^+$: 376.1577 [M+H]⁺
 found: 376.1573 [M+H]⁺.

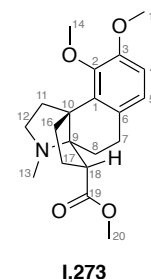
(3*R*,3*aS*,9*bR*)-methyl 8,9-dimethoxy-12-methyl-2,3,4,5-tetrahydro-1*H*-3*a*,9*b*-(epiminoethano)cyclo-penta[*a*]naphthalene-3-carboxylate (**I.273**)



To a solution of thionoamide **I.272** (96.3 mg, 0.257 mmol, 1.0 eq) in MeOH (5 mL), Raney-Ni (about 10 wt%, 0.2 mL Raney-Ni in MeOH) was added. The flask was purged with H₂ five times and stirred under H₂ atmosphere (1 atm) at room temperature for 5 h. The catalyst was removed by filtration through a pad of Celite®, which was washed with MeOH (100 mL). The filtrate was concentrated under reduced pressure and gave tertiary amine **I.273** (78.4 mg, 0.226 mmol, 88%) as a colorless oil.

$R_f = 0.78$ [DCM/MeOH, 10:1].

¹H NMR (400 MHz, CDCl₃) $\delta = 6.79$ – 6.75 (m, 1H, H-5), 6.75 – 6.70 (m, 1H, H-4), 3.88 (s, 3H, H-13), 3.84 (s, 3H, H-14), 3.72 (s, 3H, H-19), 2.99 (ddd, $J = 9.0, 7.8, 2.6$ Hz, 1H, H-12a), 2.67 (dd, $J = 12.8, 6.6$ Hz, 2H, H-7), 2.58 (dd, $J = 12.3, 6.0$ Hz, 1H, H-17), 2.54–2.41 (m, 2H, H-15a, H-12b), 2.29 (m, 2H, H-16a, H-11a), 2.25 (s, 3H, H-20), 2.15–2.06 (m, 1H, H-11b), 1.99 (q, $J = 7.1, 6.2$ Hz, 2H, H-8), 1.68 (dt, $J = 12.1, 6.2$ Hz, 1H, H-16b), 1.56 (td, $J = 12.5, 6.9$ Hz, 1H, H-15b) ppm.

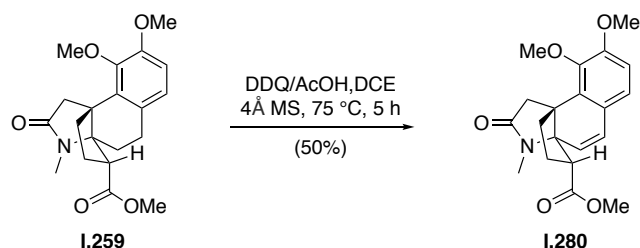


¹³C NMR (101 MHz, CDCl₃): $\delta = 174.11$ (C-18), 151.61 (C-2), 147.63 (C-3), 140.24 (C-1), 128.88 (C-6), 122.73 (C-5), 110.48 (C-4), 75.04 (C-9), 60.63 (C-14), 56.23 (C-10), 55.96 (C-13), 54.76 (C-12), 51.51 (C-19), 51.19 (C-17), 41.13 (C-15), 40.63 (C-11), 35.50 (C-20), 27.26 (C-7), 25.83 (C-8), 25.66 (C-16) ppm.

IR (ATR): $\tilde{\nu} = 2926$ (s), 1733 (s), 1486 (s), 1454 (m), 1208 (m), 1064 (m) 806 (m) cm⁻¹.

HRMS (ESI): calcd. for C₂₀H₂₈NO₄⁺: 346.2013 [M+H]⁺
 found: 346.2010 [M+H]⁺.

**Methyl (3*R*,3*aR*,9*bR*)-8,9-dimethoxy-12-methyl-11-oxo-2,3-dihydro-1*H*-3*a*,9*b*-(epiminoetha-
no)cyclopenta[*a*]naphthalene-3-carboxylate (**I.280**)**

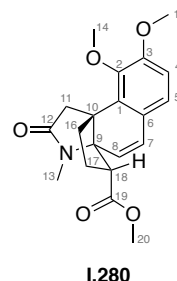


Lactam **I.259** (30.0 mg, 86.9 μmol , 1.0 eq.) was dissolved in DCE (3 mL) and 4Å MS followed by DDQ (197 mg, 869 μmol , 10 eq.) and AcOH (50.0 μL , 869 μmol , 10 eq.) were added. The mixture was heated to 75 °C for 5 h and after cooling to room temperature it was diluted with H₂O (100 mL). The mixture was extracted with EtOAc (3 \times 100 mL) and the combined organic layers were washed with aqueous saturated NaCl solution (200 mL), dried (MgSO₄) and concentrated under reduced pressure. Flash column chromatography [PE/EtOAc, 1:1 to 2:1] afforded styrene derivative **I.280** (15.4 mg, 43.1 μmol , 50%) as a colorless solid.

Crystals suitable for single-crystal X-ray analysis (Section 9.1) were obtained from recrystallization [CHCl₃] at 20 °C.

$R_f = 0.40$ [EtOAc /PE, 3:1].

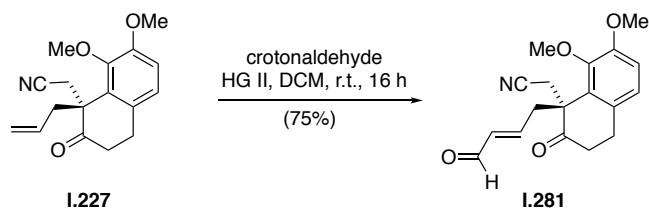
¹H NMR (400 MHz, CDCl₃) $\delta = 6.86\text{--}6.72$ (m, 2H, H-4 and H-5), 6.38 (d, $J = 10.0$ Hz, 1H, H-7), 6.23 (d, $J = 10.0$ Hz, 1H, H-8), 3.91 (s, 3H, H-14), 3.87 (s, 3H, H-15), 3.76 (s, 3H, H-20), 2.98 (d, $J = 18.1$ Hz, 1H, H-11a), 2.80–2.63 (m, 6H, H-11b, H-13, H-16a, H-18), 2.02–1.86 (m, 1H, H-17a), 1.86–1.70 (m, 2H, H-16b, H-17b) ppm.



¹³C NMR (101 MHz, CDCl₃): $\delta = 174.6$ (C-12), 172.2 (C-19), 153.2 (C-3), 146.7 (C-2), 135.2 (C-1), 125.8 (C-6), 123.0 (C-5), 122.2 (C-8), 110.8 (C-4), 73.4 (C-9), 60.6 (C-14), 56.6 (C-18), 55.7 (C-15), 52.0 (C-20), 47.9 (C-10), 46.8 (C-11), 42.0 (C-16), 26.5 (C-13), 23.1 (C-17) ppm.

IR (ATR): $\tilde{\nu} = 2946$ (w), 1733 (m), 1687 (s), 1490 (m), 1454 (m), 1390 (m), 1274 (s), 1213 (m), 1138 (m), 1071 (m), 961 (w), 818 (w) cm⁻¹.

HRMS (EI): calcd. for C₂₀H₂₄NO₅⁺: 358.1649 [M+H]⁺
 found: 358.1650 [M+H]⁺.

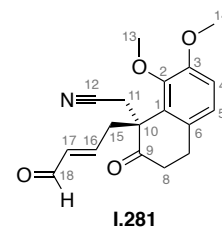
2-(7,8-Dimethoxy-2-oxo-1-(4-oxobutyl)-1,2,3,4-tetrahydronaphthalen-1-yl)acetonitrile (**I.281**)

To α -allylcyclohexanone **I.227** (100 mg, 351 μmol , 1.0 eq.) and Hoveyda–Grubbs catalyst 2nd generation (11.0 mg, 17.5 μmol , 5.0 mol%) was added degassed DCM (3 mL). Then, freshly distilled crotonaldehyde (369 mg, 450 μL , 5.26 mmol, 15 eq) was added and the reaction mixture stirred at room temperature for 16 h. After concentrating under reduced pressure, flash column chromatography [PE/EtOAc, 9:1] yielded unsaturated aldehyde **I.281** (82.7 mg, 264 μmol , 75%) as a colorless solid.

Crystals suitable for single-crystal X-ray analysis (Section 9.1) were obtained from recrystallization [PE/EtOAc, 15:1] at 0 °C.

R_f = 0.57 [PE/EtOAc, 1:1].

¹H NMR (400 MHz, CDCl₃): δ = 9.32 (d, J = 7.7 Hz, 1H, H-18), 6.96–6.86 (m, 2H, H-4, H-5), 6.33 (ddd, J = 15.3, 8.6, 6.6 Hz, 1H, H-16), 5.97 (ddt, J = 15.6, 7.7, 1.3 Hz, 1H, H-17), 3.99 (s, 3H, H-13), 3.89 (s, 3H, H-14), 3.36 (d, J = 16.4 Hz, 1H, H-11a), 3.17–2.99 (m, 4H, H-11b, H-15, H-7a), 2.92 (ddd, J = 15.8, 8.1, 5.3 Hz, 1H, H-7b), 2.80 (ddd, J = 13.5, 8.1, 5.2 Hz, 1H, H-8a), 2.66 (ddd, J = 14.1, 9.0, 5.3 Hz, 1H, H-8b) ppm.

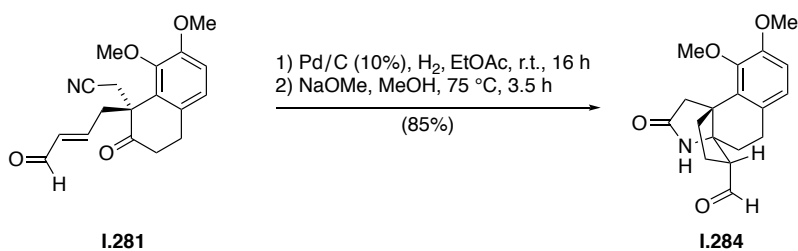


¹³C NMR (100 MHz, CDCl₃): δ = 210.0 (C-9), 193.1 (C-18), 151.6 (C-3), 151.0 (C-16), 147.7 (C-2), 135.7 (C-17), 129.6 (C-6), 128.1 (C-1), 123.9 (C-5), 117.3 (C-12), 113.1 (C-4), 60.7 (C-13), 55.8 (C-14), 53.3 (C-10), 40.4 (C-15), 39.1 (C-8), 28.2 (C-7), 25.7 (C-11) ppm.

IR (ATR): $\tilde{\nu}$ = 2943 (w), 2840 (w), 1716 (s), 1690 (s), 1487 (s), 1455 (m), 1415 (m), 1347 (w), 1275 (s) cm⁻¹.

HRMS (ESI): calcd. for C₁₈H₂₀O₄N⁺: 314.1387 [M+H]⁺
 found: 314.1390 [M+H]⁺.

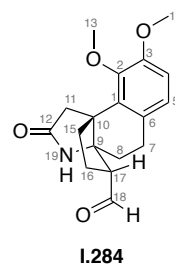
2-(7,8-Dimethoxy-2-oxo-1-(4-oxobutyl)-1,2,3,4-tetrahydronaphthalen-1-yl)acetonitrile (I.284)



A solution of the unsaturated aldehyde **I.281** (200 mg, 0.639 mmol, 1.0 eq) in dry EtOAc (7.0 mL) was added to palladium on activated charcoal (10 wt%, 20.0 mg, 2.9 mol%). The round bottom flask was purged with H₂ five times and the suspension was stirred under H₂ atmosphere at room temperature for 16 h. After removing the catalyst with a pad of celite, the pad was washed with EtOAc (50 mL) and the filtrate was concentrated under reduced pressure. The crude saturated aldehyde (185 mg crude yield) was immediately used in the next step. To a stirring solution of crude aldehyde (185 mg, assumed 0.587 mmol, 1.0 eq) in dry methanol (10 mL), NaOMe (41.2 mg, 763 μmol , 1.3 eq) was added. The solution was stirred at 75 $^\circ\text{C}$ for 3.5 h. After terminating the reaction with saturated aqueous NH₄Cl solution (25 mL), H₂O (100 mL) was added. The reaction mixture was extracted with EtOAc (3 \times 100 mL) and the combined organic layers washed with saturated aqueous NaCl solution, dried (MgSO₄) and concentrated under reduced pressure. Cascade product **I.284** (172 mg, 0.545 mmol, 85%, *dr* = 0.17:1.00) was obtained as a colorless oil.

R_f = 0.38 [EtOAc, 5% NEt₃].

¹H NMR (400 MHz, CHCl₃): δ = 9.80 (d, *J* = 0.9 Hz, 1H, H-18), 6.87–6.69 (m, 2H, H-4, H-5), 6.22 (s, 1H, H-19), 3.89 (s, 3H, H-13), 3.85 (s, 3H, H-14), 3.05–2.87 (m, 2H, H-11a, H-17), 2.81–2.63 (m, 2H, H-7), 2.63–2.53 (m, 2H, H-11b, H-15a), 2.26 (dt, *J* = 13.5, 4.3 Hz, 1H, H-8a), 2.14–1.93 (m, 3H, H-15b, H-16), 1.87 (td, *J* = 12.8, 4.8 Hz, 1H, H-8b) ppm.

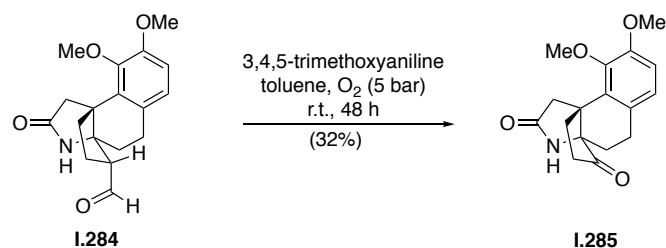


¹³C NMR (100 MHz, CHCl₃): δ = 202.6 (C-12), 176.6 (C-18), 151.7 (C-3), 147.3 (C-2), 137.5 (C-1), 126.8 (C-6), 123.4 (C-5), 111.3 (C-4), 69.5 (C-9), 60.6 (C-13), 57.1 (C-17), 55.9 (C-14), 50.3 (C-10), 46.1 (C-11), 42.0 (C-15), 32.2 (C-8), 26.1 (C-7), 24.7 (C-16) ppm.

IR (ATR): $\tilde{\nu}$ = 3230 (w), 2937 (w), 1686 (s), 1601 (w), 1487 (m), 1454 (m), 1415 (m), 1277 (m), 1099 (m), 1061 (m) cm⁻¹.

HRMS (EI): calcd. for C₁₈H₂₁O₄N⁺: 315.1471 [M]⁺
 found: 315.1470 [M]⁺.

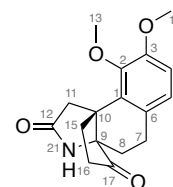
8,9-Dimethoxy-1,2,4,5-tetrahydro-3H-3a,9b-(epimenoethano)cyclopenta-[a]naphthalene-3,11-dione (I.285)



Aldehyde **I.284** (9.4 mg, 30 μ mol, 1.0 eq.) was dissolved in dry toluene (0.94 mL) and 3,4,5-trimethoxyaniline (5.5 mg, 30 μ mol, 1.0 eq.) was added. The mixture was stirred in an autoclave (purged 3 \times with O₂) under O₂ pressure (5 bar) at room temperature for 48 h. The reaction was stopped by addition of saturated, aqueous NH₄Cl solution (50 mL), the aqueous layer extracted with EtOAc (3 \times 50 mL) and the combined organic layers washed with saturated, aqueous NaCl solution (70 mL), dried (MgSO₄) and concentrated under reduced pressure. Subsequently, the obtained product was dissolved in 1 M HCl (30 mL) and the aqueous layer was extracted with EtOAc (30 mL) and washed with saturated, aqueous NaCl solution (20 mL). The combined organic layers were dried (MgSO₄) and concentrated under reduced pressure. Flash column chromatography [PE/EtOAc, 5% NEt₃ 3:1 to 1:2] afforded ketone **I.285** (2.9 mg, 0.01 mmol, 32%) as a pale brown oil.

$R_f = 0.77$ [EtOAc:PE, 3:1 + 5% NEt₃].

¹H NMR (400 MHz, CDCl₃): $\delta = 87$ – 6.75 (m, 2H, H-4, H-5), 5.72 (s, 1H, H-21), 3.95 (s, 3H, H-13), 3.87 (s, 3H, H-14), 3.08 (d, $J = 17.6$ Hz, 1H, H-11a), 2.782.71 (m, 1H, H-7), 2.68 (d, $J = 17.6$ Hz, 1H, H-11b), 2.56–2.41 (m, 3H, H-16a, H-15), 2.30–2.09 (m, 2H, H-16b, H-8a), 1.73 (ddd, $J = 13.1, 11.0, 4.5$ Hz, 1H, H-8b) ppm.



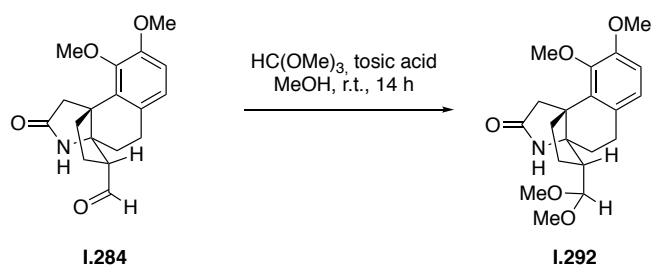
I.285

¹³C NMR (101 MHz, CDCl₃): $\delta = 215.8$ (C-17), 175.6 (C-12), 151.5 (C-3), 147.6 (C-2), 133.3 (C-1), 128.1 (C-6), 123.4 (C-5), 111.8 (C-4), 68.2 (C-9), 60.6 (C-13), 55.8 (C-14), 47.5 (C-10), 44.7 (C-11), 37.0 (C-16), 33.4 (C-15), 27.4 (C-8), 25.7 (C-7) ppm.

IR (ATR): $\tilde{\nu} = 3206$ (w), 2930 (w), 2849 (w), 2361 (w), 1746 (m), 1691 (s), 1488 (m), 1456 (m), 1417 (m), 1350 (w), 1277 (m), 1089 (m), 1065 (m), 1026 (m), 800 (m) cm⁻¹.

HRMS (EI): calcd. for C₁₇H₁₉O₄N⁺: 301.1314 [M-H]⁺
 found: 301.1324 [M-H]⁺.

3-(Dimethoxymethyl)-8,9-dimethoxy-2,3,4,5-tetrahydro-1H-3a,9b-(epiminoethano)-cyclopenta[a]-naphthalen-11-one (I.292)



To a solution of crude cascade product **I.284** (168 mg, 532 μmol , 1.0 eq.) in dry MeOH (5.5 mL) was added tosic acid (658 mg, 3.46 mmol, 6.5 eq.) and HC(OMe)_3 (0.300 mL, 2.74 mmol, 5.2 eq.) at 0 °C. After stirring a room temperature for 14 h, the reaction was quenched with saturated NaOMe solution in MeOH (6.0 mL), concentrated under reduced pressure and redissolved in Et_2O (50 mL). The organic layer was washed with saturated aqueous NaHCO_3 solution (50 mL), which was then extracted with Et_2O (4×50 mL). The combined organic layers were dried (MgSO_4) and concentrated under reduced pressure to obtain the crude protected cascade product **I.292** as a colorless oil.

The crude product could be used in the next step immediately. For analytical purposes, a sample of the product **I.292** was purified by preparative TLC [EtOAc , 5% NEt_3].

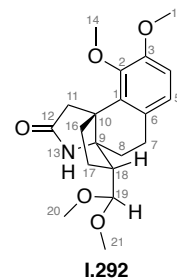
$d.r.$ = 1:6.7 (determined by integrals of H-19 in ^1H NMR).

R_f = 0.38 [EtOAc , 5% NEt_3].

^1H NMR (400 MHz, CHCl_3): δ = 6.81–6.74 (m, 2H, H-4, H-5), 5.75 (s, 1H, H-13), 4.36 (d, J = 7.6 Hz, 1H, H-19), 3.87 (s, 3H, H-14), 3.84 (s, 3H, H-15), 3.39 (s, 3H, H-20 or H-21), 3.37 (s, 3H, H-20 or H-21), 2.90 (d, J = 17.9 Hz, 1H, H-11a), 2.74 (ddd, J = 16.2, 7.4, 4.7 Hz, 1H, H-7a), 2.63 (ddd, J = 11.8, 8.3, 4.3 Hz, 1H, H-7b), 2.52 (d, J = 17.9 Hz, 1H, H-11b or H-16a), 2.49–2.44 (m, 1H, H-11b or H-16a), 2.20 (dt, J = 9.8, 7.5 Hz, 1H, H-19), 2.03–1.81 (m, 3H, H-6, H-16b), 1.76–1.66 (m, 2H, H-17) ppm.

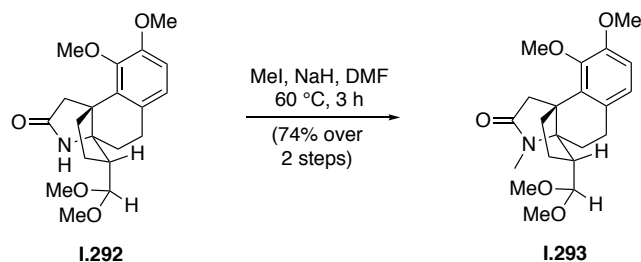
^{13}C NMR (100 MHz, CHCl_3) δ = 176.6 (C-12), 151.5 (C-3), 147.4 (C-2), 137.1 (C-1), 128.3 (C-6), 123.0 (C-5), 111.4 (C-4), 106.0 (C-19), 69.2 (C-9), 60.5 (C-14), 55.8 (C-15), 54.3 (C-20 or C-21), 53.3 (C-20 or C-21), 51.1 (C-10), 48.5 (C-19), 45.7 (C-11), 39.3 (C-16), 33.6 (C-6), 26.4 (C-17), 25.8 (C-7) ppm.

IR (ATR): = 3205 (br, w), 2925 (s), 2854 (m), 1690 (s), 1602 (w), 1487 (m), 1455 (m), 1415 (w), 1352 (w), 1277 (m), 1058 (m), 802 (w) cm^{-1} .



HRMS (EI): calc. for $C_{20}H_{28}O_5N^+$: 362.1962 [M+H]⁺
 found: 362.1964 [M+H]⁺.

(3R,3aR,9bR)-3-(Dimethoxymethyl)-8,9-dimethoxy-12-methyl-2,3,4,5-tetrahydro-1H-3a,9b-(epimino-ethano)cyclopenta[a]naphthalen-11-one (I.293)

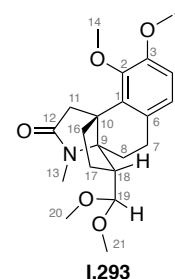


Crude protected aldehyde **I.292** (147 mg, assumed 405 μmol , 1.0 eq) was dissolved in DMF (5 mL), cooled to 0 $^\circ\text{C}$, and NaH (60 wt% suspension in mineral oil, 24.3 mg, 608 μmol , 1.5 eq) was added. After 20 min. iodomethane (37.6 μL , 608 μmol , 1.5 eq) was added, the reaction mixture was heated to 60 $^\circ\text{C}$ and stirred for 3 h at this temperature. After stopping the reaction with saturated, aqueous NaHCO_3 solution (5 mL), 10% aqueous LiCl solution (20 mL) was added and the aqueous layer was extracted with EtOAc (3×100 mL). The combined organic layers were washed with 10 wt% aqueous LiCl solution (500 mL) and saturated aqueous NaCl solution (300 mL), dried (MgSO_4) and concentrated under reduced pressure. The methylation product **I.293** (148 mg, 0.394 mmol, 74% over 2 steps) was obtained as a colorless oil.

d.r. = 10:1 (determined by integrals of H-19 in ^1H NMR).

R_f = 0.60 [EtOAc, 5% NEt_3].

^1H NMR (400 MHz, CDCl_3) of the major diastereomer: δ = 6.80–6.68 (m, 2H, H-6, H-7), 4.30 (d, J = 8.4 Hz, 1H, H-14), 3.88 (s, 3H, H-15), 3.83 (s, 3H, H-16), 3.35 (s, 3H, H-20 or H-21), 3.31 (s, 3H, H-20 or H-21), 2.95–2.84 (m, 4H, H-17a, H-19), 2.62 – 2.42 (m, 4H, H-17b, H-11a, H-4), 2.26–2.11 (m, 2H, H-3a, H-13), 1.93 (ddd, J = 14.1, 10.4, 4.1 Hz, 1H, H-3b), 1.79 (dt, J = 13.0, 7.2 Hz, 1H, H-12a), 1.75–1.65 (m, 2H, H-12b, H-11b) ppm.



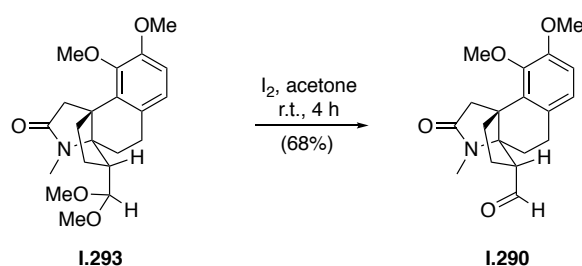
^{13}C NMR (100 MHz, CDCl_3) of the major diastereomer: δ = 207.0 (C-12), 176.1 (C-18), 151.5 (C-8), 147.5 (C-9), 137.4 (C-10), 128.2 (C-5), 122.9 (C-6), 110.9 (C-7), 104.4 (C-14), 73.5 (C-2), 60.4 (C-15), 55.8 (C-16), 53.5 (C-20 or C-21), 51.7 (C-20 or C-21), 50.4 (C-1), 46.0 (C-17), 38.2 (C-11), 31.2 (C-3), 30.9 (C-13), 27.8 (C-19), 26.2 (C-12), 15.8 (C-4) ppm.

IR (ATR): $\nu = 2927(\text{s}), 2854(\text{m}), 1682(\text{s}), 1602(\text{w}), 1488(\text{s}), 1454(\text{m}), 1418(\text{m}), 1392(\text{m}), 1277(\text{s}), 1098(\text{m}), 1068(\text{s}), 1052(\text{s}), 802(\text{w}) \text{ cm}^{-1}$.

HRMS (EI): calc. for $\text{C}_{21}\text{H}_{29}\text{O}_5\text{N}^+$: 375.2046 $[\text{M}]^+$
 found: 375.2055 $[\text{M}]^+$.

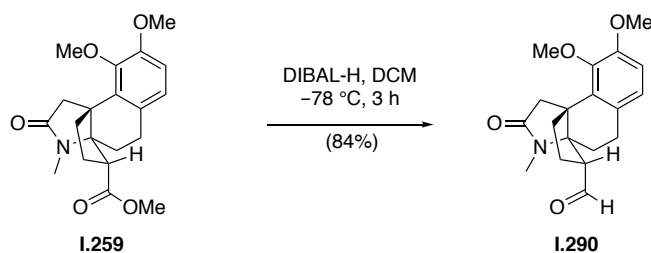
(3R,3aR,9bR)-8,9-Dimethoxy-12-methyl-11-oxo-2,3,4,5-tetrahydro-1H-3a,9b-(epiminoethano)cyclo-penta[a]naphthalene-3-carbaldehyde (I.290)

Procedure A:



Protected aldehyde **I.293** (52.5 mg, 140 μmol , 1.0 eq) was dissolved in acetone (3 mL) and iodine (3.55 mg, 14.0 μmol , 0.1 eq) was added. After 2 h, the reaction was stopped by the addition of saturated, aqueous $\text{Na}_2\text{S}_2\text{O}_7$ solution (10 mL) and the aqueous layer was extracted with DCM ($3 \times 100 \text{ mL}$). The combined organic layers were washed with saturated aqueous NaCl solution (300 mL), dried (MgSO_4) and concentrated under reduced pressure. Flash column chromatography [PE/EtOAc, 2:1 \rightarrow 1:2, +1% NEt_3] afforded aldehyde **I.290** (31.4 mg, 95.3 μmol , 68%) as a colorless oil.

Procedure B:



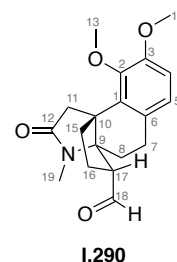
A solution of methylated lactam **I.259** (50.0 mg, 0.139 mmol, 1.0 eq) in dry DCM (5 mL) was cooled to -78°C . After 15 min. DIBAL-H (350 μL , 0.348 mmol, 2.5 eq) was added and the reaction mixture was stirred at -78°C for 3 h. Then, the reaction was quenched with EtOAc (5 mL) and stirred for another 15 min at -78°C . Aqueous 10% NaOH solution (5 mL) was added and the mixture was allowed to warm up to room temperature. The aqueous layer was extracted with EtOAc ($3 \times 50 \text{ mL}$) and the combined organic layers were washed with aqueous saturated

NaCl solution (100 mL), dried (MgSO₄) and concentrated under reduced pressure. Flash column chromatography on DAVISIL® [CHCl₃/acetone, 1:0 to 1:2] afforded aldehyde **I.290** (38.5 mg, 0.117 mmol, 84%) as a yellow oil.

d.r. = 1:1.3 (determined by integrals of H-13 in ¹H NMR).

R_f = 0.28 [DCM/MeOH, 10:1].

¹H NMR (400 MHz, CDCl₃): δ = 9.86 (d, *J* = 2.6 Hz, 1H), 9.78 (d, *J* = 3.5 Hz, 1H), 6.79–6.74 (m, 4H), 3.91 (s, 5H), 3.91 (s, 3H), 3.84 (s, 7H), 3.01 (t, *J* = 18.0 Hz, 2H), 2.92 (s, 3H), 2.85 (td, *J* = 8.5, 2.7 Hz, 1H), 2.74 (s, 3H), 2.71–2.58 (m, 5H), 2.58–2.35 (m, 4H), 2.25–2.09 (m, 3H), 2.09–1.87 (m, 6H) ppm.



¹³C NMR (101 MHz, CDCl₃): δ = 202.4, 201.9, 174.6, 173.3, 151.5, 151.5, 147.4, 147.3, 136.4, 135.5, 127.8, 127.0, 123.1, 122.8, 111.4, 111.3, 75.7, 75.4, 60.6, 60.5, 59.9, 59.0, 55.8, 49.7, 49.4, 45.8, 45.5, 39.6, 38.7, 30.0, 27.3, 26.5, 25.7, 25.4, 25.4, 25.1, 25.0 ppm.

IR (ATR): $\tilde{\nu}$ = 3854 (w), 2938 (m), 2838 (w), 2731 (w), 1714 (m), 1685 (s), 1602 (w), 1576 (w), 1488 (s), 1453 (m), 1471 (m), 1392 (m), 1355 (w), 1277 (s), 1250 (w), 1208 (w), 1100 (w), 1058 (m), 982 (w), 934 (w), 800 (w), 748 (w), 665 (w) cm⁻¹.

HRMS (ESI): calculated for C₁₉H₂₄NO₄⁺: 330.1700 [M+H]⁺
found: 330.1699 [M+H]⁺.

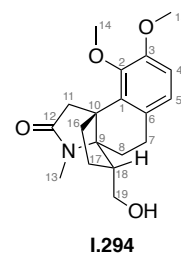
During the optimization process of the DIBAL-H reduction, the side product (3*R*,3*aS*,9*bR*)-3-(hydroxymethyl)-8,9-dimethoxy-12-methyl-2,3,4,5-tetrahydro-1*H*-3*a*,9*b*-(epiminoethano)-cyclopenta[*a*]naphthalen-11-one (**I.294**) and its epimer were isolated and characterized:

Crystals suitable for single-crystal X-ray analysis (**Section 9.1**) of both diastereomers were obtained from recrystallization [CHCl₃] at 0 °C.

d.r. = 1:5.5

R_f = 0.36 [CHCl₃/acetone, 1:1]

¹H NMR (400 MHz, CDCl₃) of the major diastereomer: δ = 6.76–6.74 (m, 2H, H-6, H-7), 3.88 (s, 3H, H-14), 3.83 (s, 3H, H-15), 3.82–3.65 (m, 2H, H-19), 2.92 (s, 3H, H-13), 2.91–2.84 (m, 1H, H-11*a*), 2.65–2.55 (m, 3H, H-7, H-16*a*), 2.54–2.50 (m, 1H, H-11*b*), 2.28–2.17 (m, 1H, H-8*a*), 2.16–2.06 (m, 1H, H-18), 1.98–1.90 (m, 1H, H-8*b*), 1.89–1.82 (m, 1H, H-17*a*), 1.81–1.71 (m, 1H, H-16*b*), 1.55–1.48 (m, 1H, H-17*b*) ppm.

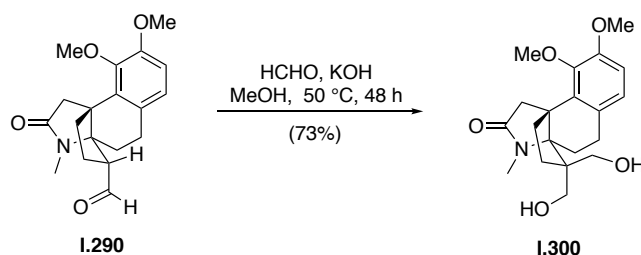


^{13}C NMR (101 MHz, CDCl_3) of the major diastereomer: δ = 175.8 (C-12), 151.7 (C-3), 147.7 (C-2), 137.6 (C-1), 128.3 (C-6), 123.1 (C-4), 111.1 (C-5), 73.9 (C-9), 63.3 (C-19), 60.6 (C-14), 56.0 (C-15), 52.2 (C-17), 50.1 (C-10), 46.4 (C-11), 38.7 (C-16), 31.3 (C-8), 27.7 (C-18 or C-13), 27.5 (C-18 or C-13), 26.0 (C-7) ppm.

IR (ATR): $\tilde{\nu}$ = 3384 (m), 2937 (m), 2361 (w), 2340 (w), 2183 (vw), 2150 (vw), 2114 (vw), 2016 (vw), 2002 (vw), 1951 (vw), 1663 (vs), 1603 (vw), 1487 (s), 1453 (m), 1417 (m), 1398 (m), 1352 (w), 1276 (s), 1210 (w), 1099 (w), 1055 (s), 973 (w), 859 (vw), 800 (w), 747 (vw), 668 (w) cm^{-1} .

HRMS (ESI): calculated for $\text{C}_{19}\text{H}_{26}\text{NO}_4^+$: 332.1856 $[\text{M}+\text{H}]^+$
found: 332.1861 $[\text{M}+\text{H}]^+$.

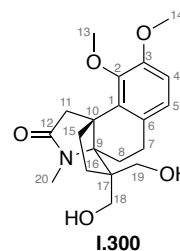
(3aR,9bR)-3,3-Bis(hydroxymethyl)-8,9-dimethoxy-12-methyl-2,3,4,5-tetrahydro-1H-3a,9b-(epiminoethano)cyclopenta[a]naphthalene-11-one (I.300)



To a solution of aldehyde **I.290** (11 mg, 33 μmol , 1 eq.) in MeOH (0.9 mL) was added KOH (20 mg, 0.33 mmol, 10 eq.) dissolved in MeOH (0.1 mL) followed by formaldehyde (37% in H_2O , 24 μL , 0.33 mmol, 10 eq.). The reaction mixture stirred for 48 h at 50 $^\circ\text{C}$. Then, the mixture was neutralized with conc. AcOH to pH = 6 and diluted with H_2O (50 mL). The aqueous layer was extracted with Et_2O (2 \times 50 mL) and CHCl_3 (2 \times 50 mL) and the combined organic layers were washed with aqueous saturated NaCl solution (100 mL), dried (MgSO_4) and concentrated under reduced pressure. Flash column chromatography [DCM/acetone, 1:0 to 1:2] afforded diol **I.300** (8.8 mg, 24 μmol , 73%) as a colorless solid.

R_f = 0.21 [CHCl_3 /acetone, 1:1]

^1H NMR (400 MHz, CDCl_3): δ = 6.76–6.69 (m, 2H, H-4, H-5), 3.91 (s, 3H, H-13), 3.82 (s, 3H, H-14), 3.80–3.60 (m, 4H, H-18, H-19), 2.98–2.94 (m, 1H, H-11a), 2.93 (s, 3H, H-20), 2.62–2.57 (m, 1H, H-11b), 2.57–2.54 (m, 1H, H-7a), 2.53–2.47 (m, 1H, H-15a), 2.47–2.40 (m, 1H, H-8a), 2.39–2.33 (m, 1H, H-7b), 2.11 (ddd, J = 14.3, 9.2, 4.2 Hz, 1H, H-15b), 1.81 (ddd, J = 17.6, 8.5, 4.3 Hz, 1H, H-16a),



1.72 (dd, $J = 13.7, 3.9$ Hz, 1H, H-8b), 1.52–1.39 (m, 1H, H-16b) ppm.

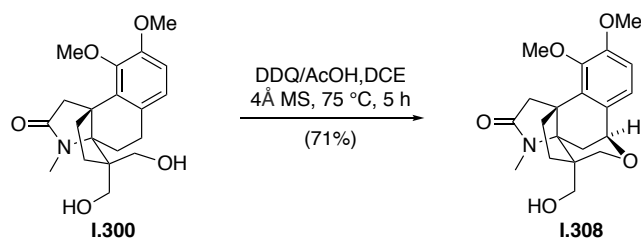
^{13}C NMR (101 MHz, CDCl_3) $\delta = 175.3$ (C-12), 151.7 (C-3), 147.4 (C-2), 138.3 (C-1), 127.4 (C-6), 122.5 (C-4), 111.5 (C-5), 76.0 (C-9), 65.1 (C-18, C-19), 60.7 (C-13), 55.2 (C-17), 55.0 (C-14), 50.2 (C-10), 50.5 (C-11), 38.0 (C-15), 30.7 (C-16), 27.6 (C-20), 25.6 (C-8), 24.7 (C-7) ppm.

C-2 is most likely superimposed with other signals and could therefore not be assigned in the ^{13}C NMR spectrum.

IR (ATR): $\tilde{\nu} = 3396$ (m), 2941 (m), 2361 (m), 2341 (m), 1654 (vs), 1489 (s), 1456 (m), 1400 (m), 1278 (s), 1086 (m), 1063 (m), 986 (w) cm^{-1} .

HRMS (ESI): calculated for $\text{C}_{20}\text{H}_{28}\text{NO}_5^+$: 362.19620 $[\text{M}+\text{H}]^+$
found: 362.19633 $[\text{M}+\text{H}]^+$.

(7*S*)-4-(Hydroxymethyl)-10,11-dimethoxy-3-methyl-4,5-dihydro-1*H*,7*H*-4,11*b*-ethano-3*a*,7-methanobenzo[6,7]oxocino[4,5-*b*]pyrrol-2(3*H*)-one (I.308)



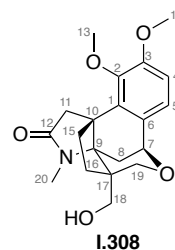
Diol **I.300** (217 mg, 0.601 mmol, 1 eq.) was suspended in dichloroethane (10 mL). DDQ (1.36 g, 6.01 mmol, 10 eq.), concentrated AcOH (344 μL , 6.01 mmol, 10 eq.) and 4 Å molecular sieves were added to the suspension and the reaction mixture was stirred at 75 °C for 5 h. The reaction mixture was allowed to cool to room temperature and 200 mL DCM were added. The organic phase was washed with 10% aqueous NaOH solution (3×100 mL) and aqueous saturated NaCl solution (100 mL), dried (MgSO_4) and concentrated under reduced pressure. Flash column chromatography [DCM/acetone, 1:0 to 0:1] afforded cyclic ether **I.308** (141 mg, 0.393 mmol, 71%) as a white solid.

Crystals suitable for single-crystal X-ray analysis (Section 9.1) were obtained from recrystallization [CHCl_3] at 0 °C.

$R_f = 0.36$ [CHCl_3 /acetone, 1:1].

^1H NMR (400 MHz, CDCl_3): $\delta = 6.95$ (d, $J = 8.3$ Hz, 1H, H-5), 6.86 (d, $J = 8.4$ Hz, 1H, H-4), 4.98 (dd, $J = 4.3, 1.7$ Hz, 1H, H-7), 4.09–3.99 (m, 1H, H-18a), 3.92 (s, 3H, H-13), 3.88 (s, 3H, H-14),

3.86 – 3.77 (m, 1H, H-18b), 3.69–3.63 (m, 1H, H-19a), 3.46–3.40 (m, 1H, H-19b), 3.23 (d, $J = 17.3$ Hz, 1H, H-11a), 3.08 (s, 3H, H-20), 3.04–2.95 (m, 1H, H-8a), 2.49–2.43 (m, 1H, H-11b), 2.35–2.25 (m, 2H, H-15), 1.60–1.51 (m, 1H, H-16a), 1.50–1.47 (m, 1H, H-10b), 1.23–1.14 (m, 1H, H-16b) ppm.

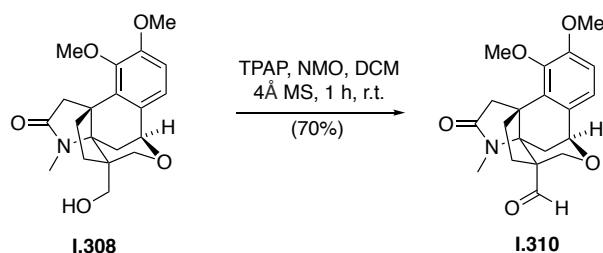


^{13}C NMR (101 MHz, CDCl_3): $\delta = 176.4$ (C-12), 153.7 (C-3), 146.0 (C-2), 140.8 (C-1), 124.9 (C-6), 124.8 (C-5), 111.3 (C-4), 73.2 (C-7), 73.1 (C-9), 69.4 (C-18), 67.1 (C-19), 60.7 (C-13), 55.9 (C-14), 51.2 (C-17), 49.4 (C-10), 45.6 (C-11), 40.9 (C-15), 30.6 (C-8), 30.3 (C-16), 29.1 (C-20) ppm.

IR (ATR): $\tilde{\nu} = 3421$ (m), 2943 (m), 2360 (w), 2340 (w), 1734 (w), 1671 (vs), 1602 (w), 1576 (w), 1559 (w), 1541 (w), 1487 (s), 1456 (m), 1421 (m), 1394 (m), 1355 (m), 1313 (m), 1275 (s), 1229 (m), 1176 (w), 1130 (w), 1103 (m), 1086 (m), 1068 (m), 1040 (m), 983 (m), 960 (w), 931 (w), 814 (w), 749 (w), 668 (w) cm^{-1} .

HRMS (ESI): calculated for $\text{C}_{20}\text{H}_{26}\text{NO}_5^+$: 360.1805 $[\text{M}+\text{H}]^+$
found: 360.1805 $[\text{M}+\text{H}]^+$.

(7S)-10,11-Dimethoxy-3-methyl-2-oxo-2,3-dihydro-1H,7H-4,11b-ethano-3a,7-methanobenzo[6,7]oxocino[4,5-b]pyrrole-4(5H)-carbaldehyde (I.310)



To a solution of primary alcohol **I.308** (141 mg, 0.393 mmol, 1.0 eq.) in DCM (10 mL) was added 4Å MS followed by NMO (460 mg, 3.93 mmol, 10 eq.) and TPAP (6.70 mg, 19.7 μmol , 0.05 eq.). The reaction mixture stirred at room temperature for 1 h. The oxidant was removed by filtration through a pad of silica that was washed with DCM/acetone (1:1, 10 mL) to afford aldehyde **I.310** (97.6 mg, 0.273 mmol, 70%) as a colorless solid.

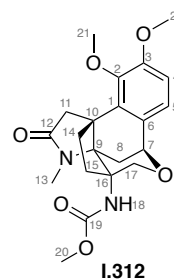
Crystals suitable for single-crystal X-ray analysis (Section 9.1) were obtained from recrystallization [CDCl_3] at room temperature.

$R_f = 0.79$ [DCM/acetone, 2:1].

aqueous NH_4Cl solution (50 mL) and extracted with DCM (3×100 mL). The combined organic layers were washed with saturated aqueous NaCl solution (200 mL), dried (MgSO_4) and concentrated under reduced pressure. Flash column chromatography [DCM/acetone, 1:0 to 2:1] afforded methyl carbamate **I.312** (43.3 mg, 108 μmol , 81%) as a colorless solid.

$R_f = 0.50$ [DCM/acetone, 2:1].

$^1\text{H NMR}$ (400 MHz, CDCl_3): $\delta = 6.94$ (d, $J = 8.3$ Hz, 1H, H-5), 6.85 (d, $J = 8.3$ Hz, 1H, H-4), 5.46 (s, 1H, H-18), 4.97–4.89 (m, 1H, H-7), 3.92 (s, 3H, H-21), 3.87 (s, 3H, H-22), 3.64 (d, $J = 10.7$ Hz, 4H, H-20, H-17a), 3.33 (d, $J = 12.9$ Hz, 1H, H-17b), 3.22 (d, $J = 17.2$ Hz, 1H, H-11a), 2.98 (s, 3H, H-13), 2.57 (dd, $J = 13.2, 4.1$ Hz, 1H, H-8a), 2.44 (d, $J = 17.2$ Hz, 1H, H-11b), 2.41–2.31 (m, 1H, H-14a), 2.31–2.12 (m, 3H, H-14b, H-15), 1.53 (dd, $J = 13.2, 1.8$ Hz, 1H, H-8b) ppm.

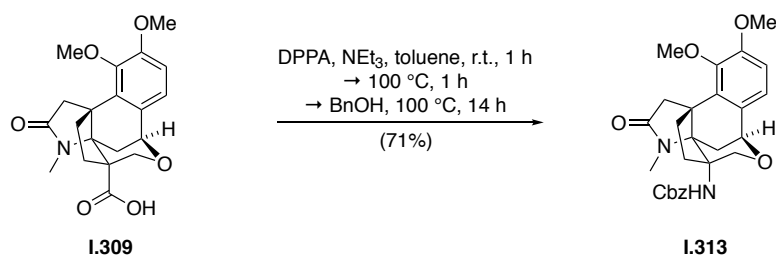


$^{13}\text{C NMR}$ (101 MHz, CDCl_3): $\delta = 174.6$ (C-12), 155.5 (C-19), 153.6 (C-3), 145.8 (C-2), 139.2 (C-6), 124.5 (C-5), 123.9 (C-1), 111.4 (C-4), 72.5 (C-7), 71.0 (C-9), 66.3 (C-17), 63.7 (C-16), 60.5 (C-21), 55.7 (C-22), 52.0 (C-20), 46.0 (C-10), 45.3 (C-11), 40.5 (C-14), 30.7 (C-15), 28.1 (C-8), 27.6 (C-13) ppm.

IR (ATR): $\tilde{\nu} = 3313$ (w), 2945 (m), 2840 (w), 1717 (m), 1676 (s), 1602 (w), 1576 (w), 1528 (m), 1488 (m), 1456 (m), 1422 (w), 1393 (w), 1356 (w), 1340 (w), 1312 (w), 1274 (s), 1251 (s), 1153 (w), 1130 (w), 1107 (w), 1074 (s), 1049 (w), 1028 (w), 1016 (w), 1002 (w), 979 (s), 1016 (w), 961 (w), 815 (m), 753 (m), 667 (w) cm^{-1} .

HRMS (EI): calcd. for $\text{C}_{21}\text{H}_{27}\text{N}_2\text{O}_6^+$ 403.1867 $[\text{M}+\text{H}]^+$
found: 403.1869 $[\text{M}+\text{H}]^+$.

Benzyl ((7*S*,11*bR*)-10,11-dimethoxy-3-methyl-2-oxo-2,3-dihydro-1*H*,7*H*-4,11*b*-ethano-3*a*,7-methano-benzo[6,7]oxocino[4,5-*b*]pyrrol-4(5*H*)-yl)carbamate (I.313)

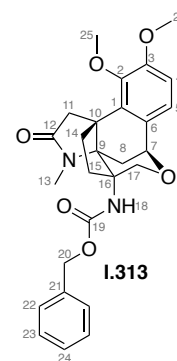


Carboxylic acid **I.309** (94.7 mg, 254 μmol , 1.0 eq.) was dissolved in toluene (3 mL) and diphenylphosphoryl azide (82.0 μL , 380 μmol , 1.5 eq.) and NEt_3 (106 μL , 762 μmol , 3 eq.) were added. The reaction was stirred at room temperature for 1 h and then heated to 100 $^\circ\text{C}$ for another 1 h. After cooling to room temperature, benzyl alcohol (132 μL , 1.27 mmol, 5 eq.) was added and the reaction was heated to 100 $^\circ\text{C}$ for additional 14 h. The reaction mixture was diluted with H_2O (200 mL) and extracted with DCM (3×200 mL). The combined organic layers were washed with saturated aqueous NaCl solution (100 mL), dried (MgSO_4) and concentrated under reduced pressure. Flash column chromatography [PE/EtOAc, 1:1 to 0:1] afforded Cbz-protected amine **I.313** (86.4 mg, 181 μmol , 71%) as a colorless solid.

Crystals suitable for single-crystal X-ray analysis (Section 9.1) were obtained from recrystallization [CHCl_3] at 20 $^\circ\text{C}$.

$R_f = 0.76$ [DCM/acetone, 1:1].

$^1\text{H NMR}$ (600 MHz, CDCl_3) $\delta = 7.41\text{--}7.30$ (m, 5H, H-22, H-23, H-24), 6.94 (d, $J = 8.3$ Hz, 1H, H-5), 6.86 (d, $J = 8.3$ Hz, 1H, H-4), 5.52 (s, 1H, H-18), 5.07 (d, $J = 3.0$ Hz, 2H, H-20), 4.97–4.89 (m, 1H, H-7), 3.92 (s, 3H, H-25), 3.87 (s, 3H, H-26), 3.64 (d, $J = 12.9$ Hz, 1H, H-17a), 3.34 (d, $J = 12.9$ Hz, 1H, H-17b), 3.22 (d, $J = 17.2$ Hz, 1H, H-11a), 2.94 (s, 3H, H-13), 2.55 (dd, $J = 13.2, 4.1$ Hz, 1H, H-11b), 2.44 (d, $J = 17.2$ Hz, 1H, H-8a), 2.39–2.11 (m, 4H, H-14, H-15), 1.56–1.49 (m, 1H, H-8b) ppm.



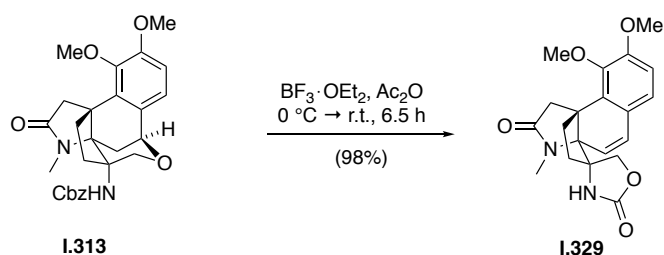
$^{13}\text{C NMR}$ (150 MHz, CDCl_3): $\delta = 174.5$ (C-12), 154.8 (C-19), 153.6 (C-3), 145.8 (C-2), 139.3 (C-1), 136.2 (C-21), 128.6 (C-22 or C-23), 128.3 (C-25), 128.2 (C-22 or C-23), 124.5 (C-5), 123.9 (C-6), 111.4 (C-4), 72.5 (C-7), 71.0 (C-9), 66.8 (C-20), 66.5 (C-17), 63.8 (C-16), 60.5 (C-25), 55.7 (C-26), 46.0 (C-10), 45.3 (C-11), 40.5 (C-14), 30.6 (C-15), 28.1 (C-8), 27.5 (C-13) ppm.

IR (ATR): $\tilde{\nu} = 3298$ (w), 2942 (m), 2838 (w), 1721 (m), 1673 (s), 1601 (w), 1576 (w), 1526 (m), 1487 (s), 1454 (m), 1421 (m), 1391 (m), 1372 (w), 1356 (w), 1340 (w), 1311 (w), 1273 (s), 1247 (s), 1172

(w), 1151 (w), 1129 (w), 1107 (m), 1080 (s), 1070 (s), 1028 (w), 1015 (w), 1002 (w), 977 (m), 959 (m), 927 (w), 891 (w), 863 (w), 834 (w), 814 (m), 751 (s), 697 (m), 665 (m) cm^{-1} .

HRMS (ESI): calcd. for $\text{C}_{19}\text{H}_{25}\text{N}_2\text{O}_5^+$ 479.2177 $[\text{M}+\text{H}]^+$
 found: 479.2178 $[\text{M}+\text{H}]^+$.

(3a'S,4R,9b'R)-8',9'-Dimethoxy-12'-methyl-1',2'-dihydrospiro[oxazolidine-4,3'-[3a,9b](epi-minoethano)cyclopenta[*a*]naphthalene]-2,11'-dione (I.329)



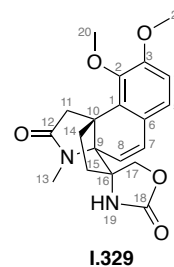
Cbz-protected amine **I.313** (22.9 mg, 47.8 μmol , 1 eq.) was dissolved in Ac_2O (1 mL) and cooled to $0\text{ }^\circ\text{C}$. After 15 min., $\text{BF}_3 \cdot \text{OEt}_2$ (150 μL , 1.42 mmol, 30 eq.) was added slowly. After 6.5 h, the reaction was quenched and diluted with wet EtOAc (1 mL) and H_2O (1 mL) followed by aqueous 10% NaOH solution (5 mL). The mixture was extracted with DCM ($3 \times 10\text{ mL}$). The combined organic layers were washed with saturated aqueous NaCl solution (10 mL), dried (MgSO_4) and concentrated under reduced pressure. Flash column chromatography [DCM/acetone, 2:1 to 0:1] afforded oxazolidinone **I.329** (17.4 mg, 47.0 μmol , 98%) as a colorless solid.

Crystals suitable for single-crystal X-ray analysis (Section 9.1) were obtained from recrystallization [CHCl_3] at $20\text{ }^\circ\text{C}$.

$R_f = 0.65$ [DCM/acetone, 1:3].

^1H NMR (600 MHz, CDCl_3) $\delta = 6.86$ (d, $J = 8.4\text{ Hz}$, 1H, H-5), 6.80 (d, $J = 8.4\text{ Hz}$, 1H, H-4), 6.62 (d, $J = 10.1\text{ Hz}$, 1H, H-7), 5.98 (d, $J = 10.1\text{ Hz}$, 1H, H-8), 5.61 (d, $J = 11.2\text{ Hz}$, 1H, H-19), 4.31 (d, $J = 9.0\text{ Hz}$, 1H, H-17a), 3.90 (m, 4H, H-17b, H-20), 3.88 (s, 3H, H-21), 2.99 (m, 4H, H-11a, H-13), 2.71 (d, $J = 18.2\text{ Hz}$, 1H, H-11b), 2.66–2.56 (m, 1H, H-14a), 2.03 (td, $J = 13.3, 12.0, 6.8\text{ Hz}$, 2H, H-15a), 1.74 (m, 2H, H-14b, H-15b).

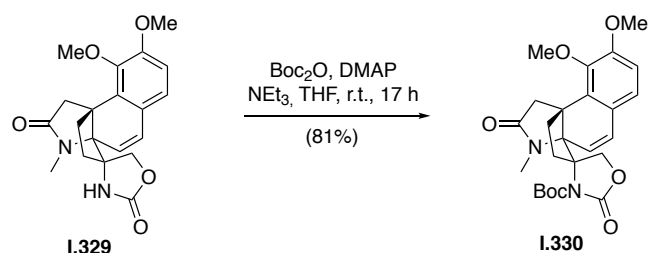
^{13}C NMR (100 MHz, CDCl_3): $\delta = 175.5$ (C-12), 158.1 (C-18), 153.6 (C-3), 146.6 (C-2), 134.5 (C-1), 130.0 (C-7), 123.6 (C-5), 122.1 (C-6), 117.4 (C-8), 111.1 (C-4), 73.4 (C-17), 73.2 (C-9), 70.9 (C-16), 60.6 (C-20), 55.7 (C-21), 48.1 (C-11), 45.6 (C-10), 39.1 (C-14), 32.2 (C-15), 28.7 (C-13) ppm.



IR (ATR): $\tilde{\nu}$ = 3266 (w), 2946 (w), 1758 (s), 1674 (s), 1596 (w), 1490 (m), 1455 (m), 1422 (m), 1390 (m), 1277 (s), 1217 (w), 1147 (w), 1090 (m), 1049 (m), 810 (w), 762 (w) cm^{-1} .

HRMS (ESI): calcd. for $\text{C}_{20}\text{H}_{23}\text{N}_2\text{O}_5^+$: 371.1601 $[\text{M}+\text{H}]^+$
found: 371.1602 $[\text{M}+\text{H}]^+$.

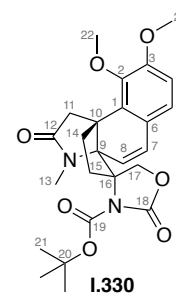
***tert*-butyl (3*a*'*S*,4*R*,9*b*'*R*)-8',9'-dimethoxy-12'-methyl-2,11'-dioxo-1',2'-dihydrospiro[oxazolidine-4,3'-[3*a*,9*b*](epiminoethano)cyclopenta[*a*]naphthalene]-3-carboxylate (I.330)**



Oxazolidinone **I.320** (12 mg, 32 μmol , 1.0 eq.) was dissolved in THF (2 mL) and Boc_2O (14 mg, 64 μmol , 2 eq.) followed by NEt_3 (22 μL , 0.61 mmol, 2 eq.) and DMAP (0.40 mg, 3.2 μmol , 0.1 eq.) were added and the reaction stirred at room temperature for 17 h. Afterwards, the reaction mixture was concentrated under reduced pressure and flash column chromatography [DCM/acetone, 1:0 to 1:1] afforded Boc-protected oxazolidinone **I.330** (12 mg, 26 μmol , 81%) as a colorless oil.

R_f = 0.65 [DCM/acetone, 5:1].

^1H NMR (400 MHz, CDCl_3): δ = 6.85 (d, J = 8.3 Hz, 1H, H-5), 6.80 (d, J = 8.4 Hz, 1H, H-4), 6.58 (d, J = 10.1 Hz, 1H, H-7), 5.95 (d, J = 10.1 Hz, 1H, H-6), 4.22 (d, J = 8.9 Hz, 1H, H-17a), 3.92 (s, 3H, H-22), 3.87 (s, 3H, H-23), 3.76 (d, J = 9.0 Hz, 1H, H-17b), 3.18 (ddd, J = 14.7, 12.7, 6.7 Hz, 1H, H-15a), 3.00 (d, J = 18.4 Hz, 1H, H-11a), 2.87–2.80 (m, 4H, H-11b, H-13), 2.73 (dd, J = 13.4, 6.6 Hz, 1H, H-14a), 1.56 (s, 10H, H-21, H-15b), 1.45 (dd, J = 8.0, 6.1 Hz, 1H, H-14b) ppm.



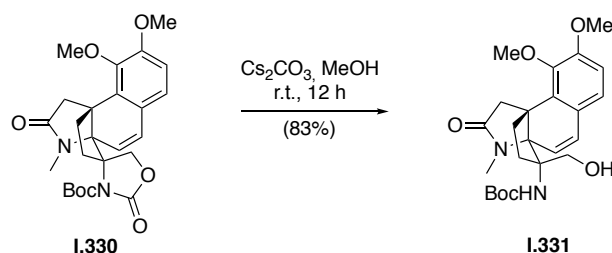
^{13}C NMR (101 MHz, CDCl_3): δ = 174.7 (C-12), 153.6 (C-3), 153.4 (C-18), 149.30 (C-19), 146.5 (C-2), 134.3 (C-1), 129.7 (C-7), 123.6 (C-5), 121.7 (C-6), 117.6 (C-8), 111.2 (C-4), 85.0 (C-20), 74.2 (C-9), 73.4 (C-16), 72.7 (C-17), 60.6 (C-22), 55.7 (C-23), 48.0 (C-11), 46.0 (C-10), 38.3 (C-14), 28.3 (C-15), 28.1 (C-13), 27.9 (C-21) ppm.

IR (ATR): $\tilde{\nu}$ = 2979 (w), 2939 (w), 1813 (s), 1734 (m), 1681 (s), 1596 (w), 1569 (w), 1490 (m), 1455

(m), 1421 (w), 1393 (w), 1370 (w), 1329 (m), 1302 (s), 1276 (s), 1257 (s), 1150 (s), 1073 (s), 1060 (s), 964 (w), 819 (w), 774 (w), 754 (m) cm^{-1} .

HRMS (ESI): calcd. for $\text{C}_{25}\text{H}_{31}\text{N}_2\text{O}_7^+$: 471.2126 $[\text{M}+\text{H}]^+$
 found: 471.2136 $[\text{M}+\text{H}]^+$.

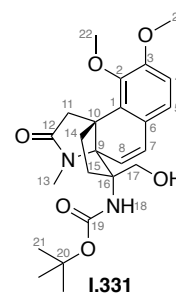
**tert-Butyl ((3*R*,3*aS*,9*bR*)-3-formyl-8,9-dimethoxy-12-methyl-11-oxo-2,3-dihydro-1*H*-3*a*,9*b*-
 (epimino- ethano)cyclopenta[*a*]naphthalen-3-yl)carbamate (I.331)**



Boc-protected oxazolidonone **I.330** (12 mg, 24 μmol , 1.0 eq.) was dissolved in MeOH (1 mL), then Cs_2CO_3 (3.9 mg, 12 μmol , 0.5 eq.) was added and the reaction stirred at room temperature for 12 h. The reaction mixture was diluted with H_2O (10 mL) and extracted with DCM (3×10 mL). The combined organic layers were washed with saturated aqueous NaCl solution (10 mL), dried (MgSO_4) and concentrated under reduced pressure. Flash column chromatography [DCM/acetone, 1:0 to 0:1] afforded aminoalcohol **I.331** (9.1 mg, 20 μmol , 83%) as a colorless oil.

$R_f = 0.88$ [acetone/DCM, 2:1].

$^1\text{H NMR}$ (400 MHz, CDCl_3) $\delta = 6.76$ (m, 2H, H-4, H-5), 6.42 (d, $J = 10.1$ Hz, 1H, H-8), 6.16 (d, $J = 10.2$ Hz, 1H, H-7), 4.64 (s, 1H, H-18), 4.25 (d, $J = 12.2$ Hz, 1H, H-17a), 3.90 (s, 3H, H-22), 3.86 (s, 3H, H-23), 3.39 (d, $J = 12.2$ Hz, 1H, H-17b), 3.04 (d, $J = 18.4$ Hz, 1H, H-11a), 2.97 (s, 3H, H-13), 2.77 (d, $J = 18.4$ Hz, 1H, H-11b), 2.46 (ddd, $J = 13.5, 6.7, 4.2$ Hz, 1H, H-14a), 2.0–2.00 (m, 1H, H-14b), 1.95 (ddd, $J = 11.3, 6.5, 4.2$ Hz, 1H, H-15a), 1.65 (td, $J = 11.5, 7.2$ Hz, 1H, H-15b), 1.45 (s, 9H, H-21) ppm.



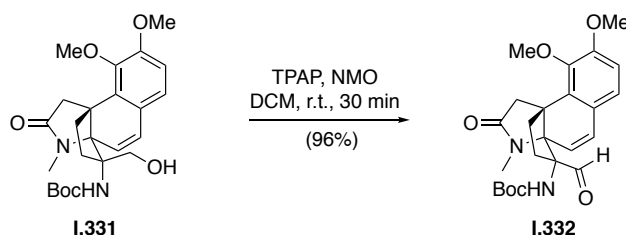
$^{13}\text{C NMR}$ (101 MHz, CDCl_3): $\delta = 175.7$ (C-12), 155.2 (C-19), 153.3 (C-3), 146.3 (C-2), 135.4 (C-1), 128.1 (C-7), 122.9 (C-5), 122.4 (C-6), 119.9 (C-8), 110.9 (C-4), 80.3 (C-20), 75.9 (C-9), 70.7 (C-16), 60.6 (C-22), 60.4 (C-17), 55.7 (C-23), 48.8 (C-11), 47.7 (C-10), 39.9 (C-14), 30.5 (C-15), 28.4 (C-21), 28.3 (C-13) ppm.

IR (ATR): $\tilde{\nu} = 3356$ (w), 2976 (w), 2939 (w), 1711 (m), 1669 (s), 1597 (w), 1570 (w), 1530 (w), 1490

(m), 1455 (m), 1421 (w), 1393 (m), 1366 (m), 1274 (s), 1249 (m), 1166 (s), 1116 (w), 1052 (m), 962 (w), 867 (w), 917 (w), 754 (m), 678 (w) cm^{-1} .

HRMS (ESI): calcd. for $\text{C}_{24}\text{H}_{33}\text{N}_2\text{O}_6^+$ 445.2333 $[\text{M}+\text{H}]^+$
found: 445.2338 $[\text{M}+\text{H}]^+$.

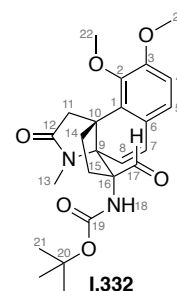
***tert*-Butyl ((3*R*,3*aS*,9*bR*)-3-formyl-8,9-dimethoxy-12-methyl-11-oxo-2,3-dihydro-1*H*-3*a*,9*b*-(epimino-ethano)cyclopenta[*a*]naphthalen-3-yl)carbamate (**I.332**)**



Alcohol **I.331** (10 mg, 23 μmol , 1.0 eq.) was dissolved in DCM (1 mL) and NMO (12 mg, 0.11 mmol, 4.5 eq.) followed by TPAP (1.2 mg, 4.7 μmol , 0.2 eq.) was added to the solution. The reaction stirred at room temperature for 30 min. Afterwards, the reaction mixture was filtered over a pad of silica and the silica was washed with DCM (3 mL) and acetone (3 mL) to afford aminoaldehyde **I.332** (9.8 mg, 22 μmol , 96%) as a colorless oil.

$R_f = 0.75$ [DCM/acetone, 2:1].

$^1\text{H NMR}$ (400 MHz, CDCl_3) $\delta = 9.55$ (s, 1H, H-17), 6.88–6.75 (m, 2H, H-4, H-5), 6.48 (d, $J = 10.0$ Hz, 1H, H-7), 5.87 (d, $J = 10.0$ Hz, 1H, H-8), 5.11 (s, 1H, H-18), 3.92 (s, 3H, H-22), 3.87 (s, 3H, H-23), 3.07 (d, $J = 18.4$ Hz, 1H, H-11a), 2.92 (s, 3H, H-13), 2.82 (d, $J = 18.5$ Hz, 1H, H-11b), 2.50 (dt, $J = 12.9, 5.1$ Hz, 1H, H-14a), 2.20–2.13 (m, 1H, 15a), 2.13–2.03 (m, 1H, H-14b), 1.94 (dt, $J = 10.7, 5.2$ Hz, 1H, H-15b), 1.45 (s, 9H, H-21) ppm.

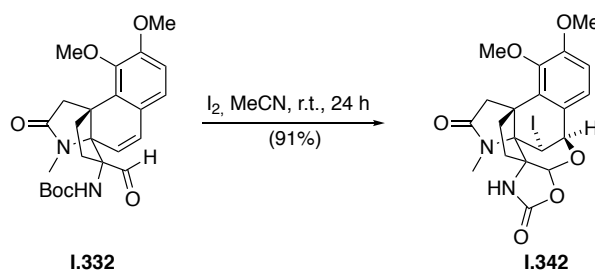


$^{13}\text{C NMR}$ (101 MHz, CDCl_3): $\delta = 198.3$ (C-17), 175.2 (C-12), 155.0 (C-19), 153.4 (C-3), 146.4 (C-2), 134.7 (C-1), 129.0 (C-7), 123.3 (C-5), 122.5 (C-6), 119.1 (C-8), 111.0 (C-4), 81.1 (C-20), 75.6 (C-9), 74.8 (C-16), 60.6 (C-22), 55.7 (C-23), 47.9 (C-11), 38.8 (C-10), 29.9 (C-14), 29.7 (C-15), 28.2 (C-21), 27.7 (C-13) ppm.

IR (ATR): $\tilde{\nu} = 3399$ (bw), 2927 (m), 2851 (w), 1734 (w), 1673 (s), 1525 (m), 1490 (m), 1455 (m), 1421 (w), 1394 (w), 1367 (w), 1276 (s), 1165 (s), 1099 (w), 1066 (m), 1046 (w), 969 (w), 817 (w), 679 (w) cm^{-1} .

HRMS (ESI): calcd. for $C_{24}H_{30}N_2O_6^+$ 443.2177 [M+H]⁺
 found: 443.2179 [M+H]⁺.

(3aR,8R,13R)-13-Iodo-4,5-dimethoxy-1-methyl-1H,8H,9aH-3a,12a-ethano-8,12b-methano-benzo[6,7]-pyrrolo[2',3':4,5]oxocino[3,2-d]oxazole-2,11(3H,12H)-dione (I.342)



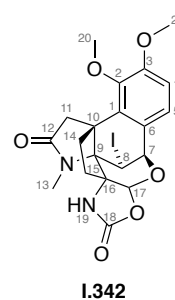
Aminoaldehyde **I.332** (3.5 mg, 7.9 μ mol, 1.0 eq.) was dissolved in MeCN/H₂O (5:1, 2.4 mL) then I₂ (8.9 mg, 79 μ mol, 10 eq.) was added and the reaction stirred at room temperature for 24 h. Afterwards, the reaction was stopped by the addition of aqueous saturated Na₂S₂O₇ (1 mL) and diluted with H₂O (10 mL). Then, the mixture was extracted with DCM (3 \times 10 mL) and the combined organic layers were washed with saturated aqueous NaCl solution (10 mL), dried (MgSO₄) and concentrated under reduced pressure. Flash column chromatography [DCM/acetone, 1:0 to 2:1] afforded hexacyclic oxazolidinone **I.342** (3.5 mg, 7.2 μ mol, 91%) as a yellow oil.

R_f = 0.61 [DCM/acetone, 2:1].

¹H NMR (400 MHz, CDCl₃): δ = 7.07 (d, J = 8.4 Hz, 1H, H-5), 6.94 (d, J = 8.4 Hz, 1H, H-4), 5.59 (d, J = 3.9 Hz, 1H, H-19), 5.19 (d, J = 3.5 Hz, 1H, H-7), 5.13 (s, 1H- H-17), 5.08 (d, J = 3.6 Hz, 1H, H-8), 3.94 (s, 3H, H-20), 3.91 (s, 3H, H-21), 3.11 (d, J = 17.5 Hz, 1H, H-11a), 3.01 (d, J = 17.7 Hz, 1H, H-11b), 2.96 (s, 3H, H-13), 2.39 (dd, J = 14.8, 9.4 Hz, 1H, H-14a), 2.16–2.06 (m, 1H, H14b), 2.06–1.97 (m, 1H, H-15a), 1.92 (dd, J = 12.8, 8.7 Hz, 1H, H-15b) ppm.

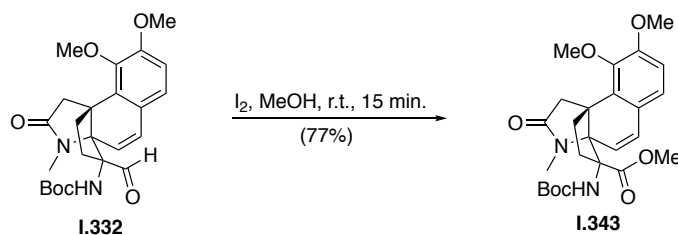
¹³C NMR (101 MHz, CDCl₃): δ = 175.3 (C-12), 157.8 (C-18), 154.3 (C-3), 145.7 (C-2), 135.9 (C-1), 126.2 (C-5), 120.4 (C-6), 112.0 (C-4), 97.4 (C-17), 76.5 (C-7), 72.0 (C-16), 70.6 (9), 60.6 (C-20), 55.7 (C-21), 47.6 (C-10), 46.3 (C-11), 40.4 (C-14), 32.5 (C-15), 27.1 (C-13), 24.4 (C-8) ppm.

IR (ATR): $\tilde{\nu}$ = 1934 (m), 2362 (w), 1778 (s), 1684 (s), 1601 (w), 1490 (m), 1457 (m), 1423 (w), 1362 (m), 1278 (s), 1212 (w), 1119 (w), 1089 (m), 1034 (s), 979 (m), 954 (w), 929 (w), 800 (w), 752 (w), 683 (w) cm⁻¹.



HRMS (ESI): calcd. for $C_{20}H_{22}IN_2O_6$: 513.0517 [M+H]⁺
 found: 513.0525 [M+H]⁺.

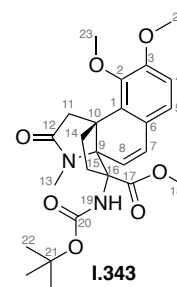
Methyl (3*R*,3*aS*,9*bR*)-3-((*tert*-butoxycarbonyl)amino)-8,9-dimethoxy-12-methyl-11-oxo-2,3-dihydro-1*H*-3*a*,9*b*-(epiminoethano)cyclopenta[*a*]naphthalene-3-carboxylate (I.343)



Aminoaldehyde **I.332** (9.8 mg, 22 μmol , 1.0 eq.) was dissolved in MeOH (2 mL), then I_2 (28.2 mg, 0.11 mmol, 10 eq.) was added and the reaction stirred at room temperature for 15 min. Afterwards, the reaction was stopped by the addition of aqueous saturated $\text{Na}_2\text{S}_2\text{O}_7$ solution (0.1 mL) and diluted with H_2O (10 mL). Then, the mixture was extracted with DCM (3×10 mL) and the combined organic layers were washed with saturated aqueous NaCl solution (10 mL), dried (MgSO_4) and concentrated under reduced pressure. Ester **I.343** (7.8 mg, 17 μmol , 77%) was obtained as a yellow oil.

$R_f = 0.65$ [DCM/acetone, 5:1].

$^1\text{H NMR}$ (400 MHz, CDCl_3) $\delta = 6.83\text{--}6.66$ (m, 2H, H-4, H-5), 6.44 (d, $J = 10.0$ Hz, 1H, H-7), 5.52 (d, $J = 10.0$ Hz, 1H, H-8), 4.95 (s, 1H, H-19), 3.94 (s, 3H, H-23), 3.86 (s, 3H, H-24), 3.77 (s, 3H, H-18), 3.16 (d, $J = 18.4$ Hz, 1H, H-11a), 3.02 (s, 3H, H-13), 2.71 (d, $J = 18.4$ Hz, 1H, H-11b), 2.40 (dd, $J = 12.5$, 5.8 Hz, 1H, H-14a), 2.36–2.27 (m, 1H, H-15a), 2.24 (dd, $J = 13.0$, 5.1 Hz, 1H, H-14b), 2.14–2.02 (m, 1H, H-15b), 1.43 (s, 9H, H-22) ppm.

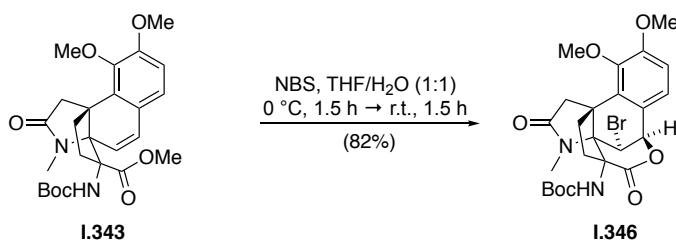


$^{13}\text{C NMR}$ (101 MHz, CDCl_3): $\delta = 175.4$ (C-12), 172.2 (C-17), 154.4 (C-20), 153.6 (C-3), 146.2 (C-2), 134.9 (C-1), 130.1 (C-7), 122.9 (C-5), 122.5 (C-6), 117.4 (C-8), 111.0 (C-4), 80.7 (C-21), 75.9 (C-9), 72.5 (C-16), 60.6 (C-23), 55.7 (C-24), 52.3 (C-18), 48.0 (C-10), 47.9 (C-11), 41.9 (C-14), 33.1 (C-15), 28.2 (C-22), 27.0 (C-13) ppm.

IR (ATR): $\tilde{\nu} = 3297$ (w), 2978 (w), 2945 (w), 2840 (w), 1789 (w), 1681 (s), 1596 (w), 1572 (w), 1491 (m), 1455 (s), 1421 (m), 1391 (m), 1367 (m), 1274 (s), 1248 (s), 1213 (m), 1163 (s), 1126 (m), 1089 (m), 1033 (m), 1063 (m), 1033 (m), 981 (m), 955 (m), 929 (w), 879 (w), 817 (m), 753 (s), 666 (w), 617 (w) cm^{-1} .

HRMS (ESI): calcd. for $C_{25}H_{33}N_2O_7^+$: 473.2282 [M+H]⁺
 found: 473.2287 [M+H]⁺.

tert-Butyl ((7R,11bR,14R)-14-bromo-10,11-dimethoxy-3-methyl-2,5-dioxo-2,3-dihydro-1H,7H-4,11b-ethano-3a,7-methanobenzo[6,7]oxocino[4,5-b]pyrrol-4(5H)-yl)carbamate (I.346)

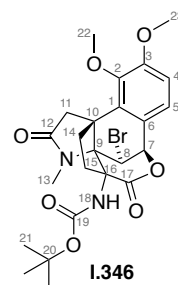


Ester **I.343** (13 mg, 28 μ mol, 1.0 eq.) was dissolved in THF (1 mL) in a flask covered with aluminium foil, then NBS (5.1 mg, 29 mmol, 1.05 eq.) in H₂O (1 mL) was added and the reaction stirred at 0 °C for 90 minutes followed by room temperature for another 90 minutes. Afterwards, the reaction was stopped by the addition of aqueous saturated Na₂S₂O₇ (0.05 mL) and diluted with H₂O (10 mL). Then, the mixture was extracted with DCM (3 \times 10 mL) and the combined organic layers were washed with saturated aqueous NaHCO₃ solution (5 \times 20 mL) and saturated aqueous NaCl solution (20 mL), dried (MgSO₄) and concentrated under reduced pressure. Flash column chromatography [PE/EtOAc, 1:0 to 2:1] afforded bromolactone **I.346** (13 mg, 23 μ mol, 82%) as a colorless solid.

R_f = 0.61 [DCM/acetone, 3:1].

The product was accompanied by 30–35% succinimide, which could not be separated at this point.

¹H NMR (400 MHz, CDCl₃) δ = 7.06 (d, J = 8.3 Hz, 1H, H-5), 6.87 (d, J = 8.4 Hz, 1H, H-4), 6.09 (d, J = 4.7 Hz, 1H, H-8), 5.65 (d, J = 4.6 Hz, 1H, H-7), 5.04 (s, 1H, H-18), 3.90 (s, 3H, H-22), 3.89 (s, 3H, H-23), 3.16 (d, J = 18.0 Hz, 1H, H-11a), 3.04 (s, 3H, H-13), 2.88 (d, J = 18.0 Hz, 1H, H-11b), 2.43–2.34 (m, 1H, H-15a), 2.34–2.26 (m, 1H, H-14a), 2.08 (td, J = 11.8, 7.2 Hz, 1H, H-15b), 1.98 (td, J = 12.1, 6.7 Hz, 1H, H-14b), 1.47 (s, 9H, H-21) ppm.



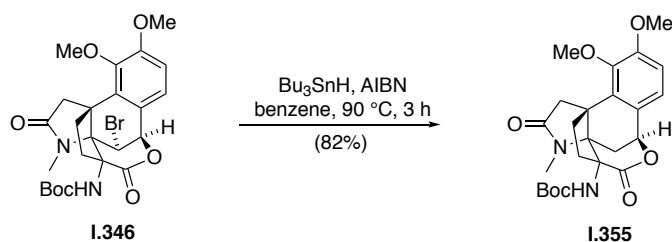
¹³C NMR (101 MHz, CDCl₃): δ = 176.0 (C-12), 169.7 (C-17), 155.5 (C-3), 154.5 (C-19), 145.8 (C-2), 135.2 (C-1), 125.5 (C-5), 122.6 (C-6), 111.2 (C-4), 82.0 (C-20), 78.6 (C-7), 75.6 (C-9), 71.2 (C-16), 60.6 (C-22), 55.7 (C-23), 49.2 (C-11), 47.4 (C-10), 44.6 (C-8), 39.6 (C-14), 38.0 (C-15), 29.7 (C-13), 28.3 (C-21) ppm.

IR (ATR): $\tilde{\nu}$ = 2928 (w), 1702 (w), 1746 (m), 1699 (s), 1684 (s), 1602 (w), 1589 (w), 1521 (w), 1491

(m), 1457 (m), 1426 (w), 1391 (w), 1369 (m), 1274 (s), 1232 (w), 1161 (m), 1121 (m), 1025 (m), 983 (m), 814 (m), 806 (m) cm^{-1} .

HRMS (ESI): calcd. for $\text{C}_{24}\text{H}_{30}\text{N}_2\text{O}_7\text{Br}^+$: 537.1231 $[\text{M}+\text{H}]^+$
 found: 537.1234 $[\text{M}+\text{H}]^+$.

***tert*-Butyl ((7*S*,11*bR*)-10,11-dimethoxy-3-methyl-2,5-dioxo-2,3-dihydro-1*H*,7*H*-4,11*b*-ethano-3*a*,7-methanobenzo[6,7]oxocino[4,5-*b*]pyrrol-4(5*H*)-yl)carbamate (**I.355**)**



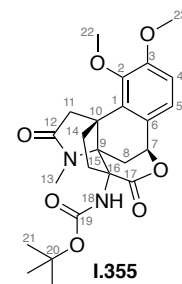
Bromide **I.346** (12.5 mg, 23.3 μmol , 1.0 eq.) was dissolved in benzene (1 mL) and AIBN (3.83 mg, 23.3 μmol , 1 eq.) followed by Bu_3SnH (63 μL , 67.7 mg, 0.233 mmol, 10 eq.) were added. The reaction mixture was degassed using three freeze-pump-thaw cycles. The reaction was then placed in a 90 $^\circ\text{C}$ oil bath and stirred at this temperature for 3 h. After cooling to room temperature, the solvent was removed under reduced pressure. Flash column chromatography on silica/ K_2CO_3 , 9:1 [DCM/acetone, 10:1 \rightarrow 2:1] afforded lactone **I.355** (8.8 mg, 19 μmol , 82%) as a colorless solid.

The compound was accompanied by 30–35% succinimide, which could not be separated at this point.

Crystals suitable for single-crystal X-ray analysis (Section 9.1) were obtained from recrystallization [CHCl_3] at 20 $^\circ\text{C}$.

$R_f = 0.51$ [DCM/acetone, 3:1].

^1H NMR (400 MHz, CDCl_3) $\delta = 7.04$ (d, $J = 8.3$ Hz, 1H, H-5), 6.83 (d, $J = 8.4$ Hz, 1H, H-4), 5.54 (d, $J = 4.5$ Hz, 1H, H-7), 5.00 (s, 1H, H-18), 3.89 (s, 3H, H-22), 3.88 (s, 3H, H-23), 3.77 (dd, $J = 13.1, 4.7$ Hz, 1H, H-8a), 3.20 (d, $J = 18.2$ Hz, 1H, H-11a), 3.03 (s, 3H, H-13), 2.80 (d, $J = 19.9$ Hz, 2H, H-11b and H-succinimide), 2.33–2.22 (m, 2H, H-14a, H-15a), 2.04–1.93 (m, 2H, H-14b, H-15b), 1.78 (d, $J = 12.9$ Hz, 1H, H-8b), 1.46 (s, 9H, H-21) ppm.



^{13}C NMR (101 MHz, CDCl_3): $\delta = 175.1$ (C-12), 171.2 (C-17), 155.4 (C-19), 154.2 (C-3), 146.6 (C-2), 135.5 (C-1), 126.2 (C-6), 124.4 (C-5), 111.1 (C-4), 81.3 (C-20), 76.2 (C-7), 72.4 (C-9), 69.3 (C-16),

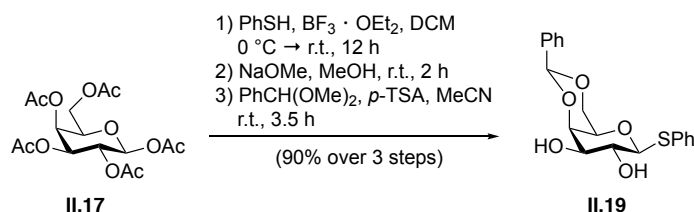
60.7 (C-22), 55.8 (C-23), 49.6 (C-10), 45.9 (C-11), 39.1 (C-14), 37.4 (C-15), 29.1 (C-8), 28.3 (C-13 and C-21) ppm.

IR (ATR): $\tilde{\nu}$ = 3339 (w), 2976 (w), 2934 (w), 1683 (s), 1603 (w), 1581 (w), 1526 (w), 1491 (m), 1457 (m), 1424 (w), 1392 (m), 1368 (m), 1329 (w), 1273 (s), 1244 (m), 1162 (m), 1125 (m), 1072 (m), 1026 (w), 1004 (w), 987 (w), 974 (w), 950 (w), 922 (w), 816 (w), 754 (m), 685 (m), 667 (w) cm^{-1} .

HRMS (ESI): calcd. for $\text{C}_{24}\text{H}_{31}\text{N}_2\text{O}_7^+$: 459.2126 $[\text{M}+\text{H}]^+$
found: 459.2129 $[\text{M}+\text{H}]^+$.

8.3 Experimental data of chapter II

(2*R*,6*S*,7*R*,8*R*,8*aR*)-2-Phenyl-6-(phenylthio)hexahydropyrano[3,2-*d*][1,3]dioxine-7,8-diol (II.19)



β -D-Galactose pentaacetate (**II.17**, 2.50 g, 6.40 mmol, 1.0 eq.) was dissolved in DCM (125 mL) and thiophenol (2.00 mL, 19.2 mmol, 3.0 eq.) was added. The mixture was cooled to 0 °C and BF₃·OEt₂ (2.40 mL, 19.2 mmol, 3.0 eq.) was added dropwise. The mixture was allowed to warm to room temperature and stirred for 12 h. Then more DCM (50 mL) was added and the organic layer was washed with 10% aqueous NaOH (3 × 50 mL), H₂O (50 mL), saturated aqueous NaCl (50 mL), dried (MgSO₄) and concentrated under reduced pressure. The crude product was immediately redissolved in MeOH (50 mL) and NaOMe was added until pH 9–10. The reaction mixture stirred at room temperature and after 4 h, it was stopped by the addition of DOWEX 50WX 2-100 (H⁺ form) and stirred for another 30 min at room temperature. All solid material was removed by filtration through a pad of Celite[®], which was washed with MeOH (20 mL) and the filtrate was concentrated under reduced pressure. The crude product was dissolved in MeCN (40 mL) at 60 °C. The mixture was allowed to cool to room temperature and benzaldehyde dimethyl acetal (2.90 mL, 19.2 mmol, 3.0 eq.) and *p*-TSA hydrate (121 mg, 0.640 mmol, 0.1 eq.) was added. The reaction mixture was stirred at room temperature for 3.5 h, then NEt₃ was added (until pH = 8–9). The solvent was removed under reduced pressure and flash column chromatography on silica gel [DCM/MeOH, 9:1] afforded galactose acetal **II.19** (2.08 g, 5.76 mmol, 90% over 3 steps) as a white powder.

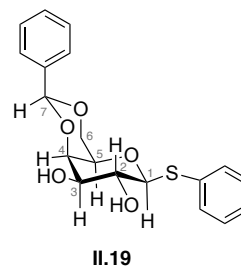
$R_f = 0.21$ [PE/EtOAc, 1:2].

$[\alpha]_D = -0.25$ ($c = 0.06$, MeOH).

mp: 155–156 °C.

¹H NMR (400 MHz, CDCl₃): $\delta = 7.71$ – 7.66 (m, 2H, H-Ar), 7.42 – 7.33 (m, 8H, H-Ar), 5.50 (s, 1H, H-7), 4.50 (d, 1H, $J = 9.2$ Hz, H-1), 4.37 (dd, 1H, $J = 12.5, 1.6$ Hz, H-6a), 4.19 (dd, 1H, $J = 1.2$ Hz, H-4), 4.02 (dd, 1H, $J = 12.5, 1.8$ Hz, H-6b), 3.72–3.62 (m, 2H, H-2, H-3), 3.56–3.49 (m, 1H, H-5), 2.73–2.58 (m, 2H, OH-2, OH-3) ppm.

^{13}C NMR (100 MHz, CDCl_3): δ = 137.7 (C-Ar), 133.8 (C-Ar), 130.9 (C-Ar), 129.5 (C-Ar), 129.1 (C-Ar), 128.4 (C-Ar), 128.3 (C-Ar), 126.6 (C-Ar), 101.5 (C-7), 87.1 (C-1), 75.5 (C-4), 73.9 (C-3), 70.1 (C-5), 69.4 (C-6), 68.8 (C-2) ppm.

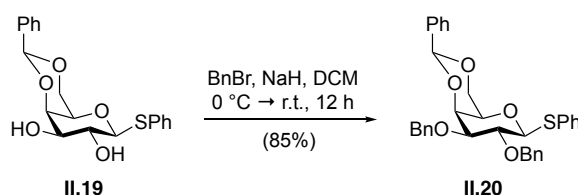


IR (ATR): $\tilde{\nu}$ = 3345 (m), 2916 (w), 1584 (w), 1481 (m), 1463 (m), 1440 (m), 1360 (m), 1264 (w), 1235 (w), 1200 (w), 1135 (m), 1122 (w), 1080 (s), 1050 (s), 1015 (s), 907 (m), 862 (m), 804 (m), 786 (w), 733 (w), 705 (m), 690 (s) cm^{-1} .

HRMS (EI): calcd. for $\text{C}_{19}\text{H}_{24}\text{O}_5\text{NS}^+$: 378.1370 $[\text{M}+\text{NH}_4]^+$
found: 378.1377 $[\text{M}+\text{NH}_4]^+$.

The analytical data matched those previously described in the literature.^[386]

(2*R*,6*S*,7*R*,8*S*,8*aS*)-7,8-bis(Benzyloxy)-2-phenyl-6-(phenylthio)hexahydropyrano[3,2-d][1,3]dioxine (II.20)



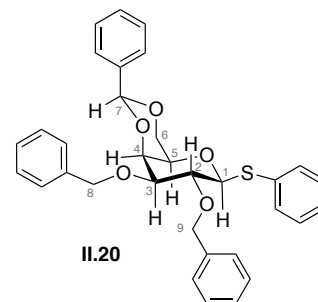
Galactose acetal **II.19** (2.06 g, 5.70 mmol, 1.0 eq.) was dissolved in DMF (40 mL) and cooled to 0 °C. After 15 min., NaH (1.64 g, 41.1 mmol, 7.2 eq.) was added and stirred for 20 min at this temperature. Then benzyl bromide (2.40 mL, 20.5 mmol, 3.6 eq.) was added and the mixture was slowly allowed to warm to room temperature and stirred for 12 h. Ice-cold H_2O (30 mL) was added and the aqueous layer was extracted with DCM (3×50 mL). The organic layer was washed with saturated aqueous NaCl solution (50 mL), dried (MgSO_4) and concentrated under reduced pressure. Flash column chromatography on silica gel [PE/EtOAc, 4:1] afforded fully protected galactose **II.20** (2.61 g, 4.83 mmol, 85%) as a white powder.

R_f = 0.49 [PE/EtOAc, 2:1].

$[\alpha]_D = -0.12$ ($c = 0.09$, DCM).

mp: 172–173 °C.

¹H NMR (400 MHz, CDCl₃): δ = 7.74–7.68 (m, 2H, H-Ar), 7.56–7.51 (m, 2H, H-Ar), 7.44–7.27 (m, 13H, H-Ar), 7.24–7.16 (m, 3H, H-Ar), 5.50 (s, 1H, H-7), 4.72 (d, 2H, J = 2.3 Hz, H-8), 4.70 (d, 2H, J = 3.8 Hz, H-9), 4.62 (d, 1H, J = 9.5 Hz, H-1), 4.38 (dd, 1H, J = 12.3, 1.6 Hz, H-6a), 4.16 (d, 1H, J = 2.9 Hz, H-4), 3.99 (dd, 1H, J = 12.3, 1.6 Hz, H-6b), 3.90 (t, 1H, J = 9.4 Hz, H-2), 3.63 (dd, 1H, J = 9.2, 3.4 Hz, H-3), 3.43 (dd, 1H, J = 1.5 Hz, H-5) ppm.



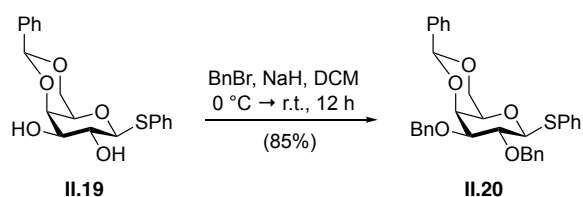
¹³C NMR (100 MHz, CDCl₃): δ = 138.6 (C-Ar), 138.2 (C-Ar), 138.0 (C-Ar), 132.9 (C-Ar), 132.8 (C-Ar), 129.2 (C-Ar), 129.0 (C-Ar), 128.6 – 127.6 (C-Ar), 126.8 (C-Ar), 101.5 (C-7), 86.7 (C-1), 81.5 (C-3), 75.6 (C-9), 75.5 (C-2), 73.9 (C-4), 72.0 (C-8), 70.0 (C-5), 69.6 (C-6) ppm.

IR (ATR): $\tilde{\nu}$ = 3368 (br, w), 2863 (w), 1585 (w), 1497 (w), 1482 (w), 1453 (m), 1441 (w), 1398 (w), 1366 (m), 1355 (w), 1342 (w), 1281 (w), 1250 (w), 1214 (w), 1168 (m), 1130 (m), 1091 (s), 1078 (m), 1056 (s), 1026 (m), 1000 (m), 898 (w), 867 (w), 814 (m), 730 (s), 695 (s) cm⁻¹.

HRMS (ESI): calcd. for C₃₃H₃₆O₅NS⁺: 558.2309 [M+NH₄]⁺
found: 558.2321 [M+NH₄]⁺.

The analytical data matched those previously described in the literature.^[399]

2,3-Di-O-benzyl-4,6-O-benzylidene- α,β -D-galactopyranose (II.21)



Protected galactose **II.20** (2.61 g, 4.83 mmol, 1.0 eq.) was dissolved in acetone (80 mL). Then H₂O (7.7 mL) was added and the mixture was cooled to 0 °C. NBS (1.02 g, 8.70 mmol, 1.8 eq.) was added and the color of the mixture changed to yellow. After 1 h, the yellow color disappeared and saturated aqueous Na₂S₂O₃ solution (40 mL) was added. The aqueous layer was extracted with DCM (2 × 50 mL) and the combined organic layers were washed with saturated aqueous Na₂S₂O₃ (40 mL), saturated aqueous NaCl solution (40 mL), dried (MgSO₄) and concentrated under reduced pressure. Flash column chromatography on silica gel [PE/EtOAc, 1:1] afforded hemiacetal **II.21** (1.93 g, 4.30 mmol, 89%) as a white powder.

The compound was obtained as an inseparable mix of diastereomers. Thus NMR signals could not be assigned. All signals match the data reported in the literature.^[401]

$R_f = 0.35$ [PE/EtOAc, 2:1].

$[\alpha]_D = +0.50$ ($c = 0.08$, MeOH).

mp: 154–155°C.

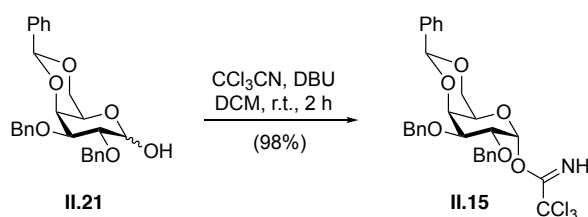
¹H NMR (400 MHz, CDCl₃): $\delta = 7.59$ – 7.51 (m, 4H), 7.45 – 7.27 (m, 26H), 5.50 (s, 1H), 5.49 (s, 1H), 5.38 – 5.35 (m, 1H), 4.91 – 4.68 (m, 8H), 4.65 (t, 1H, $J = 7.4$ Hz), 4.31 (d, 1H, $J = 12.4$ Hz), 4.25 – 4.17 (m, 2H), 4.12 – 4.04 (m, 2H), 4.02 – 3.95 (m, 3H), 3.84 – 3.77 (m, 2H), 3.66 – 3.43 (m, 2H), 3.32 – 3.27 (m, 1H), 3.19 – 3.04 (m, 1H) ppm.

¹³C NMR (100 MHz, CDCl₃): $\delta = 138.7$, 138.6 , 138.4 , 138.3 , 137.9 , 137.8 , 129.0 , 128.5 , 128.4 , 128.3 , 128.2 , 128.1 , 127.9 , 127.7 , 126.5 , 126.4 , 101.2 , 101.1 , 97.6 , 92.5 , 80.0 , 79.4 , 75.9 , 75.8 , 75.3 , 74.4 , 73.9 , 73.8 , 72.0 , 71.9 , 69.6 , 69.4 , 66.8 , 62.8 ppm.

IR (ATR): $\tilde{\nu} = 3376$ (br, w), 2914 (w), 1454 (m), 1098 (s), 739 (s), 698 (s) cm⁻¹.

HRMS (ESI): calcd. for C₂₇H₃₂O₆N⁺: 466.2224 [M+NH₄]⁺
found: 466.2235 [M+NH₄]⁺.

(2R,6R,7R,8S,8aS)-7,8-bis(Benzyloxy)-2-phenylhexahydropyrano[3,2-d][1,3]dioxin-6-yl 2,2,2-trichloroacetimidate (II.15)



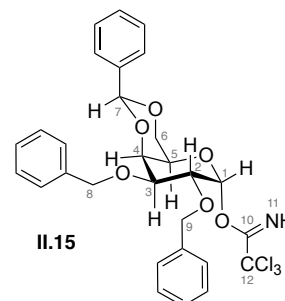
Hemiacetal **II.21** (750 mg, 1.67 mmol, 1.0 eq.) was dissolved in DCM (13 mL) and CCl₃CN (1.30 mL, 16.7 mmol, 10 eq.) followed by DBU (100 μ L, 0.669 mmol, 0.4 eq.) were added. The mixture was stirred at room temperature for 2 h. Then the solvent was removed under reduced pressure and the crude product was purified by flash column chromatography on silica gel [PE/EtOAc, 3:2 + 1% NEt₃] to give trichloroacetimidate **II.15** (974 mg, 1.64 mmol, 98%) as a white powder.

$R_f = 0.58$ [PE/EtOAc, 2:1].

$[\alpha]_D = +31.4$ ($c = 4.3$, DCM)

mp: 137–138 °C.

$^1\text{H NMR}$ (400 MHz, CDCl_3): $\delta = 8.58$ (s, 1H, H-11), 7.60–7.49 (m, 2H, H-Ar), 7.45–7.28 (m, 13H, H-Ar), 6.65 (d, 1H, $J = 3.3$ Hz, H-1), 5.53 (s, 1H, H-7), 4.87–4.74 (m, 4H, H-8, H-9), 4.34–4.26 (m, 3H, H-2, H-4, H-6a), 4.09 (dd, 1H, $J = 10.1, 3.3$ Hz, H-3), 4.02 (dd, 1H, $J = 12.7, 1.8$ Hz, H-6b), 3.85 (s, 1H, H-5) ppm.



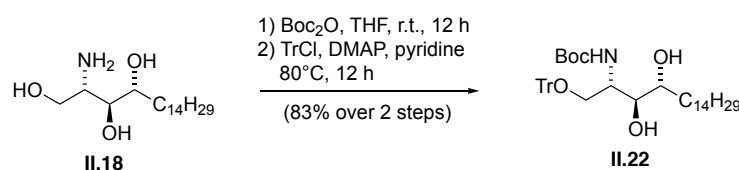
$^{13}\text{C NMR}$ (100 MHz, CDCl_3): $\delta = 161.1$ (C-10), 138.5 (C-Ar), 138.4 (C-Ar), 137.7 (C-Ar), 129.1 (C-Ar), 128.4–127.5 (C-Ar), 126.5 (C-Ar), 101.2 (C-7), 95.7 (C-1), 91.5 (C-12), 75.2 (C-2), 74.8 (C-3), 74.6 (C-4), 73.2 (C-9), 72.3 (C-8), 69.2 (C-6), 65.4 (C-5) ppm.

IR (ATR): $\tilde{\nu} = 3344$ (w), 2918 (w), 2251 (w), 2163 (w), 1998 (w), 1727 (m), 1497 (w), 1455 (m), 1364 (w), 1099 (s), 1051 (m), 1028 (m), 824 (m), 739 (m), 698 (s) cm^{-1} .

HRMS (ESI): calcd. for $\text{C}_{29}\text{H}_{29}\text{O}_6\text{Cl}_3\text{N}^+$: 592.1055 $[\text{M}+\text{H}]^+$
found: 592.1079 $[\text{M}+\text{H}]^+$.

The analytical data matched those previously described in the literature.^[401]

***tert*-Butyl-((2*S*,3*S*,4*R*)-3,4-dihydroxy-1-(trityloxy)octadecan-2-yl)carbamate (II.22)**



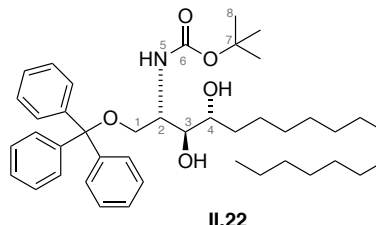
Boc_2O (1.13 g, 5.19 mmol, 1.1 eq.) and phytosphingosine **II.18** (1.50 g, 4.72 mmol, 1.0 eq.) were dissolved in THF (50 mL) and stirred at room temperature for 12 h. The reaction was stopped by the addition of 0.5 M aqueous HCl (50 mL) and the aqueous layer was extracted with EtOAc (3 \times 100 mL). The combined organic layers were washed with H_2O (100 mL) and saturated aqueous NaCl solution (100 mL), dried (MgSO_4) and concentrated under reduced pressure. The residue was dissolved in pyridine (60 mL), and TrCl (1.32 g, 4.72 mmol, 1.0 eq.) followed by DMAP (28.8 mg, 0.236 mmol, 0.05 eq.) were added. The mixture was stirred at 80 °C for 12 h. Then a second portion of TrCl (395 mg, 1.42 mmol, 0.3 eq.) was added and, after additional 2 h,

the solvent was removed under reduced pressure. Flash column chromatography on silica gel [PE/EtOAc, 4:1] afforded diol **II.22** (2.55 g, 3.87 mmol, 82% over two steps) as a colorless oil.

$R_f = 0.40$ [PE/EtOAc, 4:1].

$[\alpha]_D = +0.02$ ($c = 0.1$, MeOH).

$^1\text{H NMR}$ (400 MHz, CDCl_3): $\delta = 7.43\text{--}7.40$ (m, 6H, H-Ar), 7.34–7.29 (m, 6H, H-Ar), 7.27–7.23 (m, 3H, H-Ar), 5.18 (d, 1H, $J = 8.9$ Hz, H-5), 3.95 (q, $J = 4.3$ Hz, 1H, H-2), 3.60 (dt, 1H, $J = 8.2, 5.5$ Hz, H-3), 3.40–3.39 (m, 3H, H-1, H-4), 2.80 (d, 1H, $J = 8.1$ Hz, OH-3), 2.02 (d, 1H, $J = 7.6$ Hz, OH-4), 1.67–1.62 (m, 1H, H-alkyl), 1.46 (m, 10H, H-8, H-alkyl), 1.44–1.05 (m, 25H, H-alkyl), 0.88 (t, $J = 6.4$ Hz, H-alkyl) ppm.

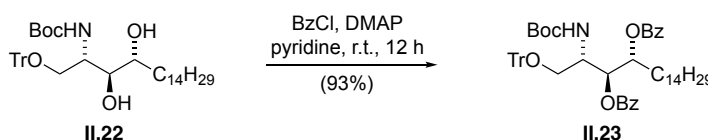


$^{13}\text{C NMR}$ (100 MHz, CDCl_3): $\delta = 155.8$ (C-6), 143.4 (C-Ar), 128.6 (C-Ar), 128.2 (C-Ar), 127.5 (C-Ar), 87.7 (C-Ar), 79.8 (C-7), 76.0 (C-3), 73.3 (C-4), 63.4 (C-1), 51.2 (C-2), 33.2–29.5 (C-alkyl), 28.6 (C-8), 26.0 (C-alkyl), 22.9 (C-alkyl), 14.3 (C-alkyl) ppm.

IR (ATR): $\tilde{\nu} = 3441$ (w), 1923 (s), 2853 (m), 1692 (m), 1492 (m), 1449 (m), 1392 (w), 1366 (m), 1319 (w), 1246 (w), 1169 (m), 1058 (m), 1001 (m), 899 (w), 862 (w), 761 (m), 745 (m), 703 (s) cm^{-1} .

HRMS (ESI): calcd. for $\text{C}_{42}\text{H}_{61}\text{NO}_5\text{Cl}$: 694.4244 $[\text{M}+\text{Cl}]^-$
found: 694.4283 $[\text{M}+\text{Cl}]^-$.

(2*S*,3*S*,4*R*)-2-((*tert*-Butoxycarbonyl)amino)-1-(trityloxy)octadecane-3,4-diyl dibenzoate (II.23)



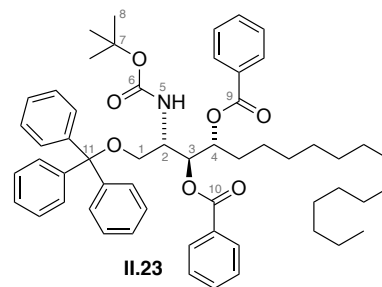
To a solution of diol **II.22** (1.21 g, 1.84 mmol, 1.0 eq.) in pyridine (84 mL) was added benzoyl chloride (1.28 mL, 11.0 mmol, 6.0 eq.) and DMAP (17.9 mg, 150 μmol , 0.08 eq.). The mixture was stirred at room temperature for 12 h. Then iced-cold H_2O (50 mL) was added and the aqueous layer was extracted with DCM (3×100 mL). The combined organic layers were washed with saturated aqueous NaHCO_3 (100 mL) and saturated aqueous NaCl (100 mL) and concentrated under reduced pressure. Flash column chromatography on silica gel [PE/EtOAc, 10:0→10:1] afforded protected phytosphingosine **II.23** (1.48 g, 1.70 mmol, 93%) as a colorless oil.

$R_f = 0.46$ [PE/EtOAc, 9:1 + 1% NEt₃].

$[\alpha]_D = +0.14$ ($c = 0.08$, MeOH).

¹H NMR (400 MHz, CDCl₃): $\delta = 7.96$ – 7.90 (m, 2H, H-Ar), 7.83 (dd, 2H, $J = 8.3, 1.4$ Hz, H-Ar), 7.59– 7.51 (m, 2H, H-Ar), 7.43– 7.28 (m, 10H, H-21, H-Ar), 7.19– 7.08 (m, 9H, H-Ar), 5.72 (dd, 1H, $J = 9.0, 2.9$ Hz, H-3), 5.49 (dt, 1H, $J = 9.5, 3.1$ Hz, H-4), 5.07 (d, 1H, $J = 9.9$ Hz, NH-5), 4.33– 4.24 (m, 1H, H-2), 3.32 (dd, 1H, $J = 9.6, 3.1$ Hz, H-1a), 3.20 (dd, 1H, $J = 9.6, 4.3$ Hz, H-1b), 1.95– 1.78 (m, 2H, H-alkyl), 1.48 (s, 9H, H-8), 1.43– 1.17 (m, 24H, H-alkyl), 0.88 (t, 3H, $J = 6.9$ Hz, H-alkyl) ppm.

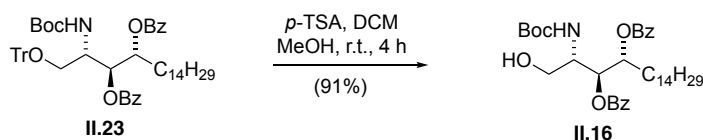
¹³C NMR (100 MHz, CDCl₃): $\delta = 166.3$ (C-9), 165.2 (C-10), 155.5 (C-6), 143.5 (C-Ar), 133.1 (C-Ar), 133.0 (C-Ar), 130.0 (C-Ar), 129.9 (C-Ar), 129.5 (C-Ar), 128.7 (C-Ar), 128.4 (C-Ar), 127.9 (C-Ar), 127.0 (C-Ar), 86.8 (C-11), 79.9 (C-7), 73.9 (C-4), 72.9 (C-3), 62.2 (C-1), 50.6 (C-2), 32.1– 29.4 (C-alkyl), 28.7 (C-alkyl), 28.5 (C-8), 25.7– 22.8 (C-alkyl), 14.3 (C-alkyl) ppm.



IR (ATR): $\tilde{\nu} = 3352$ (br, w), 2925 (m), 2854 (w), 1717 (m), 1602 (w), 1492 (w), 1450 (m), 1367 (m), 1315 (w), 1262 (m), 1173 (m), 1094 (m), 1068 (m), 1026 (m), 899 (w), 756 (m), 703 (s) cm⁻¹.

HRMS (ESI): calcd. for C₅₆H₇₃N₂O₇⁺: 885.5412 [M+NH₄]⁺
found: 885.5439 [M+NH₄]⁺.

(2*S*,3*S*,4*R*)-2-((*tert*-Butoxycarbonyl)amino)-1-hydroxyoctadecane-3,4-diyl dibenzoate (II.16)



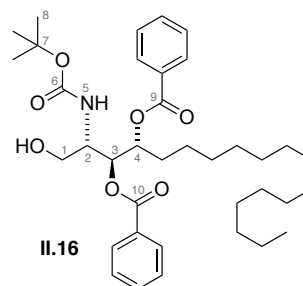
To a solution of protected phytosphingosine **II.23** (1.48 g, 1.70 mmol, 1.0 eq.) in DCM (28 mL) and MeOH (28 mL) was added *p*-TSA (325 mg, 1.70 mmol, 1.0 eq.). The mixture was stirred at room temperature for 5 h, then saturated aqueous NaHCO₃ (30 mL) was added and the aqueous layer was extracted with DCM (3 × 100 mL). The combined organic layers were washed with saturated aqueous NaHCO₃ solution (100 mL) and saturated aqueous NaCl solution (100 mL), dried (MgSO₄) and concentrated under reduced pressure. Flash column chromatography

[PE/EtOAc, 10:1 to 3:1] afforded primary alcohol **II.16** (968 mg, 1.55 mmol, 91%) as a colorless oil.

$R_f = 0.54$ [PE/EtOAc, 2:1 + 1% NEt₃].

$[\alpha]_D = +0.08$ ($c = 0.09$, MeOH).

¹H NMR (400 MHz, CDCl₃): $\delta = 8.08$ – 8.03 (m, 2H, H-Ar), 7.97 – 7.93 (m, 2H, H-Ar), 7.63 (tt, 1H, $J = 7.4, 1.3$ Hz, H-Ar), 7.54 – 7.47 (m, 3H, H-Ar), 7.37 (t, 2H, $J = 7.8$ Hz, H-Ar), 5.50 (dt, 1H, $J = 9.3, 3.1$ Hz, H-4), 5.40 (dd, 1H, $J = 9.5, 2.6$ Hz, H-3), 5.35 (d, 1H, $J = 9.8$ Hz, NH-5), 4.03 (t, 1H, $J = 9.6$ Hz, H-2), 3.65 (s, 2H, H-1), 2.62 (s, 1H, OH-1), 2.10 – 1.93 (m, 2H, H-alkyl), 1.48 (s, 9H, H-8), 1.44 – 1.11 (m, 24H, H-alkyl), 0.87 (t, 3H, $J = 6.8$ Hz, H-alkyl) ppm.



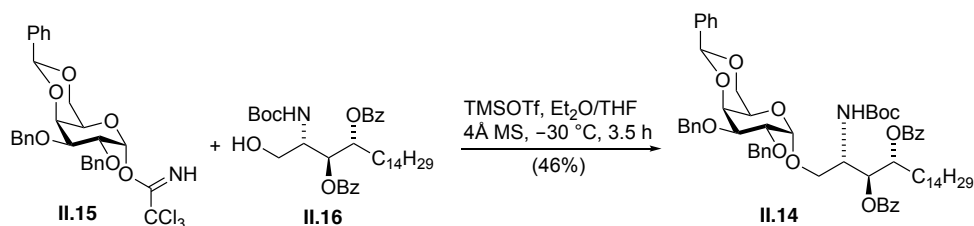
¹³C NMR (100 MHz, CDCl₃): $\delta = 167.2$ (C-10), 166.3 (C-9), 155.6 (C-Ar), 133.9 (C-6), 133.2 (C-Ar), 130.1 (C-Ar), 130.1 (C-Ar), 129.8 (C-Ar), 129.3 (C-Ar), 128.8 (C-Ar), 128.5 (C-Ar), 80.2 (C-7), 74.0 (C-3), 73.9 (C-4), 61.8 (C-1), 51.6 (C-2), 32.1 – 29.4 (C-alkyl), 28.6 (C-alkyl), 28.5 – 22.8 (C-alkyl), 14.3 (C-alkyl) ppm.

IR (ATR): $\tilde{\nu} = 3377$ (br, w), 2924 (s), 2854 (m), 1719 (s), 1602 (w), 1505 (w), 1452 (m), 1392 (w), 1366 (w), 1315 (m), 1279 (s), 1173 (m), 1108 (m), 1069 (m), 1026 (m), 711 (s) cm⁻¹.

HRMS (ESI): calcd. for C₃₇H₅₆NO₇⁺: 626.4052 [M+H]⁺
found: 626.4072 [M+H]⁺.

The analytical data matched those previously described in the literature.^[365]

(2*S*,3*S*,4*R*)-1-(((2*R*,6*S*,7*R*,8*S*,8*aS*)-7,8-*bis*(Benzyloxy)-2-phenylhexahydropyrano[3,2-*d*][1,3]-dioxin-6-yl)oxy)-2-((*tert*-butoxycarbonyl)amino)octadecane-3,4-diyl dibenzoate (**II.14**)

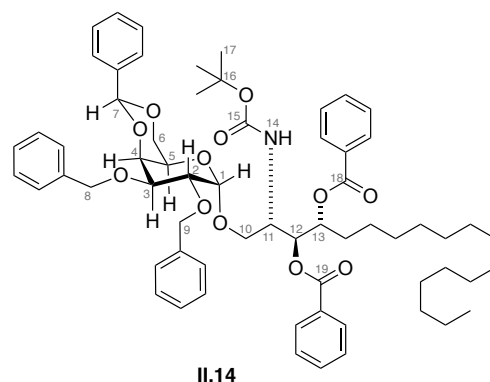


Galactosyl donor **II.28** (450 mg, 0.759 mmol, 1.5 eq.) and acceptor **II.16** (316 mg, 0.506 mmol, 1.0 eq.) were combined and co-evaporated with toluene (3×5 mL) and with THF (1×5 mL), dried under high vacuum and then dissolved in Et₂O (8.4 mL) and THF (4.2 mL). The mixture was stirred with freshly activated 4Å MS at room temperature for 30 min, before the reaction vessel was cooled to -30 °C and TMSOTf (5.2 μL, 29 μM, 0.056 eq.) was added. After 2.5 h a second portion of trichloroacetimidate **II.15** (450 mg, 0.759 mmol, 1.5 eq.) and after 15 min. TMSOTf (5.2 μL, 29 μM, 0.056 eq.) was added slowly. After 1 h at this temperature, the mixture was allowed to warm to -10 °C and after an additional 0.5 h the reaction was stopped by the addition of NEt₃ (1 mL). Then the reaction mixture was allowed to warm to room temperature and EtOAc (10 mL) was added. All solid material was removed by filtration through a pad of Celite[®], which was washed with EtOAc (20 mL). Saturated aqueous NaHCO₃ (10 mL) was added to the filtrate and the aqueous layer was extracted with EtOAc (3×20 mL). The combined organic layers were dried (MgSO₄) and concentrated under reduced pressure. Flash column chromatography [PE/EtOAc, 100:0 to 0:1] afforded protected glycoside **II.14** (249 mg, 0.235 mmol, 46%) as a colorless oil.

$R_f = 0.69$ [PE/EtOAc, 2:1].

$[\alpha]_D = +0.19$ ($c = 0.06$, MeOH).

¹H NMR (400 MHz, CDCl₃): $\delta = 8.05$ – 7.92 (m, 4H, H-Ar), 7.65 – 7.13 (m, 21H, H-Ar), 5.60 (dd, 1H, $J = 8.6, 3.2$ Hz, H-12), 5.46 (s, 1H, H-7), 5.44 – 5.38 (m, 1H, H-13), 5.38 – 5.32 (m, 1H, NH-14), 4.86 (d, 1H, $J = 3.6$ Hz, H-1), 4.78 – 4.59 (m, 4H, H-8, H-9), 4.30 – 4.19 (m, 2H, H-11, H-6a), 4.16 (d, 1H, $J = 3.4$ Hz, H-4), 4.06 – 3.99 (m, 2H, H-2, H-6b), 3.93 – 3.88 (m, 1H, H-3), 3.86 – 3.79 (m, 1H, H-10a), 3.77 – 3.69 (m, 2H, H-10b, H-5), 2.02 – 1.79 (m, 2H, H-alkyl), 1.47 (s, 9H, H-17), 1.37 – 1.18 (m, 24H, H-alkyl), 0.88 (t, 3H, $J = 6.9$ Hz, H-alkyl) ppm.



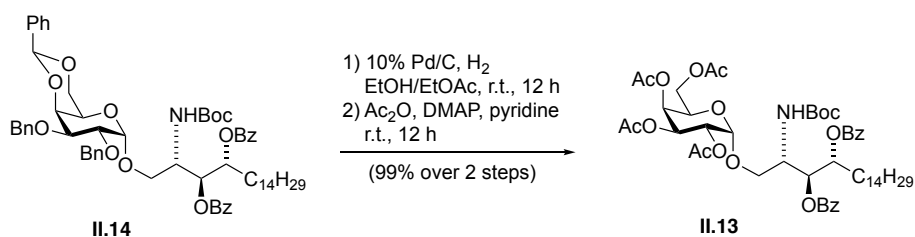
^{13}C NMR (100 MHz, CDCl_3): δ = 166.3 (C-19), 165.4 (C-15, C-19), 139.0–126.4 (C-Ar), 101.0 (C-7), 100.4 (C-1), 80.1 (C-16), 76.0 (C-3), 75.8 (C-2), 74.8 (C-4), 73.9 (C-13), 73.6 (C-9), 73.1 (C-12), 72.2 (C-8), 69.8 (C-10), 69.6 (C-6), 63.5 (C-5), 50.7 (C-11), 32.1–29.4 (C-alkyl), 28.8 (C-alkyl), 28.5 (C-17), 25.8–22.8 (C-alkyl), 14.3 (C-alkyl) ppm.

IR (ATR): $\tilde{\nu}$ = 2924 (m), 2854 (w), 1715 (m), 1602 (w), 1497 (w), 1452 (m), 1392 (w), 1366 (m), 1314 (m), 1258 (s), 1173 (m), 1095 (s), 1068 (s), 1064 (s), 1025 (s), 798 (m), 740 (m), 710 (s), 696 (s) cm^{-1} .

HRMS (ESI): calcd. for $\text{C}_{64}\text{H}_{85}\text{O}_{12}\text{N}_2^+$: 1073.6097 $[\text{M}+\text{NH}_4]^+$
found: 1073.6110 $[\text{M}+\text{NH}_4]^+$.

The analytical data matched those previously described in the literature.^[365]

(2R,3S,4S,5R,6S)-2-(Acetoxymethyl)-6-(((2S,3S,4R)-3,4-bis(benzoyloxy)-2-((tert-butoxycarbonyl)-amino)octadecyl)oxy)tetrahydro-2H-pyran-3,4,5-triyl triacetate (II.13)

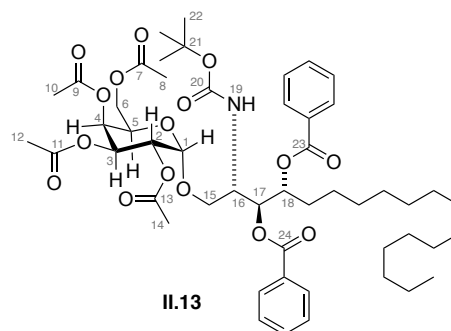


Protected glycoside **II.14** (249 mg, 0.235 mmol, 1.0 eq.) was dissolved in ethanol/EtOAc (1:1, 12.6 mL) and 10% Pd/C (250 mg, 10 wt%, 0.01 eq.) was added. The mixture was stirred vigorously under H_2 -atmosphere at room temperature for 12 h. Then the solution was diluted with ethanol/EtOAc (1:1, 10 mL) and all solid material was removed by filtration through a pad of Celite[®], which was washed with ethanol/EtOAc (1:1, 20 mL). The filtrate was concentrated under reduced pressure and immediately dissolved in pyridine/ Ac_2O (1:1, 5 mL) and DMAP (1.44 mg, 11.8 μmol , 0.05 eq.) was added. The reaction mixture was stirred at room temperature for 12 h. Then the solvent was removed under reduced pressure and the crude product was dissolved in EtOAc (20 mL). The organic layer was washed with saturated aqueous NaCl solution (20 mL), dried (MgSO_4) and the solvent was removed under reduced pressure. Flash column chromatography on silica gel (PE/EtOAc, 10:1 to 1:1) afforded acetylated glycoside **II.13** (224 mg, 0.234 mmol, 99% over 2 steps) as a colorless oil.

R_f = 0.39 [PE/EtOAc, 2:1].

$[\alpha]_D = +0.25$ (c = 0.04, MeOH).

¹H NMR (400 MHz, acetone-*d*₆): δ = 8.11–8.04 (m, 2H, H-Ar), 8.02–7.95 (m, 2H, H-Ar), 7.71–7.65 (m, 1H, H-Ar), 7.64–7.59 (m, 1H, H-Ar), 7.54 (t, 2H, J = 7.8 Hz, H-Ar), 7.47 (t, 2H, J = 7.8 Hz, H-Ar), 6.84 (d, 1H, J = 9.6 Hz, NH-19), 5.71 (dd, 1H, J = 9.1, 3.0 Hz, H-17), 5.53 (dt, 1H, J = 10.2, 2.9 Hz, H-18), 5.42 (dd, 1H, J = 3.5, 1.3 Hz, H-4), 5.35 (dd, 1H, J = 10.6, 3.5 Hz, H-2), 5.03–4.98 (m, 2H, H-1, H-3), 4.44 (t, 1H, J = 6.5 Hz, H-5), 4.37 (tdd, 1H J = 9.0 Hz, 4.8, 2.9 Hz, H-16), 4.14–4.00 (m, 2H, H-6), 3.96 (dd, 1H, J = 10.4, 2.9 Hz, H-15a), 3.70 (dd, 1H, J = 10.4, 4.8 Hz, H-15b), 2.09 (s, 3H, H-Ac), 2.01–1.96 (m, 2H, H-alkyl), 1.94 (s, 3H, H-Ac), 1.92 (s, 3H, H-1Ac), 1.91 (s, 3H, H-Ac), 1.47 (s, 9H, H-22), 1.40–1.08 (m, 24H, H-alkyl), 0.87 (t, 3H, J = 6.8 Hz, H-alkyl) ppm.



¹³C NMR (100 MHz, acetone-*d*₆): δ = 170.7 (C-9, C-11), 170.4 (C-7), 170.2 (C-13), 166.3 (C-23), 165.7 (C-24), 156.4 (C-20), 134.2 (C-Ar), 133.9 (C-Ar), 131.1 (C-Ar), 130.9 (C-Ar), 130.5 (C-Ar), 130.3 (C-Ar), 129.5 (C-Ar), 129.3 (C-Ar), 97.6 (C-1), 79.4 (C-21), 74.5 (C-18), 73.6 (C-17), 68.8 (C-4), 68.5 (C-15), 68.4 (C-2, C-3), 67.3 (C-5), 62.2 (C-6), 51.1 (C-16), 32.6–29.3 (C-alkyl), 28.7 (C-22), 26.4–23.3 (C-alkyl), 20.6 (C-12), 20.6 (C-8, C-14), 20.5 (C-10), 14.4 (C-alkyl) ppm.

IR (ATR): $\tilde{\nu}$ = 2924 (m), 2854 (w), 1715 (m), 1602 (w), 1497 (w), 1452 (m), 1392 (w), 1366 (m), 1314 (m), 1258 (s), 1173 (m), 1095 (s), 1068 (s), 1064 (s), 1025 (s), 798 (m), 740 (m), 710 (s), 696 (s) cm^{-1} .

HRMS (ESI): calcd. for $\text{C}_{51}\text{H}_{77}\text{O}_{16}\text{N}_2^+$: 973.5268 $[\text{M}+\text{NH}_4]^+$
 found: 973.5290 $[\text{M}+\text{NH}_4]^+$.

The analytical data matched those previously described in the literature.^[365]

(2*R*,3*S*,4*S*,5*R*,6*S*)-2-(Acetoxymethyl)-6-(((2*S*,3*S*,4*R*)-3,4-*bis*(benzoyloxy)-2-(4-((*E*)-(4-heptylphenyl)-diazenyl)benzamido)octadecyl)oxy)tetrahydro-2*H*-pyran-3,4,5-triyl triacetate (II.46)

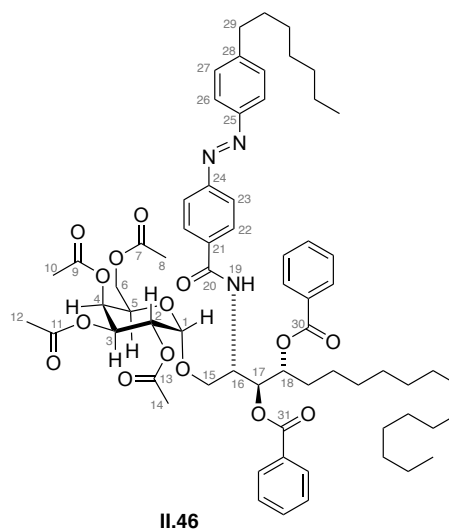


Acetylated glycoside **II.31** (66.7 mg, 69.7 μmol , 1.0 eq.) was dissolved in DCM (0.75 mL) and the mixture was cooled to 0 °C. TFA (0.75 mL) was added and the mixture was stirred at 0 °C and after 2 h the solvent was removed under reduced pressure. The crude product was immediately dissolved in DCM (3.4 mL) and FAAzo-1 (33.9 mg, 0.105 mmol, 1.5 eq.) followed by HBTU (39.6 mg, 0.105 mmol, 1.5 eq.) and *N*-methylmorpholine (97.3 μL , 1.05 mmol, 15 eq.) were added at room temperature. After 12 h, the solvent was removed under reduced pressure and the crude product was purified by flash column chromatography [PE/EtOAc, 100:0 to 1:1] to give protected glycosphingolipid **II.46** (60.9 mg, 52.4 μmol , 75% over 2 steps) as a yellow viscous oil.

$R_f = 0.40$ [PE/EtOAc, 2:1].

¹H NMR (400 MHz, CDCl₃): $\delta = 8.12$ (d, 2H, $J = 8.5$ Hz, H-22), 8.06–8.00 (m, 4H, H-Bz, H-23), 7.97–7.93 (m, 2H, H-35), 7.89 (d, 2H, $J = 8.3$ Hz, H-26), 7.67–7.60 (m, 1H, H-Bz), 7.56–7.52 (m, 1H, H-Bz), 7.49 (t, 2H, $J = 7.7$ Hz, H-Bz), 7.39 (t, 2H, $J = 7.8$ Hz, H-Bz), 7.36–7.31 (m, 2H, H-27), 5.88 (dd, 1H, $J = 9.4, 2.8$ Hz, H-17), 5.47–5.42 (m, 1H, H-18), 5.42–5.37 (m, 2H, H-3, H-4), 5.18–5.12 (m, 1H, H-2), 4.92 (d, 1H, $J = 3.6$ Hz, H-1), 4.91–4.84 (m, 1H, H-16), 4.14 (t, 1H, H-5), 4.00–3.93 (m, 2H, H-6), 3.92–3.87 (m, 1H, H-15a), 3.66 (dd, 1H, $J = 11.0, 2.8$ Hz, H-15b), 2.70 (t, 2H, $J = 7.6$ Hz, H-29), 2.10 (s, 3H, H-10 or H-12), 2.02–1.96 (m, 5H, H-10 or H-12, H-alkyl), 1.94 (s, 3H, H-14), 1.90 (s, 3H, H-8), 1.72–1.62 (m, 2H, H-alkyl), 1.35–1.10 (m, 30H, H-alkyl), 0.92–0.82 (m, 6H, H-alkyl) ppm.

¹³C NMR (100 MHz, CDCl₃): $\delta = 170.7$ (C-13), 170.5 (C-7), 170.3 (C-9, C-11), 166.8 (C-30), 166.5 (C-20), 165.4 (C-31), 154.8 (C-24), 151.0 (C-25), 147.5 (C-28), 135.1 (C-21), 133.7 (C-Bz), 133.3 (C-Bz), 130.0 (C-Bz, C-Bz), 129.8 (C-Bz), 129.4 (C-Bz), 129.3 (C-27), 128.8 (C-Bz), 128.5 (C-22), 123.3 (C-26), 123.1 (C-23), 97.6 (C-1), 74.2 (C-18), 72.0 (C-17), 68.1 (C-4), 67.8 (C-15), 67.6 (C-2, C-3), 67.0

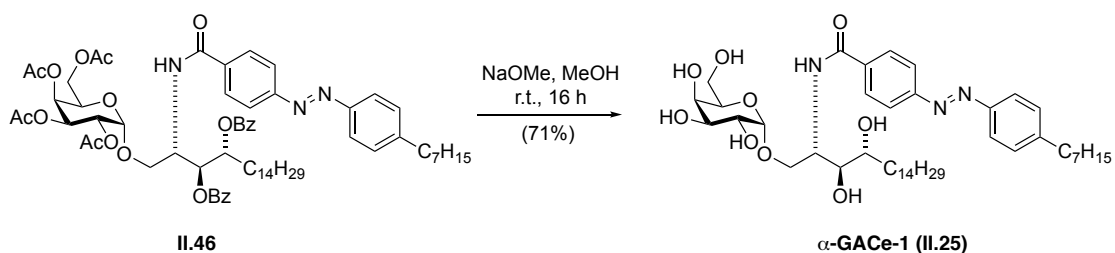


(C-5), 61.9 (C-6), 49.4 (C-16), 36.1 (C-29), 32.0–31.9 (C-alkyl), 31.4 (C-alkyl), 29.9–29.3 (C-alkyl), 28.2 (C-alkyl), 22.8 (C-alkyl), 20.8–20.6 (C-8, C-10, C-12, C-14), 14.3 (C-alkyl) ppm.

IR (ATR): $\tilde{\nu}$ = 2924 (m), 2854 (w), 1748 (m), 1724 (m), 1663 (m), 1602 (w), 1530 (m), 1492 (w), 1451 (m), 1370 (m), 1315 (w), 1223 (s), 1177 (m), 1153 (m), 1094 (m), 1068 (s), 1026 (s), 953 (w), 906 (w), 861 (m), 803 (m), 754 (s), 710 (s) cm^{-1} .

HRMS (ESI): calcd. for $\text{C}_{66}\text{H}_{91}\text{N}_4\text{O}_{15}^+$: 1179.6475 $[\text{M}+\text{NH}_4]^+$
found: 1179.6491 $[\text{M}+\text{NH}_4]^+$.

***N*-((2*S*,3*S*,4*R*)-3,4-Dihydroxy-1-(((2*S*,3*R*,4*S*,5*R*,6*R*)-3,4,5-trihydroxy-6-(hydroxymethyl)tetrahydro-2*H*-pyran-2-yl)oxy)octadecan-2-yl)-4-((*E*)-(4-heptylphenyl)diazenyl)benzamide (α -GACe-1, **II.25**)**

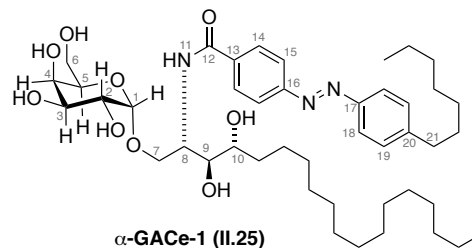


Protected glycosphingolipid **II.46** (60.9 mg, 52.4 μmol , 1.0 eq.) was dissolved in MeOH (14 mL) and NaOMe was added until pH 9–10. The reaction mixture was stirred at room temperature for 12 h. Then a second portion of NaOMe was added and stirred for additional 4 h at room temperature. The reaction was stopped by the addition of DOWEX 50WX 2-100 (H^+ form) and stirred for another 30 min at room temperature. All solid material was removed by filtration through a pad of Celite[®], which was washed with MeOH (20 mL) and the filtrate was concentrated under reduced pressure. Flash column chromatography [$\text{CHCl}_3/\text{MeOH}$, 19:1 to 9:1] afforded α -GACe-1 (**II.25**, 29.0 mg, 37.1 μmol , 71%) as yellow viscous oil.

Compound **II.25** was isolated as a 5:1 mixture of *trans*-/*cis*-isomers.

R_f = 0.20 [DCM/MeOH , 9:1].

¹H NMR (800 MHz, pyridine-*d*₅): δ = 9.05 (d, 1H, J = 7.6 Hz, NH-11), 8.41 (d, 2H, J = 8.0 Hz, H-14), 8.09 (d, 2H, J = 7.9 Hz, H-18), 8.05 (d, 2H, J = H-15), 7.42 (d, 2H, J = 8.0 Hz, H-19), 7.09 (d, J = 6.8 Hz, 1H, OH-2), 6.76 (d, 1H, J = 6.6 Hz, OH-9), 6.71–6.63 (m, 1H, OH-3), 6.59–6.50 (m, 1H, OH-6), 6.40–6.29 (m, 1H, OH-4), 6.22 (d, 1H, J = 6.8 Hz, OH-10), 5.63 (d, 1H, J = 2.7 Hz, H-1), 5.54–5.45 (m, 1H, H-8), 4.84–4.74 (m, 1H, H-7a), 4.73–4.64 (m, 1H, H-2), 4.60–4.29 (m, 8H, H-7b, H-3, H-9, H-4, H-10, H-5, H-6), 2.64 (t, 2H, J = 7.7 Hz, H-21), 2.38–2.28 (m, 1H, H-alkyl), 1.99–1.86 (m, 2H, H-alkyl), 1.75–1.66 (m, 1H, H-alkyl), 1.63–1.55 (m, 2H, H-alkyl), 1.49–1.35 (m, 2H, H-alkyl), 1.35–1.13 (m, 28H, H-alkyl), 0.91–0.83 (m, 6H, H-alkyl) ppm.

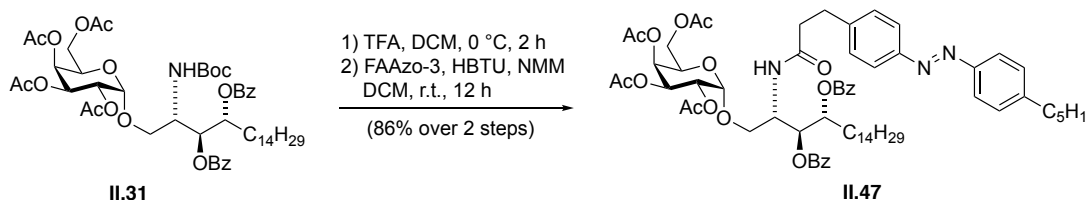


¹³C NMR (200 MHz, pyridine-*d*₅): δ = 167.5 (C-12), 154.8 (C-16), 151.8 (C-17), 148.1 (C-20), 138.4 (C-13), 130.2 (C-19), 129.7 (C-14), 124.1 (C-18), 123.4 (C-15), 102.0 (C-1), 76.7 (C-9), 73.6 (C-5), 73.0 (C-10), 72.1 (C-3), 71.6 (C-4), 70.8 (C-2), 68.6 (C-7), 63.2 (C-6), 53.1 (C-8), 36.5 (C-21), 34.9 (C-alkyl), 32.6–32.5 (C-alkyl), 31.9 (C-alkyl), 30.8 (C-alkyl), 30.6–29.8 (C-alkyl), 26.9 (C-alkyl), 23.4–20.2 (C-alkyl), 14.8–14.7 (C-alkyl) ppm.

IR (ATR): $\tilde{\nu}$ = 3570 (w), 3458 (m), 3288 (m), 2955 (m), 2920 (s), 2850 (m), 1635 (s), 1606 (m), 1538 (m), 1492 (w), 1468 (m), 1407 (w), 1347 (m), 1294 (m), 1224 (m), 1140 (m), 1065 (s), 1039 (s), 1013 (m), 974 (m), 950 (w), 892 (w), 858 (m), 804 (m), 772 (m), 720 (s), 696 (m) cm^{-1} .

HRMS (ESI): calcd. for $\text{C}_{44}\text{H}_{72}\text{N}_3\text{O}_9^+$: 786.5263 $[\text{M}+\text{H}]^+$
found: 786.5285 $[\text{M}+\text{H}]^+$.

(2R,3S,4S,5R,6S)-2-(Acetoxymethyl)-6-(((2S,3S,4R)-3,4-bis(benzoyloxy)-2-(3-(4-((E)-(4-pentylphenyl)diazenyl)phenyl)propanamido)octadecyl)oxy)tetrahydro-2H-pyran-3,4,5-triyl triacetate (II.47)

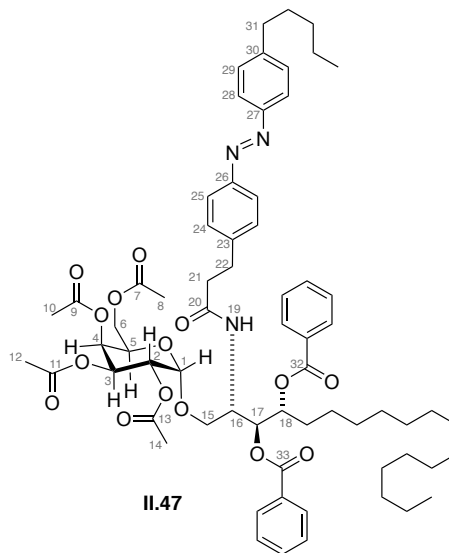


Acetylated glycoside **II.31** (66.7 mg, 69.7 μmol , 1.0 eq.) was dissolved in DCM (0.75 mL) and the mixture was cooled to 0 °C. Then TFA (0.75 mL) was added and the mixture was stirred at 0 °C and after 2 h the solvent was removed under reduced pressure. The crude product was dissolved in

DCM (3.4 mL) and FAAzo-3 (21.0 mg, 64.7 μmol , 0.93 eq.) followed by HBTU (39.6 mg, 0.105 mmol, 1.5 eq.) and *N*-methylmorpholine (97.3 μL , 1.05 mmol, 15 eq.) were added and stirred at room temperature for 12 h. Afterwards, the solvent was removed under reduced pressure and the crude product was purified *via* flash column chromatography [PE/EtOAc, 100:0 to 1:1] to give protected glycosphingolipid **II.47** (69.9 mg, 60.1 μmol , 86% over 2 steps) as yellow viscous oil.

$R_f = 0.29$ [PE/EtOAc = 2:1].

$^1\text{H NMR}$ (400 MHz, CDCl_3): $\delta = 8.01\text{--}7.95$ (m, 2H, H-Bz), 7.93–7.88 (m, 2H, H-Bz), 7.85 (d, 2H, $J = 8.2$ Hz, H-25), 7.78 (d, 2H, $J = 8.2$ Hz, H-28), 7.59 (t, 1H, $J = 7.4$ Hz, Bz), 7.52 (t, 1H, $J = 7.4$ Hz, H-Bz), 7.49–7.41 (m, 4H, H-24, H-Bz), 7.36 (t, 2H, $J = 7.6$ Hz, H-Bz), 7.28 (d, 2H, $J = 8.2$ Hz, H-29), 6.72 (d, 1H, $J = 9.7$ Hz, NH-19), 5.66 (dd, 1H, $J = 9.8, 2.4$ Hz, H-17), 5.41 (d, 1H, $J = 3.3$ Hz, H-4), 5.32 (dd, 1H, $J = 10.9, 3.4$ Hz, H-3), 5.24–5.19 (m, 1H, H-18), 5.13 (dd, 1H, $J = 10.9, 3.6$ Hz, H-2), 4.77 (d, 1H, $J = 3.6$ Hz, H-1), 4.66–4.56 (m, 1H, H-16), 4.08–4.01 (m, 1H, H-5), 4.01–3.91 (m, 2H, H-6), 3.67 (dd, 1H, $J = 11.0, 2.9$ Hz, H-15a), 3.48 (dd, 1H, $J = 11.3, 2.8$ Hz, H-15b), 3.14 (t, 2H, $J = 7.7$ Hz, H-22), 2.80–2.71 (m, 2H, H-21), 2.66 (t, 3H, $J = 7.7$ Hz, H-31), 2.09 (s, 3H, H-10), 1.99 (d, 6H, $J = 2.6$ Hz, H-8, H-12), 1.92 (s, 3H, H-14), 1.88 (d, 2H, $J = 6.7$ Hz, H-alkyl), 1.65 (p, 2H, $J = 7.4$ Hz, H-alkyl), 1.45–1.10 (m, 30H, H-alkyl), 0.97–0.77 (m, 8H, H-alkyl) ppm.

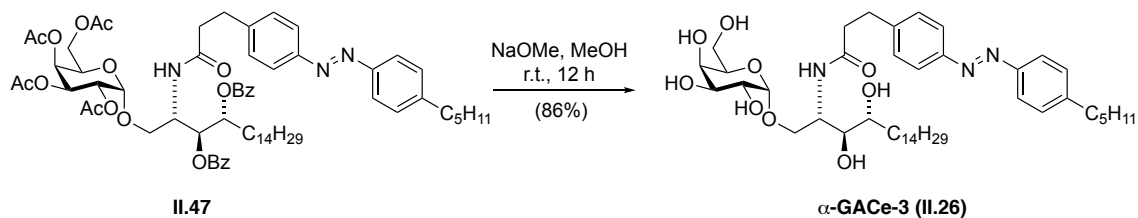


$^{13}\text{C NMR}$ (100 MHz, CDCl_3): $\delta = 171.8$ (C-20), 170.7 (C-13), 170.5 (C-7), 170.3 (C-11), 170.2 (C-9), 166.6 (C-32), 165.1 (C-33), 151.4 (C-26), 151.0 (C-27), 146.4 (C-30), 143.7 (C-23), 133.6 (C-Bz), 133.2 (C-Bz), 130.0 (C-Bz), 129.9 (C-Bz), 129.7 (C-Bz), 129.4 (C-Bz), 129.2 (C-24), 129.1 (C-29), 128.7 (C-Bz), 128.4 (C-Bz), 123.1 (C-25), 122.9 (C-28), 97.4 (C-1), 74.3 (C-18), 71.6 (C-17), 68.1 (C-4), 67.6 (C-3), 67.2 (C-2), 66.9 (C-5), 62.0 (C-6), 48.4 (C-16), 37.8 (C-21), 35.9 (C-31), 32.0 (C-alkyl), 31.6 (C-alkyl), 31.4 (C-22), 31.1 (C-alkyl), 29.8–29.4 (C-alkyl), 28.1 (C-alkyl), 25.7 (C-alkyl), 22.8 (C-alkyl), 22.6 (C-alkyl), 20.8 (C-8, C-12), 20.7 (C-10), 20.6 (C-14), 14.2 (C-alkyl), 14.1 (C-alkyl) ppm.

IR (ATR): $\tilde{\nu} = 2925$ (w), 2854 (w), 1748 (m), 1728 (m), 1674 (w), 1602 (w), 1529 (w), 1451 (w), 1370 (w), 1315 (w), 1222 (s), 1176 (w), 1156 (w), 1095 (m), 1068 (m), 1026 (m), 953 (w), 907 (w), 848 (w), 803 (w), 752 (s), 710 (s), 666 (m) cm^{-1} .

HRMS (ESI): calcd. for $\text{C}_{66}\text{H}_{88}\text{O}_{15}\text{N}_3^+$: 1162.6210 $[\text{M}+\text{H}]^+$
 found: 1162.6223 $[\text{M}+\text{H}]^+$.

N-((2*S*,3*S*,4*R*)-3,4-Dihydroxy-1-(((2*S*,3*R*,4*S*,5*R*,6*R*)-3,4,5-trihydroxy-6-(hydroxymethyl)tetrahydro-2*H*-pyran-2-yl)oxy)octadecan-2-yl)-3-(4-((*E*)-(4-pentylphenyl)diazenyl)phenyl)propanamide (α -GACe-3, **II.26**)



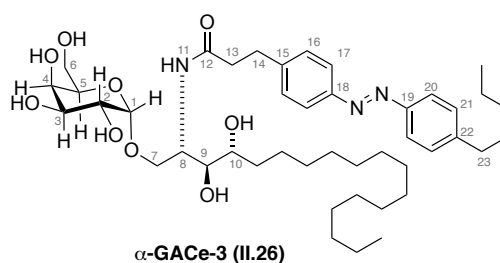
Protected glycosphingolipid **II.47** (69.9 mg, 60.1 μ mol, 1.0 eq.) was dissolved in MeOH (14 mL) and NaOMe was added until pH 9–10. The reaction mixture was stirred at room temperature for 12 h. Afterwards, it was stopped by the addition of DOWEX 50WX 2-100 (H⁺ form) and stirred for another 30 min at room temperature. All solid material was removed by filtration through a pad of Celite[®], which was washed with MeOH (20 mL) and the filtrate was concentrated under reduced pressure. Flash column chromatography [CHCl₃/MeOH, 9:1] afforded α -GACe-3 (**II.26**, 40.6 mg, 51.7 μ mol, 86%) as yellow viscous oil.

Compound was obtained as a 10:1 mixture of *trans*-/*cis*-isomers. ¹H NMR signal of H-1 underneath solvent signal; conformation at the anomeric center was confirmed by coupling of H-2 to H-1 ($J = 3.8$ Hz).

$R_f = 0.17$ [DCM/MeOH, 9:1].

¹H NMR (800 MHz, CD₃OD): $\delta = 7.88$ – 7.82 (m, 4H, H-17, H-20), 7.43 (d, 2H, $J = 8.4$ Hz, H-16), 7.37 (d, 2H, $J = 8.2$ Hz, H-21), 4.90–4.88 (m, 1H, H-1), 4.22 (dt, 1H, $J = 6.3, 4.6$ Hz, H-8), 3.90–3.86 (m, 2H, H-4, H-7a), 3.83 (t, 1H, $J = 6.1$ Hz, H-5), 3.80 (dd, 1H, $J = 10.0, 3.8$ Hz, H-2), 3.76–3.68 (m, 4H, H-3, H-6, H-7b), 3.56 (t, 1H, $J = 6.1$ Hz, H-9), 3.51–3.48 (m, 1H, H-10), 3.09–3.01 (m, 2H, H-14), 2.72 (t, 2H, $J = 7.8$ Hz, H-23), 1.94 (td, 2H, $J = 7.5, 3.5$ Hz, H-13), 1.70 (p, 2H, $J = 7.5$ Hz, H-alkyl), 1.42–1.16 (m, 30H, H-alkyl), 0.94 (t, 3H, $J = 7.0$ Hz, H-alkyl), 0.91 (t, 3H, $J = 7.2$ Hz, H-alkyl) ppm.

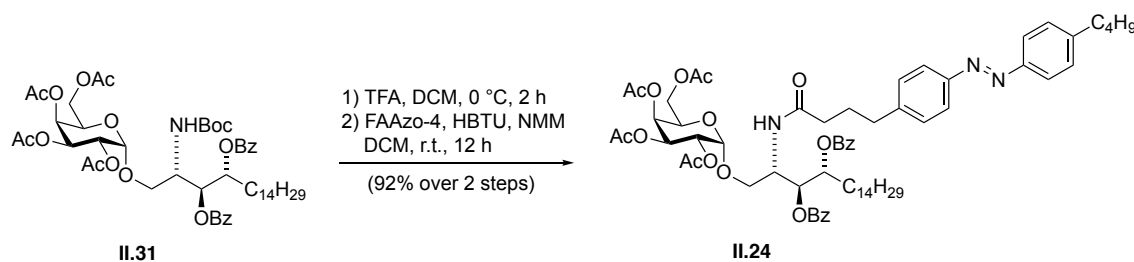
¹³C NMR (200 MHz, CD₃OD): $\delta = 1.74.5$ (C-12), 152.6 (C-18), 152.3 (C-19), 147.9 (C-22), 145.7 (C-15), 130.3 (C-16), 130.2 (C-21), 123.9–123.8 (C-17, C-20), 101.1 (C-1), 75.5 (C-9), 72.9 (C-10), 72.6 (C-5), 71.5 (C-3), 71.1 (C-4), 70.2 (C-2), 68.2 (C-13), 62.8 (C-6), 52.0 (C-2), 38.4 (C-13), 36.8 (C-23), 33.1 (C-alkyl), 32.6 (C-alkyl), 32.6 (C-14), 31.4–23.7 (C-alkyl), 23.6 (C-alkyl), 14.5 (C-alkyl), 14.4 (C-alkyl) ppm.



IR (ATR): $\tilde{\nu}$ = 3386 (br, w), 2955 (s), 2922 (s), 2854 (m), 1653 (w), 1558 (w), 1458 (m), 1378 (m), 1155 (w), 1058 (m), 721 (m) cm^{-1} .

HRMS (ESI): calcd. for $\text{C}_{44}\text{H}_{72}\text{N}_3\text{O}_9^+$: 789.5263 $[\text{M}+\text{H}]^+$
 found: 789.5283 $[\text{M}+\text{H}]^+$.

(2R,3S,4S,5R,6S)-2-(Acetoxymethyl)-6-(((2S,3S,4R)-3,4-bis(benzoyloxy)-2-(4-(4-((E)-(4-butylphenyl)diazenyl)phenyl)butanamido)octadecyl)oxy)tetrahydro-2H-pyran-3,4,5-triyl triacetate (II.24)



Acetylated glycoside **II.31** (73.4 mg, 76.8 μmol , 1.0 eq.) was dissolved in DCM (0.75 mL) and cooled to 0 °C. Then TFA (0.75 mL) was added and the reaction mixture stirred at 0 °C for 2 h. Afterwards, the solvent was removed under reduced pressure and the crude product was immediately redissolved in DCM (3.7 mL). FAAzo-4 (37.4 mg, 0.115 mmol, 1.5 eq.) followed by HBTU (43.7 mg, 0.115 mmol, 1.5 eq.) and *N*-methylmorpholine (110 μL , 1.15 mmol, 15 eq.) were added and the reaction stirred at room temperature for 12 h. The solvent was removed under reduced pressure and the crude product was purified *via* flash column chromatography [PE/EtOAc, 100:0 \rightarrow 1:1] to give protected glycosphingolipid **II.24** (82.5 mg, 71.0 μmol , 92% over 2 steps) as a yellow oil.

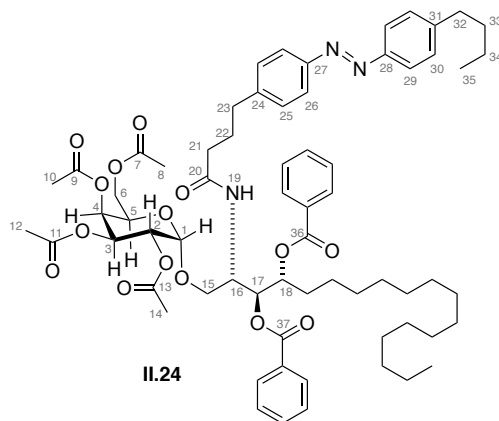
Compound **II.24** was isolated as an 8:1 mixture of *trans*-/*cis*-isomers.

R_f = 0.34 [PE/EtOAc, 2:1].

$^1\text{H NMR}$ (400 MHz, CDCl_3): δ = 8.02–7.97 (m, 2H, H-Bz), 7.94–7.89 (m, 2H, H-Bz), 7.86–7.80 (m, 4H, H-26, H-29), 7.64–7.58 (m, 1H, H-Bz), 7.56–7.50 (m, 1H, H-Bz), 7.47 (t, 2H, J = 7.7 Hz, H-Bz), 7.41–7.34 (m, 4H, H-25, H-Bz), 7.31 (d, 2H, J = 8.4 Hz, H-30), 6.60 (d, 1H, J = 9.6 Hz, NH-19), 5.69 (dd, 1H, J = 9.7, 2.6 Hz, H-17), 5.43–5.40 (m, 1H, H-4), 5.36–5.29 (m, 2H, H-3, H-18), 4.81 (d, 1H, J = 3.6 Hz, H-1), 4.10 (t, 1H, J = 6.4 Hz, H-5), 4.06–3.93 (m, 2H, H-6), 5.14 (dd, 1H, J = 10.9, 3.6 Hz, H-2), 4.67–4.59 (m, 1H, H-16), 3.74 (dd, 1H, J = 10.8, 2.9 Hz, H-15a), 3.50 (dd, 1H, J = 10.9, 2.7 Hz, H-15b), 2.83–2.77 (m, 2H, H-23), 2.68 (t, 2H, J = 7.8 Hz, H-32), 2.42 (t, 2H, J = 7.5 Hz, H-21), 2.14–2.07 (m, 5H, H-10, H-22), 1.99 (s, 3H, H-12), 1.97 (s, 3H, H-8), 1.94–

1.87 (m, 5H, H-14, H-alkyl), 1.67–1.60 (m, 2H, H-33), 1.42–1.35 (m, 2H, H-34), 1.31–1.09 (m, 24H, H-alkyl), 0.94 (t, 3H, $J = 7.4$ Hz, H-alkyl), 0.89–0.84 (m, 3H, H-alkyl) ppm.

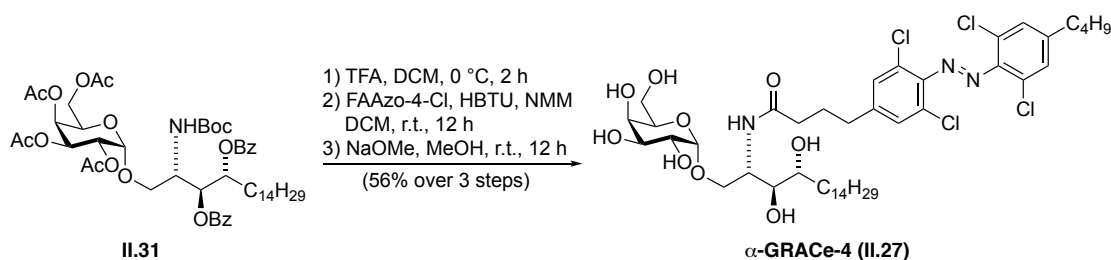
^{13}C NMR (100 MHz, CDCl_3): $\delta = 172.6$ (C-20), 170.8 (C-13), 170.6 (C-7), 170.4 (C-11), 170.3 (C-9), 166.7 (C-36), 165.2 (C-37), 151.4 (C-27), 151.1 (C-28), 146.4 (C-31), 144.8 (C-24), 133.7 (C-Bz), 133.3 (C-Bz), 130.0 (C-Bz), 129.9 (C-Bz), 129.8 (C-Bz), 129.4 (C-Bz), 129.3 (C-25), 129.2 (C-30), 128.8 (C-Bz), 128.5 (C-Bz), 123.0 (C-26), 122.9 (C-29), 97.5 (C-1), 74.3 (C-18), 71.7 (C-17), 68.1 (C-4), 67.7 (C-3), 67.5 (C-15), 67.3 (C-2), 66.9 (C-5), 61.9 (C-6), 48.5 (C-16), 36.1 (C-21), 35.7 (C-32), 35.3 (C-23), 33.6 (C-33), 32.1 – 29.5 (C-alkyl), 28.1 (C-alkyl), 27.2 (C-22), 25.9 – 22.8 (C-alkyl), 22.5 (C-34), 20.8–20.7 (C-8, C-10, C-12, C-14), 14.3 (C-alkyl), 14.1 (C-alkyl) ppm.



IR (ATR): $\tilde{\nu} = 2925$ (m), 2363 (w), 1753 (m), 1260 (s), 1070 (m), 799 (m), 712 (w) cm^{-1} .

HRMS (ESI): calcd. for $\text{C}_{66}\text{H}_{88}\text{O}_{15}\text{N}_3^+$: 1162.6210 $[\text{M}+\text{H}]^+$
found: 1162.6249 $[\text{M}+\text{H}]^+$.

4-(4-((*E*)-(4-Butylphenyl)diazenyl)phenyl)-*N*-((2*S*,3*S*,4*R*)-3,4-dihydroxy-1-(((2*S*,3*R*,4*S*,5*R*,6*R*)-3,4,5-trihydroxy-6-(hydroxymethyl)tetrahydro-2*H*-pyran-2-yl)oxy)octadecan-2-yl)butanamide (α -GACe-4, **II.12)**



Protected glycosphingolipid **II.24** (82.5 mg, 71.0 μmol , 1.0 eq.) was dissolved in MeOH (14 mL) and NaOMe was added until pH 9–10 and reaction mixture was stirred at room temperature for 12 h. The reaction was stopped by the addition of DOWEX 50WX 2-100 (H^+ form) and stirred for another 30 min at room temperature. All solid material was removed by filtration through a pad of Celite[®], which was washed with MeOH (20 mL) and the filtrate was concentrated under reduced pressure. Flash column chromatography [DCM/MeOH, 9:1] afforded (α -GACe-4 (**II.12**, 48.0 mg, 61.1 μmol , 86%) as yellow viscous oil.

Compound **II.12** was isolated as a 14:1 mixture of *trans*-/*cis*-isomers.

$R_f = 0.15$ [DCM/MeOH, 9:1].

$^1\text{H NMR}$ (800 MHz, CD_3OD): $\delta = 7.83\text{--}7.80$

(m, 4H, H-18, H-21), 7.39 (d, 2H, $J = 8.3$ Hz,

H-17), 7.35 (d, 2H, $J = 8.3$ Hz, H-22), 4.87 (d,

1H, $J = 3.8$ Hz, H-1), 4.23–4.21 (m, 1H, H-8),

3.90 (dd, 1H, $J = 10.6, 4.1$ Hz, H-7a), 3.87 (d,

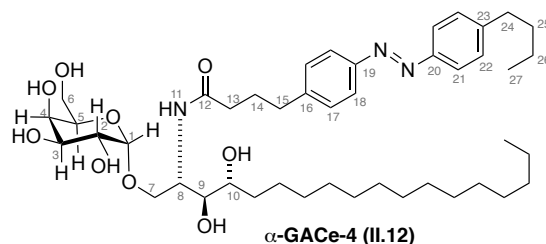
1H, $J = 2.5$ Hz, H-4), 3.84–3.83 (m, 1H, H-5), 3.79 (dd, 1H, $J = 10.0, 3.9$ Hz, H-2), 3.74 (dd, 1H,

$J = 10.1$ Hz, 3.3 Hz, H-3), 3.73–3.66 (m, 3H, H-7b, H-6), 3.63 (t, 1H, $J = 6.2$ Hz, H-9), 3.58–3.55

(m, 1H, H-4), 2.74 (t, 2H, $J = 7.8$ Hz, H-15), 2.71 (t, 2H, $J = 7.8$ Hz, H-24), 2.31 (td, 2H, $J = 7.4,$

3.8 Hz, H-13), 1.99 (td, 2H, $J = 7.6, 3.7$, H-14), 1.69–1.64 (m, 2H, H-25), 1.42–1.38 (m, 2H, H-26),

1.36–1.19 (m, 26H, H-alkyl), 0.97 (t, 3H, $J = 7.4$ Hz, H-27), 0.88 (t, 3H, $J = 7.2$ Hz, H-alkyl) ppm.



$^{13}\text{C NMR}$ (200 MHz, CD_3OD): $\delta = 175.3$ (C-12), 152.5 (C-19), 152.3 (C-20), 147.8 (C-23), 146.6

(C-16), 130.3 (C-17), 130.2 (C-22), 123.9–123.8 (C-18, C-21), 101.2 (C-1), 75.4 (C-9), 72.9 (C-10),

72.7 (C-5), 71.5 (C-3), 71.1 (C-4), 70.2 (C-2), 68.3 (C-7), 62.8 (C-6), 52.0 (C-8), 36.6 (C-13), 36.5 (C-

24), 36.2 (C-15), 34.8 (C-25), 33.07–30.5 (C-alkyl), 28.7 (C-14), 27.1–23.7 (C-alkyl), 23.4 (C-26), 14.5

(C-alkyl), 14.3 (C-27) ppm.

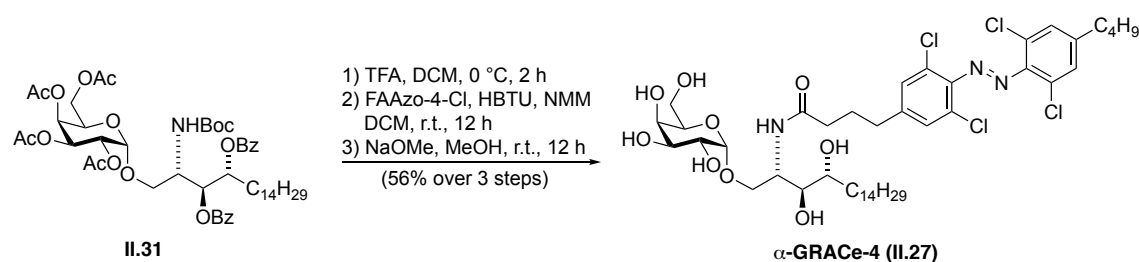
IR (ATR): $\tilde{\nu} = 3790$ (w), 3663 (w), 3288 (m), 2921 (s), 2851 (m), 1725 (w), 1658 (m), 1642 (m),

1564 (w), 1551 (w), 1468 (m), 1151 (m), 1031 (m) cm^{-1} .

HRMS (ESI): calcd. for $\text{C}_{44}\text{H}_{72}\text{O}_9\text{N}_3^+$: 786.5263 $[\text{M}+\text{H}]^+$

found: 786.5287 $[\text{M}+\text{H}]^+$.

4-(4-((*E*)-(4-Butyl-2,6-dichlorophenyl)diazenyl)-3,5-dichlorophenyl)-*N*-((2*S*,3*S*,4*R*)-3,4-dihydroxy-1-(((2*S*,3*R*,4*S*,5*R*,6*R*)-3,4,5-trihydroxy-6-(hydroxymethyl)tetrahydro-2*H*-pyran-2-yl)oxy)octadecan-2-yl)butanamide (α -GRaCe-4, **II.27**)



Acetylated glycoside **II.31** (66.7 mg, 69.7 μmol , 1.0 eq.) was dissolved in DCM (0.75 mL) and the mixture was cooled to 0 °C. Then TFA (0.75 mL) was added and the reaction stirred at 0 °C for 2 h. The solvent was removed under reduced pressure and the crude product was immediately redissolved in DCM (3.4 mL). Red FAAzo-4 (48.3 mg, 0.105 mmol, 1.5 eq.) followed by HBTU (39.6 mg, 0.105 mmol, 1.5 eq.) and *N*-methylmorpholine (97.3 μL , 1.05 mmol, 15 eq.) were added and the reaction stirred at room temperature for 12 h. The solvent was removed under reduced pressure and the crude product ($R_f = 0.29$ [PE/EtOAc, 2:1]) was filtered over a plug of silica and directly used in the next step. The crude material was dissolved in MeOH (14 mL) and NaOMe was added until pH 9–10. The reaction mixture stirred at room temperature for 12 h. Afterwards, it was stopped by the addition of DOWEX 50WX 2-100 (H^+ form) and stirred for another 30 min at room temperature. All solid material was removed by filtration through a pad of Celite®, which was washed with MeOH (20 mL), and the filtrate was concentrated under reduced pressure. Flash column chromatography [$\text{CHCl}_3/\text{MeOH}$, 19:1 to 9:1] afforded α -GRACe-4 (**II.27**, 36.1 mg, 39.1 μmol , 56% over 3 steps) as a yellow viscous oil.

Compound **II.27** was isolated as a 1.7:1 mixture of *trans*-/*cis*-isomers, thus NMR signals could not be assigned.

$R_f = 0.17$ [DCM/MeOH, 9:1].

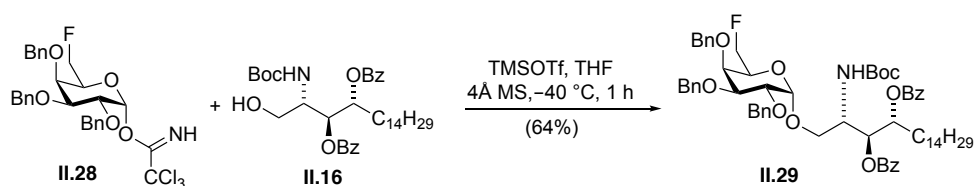
^1H NMR (800 MHz, CD_3OD): $\delta = 7.46$ (s, 2H), 7.42 (s, 2H), 7.27 (s, 1H), 7.23 (s, 1H), 4.90 (dd, $J = 9.1, 3.8$ Hz, 2H), 4.26 (ddt, $J = 8.0, 6.2, 4.7$ Hz, 2H), 3.96–3.89 (m, 4H), 3.87 (dddd, $J = 14.1, 6.7, 5.2, 1.3$ Hz, 2H), 3.81 (ddd, $J = 10.1, 6.3, 3.8$ Hz, 2H), 3.80–3.69 (m, 7H), 3.64 (dt, $J = 23.4, 6.1$ Hz, 2H), 3.58 (dddd, $J = 18.1, 9.8, 6.0, 2.4$ Hz, 2H), 2.74 (td, $J = 7.5, 2.5$ Hz, 2H), 2.73–2.70 (m, 2H), 2.66–2.60 (m, 3H), 2.34 (td, $J = 7.3, 4.5$ Hz, 2H), 2.29 (td, $J = 7.3, 3.1$ Hz, 1H), 2.01 (p, $J = 7.6$ Hz, 2H), 1.95–1.90 (m, 1H), 1.71–1.65 (m, 3H), 1.63–1.55 (m, 4H), 1.47–1.39 (m, 3H), 1.39–1.24 (m, 45H), 1.01 (t, $J = 7.4$ Hz, 3H), 0.96 (t, $J = 7.4$ Hz, 2H), 0.92 (dt, $J = 11.8, 7.2$ Hz, 6H) ppm.

^{13}C NMR (200 MHz, CD_3OD): $\delta = 175.0, 174.9, 147.6, 147.5, 147.3, 147.1, 146.8, 146.5, 146.5, 130.7, 130.6, 130.4, 130.4, 128.3, 128.3, 126.8, 126.7, 101.2, 101.1, 75.4, 72.9, 72.6, 71.5, 71.1, 70.2, 70.2, 68.3, 68.3, 62.8, 52.0, 49.0, 36.3, 35.8, 35.5, 35.4, 35.2, 34.2, 33.1, 32.9, 30.9, 30.8, 30.8, 30.5, 28.2, 28.1, 27.0, 27.0, 23.7, 23.3, 23.2, 14.5, 14.2$ ppm.

IR (ATR): $\tilde{\nu} = 3396$ (br, m), 2924 (m), 2853 (w), 1641 (m), 1591 (w), 1548 (w), 1466 (w), 1401 (w), 1149 (m), 1030 (m), 844 (s) cm^{-1} .

HRMS (ESI): calcd. for $\text{C}_{44}\text{H}_{68}\text{Cl}_4\text{N}_3\text{O}_9^+$: 922.3704 [M+H]⁺
found: 922.3723 [M+H]⁺.

(2*S*,3*S*,4*R*)-2-((*tert*-Butoxycarbonyl)amino)-1-(((2*S*,3*R*,4*S*,5*R*,6*S*)-3,4,5-tris(benzyloxy)-6-(fluoromethyl)tetrahydro-2*H*-pyran-2-yl)oxy)octadecane-3,4-diyl dibenzoate (**II.29**)

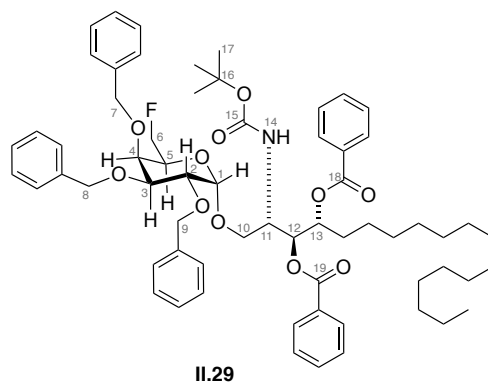


Fluorinated galactosyl donor **II.28** (72 mg, 119 μmol , 1.5 eq.) and acceptor **II.16** (50 mg, 80 μmol , 1.0 eq.) were combined and co-evaporated with toluene ($3 \times 5 \text{ mL}$) and with THF ($1 \times 5 \text{ mL}$), dried under high vacuum and then dissolved in THF (8.0 mL) under argon. The mixture was stirred with freshly activated 4Å MS at room temperature for 30 min, before the reaction vessel was cooled to -40°C . TMSOTf (4.4 mL, 24 μmol , 0.3 eq.) was added and the reaction mixture was stirred at -40°C for 1 h. The reaction mixture was diluted with THF (10 mL), quenched by the addition of NEt_3 and filtered through a pad of celite. The solvents were removed under reduced pressure and the crude product was purified by flash chromatography on silica (PE/EtOAc, 6:1) to give **II.29** (54 mg, 51 μmol , 64%) as a colorless oil.

$R_f = 0.76$ [PE:EtOAc, 2:1].

$[\alpha]_{\text{D}}^{20} = +0.47$ ($c = 2.9$, DCM).

$^1\text{H NMR}$ (599 MHz, CDCl_3) $\delta = 8.05\text{--}7.95$ (m, 4H, H-Ar), 7.60–7.16 (m, 21H, H-Ar), 5.62 (dd, $J = 8.7$, 3.2 Hz, 1H, H-12), 5.48 (d, $J = 9.8$ Hz, 1H, H-13), 5.33 (d, $J = 9.9$ Hz, 1H, NH-14), 4.93 (d, $J = 11.5$ Hz, 1H, $-\text{CH}_2\text{-Ph}$), 4.83–4.78 (m, 1H, H-1), 4.69 (d, $J = 11.7$ Hz, 1H, $-\text{CH}_2\text{-Ph}$), 4.64 (d, $J = 3.4$ Hz, 2H, $-\text{CH}_2\text{-Ph}$), 4.57 (d, $J = 11.4$ Hz, 1H, $-\text{CH}_2\text{-Ph}$), 4.50–4.21 (m, 3H, H-6, H-11), 4.13–4.05 (m, 1H, H-5), 4.00 (dd, $J = 9.5$, 3.6 Hz, 1H, H-2), 3.92–3.87 (m, 2H, H-3, H-4), 3.79–3.71 (m, 2H, H-10), 1.98–1.79 (m, 1H, H-alkyl), 1.47 (s, 9H, H-17), 1.42 – 1.18 (m, 19H, H-alkyl), 0.89 (t, $J = 6.9$ Hz, 3H, H-alkyl).



$^{13}\text{C NMR}$ (151 MHz, CDCl_3) $\delta = 166.2$ (C-18), 165.4 (C-19), 155.5 (C-14), 138.9 (C-Ar), 138.6 (C-Ar), 138.3 (C-Ar), 133.4 (C-Ar), 133.0 (C-Ar), 130.3 (C-Ar), 123.0 (C-Ar), 129.9 (C-Ar), 128.6 (C-Ar), 128.5 (C-Ar), 128.4 (C-Ar), 128.2 (C-Ar), 127.9 (C-Ar), 127.6 (C-Ar), 99.3 (C-1), 82.3 (d, $J = 167.8$ Hz, C-6), 80.0 (C-16), 78.5 (C-3), 76.6 (C-2), 74.8 (CH₂-Ph), 74.6 (C-4), 73.8 (C-13), 73.6 (CH₂-Ph), 73.3 (CH₂-Ph), 73.2 (C-12), 69.7 (d, $J = 23.0$ Hz, C-5), 69.1 (C-10), 50.6 (C-11), 32.1 (C-

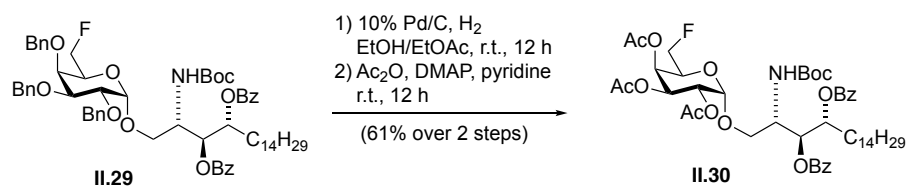
alkyl), 29.8 (C-alkyl), 29.7 (C-alkyl), 29.5 (C-alkyl), 28.9 (C-alkyl), 28.5 (C-17), 27.1 (C-alkyl), 25.8 (C-alkyl), 22.8 (C-alkyl), 14.3 (C-alkyl) ppm.

^{19}F NMR (377 MHz, CDCl_3) $\delta = -229.50$ (td, $J = 46.8, 12.3$ Hz, F-6).

IR (ATR): $\tilde{\nu} = 2925$ (s), 2854 (m), 1718 (s), 1602 (w), 1585 (w), 1497 (m), 1453 (m), 1392 (w), 1366 (m), 1343 (w), 1315 (m), 1263 (s), 1159 (m), 1097 (s), 1069 (s), 1042 (m), 1027 (s), 913 (w), 866 (w), 736 (m), 712 (s), 698 (m) cm^{-1} .

HRMS (ESI): calcd. for $\text{C}_{64}\text{H}_{86}\text{FN}_2\text{O}_{11}^+$: 1077.6210 $[\text{M}+\text{NH}_4]^+$
found: 1077.6237 $[\text{M}+\text{NH}_4]^+$.

(2*S*,3*R*,4*S*,5*R*,6*S*)-2-(((2*S*,3*S*,4*R*)-3,4-bis(Benzoyloxy)-2-((tert-butoxycarbonyl)amino)octadecyl)oxy)-6-(fluoromethyl)tetrahydro-2*H*-pyran-3,4,5-triyl triacetate (II.30**)**

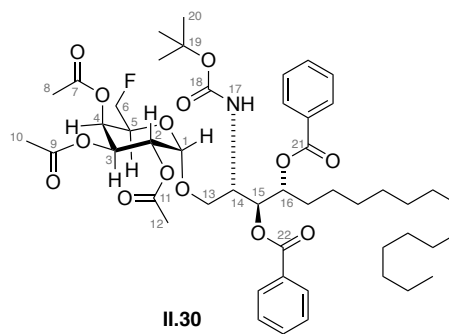


Protected glycoside **II.29** (28.6 mg, 27.0 μmol , 1.0 eq.) was dissolved in EtOH/EtOAc (1:1, 2 mL) and 10% palladium on activated charcoal (28.6 mg, 100 wt%, 0.1 eq.) was added. The mixture was stirred vigorously under H_2 -atmosphere at room temperature for 12 h. Then the solution was diluted with EtOH/EtOAc (1:1, 10 mL) and all solid material was removed by filtration through a pad of Celite[®], which was washed with EtOH/EtOAc (1:1, 20 mL) and the filtrate was concentrated under reduced pressure. The crude product was dissolved in pyridine (1 mL) and Ac_2O (0.2 mL) and DMAP (0.165 mg, 1.35 μmol , 0.05 eq.) were added. The reaction mixture was stirred at room temperature for 12 h, then the solvent was removed under reduced pressure and the crude product was dissolved in EtOAc (10 mL). The organic layer was washed with saturated aqueous NaCl solution (20 mL), dried (MgSO_4) and the solvent was removed under reduced pressure. Flash column chromatography on silica gel [PE/EtOAc, 10:1 to 1:1] afforded acetylated glycoside **II.30** (15 mg, 0.0164 mmol, 61% over 2 steps) as a colorless oil.

$R_f = 0.31$ [PE/EtOAc, 4:1].

$[\alpha]_{\text{D}}^{20} = +0.74$ ($c = 1$, DCM).

¹H NMR (400 MHz, acetone-*d*₆): δ = 8.01–7.96 (m, 2H, H-Bz), 7.92 (dd, J = 8.0, 1.4 Hz, 2H, H-Bz), 7.63–7.56 (m, 1H, H-Bz), 7.56–7.49 (m, 1H, H-Bz), 7.46 (t, J = 7.8 Hz, 2H, H-Bz), 7.37 (t, J = 7.6 Hz, 2H, H-Bz), 5.63 (dd, J = 9.5, 2.7 Hz, 1H, H-15), 5.55–5.47 (m, 1H, H-4), 5.43 (dt, J = 10.0, 3.0 Hz, 1H, H-16), 5.30 (dd, J = 10.9, 3.3 Hz, 1H, H-2), 5.21–5.13 (m, 1H, NH-17, H-3), 4.84 (d, J = 3.7 Hz, 1H, H-1), 4.45–4.35 (m, 2H, H-6), 4.35–4.17 (m, 2H, H-5, H-14), 3.80 (dd, J = 10.9, 3.0 Hz, 1H, H-13a), 3.53–3.42 (m, 1H, H-13b), 2.10 (s, 3H, H-Ac), 1.99 (s, 3H, H-Ac), 1.97 (s, 3H, H-Ac), 1.51 (s, 9H, H-20), 1.32–1.17 (m, 25H, H-alkyl), 0.87 (dp, J = 5.7, 3.1 Hz, 6H, H-alkyl) ppm.



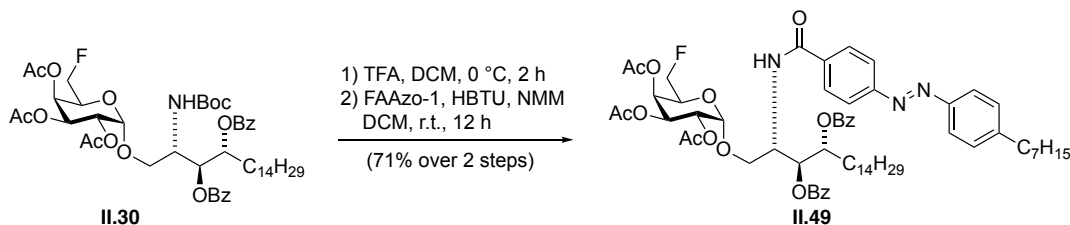
¹³C NMR (100 MHz, acetone-*d*₆): δ = 170.8 (C-Ac), 170.3 (C-Ac), 170.2 (C-Ac), 166.3 (C-21), 165.2 (C-22), 155.3 (C-Bz), 133.6 (C-Bz), 133.1 (C-Bz), 130.1 (C-Bz), 129.9 (C-Bz), 129.8 (C-Bz), 129.6 (C-Bz), 128.7 (C-Bz), 128.5 (C-Bz), 125.7 (C-Bz), 97.5 (C-1), 81.3 (d, J = 171.8 Hz, C-6), 80.5 (C-16), 77.4 (C-15), 77.2 (C-4), 76.8 (C-13), 72.1 (C-2), 68.0 (C-3), 67.45 (d, J = 22.8 Hz, C-5), 50.9 (C-14), 34.3 (C-alkyl), 32.1 (C-alkyl), 30.5 (C-alkyl), 29.8–29.4 (C-alkyl), 28.5 (C-alkyl), 28.4 (C-alkyl), 25.9 (C-alkyl), 22.8 (C-alkyl), 22.5 (C-alkyl), 20.8 (C-Ac), 20.7 (C-Ac), 20.7 (C-Ac), 15.4 (C-alkyl), 14.3 (C-alkyl), 14.2 (C-alkyl) ppm.

¹⁹F NMR (377 MHz, acetone-*d*₆) δ = –231.07 (td, J = 46.4, 14.2 Hz, F-6).

IR (ATR): $\tilde{\nu}$ = 3369 (bw), 2925 (s), 2854 (m), 1750 (s), 1717 (s), 1602 (w), 1507 (w), 1452 (m), 1369 (m), 1315 (w), 1279 (s), 1248 (s), 1226 (s), 1173 (m), 1096 (m), 1069 (s), 1026 (m), 951 (w), 712 (m) cm^{-1} .

HRMS (ESI): calcd. for $\text{C}_{49}\text{H}_{74}\text{O}_{14}\text{N}_2\text{F}^+$: 933.5119 $[\text{M}+\text{NH}_4]^+$
 found: 933.5149 $[\text{M}+\text{NH}_4]^+$.

(2*S*,3*R*,4*S*,5*R*,6*S*)-2-(((2*S*,3*S*,4*R*)-3,4-Bis(benzoyloxy)-2-(3-(4-((*E*)-(4-pentylphenyl)diaz-enyl)phenyl)-propanamido)octadecyl)oxy)-6-(fluoromethyl)tetrahydro-2*H*-pyran-3,4,5-triyl triacetate (II.49)



Acetylated glycoside **II.30** (22.0 mg, 23.0 μmol , 1.0 eq.) was dissolved in DCM (1 mL) and the mixture was cooled to 0 °C. Then TFA (1 mL) was added and after 2 h, the solvent was removed under reduced pressure. The crude product was dissolved in DCM (1.3 mL), and FAAzo-1 (11.2 mg, 34.5 μmol , 1.5 eq.) followed by HBTU (13.1 mg, 34.5 μmol , 1.5 eq.) and *N*-methylmorpholine (38.0 μL , 34.5 μmol , 1.5 eq.) were added at room temperature. After 12 h the solvent was removed under reduced pressure and the crude product was purified *via* flash column chromatography [PE/EtOAc, 100:0 to 1:1] to give protected glycosphingolipid **II.49** (18.3 mg, 16.3 μmol , 71% over 2 steps) as a yellow viscous oil.

$R_f = 0.63$ [PE/EtOAc, 2:1].

$^1\text{H NMR}$ (800 MHz, CD_3OD): $\delta = 8.08\text{--}8.04$ (m, 4H), 8.03–8.00 (m, 2H), 7.99–7.97 (m, 2H), 7.90 - 7.88 (m, 2H), 7.62 (tt, $J = 7.4, 1.3$ Hz, 1H), 7.55 (tt, $J = 7.4, 1.3$ Hz, 1H), 7.51–7.48 (m, 2H), 7.42–7.39 (m, 2H), 7.35–7.33 (m, 2H), 5.77 (dd, $J = 8.9, 3.1$ Hz, 1H), 5.50–5.44 (m, 2H), 5.33 (dd, $J = 10.9, 3.4$ Hz, 1H), 5.16 (dd, $J = 10.9, 3.7$ Hz, 1H), 4.95 (d, $J = 3.7$ Hz, 1H), 4.87 (tt, $J = 9.1, 3.4$ Hz, 1H), 4.40–4.22 (m, 3H), 3.90 (dd, $J = 11.4, 3.5$ Hz, 1H), 3.73 (dd, $J = 11.4, 3.4$ Hz, 1H), 2.70 (t, $J = 7.8$ Hz, 2H), 2.10 (s, 3H), 1.99 (s, 3H), 1.98–1.94 (m, 1H), 1.93 (s, 3H), 1.70–1.64 (m, 2H), 1.40–1.12 (m, 21H), 0.88 (dt, $J = 20.3, 7.1$ Hz, 6H) ppm.

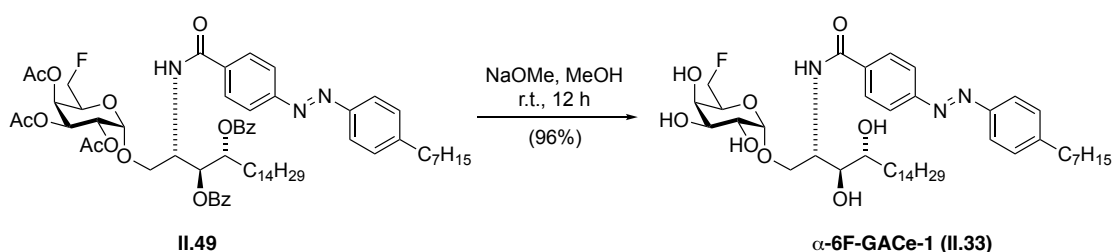
$^{13}\text{C NMR}$ (200 MHz, CD_3OD): $\delta = 170.7, 170.2, 166.7, 166.5, 165.5, 154.9, 151.1, 147.5, 135.2, 133.7, 133.3, 130.0, 129.9, 129.4, 129.3, 128.8, 128.6, 128.4, 123.3, 123.2, 97.9, 81.4$ (d, $J = 172.1$ Hz), 77.2, 74.1, 72.7, 68.4, 68.1, 68.2, 67.9 (d, $J = 22.3$ Hz), 67.5, 67.5, 49.5, 36.1, 32.1, 32.0, 31.4, 29.8, 29.8, 29.7, 29.7, 29.6, 29.5, 29.4, 29.3, 28.7, 25.6, 22.8, 20.8, 20.7, 20.7, 14.3, 1.3 ppm.

$^{19}\text{F NMR}$ (377 MHz, CD_3OD) $\delta = -231.07$ (td, $J = 46.5, 14.2$ Hz).

IR (ATR): $\tilde{\nu}$ = 2926 (s), 2854 (m), 1752 (s), 1726 (s), 1666 (m), 1602 (w), 1531 (w), 1492 (w), 1452 (m), 1372 (m), 1316 (w), 1254 (s), 1227 (s), 1177 (w), 1153 (w), 1108 (w), 1070 (s), 1027 (m), 948 (w), 861 (w), 712 (m) cm^{-1} .

HRMS (ESI): calcd. for $\text{C}_{64}\text{H}_{88}\text{FN}_4\text{O}_{13}^+$: 1139.6326 $[\text{M}+\text{NH}_4]^+$
 found: 1139.6350 $[\text{M}+\text{HH}_4]^+$.

***N*-((2*S*,3*S*,4*R*)-1-(((2*S*,3*R*,4*S*,5*R*,6*S*)-6-(Fluoromethyl)-3,4,5-trihydroxytetrahydro-2*H*-pyran-2-yl)oxy)-3,4-dihydroxyoctadecan-2-yl)-3-(4-((*E*)-(4-pentylphenyl)diazenyl)phenyl)propanamide (α -6*F*-GACe-1, **II.33**)**



Protected glycosphingolipid **II.49** (18.3 mg, 16.5 μmol , 1.0 eq.) was dissolved in MeOH (1 mL) and NaOMe was added at room temperature until pH 9–10. After 12 h, it was stopped by the addition of DOWEX 50WX 2-100 (H^+ form) and stirred for another 30 min. at room temperature. All solid material was removed by filtration through a pad of Celite[®], which was washed with MeOH (5 mL) and the filtrate was concentrated under reduced pressure. Flash column chromatography [DCM/MeOH, 9:1] afforded 6*F*- α -GACe-1 (**II.33**, 12.5 mg, 15.8 μmol , 96%) as a yellow viscous oil.

R_f = 0.50 [DCM/MeOH, 10:1].

^1H NMR (800 MHz, CD_3OD): δ = 8.02–8.00 (m, 2H), 7.98–7.96 (m, 2H), 7.90–7.87 (m, 2H), 7.40–7.38 (m, 2H), 4.96 (d, J = 3.6 Hz, 1H), 4.59–4.44 (m, 3H), 4.11 (dtd, J = 12.8, 6.1, 5.4, 2.7 Hz, 1H), 4.03 (dd, J = 10.8, 4.3 Hz, 1H), 3.67 (ddd, J = 9.9, 5.7, 2.4 Hz, 1H), 3.35–3.33 (m, 2H), 3.29 (p, J = 1.7 Hz, 1H), 2.75–2.70 (m, 2H), 1.73–1.66 (m, 3H), 1.58–1.51 (m, 1H), 1.51–1.43 (m, 1H), 1.41–1.18 (m, 33H), 0.91 (t, J = 7.1 Hz, 3H), 0.89 (t, J = 7.3 Hz, 3H) ppm.

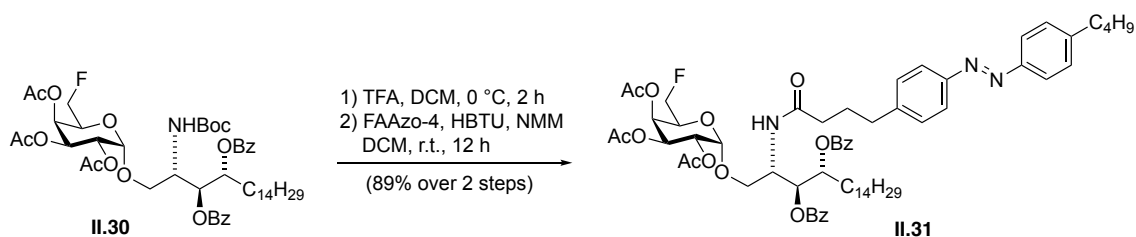
^{13}C NMR (200 MHz, CD_3OD): δ = 169.1, 155.8, 152.3, 148.8, 137.6, 130.4, 129.6, 124.2, 123.6, 101.2, 83.9 (d, J = 167.0 Hz), 75.0, 72.8, 71.1, 71.0 (d, J = 22.1 Hz), 70.5, 70.5, 70.1, 68.2, 52.9, 36.9, 33.1, 33.0, 32.7, 32.5, 30.9–30.7, 30.6, 30.5, 30.4, 30.3, 26.7, 23.8, 23.7, 14.5, 14.4 ppm.

^{19}F NMR (377 MHz, CD_3OD) δ = –231.33–(–231.69) (m).

IR (ATR): $\tilde{\nu}$ = 3284 (bw), 2924 (s), 2853 (s), 2362 (w), 2168 (m), 1734 (w), 1635 (m), 1540 (m), 1458 (m), 1025 (s), 859 (m), 727 (m), 668 (m) cm^{-1} .

HRMS (ESI): calcd. for $\text{C}_{44}\text{H}_{71}\text{N}_3\text{O}_8\text{F}^+$: 788.5220 $[\text{M}+\text{H}]^+$
found: 788.5244 $[\text{M}+\text{H}]^+$.

(2*S*,3*R*,4*S*,5*R*,6*S*)-2-(((2*S*,3*S*,4*R*)-3,4-bis(Benzyloxy)-2-(4-(4-((*E*)-(4-butylphenyl)diaz-enyl)phenyl)-butanamido)octadecyl)oxy)-6-(fluoromethyl)tetrahydro-2*H*-pyran-3,4,5-triyl triacetate (II.31)



Acetylated glycoside **II.30** (15.0 mg, 16.4 μmol , 1.0 eq.) was dissolved in DCM (0.5 mL) and cooled to 0 °C. Then TFA (0.5 mL) was added and the reaction mixture was stirred at 0 °C and after 2 h the solvent was removed under reduced pressure. The crude product was dissolved in DCM (1 mL) and FAAzo-4 (7.97 mg, 24.6 μmol , 1.5 eq.) followed by HBTU (9.33 mg, 24.6 μmol , 1.5 eq.) and *N*-methylmorpholine (27.0 μL , 246 μmol , 15 eq.) was added and the reaction stirred at room temperature. After 12 h the solvent was removed under reduced pressure and the crude product was purified *via* flash column chromatography [PE/EtOAc, 100:0 to 1:1] to give protected glycosphingolipid **II.31** (16.4 mg, 14.6 μmol , 89% over 2 steps) as yellow viscous oil.

R_f = 0.53 [PE/EtOAc, 2:1].

¹H NMR (600 MHz, CDCl_3): δ = 8.00 (dd, J = 8.4, 1.3 Hz, 2H), 7.96–7.92 (m, 2H), 7.86–7.80 (m, 4H), 7.60 (ddt, J = 8.7, 7.2, 1.3 Hz, 1H), 7.53 (ddt, J = 8.8, 7.1, 1.3 Hz, 1H), 7.49–7.44 (m, 2H), 7.41–7.35 (m, 4H), 7.33–7.29 (m, 2H), 6.40 (d, J = 9.5 Hz, 1H), 5.65 (dd, J = 9.2, 2.8 Hz, 1H), 5.45 (dd, J = 3.4, 1.3 Hz, 1H), 5.37–5.29 (m, 2H), 5.15 (dd, J = 10.9, 3.7 Hz, 1H), 4.86 (d, J = 3.7 Hz, 1H), 4.64 (ddt, J = 9.5, 6.3, 3.0 Hz, 1H), 4.40–4.23 (m, 2H), 4.22–4.16 (m, 1H), 3.76 (dd, J = 11.2, 3.1 Hz, 1H), 3.60 (dd, J = 11.2, 3.1 Hz, 1H), 2.83–2.77 (m, 2H), 2.72–2.66 (m, 2H), 2.39 (t, J = 7.5 Hz, 2H), 2.09 (s, 4H), 1.99 (s, 3H), 1.93 (s, 3H), 1.69–1.60 (m, 2H), 1.39 (dtt, J = 14.7, 9.3, 5.4 Hz, 3H), 1.34–1.16 (m, 30H), 0.94 (t, J = 7.4 Hz, 3H), 0.87 (t, J = 7.1 Hz, 3H) ppm.

¹³C NMR (201 MHz, CDCl_3): δ = 172.5, 170.7, 170.2, 170.2, 166.6, 165.3, 151.4, 151.1, 146.4, 144.8, 133.7, 133.2, 130.1, 130.0, 129.8, 129.5, 129.3, 129.2, 128.8, 128.5, 126.7, 123.0, 122.9, 97.8,

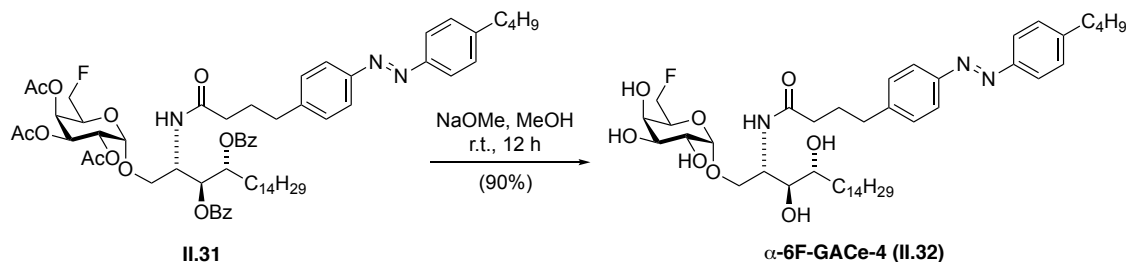
81.5 (d, $J = 171.9$ Hz), 74.1, 72.2, 68.3, 68.1, 68.0, 67.8 (d, $J = 22.3$ Hz), 67.6, 67.3, 48.6, 36.1, 35.7, 35.3, 33.6, 32.1, 29.8, 29.8, 29.8, 29.7, 29.7, 29.5, 28.4, 27.1, 25.8, 22.8, 22.5, 20.8, 20.7, 14.3, 14.1 ppm.

^{19}F NMR (377 MHz, CHCl_3) $\delta = -230.43$ (td, $J = 46.5, 14.7$ Hz).

IR (ATR): $\tilde{\nu} = 3370$ (w), 2925 (s), 2854 (m), 1726 (s), 1751 (s), 1679 (m), 1602 (w), 1529, 1452, 1372, 1315, 1279 (s), 1249 (s), 1226 (s), 1177 (w), 1156 (s), 1109 (m), 1096 (m), 1070 (s), 1026 (w), 951 (w), 845 (w), 712 (m) cm^{-1} .

HRMS (ESI): calcd. for $\text{C}_{64}\text{H}_{85}\text{FN}_3\text{O}_{13}^+$: 1122.6061 $[\text{M}+\text{H}]^+$
found: 1122.6100 $[\text{M}+\text{H}]^+$.

4-(4-((*E*)-(4-Butylphenyl)diazenyl)phenyl)-*N*-((2*S*,3*S*,4*R*)-1-(((2*S*,3*R*,4*S*,5*R*,6*S*)-6-(fluoromethyl)-3,4,5-trihydroxytetrahydro-2*H*-pyran-2-yl)oxy)-3,4-dihydroxyoctadecan-2-yl)butanamide (α -6F-GACe-4, **II.32**)



Protected glycosphingolipid **II.31** (16.4 mg, 14.6 μmol , 1.0 eq.) was dissolved in MeOH (1 mL) and NaOMe was added until pH 9–10. The reaction mixture was stirred at room temperature and after 12 h, it was stopped by the addition of DOWEX 50WX 2-100 (H^+ form) and stirred for another 30 min. at room temperature. All solid material was removed by filtration through a pad of Celite[®], which was washed with MeOH (5 mL), and the filtrate was concentrated under reduced pressure. Flash column chromatography [$\text{CHCl}_3/\text{MeOH}$, 9:1] afforded α -6F-GACe-4 **II.32** (10.3 mg, 13.1 μmol , 90%) as yellow viscous oil.

$R_f = 0.47$ [DCM/MeOH , 10:1].

^1H NMR (800 MHz, CD_3OD): $\delta = 7.84$ – 7.81 (m, 4H), 7.40– 7.34 (m, 4H), 4.60– 4.44 (m, 2H), 4.21 (dt, $J = 6.8, 4.2$ Hz, 1H), 4.09 (dddd, $J = 14.8, 6.2, 4.8, 1.2$ Hz, 1H), 3.90– 3.84 (m, 2H), 3.82– 3.76 (m, 2H), 3.74– 3.69 (m, 1H), 3.65 (dd, $J = 6.8, 5.6$ Hz, 1H), 3.57 (ddd, $J = 10.0, 5.7, 2.4$ Hz, 1H), 3.34 (dq, $J = 4.5, 1.6$ Hz, 1H), 2.73 (dt, $J = 19.6, 7.8$ Hz, 4H), 2.34– 2.27 (m, 2H), 2.02– 1.96 (m,

2H), 1.71–1.60 (m, 4H), 1.47–1.36 (m, 3H), 1.36–1.18 (m, 17H), 0.97 (t, $J = 7.4$ Hz, 3H), 0.89 (t, $J = 7.2$ Hz, 3H) ppm.

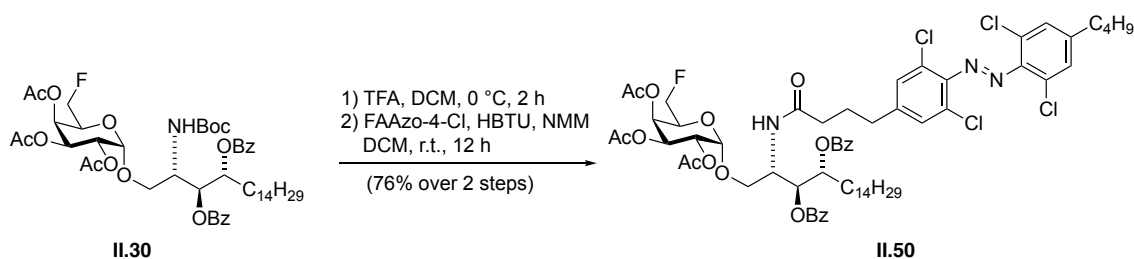
^{13}C NMR (200 MHz, CD_3OD): $\delta = 175.2, 152.5, 152.3, 147.8, 146.6, 131.2, 130.3, 130.2, 128.7, 123.9, 123.8, 101.0, 84.0$ (d, $J = 167.2$ Hz), $75.1, 70.9$ (d, $J = 21.6$ Hz), $70.6, 70.5, 70.1, 68.3, 51.8, 36.6, 36.5, 36.2, 34.8, 33.1, 32.7, 30.9, 30.8, 30.8, 30.5, 28.7, 27.1, 23.7, 23.4, 14.5, 14.3$ ppm.

^{19}F NMR (377 MHz, CD_3OD) $\delta = -231.30$ (td, $J = 47.4, 14.9$ Hz).

IR (ATR): $\tilde{\nu} = 3302$ (bw), 2922 (s), 2852 (s), 2362 (w), 2168 (m), 2138 (w), 1647 (m), 1601 (w), 1545 (m), 1476 (m), 1379 (m), 1260 (w), 1156 (m), 1076 (s), 1028 (s), 840 (m), 798 (m), 727 (m), 716 (w), 668 (w) cm^{-1} .

HRMS (ESI): calcd. for $\text{C}_{44}\text{H}_{71}\text{N}_3\text{O}_8\text{F}^+$: 788.5220 $[\text{M}+\text{H}]^+$
found: 788.5244 $[\text{M}+\text{H}]^+$.

(2*S*,3*R*,4*S*,5*R*,6*S*)-2-(((2*S*,3*S*,4*R*)-3,4-Bis(benzoyloxy)-2-(4-(4-((*E*)-(4-butyl-2,6-dichlorophenyl)diazenyl)-3,5-dichlorophenyl)butanamido)octadecyl)oxy)-6-(fluoromethyl)tetrahydro-2*H*-pyran-3,4,5-triyl triacetate (**II.50**)



Acetylated glycoside **II.30** (19.0 mg, 19.9 μmol , 1.0 eq.) was dissolved in DCM (1.0 mL) and the mixture was cooled to 0°C . Then TFA (1.0 mL) was added and the reaction was stirred for 2 h at this temperature. Afterwards the solvent was removed under reduced pressure and the crude product was immediately dissolved in DCM (1.3 mL). FAAzo-4-Cl (13.7 mg, 29.8 μmol , 1.5 eq.) followed by HBTU (11.3 mg, 29.8 mmol, 1.5 eq.) and *N*-methylmorpholine (32.0 μL , 1.5 mmol, 15 eq.) were added and the reaction stirred at room temperature. After 12 h the solvent was removed under reduced pressure and the crude product was purified *via* flash column chromatography [PE/EtOAc, 10:1 \rightarrow 1:1] to give protected glycosphingolipid **II.50** (19.2 mg, 15.2 μmol , 76% over 2 steps) as yellow viscous oil.

Compound **II.50** was isolated as a 2.2:1 mixture of *trans*-/*cis*-isomers.

$R_f = 0.50$ [PE/EtOAc, 2:1].

$^1\text{H NMR}$ (800 MHz, CDCl_3): $\delta = 8.01$ (ddd, $J = 8.4, 5.1, 1.4$ Hz, 2H), 7.95 (ddd, $J = 10.0, 8.4, 1.4$ Hz, 2H), 7.63–7.59 (m, 1H), 7.56–7.52 (m, 1H), 7.49–7.46 (m, 2H), 7.41–7.37 (m, 2H), 7.34 (s, 1H), 6.45–6.40 (m, 1H), 5.62 (ddd, $J = 11.3, 9.0, 2.9$ Hz, 1H), 5.45 (ddd, $J = 8.2, 3.4, 1.3$ Hz, 1H), 5.32 (ddd, $J = 17.9, 10.5, 7.0, 3.3$ Hz, 2H), 5.15 (ddd, $J = 11.0, 7.3, 3.7$ Hz, 1H), 4.87 (dd, $J = 6.2, 3.7$ Hz, 1H), 4.66–4.59 (m, 1H), 4.39–4.33 (m, 1H), 4.33–4.26 (m, 1H), 4.26–4.19 (m, 1H), 3.76 (ddd, $J = 17.8, 11.2, 3.1$ Hz, 1H), 3.65 (ddd, $J = 10.7, 7.2, 3.3$ Hz, 1H), 2.74 (dt, $J = 8.6, 6.3$ Hz, 1H), 2.66–2.59 (m, 2H), 2.56–2.51 (m, 1H), 2.39 (t, $J = 7.3$ Hz, 2H), 2.36 (t, $J = 7.4$ Hz, 1H), 2.10 (s, 3H), 2.10 (s, 3H), 1.99 (s, 3H), 1.93 (s, 2H), 1.92 (s, 1H), 1.65–1.60 (m, 1H), 1.60–1.54 (m, 1H), 1.39 (dt, $J = 15.0, 7.4$ Hz, 1H), 1.36–1.30 (m, 1H), 1.28–1.16 (m, 25H), 0.94 (dt, $J = 25.7, 7.4$ Hz, 3H), 0.87 (td, $J = 7.2, 5.2$ Hz, 3H) ppm.

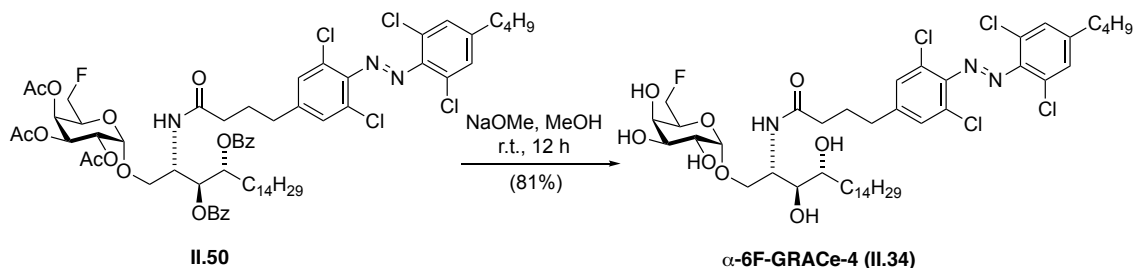
$^{13}\text{C NMR}$ (201 MHz, CDCl_3): $\delta = 172.2, 170.7, 170.2, 166.6, 165.3, 146.4, 146.1, 145.8, 145.7, 145.5, 145.3, 144.3, 143.9, 133.7, 133.3, 130.0, 130.0, 129.9, 129.6, 129.5, 129.4, 129.2, 129.1, 128.8, 128.5, 127.5, 127.5, 97.9, 81.5$ (d, $J = 171.7$ Hz), 77.2, 74.1, 72.4, 72.3, 68.4, 68.0, 67.9 (d, $J = 22.3$ Hz), 67.6, 67.4, 48.7, 35.8, 35.0, 34.8, 34.6, 34.4, 33.1, 32.9, 32.1, 30.5, 29.8, 29.8, 29.8, 29.7, 29.7, 29.5, 28.5, 26.4, 25.8, 22.8, 22.3, 20.8, 20.7, 14.3, 14.0 ppm.

$^{19}\text{F NMR}$ (377 MHz, CDCl_3) $\delta = -230.25$ (td, $J = 46.2, 14.3$ Hz).

IR (ATR): $\tilde{\nu} = 2926$ (s), 2854 (m), 1751 (m), 1726 (m), 1679 (w), 1588 (w), 1530 (w), 1452 (w), 1372 (w), 1315 (w), 1250 (s), 1227 (s), 1177 (w), 1155 (w), 1070 (s), 1026 (m), 953 (w), 807 (w), 712 (m) cm^{-1} .

HRMS (ESI): calcd. for $\text{C}_{64}\text{H}_{84}\text{Cl}_4\text{FN}_4\text{O}_{13}^+$: 1275.4768 $[\text{M}+\text{NH}_4]^+$
found: 1275.4798 $[\text{M}+\text{NH}_4]^+$.

4-(4-((*E*)-(4-Butyl-2,6-dichlorophenyl)diazenyl)-3,5-dichlorophenyl)-*N*-((2*S*,3*S*,4*R*)-1-(((2*S*,3*R*,4*S*,5*R*,6*S*)-6-(fluoromethyl)-3,4,5-trihydroxytetrahydro-2*H*-pyran-2-yl)oxy)-3,4-dihydroxyoctadecan-2-yl)butanamide (α -6F-GRACe-4, **II.34**)



Protected glycosphingolipid **II.50** (17.3 mg, 15.2 μ mol, 1.0 eq.) was dissolved in MeOH (1 mL) and NaOMe was added at room temperature until pH 9–10. After 12 h, the reaction was stopped by the addition of DOWEX 50WX 2-100 (H⁺ form) and stirred for another 30 min. at room temperature. All solid material was removed by filtration through a pad of Celite®, which was washed with MeOH (20 mL) and the filtrate was concentrated under reduced pressure. Flash column chromatography [CHCl₃/MeOH, 9:1] afforded α -6F-GRACe-4 (**II.34**, 11.4 mg, 12.3 μ mol, 81%) as yellow viscous oil.

Compound **II.34** was isolated as a 2.2:1 mixture of *trans*-/*cis*-isomers.

R_f = 0.45 [DCM/MeOH, 10:1].

¹H NMR (800 MHz, CD₃OD): δ = 7.45 (s, 1H), 7.41 (d, J = 0.7 Hz, 1H), 4.63–4.47 (m, 2H), 4.23 (tt, J = 6.8, 4.3 Hz, 1H), 4.16–4.08 (m, 1H), 3.94–3.86 (m, 2H), 3.85–3.77 (m, 2H), 3.72 (ddd, J = 15.7, 10.5, 4.6 Hz, 1H), 3.66 (dd, J = 6.8, 5.7 Hz, 1H), 3.57 (dddd, J = 18.2, 9.9, 5.8, 2.4 Hz, 1H), 2.72 (dt, J = 15.7, 7.4 Hz, 2H), 2.62 (dt, J = 11.8, 7.8 Hz, 1H), 2.32 (ddd, J = 10.3, 6.6, 2.9 Hz, 1H), 2.00 (dtd, J = 15.2, 8.5, 7.9, 4.1 Hz, 1H), 1.97–1.88 (m, 1H), 1.72–1.52 (m, 2H), 1.47–1.39 (m, 2H), 1.39–1.22 (m, 26H), 0.98 (dt, J = 35.1, 7.4 Hz, 2H), 0.94–0.88 (m, 3H) ppm.

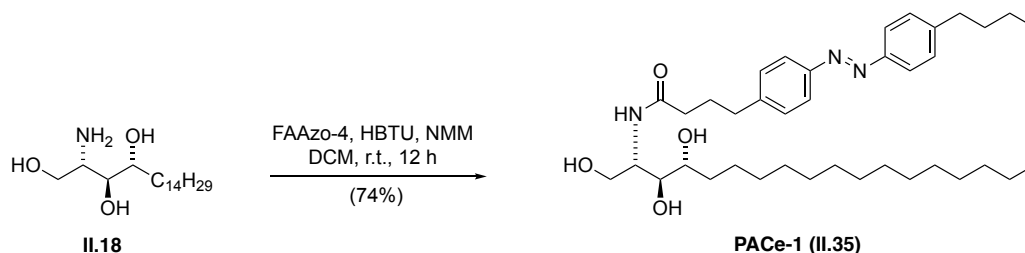
¹³C NMR (200 MHz, CD₃OD): δ = 174.9, 174.9, 147.7, 147.5, 147.3, 147.1, 146.8, 146.5, 146.5, 146.4, 130.7, 130.6, 130.4, 130.4, 128.3, 128.3, 126.8, 126.7, 101.0, 84.4, 84.4, 83.6, 83.6, 75.2, 75.1, 72.9, 71.1, 71.0, 70.9, 70.6, 70.5, 70.1, 68.3, 51.9, 51.8, 49.0, 36.3, 36.2, 35.8, 35.5, 35.4, 35.2, 34.3, 34.1, 33.1, 32.9, 32.8, 30.9, 30.8, 30.5, 28.2, 28.0, 27.0, 23.8, 23.3, 23.2, 14.5, 14.2 ppm.

¹⁹F NMR (377 MHz, CD₃OD) δ = –231.18 (td, J = 48.3, 47.7, 15.3 Hz).

IR (ATR): $\tilde{\nu}$ = 3308 (bm), 2922 (s), 2852 (s), 1643 (m), 1591 (m), 1549 (m), 1466 (m), 1401 (m), 1379 (m), 1347 (m), 1260 (m), 1207 (m), 1153 (m), 1079 (s), 1028 (s), 1004 (s), 979 (s), 858 (m), 802 (m), 726 (m), 692 (m) cm⁻¹.

HRMS (ESI): calcd. for $C_{44}H_{65}N_3O_8F$: 922.3515 [M-H]⁻
 found: 922.3531 [M-H]⁻.

4-(4-((*E*)-(4-Butylphenyl)diazenyl)phenyl)-*N*-((2*S*,3*S*,4*R*)-1,3,4-trihydroxyoctadecan-2-yl)butanamide (PACe-1, II.35)

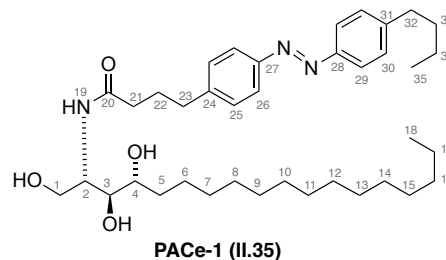


Phytosphingosine **II.18** (4.3 mg, 14 μ mol, 1.0 eq.) was dissolved in DCM (1 mL) and FAAzo-4 (4.4 mg, 14 μ mol, 1 eq.) followed by HBTU (7.7 mg, 21 μ mol, 1.5 eq.) and *N*-methylmorpholine (22 μ L, 0.20 mmol, 15 eq.) were added and the reaction stirred at room temperature. After 12 h the solvent was removed under reduced pressure and the crude product was purified *via* flash column chromatography [DCM/MeOH, 10:0 to 10:1] to give PACe-1 **II.35** (8.3 mg, 13 μ mol, 93%) as yellow viscous oil.

$R_f = 0.82$ [DCM/MeOH, 10:1].

¹H NMR (400 MHz, $CDCl_3$): $\delta = 7.82$ (d, $J = 8.1$ Hz, 4H, H-26 and H-29), 7.31 (d, $J = 8.1$ Hz, 4H, H-25 and H-30), 6.39 (d, $J = 7.6$ Hz, 1H, H-19), 4.14 (td, $J = 5.4, 2.9$ Hz, 1H, H-2), 3.90 (dd, $J = 11.5, 2.7$ Hz, 1H, H-1a), 3.71 (dd, $J = 11.6, 5.5$ Hz, 1H, H-1b), 3.61 (dt, $J = 8.8, 4.8$ Hz, 1H, H-4), 3.55 (dd, $J = 6.8, 3.1$ Hz, 1H, H-3), 2.73 (t, $J = 7.4$ Hz, 2H, H-23), 2.68 (t, $J = 7.7$ Hz, 2H, H-32), 2.26 (t, $J = 7.4$ Hz, 2H, H-21), 2.02 (p, $J = 7.5$ Hz, 2H, H-22), 1.69 – 1.59 (m, 2H, H-33), 1.37 (dt, $J = 14.8, 7.5$ Hz, 2H, H-34), 1.24 (s, 24H, H6–17), 0.94 (t, $J = 7.4$ Hz, 3H, H-35), 0.87 (t, $J = 7.1$ Hz, 3H, H-18) ppm.

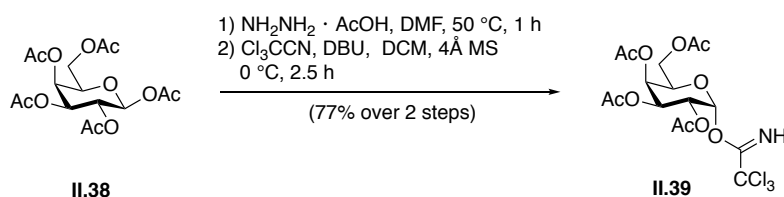
¹³C NMR (100 MHz, $CDCl_3$): $\delta = 173.8$ (C-20), 151.3 (C-27 or C-28), 150.9 (C-27 or C-28), 146.4 (C-31), 144.4 (C-24), 129.2 (C-25), 129.1 (C-30), 122.8 (C-26 and C-29), 76.6 (C-3), 72.6 (C-4), 61.8 (C-1), 53.1 (C-2), 35.6 (C-21 and C-32), 35.0 (C-23), 33.5 (C-33), 33.3 – 29.4 (C-6 – C-17), 26.8 (C-22), 25.6 (C-5), 22.7 (C-6 – C-17), 22.3 (C-34), 14.1 (C-18), 13.9 (C-35) ppm.



IR (ATR): $\tilde{\nu}$ = 3295 (bm), 2956 (m), 1919 (s), 2851 (s), 1636 (m), 1603 (w), 1542 (w), 1498 (w), 1468 (m), 1481 (w), 1378 (w), 1156 (w), 1068 (w), 840 (w), 721 (w) cm^{-1} .

HRMS (ESI): calcd. for $\text{C}_{38}\text{H}_{62}\text{N}_3\text{O}_4^+$: 624.4735 $[\text{M}+\text{H}]^+$
found: 624.4738 $[\text{M}+\text{H}]^+$.

(2R,3S,4S,5R,6R)-2-(Acetoxymethyl)-6-(2,2,2-trichloro-1-iminoethoxy)tetrahydro-2H-pyran-3,4,5-triyl triacetate (II.39)

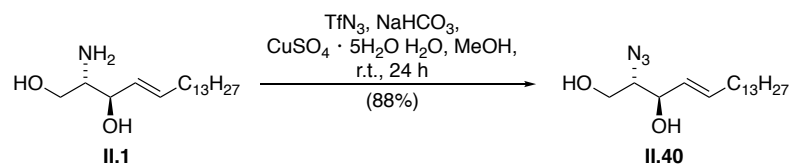


β -D-Galactose pentaacetate (**II.38**, 1.00 g, 2.56 mmol, 1.0 eq.) was dissolved in DMF (25 mL), hydrazine acetate (295 mg, 3.20 mmol, 1.25 eq.) was added and the reaction was heated to 50 °C. After 1 h, the reaction was allowed to cool to room temperature. EtOAc (200 mL) was added and the organic phase was washed with H_2O (3×100 mL), 0.2 M aqueous HCl (100 mL), saturated NaHCO_3 (100 mL), saturated aqueous NaCl (100 mL) and dried (MgSO_4) and concentrated under reduced pressure. The crude reaction mixture was dissolved in DCM (20 mL) and cooled to 0 °C. CCl_3CN (2.9 mL, 25.6 mmol, 10 eq.) was added and after 1 h, DBU (77 μL , 0.512 mmol, 0.2 eq.) was added and the reaction stirred for 2 h. Then the solvent was removed under reduced pressure and the crude product was purified by flash column chromatography on silica gel [PE/EtOAc, 1:1] to give trichloroacetimidate (**II.39**, 974 mg, 1.98 mmol, 77% over two steps) as white foam.

^1H NMR (400 MHz, CDCl_3): δ = 8.67 (s, 1H), 6.60 (d, J = 3.4 Hz, 1H), 5.61–5.54 (m, 1H), 5.45–5.31 (m, 2H), 4.51–4.40 (m, 1H), 4.17 (dd, J = 11.3, 6.6 Hz, 1H), 4.12–4.05 (m, 1H), 2.17 (s, 3H), 2.03 (s, 3H), 2.02 (s, 3H), 2.02 (s, 3H) ppm.

HRMS (ESI): calcd. for $\text{C}_{14}\text{H}_{24}\text{N}_2\text{O}_{10}\text{Cl}_3^+$: 509.0461 $[\text{M}+\text{H}]^+$
found: 509.0499 $[\text{M}+\text{H}]^+$.

The analytical data matched those previously described in the literature.^[402]

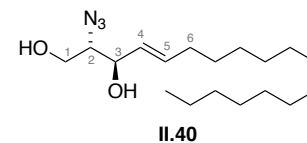
(2*S*,3*R*,*E*)-2-Azido-octadec-4-ene-1,3-diol (II.40)

D-erythro-sphingosine (**II.1**, 275 mg, 0.920 mmol, 1 eq.), NaHCO₃ (312 mg, 3.72 mg, 4 eq.) and CuSO₄·H₂O (8.80 mg, 40.0 μmol, 5 mol%) were dissolved in H₂O (1.2 mL). The emulsion was cooled to 0 °C and freshly prepared TfN₃^[403] (2 M in toluene, 2.00 mL, 4.00 mmol, 4.3 eq.) was added. MeOH (2 mL) was added and the reaction was slowly allowed to warm to r.t. After 24 h, H₂O (20 mL) was added and the reaction mixture was extracted with EtOAc (3 × 20 mL), dried (MgSO₄) and concentrated under reduced pressure. Flash column chromatography [PE/EtOAc, 10:1 to 0:1] afforded azidosphingosine (**II.40**, 263 mg, 0.806 mmol, 88%) as a yellow oil.

R_f = 0.66 [PE/EtOAc, 1:1].

[α]_D²⁰ = -0.14 (c = 1, DCM).

¹H NMR (400 MHz, CDCl₃): δ = 5.86–5.78 (m, 1H, H-5), 5.53 (ddt, *J* = 15.4, 7.4, 1.5 Hz, 1H, H-4), 4.27–4.23 (m, 1H, H-3), 3.78 (dd, *J* = 5.2, 3.9 Hz, 2H, H-1), 3.51 (q, *J* = 5.4 Hz, 1H, H-2), 2.14–2.00 (m, 2H, H-6), 1.47–1.32 (m, 2H, H-alkyl), 1.32–1.19 (m, 21H, H-alkyl), 0.88 (t, *J* = 6.8 Hz, 3H, H-alkyl) ppm.

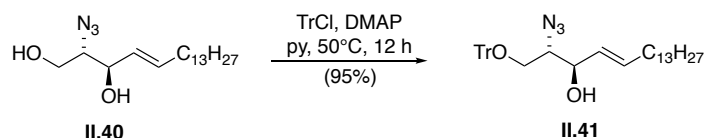


¹³C NMR (101 MHz, CDCl₃): δ = 136.1 (C-5), 127.9 (C-4), 73.8 (C-3), 66.7 (C-2), 62.6 (C-1), 32.3 (C-6), 31.9 (C-alkyl), 29.7 – 29.2 (C-alkyl), 28.9 (C-7), 14.1 (C-alkyl) ppm.

IR (ATR): $\tilde{\nu}$ = 3351 (w), 2919 (s), 2851 (s), 2100 (m), 1669 (w), 1467 (m), 1379 (m), 1266 (m), 1235 (m), 1195 (m), 1154 (m), 1003 (m), 971 (m), 704 (w) cm⁻¹.

HRMS (EI): calcd. for C₁₈H₃₄O₂N₃: 324.2657 [M-H]⁻

found: 324.2658 [M-H]⁻.

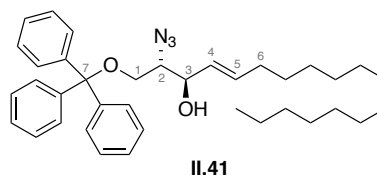
(2*S*,3*R*,*E*)-2-Azido-1-(trityloxy)octadec-4-en-3-ol (II.41)

Azide **II.40** (263 mg, 0.806 mmol, 1 eq.) was dissolved in pyridine (3 mL) and TrCl (274 mg, 0.887 mmol, 1.1 eq.) followed by DMAP (4.92 mg, 40.3 μ mol, 0.05 eq.) were added. The mixture was stirred at 50 °C for 12 h. Afterwards, the solvent was removed under reduced pressure. The crude product was purified by flash column chromatography on silica gel [PE/EtOAc, 10:1 to 3:1] to give protected alcohol **II.41** (437 mg, 0.771 mmol, 95%) as a colorless oil.

$R_f = 0.65$ [PE/EtOAc, 7:1].

$[\alpha]_D^{20} = 0.01$ ($c = 1$, DCM).

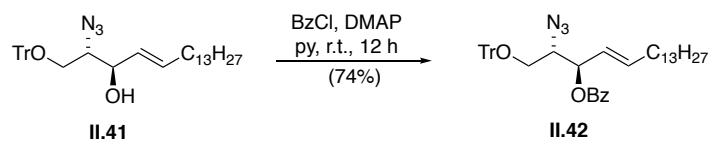
¹H NMR (400 MHz, CD₃CN): $\delta = 7.37$ – 7.32 (m, 6H, H-Ar), 7.21 (q, $J = 6.8, 6.1$ Hz, 6H, H-Ar), 7.16 (t, $J = 7.1$ Hz, 3H, H-Ar), 5.46 (dt, $J = 14.3, 6.8$ Hz, 1H, H-5), 5.22 (dd, $J = 15.5, 7.1$ Hz, 1H, H-4), 3.97 (t, $J = 6.2$ Hz, 1H, H-3), 3.49 (dt, $J = 8.6, 4.4$ Hz, 1H, H-2), 3.14–3.06 (m, 1H, H-1a), 3.01 (dd, $J = 9.9, 7.7$ Hz, 1H, H-1b), 3.14–3.06 (m, 2H), 3.01 (dd, $J = 9.9, 7.7$ Hz, 1H), 1.83 (dq, $J = 5.2, 2.6$ Hz, 2H, H-6), 1.01–1.21 (d, $J = 13.9$ Hz, 22H, H-alkyl), 0.77 (t, $J = 6.6$ Hz, 3H, H-alkyl) ppm.



¹³C NMR (101 MHz, CD₃CN): $\delta = 144.8$ (C-Ar), 134.7 (C-5), 129.9 (C-4), 129.6 (C-Ar), 129.4 (C-Ar), 128.1 (C-Ar), 87.8 (C-alkyl), 73.0 (C-3), 67.2 (C-2), 64.2 (C-1), 32.7 (C-6), 32.6–29.7 (C-alkyl), 23.3 (C-alkyl), 14.4 (C-alkyl) ppm.

IR (ATR): $\tilde{\nu} = 3422$ (bw), 3059 (w), 3033 (w), 2924 (s), 2954 (m), 2362 (w), 2098 (m), 1669 (w), 15098 (w), 1491 (w), 1448 (m), 1271 (w), 1221 (w), 1184 (w), 1155 (w), 1077 (m), 1033 (w), 1015 (w), 972 (w), 989 (w), 764 (m), 746 (m), 702 (s) cm⁻¹.

HRMS (EI): calcd. For C₃₇H₄₈N₃O₂⁻ : 566.3752 [M-H]⁻
 found: : 566.3746 [M-H]⁻.

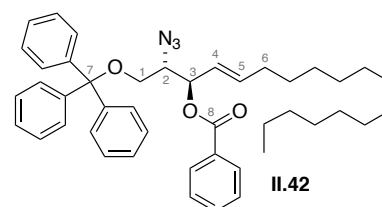
(2*S*,3*R*,*E*)-2-Azido-1-(trityloxy)octadec-4-en-3-yl benzoate (II.42)

To a solution of secondary alcohol **II.41** (437 mg, 0.771 mmol, 1 eq.) in pyridine (12 mL) were added benzoylchloride (0.187 mL, 1.54 mmol, 2 eq.) and DMAP (4.71 mg, 38.6 μmol , 0.05 eq.). The mixture was stirred at room temperature for 12 h. The solvent was removed under reduced pressure and flash column chromatography on silica gel [PE/EtOAc, 1:0 to 2:1] afforded protected *D-erythro*-sphingosine **II.42** (383 mg, 0.570 mmol, 74%) as a colorless oil.

$R_f = 0.79$ [PE/EtOAc, 7:1]

$[\alpha]_D = -0.003$ ($c = 1$, DCM).

$^1\text{H NMR}$ (400 MHz, CDCl_3): $\delta = 7.91\text{--}7.85$ (m, 2H, H-Ar), 7.53–7.45 (m, 1H, H-Ar), 7.39–7.32 (m, 6H, H-Ar), 7.24–7.17 (m, 6H, H-Ar), 7.17–7.11 (m, 3H, H-Ar), 5.74 (dt, $J = 15.4$, 6.7 Hz, 1H, H-5), 5.56 (dd, $J = 7.9$, 4.8 Hz, 1H, H-3), 5.35 (ddt, $J = 15.4$, 7.9, 1.5 Hz, 1H, H-4), 3.79 (dt, $J = 6.8$, 5.0 Hz,

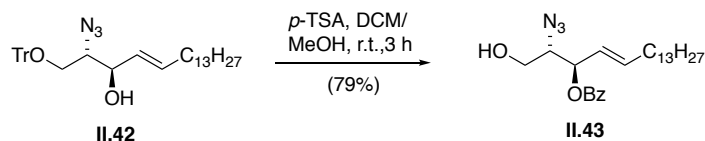


1H, H-2), 3.22 (dd, $J = 9.8$, 6.8 Hz, 1H, H-1a), 3.12 (dd, $J = 9.8$, 5.2 Hz, 1H, H-1b), 1.89 (qt, $J = 7.0$, 1.7 Hz, 2H, H-6), 1.29–1.06 (m, 22H, H-alkyl), 0.86–0.74 (m, 3H, H-alkyl) ppm.

$^{13}\text{C NMR}$ (101 MHz, CDCl_3): $\delta = 165.3$ (C-8), 143.6 (C-5), 138.5 (C-Ar), 133.2 (C-Ar), 129.9 (C-Ar), 129.8 (C-Ar), 128.7 (C-Ar), 128.5 (C-Ar), 128.2 (C-Ar), 128.0 (C-Ar), 127.3 (C-Ar), 123.2 (C-4), 87.3 (C-7), 74.9 (C-3), 64.6 (C-2), 63.0 (C-1), 32.4 (C-alkyl), 32.1 (C-alkyl), 29.9–29.3 (C-alkyl), 28.8 (C-alkyl), 22.9 (C-alkyl), 14.3 (C-alkyl) ppm.

IR (ATR): $\tilde{\nu} = 2924$ (m), 2853 (m), 2098 (m), 1723 (m), 1602 (w), 1491 (w), 1466 (w), 1450 (m), 1315 (w), 1263 (s), 1177 (w), 1154 (w), 1092 (m), 1069 (m), 1026 (m), 970 (m), 899 (w), 774 (w), 764 (m), 741 (m), 703 (s) cm^{-1} .

HRMS (ESI): calcd. for $\text{C}_{44}\text{H}_{57}\text{N}_4\text{O}_3^+$ 689.4425 $[\text{M}+\text{NH}_4^+]$
 found: 689.4442 $[\text{M}+\text{NH}_4^+]$.

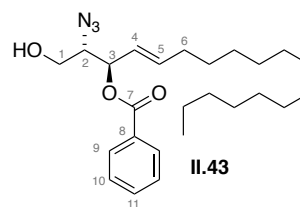
(2*S*,3*R*,*E*)-2-Azido-1-hydroxyoctadec-4-en-3-yl benzoate (II.43)

To a solution of protected *D-erythro*-sphingosine (**II.42**, 72.6 mg, 0.108 mmol, 1 eq.) in DCM (1 mL) and MeOH (1 mL) was added *p*-toluenesulfonic acid hydrate (20.5 mg, 0.108 mmol, 1.0 eq.). The mixture was removed under reduced pressure and the crude product was purified by flash column chromatography [PE/EtOAc, 10:1 to 3:1] to give primary alcohol (**II.43**, 27.6 mg, 85.1 μ mol, 79%) as a colorless oil.

$R_f = 0.66$ [PE/EtOAc, 4:1].

$[\alpha]_D^{20} = -0.38$ ($c = 1$, DCM).

$^1\text{H NMR}$ (400 MHz, CDCl_3): $\delta = 8.06$ (d, $J = 7.7$ Hz, 2H, H-Ar), 7.59 (t, $J = 7.4$ Hz, 1H, H-Ar), 7.46 (t, $J = 7.6$ Hz, 2H, H-Ar), 5.96 (ddd, $J = 13.8, 8.7, 4.3$ Hz, 1H, H-5), 5.68–5.57 (m, 2H, H-4 and H-3), 3.85–3.70 (m, 2H, H-2 and H-1a), 3.63 (dd, $J = 11.6, 7.0$ Hz, 1H, H-1b), 2.08 (q, $J = 7.1$ Hz, 2H, H-6), 1.57 (bs, 1H, OH), 1.39 (t, $J = 7.2$ Hz, 2H, H-alkyl), 1.24 (d, $J = 3.7$ Hz, 16H, H-alkyl), 0.88 (t, $J = 6.7$ Hz, 3H, H-alkyl) ppm.

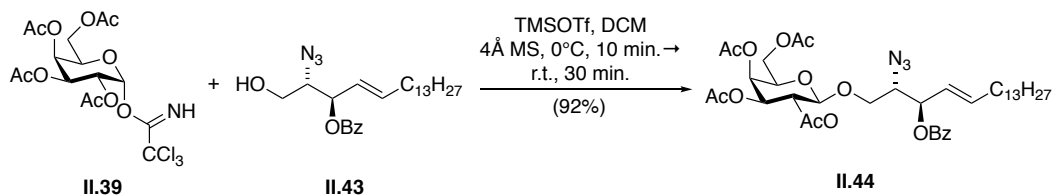


$^{13}\text{C NMR}$ (101 MHz, CDCl_3): $\delta = 165.5$ (C-7), 138.7 (C-Ar), 133.4 (C-Ar), 129.8 (C-5), 129.7 (C-Ar), 128.5 (C-Ar), 123.2 (C-4), 74.6 (C-3), 66.2 (C-2), 62.0 (C-1), 32.4 (C-6), 31.9–28.7 (C-alkyl), 22.7 (C-alkyl), 14.1 (C-alkyl) ppm.

IR (ATR): $\tilde{\nu} = 3428$ (bw), 2923 (s), 2853 (s), 2168 (w), 2101 (s), 1722 (s), 1602 (w), 1452 (m), 1316 (m), 1265 (s), 1177 (m), 1110 (s), 1068 (s), 1026 (m), 970 (m), 860 (w), 710 (s), 686 (m) cm^{-1} .

HRMS (EI): calcd. for $\text{C}_{25}\text{H}_{43}\text{N}_4\text{O}_3^-$ 447.3330 $[\text{M}+\text{NH}_4^+]$
 found: 447.3336 $[\text{M}+\text{NH}_4^+]$

(2*R*,3*S*,4*S*,5*R*,6*R*)-2-(Acetoxymethyl)-6-(((2*S*,3*R*,*E*)-2-azido-3-(benzyloxy)octadec-4-en-1-yl)oxy)tetrahydro-2*H*-pyran-3,4,5-triyl triacetate (**II.44**)

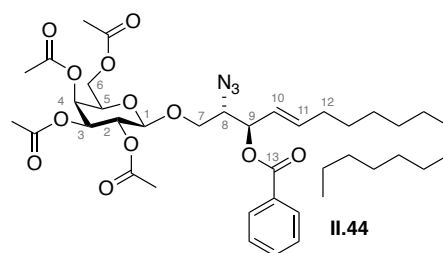


Galactosyl donor **II.39** (225 mg, 0.456 mmol, 2.3 eq.) and acceptor **II.43** (100 mg, 0.198 mmol, 1.0 eq.) were combined and co-evaporated with toluene (3×5 mL) and with THF (1×5 mL), dried under high vacuum and then dissolved in DCM (0.8 mL). The mixture was stirred with freshly activated 4Å MS at room temperature for 30 min, before the reaction vessel was cooled to 0 °C and TESOTf (0.8 M in DCM, 31.7 μ L, 39.6 μ mol, 0.2 eq.) were added. After 10 min. the reaction was allowed to warm to room temperature and after an additional 30 min. the reaction was diluted with DCM and washed with saturated aqueous NaHCO₃ solution (10 mL). The aqueous layer was extracted with DCM (3×20 mL) and the combined organic phases were dried (MgSO₄) and concentrated under reduced pressure. Flash column chromatography (PE/EtOAc, 100:0 to 2:1) afforded protected glycoside (**II.44**, 139 mg, 0.182 mmol, 92%) as a colorless oil.

$R_f = 0.50$ [PE/EtOAc, 2:1].

$[\alpha]_D^{20} = -0.13$ ($c = 1$, DCM)

¹H NMR (600 MHz, CDCl₃): $\delta = 8.08$ – 8.02 (m, 2H, H-Bz), 7.57 (t, $J = 7.4$ Hz, 1H, H-Bz), 7.45 (t, $J = 7.6$ Hz, 2H, H-Bz), 5.93 (dt, $J = 13.6$, 6.7 Hz, 1H, H-11), 5.63–5.51 (m, 2H, H-3, H-10), 5.38 (d, $J = 3.4$ Hz, 1H, H-4), 5.23 (dd, $J = 10.5$, 7.9 Hz, 1H, H-2), 5.01 (dd, $J = 10.4$, 3.5 Hz, 1H, H-3), 4.49 (d, $J = 8.0$ Hz, 1H, H-1), 4.17–



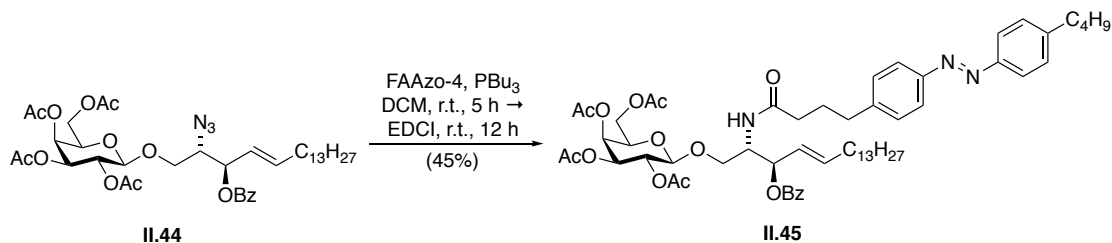
4.04 (m, 2H, H-6), 3.92 (m, 3H, H-5, H-7a, H-8), 3.58 (dd, $J = 9.1$, 4.8 Hz, 1H, H-7b), 2.15 (s, 3H, H-Ac), 2.10 (s, 3H, H-Ac), 2.09–2.03 (m, 3H, H-alkyl), 2.02 (s, 3H, H-Ac), 1.98 (s, 4H, H-Ac, H-alkyl), 1.37 (q, $J = 7.0$ Hz, 2H, H-alkyl), 1.24 (d, $J = 4.7$ Hz, 23H, H-alkyl), 0.87 (t, $J = 6.7$ Hz, 3H, H-alkyl).

¹³C NMR (101 MHz, CDCl₃): $\delta = 170.3$ (C-Ac), 170.2 (C-Ac), 170.14 (C-Ac), 169.3 (C-Ac), 165.1 (C-13), 139.1 (C-10), 133.2 (C-Bz), 129.9 (C-Bz), 129.7 (C-Bz), 128.4 (C-Bz), 122.62 (C-11), 101.0 (C-1), 74.7 (C-9), 70.8 (C-3 and C-5), 68.5 (C-2), 68.0 (C-7), 66.9 (C-4), 63.5 (C-8), 61.1 (C-6), 32.4 (C-alkyl), 31.9–29.1 (C-alkyl), 28.7 (C-alkyl), 22.7 (C-Ac), 20.7 (C-Ac), 20.7 (C-Ac), 20.6 (C-Ac), 14.1 (C-alkyl) ppm.

IR (ATR): $\tilde{\nu}$ = 3428 (w), 3353 (w), 3296 (w), 1926 (m), 2854 (m), 2108 (m), 1726 (s), 1726 (s), 1601 (w), 1452 (w), 1370 (m), 1317 (w), 1252 (s), 1224 (s), 1176 (w), 1070 (m), 1026 (w), 973 (w), 957 (w), 916 (w), 827 (m), 713 (m) cm^{-1} .

HRMS (EI): calcd. for $\text{C}_{39}\text{H}_{61}\text{N}_4\text{O}_{12}^+$: 777.4280 $[\text{M}+\text{NH}_4]^+$
found: 777.4297 $[\text{M}+\text{NH}_4]^+$.

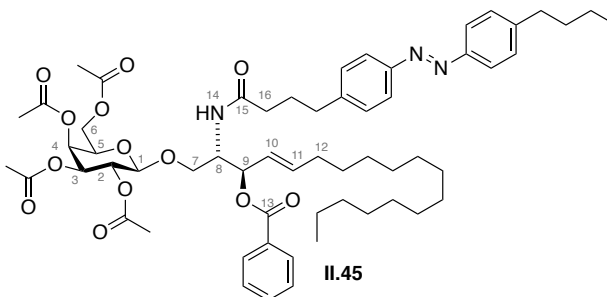
4-(4-((*E*)-(4-Butylphenyl)diazenyl)phenyl)-*N*-((2*S*,3*R*,*E*)-3-hydroxy-1-(((2*R*,3*R*,4*S*,5*R*,6*R*)-3,4,5-trihydroxy-6-(hydroxymethyl)tetrahydro-2*H*-pyran-2-yl)oxy)octadec-4-en-2-yl)butanamide (II.45)



Glycoside **II.44** (23.9 mg, 31.5 μmol , 1 eq.) and FAAzo-4 (15.3 mg, 47.2 μmol , 1.5 eq.) were dissolved in DCM (1 mL). Bu_3P (11.6 μL , 47.2 μmol , 1.5 eq.) was added and the reaction stirred for 6 h at room temperature. Then EDCI (22.0 mg, 142 μmol , 3 eq.) was added and the reaction mixture stirred at room temperature for another 12 h. The solvent was removed under reduced pressure and purification *via* flash column chromatography [PE/EtOAc, 10:1 to 0:1] afforded amide **II.45** (14.8 mg, 14.2 μmol , 45%) as a yellow oil.

R_f = 0.60 [PE/EtOAc, 1:2].

$^1\text{H NMR}$ (600 MHz, CDCl_3): δ = 8.05–8.01 (m, 2H, H-Bz), 7.83–7.80 (m, 4H, H-Ar), 7.58–7.53 (m, 1H, H-Bz), 7.46–7.42 (m, 2H, H-Bz), 7.33–7.29 (m, 4H, H-Ar), 5.89 (dtd, J = 15.2, 6.7, 0.8 Hz, 1H, H-11), 5.78 (d, J = 9.1 Hz, 1H, NH-14), 5.59–5.54 (m, 1H, H-9), 5.50 (ddt, J = 15.3, 7.6, 1.5 Hz, 1H, H-10), 5.35 (dd, J = 3.4, 1.2 Hz, 1H, H-4), 5.15 (dd, J = 10.5, 7.8 Hz, 1H, H-2), 4.99 (dd, J = 10.5, 3.4 Hz, 1H, H-3), 4.54–4.48 (m, 1H, H-8), 4.44 (d, J = 7.9 Hz, 1H, H-1), 4.07–4.00 (m, 2H, H-6a and H-7a), 3.96 (dd, J = 11.3, 6.3 Hz, 1H, H-H-6b), 3.85 (ddd, J = 7.4, 6.4, 1.3 Hz, 1H, H-5), 3.68 (dd, J = 10.1, 4.3 Hz, 1H, H-7b),



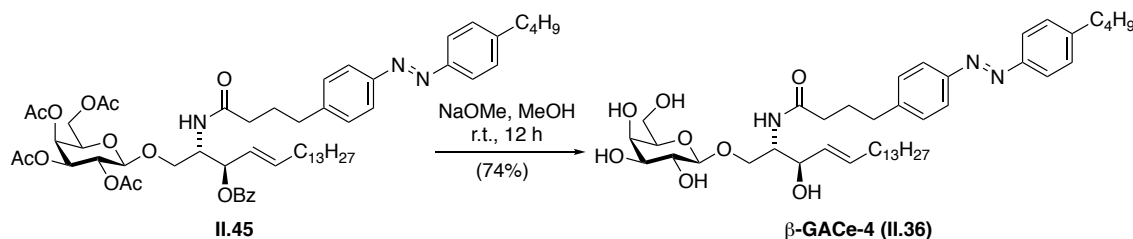
2.78–2.71 (m, 2H, H-alkyl), 2.71–2.65 (m, 3H, H-Ac), 2.10–2.13 (m, 3H, H-12), 2.07–1.99 (m, 4H, H-alkyl), 1.97 (s, 2H, H-Ac), 1.96 (s, 3H, H-Ac), 1.94 (s, 3H, H-Ac), 1.68–1.61 (m, 2H, H-alkyl), 1.38 (h, $J = 7.4$ Hz, 3H, H-alkyl), 1.35–1.17 (m, 27H, H-alkyl), 0.94 (t, $J = 7.4$ Hz, 3H, H-alkyl), 0.87 (t, $J = 7.1$ Hz, 3H, H-alkyl) ppm.

^{13}C NMR (151 MHz, CDCl_3): $\delta = 172.3$ (C-15), 170.4 (C-Ac), 170.3 (C-Ac), 170.2 (C-Ac), 169.7 (C-Ac), 165.4 (C-13), 151.4 (C-Ar), 151.1 (C-Ar), 146.5 (C-Ar), 144.8 (C-Ar), 137.7 (C-11), 133.2 (C-Bz), 129.8 (C-Bz), 129.3 (C-Ar), 129.2 (C-Ar), 128.6 (C-Bz), 124.8 (C-Ar), 123.0 (C-Ar), 122.9 (C-Ar), 101.1 (C-1), 74.5 (C-9), 70.9 (C-3 and C-5), 70.8 (C-2), 69.0 (C-7), 67.3 (C-4), 67.0 (C-6), 61.2 (C-8), 51.0 (C-16), 36.0 (C-alkyl), 35.7 (C-alkyl), 35.2 (C-alkyl), 33.6 (C-alkyl), 32.5 (C-alkyl), 32.1 (C-alkyl), 29.8 (C-alkyl), 29.6 (C-alkyl), 29.5 (C-alkyl), 29.4 (C-alkyl), 29.1 (C-alkyl), 27.1 (C-12), 22.8 (C-alkyl), 22.5 (C-alkyl), 20.9 (C-Ac), 20.8 (C-Ac), 20.7 (C-Ac), 14.3 (C-alkyl), 14.1 (C-alkyl) ppm.

IR (ATR): $\tilde{\nu} = 2926$ (m), 2854 (w), 1753 (s), 1672 (w), 1602 (w), 1531 (w), 1452 (w), 1369 (m), 1224 (s), 1176 (w), 1071 (m), 968 (w), 846 (w), 714 (m) cm^{-1} .

HRMS (ESI): calcd. for $\text{C}_{59}\text{H}_{82}\text{N}_3\text{O}_{13}^+$: 1040.5842 $[\text{M}+\text{H}]^+$
found: 1040.5880 $[\text{M}+\text{H}]^+$.

(2*R*,3*S*,4*S*,5*R*,6*R*)-2-(Acetoxymethyl)-6-(((2*S*,3*R*,*E*)-3-(benzoyloxy)-2-(4-(4-((*E*)-(4-butylphenyl)di-azeryl)phenyl)butanamido)octadec-4-en-1-yl)oxy)tetrahydro-2*H*-pyran-3,4,5-triyl triacetate (β -GACe-4, **II.36**)



Protected glycosphingolipid (**II.45**, 13.6 mg, 13.1 μmol , 1.0 eq.) was dissolved in MeOH (1.5 mL) and NaOMe was added until pH 9–10. The reaction mixture was stirred at room temperature for 12 h. The reaction was stopped by the addition of DOWEX 50WX 2-100 (H^+ form) and stirred for another 30 min. at room temperature. All solid material was removed by filtration through a pad of Celite[®], which was washed with MeOH (5 mL) and the filtrate was concentrated under reduced pressure. Flash column chromatography [$\text{CHCl}_3/\text{MeOH}$, 10:1] afforded β -GACe-4 (**II.36**, 7.4 mg, 9.63 μmol , 74%) as yellow viscous oil.

$R_f = 0.34$ [DCM: MeOH 10:1]

$^1\text{H NMR}$ (800 MHz, CD_3OD): $\delta = 7.85\text{--}7.80$ (m, 4H), 7.42–7.33 (m, 4H), 5.69 (dtd, $J = 15.3, 6.7, 0.9$ Hz, 1H), 5.46 (ddt, $J = 15.3, 7.8, 1.5$ Hz, 1H), 4.23 (d, $J = 7.7$ Hz, 1H), 4.18 (dd, $J = 10.1, 4.9$ Hz, 1H), 4.10 (t, $J = 8.1$ Hz, 1H), 4.01 (ddd, $J = 8.3, 4.9, 3.3$ Hz, 1H), 3.83 (dd, $J = 3.4, 1.1$ Hz, 1H), 3.77 (dd, $J = 11.4, 7.0$ Hz, 1H), 3.72 (dd, $J = 11.4, 5.2$ Hz, 1H), 3.63 (dd, $J = 10.2, 3.3$ Hz, 1H), 3.59–3.55 (m, 1H), 3.55–3.51 (m, 1H), 3.48 (dd, $J = 9.7, 3.4$ Hz, 1H), 2.76–2.68 (m, 4H), 2.26 (t, $J = 7.5$ Hz, 2H), 2.02–1.93 (m, 4H), 1.71–1.64 (m, 2H), 1.41 (dt, $J = 15.0, 7.4$ Hz, 2H), 1.35–1.16 (m, 33H), 0.97 (t, $J = 7.4$ Hz, 3H), 0.88 (t, $J = 7.2$ Hz, 3H) ppm.

$^{13}\text{C NMR}$ (101 MHz, CDCl_3): $\delta = 175.5, 152.5, 152.3, 147.8, 146.7, 135.2, 131.3, 130.3, 130.2, 123.9, 123.8, 105.4$ (C-1), 76.8, 74.9, 73.1, 72.7, 70.3, 70.0, 62.6, 54.9, 49.0, 36.8, 36.5, 36.2, 34.8, 33.4, 33.1, 30.8, 30.8, 30.7, 30.5, 30.4, 30.4, 28.8, 23.8, 23.4, 14.5, 14.3 ppm.

IR (ATR): $\tilde{\nu} = 3288$ (bm), 2924 (s), 2852 (m), 2168 (m), 1745 (m), 1558 (w), 1465 (m), 1003 (s), 727 (m) cm^{-1} .

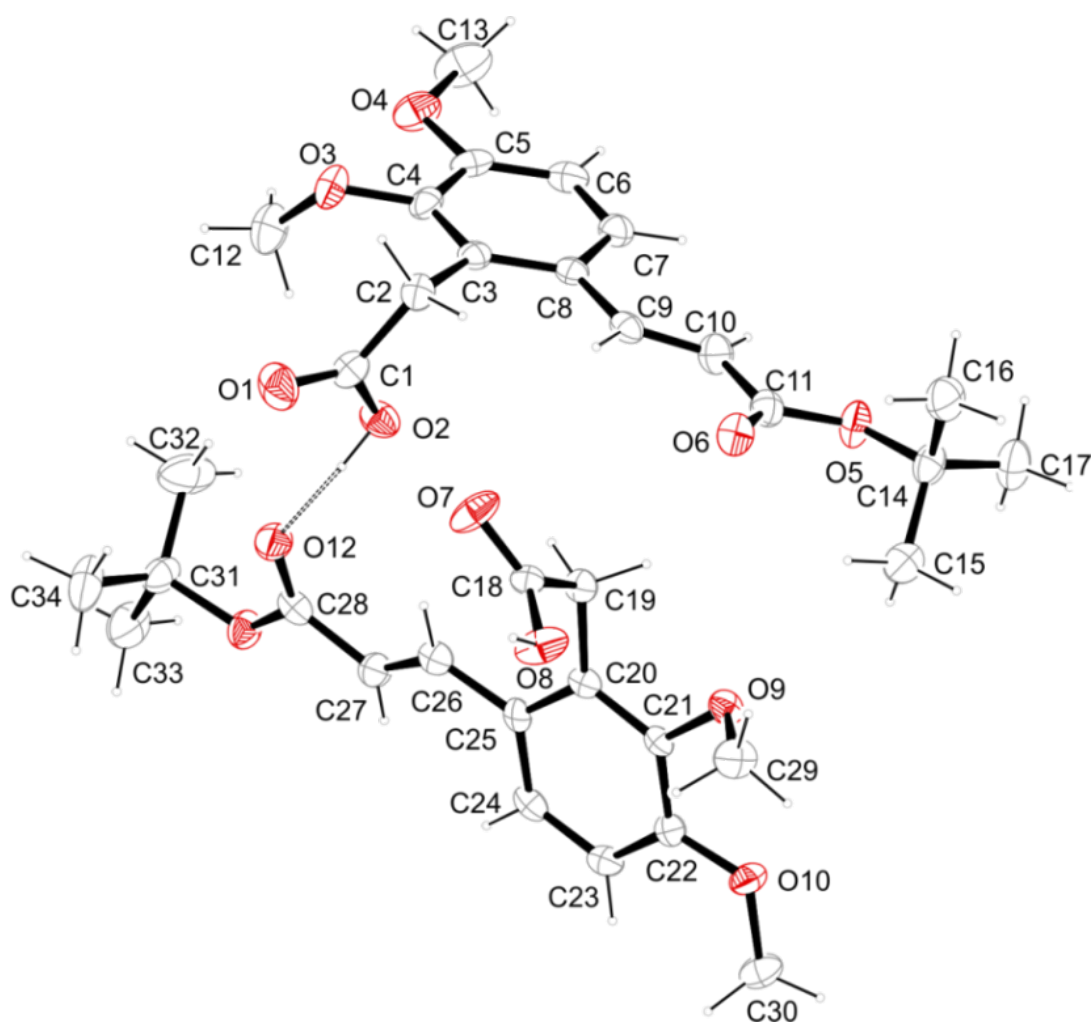
HRMS (EI): calcd. for $\text{C}_{44}\text{H}_{70}\text{N}_3\text{O}_8^+$: 768.5167 $[\text{M}+\text{H}]^+$
found: 768.5157 $[\text{M}+\text{H}]^+$.

9 Appendix

9.1 Single-crystal X-ray analysis

All single-crystal X-ray analyses were carried out by Dr. Peter Mayer in the analytic department. The data collections were performed on an Oxford Diffraction Xcalibur, Bruker D8Quest or Bruker D8Venture diffractometer and MoK α -radiation ($\lambda = 0.71073 \text{ \AA}$, graphite monochromator). The CrysAlisPro software was applied for the integration, scaling and multi-scan absorption correction of the data. The structures were solved by direct methods with SIR97 and refined by least-squares methods against F_2 with SHELXL-97. All non-hydrogen atoms were refined anisotropically. The hydrogen atoms were placed in ideal geometry riding on their parent atoms.

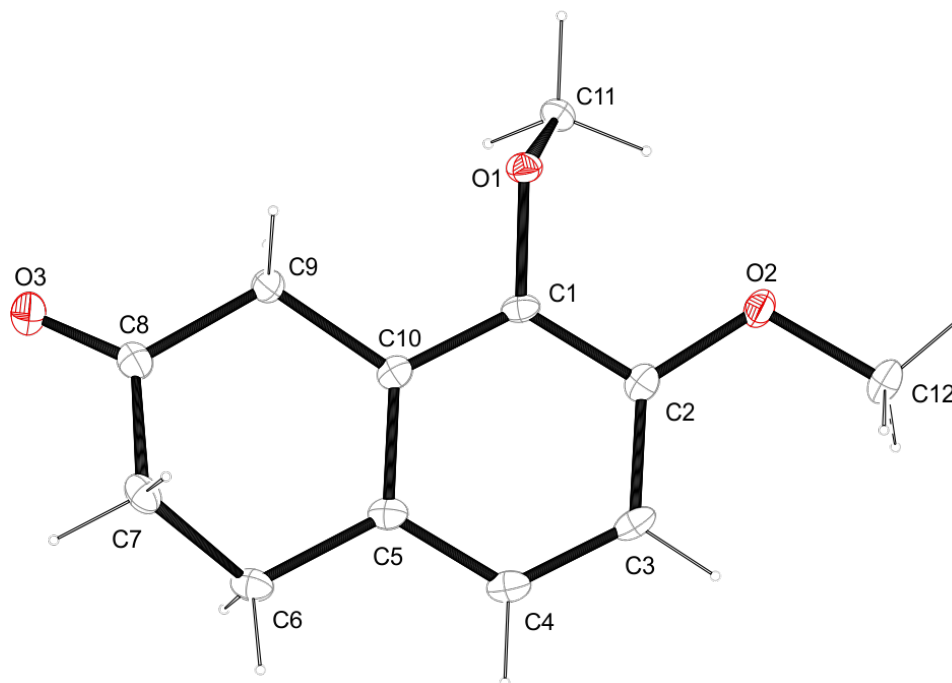
Single-crystal X-ray analysis of compound I.224



net formula	$C_{17}H_{22}O_6$
M_r/g mol⁻¹	322.353
crystal size/mm	0.131 × 0.084 × 0.027
T/K	100(2)
radiation	'Mo $K\alpha$
diffractometer	'Bruker D8Venture'
crystal system	monoclinic
space group	$P2_1/n$
a/Å	16.8852(14)
b/Å	12.1795(11)
c/Å	18.4136(13)

$\alpha/^\circ$	90
$\beta/^\circ$	116.451(2)
$\gamma/^\circ$	90
$V/\text{\AA}^3$	3390.4(5)
Z	8
calc. density/g cm⁻³	1.26307(19)
μ/mm^{-1}	0.095
absorption correction	multi-scan
transmission factor range	0.8543–0.9579
refls. measured	19953
R_{int}	0.0742
mean $\sigma(I)/I$	0.0743
θ range	2.98–25.04
observed refls.	3640
x, y (weighting scheme)	0.0593, 0
hydrogen refinement	mixed
refls in refinement	5976
parameters	431
restraints	0
$R(F_{\text{obs}})$	0.0468
$R_w(F^2)$	0.1195

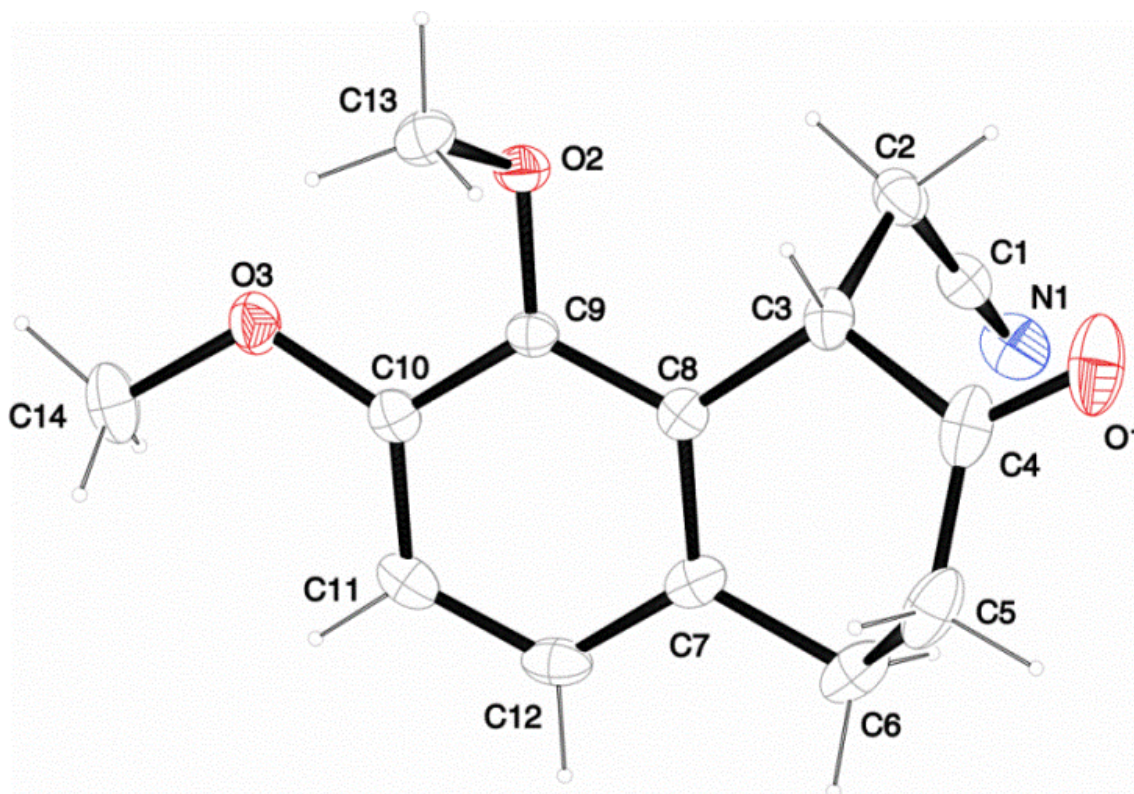
Single-crystal X-ray analysis of compound I.219



net formula	C ₁₂ H ₁₄ O ₃
Mr/g mol⁻¹	206.23
crystal size/mm	0.100 × 0.040 × 0.030
T/K	100(2)
radiation	MoKα
diffractometer	'Bruker D8Venture'
crystal system	monoclinic
space group	'C c'
a/Å	4.2298(2)
b/Å	19.7579(11)
c/Å	12.2515(6)
α/°	90
β/°	97.8156(18)
γ/°	90
V/Å³	1014.37(9)
Z	4

calc. density/g cm⁻³	1.350
μ/mm^{-1}	0.096
absorption correction	multi-scan
transmission factor range	0.8529–0.9585
refls. measured	6169
<i>Rint</i>	0.0331
mean $\sigma(I)/I$	0.0308
θ range	3.940–26.38
observed refls.	1631
<i>x, y</i> (weighting scheme)	0.0465, 0.2317
hydrogen refinement	constr
refls in refinement	0.1(15)
parameters	1775
restraints	139
<i>R(Fobs)</i>	2
<i>Rw(F2)</i>	0.0332

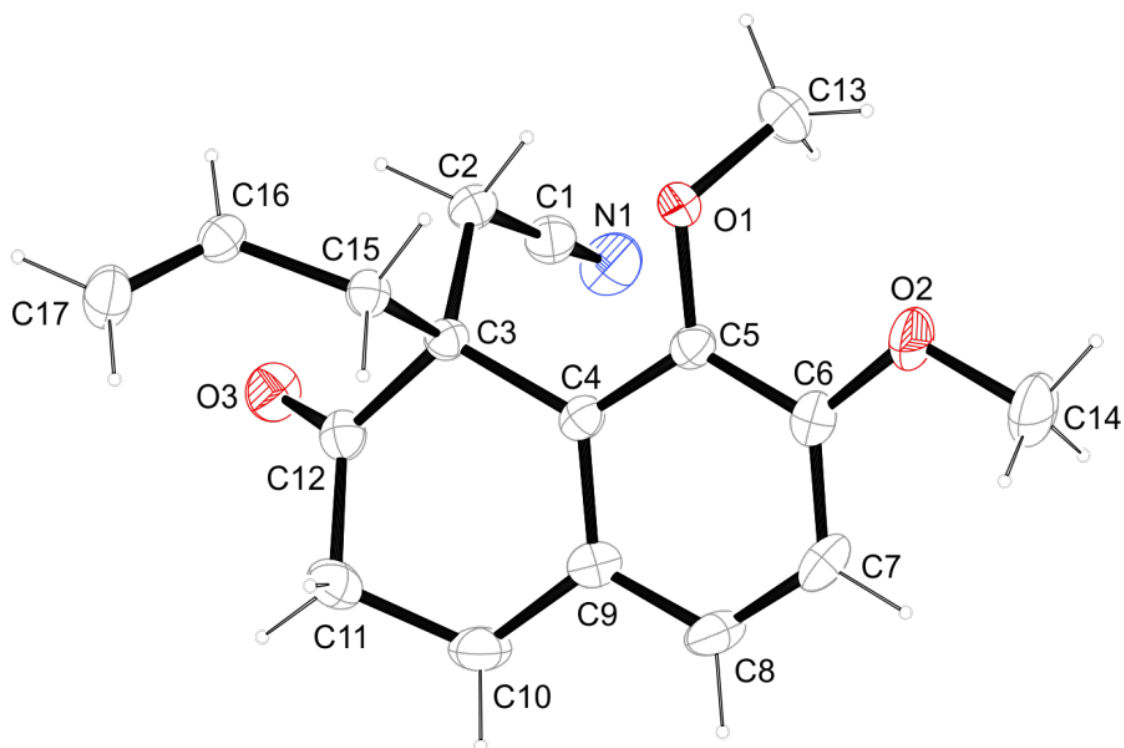
Single-crystal X-ray analysis of compound I.226.



net formula	$C_{14}H_{15}NO_3$
<i>Mr</i>/g mol⁻¹	245.274
crystal size/mm	0.388 × 0.284 × 0.270
<i>T</i>/K	200(2)
radiation	'MoK α
diffractometer	'Bruker D8Quest'
crystal system	monoclinic
space group	$P2_1/c$
<i>a</i>/Å	7.2350(2)
<i>b</i>/Å	11.4719(4)
<i>c</i>/Å	14.8725(5)
α/°	90
β/°	95.298(2)

γ/°	90
$V/\text{Å}^3$	1229.13(7)
Z	4
calc. density/g cm⁻³	1.32547(8)
μ/mm^{-1}	0.094
absorption correction	'multi-scan'
transmission factor range	0.8791–0.9144
refls. measured	19144
R_{int}	0.0330
mean $\sigma(I)/I$	0.0212
θ range	2.75–27.60
observed refls.	2335
x, y (weighting scheme)	0.0512, 0.3930
hydrogen refinement	constr
refls in refinement	2823
parameters	165
restraints	0
$R(F_{obs})$	0.0438
$R_w(F_2)$	0.1140

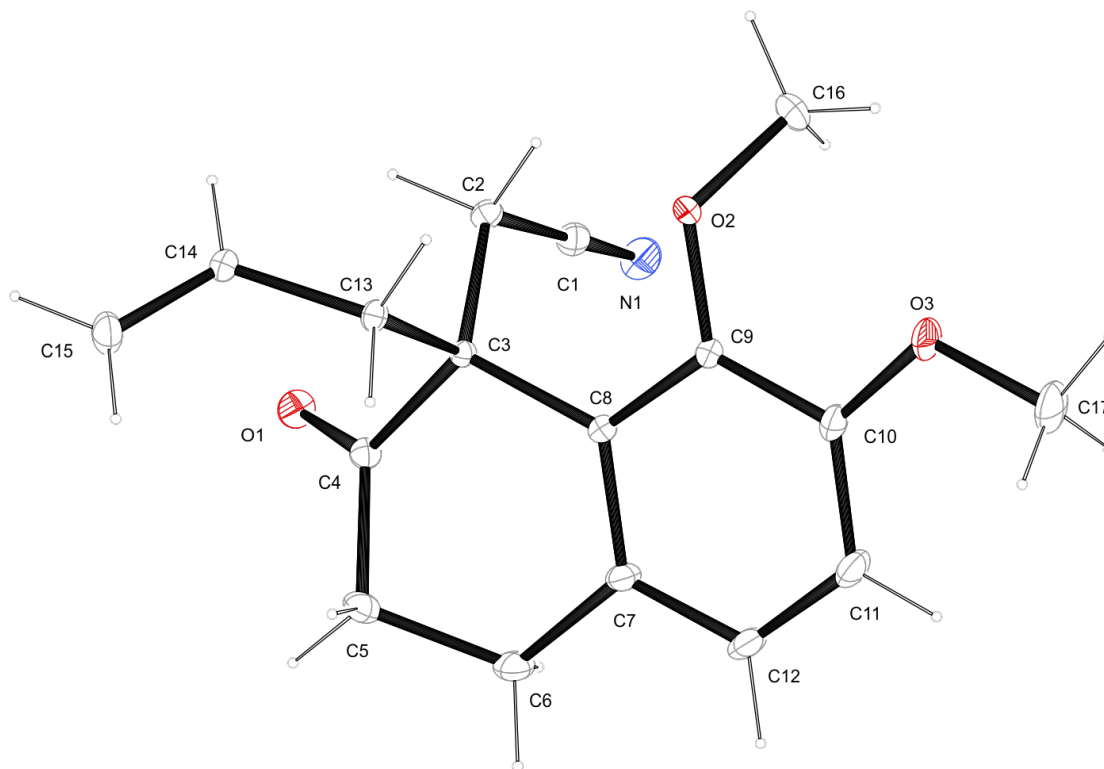
Single-crystal X-ray analysis of compound I.227 (racemic).



net formula	$C_{17}H_{19}NO_3$
Mr/g mol⁻¹	285.338
crystal size/mm	0.17 × 0.14 × 0.12
T/K	123(2)
radiation	'Mo $K\alpha$
diffractometer	'Bruker D8Venture'
crystal system	orthorhombic
space group	$P2_12_12_1$
a/Å	7.6671(6)
b/Å	8.3382(6)
c/Å	23.4368(18)
α/°	90
β/°	90
γ/°	90

V/Å³	1498.3(2)
Z	4
calc. density/g cm⁻³	1.26496(17)
μ/mm⁻¹	0.087
absorption correction	multi-scan
transmission factor range	0.9276–0.9585
refls. measured	17807
Rint	0.0274
mean σ(I)/I	0.0202
θ range	3.17–26.43
observed refls.	2776
x, y (weighting scheme)	0.0408, 0.3090
hydrogen refinement	constr
Flack parameter	–0.1(10)
refls in refinement	3051
parameters	192
restraints	0
R(Fobs)	0.0326

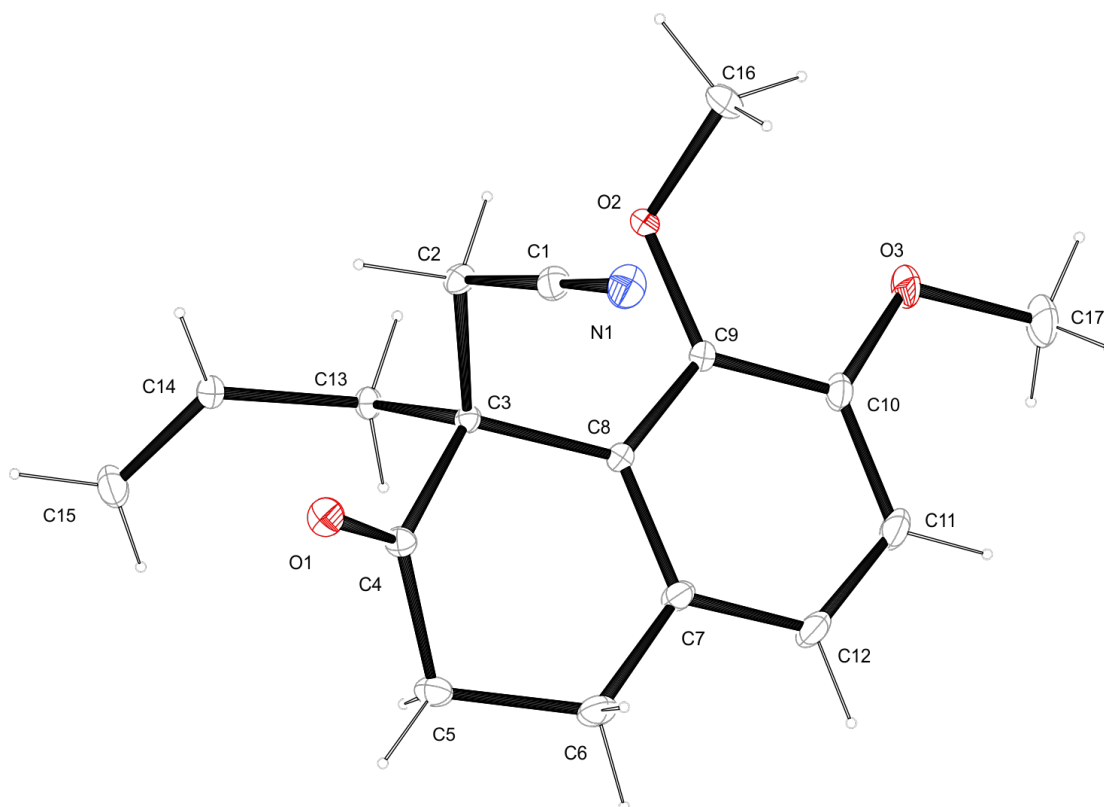
Single-crystal X-ray analysis of compound (R)-I.227.



net formula	$C_{17}H_{19}NO_3$
Mr/g mol⁻¹	285.33
crystal size/mm	0.10 × 0.10 × 0.09
T/K	100(2)
radiation	MoK α
diffractometer	'Bruker D8Venture'
crystal system	orthorhombic
space group	'P 21 21 21'
a/Å	7.6599(2)
b/Å	8.3420(2)
c/Å	23.4353(7)
α/°	90
β/°	90
γ/°	90
V/Å³	1497.49(7)
Z	4
calc. density/g cm⁻³	1.266
μ/mm⁻¹	0.087
absorption correction	Multi-Scan
transmission factor range	0.8862–0.9634
refls. measured	49074
Rint	0.0477

mean $\sigma(I)/I$	0.0350
θ range	3.177–36.36
observed refls.	6781
x, y (weighting scheme)	0.0488, 0.2654
hydrogen refinement	constr
Flack parameter	–0.1(2)
refls in refinement	7261
parameters	192
restraints	0
R(Fobs)	0.0425

C3: R

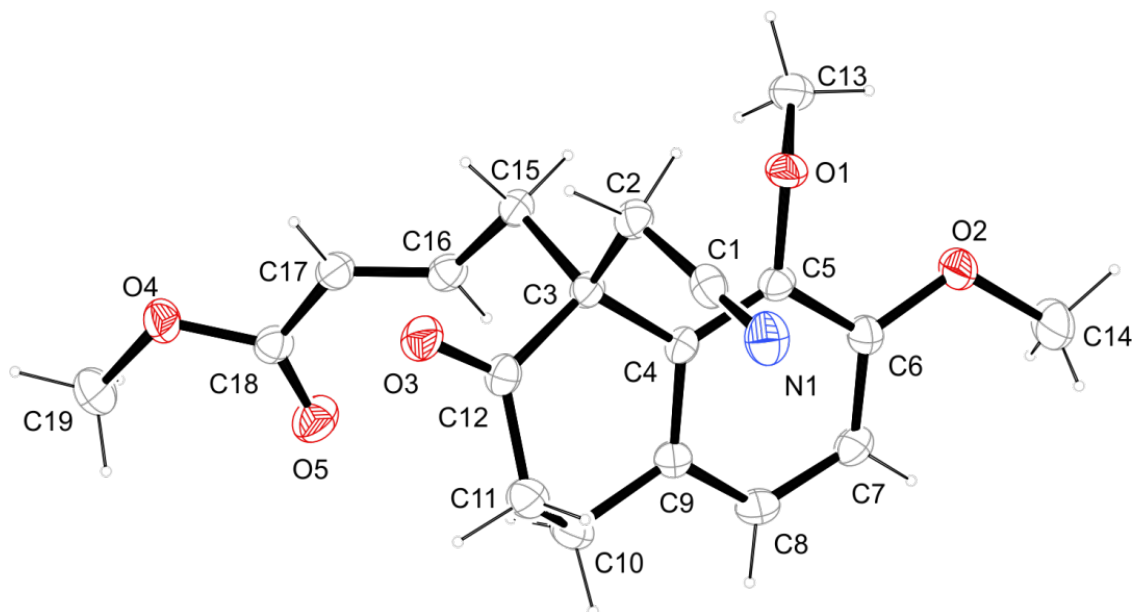
Single-crystal X-ray analysis of compound (*S*)-I.227

net formula	$C_{17}H_{19}NO_3$
Mr/g mol⁻¹	285.33
crystal size/mm	0.100 × 0.100 × 0.090
T/K	100(2)
radiation	MoK α
diffractometer	'Bruker D8Venture'
crystal system	orthorhombic
space group	'P 21 21 21'
a/Å	7.6610(2)
b/Å	8.3423(2)
c/Å	23.4440(5)
α/°	90
β/°	90
γ/°	90
V/Å³	1498.31(6)

Z	4
calc. density/g cm⁻³	1.265
μ/mm⁻¹	0.087
absorption correction	Multi-Scan
transmission factor range	0.9091–0.9666
refls. measured	66705
Rint	0.0391
mean $\sigma(I)/I$	0.0270
θ range	2.997–42.15
observed refls.	6833
x, y (weighting scheme)	0.0540, 0.2317
hydrogen refinement	constr
Flack parameter	–0.09(19)
refls in refinement	7261
parameters	192
restraints	0
R(Fobs)	0.0388

C3: S

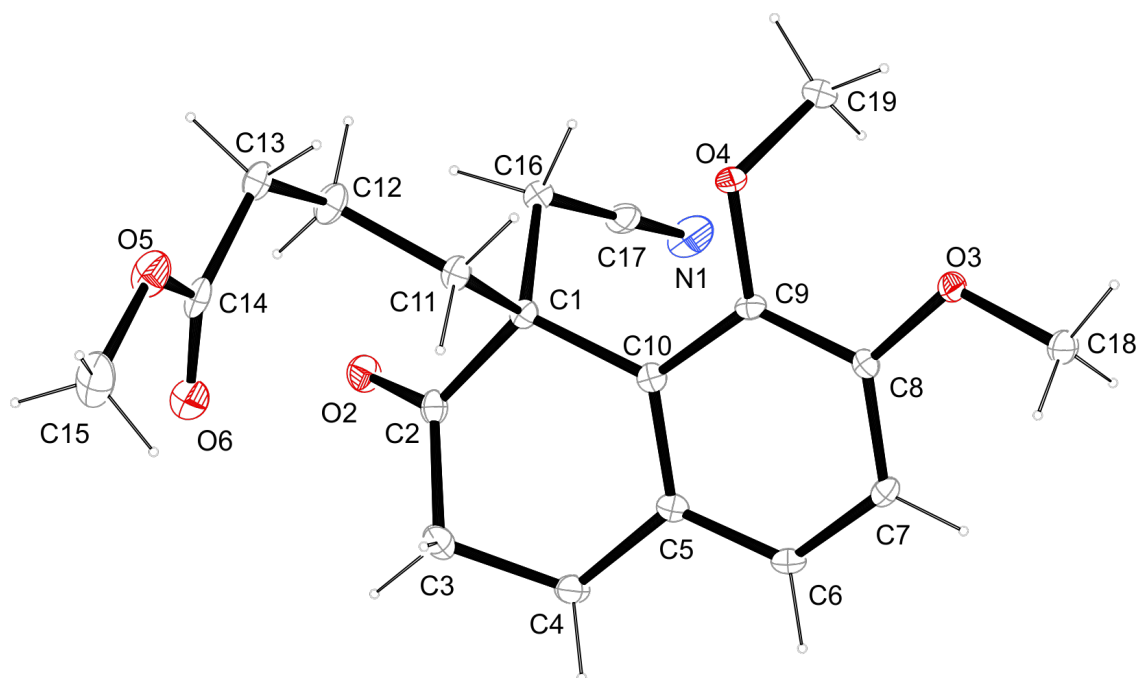
Single-crystal X-ray analysis of compound I.218.



net formula	$C_{19}H_{21}NO_5$
<i>M</i>, g mol⁻¹	343.374
crystal size/mm	0.483 × 0.451 × 0.356
<i>T</i>/K	123(2)
radiation	MoKα
diffractometer	'Oxford XCalibur'
crystal system	triclinic
space group	$\bar{P}1$
<i>a</i>/Å	7.6302(6)
<i>b</i>/Å	8.8519(6)
<i>c</i>/Å	12.7508(9)
α/°	87.503(6)
β/°	87.653(6)
γ/°	87.251(6)
<i>V</i>/Å³	858.75(11)
<i>Z</i>	2
calc. density/g cm⁻³	1.32796(17)
μ/mm⁻¹	0.096

absorption correction	'multi-scan'
transmission factor range	0.97201–1.00000
refls. measured	4728
R_{int}	0.0155
mean $\sigma(I)/I$	0.0340
θ range	4.57–26.37
observed refls.	2838
x, y (weighting scheme)	0.0420, 0.2630
hydrogen refinement	constr
refls in refinement	3462
parameters	229
restraints	0
$R(F_{\text{obs}})$	0.0397
$R_w(F^2)$	0.1023

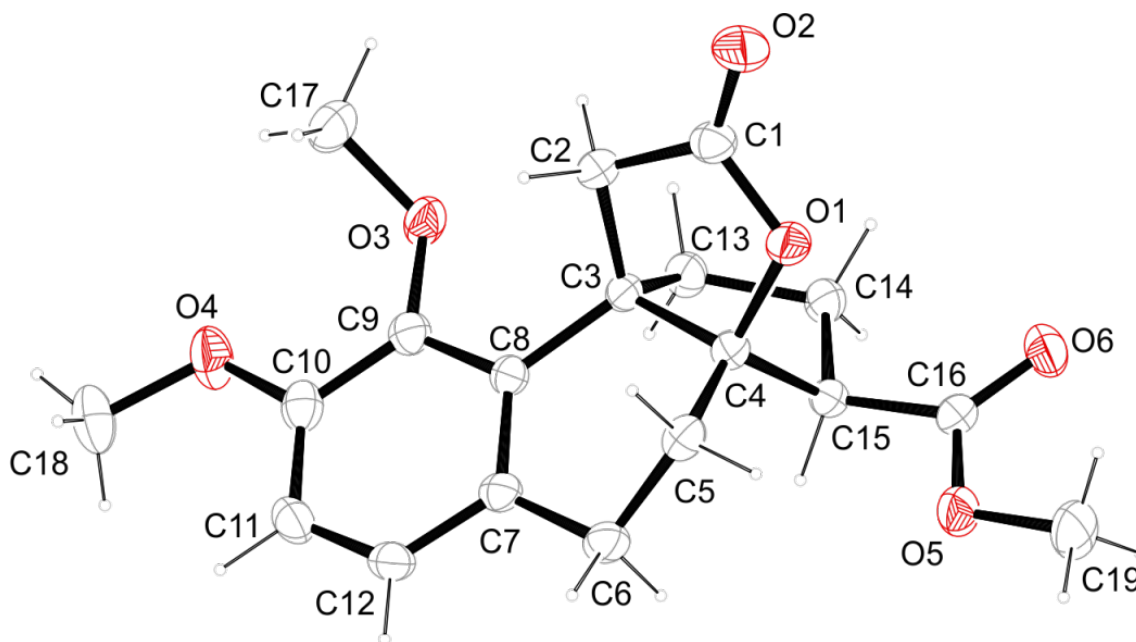
Single-crystal X-ray analysis of compound I.251.



net formula	$C_{19}H_{23}NO_5$
<i>M</i>,/g mol⁻¹	345.38
crystal size/mm	0.100 × 0.090 × 0.010
<i>T</i>/K	100(2)
radiation	MoKα
diffractometer	'Bruker D8Venture'
crystal system	monoclinic
space group	'P 21/c'
<i>a</i>/Å	16.1951(7)
<i>b</i>/Å	8.3508(4)
<i>c</i>/Å	13.1442(6)
α/°	90
β/°	102.4370(10)
γ/°	90
<i>V</i>/Å³	1735.93(14)
<i>Z</i>	4

calc. density/g cm⁻³	1.322
μ/mm^{-1}	0.096
absorption correction	multi-scan
transmission factor range	0.8970–0.9579
refls. measured	19934
R_{int}	0.0461
mean $\sigma(I)/I$	0.0266
θ range	3.041–25.04
observed refls.	2472
x, y (weighting scheme)	0.0407, 0.7699
hydrogen refinement	constr
refls in refinement	3072
parameters	229
restraints	0
$R(F_{\text{obs}})$	0.0353
$R_w(F^2)$	0.0909

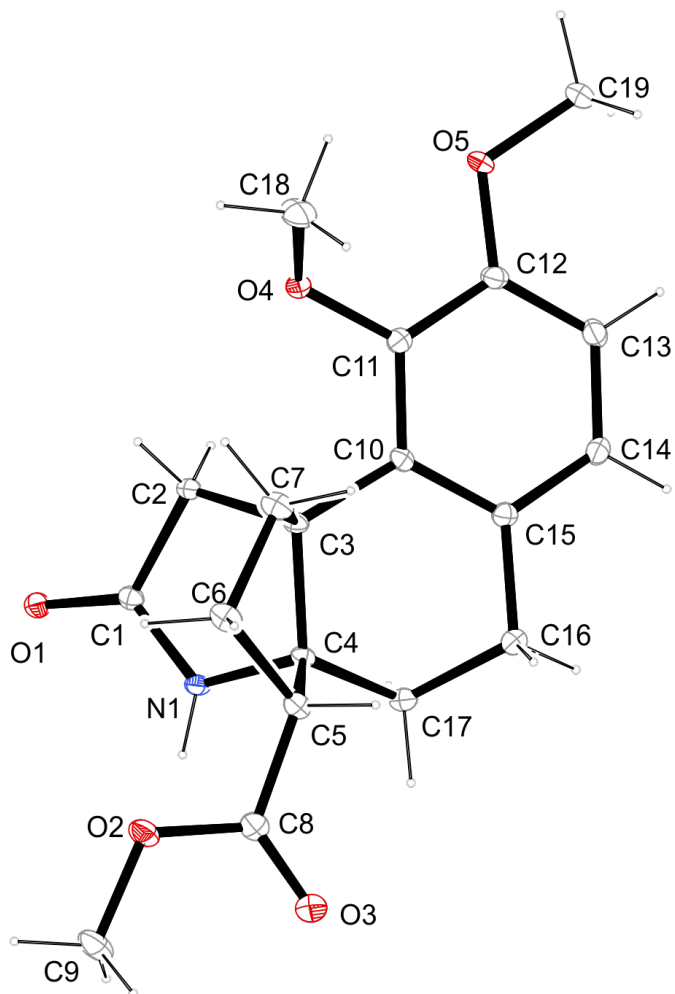
Single-crystal X-ray analysis of compound I.254.



net formula	$C_{19}H_{22}O_6$
$M_r/g\ mol^{-1}$	346.374
crystal size/mm	$0.182 \times 0.095 \times 0.054$
T/K	173(2)
radiation	'Mo K α
diffractometer	'Bruker D8Venture'
crystal system	monoclinic
space group	$P2_1/c$
$a/\text{\AA}$	8.9536(5)
$b/\text{\AA}$	13.8303(7)
$c/\text{\AA}$	13.3248(6)
$\alpha/^\circ$	90
$\beta/^\circ$	94.6825(16)
$\gamma/^\circ$	90
$V/\text{\AA}^3$	1644.52(14)
Z	4
calc. density/ $g\ cm^{-3}$	1.39901(12)
μ/mm^{-1}	0.104
absorption correction	multi-scan
transmission factor range	0.9257–0.9585
refls. measured	32974
R_{int}	0.0386

mean $\sigma(I)/I$	0.0186
θ range	3.21–26.42
observed refls.	2795
x, y (weighting scheme)	0.0414, 0.9448
hydrogen refinement	constr
refls in refinement	3350
parameters	229
restraints	0
$R(F_{\text{obs}})$	0.0378
$R_w(F^2)$	0.0984

Single-crystal X-ray analysis of compound I.260.



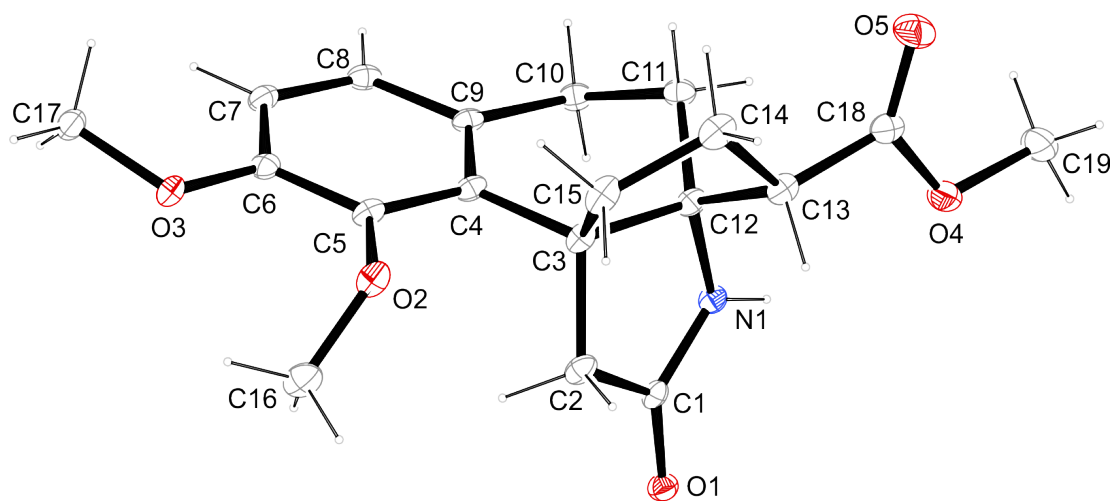
net formula	$C_{19}H_{23}NO_5$
$C_{19}H_{23}NO_5$	345.38
$M_r/g\ mol^{-1}$	$0.100 \times 0.080 \times 0.040$
345.38	100(2)
crystal size/mm	MoKa
$0.100 \times 0.080 \times 0.040$	'Bruker D8Venture'
T/K	monoclinic
100(2)	'C 2'
radiation	25.0443(7)
MoKa	6.8179(2)
diffractometer	10.1504(3)
'Bruker D8Venture'	90
crystal system	96.3846(9)
monoclinic	90

space group	1722.43(9)
'C 2'	4
<i>a</i>/Å	1.332
25.0443(7)	0.096
<i>b</i>/Å	multi-scan
6.8179(2)	0.9095–0.9585
<i>c</i>/Å	16167
10.1504(3)	0.0317
α/°	0.0257
90	3.098–26.43
β/°	3359
96.3846(9)	0.0438, 0.6259
γ/°	mixed
90	0.2(3)
<i>V</i>/Å³	3536
1722.43(9)	233
<i>Z</i>	1
4	0.0325
calc. density/g cm⁻³	0.0785
1.332	1.057
μ/mm⁻¹	0.001
0.096	0.183

C-H: constr

N-H: refall

Single-crystal X-ray analysis of compound I.261.



net formula	$C_{19}H_{23}NO_5$
M_r/g mol⁻¹	345.390
crystal size/mm	0.110 × 0.070 × 0.050
T/K	100(2)
radiation	'Mo K α
diffractometer	'Bruker D8Venture'
crystal system	monoclinic
space group	$P2_1/c$
a/Å	7.6612(4)
b/Å	20.3093(9)
c/Å	10.7852(5)
α/°	90
β/°	90.6667(15)
γ/°	90
V/Å³	1677.99(14)
Z	4
calc. density/g cm⁻³	1.36721(11)
μ/mm⁻¹	0.099
absorption correction	multi-scan
transmission factor range	0.9061–0.9585
refls. measured	19936
R_{int}	0.0377
mean $\sigma(I)/I$	0.0301
θ range	3.33–26.42
observed refls.	2669

<i>x, y (weighting scheme)</i>	0.0396, 0.8950
hydrogen refinement	mixed
refls in refinement	3432
parameters	233
restraints	0
<i>R</i>(<i>F</i>_{obs})	0.0419
<i>R</i>_w(<i>F</i>²)	0.1013
<i>S</i>	1.053
1.062	0.001
shift/error_{max}	0.358
0.001	-0.190

C-H: constr, N-H: refall.

Single-crystal X-ray analysis of compound I.259.

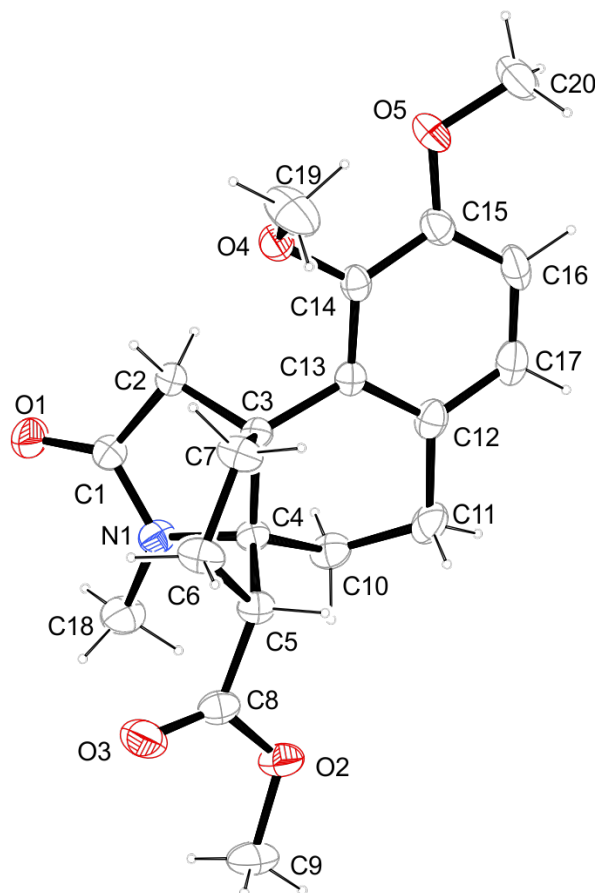
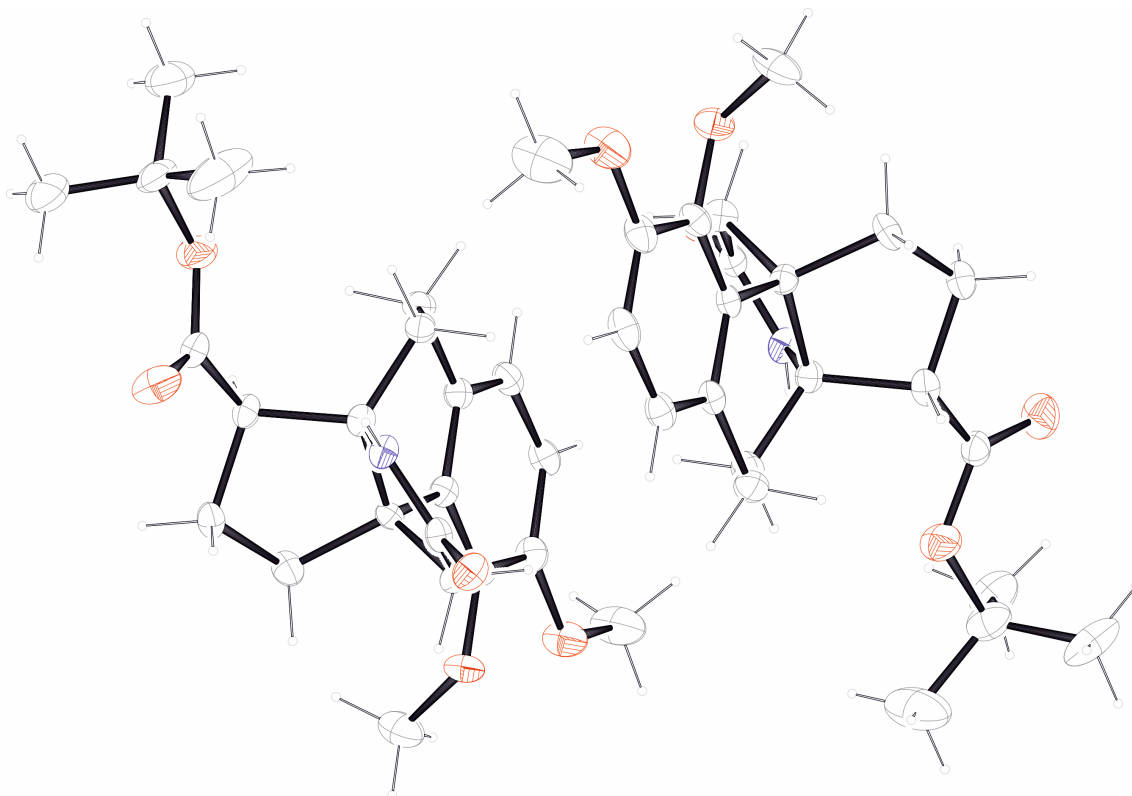


Table 9.1 Crystallographic data for lactam I.259.

net formula	$C_{19}H_{22}O_6$
$M_r/g\ mol^{-1}$	359.416
crystal size/mm	$0.294 \times 0.153 \times 0.092$
T/K	173(2)
radiation	'Mo K α
diffractometer	'Bruker D8Quest'
crystal system	orthorhombic
space group	<i>Pbca</i>
$a/\text{\AA}$	11.5962(5)
$b/\text{\AA}$	14.1871(7)
$c/\text{\AA}$	21.2925(9)
$\alpha/^\circ$	90
$\beta/^\circ$	90
$\gamma/^\circ$	90
$V/\text{\AA}^3$	3503.0(3)
Z	8

calc. density/g cm⁻³	1.36302(12)
μ/mm⁻¹	0.098
absorption correction	multi-scan
transmission factor range	0.9079–0.9580
refls. measured	61699
R_{int}	0.0583
mean $\sigma(I)/I$	0.0202
θ range	2.46–25.41
observed refls.	2628
x, y (weighting scheme)	0.0469, 2.1055
hydrogen refinement	constr
refls in refinement	3203
parameters	239
restraints	0
$R(F_{\text{obs}})$	0.0425
$R_w(F^2)$	0.1077
S	S
1.062	1.062
shift/error_{max}	shift/error _{max}
0.001	0.001

Single-crystal X-ray analysis of compound I.267.



net formula	$C_{22}H_{29}NO_5$
$C_{20}H_{23}NO_5$	387.46
$M_r/g\ mol^{-1}$	$0.100 \times 0.070 \times 0.040$
357.39	123.(2)
crystal size/mm	MoKa
$0.100 \times 0.040 \times 0.030$	'Bruker D8 Venture TXS'
T/K	monoclinic
100.(2)	'P 1 21 1'
radiation	9.7651(2)
'Mo Ka	19.5668(5)
diffractometer	11.8470(3)
'Bruker D8 Venture TXS'	90
crystal system	92.1790(10)
orthorhombic	90
space group	2261.99(9)
'P 21 21 21'	4
a/Å	1.138
10.8766(6)	0.080
b/Å	Multi-Scan

14.6810(9)	0.9358–0.9705
c/Å	9220
21.6036(13)	0.0362
α/°	0.0344
90	3.374–26.372
β/°	8053
90	0.0728, 1.1613
γ/°	H(C) constr, H(N) refall
90	–0.4(3)
V/Å³	9220
3449.6(4)	523
Z	1
8	0.0493
calc. density/g cm⁻³	0.1458
1.376	1.087
μ/mm⁻¹	0.001
0.099	0.313

Single-crystal X-ray analysis of compound I.280.

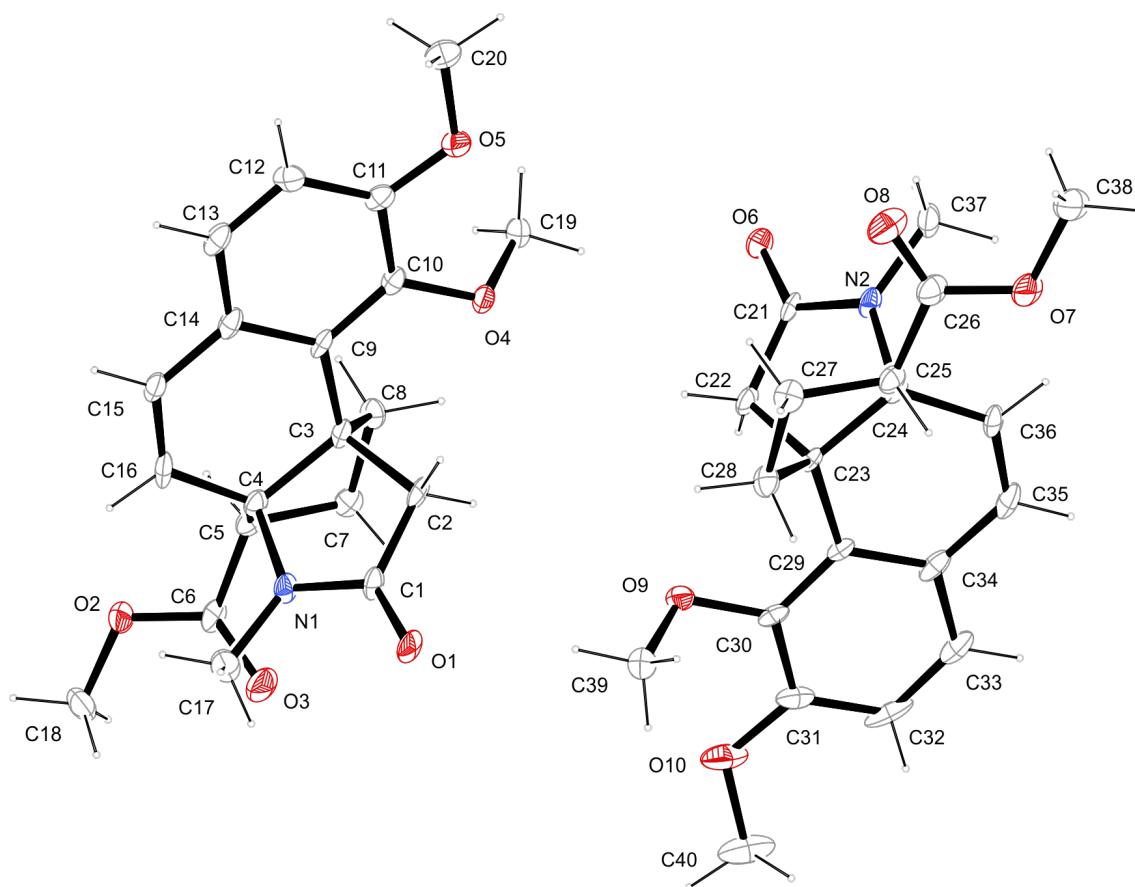


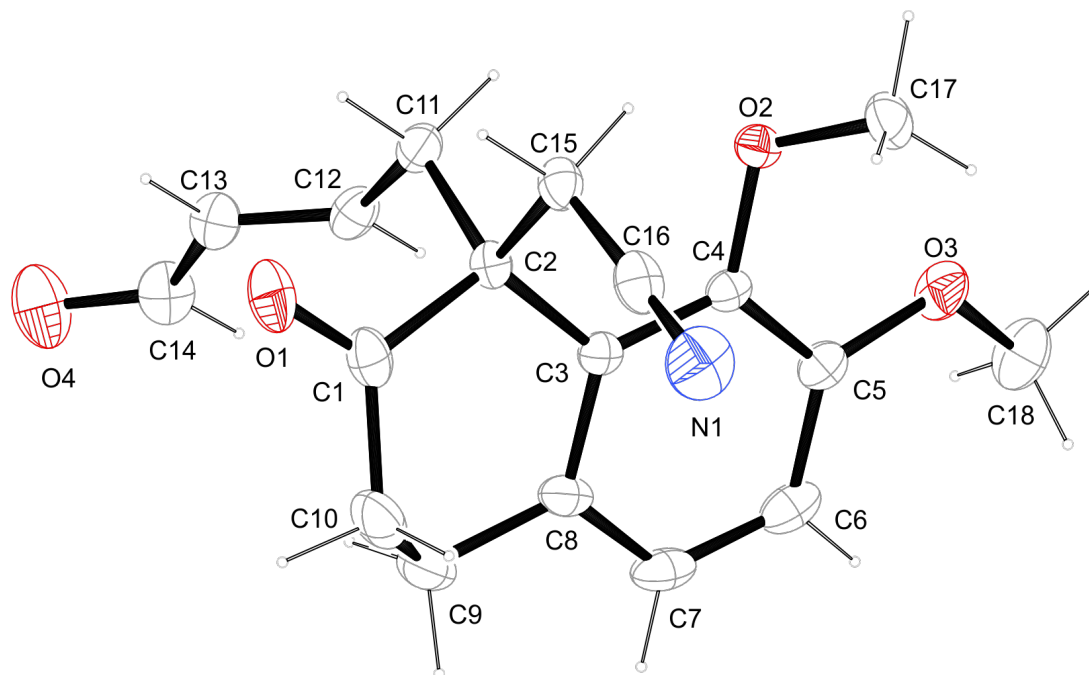
Table 9.2 Crystallographic data for styrene I.280.

net formula	$C_{20}H_{23}NO_5$
M_r/g mol⁻¹	357.39
crystal size/mm	0.100 × 0.040 × 0.030
T/K	100.(2)
radiation	'Mo K α
diffractometer	'Bruker D8 Venture TXS'
crystal system	orthorhombic
space group	'P 21 21 21'
a/Å	10.8766(6)
b/Å	14.6810(9)
c/Å	21.6036(13)
α/°	90
β/°	90
γ/°	90
V/Å³	3449.6(4)
Z	8
calc. density/g cm⁻³	1.376

μ/mm^{-1}	0.099
absorption correction	Multi-Scan
transmission factor range	0.89–1.00
refls. measured	60717
R_{int}	0.0886
mean $\sigma(I)/I$	0.0434
θ range	1.68–25.41
observed refls.	5493
x, y (weighting scheme)	0.0750, 7.4803
hydrogen refinement	constr
Flack parameter	0.500000
refls in refinement	6329
parameters	477
restraints	0
$R(F_{\text{obs}})$	0.0787
$R_w(F^2)$	0.1963
S	1.106
shift/error _{max}	0.001
max electron density/e \AA^{-3}	0.536

Structure refined as a racemic twin.

Single-crystal X-ray analysis of compound I.281.



net formula	$C_{18}H_{19}NO_4$
M_r/g mol⁻¹	313.348
crystal size/mm	0.348 \diamond 0.319 \diamond 0.131
T/K	173(2)
radiation	MoK α
diffractometer	'Oxford XCalibur'
crystal system	orthorhombic
space group	'P n a 21'
$a/\text{\AA}$	8.0956(3)
$b/\text{\AA}$	17.2610(8)
$c/\text{\AA}$	11.5189(5)
α°	90
β°	90
γ°	90
$V/\text{\AA}^3$	1609.63(12)
Z	4

calc. density/g cm⁻³	1.29305(10)
μ/mm^{-1}	0.092
absorption correction	'multi-scan'
transmission factor range	0.95975–1.00000
refls. measured	7591
R_{int}	0.0305
mean $\sigma(I)/I$	0.0395
θ range	4.254–25.341
observed refls.	2437
x, y (weighting scheme)	0.0336, 0.0140
hydrogen refinement	constr
refls in refinement	0.3(14)
parameters	2873
restraints	211
$R(F_{\text{obs}})$	1
$R_w(F^2)$	0.0361

Single-crystal X-ray Analysis of compounds I.294 and I.295

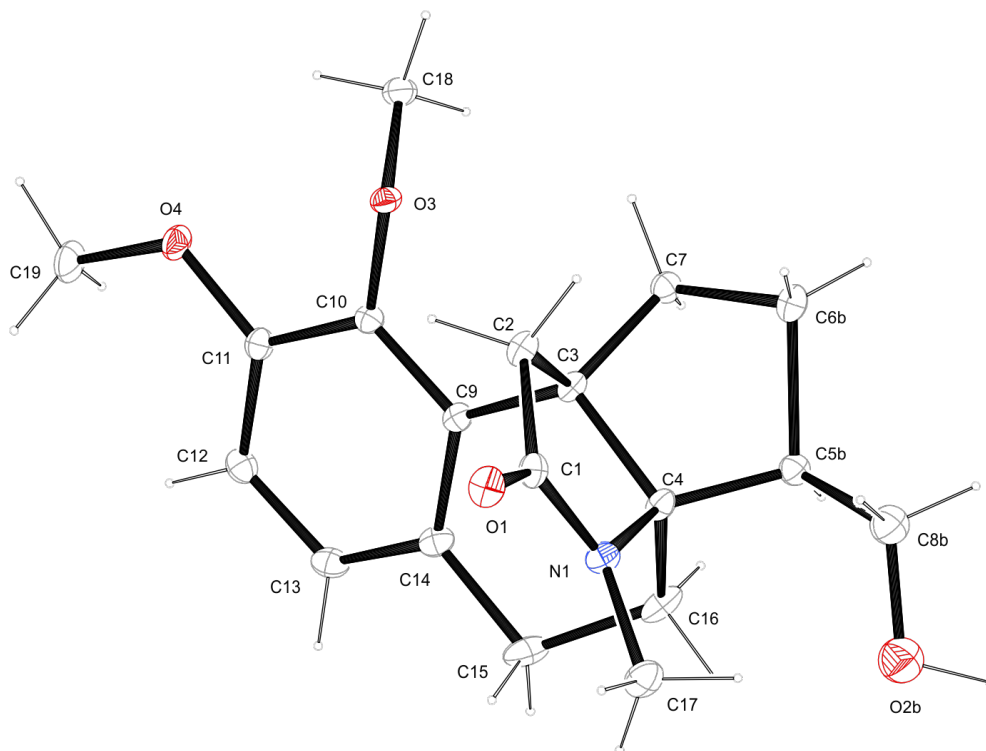


Figure III.1 Crystal structure of major component **I.294**.

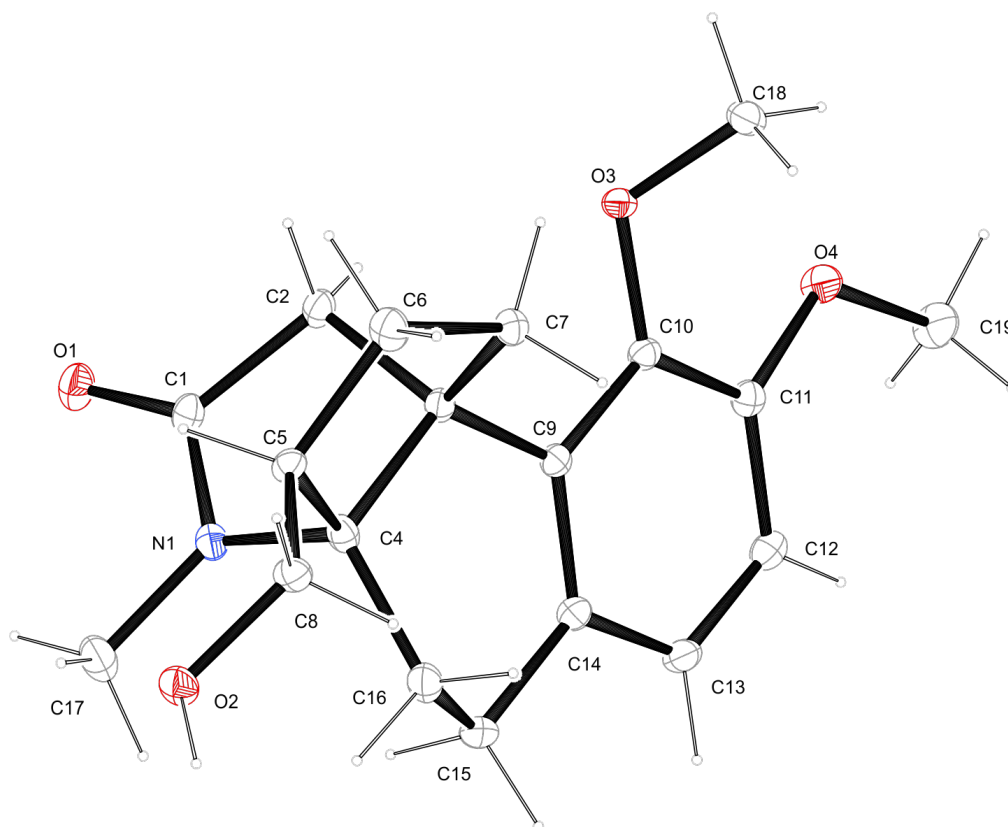
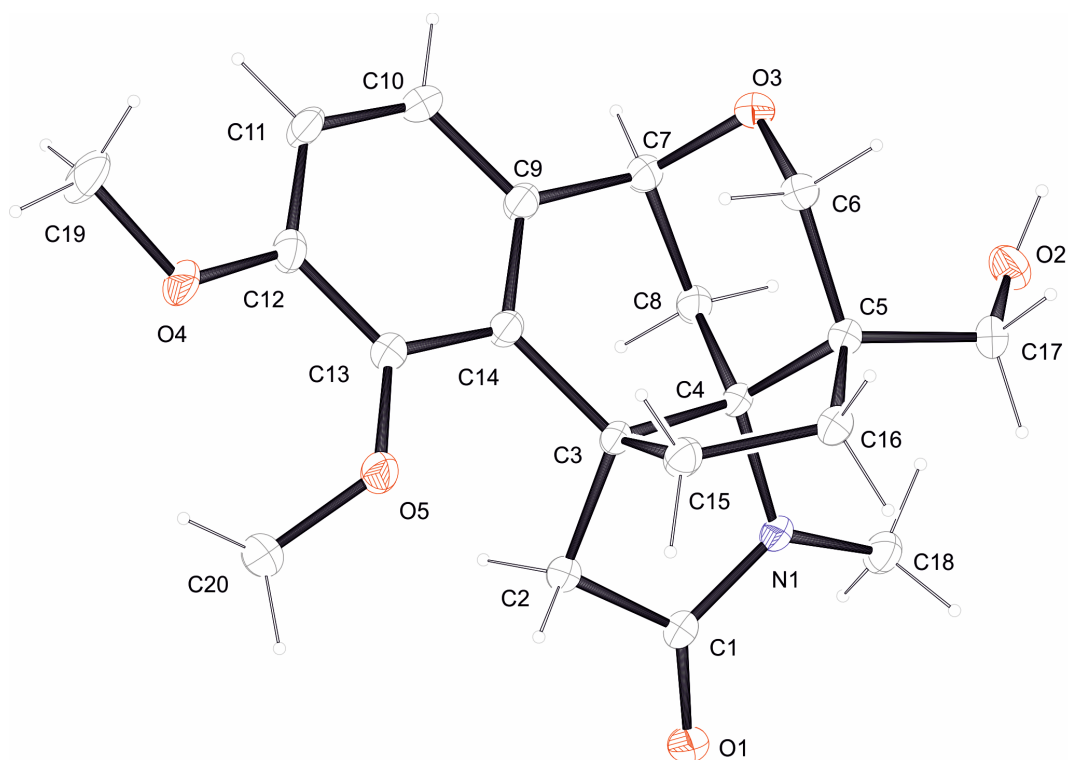


Figure III.2 Crystal structure of minor component **I.295**.

net formula	C ₁₉ H ₂₅ NO ₄
<i>M_r</i>/g mol⁻¹	331.40
crystal size/mm	0.100 × 0.070 × 0.040
<i>T</i>/K	100.(2)
radiation	MoKα
diffractometer	'Bruker D8 Venture TXS'
crystal system	orthorhombic
space group	'P b c a'
<i>a</i>/Å	11.022(3)
<i>b</i>/Å	14.897(4)
<i>c</i>/Å	20.167(5)
α/°	90
β/°	90
γ/°	90
<i>V</i>/Å³	3311.3(14)
<i>Z</i>	8
calc. density/g cm⁻³	1.330
μ/mm⁻¹	0.093
absorption correction	Multi-Scan
transmission factor range	0.8998–0.9457
refls. measured	53585
<i>R</i>_{int}	0.0641
mean σ(<i>I</i>)/<i>I</i>	0.0254
θ range	3.401–27.102
observed refls.	3155
<i>x</i>, <i>y</i> (weighting scheme)	0.0610, 2.2953
hydrogen refinement	C-H: constr, O-H: noref
refls in refinement	3621
parameters	234
restraints	0
<i>R</i>(<i>F</i>_{obs})	0.0481
<i>R</i>_w(<i>F</i>²)	0.1303
<i>S</i>	1.065
shift/error_{max}	0.001
max electron density/e Å⁻³	0.337
min electron density/e Å⁻³	-0.286

Structure disordered, major product 82%, minor product 18%.

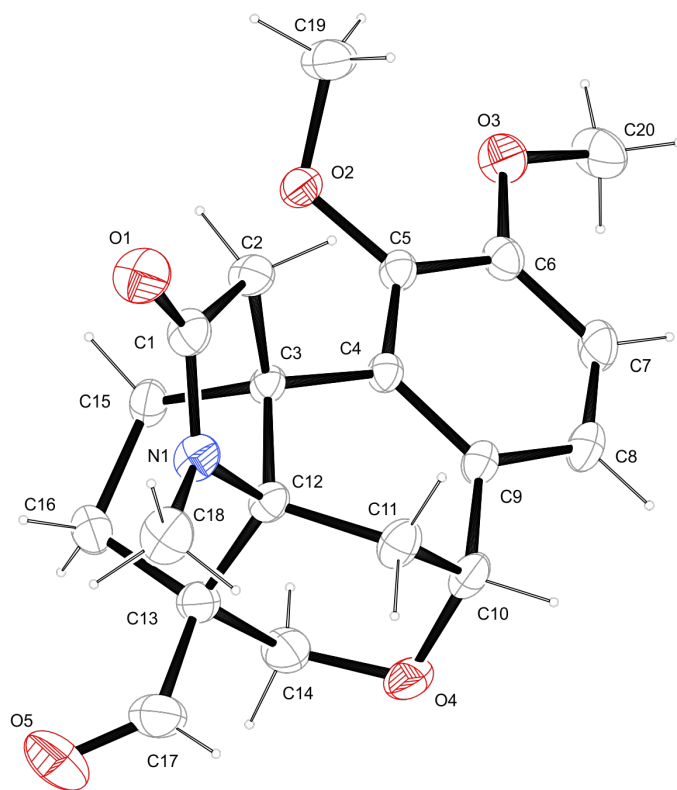
Single-crystal X-ray analysis of compound I.308.



net formula	$C_{21}H_{27}Cl_2NO_5$
M_r/g mol⁻¹	444.33
crystal size/mm	0.090 × 0.060 × 0.040
T/K	100.(2)
radiation	MoK α
diffractometer	'Bruker D8 Venture TXS'
crystal system	triclinic
space group	'P -1'
a/Å	8.3263(5)
b/Å	11.3620(7)
c/Å	12.3017(6)
α/°	69.648(2)
β/°	83.394(2)
γ/°	70.160(2)
V/Å³	1026.36(10)
Z	2
calc. density/g cm⁻³	1.438
μ/mm⁻¹	0.350
absorption correction	Multi-Scan
transmission factor range	0.7750–0.9705

refls. measured	12197
R_{int}	0.0419
mean $\sigma(I)/I$	0.0483
θ range	3.442–26.372
observed refls.	3604
x, y (weighting scheme)	0.0358, 0.7268
hydrogen refinement	H(C) constr, H(O) refall
refls in refinement	4170
parameters	269
restraints	0
R(F_{obs})	0.0403
R_w(F²)	0.1053
S	1.035
shift/error_{max}	0.001
max electron density/e \AA^{-3}	0.391
min electron density/e \AA^{-3}	–0.447

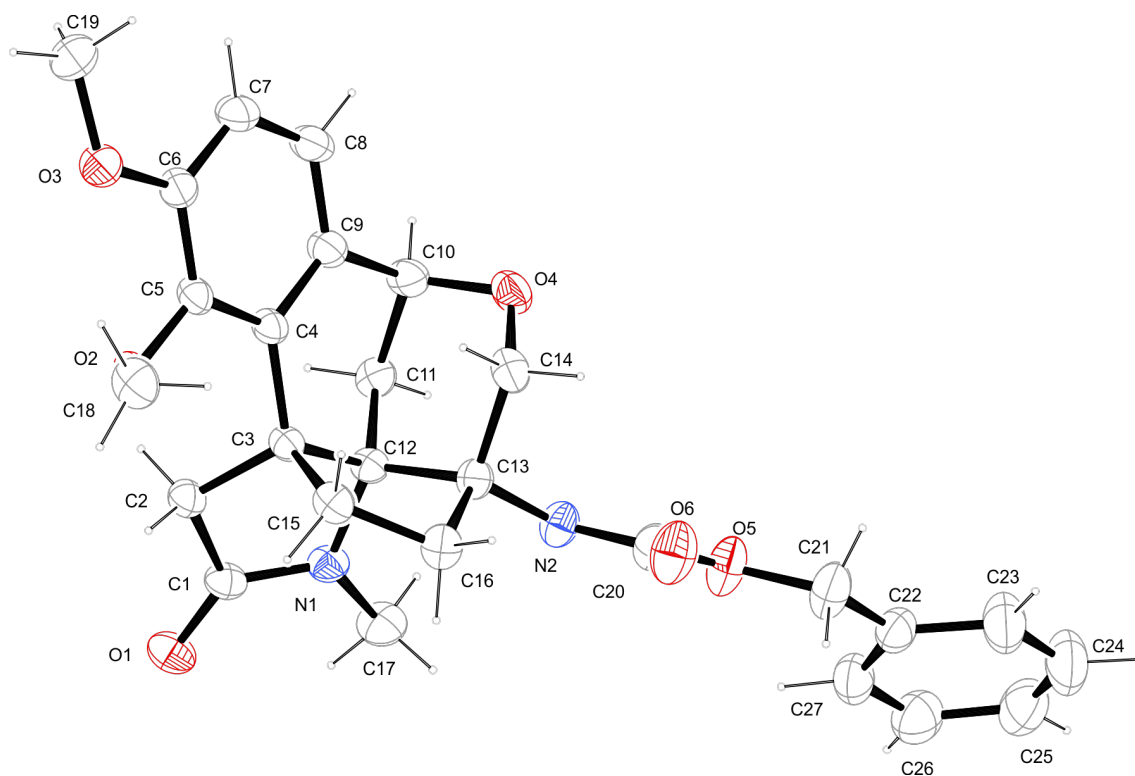
Single-crystal X-ray analysis of compound I.290.



net formula	$C_{20}H_{23}NO_5$
M_r/g mol⁻¹	357.39
crystal size/mm	0.100 × 0.090 × 0.070
T/K	298.(2)
radiation	MoK α
diffractometer	'Bruker D8 Venture TXS'
crystal system	triclinic
space group	'P -1'
a/Å	7.9677(2)
b/Å	9.2454(2)
c/Å	11.7448(3)
α/°	83.4692(8)
β/°	88.5722(9)
γ/°	80.9664(9)
V/Å³	848.88(4)
Z	2
calc. density/g cm⁻³	1.398
μ/mm⁻¹	0.100
absorption correction	Multi-Scan

transmission factor range	0.9304–0.9590
refls. measured	16616
R_{int}	0.0285
mean $\sigma(I)/I$	0.0301
θ range	3.112–27.485
observed refls.	3287
x, y (weighting scheme)	0.0585, 0.3339
hydrogen refinement	constr
refls in refinement	3871
parameters	238
restraints	0
$R(F_{\text{obs}})$	0.0485
$R_w(F^2)$	0.1355
S	1.070
shift/error_{max}	0.001
max electron density/e \AA^{-3}	0.232
min electron density/e \AA^{-3}	–0.218

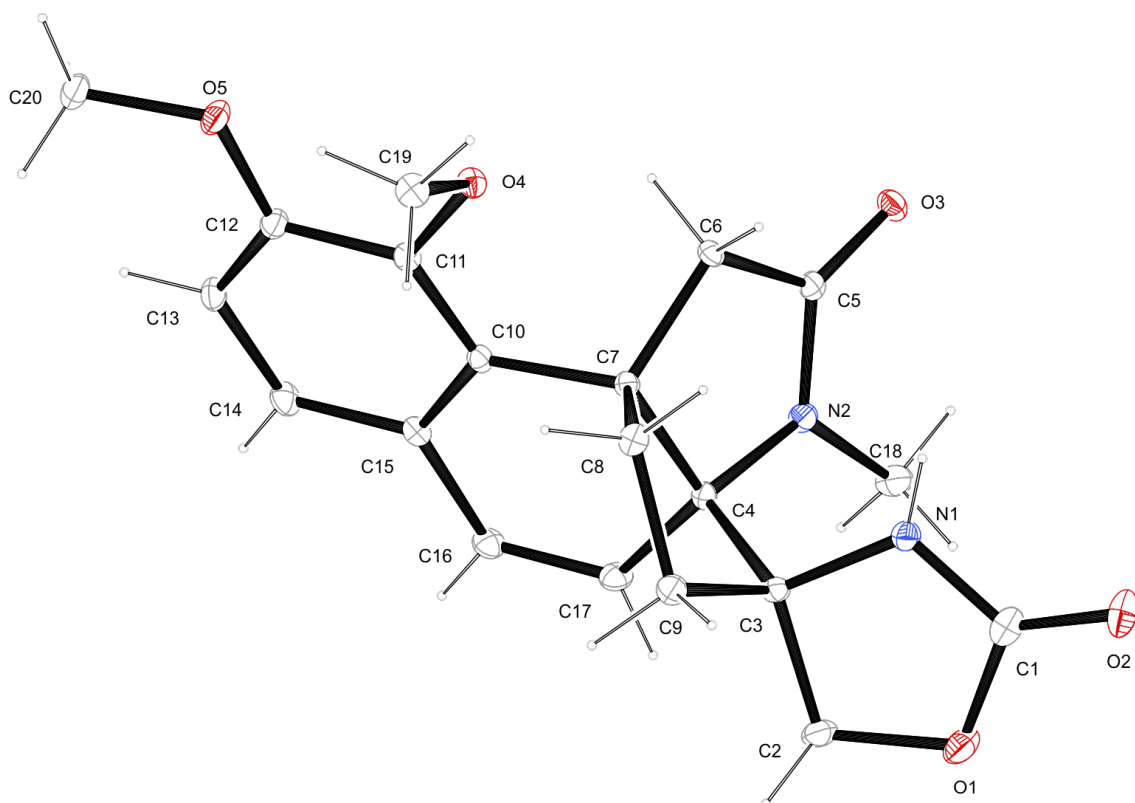
Single-crystal X-ray analysis of compound I.313.



net formula	$C_{27}H_{30}N_2O_6$
M_r/g mol⁻¹	478.53
crystal size/mm	0.100 × 0.100 × 0.030
T/K	298.(2)
radiation	MoK α
diffractometer	'Bruker D8 Venture TXS'
crystal system	monoclinic
space group	'P 1 21/c 1'
a/Å	13.4422(4)
b/Å	11.6532(4)
c/Å	15.2777(5)
α/°	90
β/°	99.7940(10)
γ/°	90
V/Å³	2358.29(13)
Z	4
calc. density/g cm⁻³	1.348
μ/mm⁻¹	0.096
absorption correction	Multi-Scan
transmission factor range	0.9101–0.9590

refls. measured	45381
R_{int}	0.0405
mean $\sigma(I)/I$	0.0259
θ range	3.076–27.494
observed refls.	4408
x, y (weighting scheme)	0.0640, 1.3189
hydrogen refinement	mixed
Flack parameter	5391
refls in refinement	323
parameters	0
restraints	0.0575
$R(F_{\text{obs}})$	0.1627
$R_w(F^2)$	1.072
S	0.001
shift/error_{max}	0.375
max electron density/e \AA^{-3}	-0.187

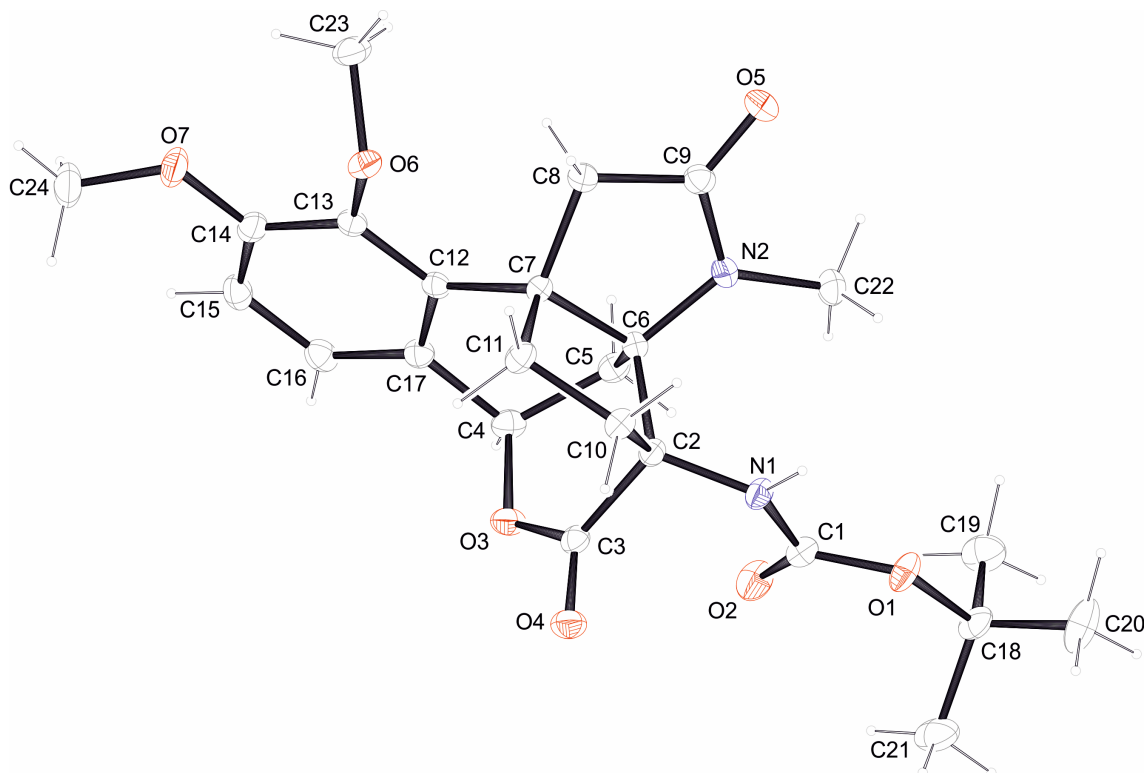
Single-crystal X-ray analysis of compound I.329.



net formula	$C_{20}H_{22}N_2O_5$
M_r/g mol⁻¹	370.39
crystal size/mm	0.090 × 0.060 × 0.040
T/K	100.(2)
radiation	MoK α
diffractometer	'Bruker D8 Venture TXS'
crystal system	orthorhombic
space group	'P b c a'
a/Å	8.246(5)
b/Å	18.285(11)
c/Å	22.344(15)
α/°	90
β/°	90
γ/°	90
V/Å³	3369.(4)
Z	8
calc. density/g cm⁻³	1.461
μ/mm⁻¹	0.106

absorption correction	Multi-Scan
transmission factor range	0.9167–0.9590
refls. measured	4372
R_{int}	0.0000
mean $\sigma(I)/I$	0.0439
θ range	3.648–27.483
observed refls.	3702
x, y (weighting scheme)	0.0396, 5.2315
hydrogen refinement	C-H: constr, N-H: refall
refls in refinement	4372
parameters	252
restraints	0
$R(F_{\text{obs}})$	0.0614
$R_w(F^2)$	0.1544
S	1.098
shift/error_{max}	0.001
max electron density/e \AA^{-3}	0.427
min electron density/e \AA^{-3}	–0.285

Single-crystal X-ray analysis of compound I.355.

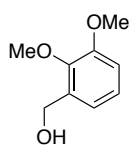


net formula	$C_{24}H_{32}N_2O_8$
M_r/g mol⁻¹	476.51
crystal size/mm	0.100 × 0.060 × 0.040
T/K	100.(2)
radiation	MoK α
diffractometer	'Bruker D8 Venture TXS'
crystal system	monoclinic
space group	'P 1 21/c 1'
a/Å	10.0419(7)
b/Å	18.4401(10)
c/Å	12.5503(7)
α/°	90
β/°	93.409(2)
γ/°	90
V/Å³	2319.9(2)
Z	4
calc. density/g cm⁻³	1.364
μ/mm⁻¹	0.103
absorption correction	Multi-Scan

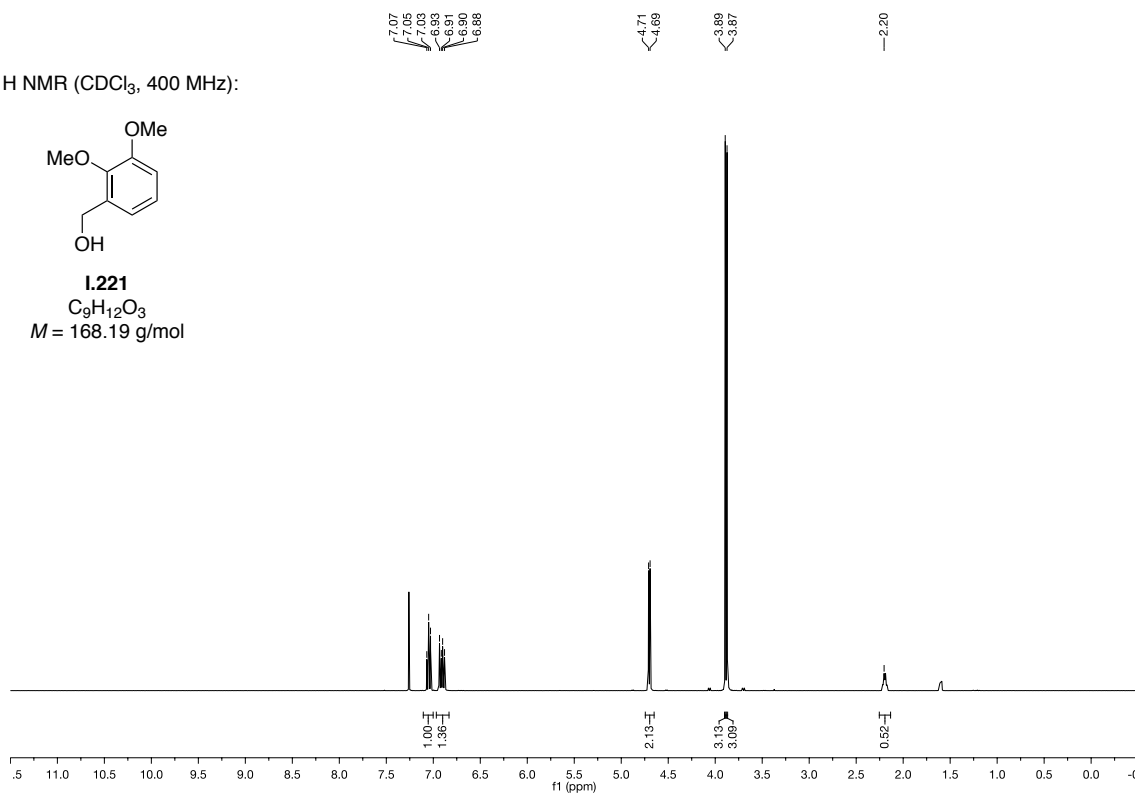
transmission factor range	0.9250–0.9705
refls. measured	20766
R_{int}	0.0399
mean $\sigma(I)/I$	0.0339
θ range	3.252–26.372
observed refls.	4076
x, y (weighting scheme)	0.0397, 1.4833
hydrogen refinement	H(C) const, H(N/O) refall
refls in refinement	4735
parameters	325
restraints	0
$R(F_{\text{obs}})$	0.0402
$R_w(F^2)$	0.1021
S	1.052
shift/error_{max}	0.001
max electron density/e \AA^{-3}	0.360

9.2 NMR spectra of chapter I

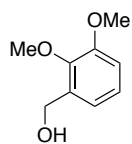
$^1\text{H NMR}$ (CDCl_3 , 400 MHz):



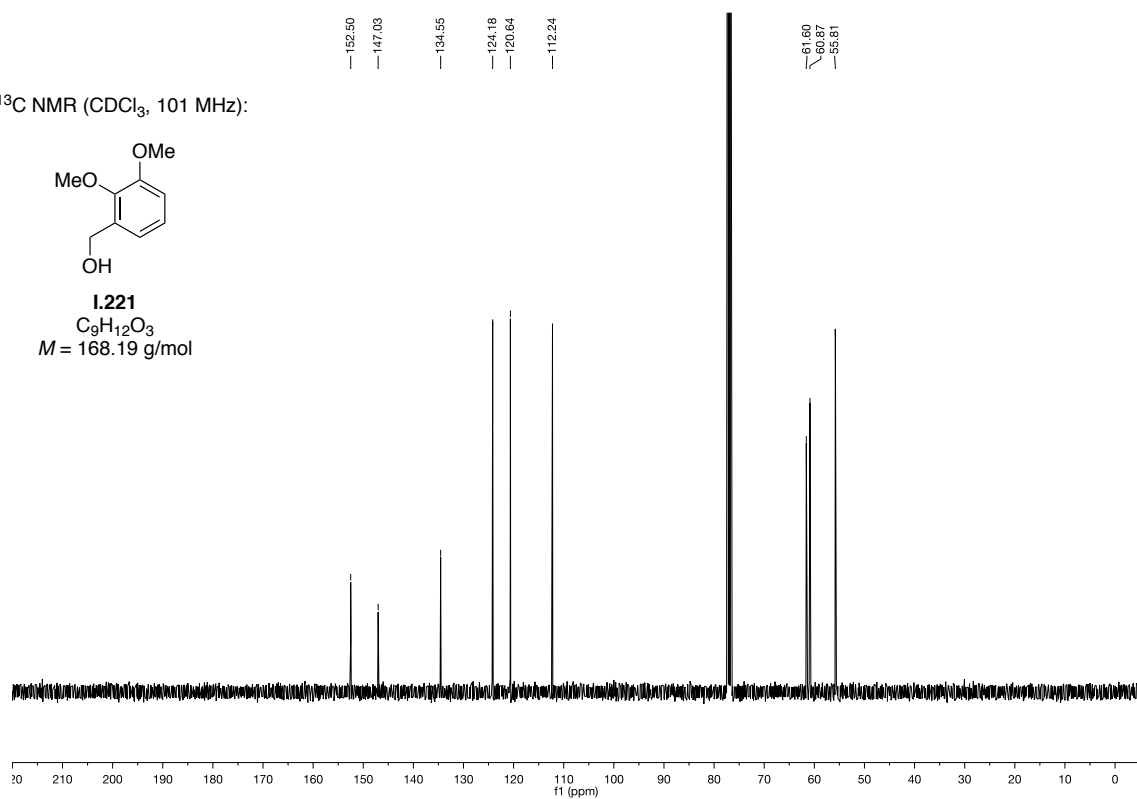
1.221
 $\text{C}_9\text{H}_{12}\text{O}_3$
 $M = 168.19$ g/mol



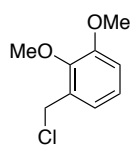
$^{13}\text{C NMR}$ (CDCl_3 , 101 MHz):



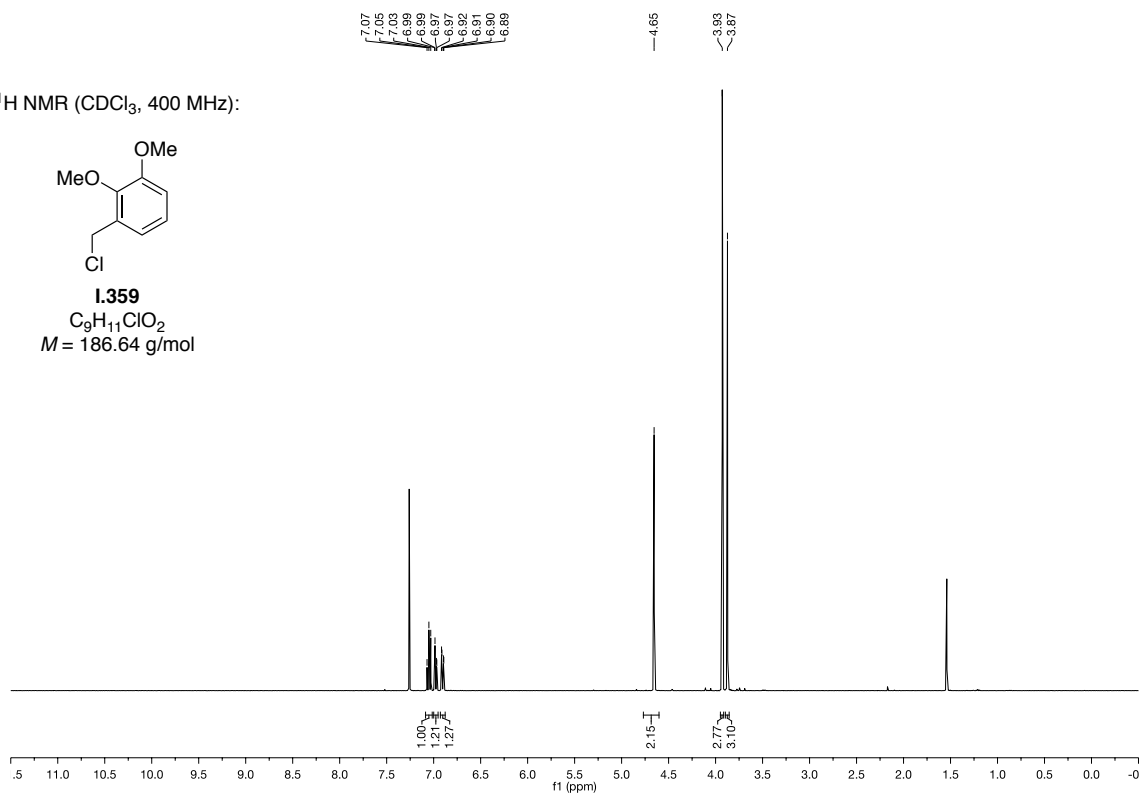
1.221
 $\text{C}_9\text{H}_{12}\text{O}_3$
 $M = 168.19$ g/mol



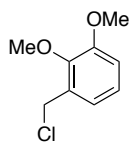
^1H NMR (CDCl_3 , 400 MHz):



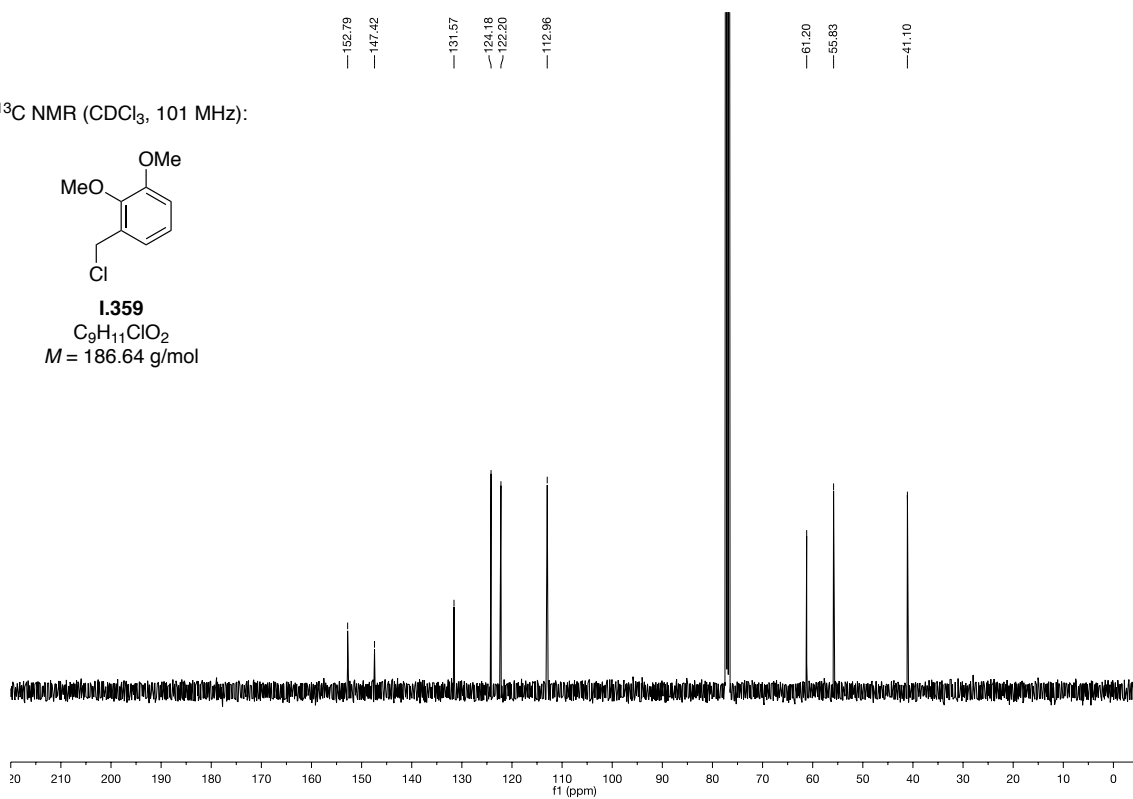
1.359
 $\text{C}_9\text{H}_{11}\text{ClO}_2$
 $M = 186.64$ g/mol



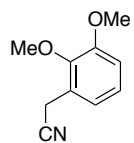
^{13}C NMR (CDCl_3 , 101 MHz):



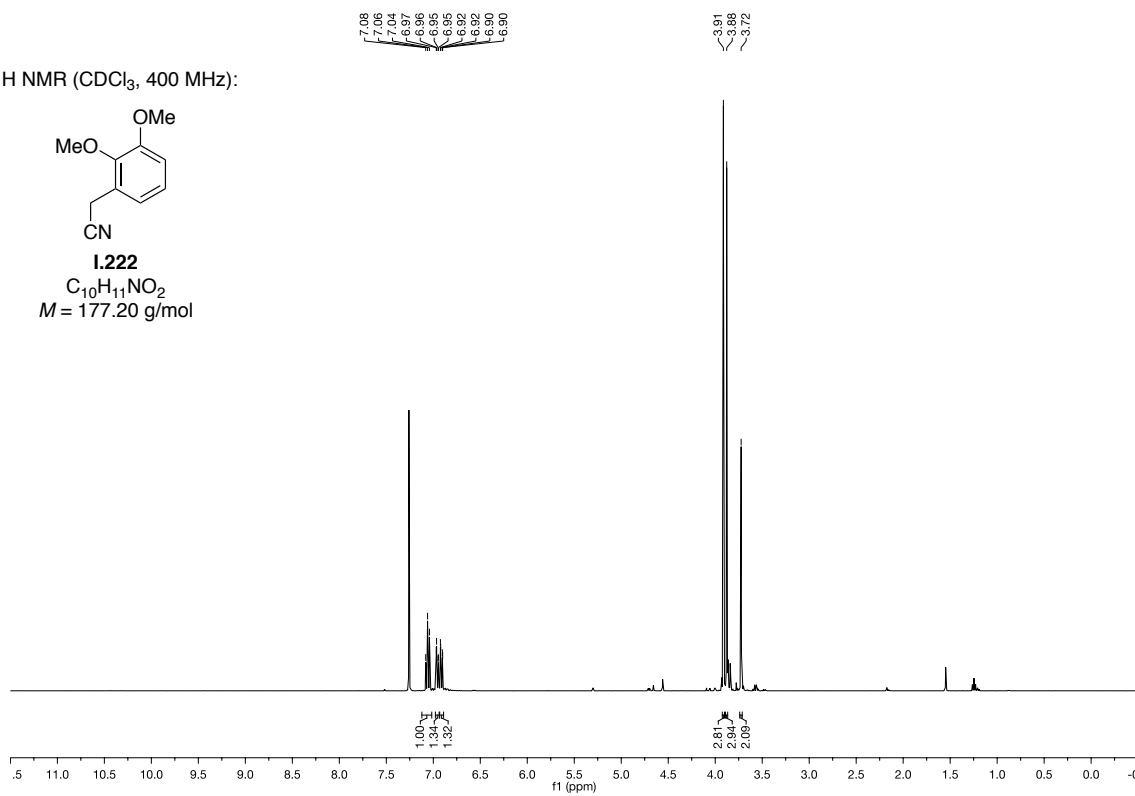
1.359
 $\text{C}_9\text{H}_{11}\text{ClO}_2$
 $M = 186.64$ g/mol



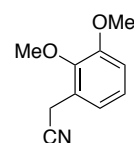
$^1\text{H NMR}$ (CDCl_3 , 400 MHz):



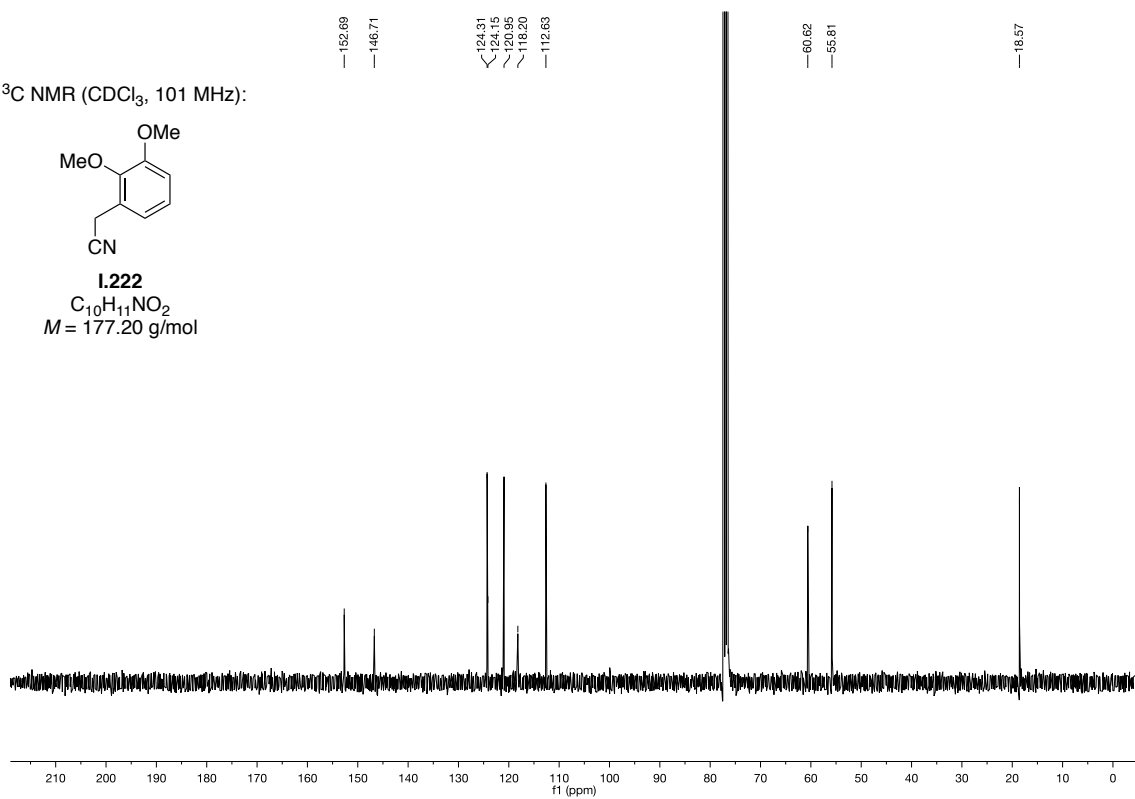
1.222
 $\text{C}_{10}\text{H}_{11}\text{NO}_2$
 $M = 177.20 \text{ g/mol}$



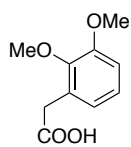
$^{13}\text{C NMR}$ (CDCl_3 , 101 MHz):



1.222
 $\text{C}_{10}\text{H}_{11}\text{NO}_2$
 $M = 177.20 \text{ g/mol}$



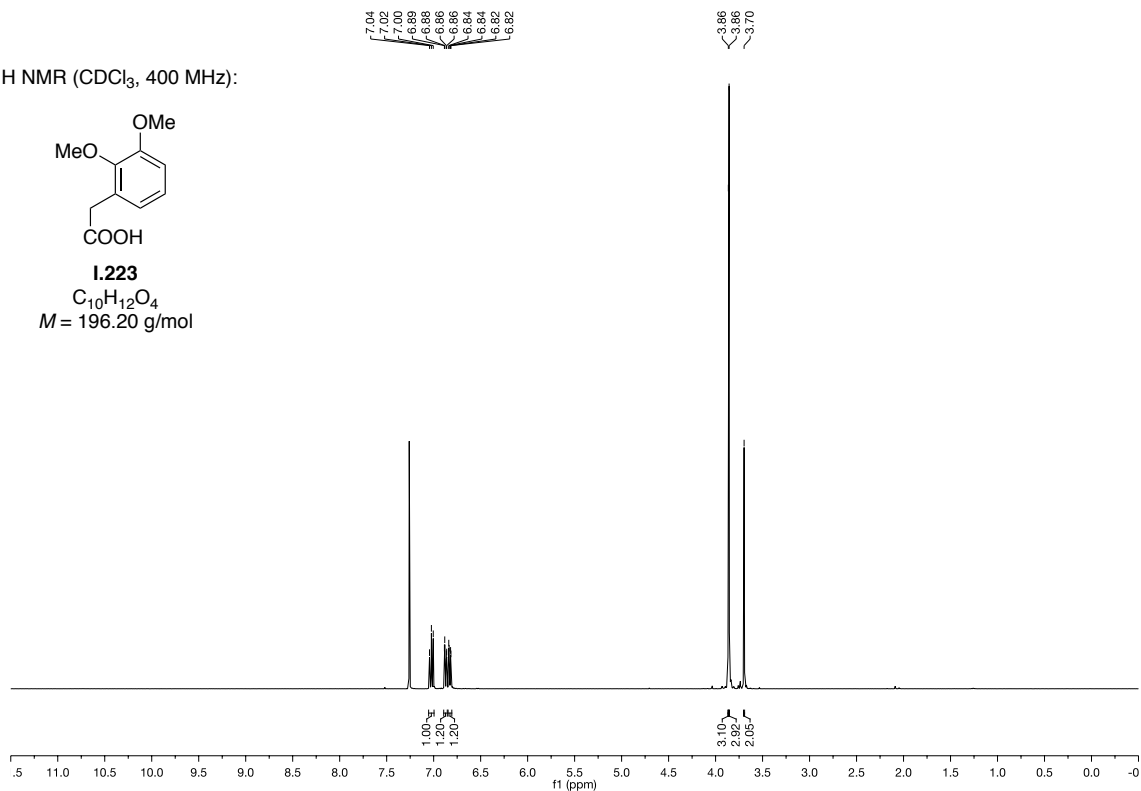
^1H NMR (CDCl_3 , 400 MHz):



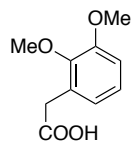
1.223

$\text{C}_{10}\text{H}_{12}\text{O}_4$

$M = 196.20$ g/mol



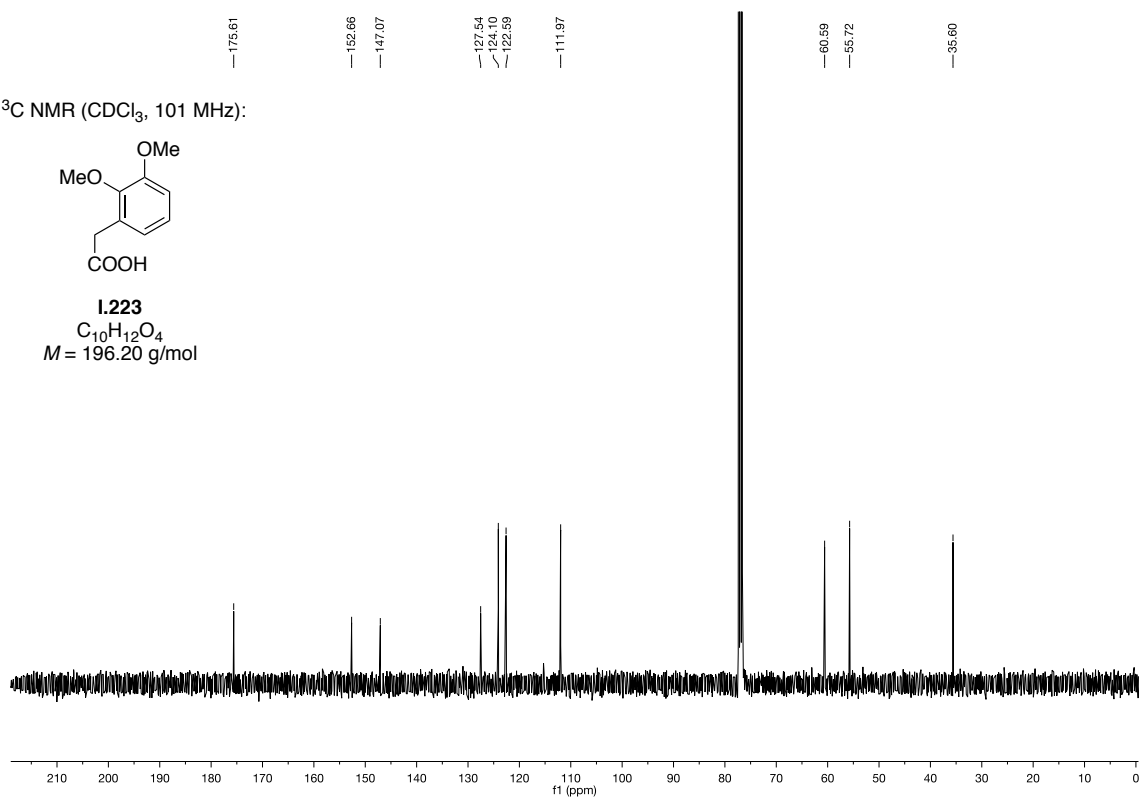
^{13}C NMR (CDCl_3 , 101 MHz):

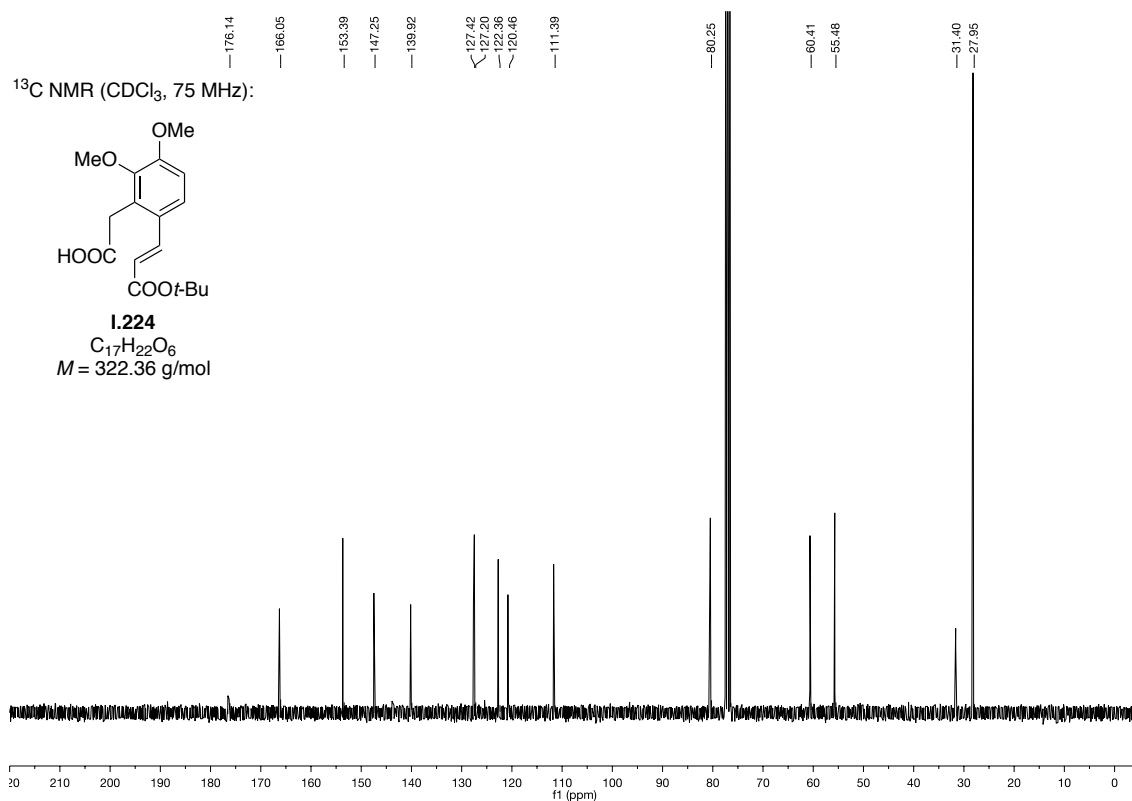
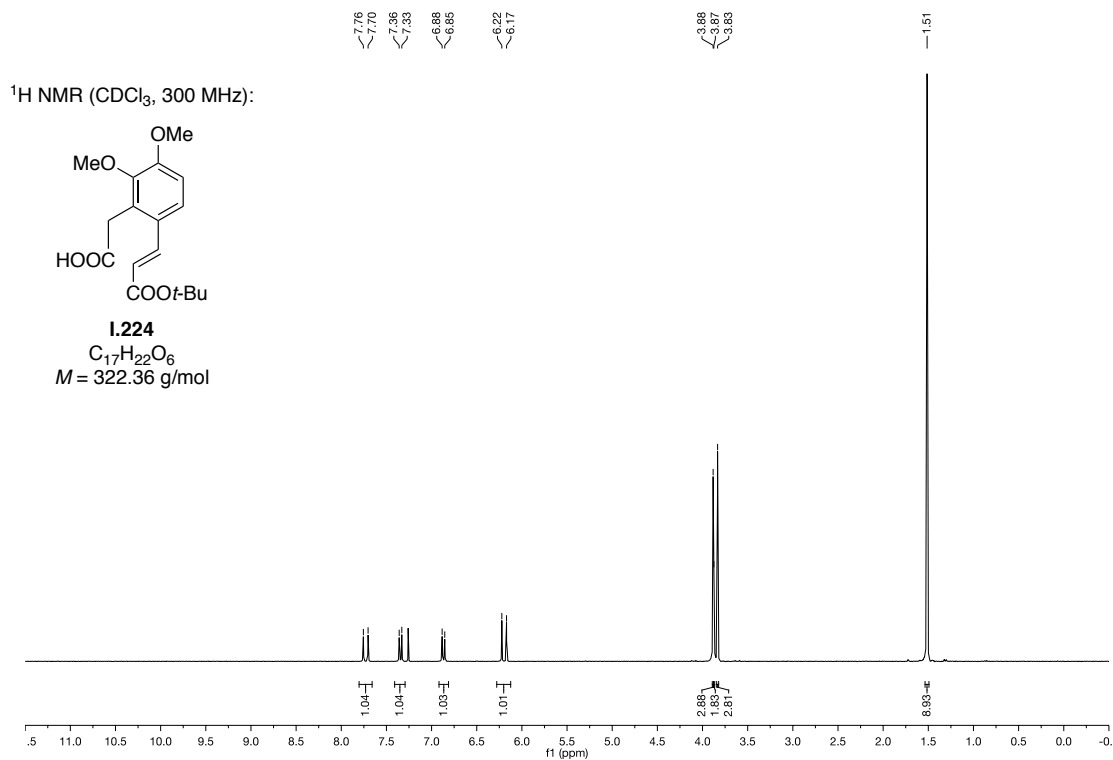


1.223

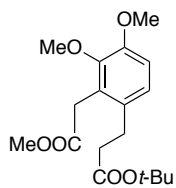
$\text{C}_{10}\text{H}_{12}\text{O}_4$

$M = 196.20$ g/mol

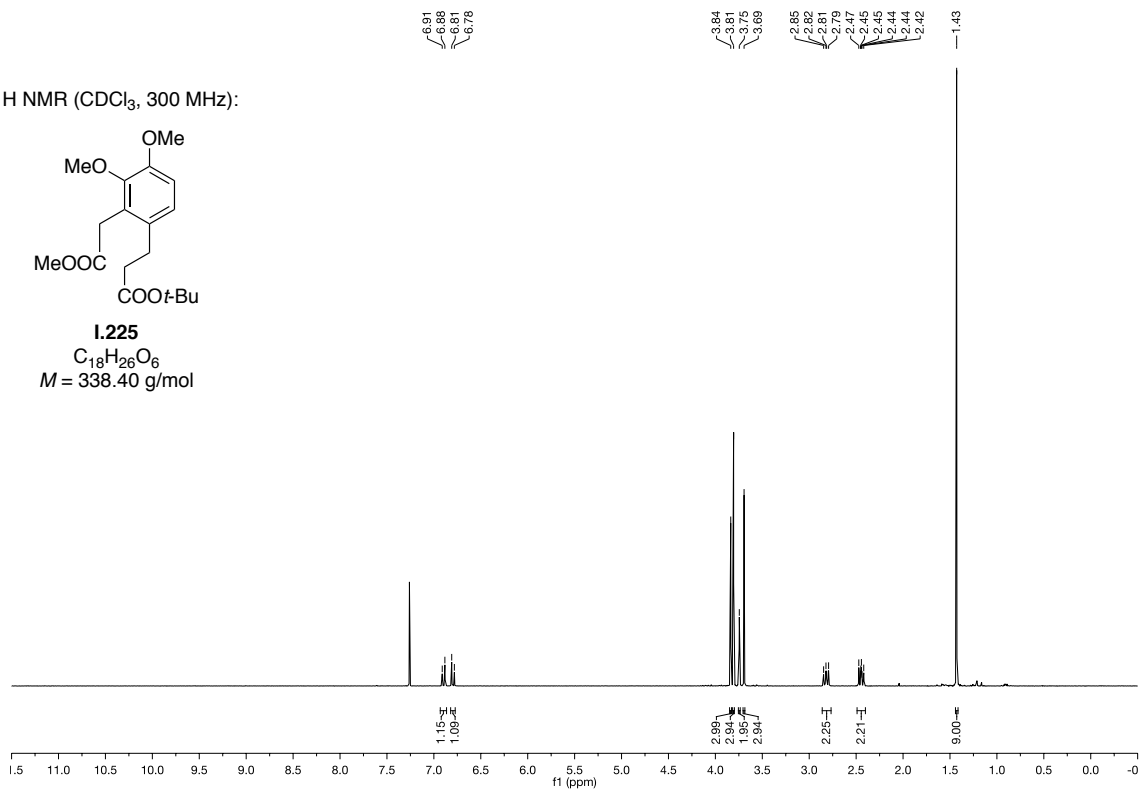




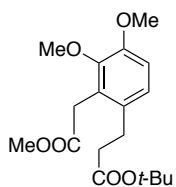
¹H NMR (CDCl₃, 300 MHz):



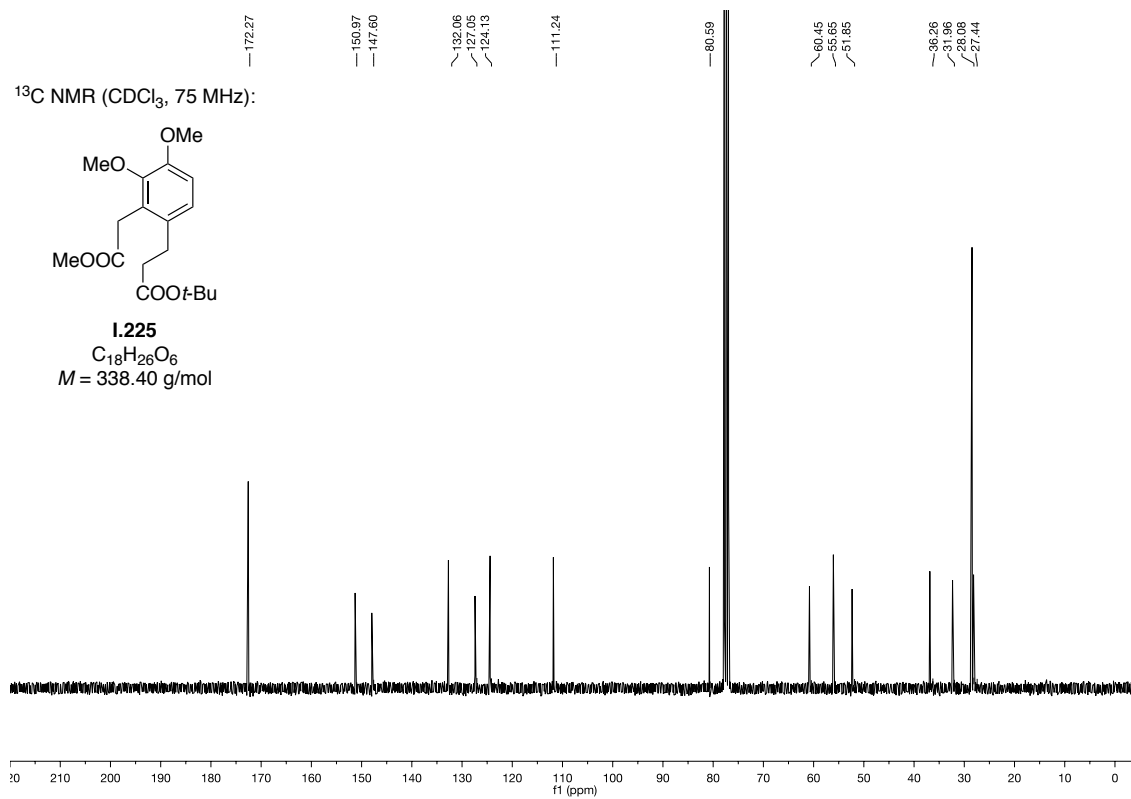
1.225
 $C_{18}H_{26}O_6$
 $M = 338.40$ g/mol



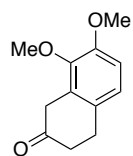
¹³C NMR (CDCl₃, 75 MHz):



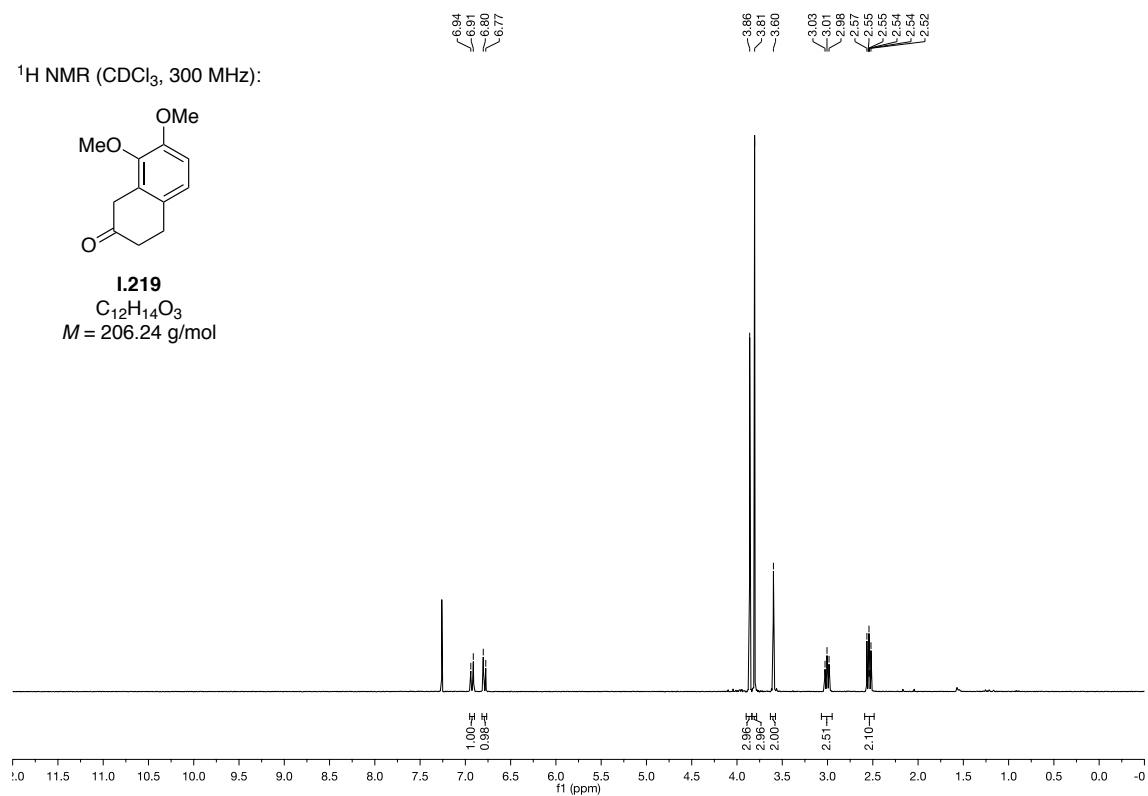
1.225
 $C_{18}H_{26}O_6$
 $M = 338.40$ g/mol



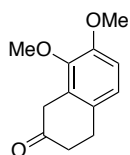
¹H NMR (CDCl₃, 300 MHz):



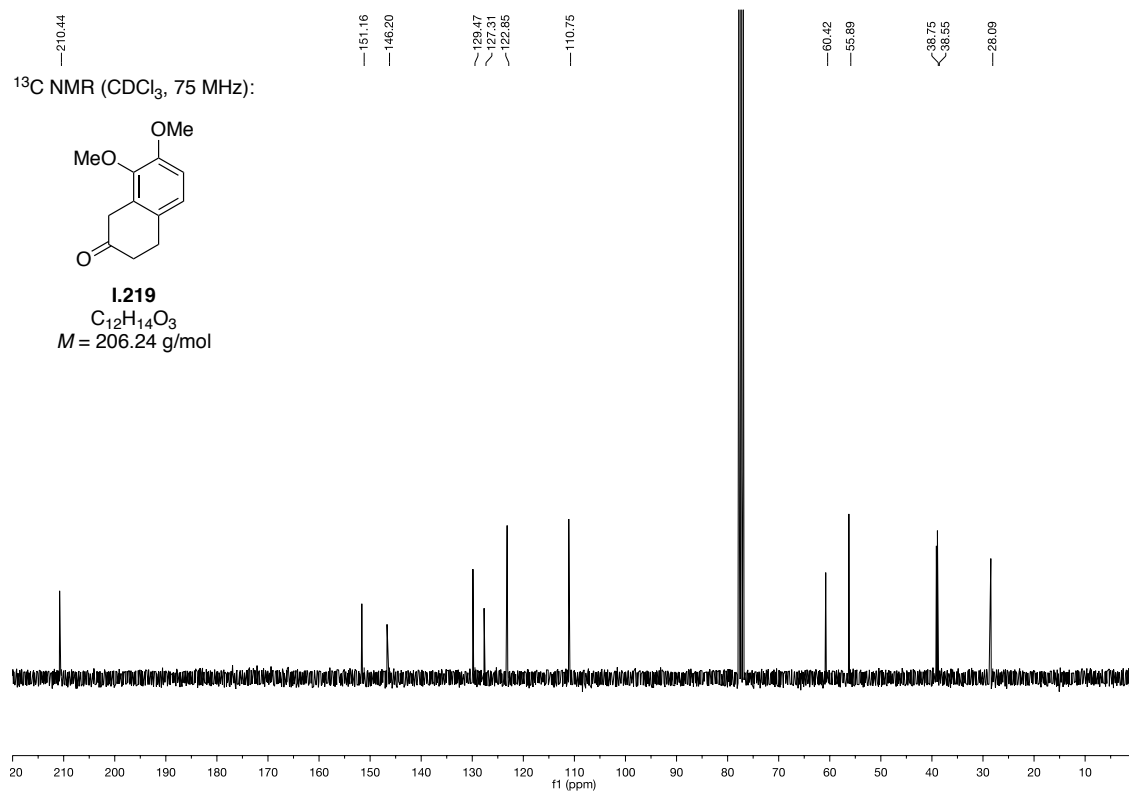
1.219
C₁₂H₁₄O₃
M = 206.24 g/mol

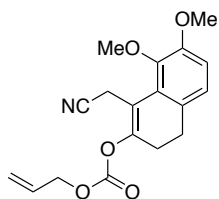


¹³C NMR (CDCl₃, 75 MHz):

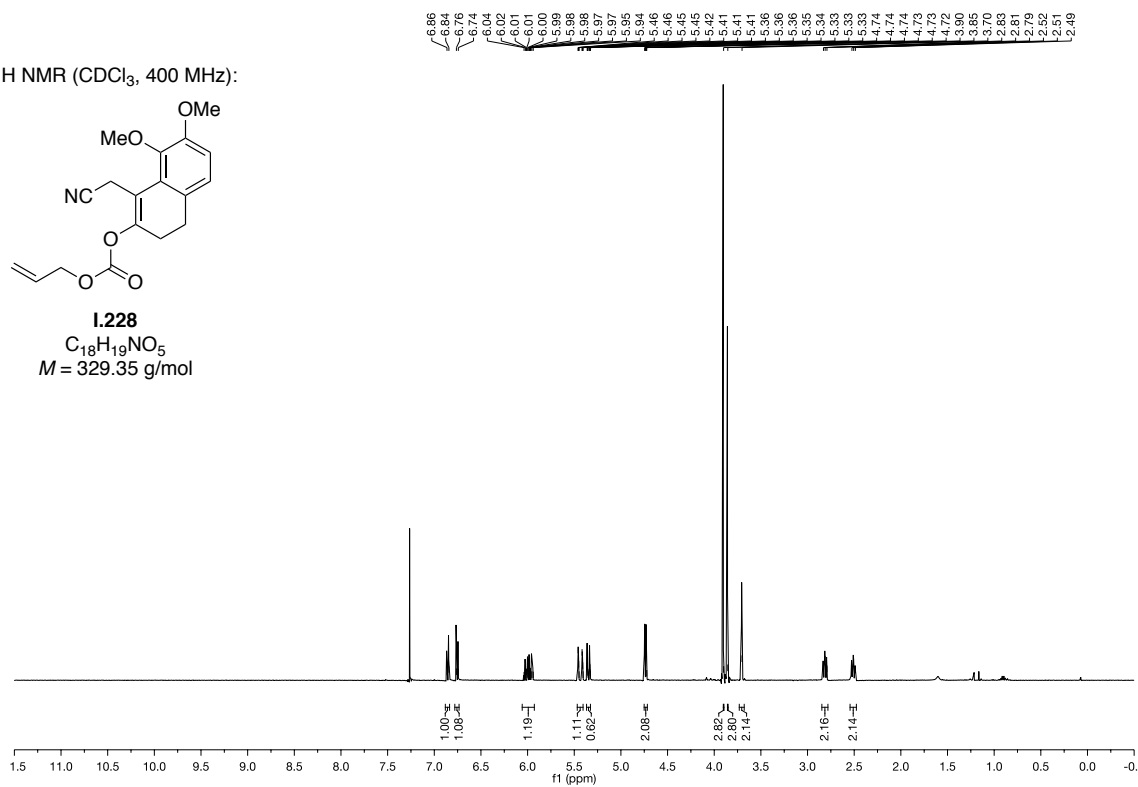
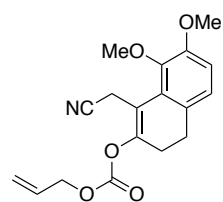


1.219
C₁₂H₁₄O₃
M = 206.24 g/mol

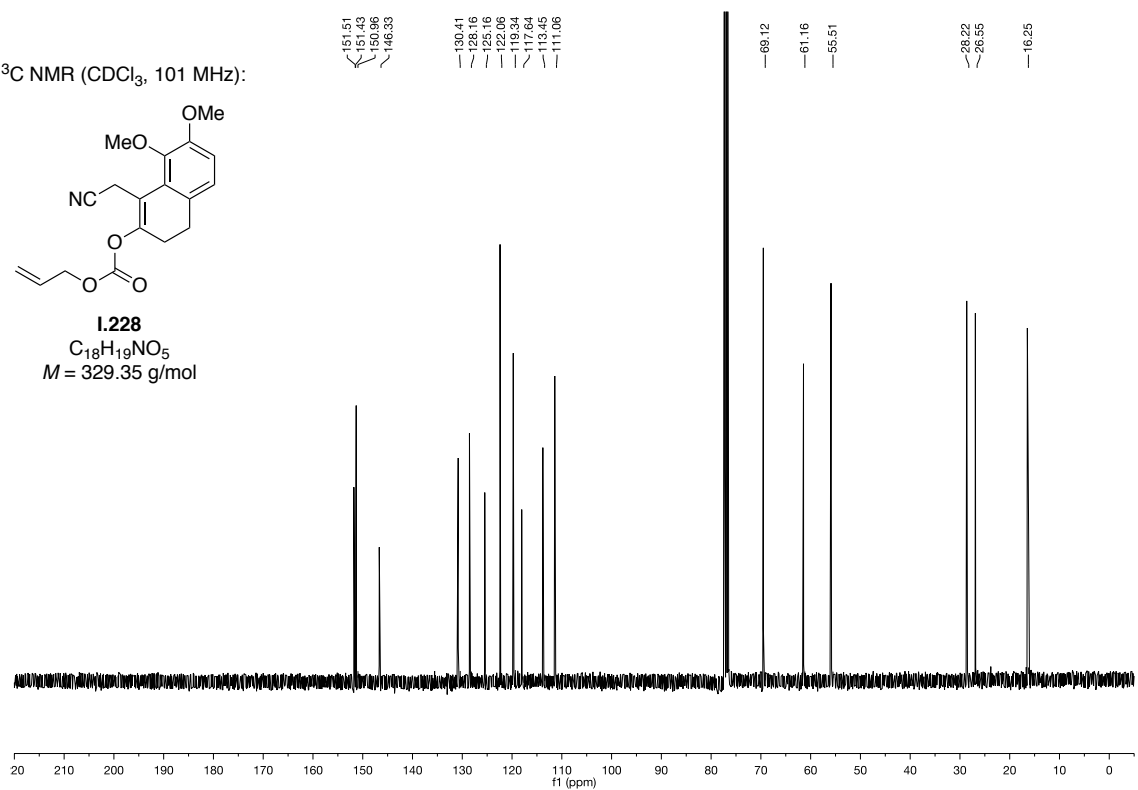


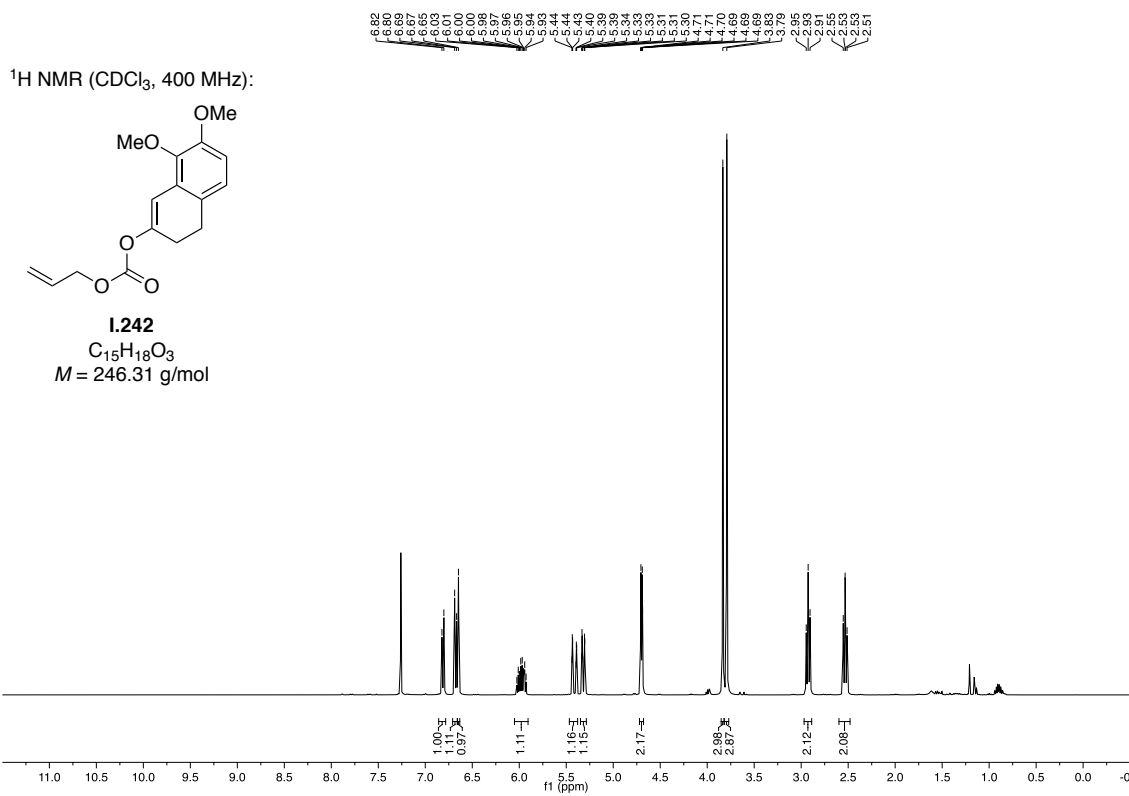
$^1\text{H NMR}$ (CDCl_3 , 400 MHz):

1.228
 $\text{C}_{18}\text{H}_{19}\text{NO}_5$
 $M = 329.35 \text{ g/mol}$

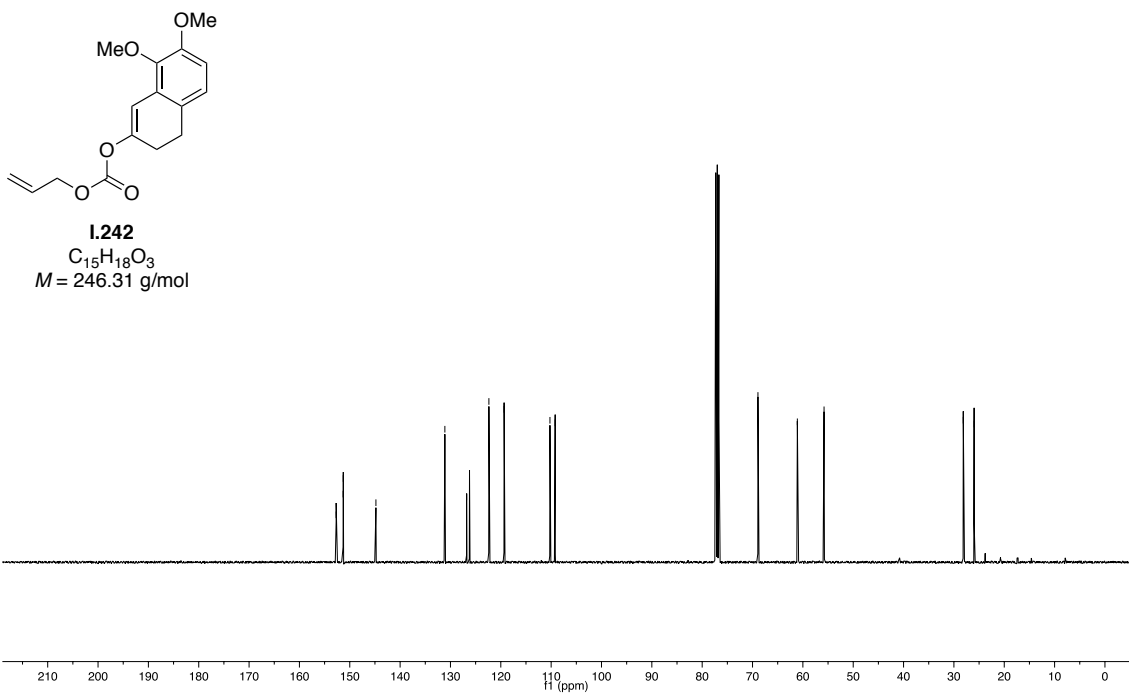
 $^{13}\text{C NMR}$ (CDCl_3 , 101 MHz):

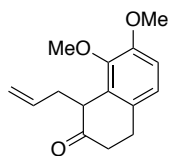
1.228
 $\text{C}_{18}\text{H}_{19}\text{NO}_5$
 $M = 329.35 \text{ g/mol}$



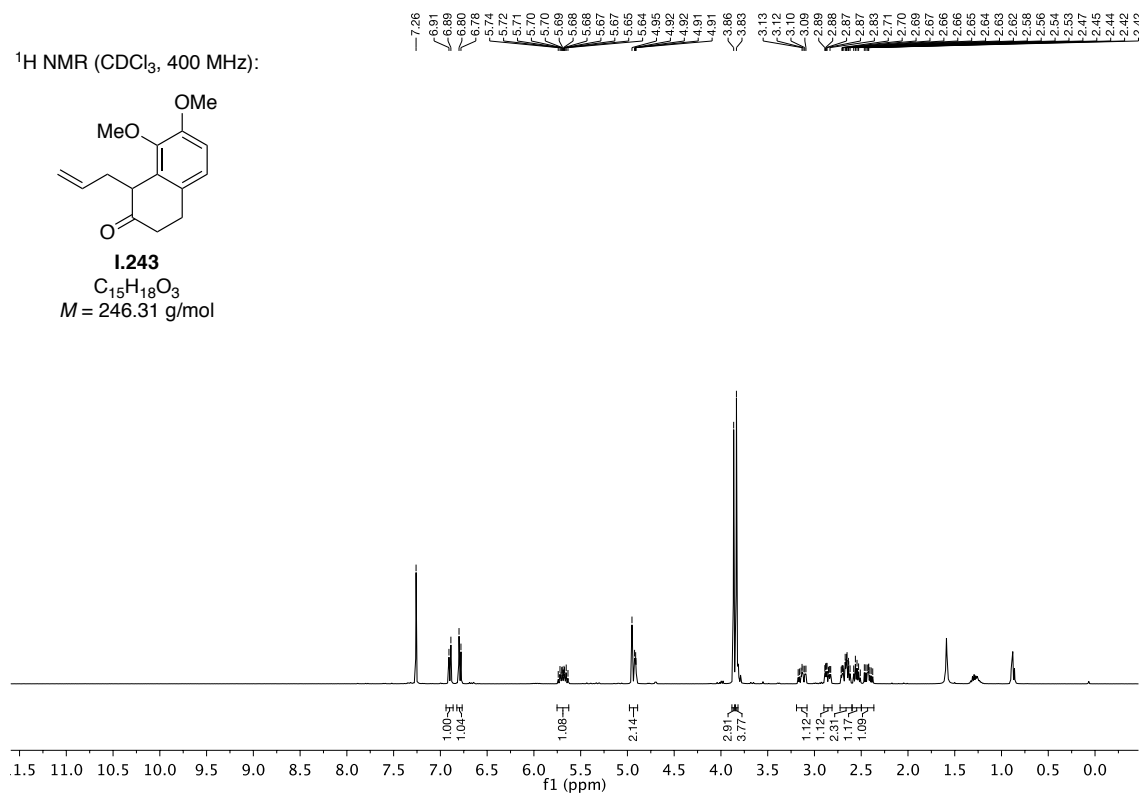
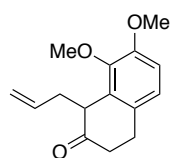


¹³C NMR (CDCl₃, 101 MHz):

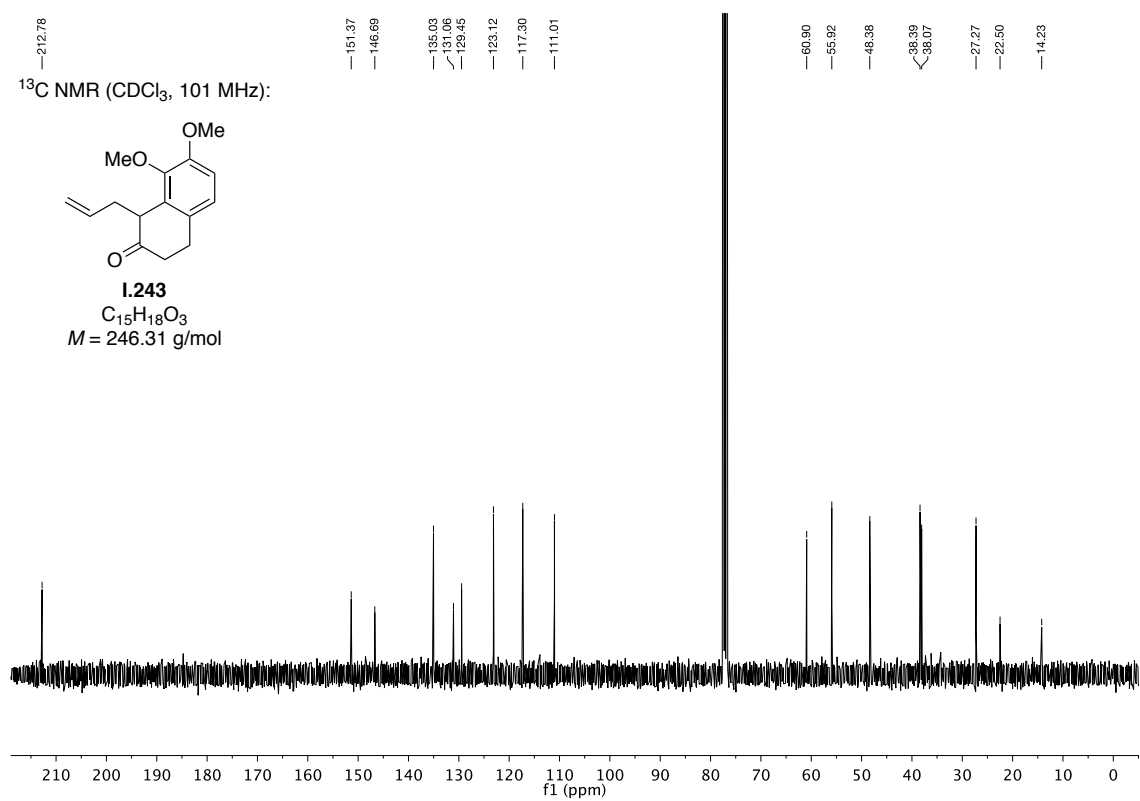


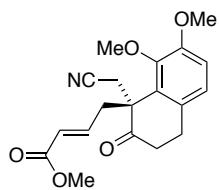
^1H NMR (CDCl_3 , 400 MHz):

1.243
 $\text{C}_{15}\text{H}_{18}\text{O}_3$
 $M = 246.31$ g/mol

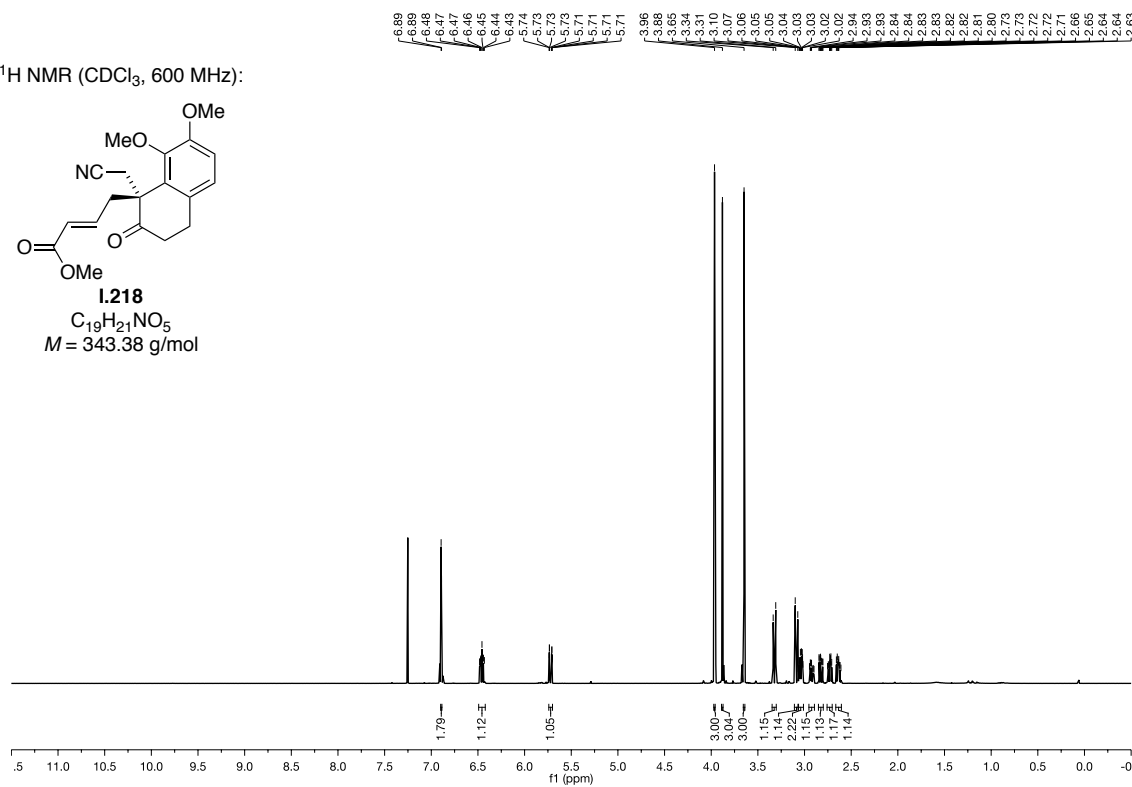
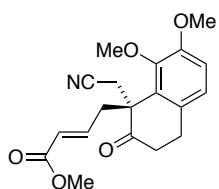
 ^{13}C NMR (CDCl_3 , 101 MHz):

1.243
 $\text{C}_{15}\text{H}_{18}\text{O}_3$
 $M = 246.31$ g/mol

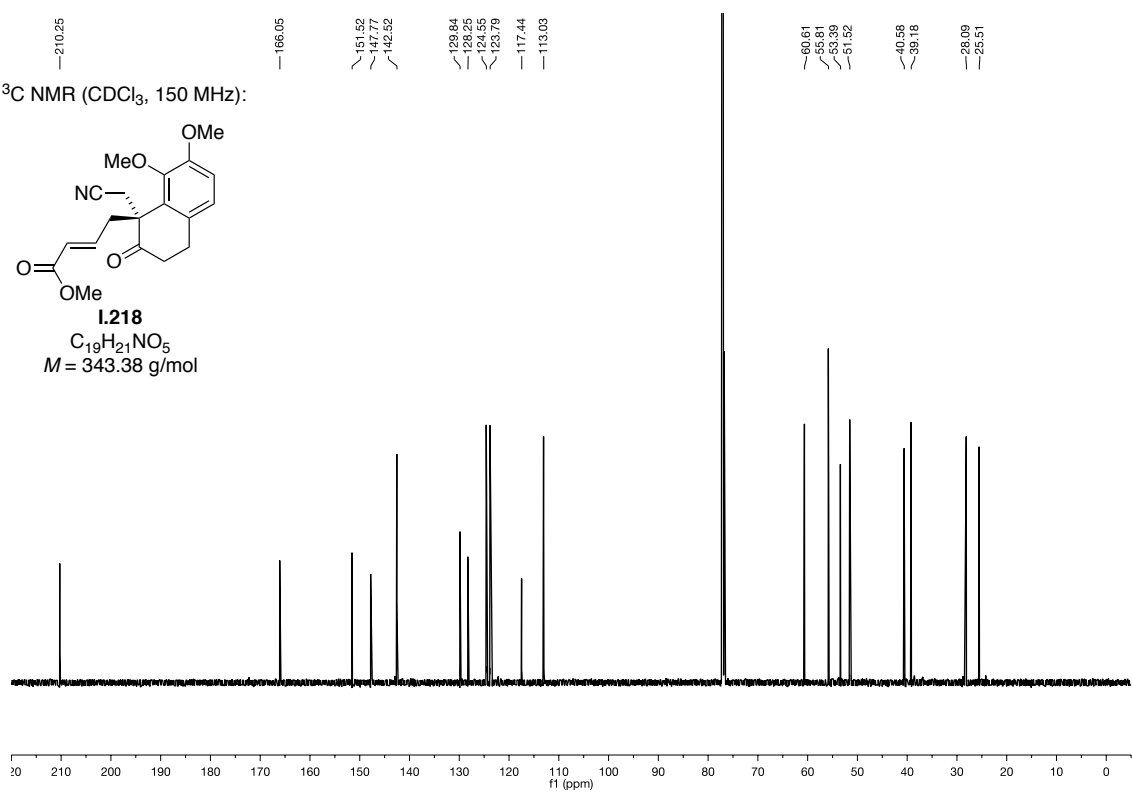


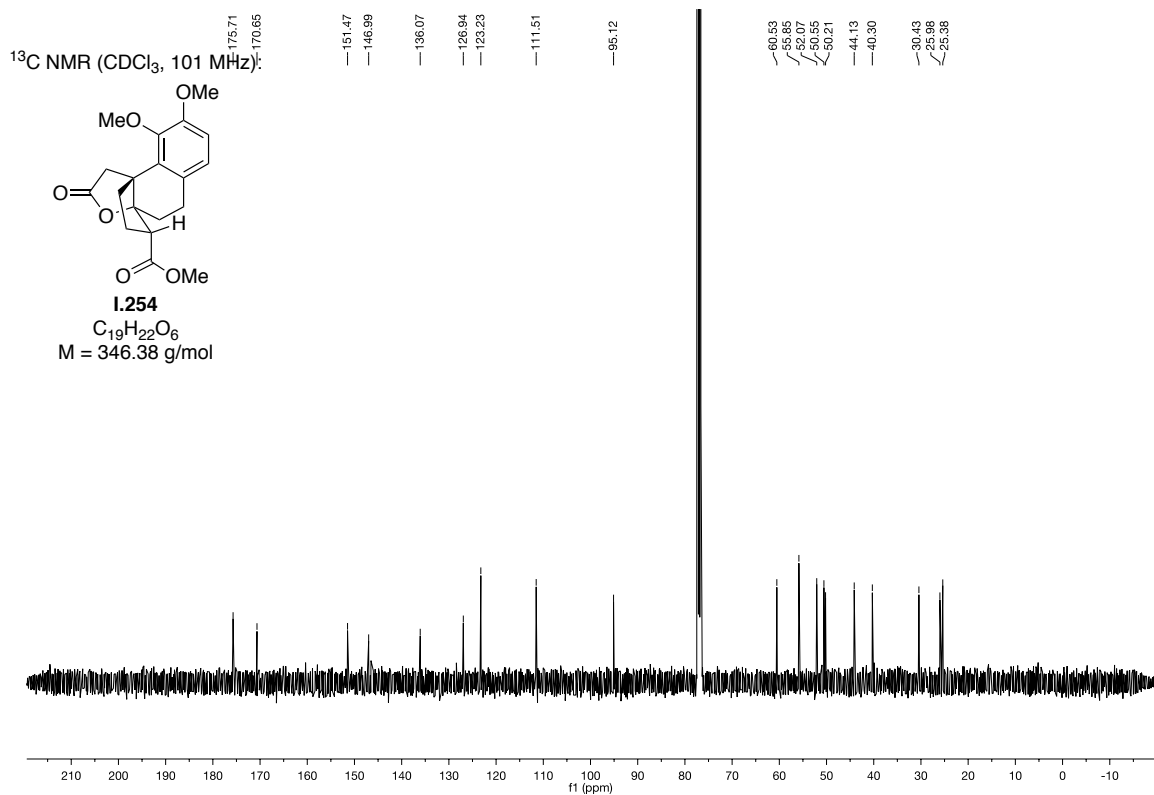
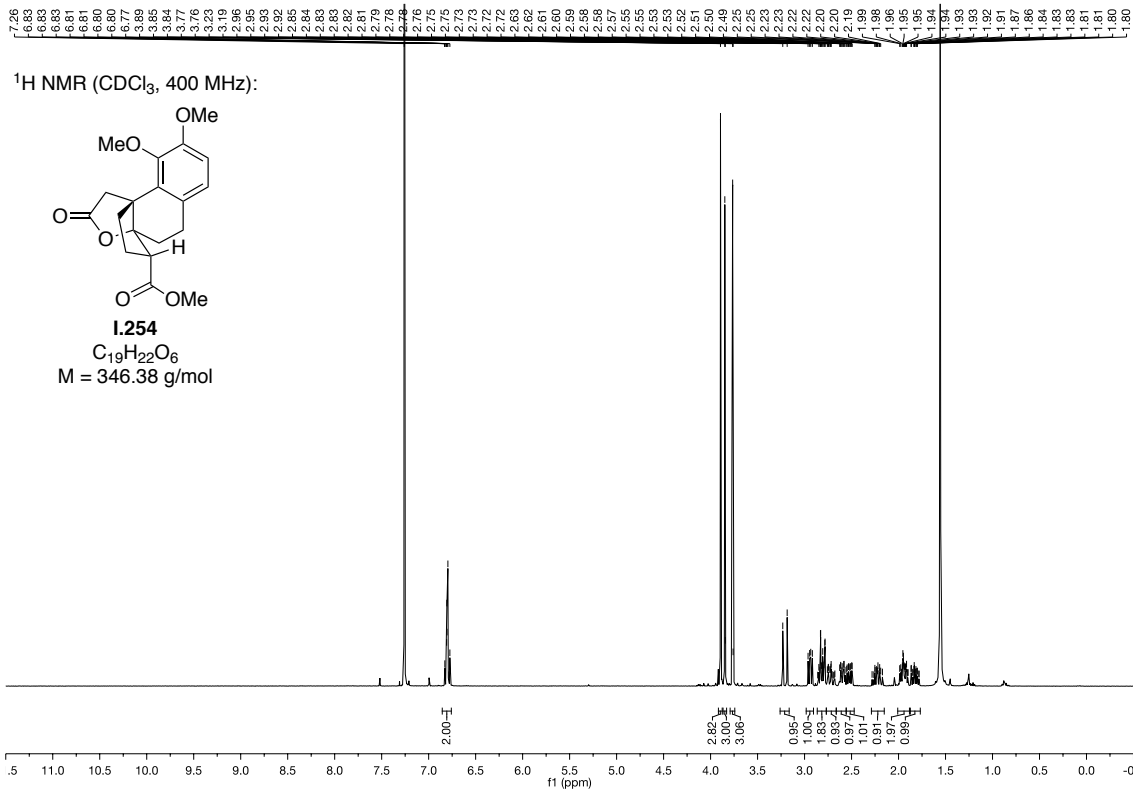
¹H NMR (CDCl₃, 600 MHz):

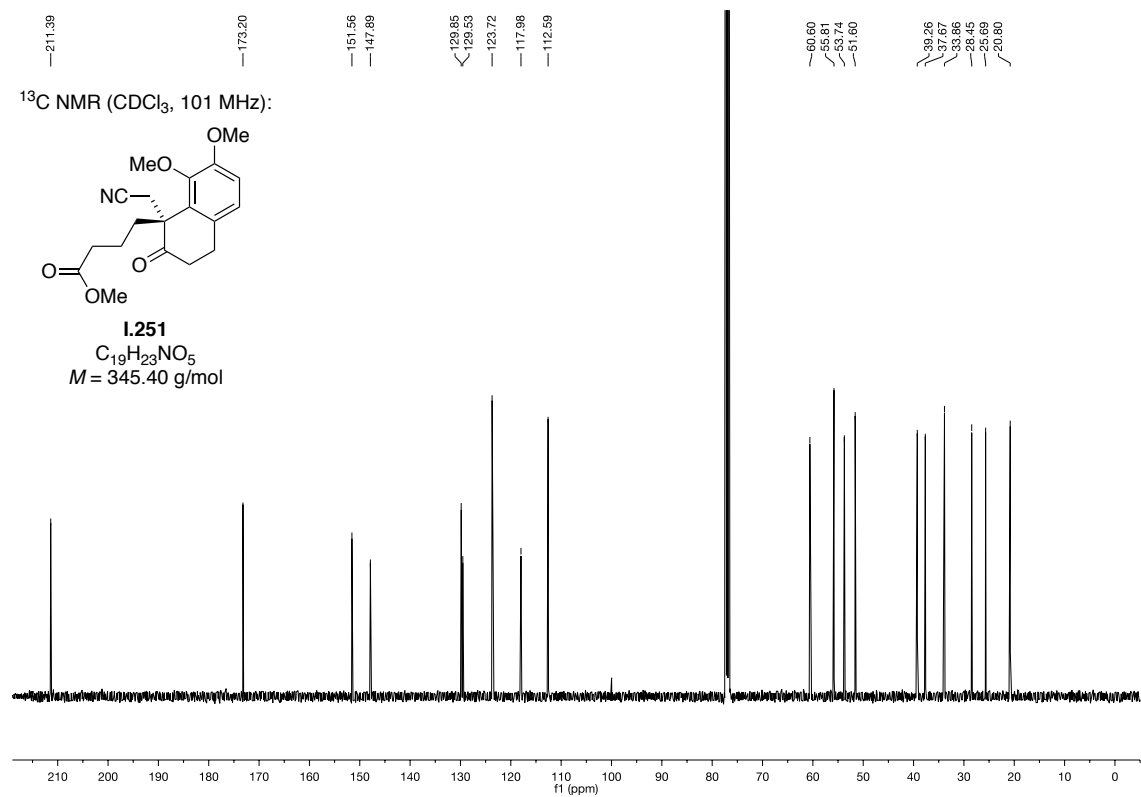
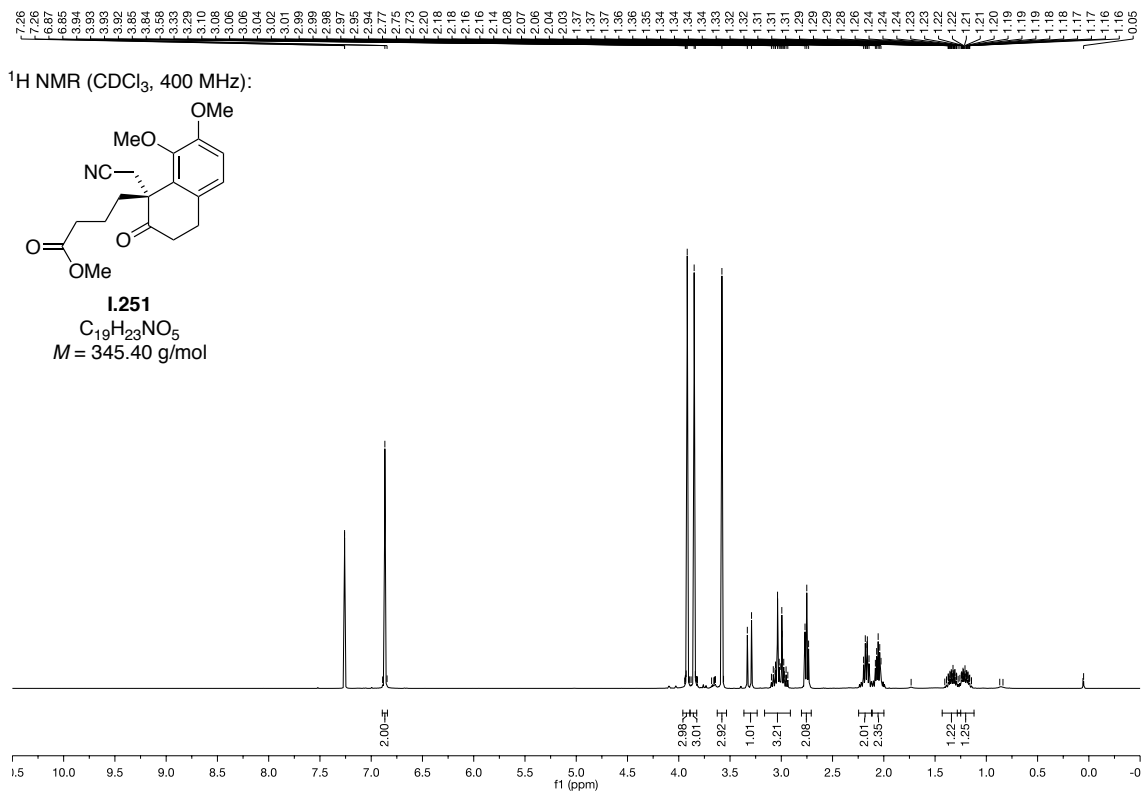
I.218
 C₁₉H₂₁NO₅
 M = 343.38 g/mol

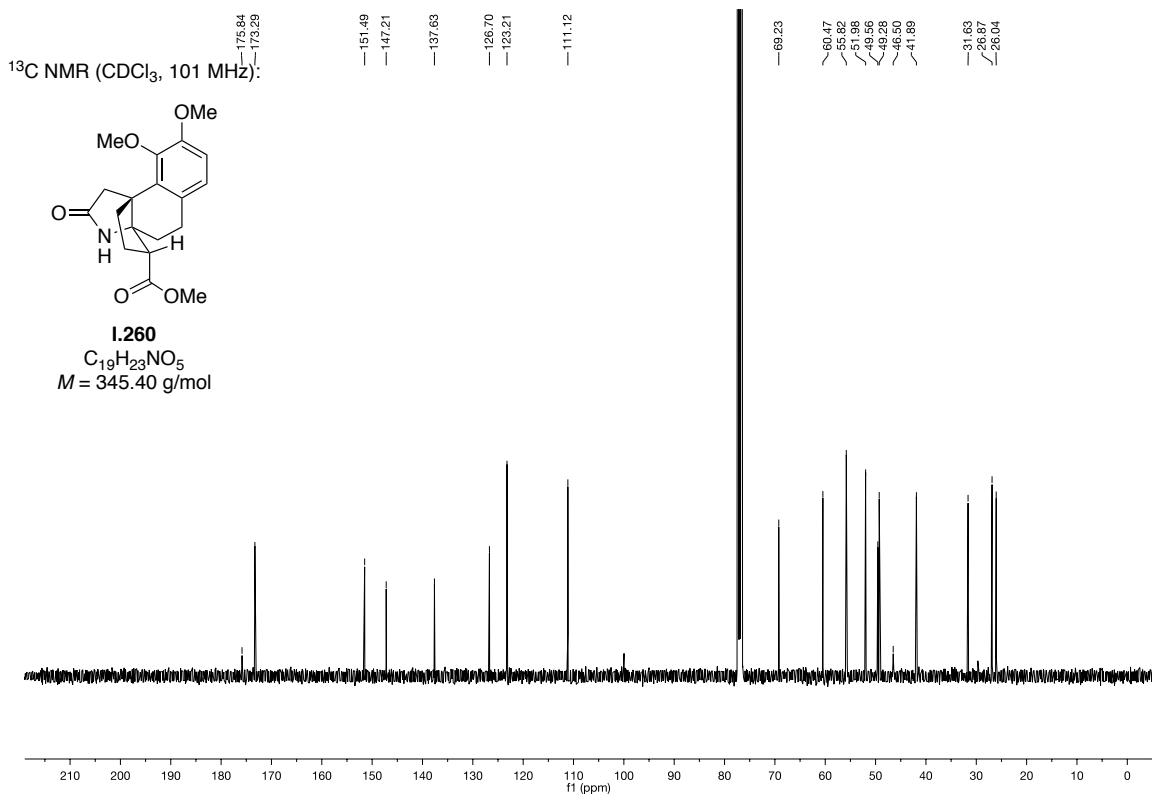
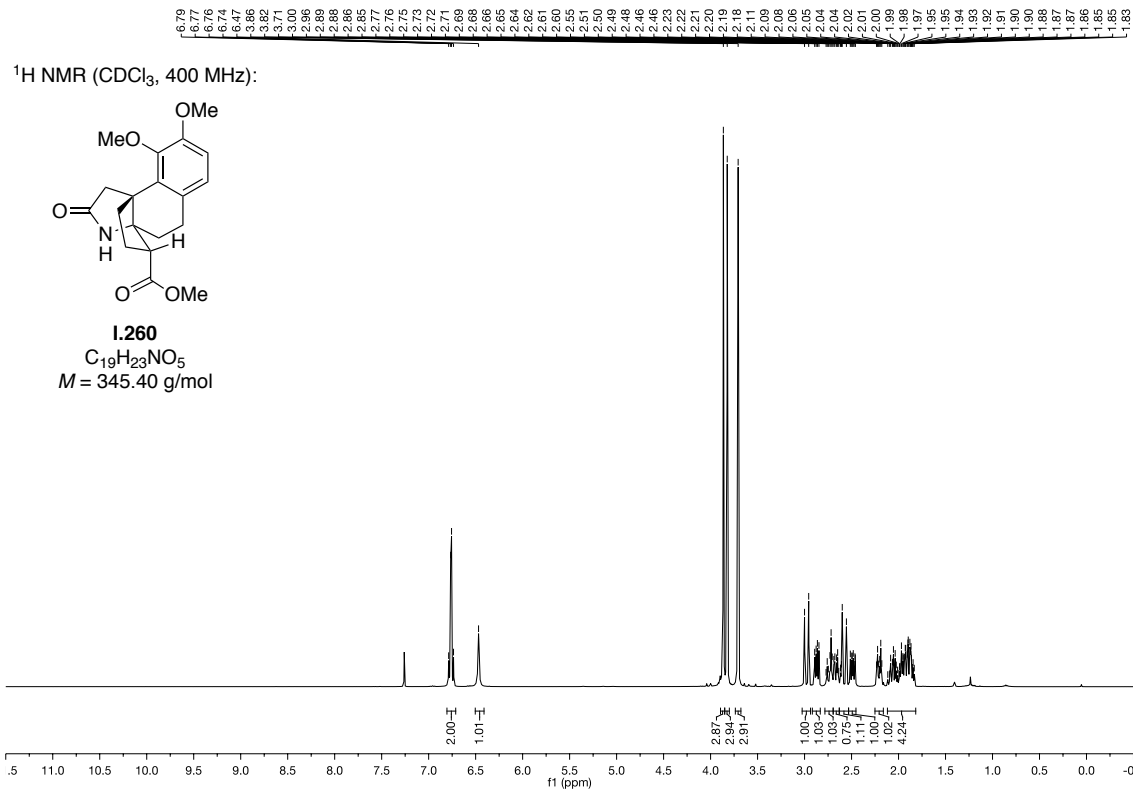
¹³C NMR (CDCl₃, 150 MHz):

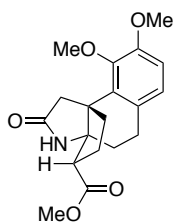
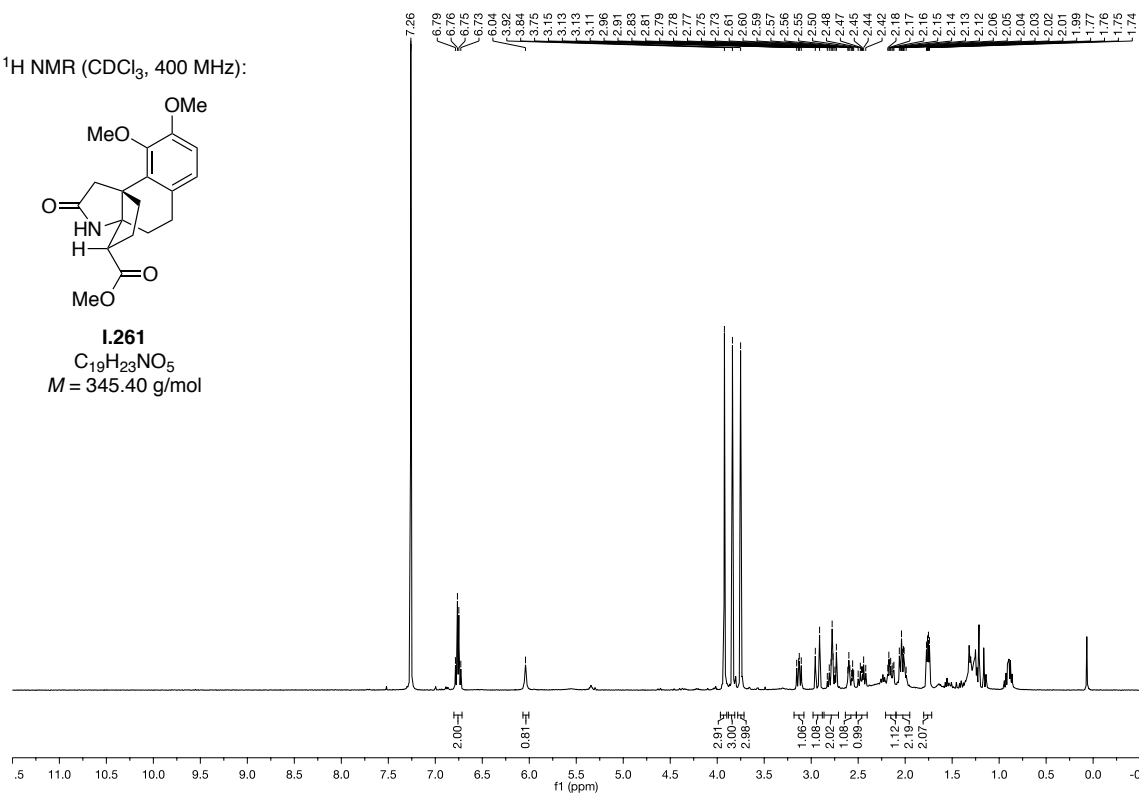
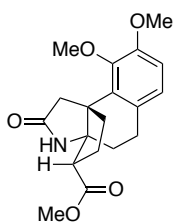
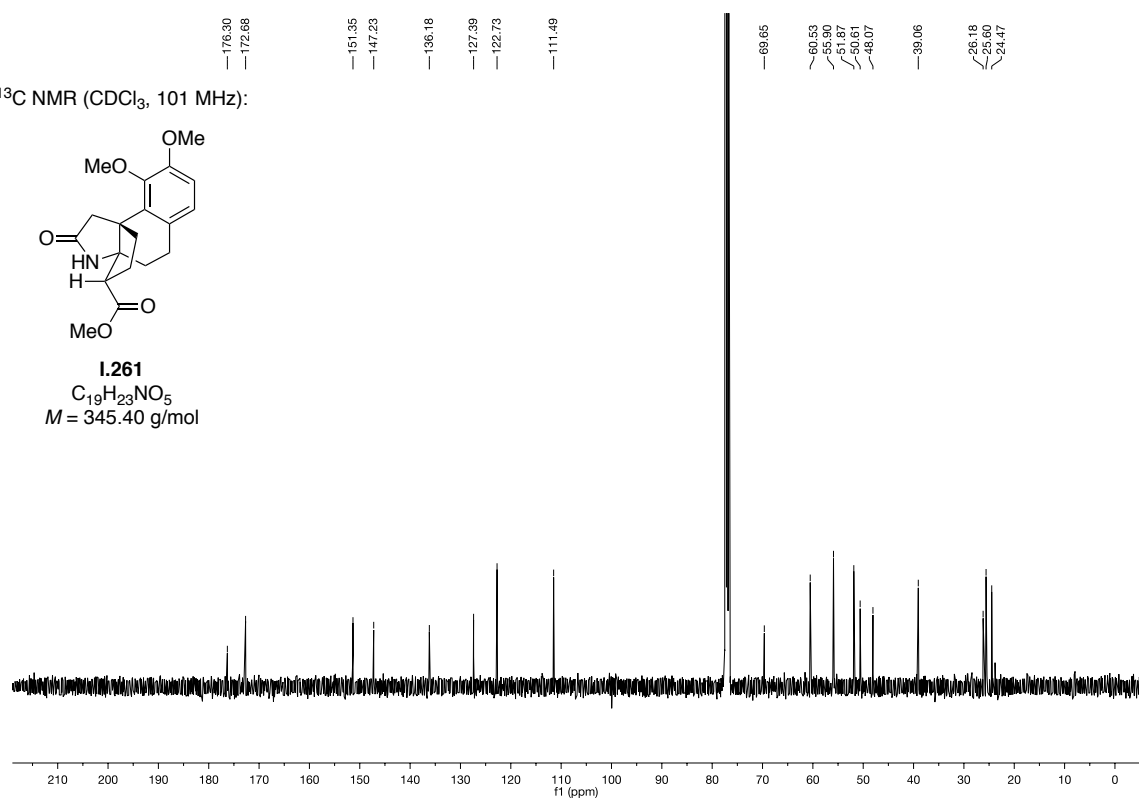
I.218
 C₁₉H₂₁NO₅
 M = 343.38 g/mol

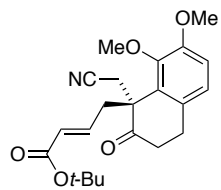




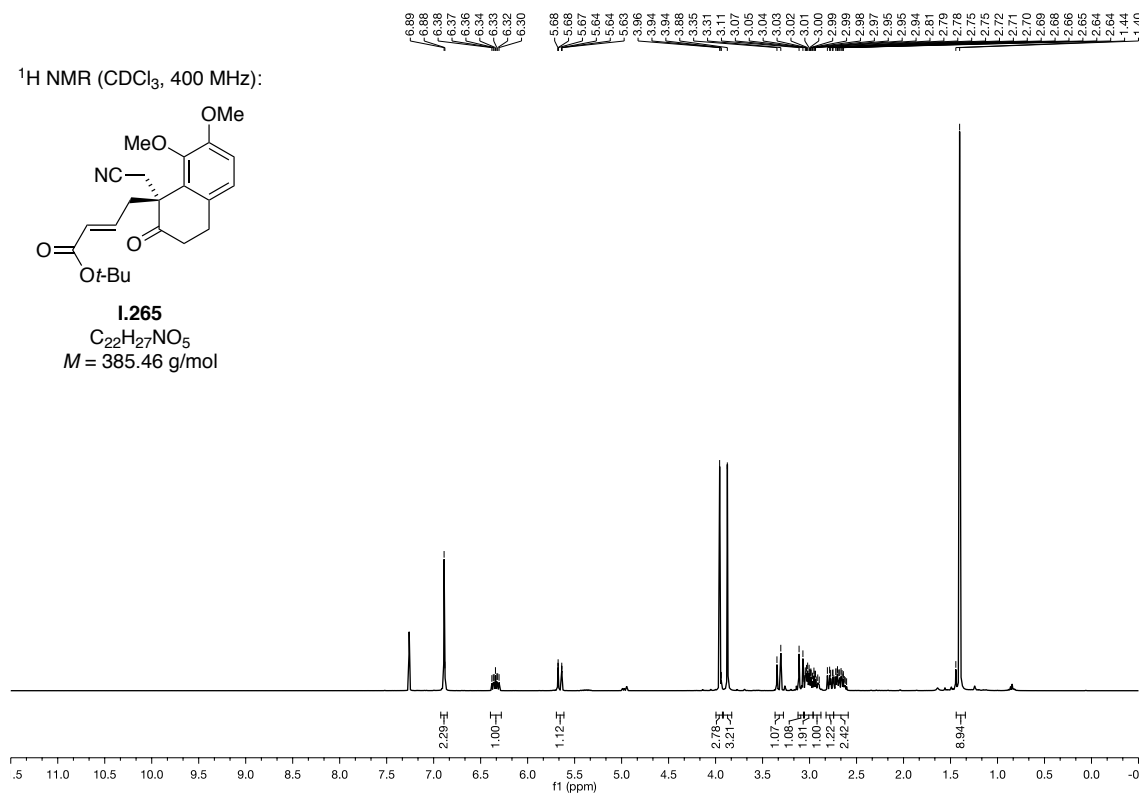
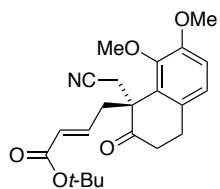




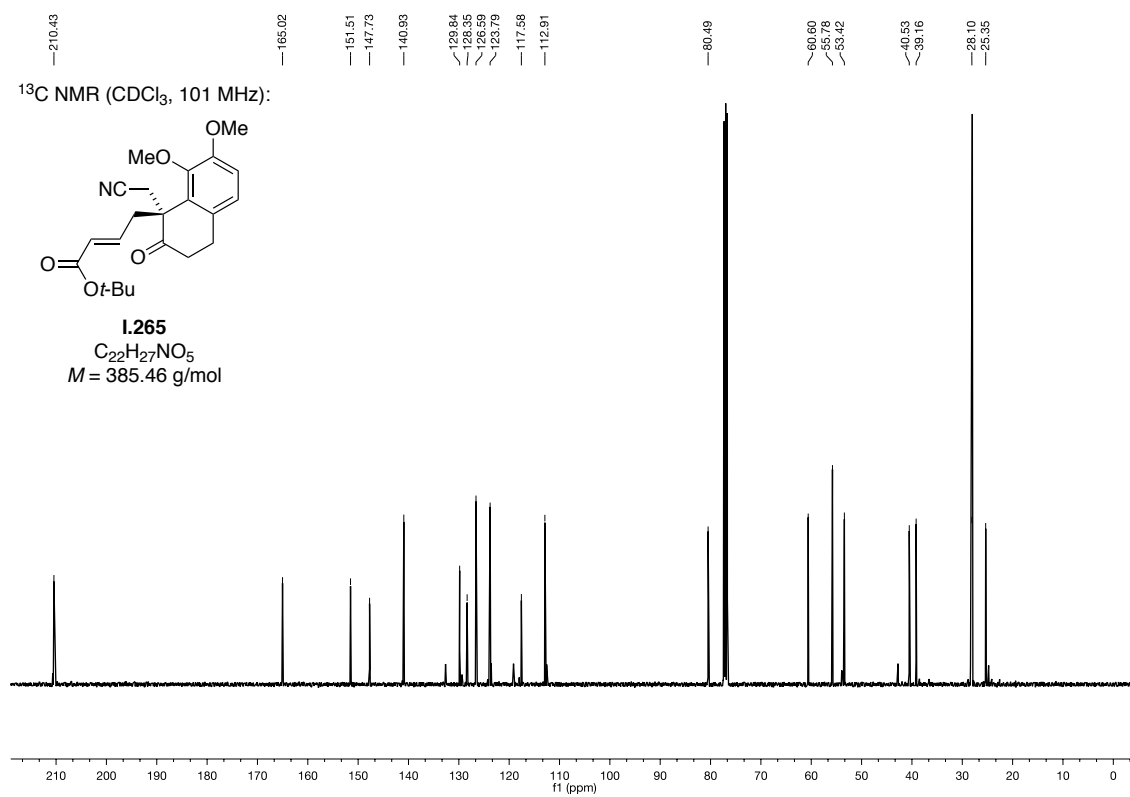
^1H NMR (CDCl_3 , 400 MHz):**I.261**
 $\text{C}_{19}\text{H}_{23}\text{NO}_5$
 $M = 345.40 \text{ g/mol}$
 ^{13}C NMR (CDCl_3 , 101 MHz):**I.261**
 $\text{C}_{19}\text{H}_{23}\text{NO}_5$
 $M = 345.40 \text{ g/mol}$


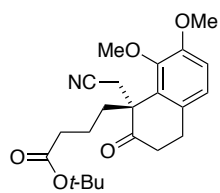
^1H NMR (CDCl_3 , 400 MHz):

1.265
 $\text{C}_{22}\text{H}_{27}\text{NO}_5$
 $M = 385.46 \text{ g/mol}$

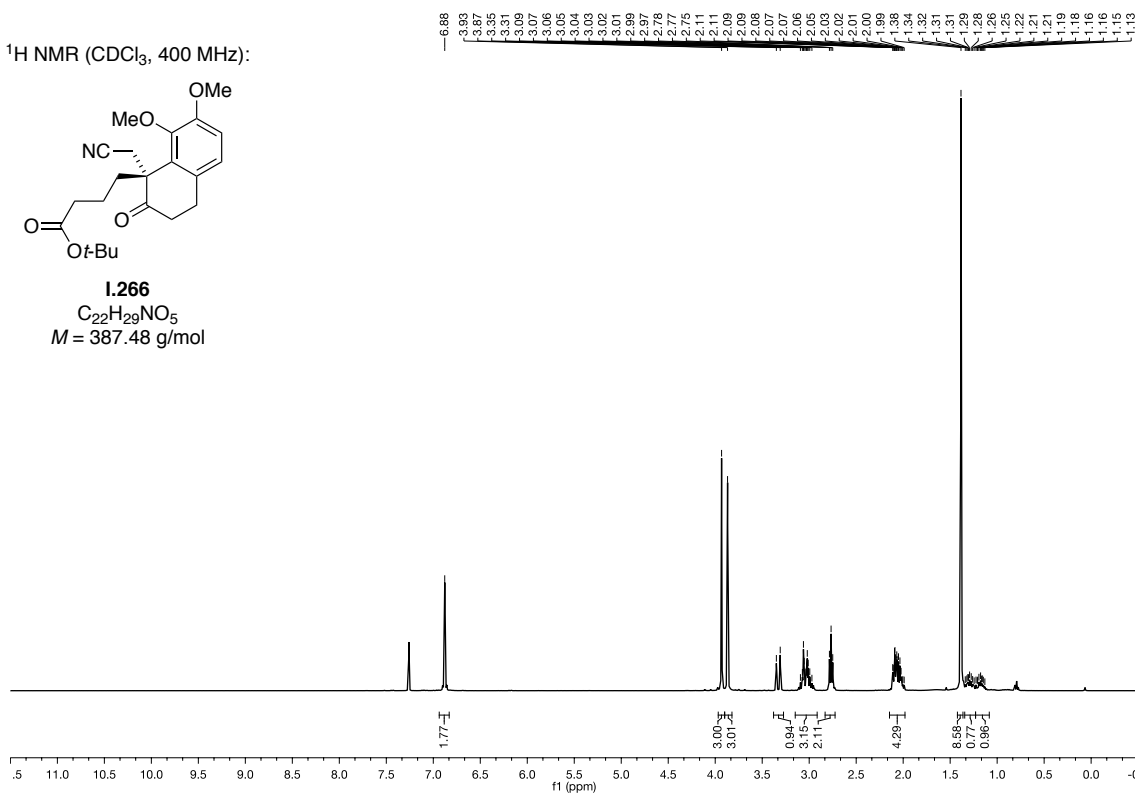
 ^{13}C NMR (CDCl_3 , 101 MHz):

1.265
 $\text{C}_{22}\text{H}_{27}\text{NO}_5$
 $M = 385.46 \text{ g/mol}$

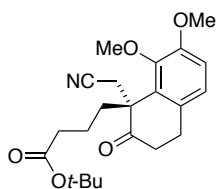


^1H NMR (CDCl_3 , 400 MHz):

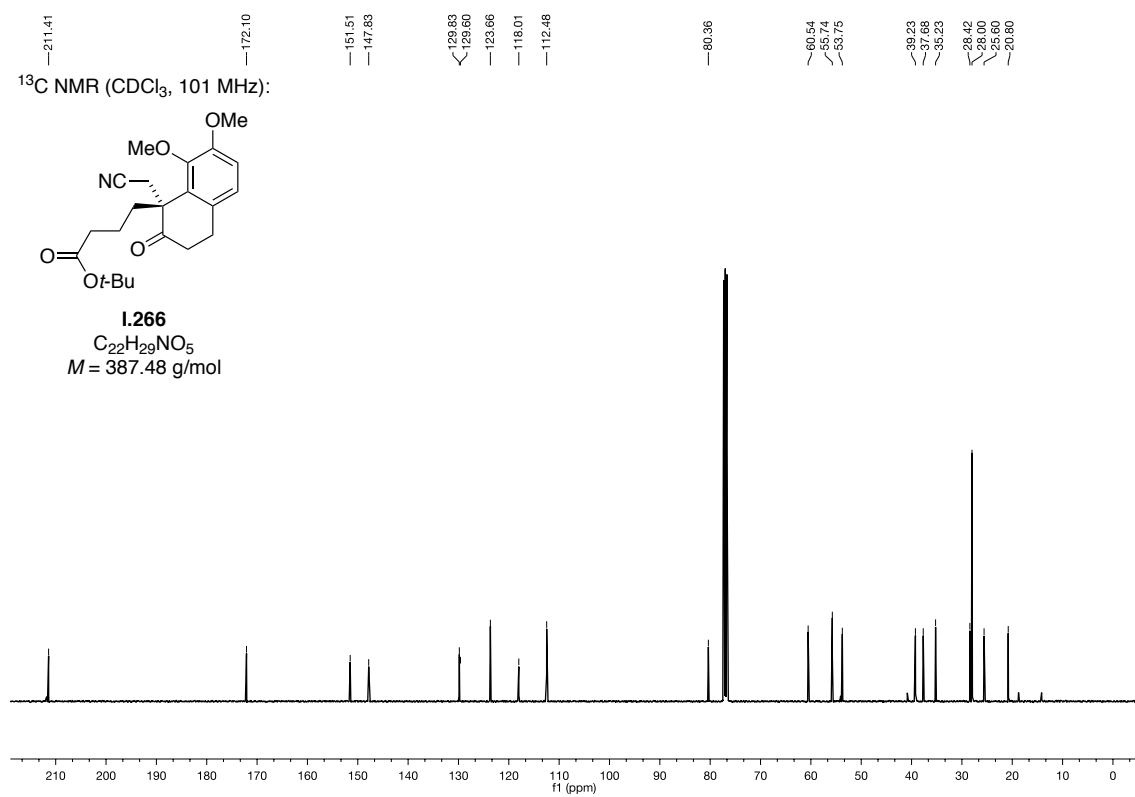
1.266
 $\text{C}_{22}\text{H}_{29}\text{NO}_5$
 $M = 387.48$ g/mol

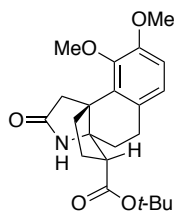


^{13}C NMR (CDCl_3 , 101 MHz):

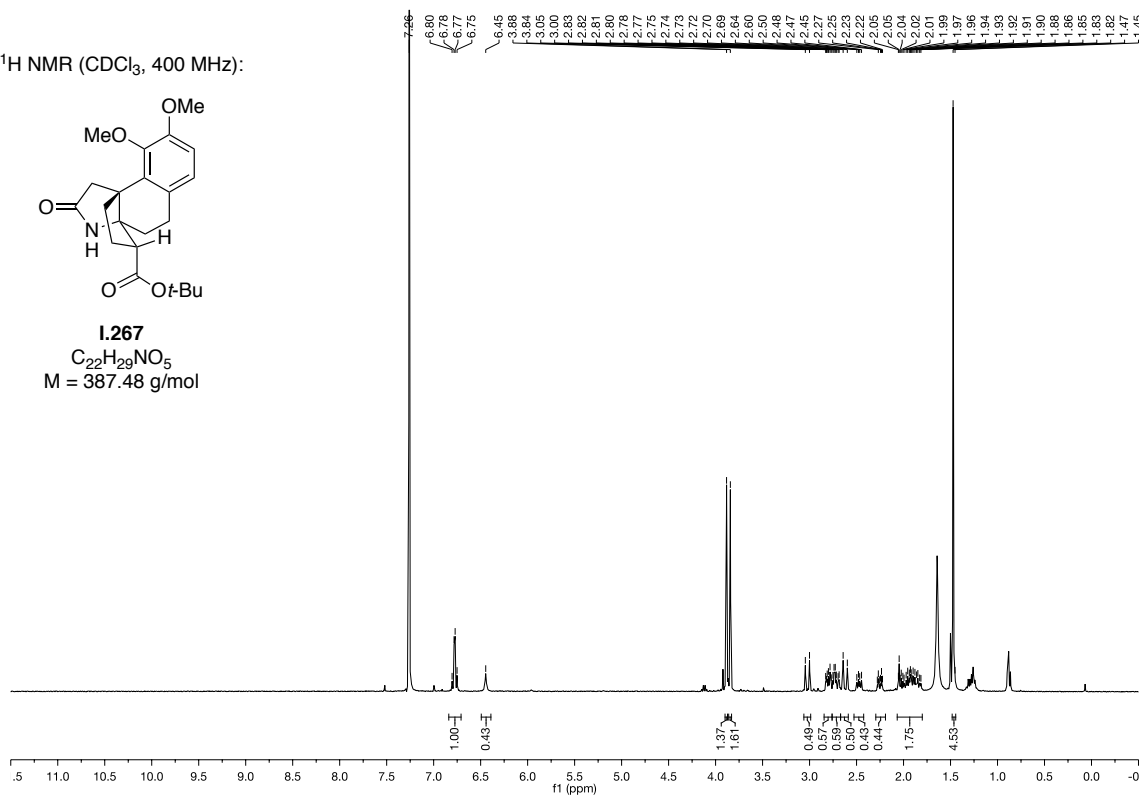
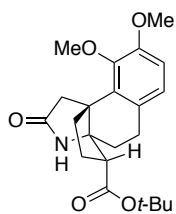


1.266
 $\text{C}_{22}\text{H}_{29}\text{NO}_5$
 $M = 387.48$ g/mol

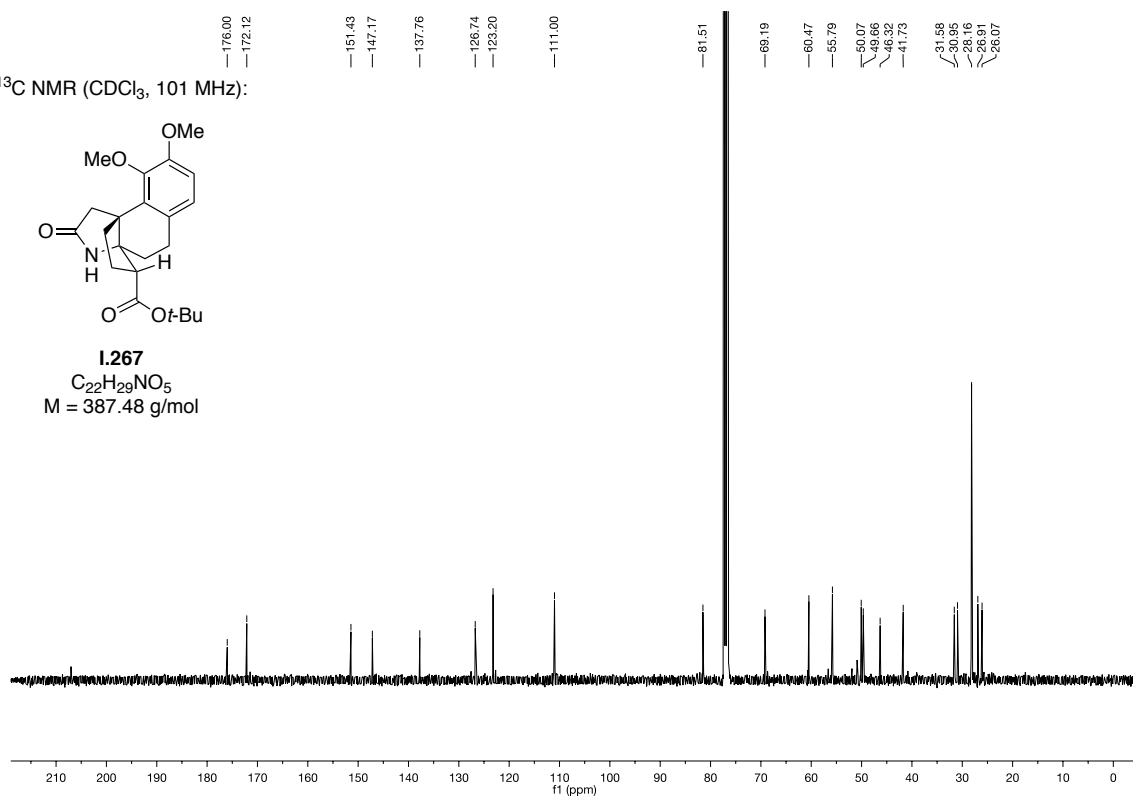


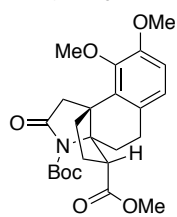
^1H NMR (CDCl_3 , 400 MHz):

1.267
 $\text{C}_{22}\text{H}_{29}\text{NO}_5$
 $M = 387.48 \text{ g/mol}$

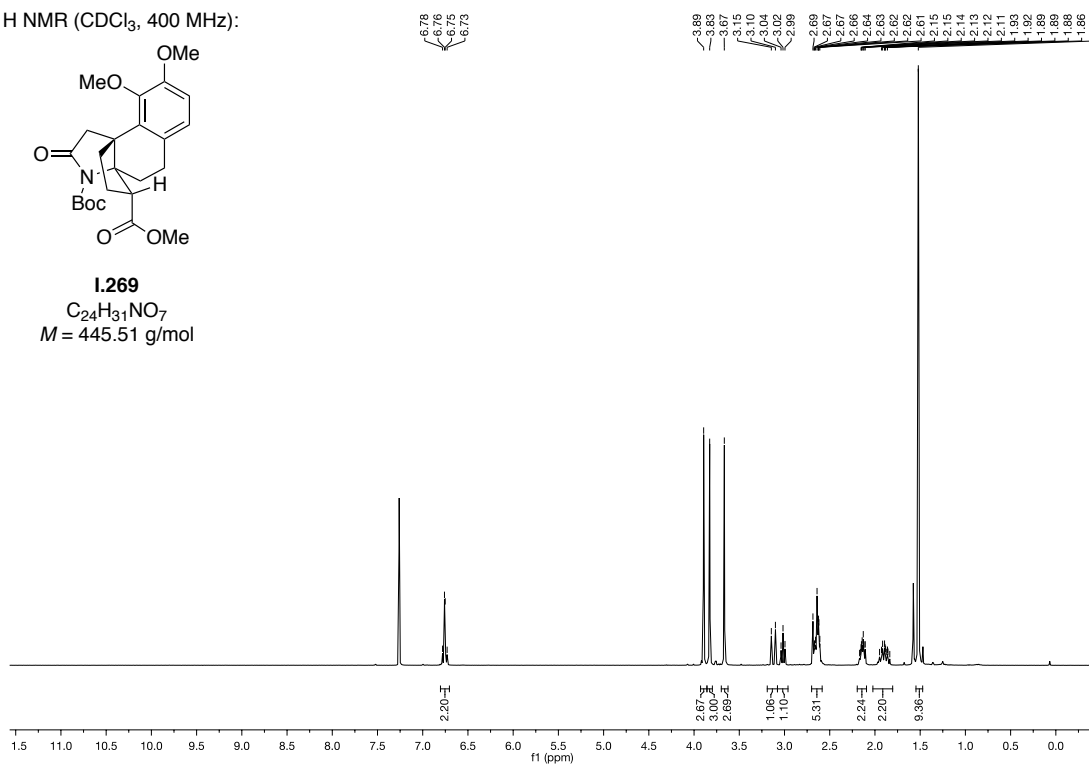
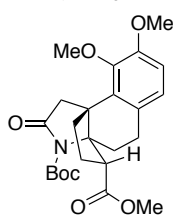
 ^{13}C NMR (CDCl_3 , 101 MHz):

1.267
 $\text{C}_{22}\text{H}_{29}\text{NO}_5$
 $M = 387.48 \text{ g/mol}$

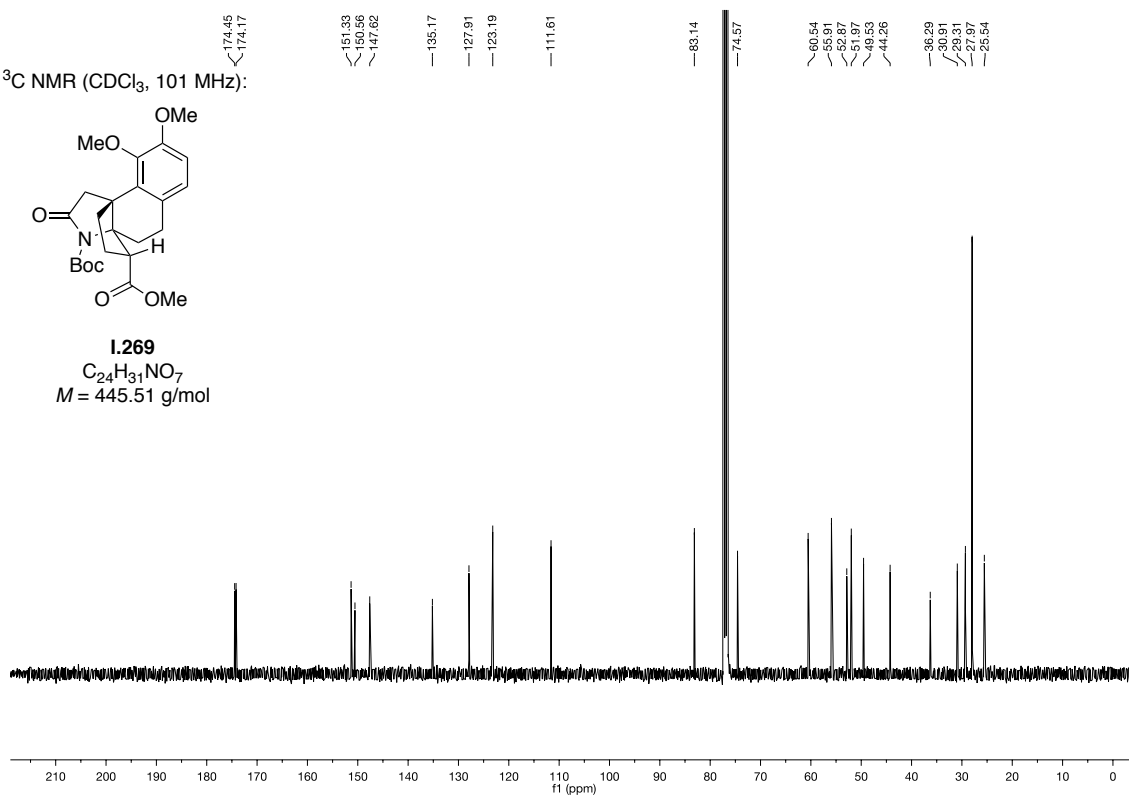


$^1\text{H NMR}$ (CDCl_3 , 400 MHz):

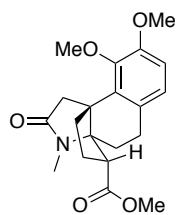
1.269
 $\text{C}_{24}\text{H}_{31}\text{NO}_7$
 $M = 445.51 \text{ g/mol}$

 $^{13}\text{C NMR}$ (CDCl_3 , 101 MHz):

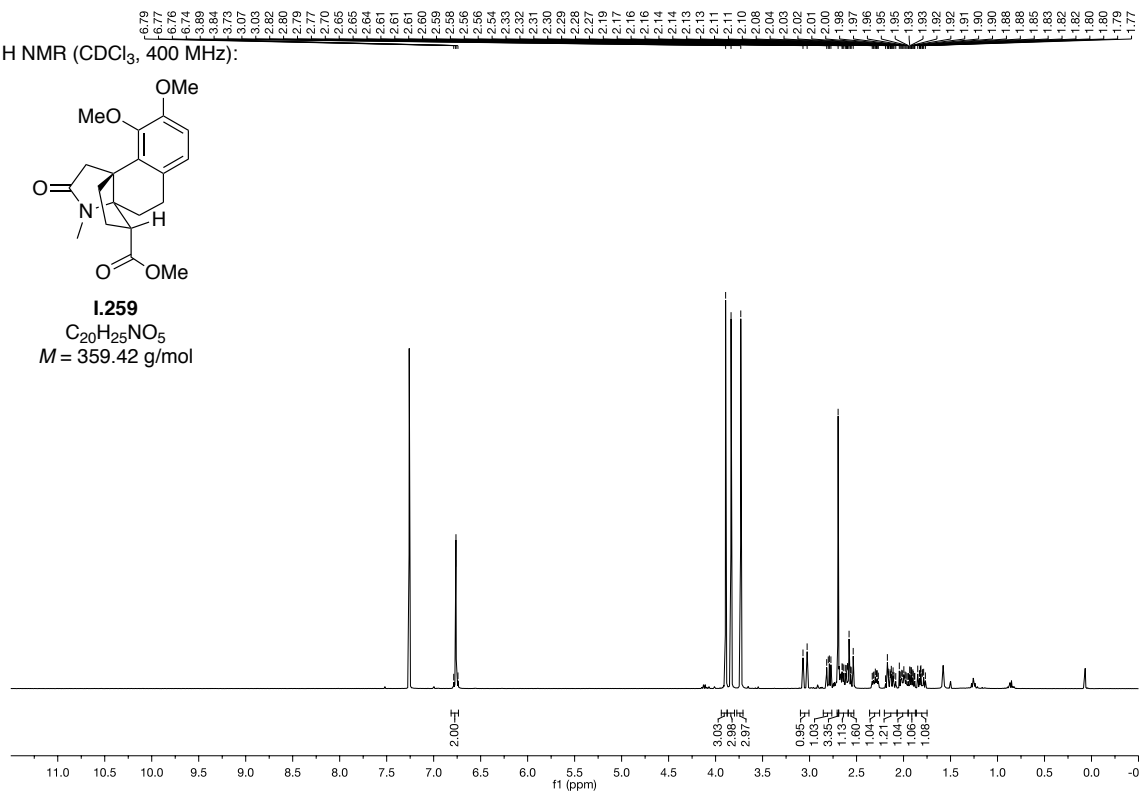
1.269
 $\text{C}_{24}\text{H}_{31}\text{NO}_7$
 $M = 445.51 \text{ g/mol}$



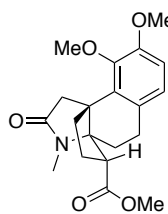
¹H NMR (CDCl₃, 400 MHz):



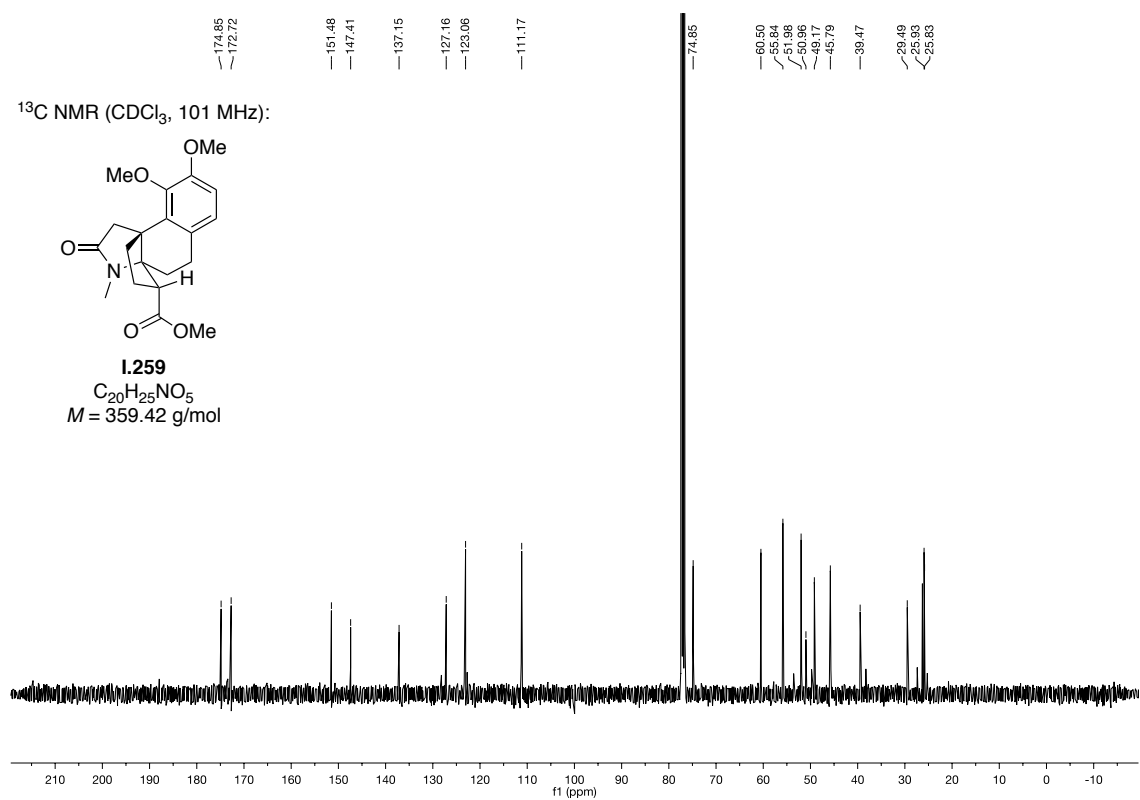
1.259
C₂₀H₂₅NO₅
M = 359.42 g/mol

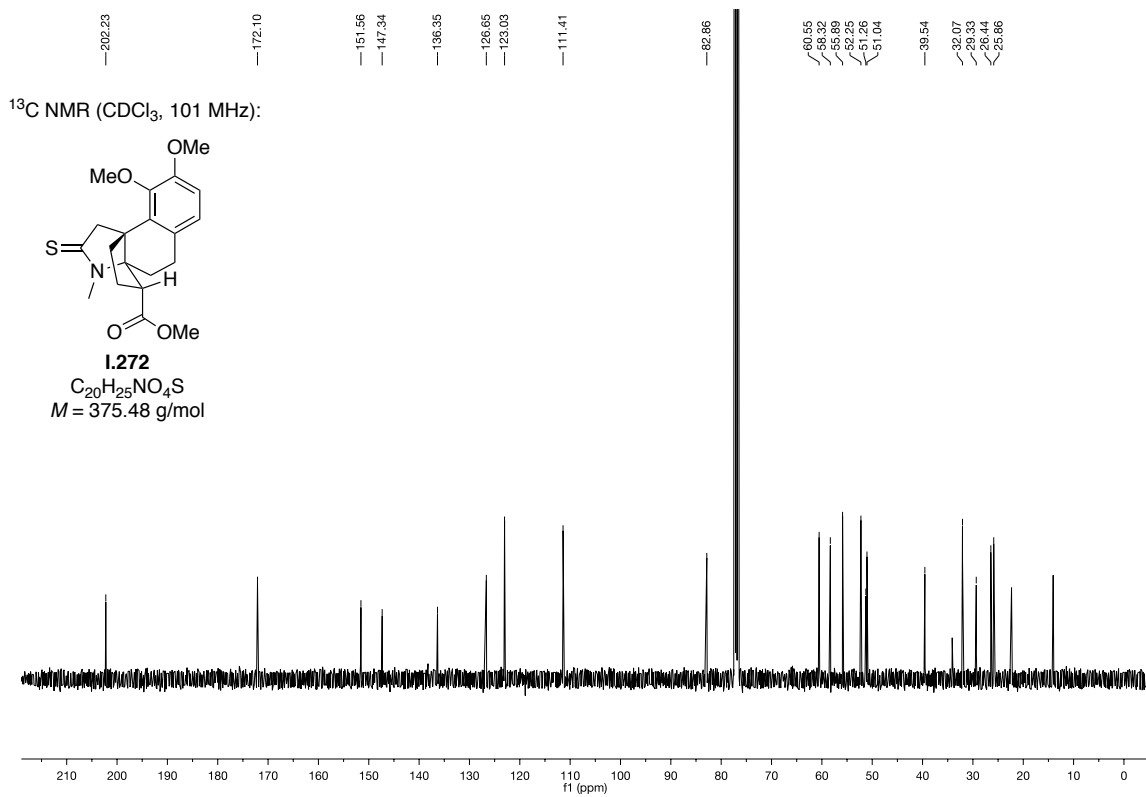
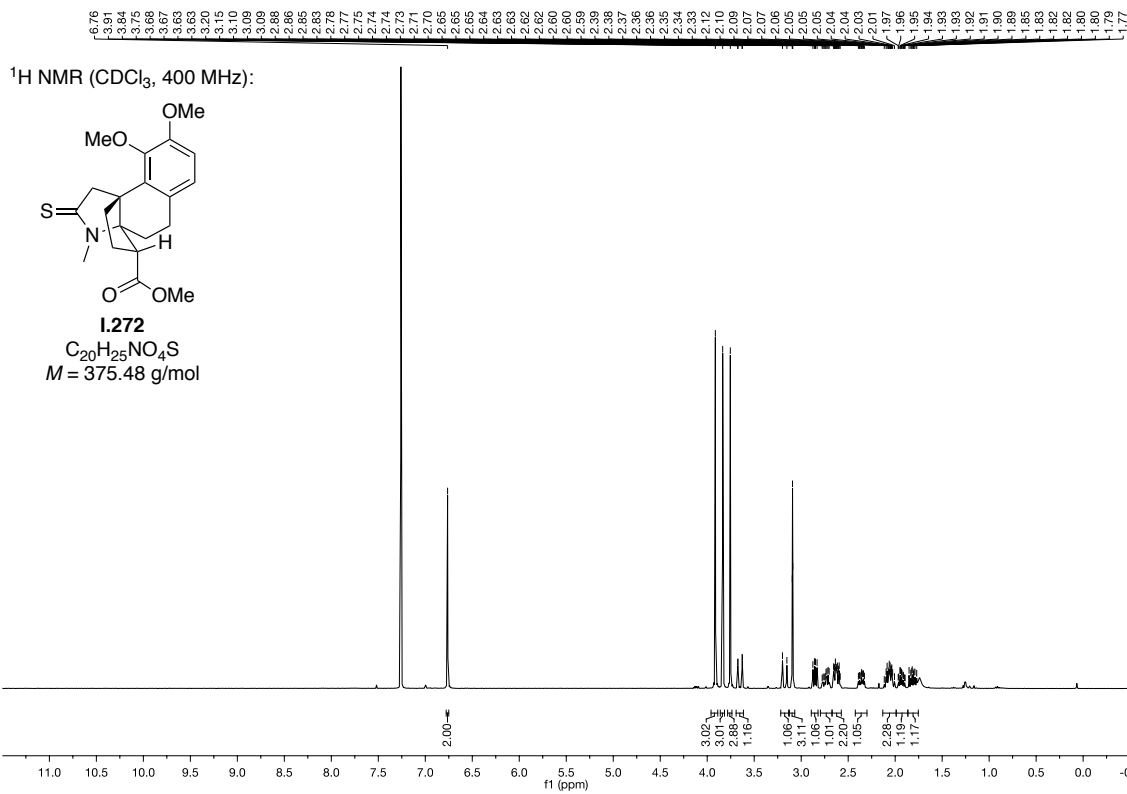


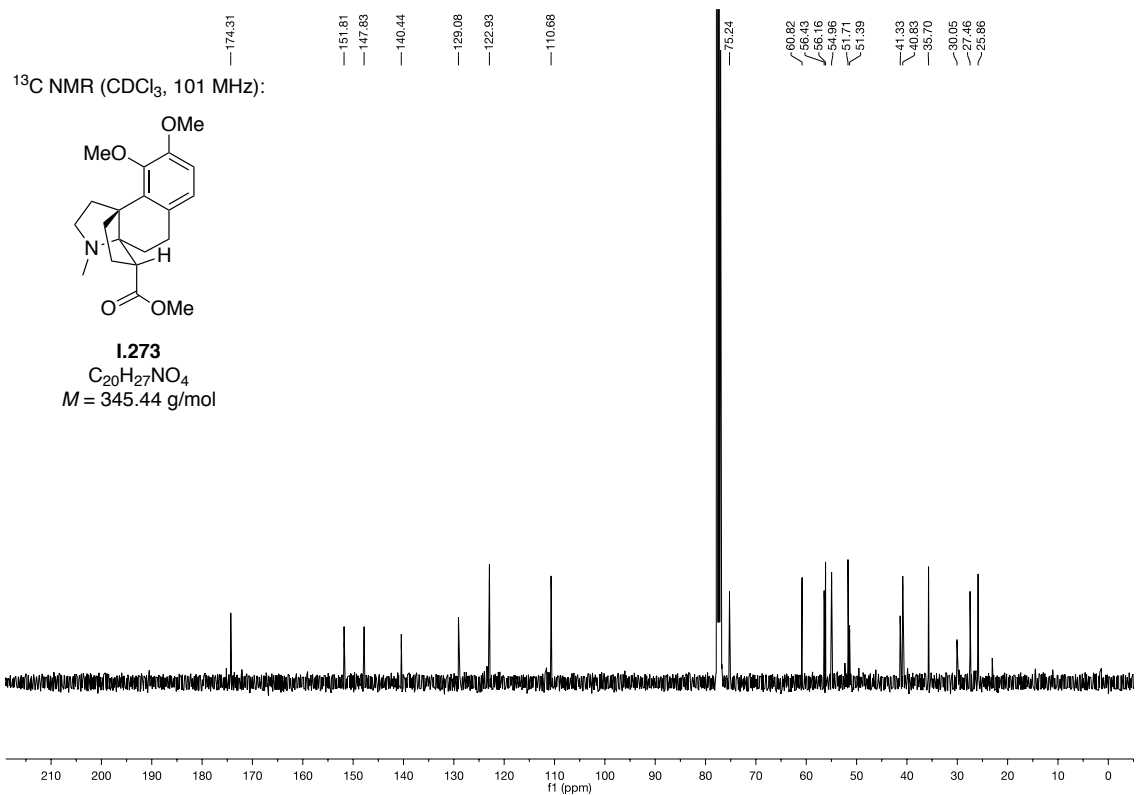
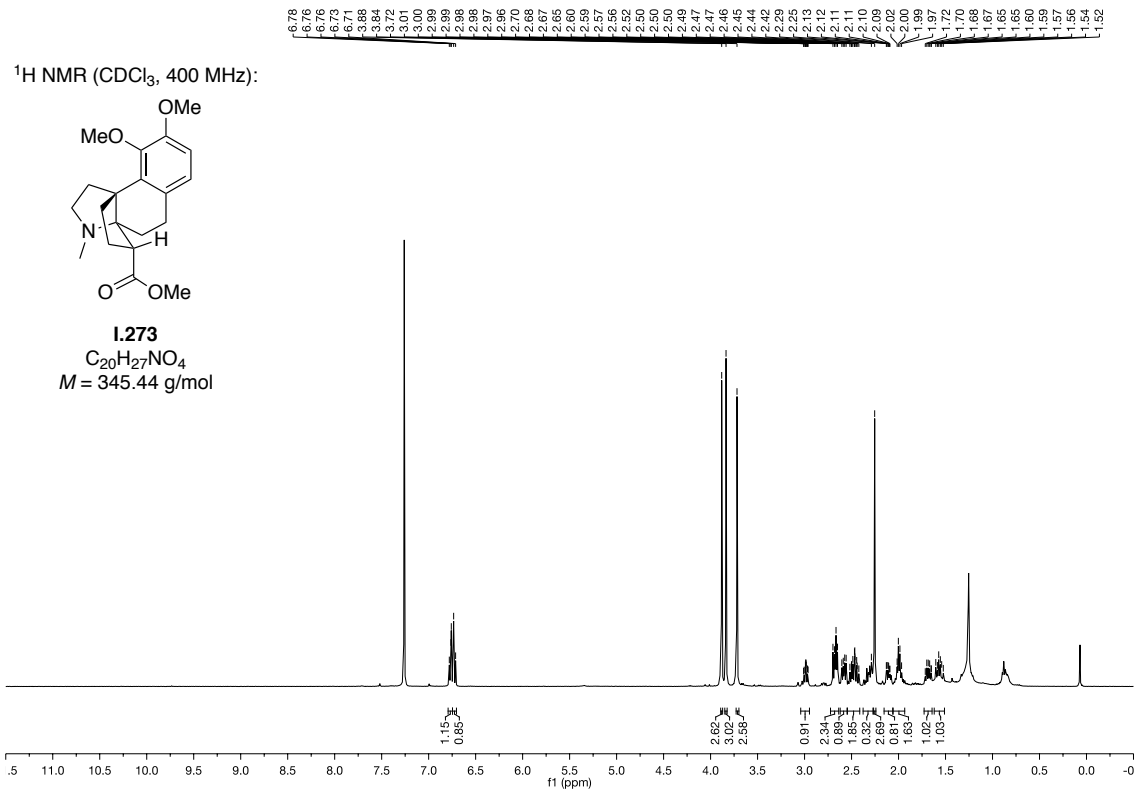
¹³C NMR (CDCl₃, 101 MHz):

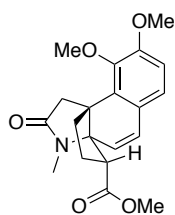


1.259
C₂₀H₂₅NO₅
M = 359.42 g/mol

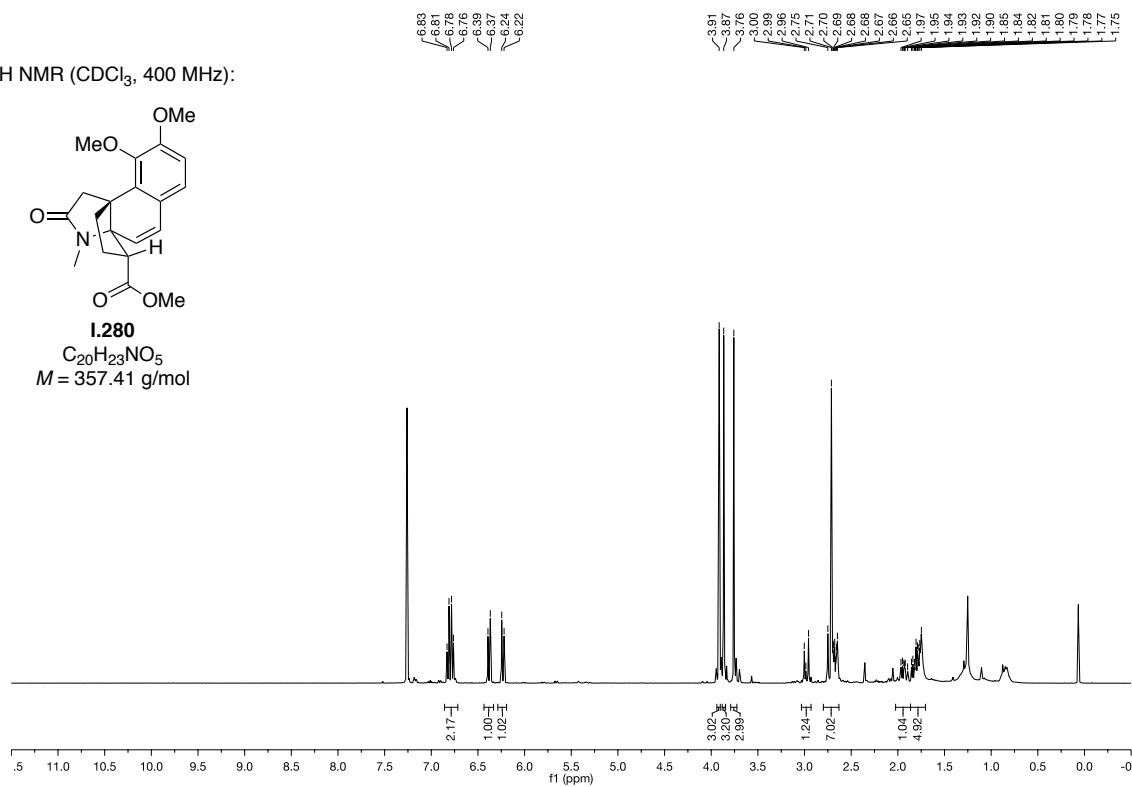
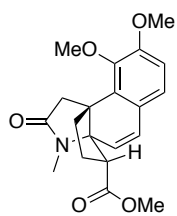




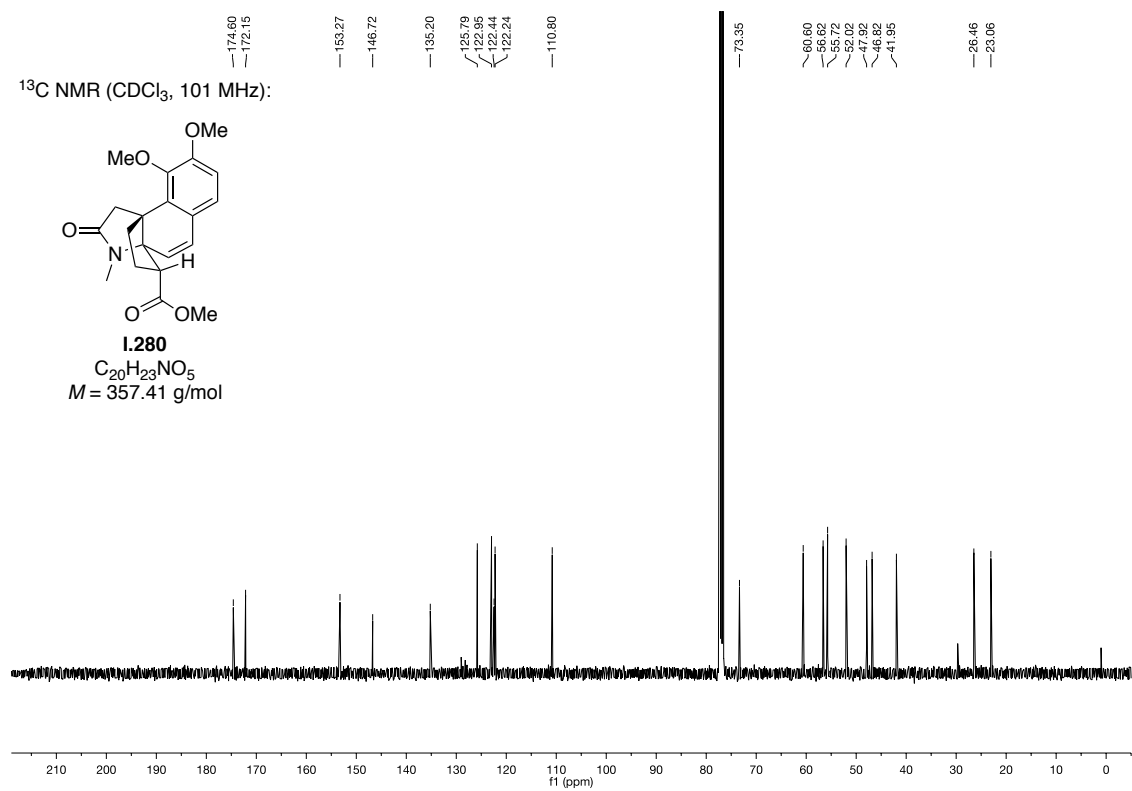


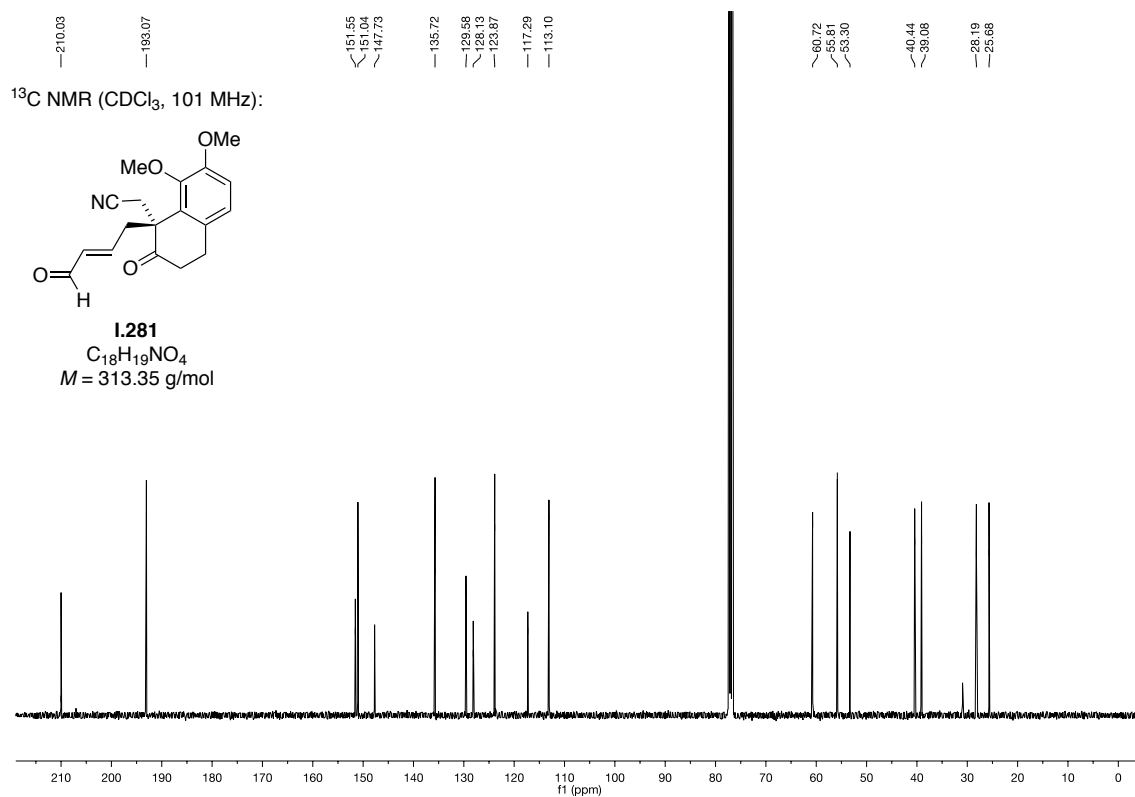
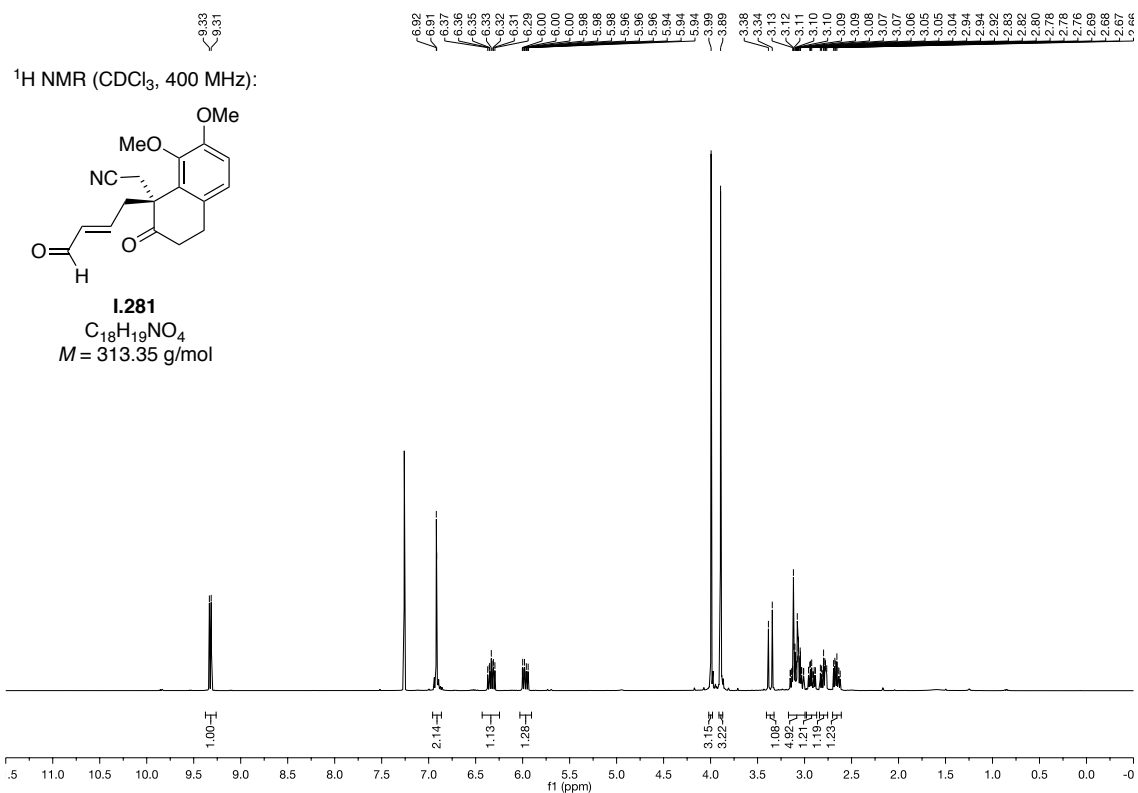
^1H NMR (CDCl_3 , 400 MHz):

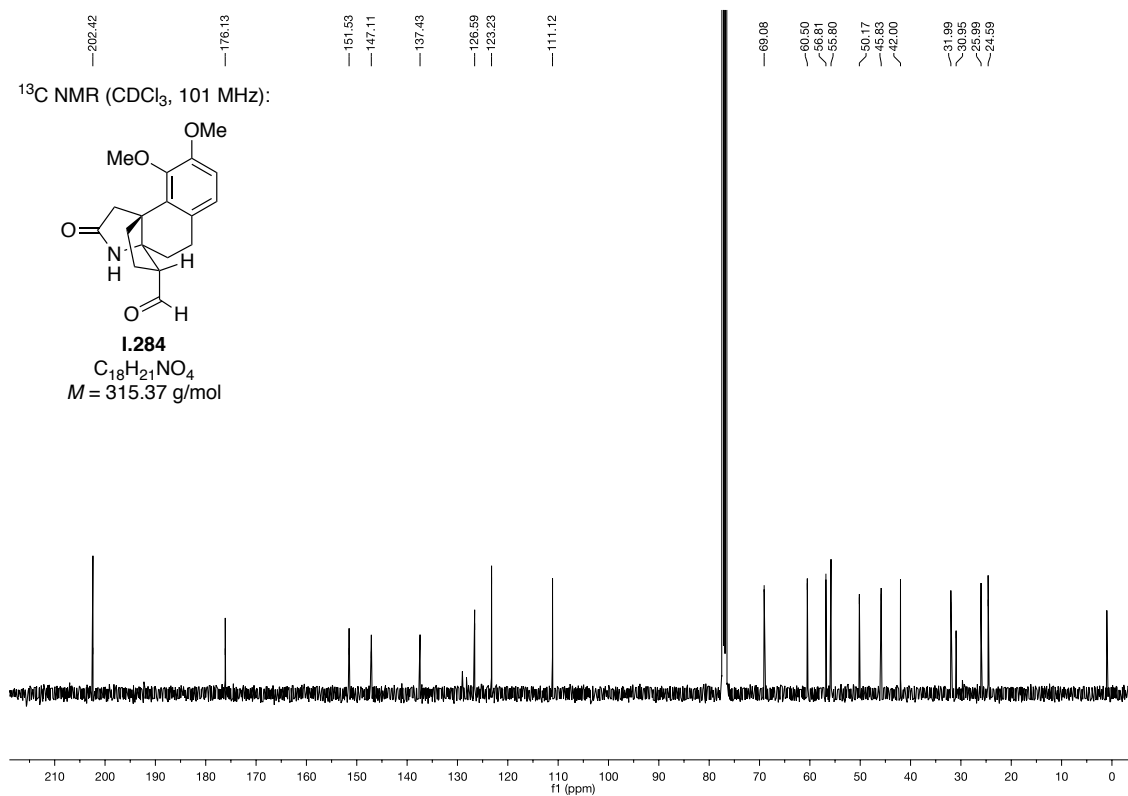
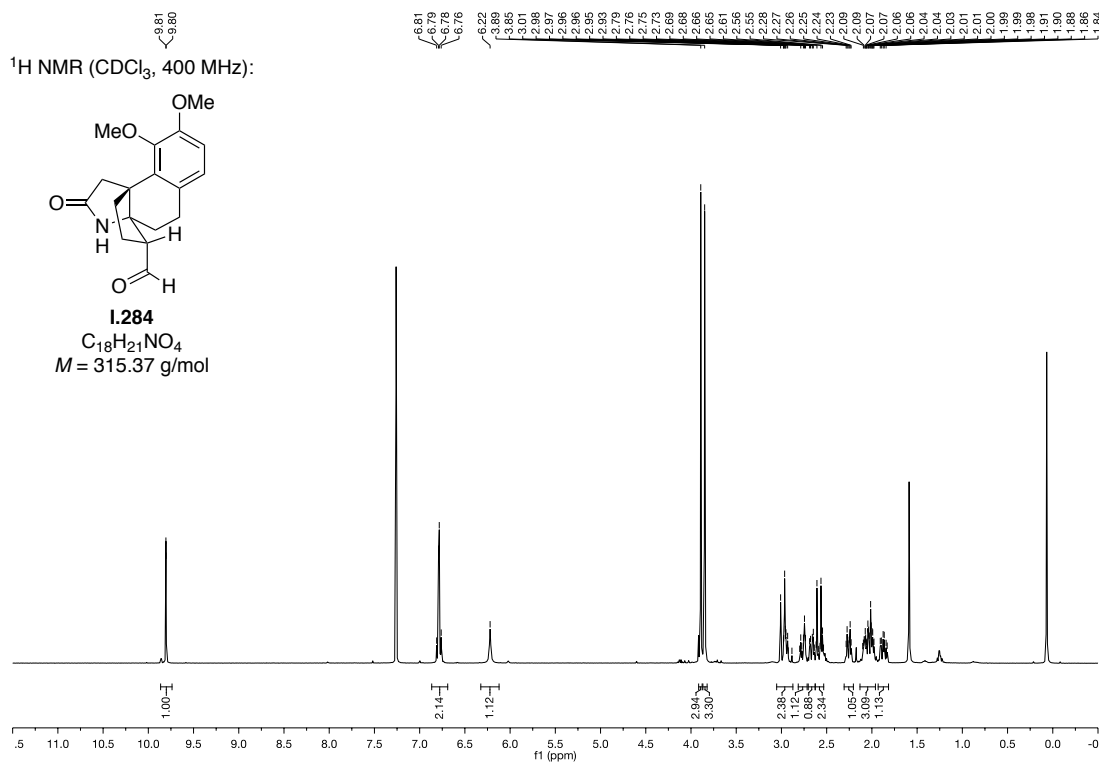
1.280
 $\text{C}_{20}\text{H}_{23}\text{NO}_5$
 $M = 357.41$ g/mol

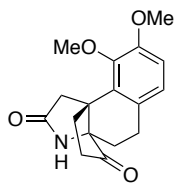
 ^{13}C NMR (CDCl_3 , 101 MHz):

1.280
 $\text{C}_{20}\text{H}_{23}\text{NO}_5$
 $M = 357.41$ g/mol

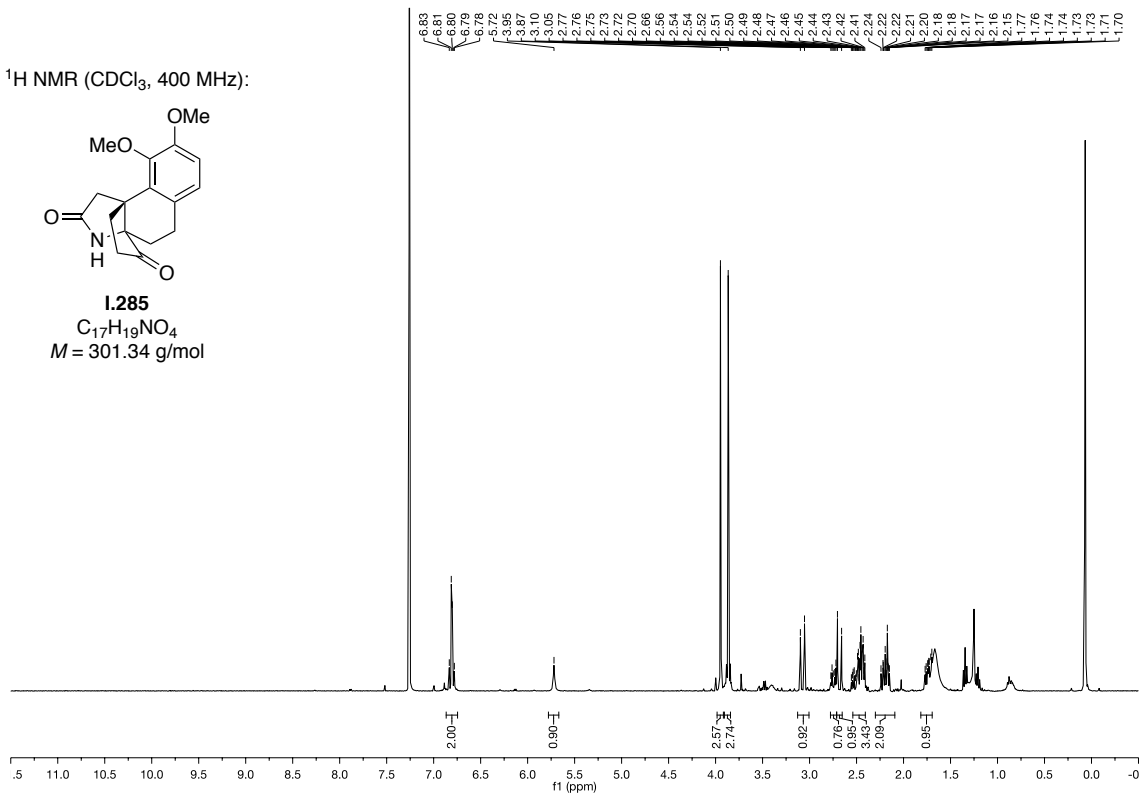
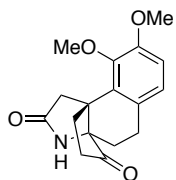




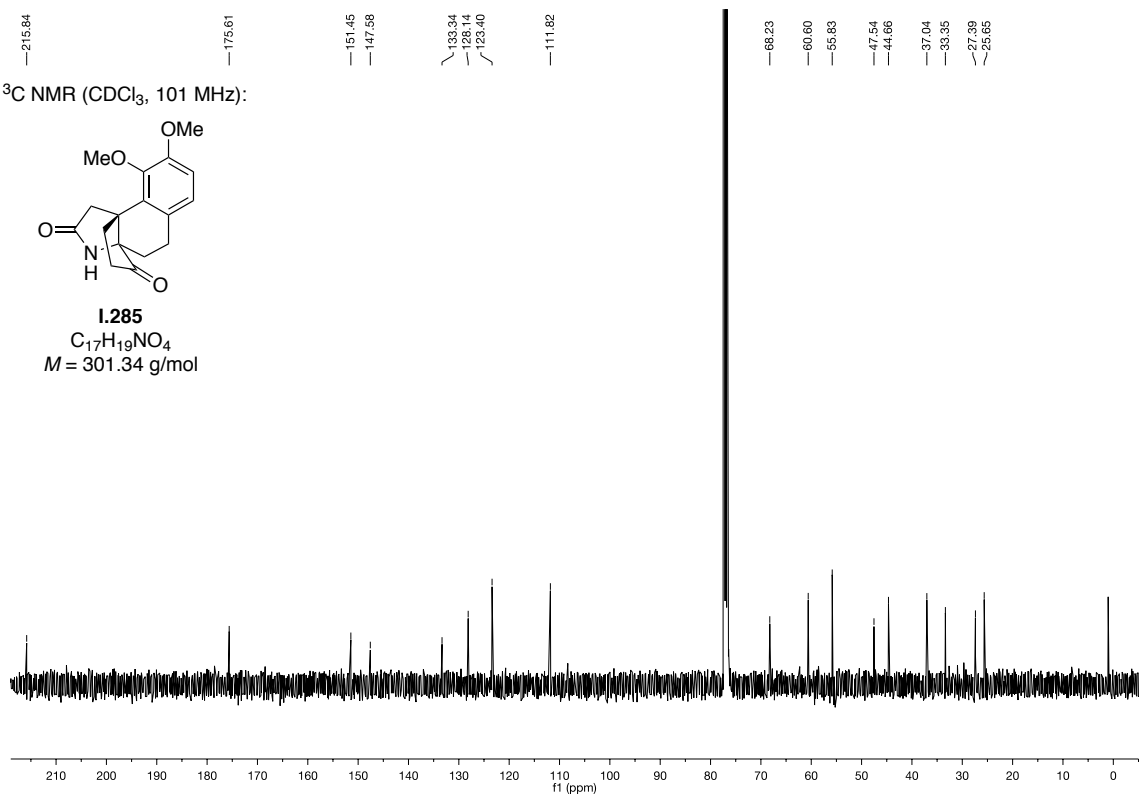


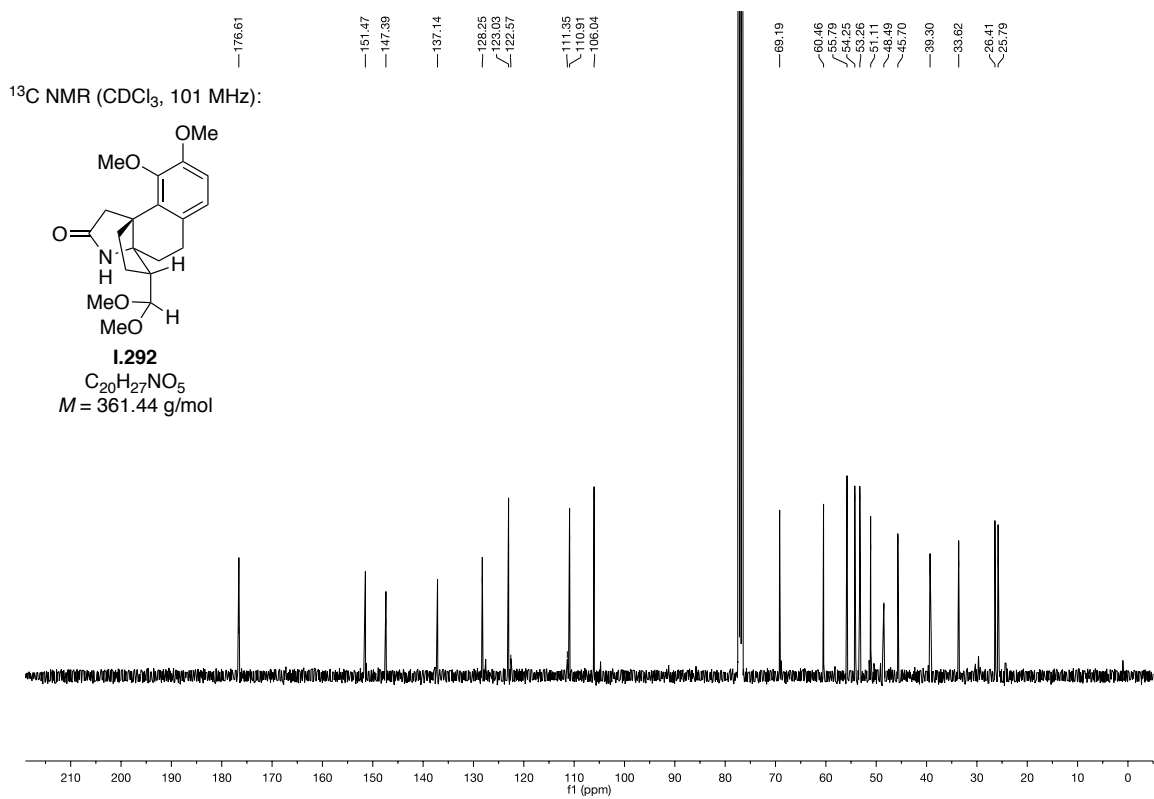
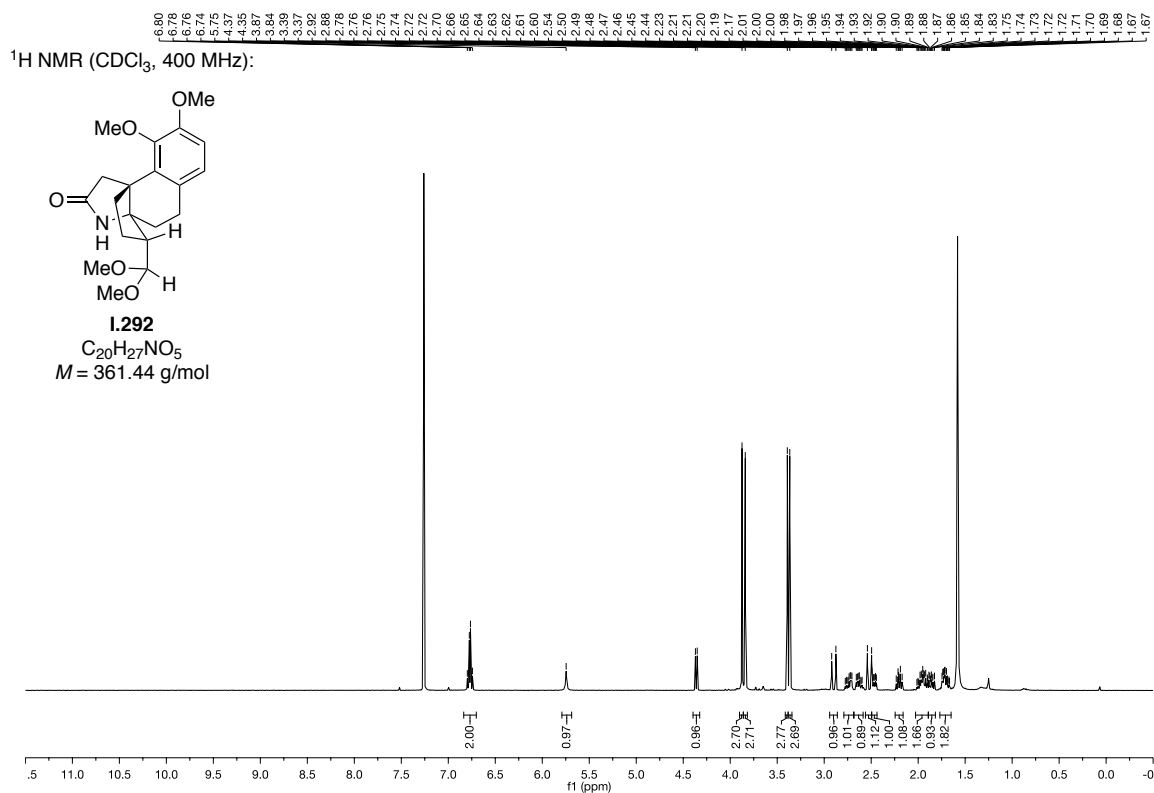
¹H NMR (CDCl₃, 400 MHz):

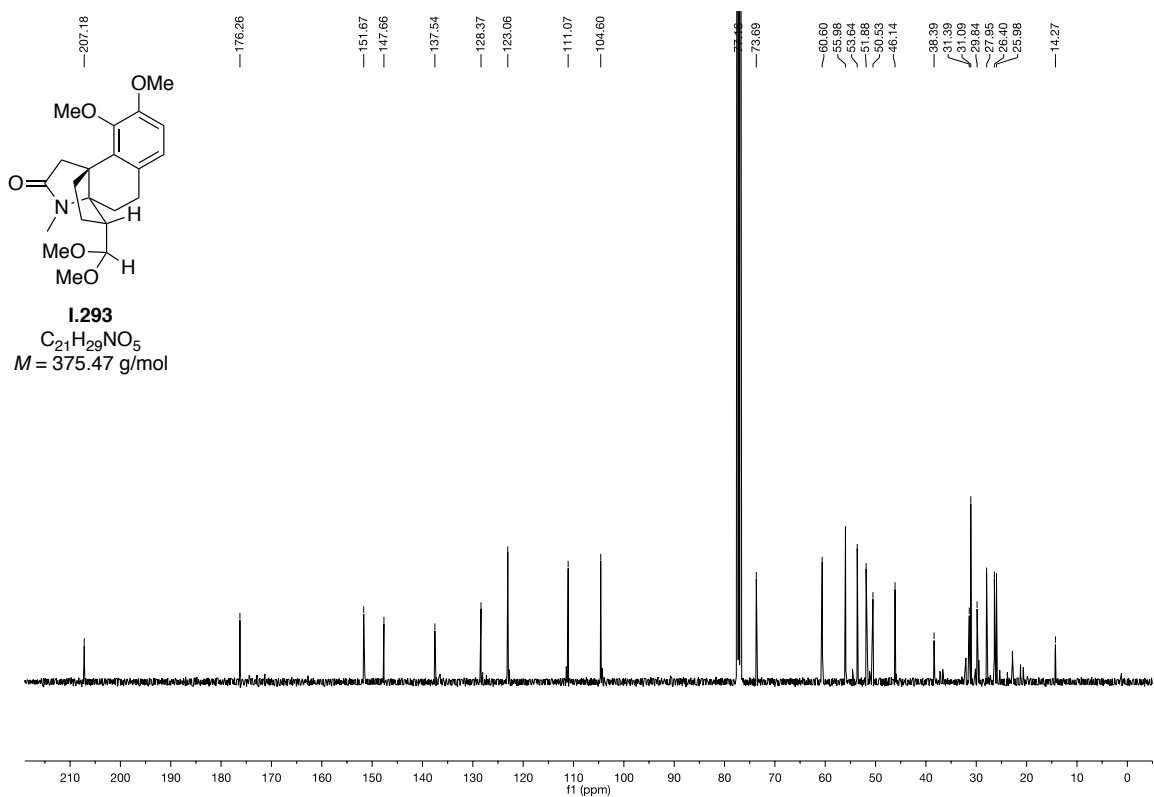
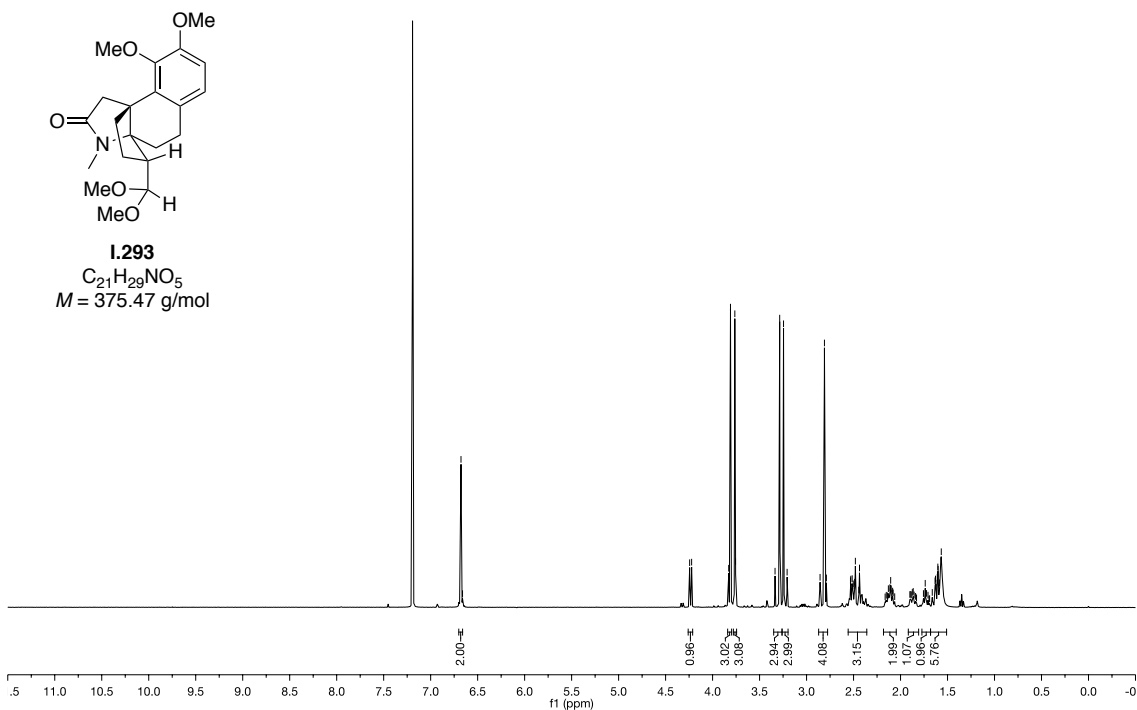
1.285
C₁₇H₁₉NO₄
M = 301.34 g/mol

¹³C NMR (CDCl₃, 101 MHz):

1.285
C₁₇H₁₉NO₄
M = 301.34 g/mol

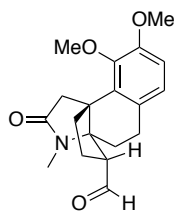




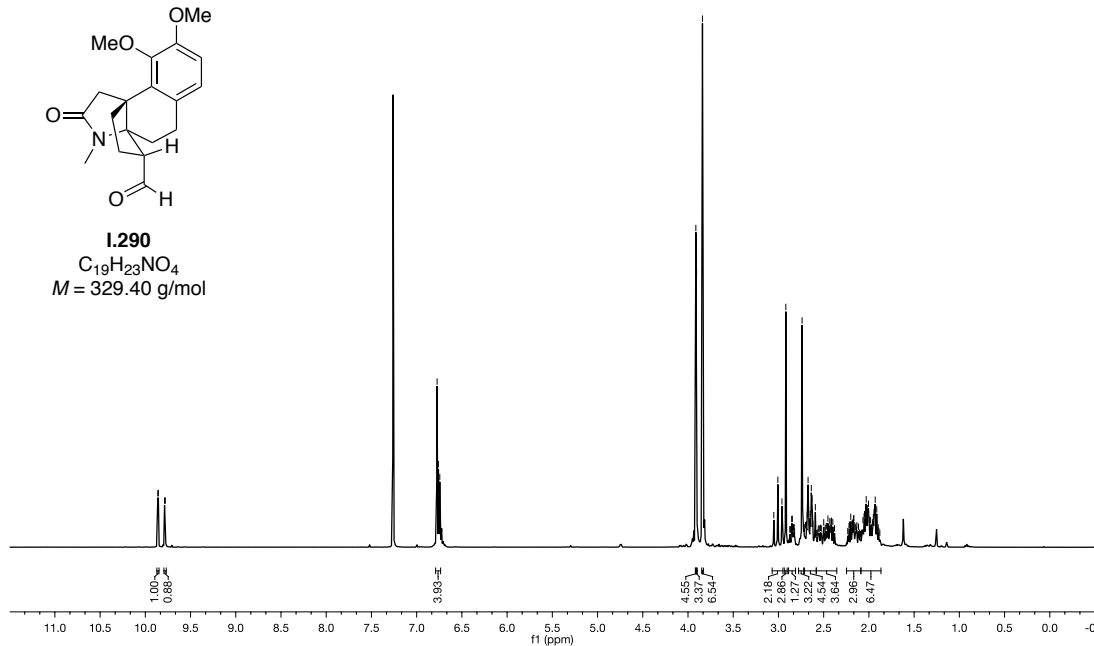
$^1\text{H NMR}$ (CDCl_3 , 400 MHz):

1.96, 1.94, 1.91, 1.89, 1.87, 1.85, 1.83, 1.81, 1.79, 1.77, 1.75, 1.73, 1.71, 1.69, 1.67, 1.65, 1.63, 1.61, 1.59, 1.57, 1.55, 1.53, 1.51, 1.49, 1.47, 1.45, 1.43, 1.41, 1.39, 1.37, 1.35, 1.33, 1.31, 1.29, 1.27, 1.25, 1.23, 1.21, 1.19, 1.17, 1.15, 1.13, 1.11, 1.09, 1.07, 1.05, 1.03, 1.01, 0.99, 0.97, 0.95, 0.93, 0.91, 0.89, 0.87, 0.85, 0.83, 0.81, 0.79, 0.77, 0.75, 0.73, 0.71, 0.69, 0.67, 0.65, 0.63, 0.61, 0.59, 0.57, 0.55, 0.53, 0.51, 0.49, 0.47, 0.45, 0.43, 0.41, 0.39, 0.37, 0.35, 0.33, 0.31, 0.29, 0.27, 0.25, 0.23, 0.21, 0.19, 0.17, 0.15, 0.13, 0.11, 0.09, 0.07, 0.05, 0.03, 0.01, -0.01, -0.03, -0.05, -0.07, -0.09, -0.11, -0.13, -0.15, -0.17, -0.19, -0.21, -0.23, -0.25, -0.27, -0.29, -0.31, -0.33, -0.35, -0.37, -0.39, -0.41, -0.43, -0.45, -0.47, -0.49, -0.51, -0.53, -0.55, -0.57, -0.59, -0.61, -0.63, -0.65, -0.67, -0.69, -0.71, -0.73, -0.75, -0.77, -0.79, -0.81, -0.83, -0.85, -0.87, -0.89, -0.91, -0.93, -0.95, -0.97, -0.99, -1.01, -1.03, -1.05, -1.07, -1.09, -1.11, -1.13, -1.15, -1.17, -1.19, -1.21, -1.23, -1.25, -1.27, -1.29, -1.31, -1.33, -1.35, -1.37, -1.39, -1.41, -1.43, -1.45, -1.47, -1.49, -1.51, -1.53, -1.55, -1.57, -1.59, -1.61, -1.63, -1.65, -1.67, -1.69, -1.71, -1.73, -1.75, -1.77, -1.79, -1.81, -1.83, -1.85, -1.87, -1.89, -1.91, -1.93, -1.95, -1.96, -1.94, -1.92, -1.90, -1.89

¹H NMR (CDCl₃, 400 MHz):

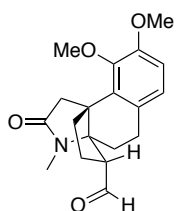


1.290
C₁₉H₂₃NO₄
M = 329.40 g/mol

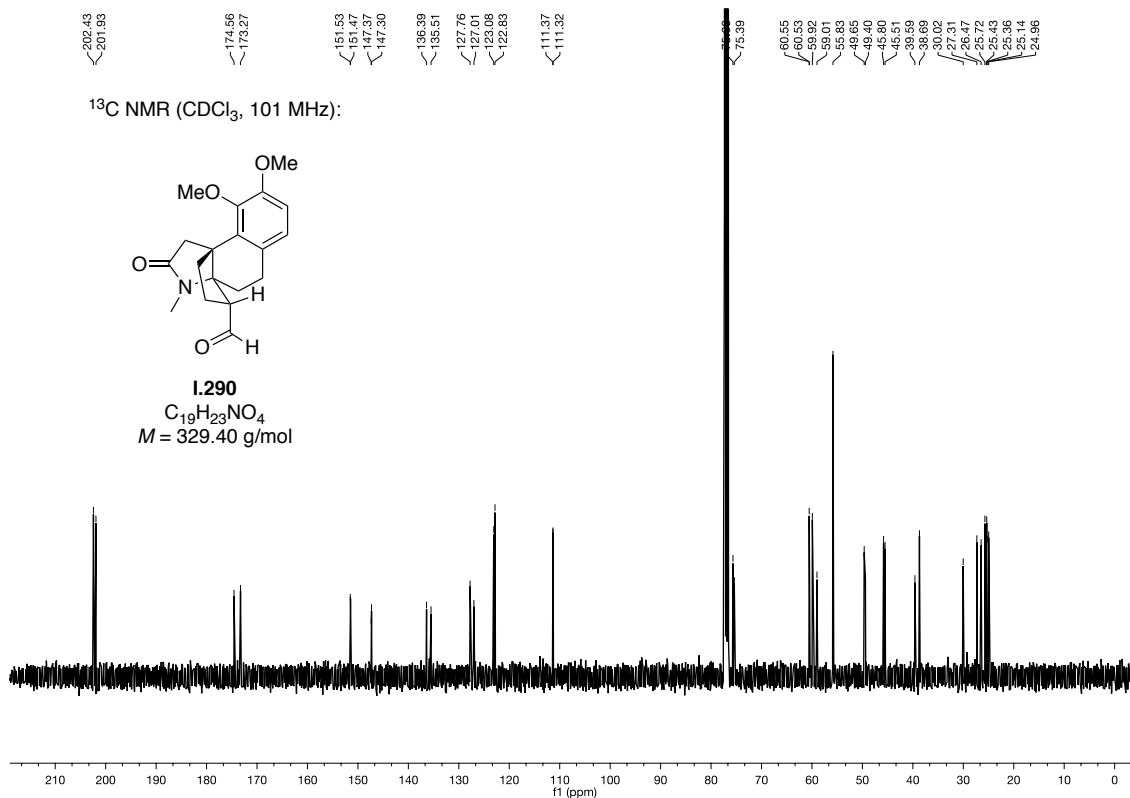


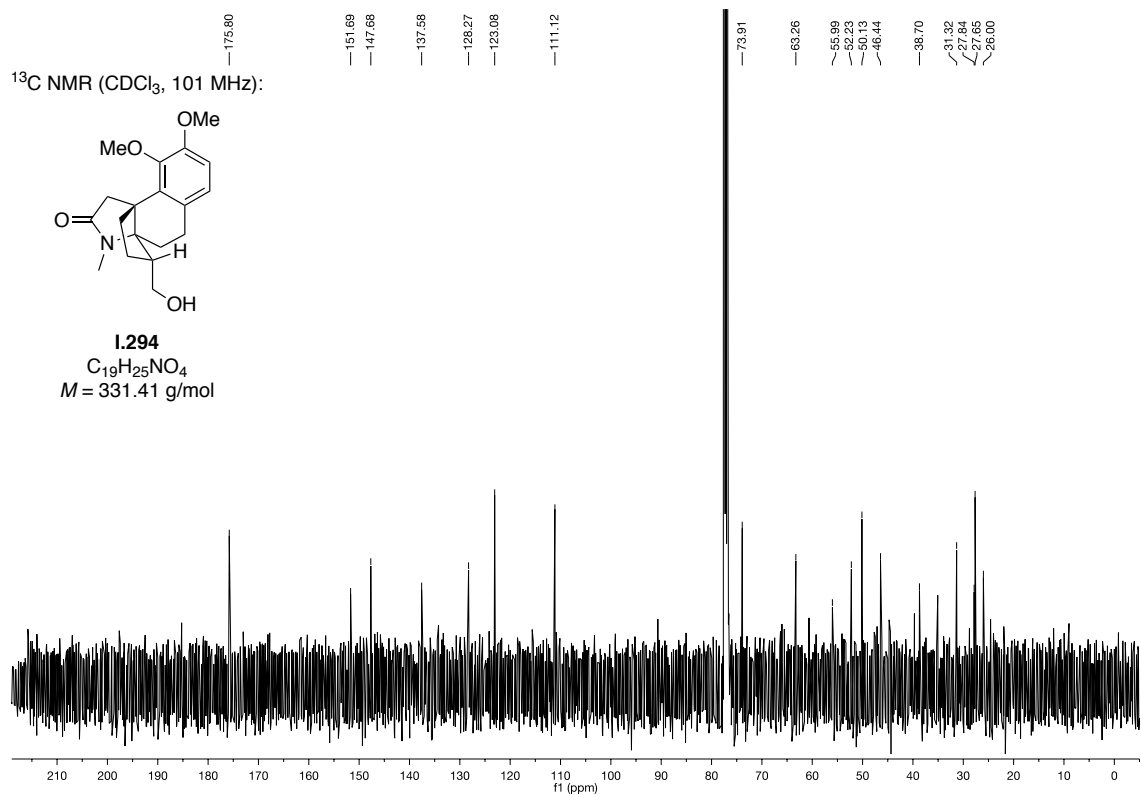
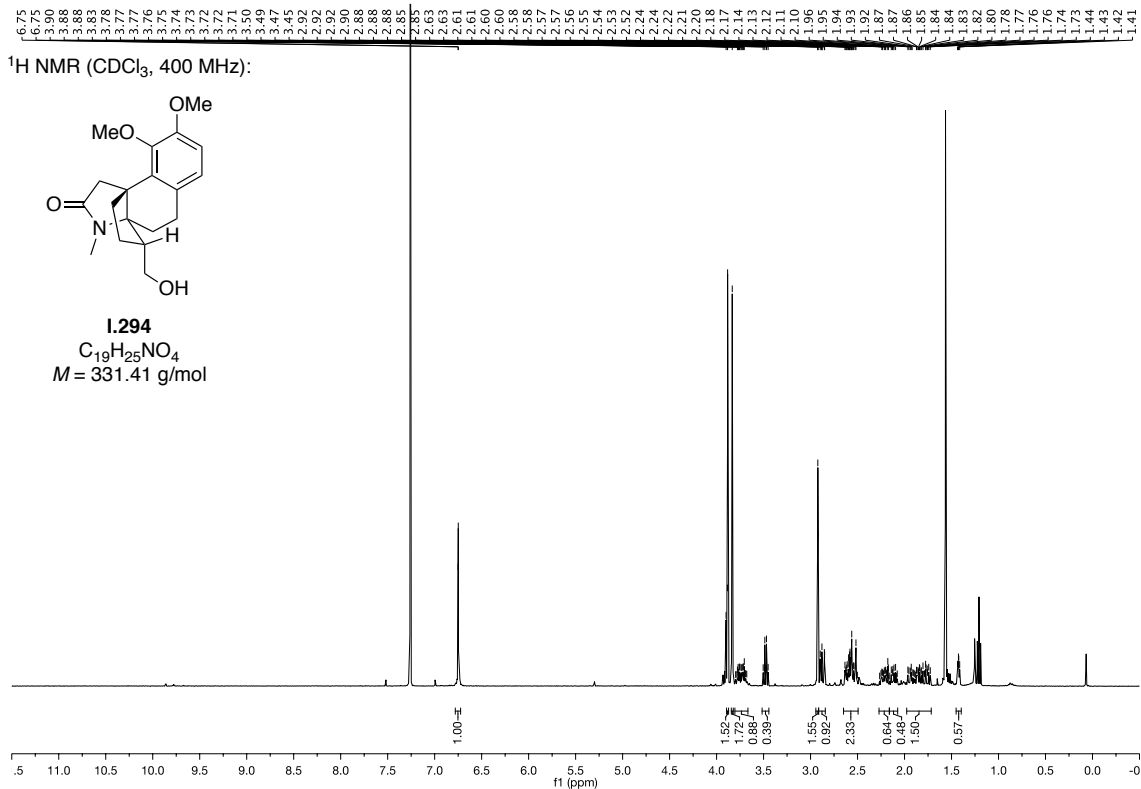
202.43, 201.93, 174.96, 173.27, 151.65, 151.37, 147.37, 147.30, 136.99, 135.51, 127.76, 127.01, 123.08, 122.83, 111.97, 111.32, 75.39, 60.55, 59.92, 59.01, 55.83, 49.65, 49.40, 45.80, 45.51, 39.93, 38.69, 30.02, 27.31, 26.47, 25.72, 25.43, 24.36, 24.36, 24.36

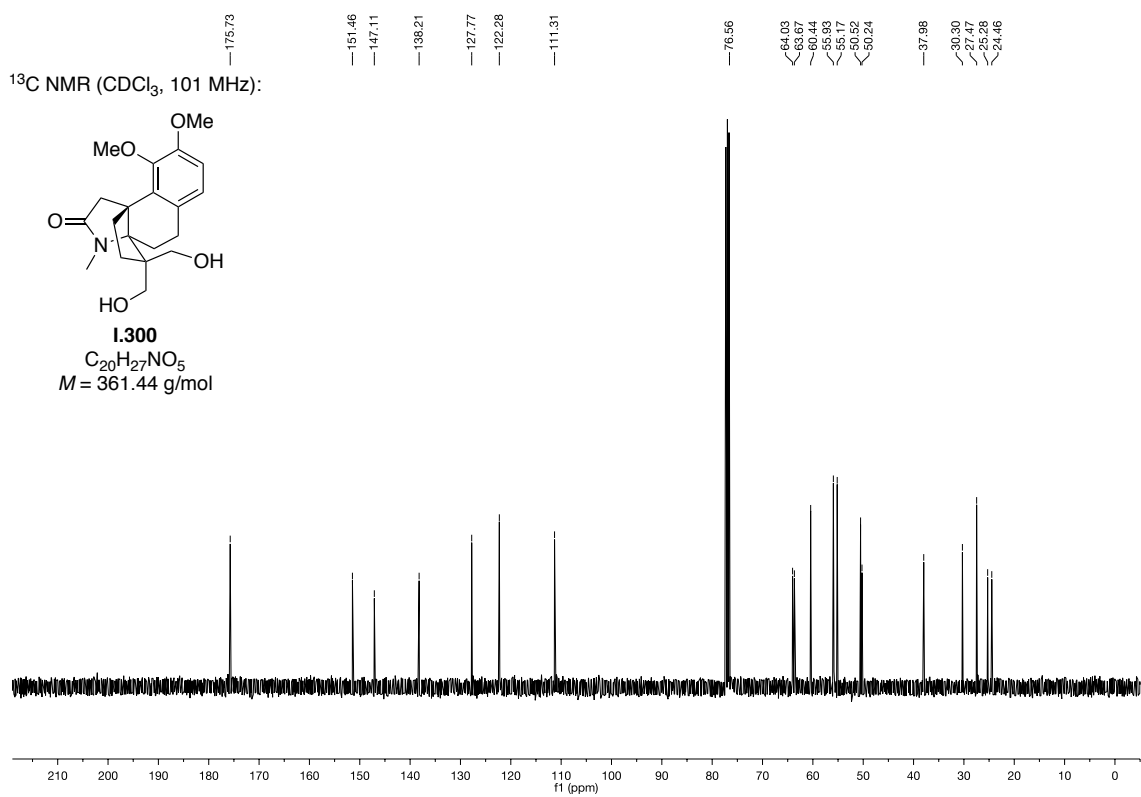
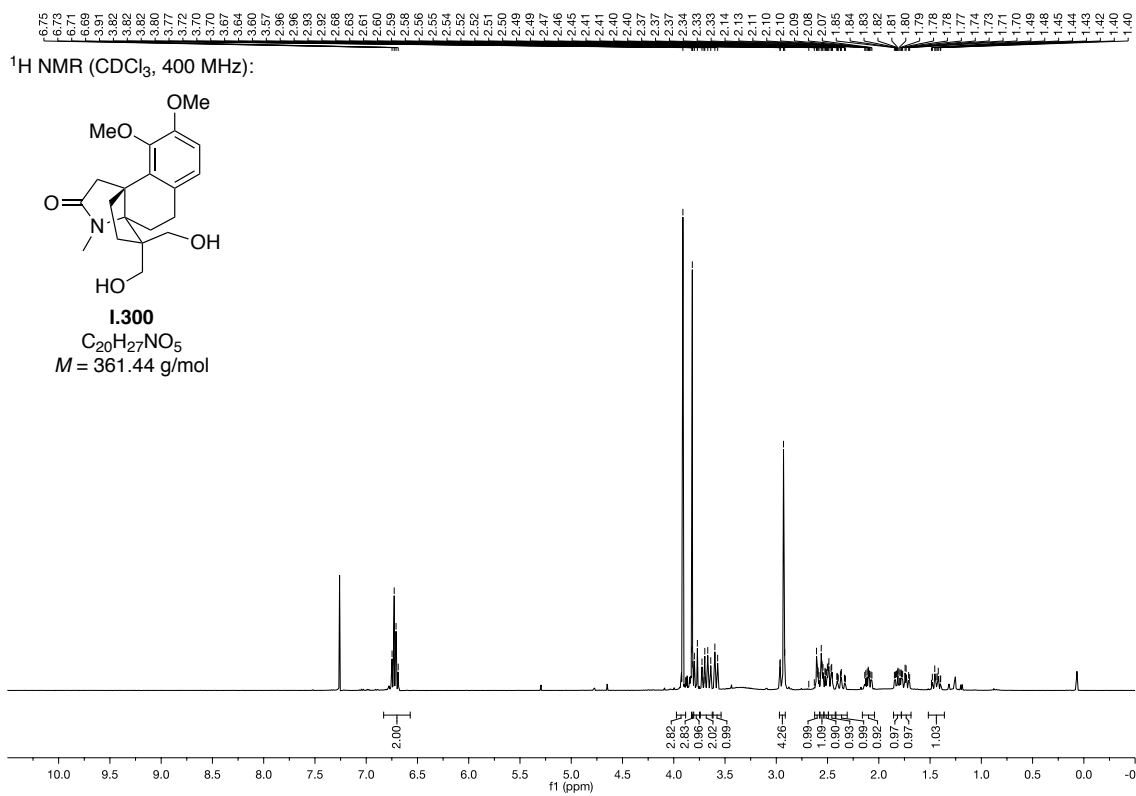
¹³C NMR (CDCl₃, 101 MHz):



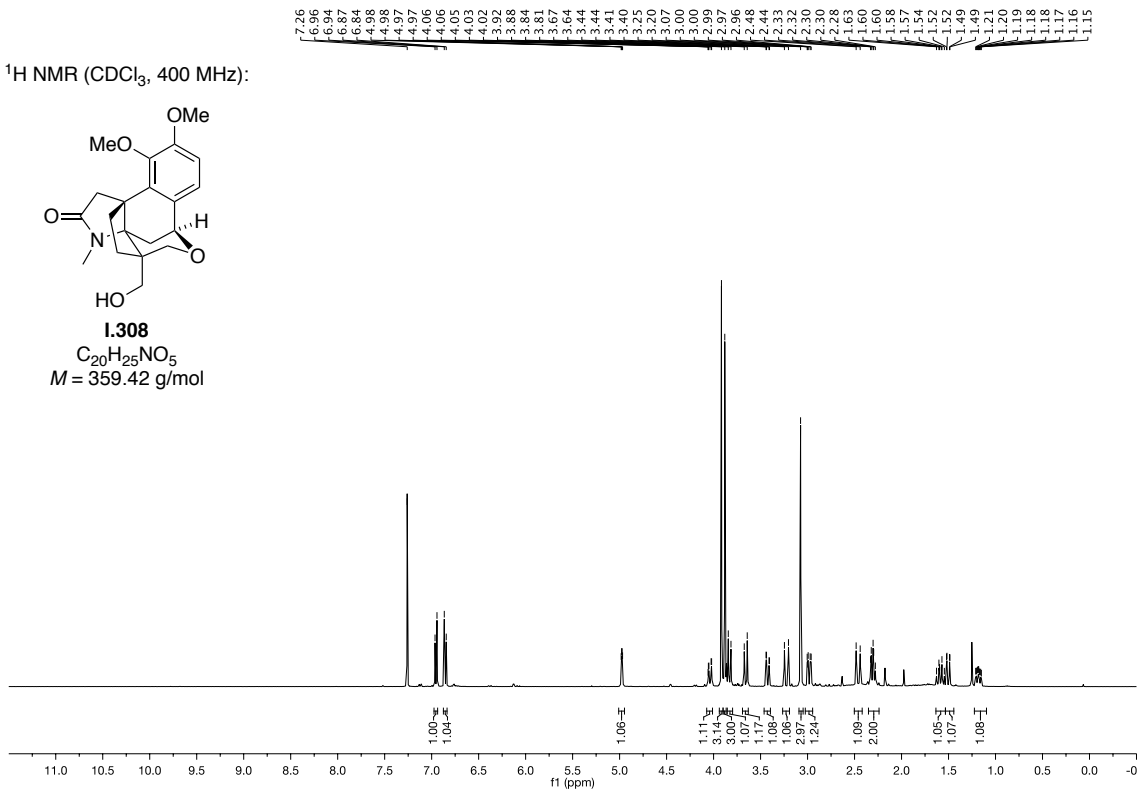
1.290
C₁₉H₂₃NO₄
M = 329.40 g/mol



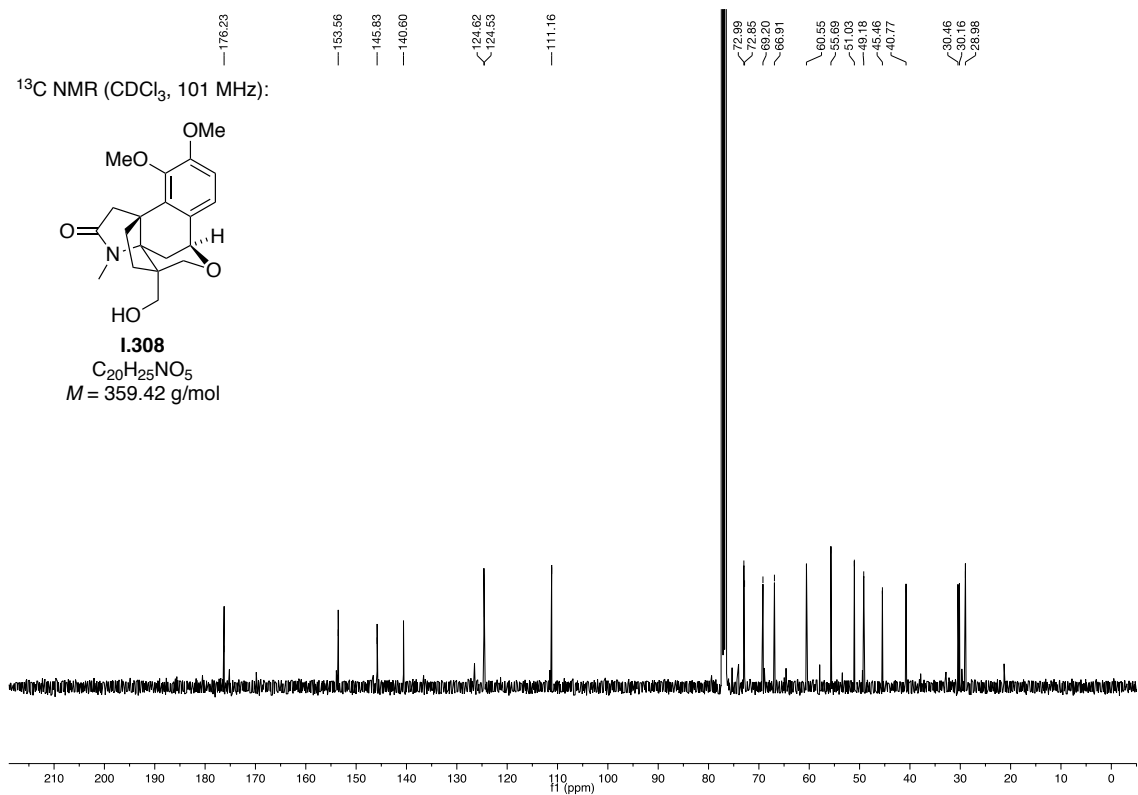
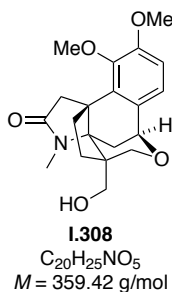


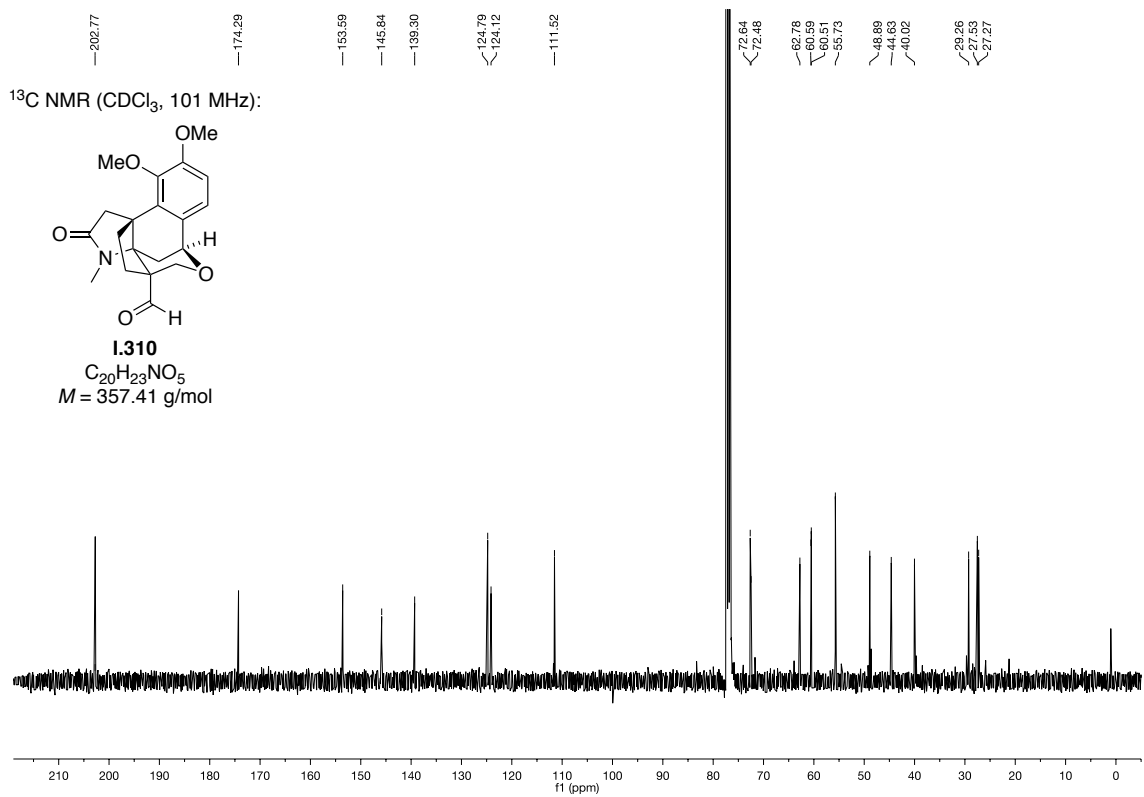
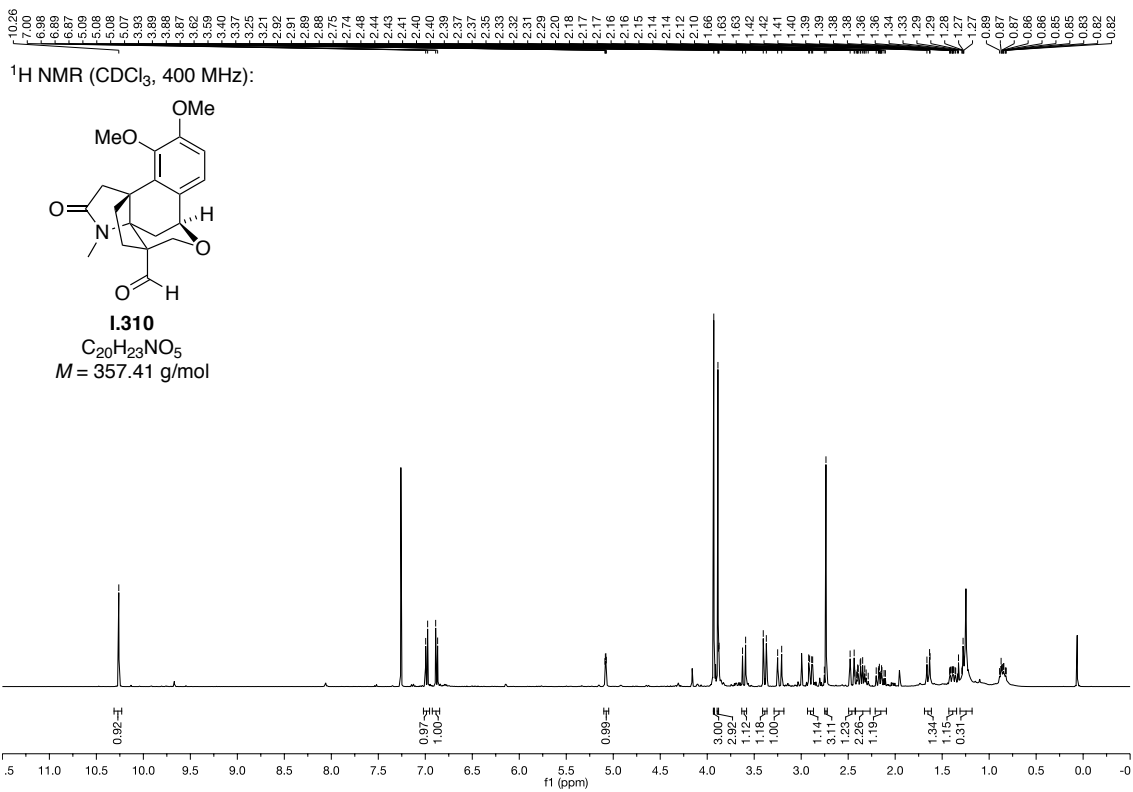


¹H NMR (CDCl₃, 400 MHz):

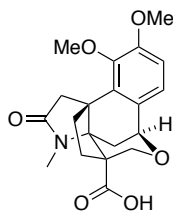


¹³C NMR (CDCl₃, 101 MHz):

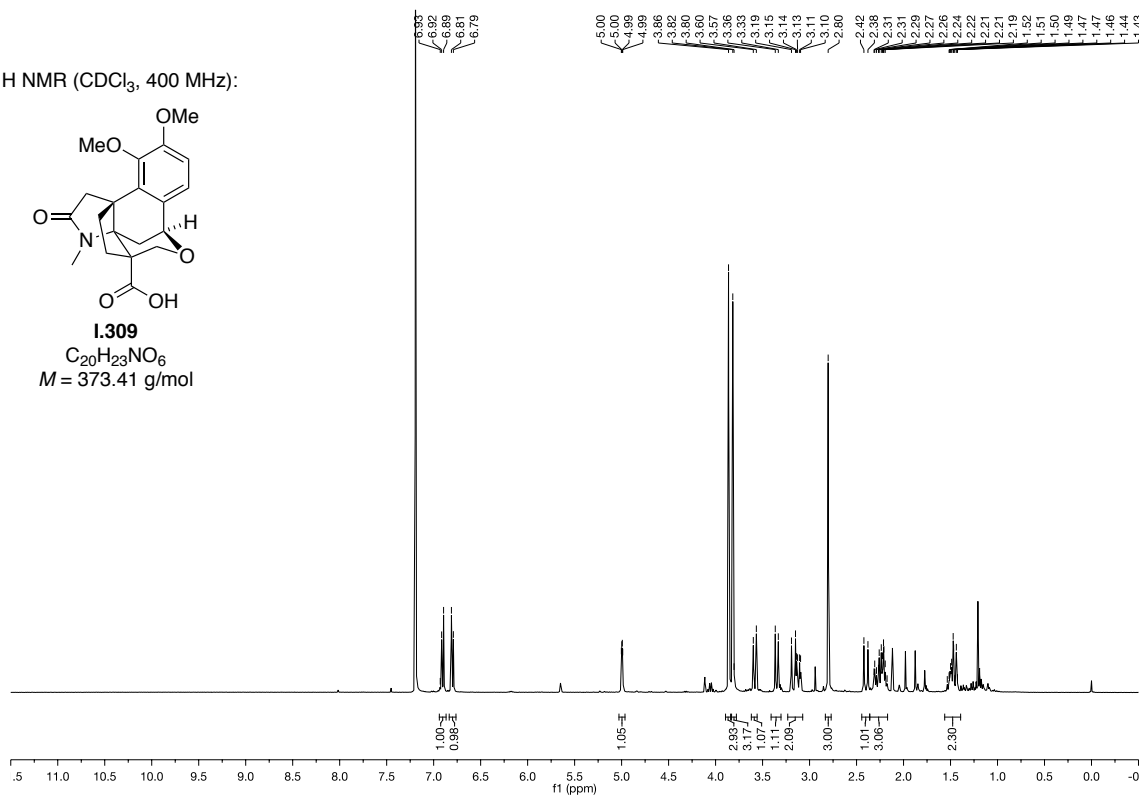




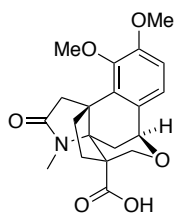
¹H NMR (CDCl₃, 400 MHz):



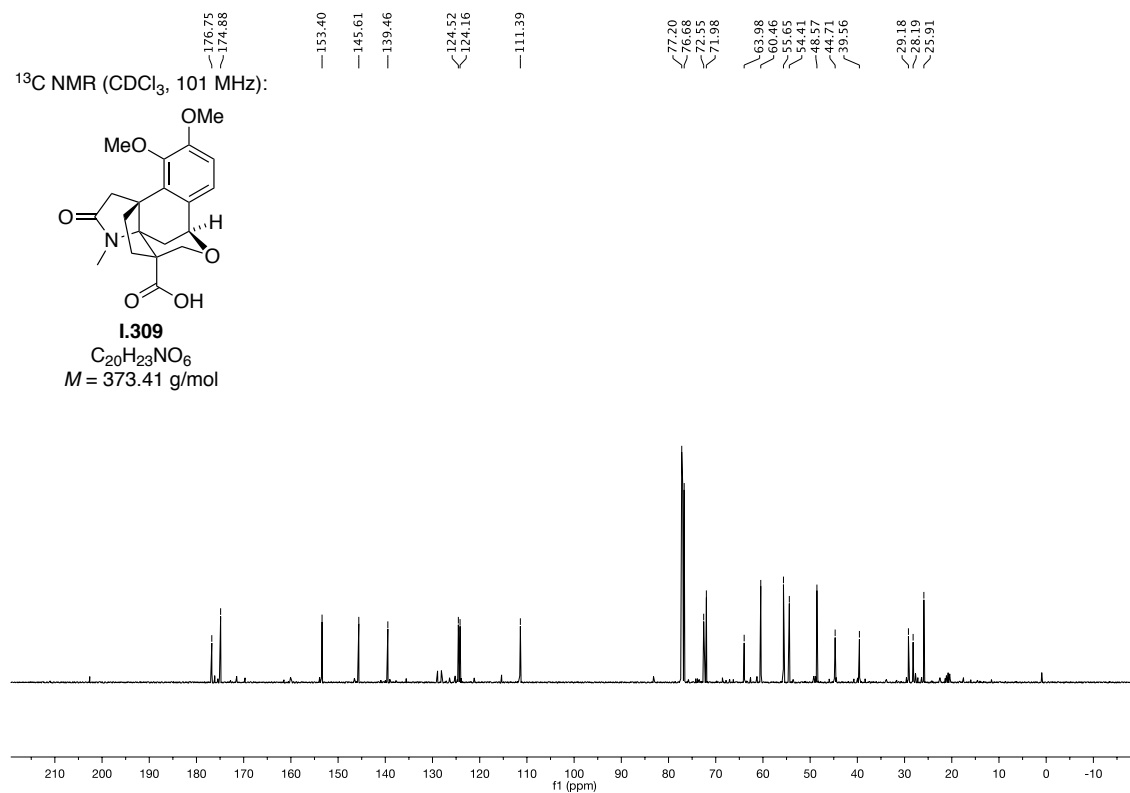
1.309
 $C_{20}H_{23}NO_6$
 $M = 373.41$ g/mol

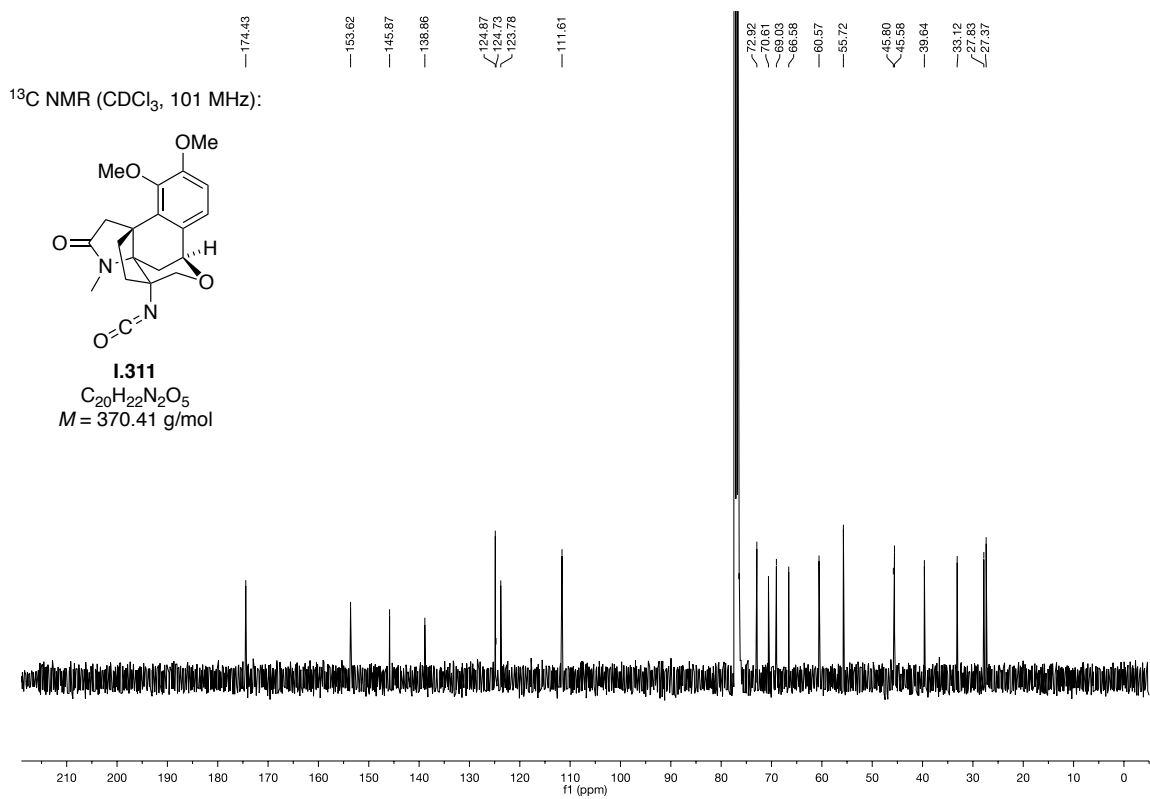
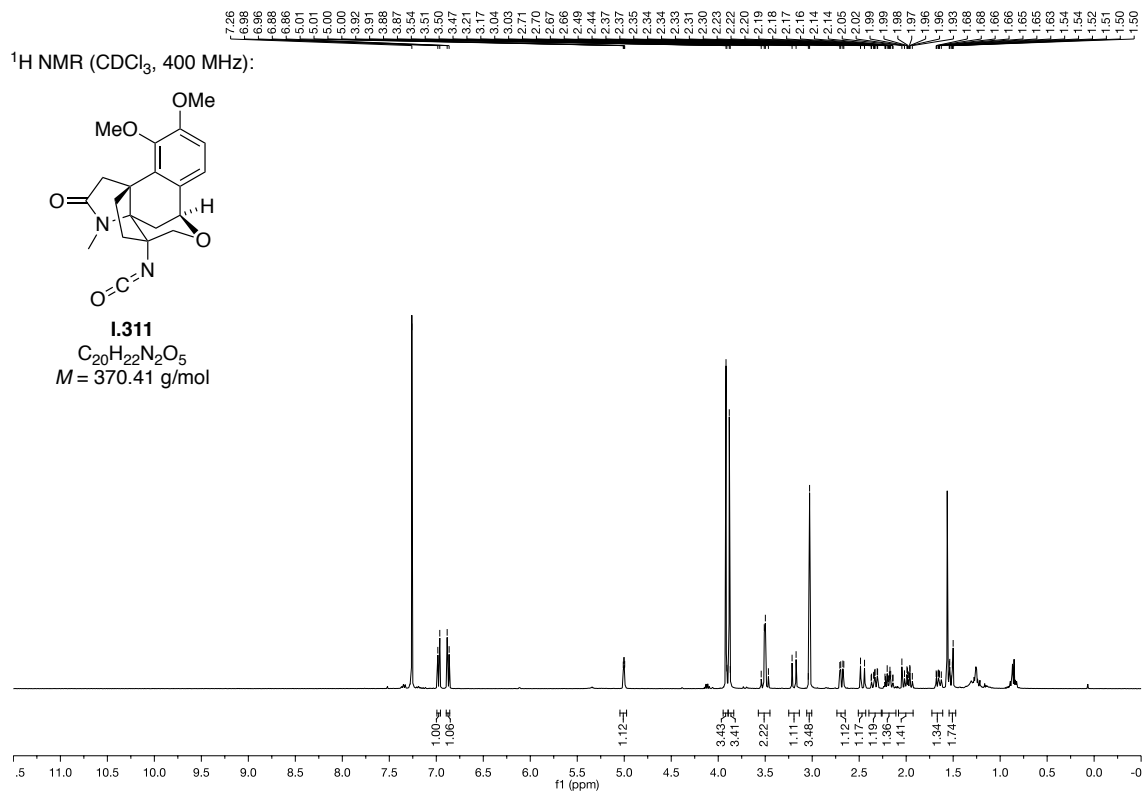


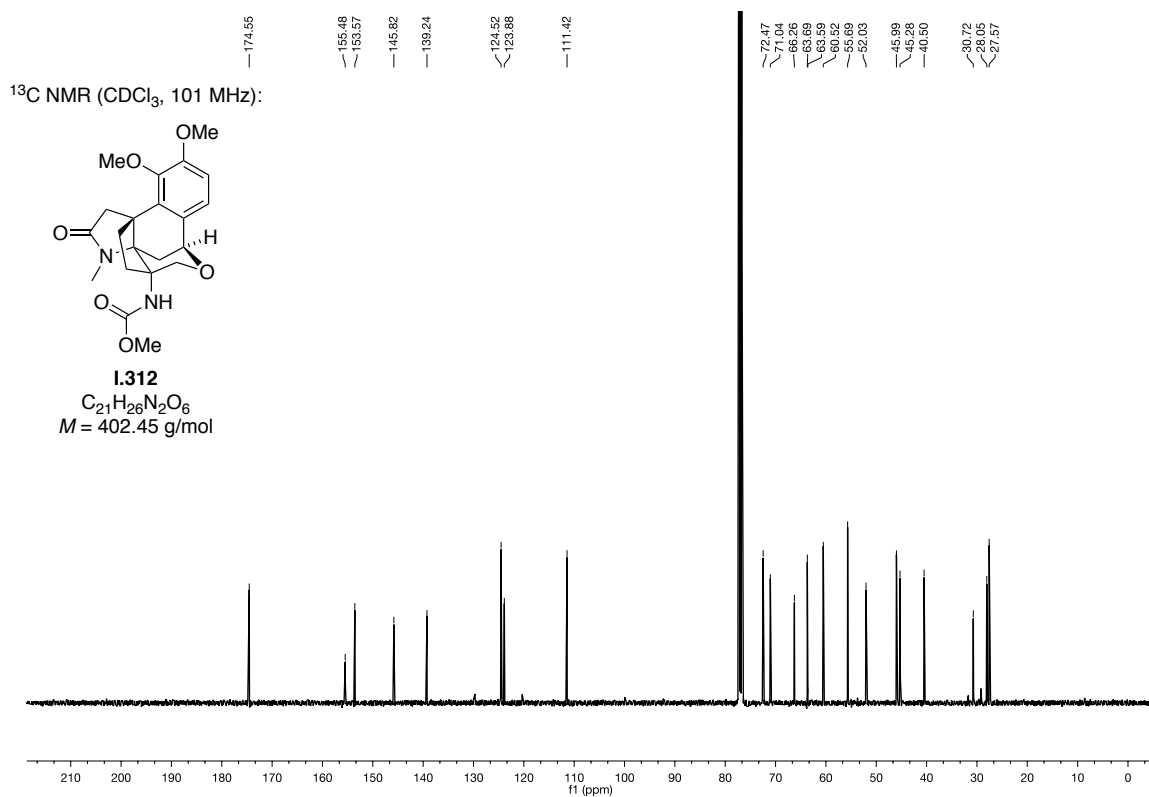
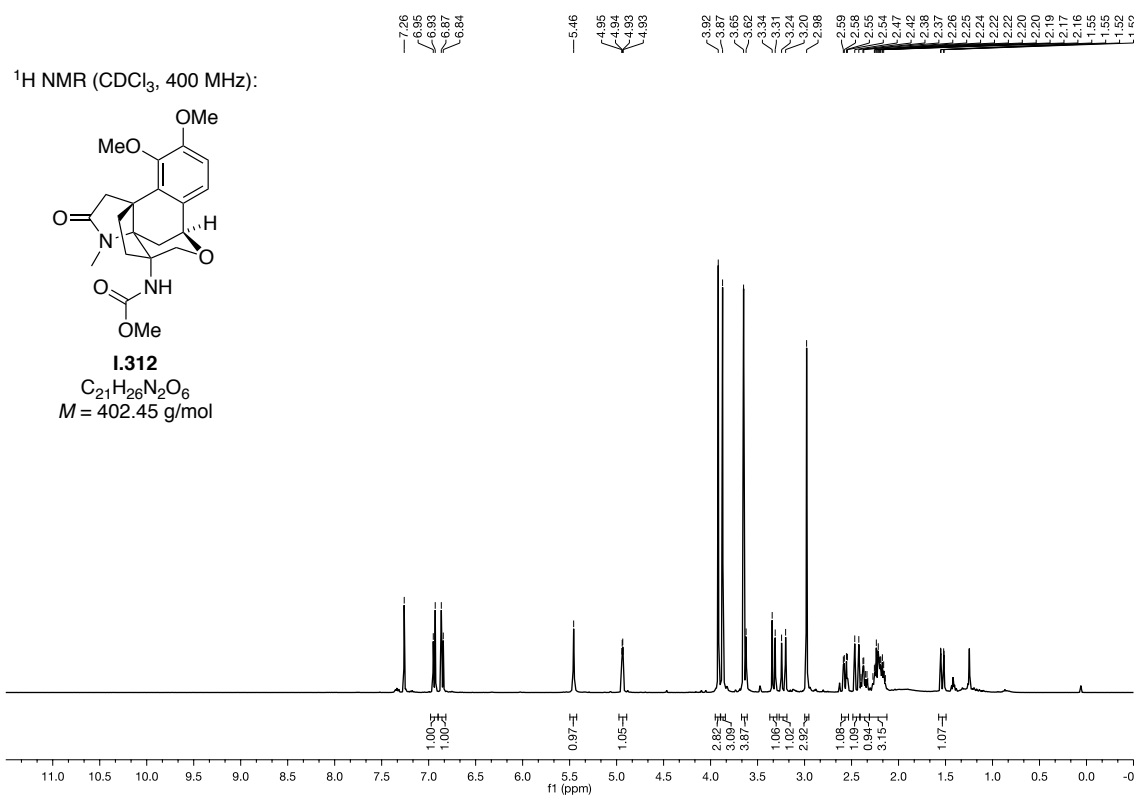
¹³C NMR (CDCl₃, 101 MHz):

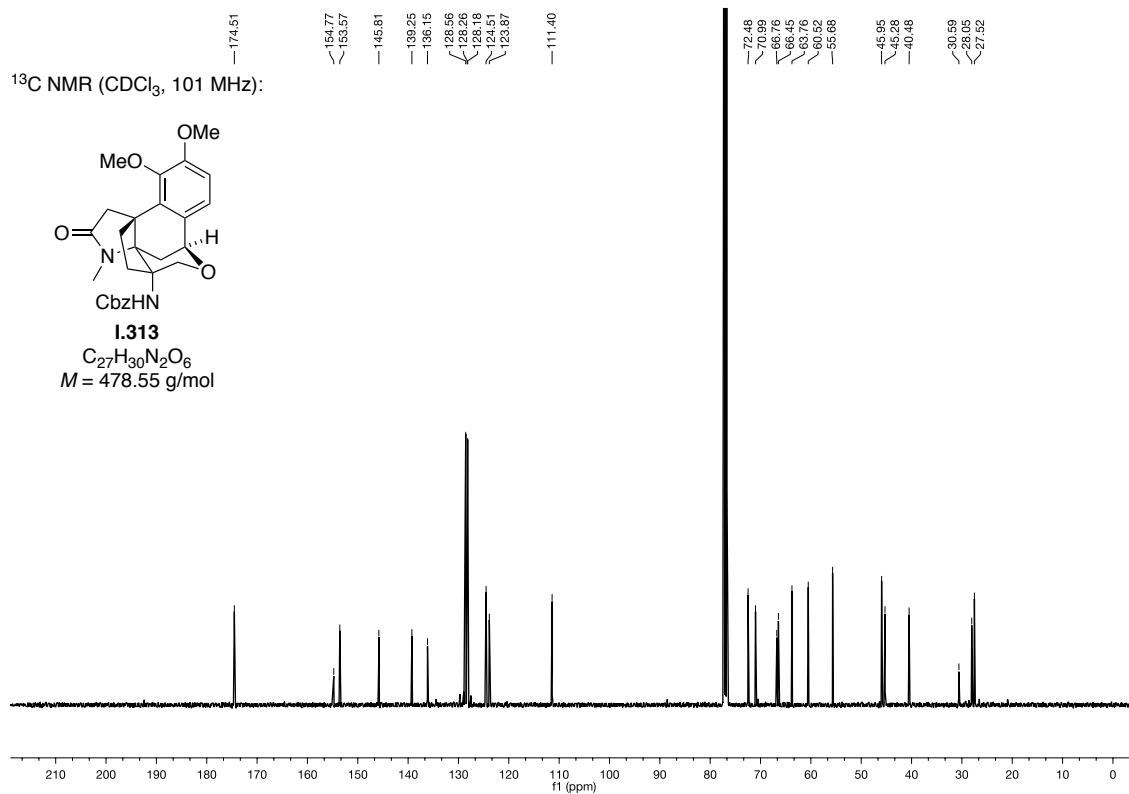
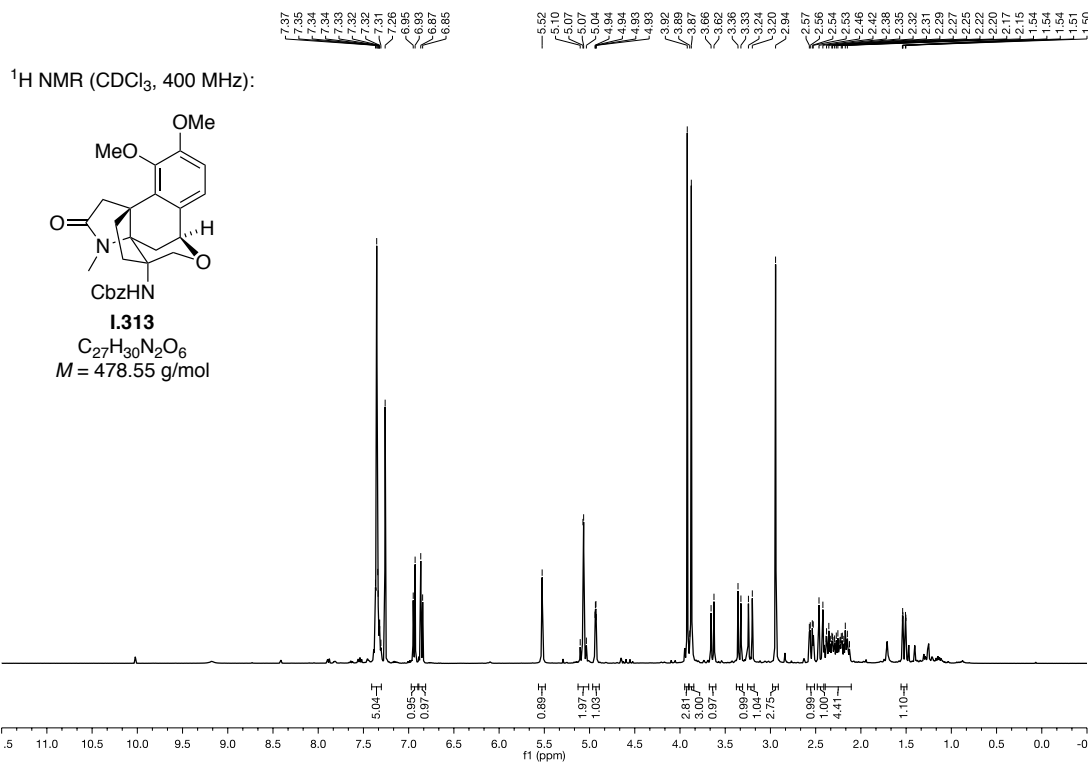


1.309
 $C_{20}H_{23}NO_6$
 $M = 373.41$ g/mol

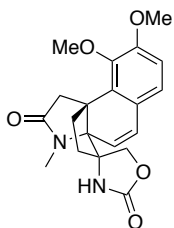




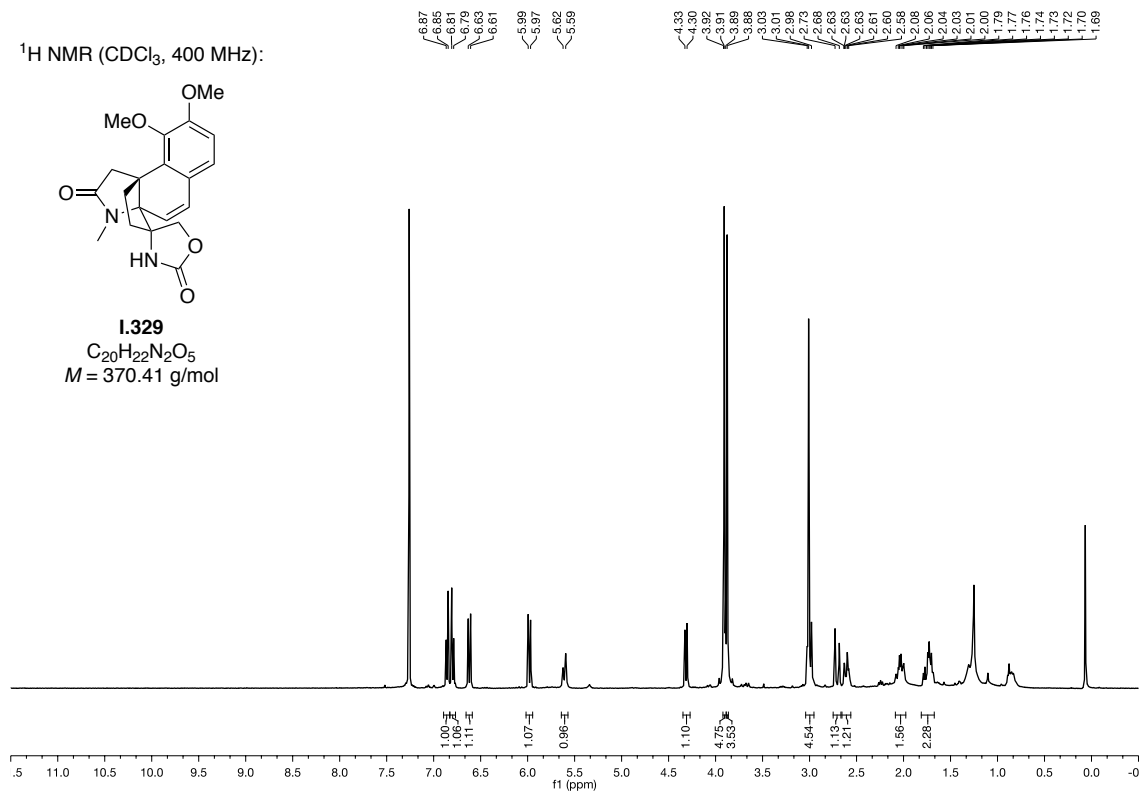




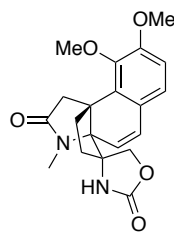
¹H NMR (CDCl₃, 400 MHz):



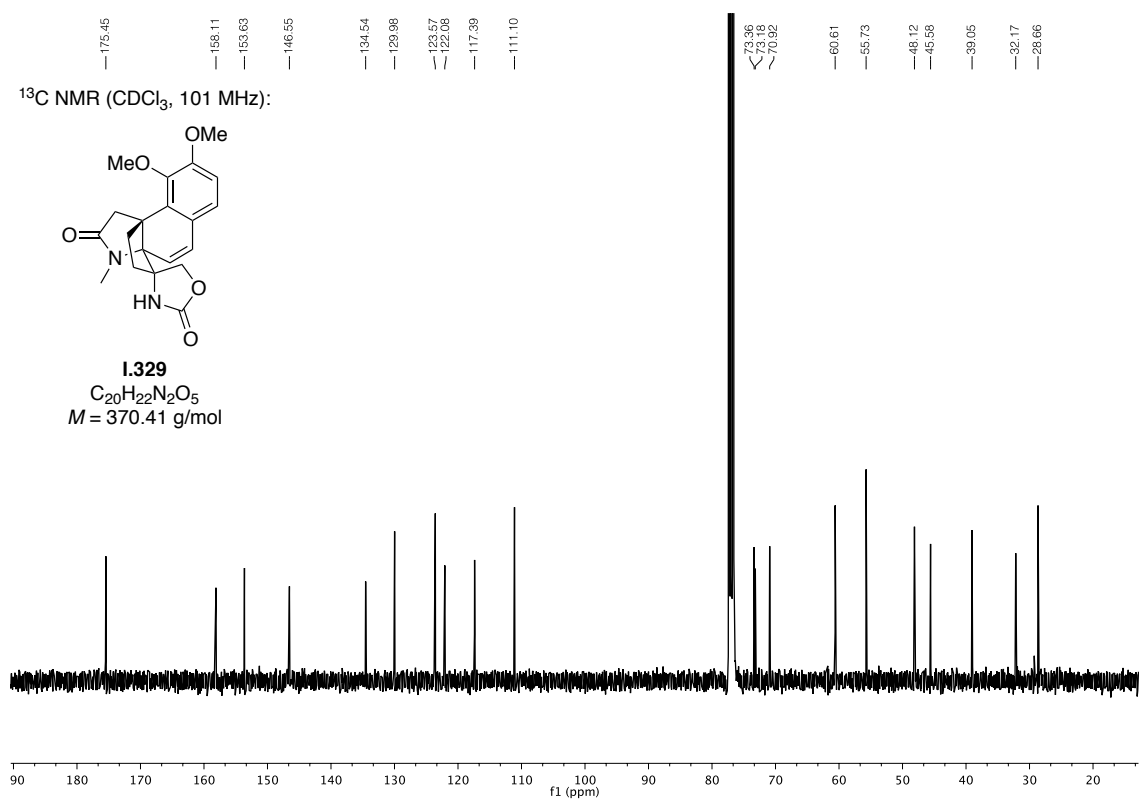
1.329
 C₂₀H₂₂N₂O₅
 M = 370.41 g/mol

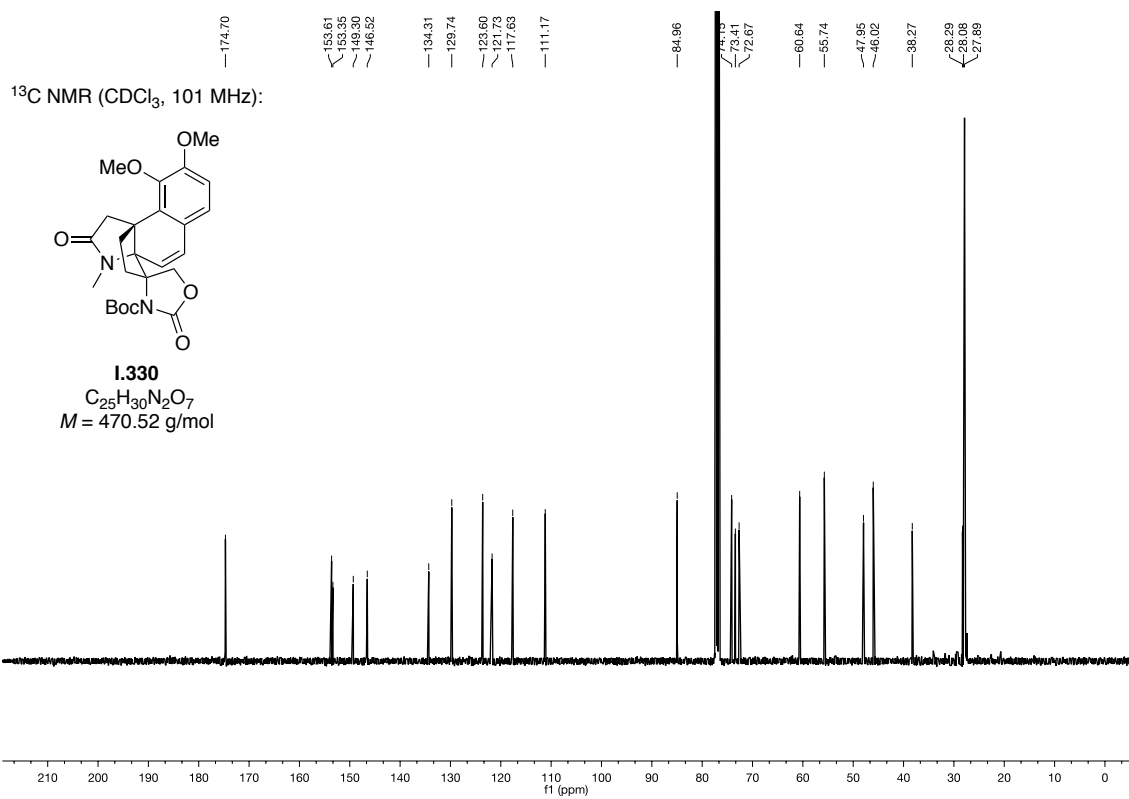
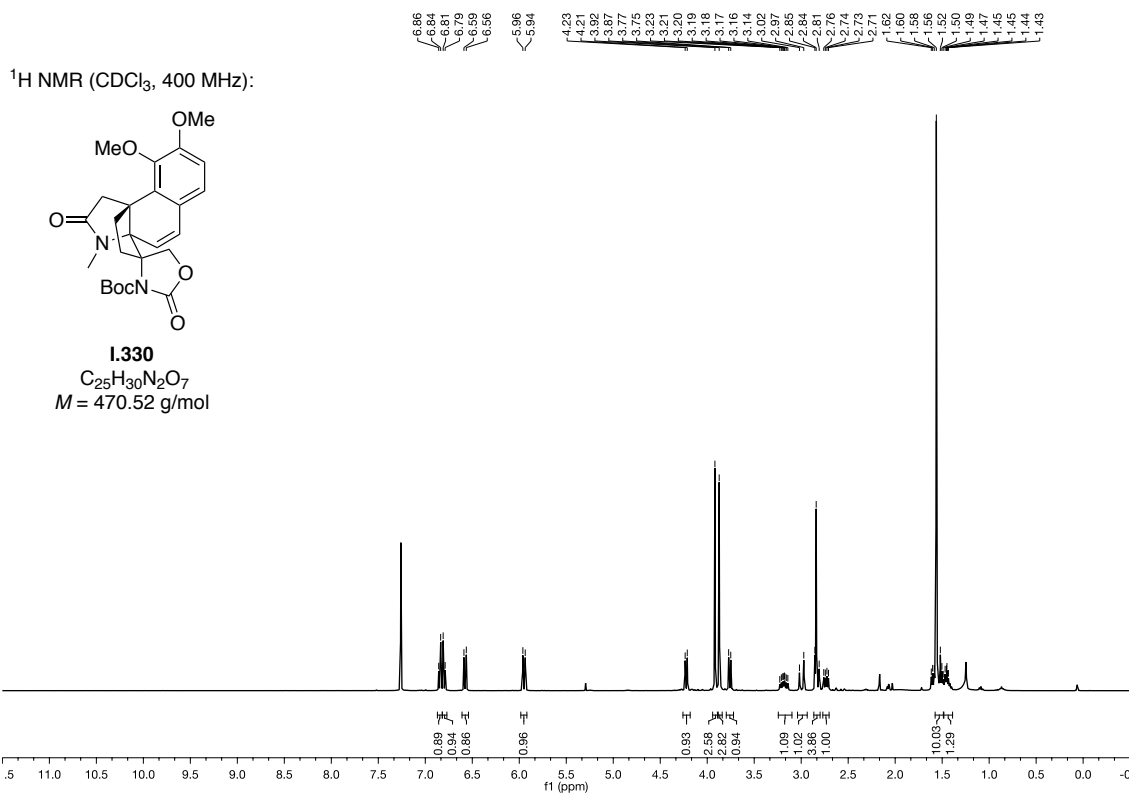


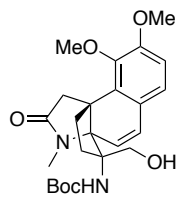
¹³C NMR (CDCl₃, 101 MHz):



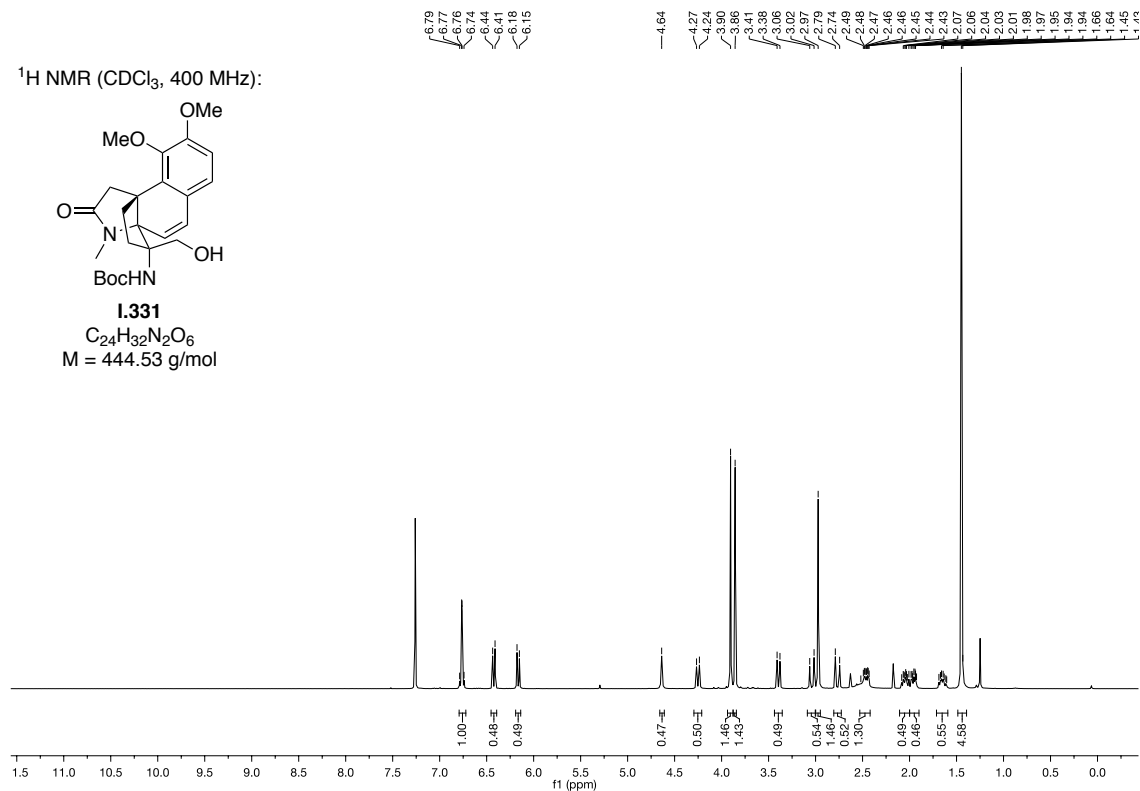
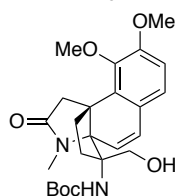
1.329
 C₂₀H₂₂N₂O₅
 M = 370.41 g/mol



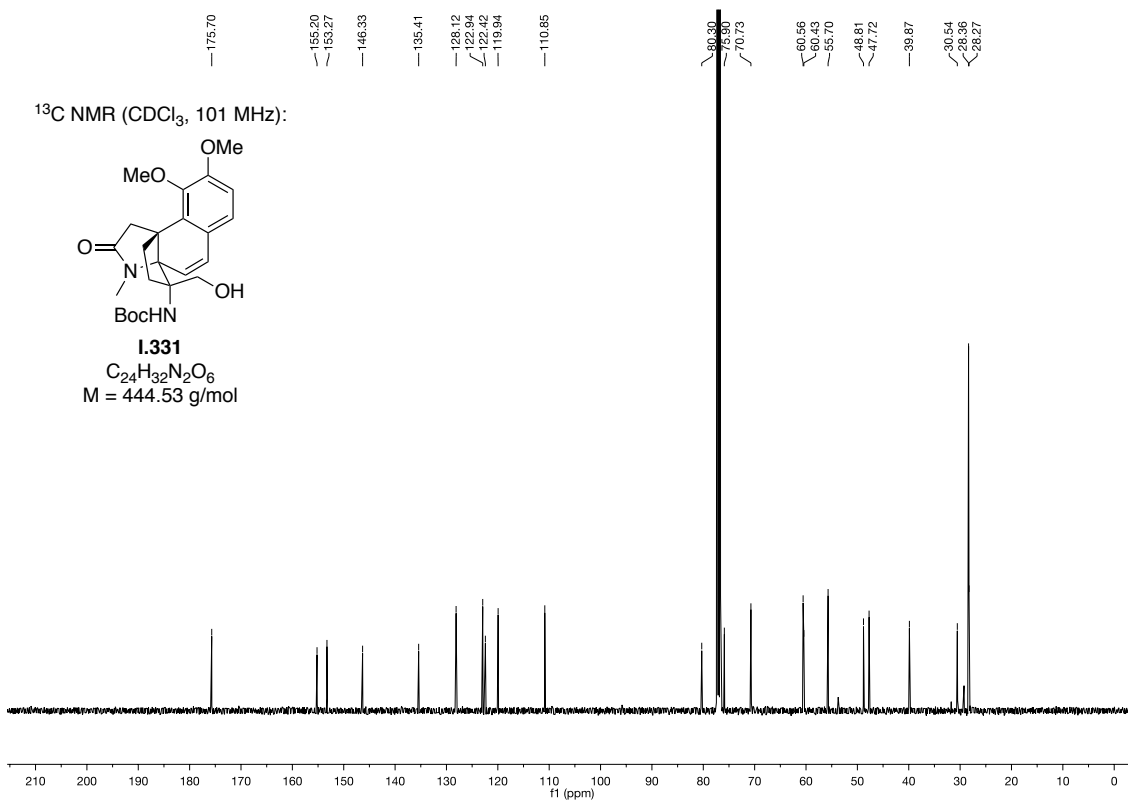


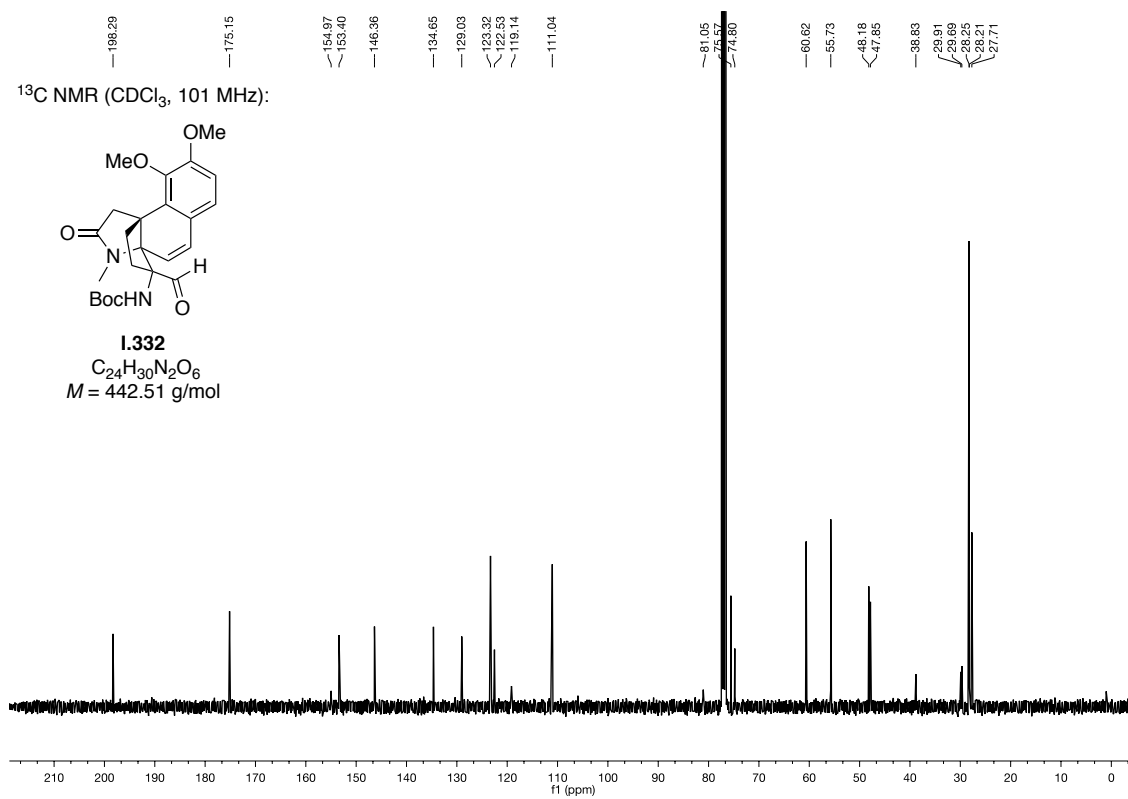
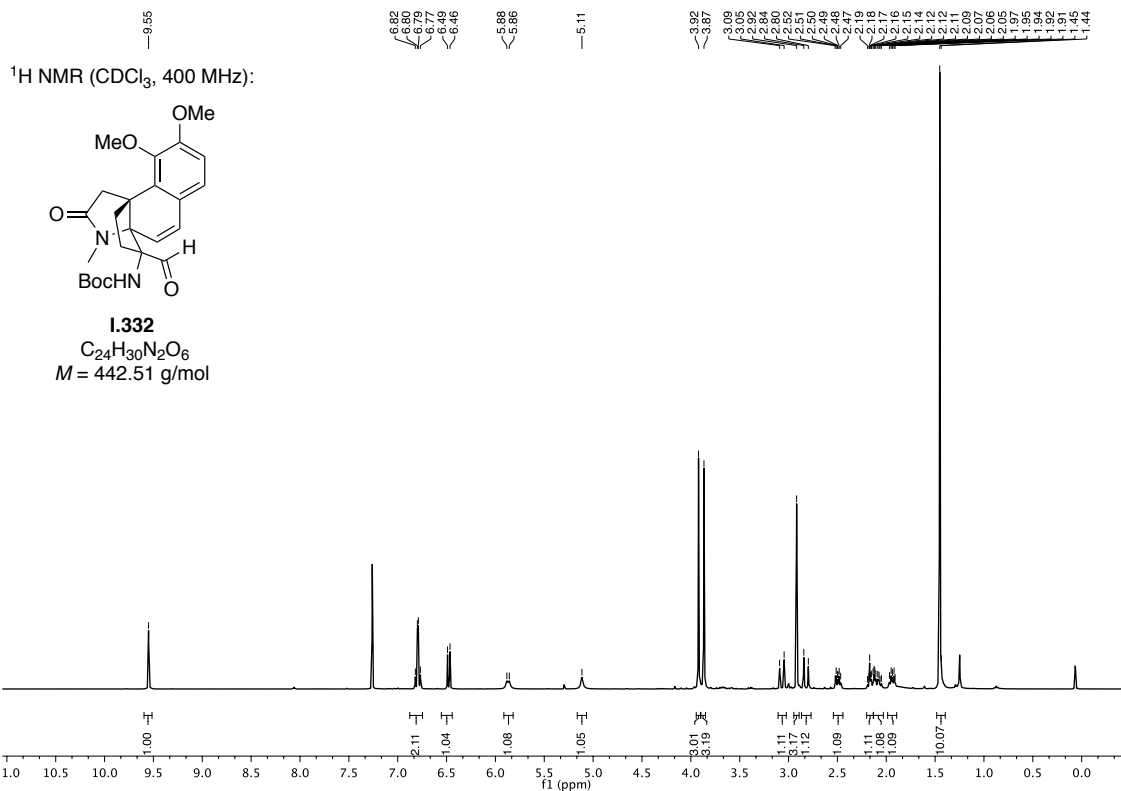
^1H NMR (CDCl_3 , 400 MHz):

1.331
 $\text{C}_{24}\text{H}_{32}\text{N}_2\text{O}_6$
 $M = 444.53 \text{ g/mol}$

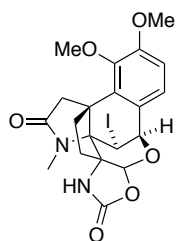
 ^{13}C NMR (CDCl_3 , 101 MHz):

1.331
 $\text{C}_{24}\text{H}_{32}\text{N}_2\text{O}_6$
 $M = 444.53 \text{ g/mol}$

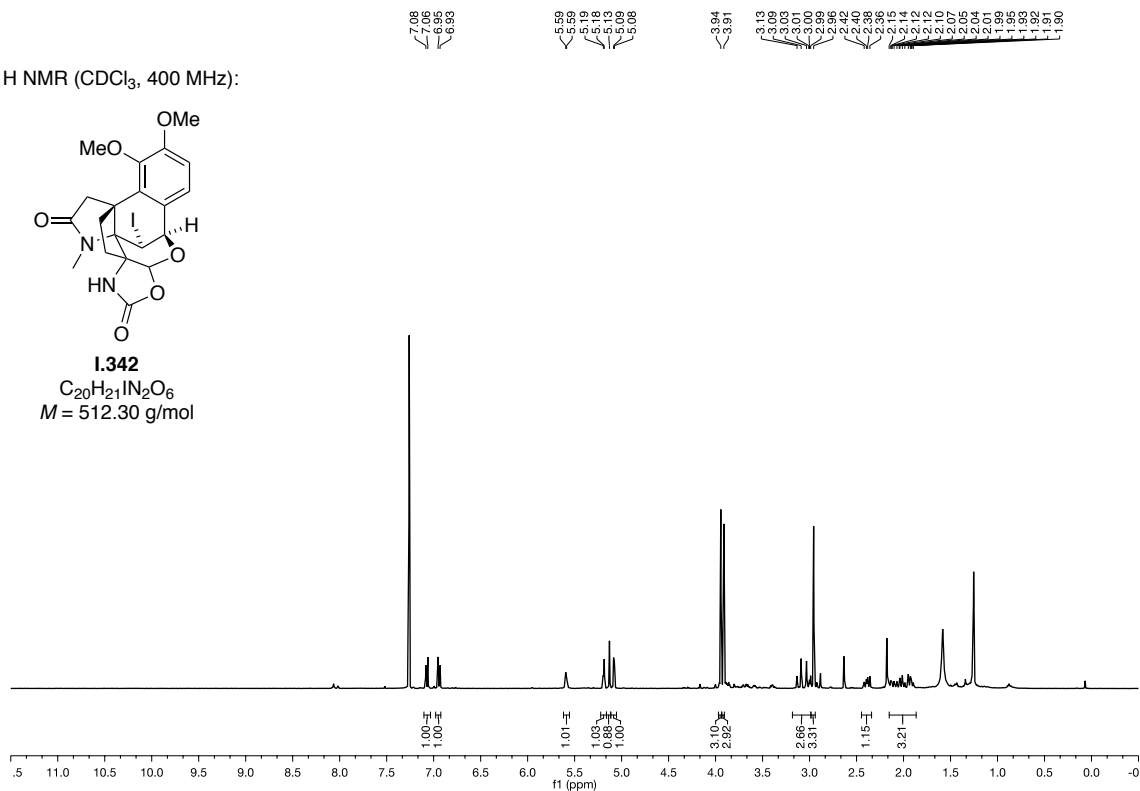




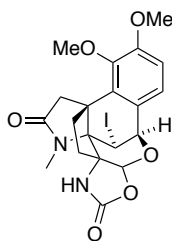
¹H NMR (CDCl₃, 400 MHz):



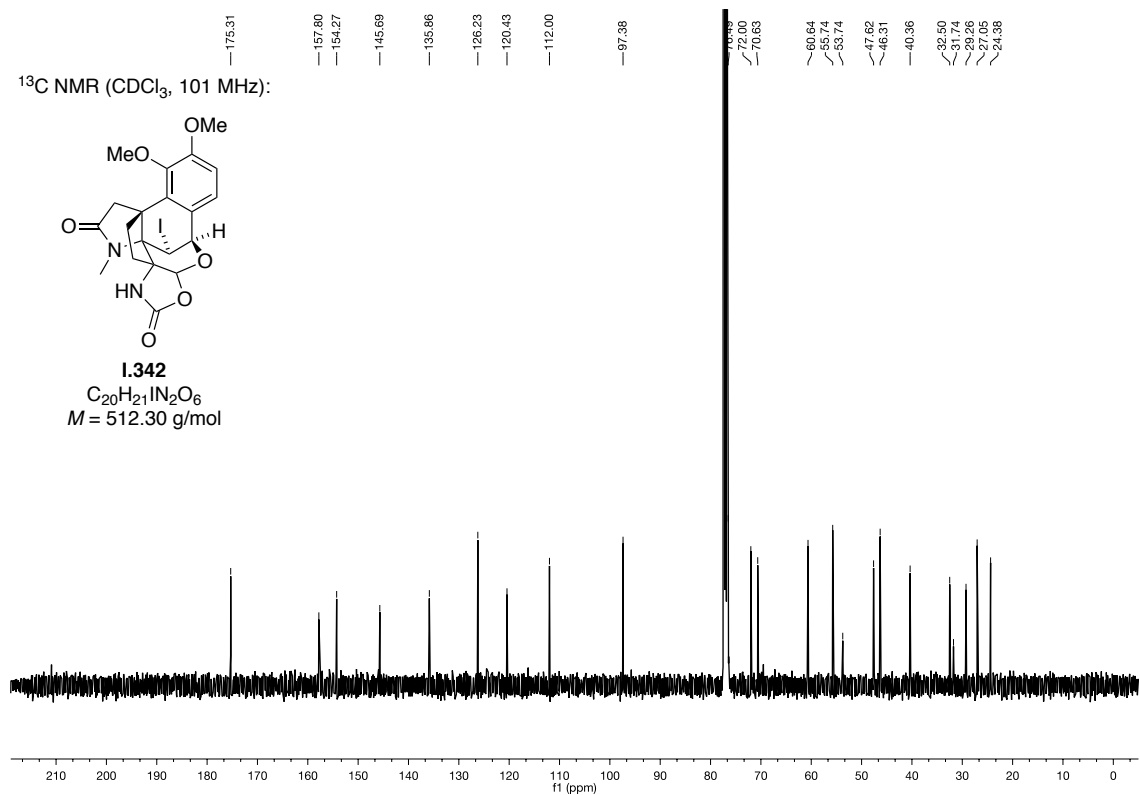
1.342
 $C_{20}H_{21}N_2O_6$
 $M = 512.30$ g/mol

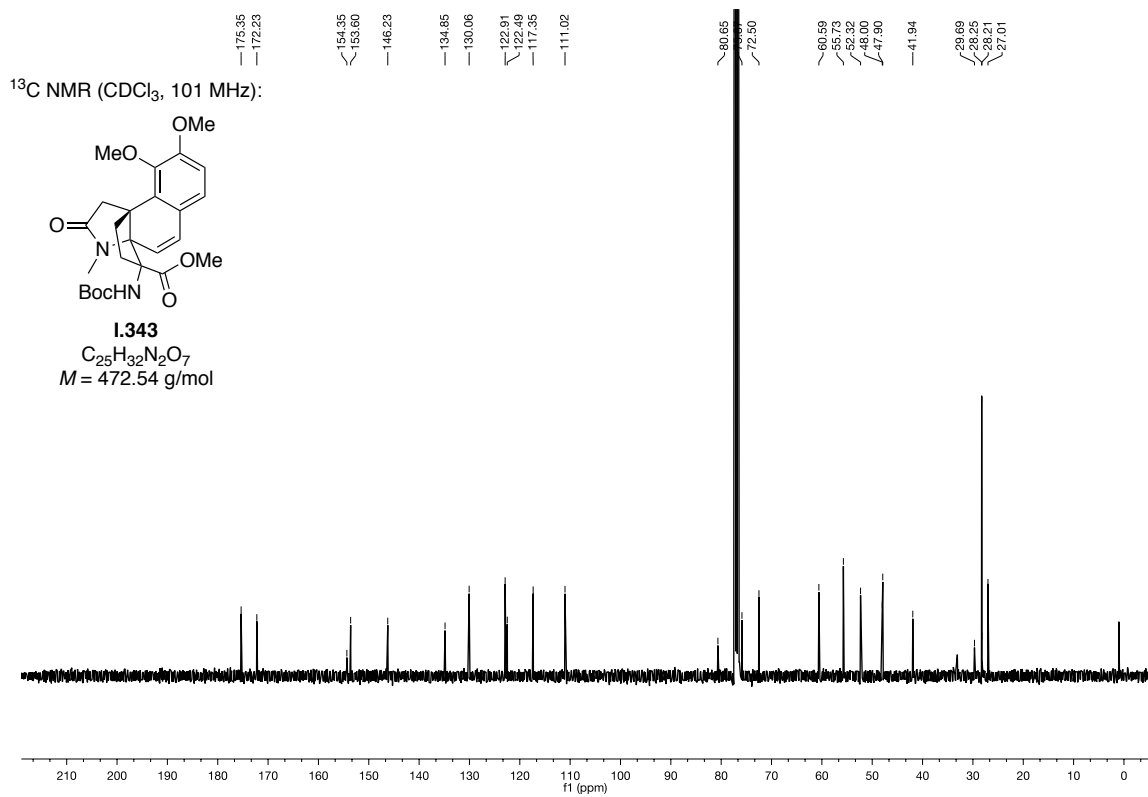
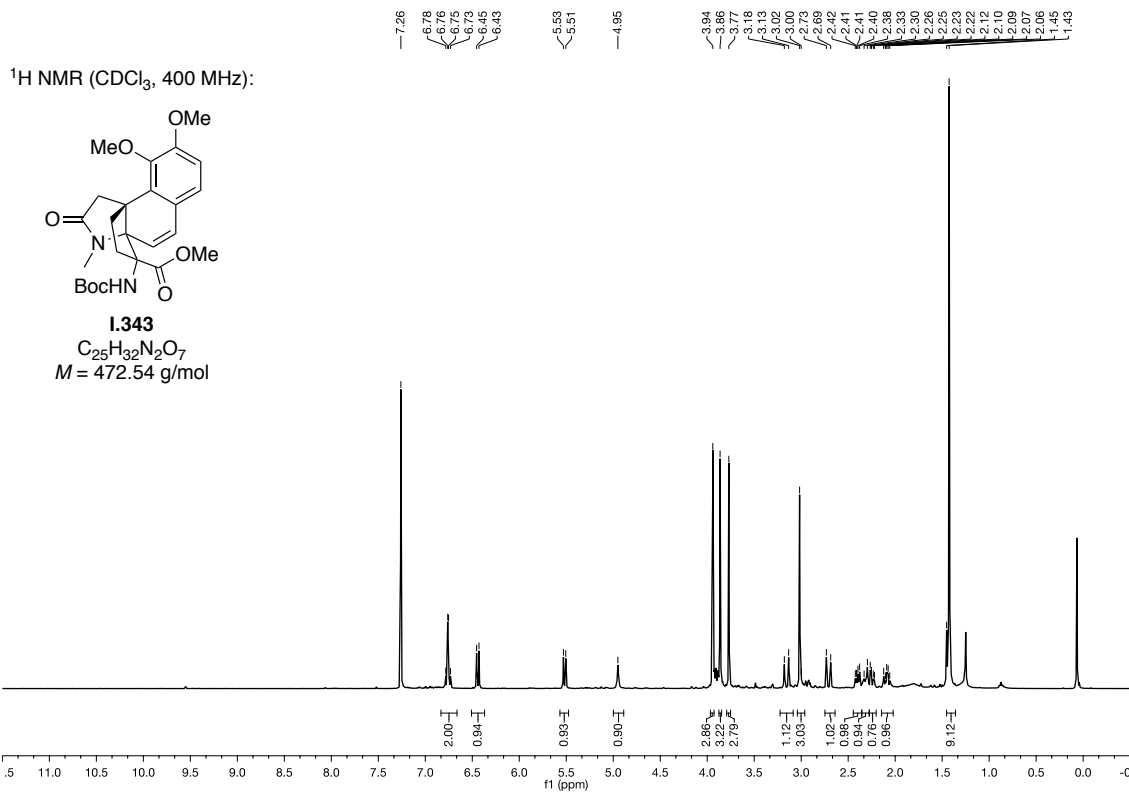


¹³C NMR (CDCl₃, 101 MHz):



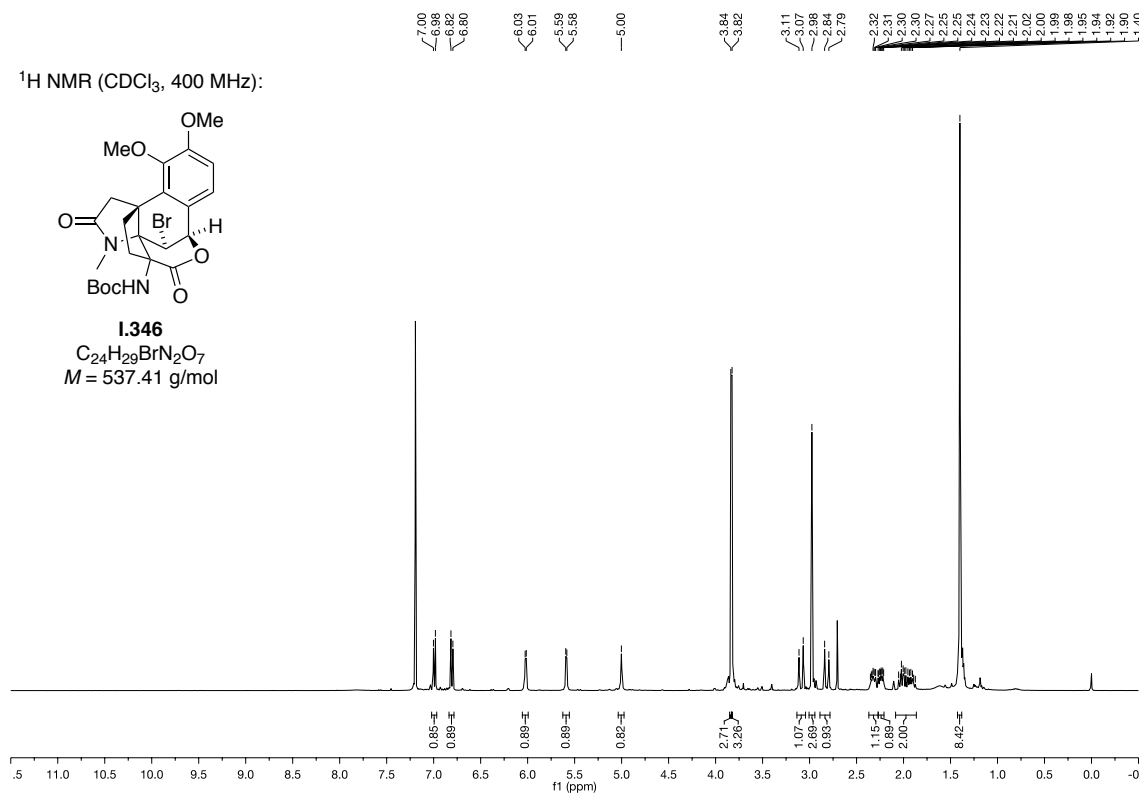
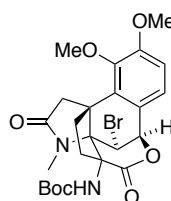
1.342
 $C_{20}H_{21}N_2O_6$
 $M = 512.30$ g/mol



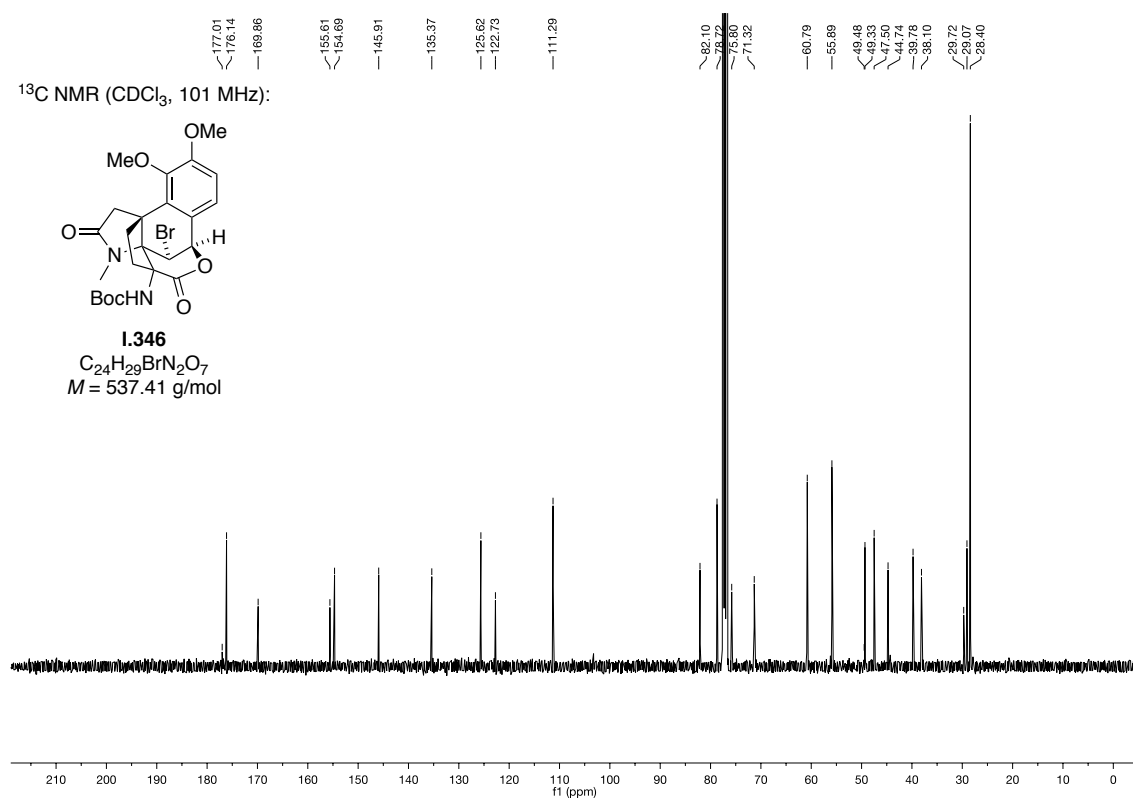


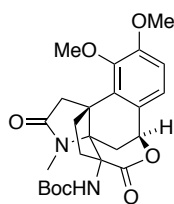
^1H NMR (CDCl_3 , 400 MHz):

1.346
 $\text{C}_{24}\text{H}_{29}\text{BrN}_2\text{O}_7$
 $M = 537.41$ g/mol

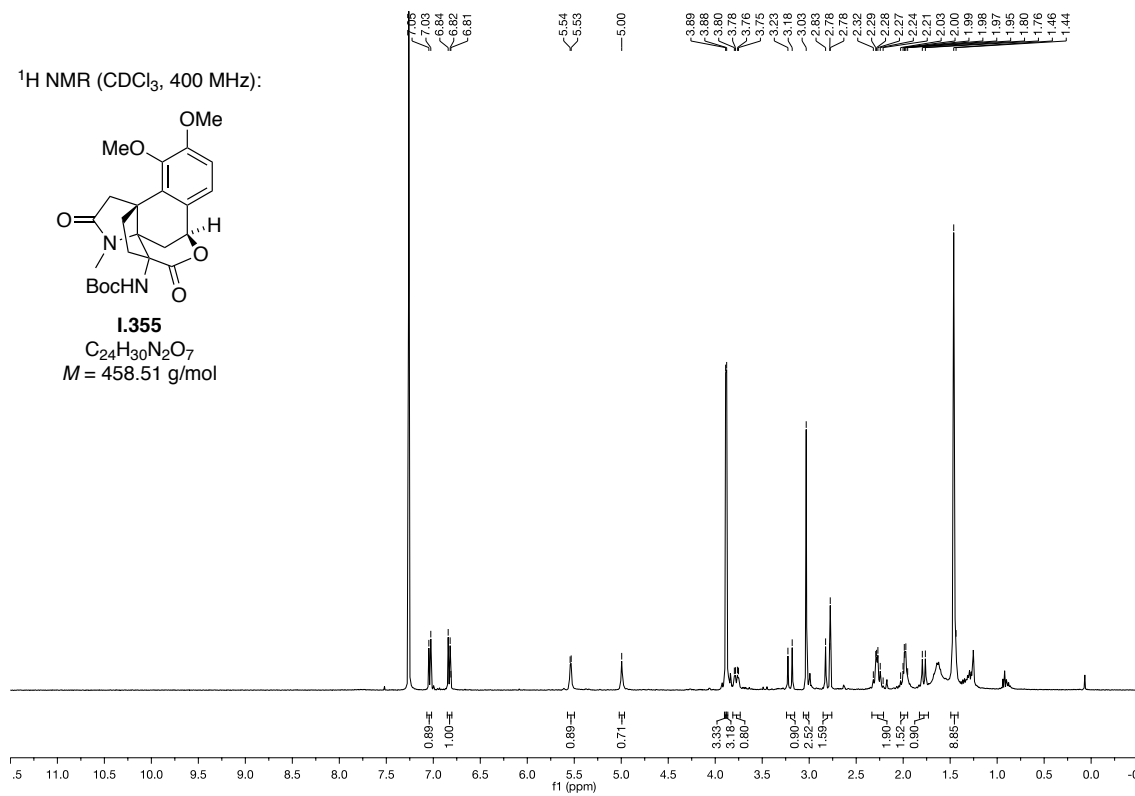
 ^{13}C NMR (CDCl_3 , 101 MHz):

1.346
 $\text{C}_{24}\text{H}_{29}\text{BrN}_2\text{O}_7$
 $M = 537.41$ g/mol

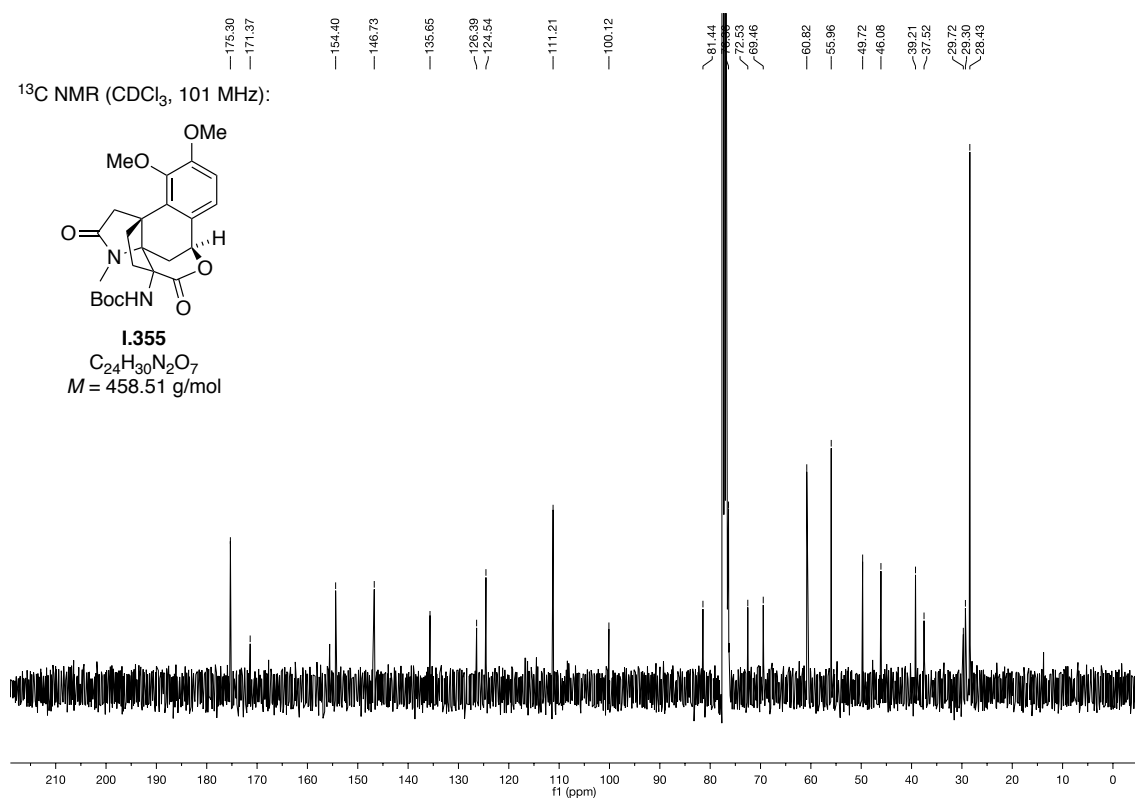


¹H NMR (CDCl₃, 400 MHz):

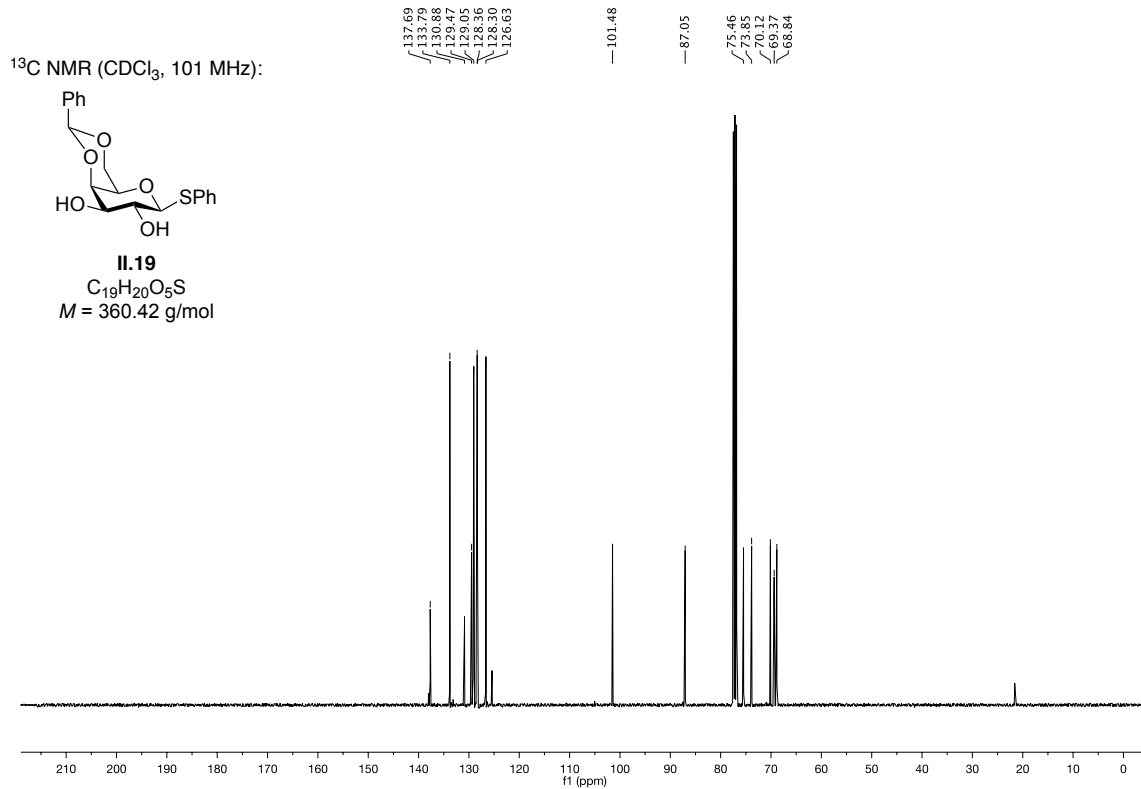
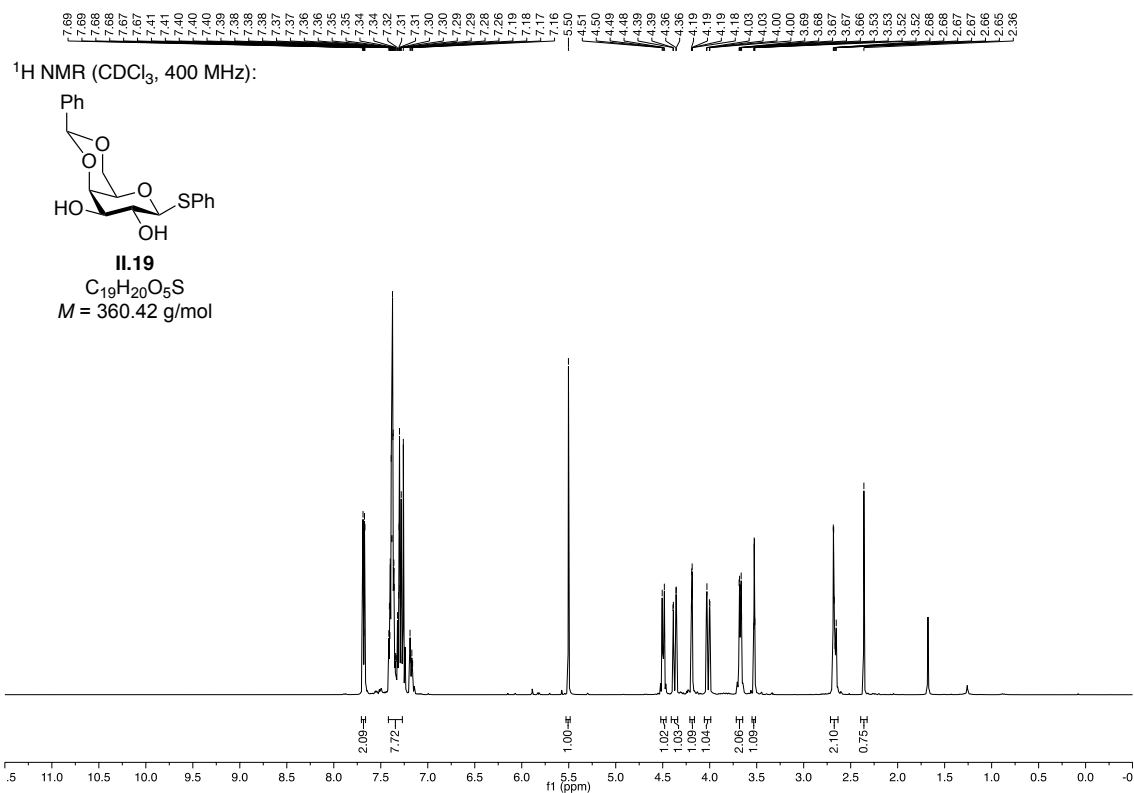
1.355
 $C_{24}H_{30}N_2O_7$
 $M = 458.51$ g/mol

¹³C NMR (CDCl₃, 101 MHz):

1.355
 $C_{24}H_{30}N_2O_7$
 $M = 458.51$ g/mol

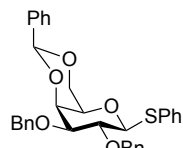


9.3 NMR spectra of chapter II

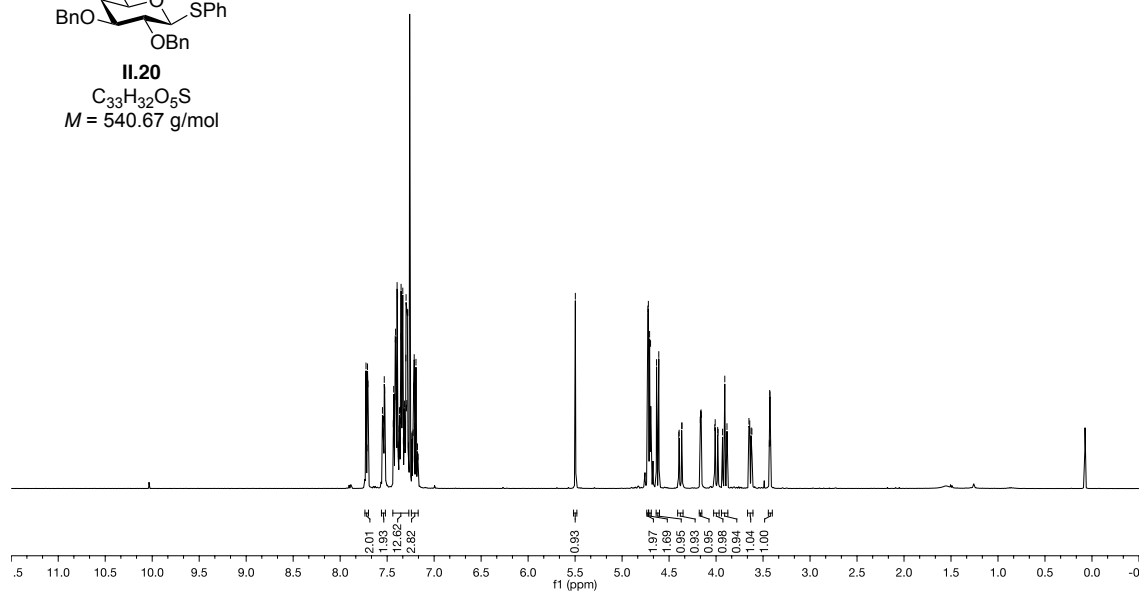


7.73
7.72
7.72
7.71
7.70
7.65
7.64
7.64
7.63
7.63
7.43
7.43
7.42
7.41
7.41
7.41
7.40
7.39
7.38
7.37
7.37
7.36
7.36
7.35
7.35
7.34
7.34
7.33
7.33
7.32
7.32
7.31
7.31
7.30
7.30
7.29
7.29
7.28
7.24
7.24
7.22
7.22
7.21
7.21
7.20
7.20
5.50
4.73
4.72
4.71
4.71
4.63
4.61
4.40
4.40
4.39
4.37
4.36
4.17
4.17
4.16
4.16
4.01
4.01
3.98
3.98
3.93
3.93
3.65
3.65
3.64
3.63
3.43
3.43
3.42

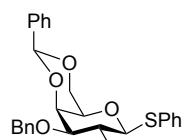
$^1\text{H NMR}$ (CDCl_3 , 400 MHz):



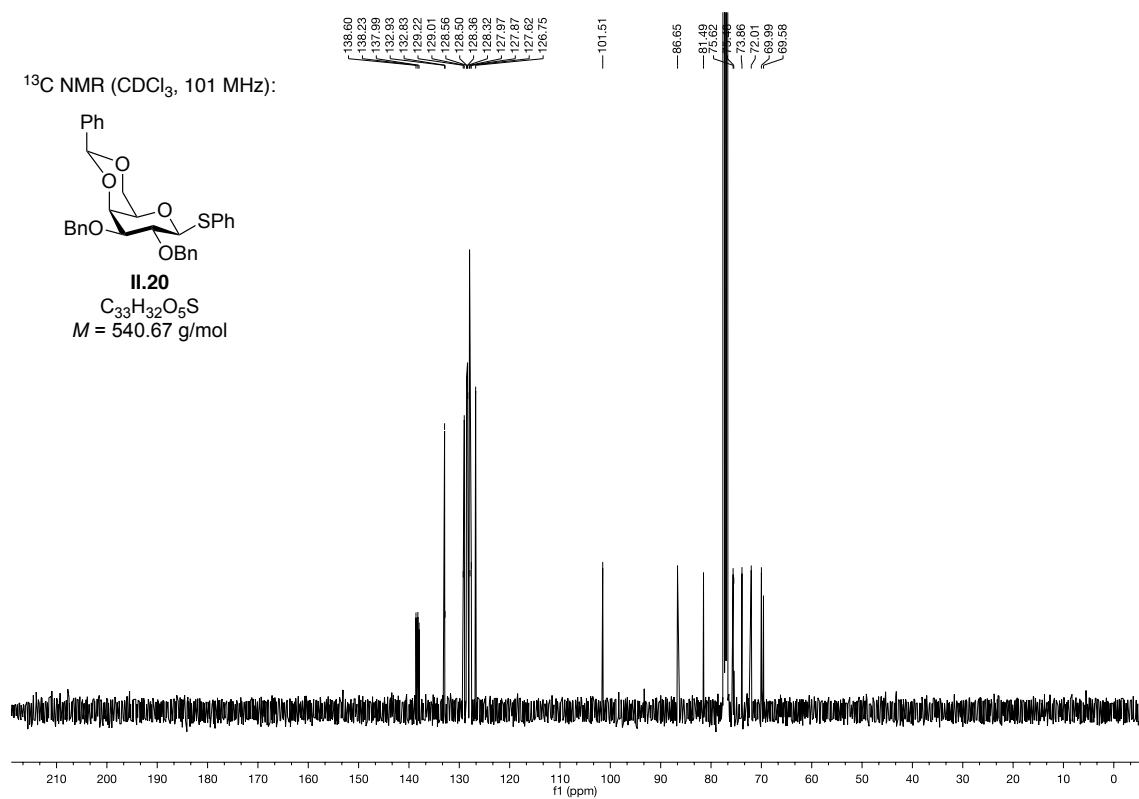
II.20
 $\text{C}_{33}\text{H}_{32}\text{O}_5\text{S}$
 $M = 540.67 \text{ g/mol}$

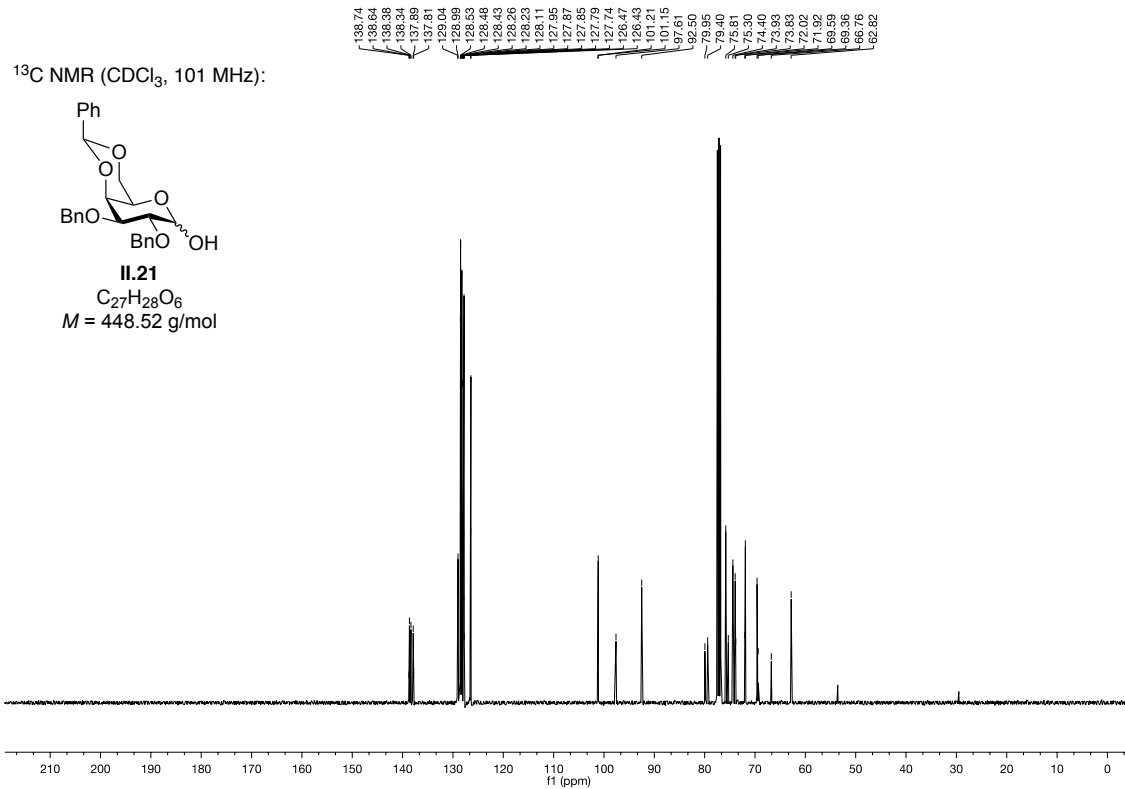
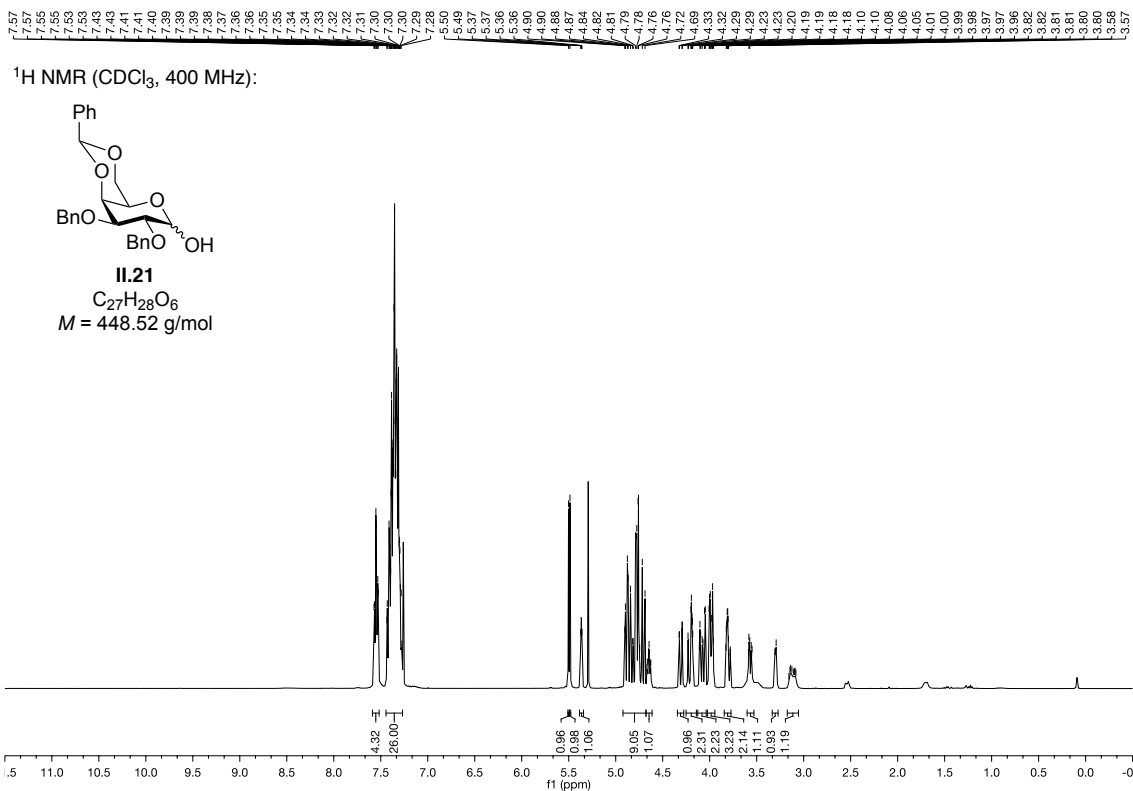


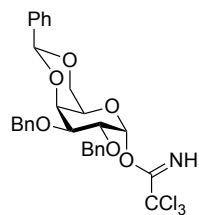
$^{13}\text{C NMR}$ (CDCl_3 , 101 MHz):



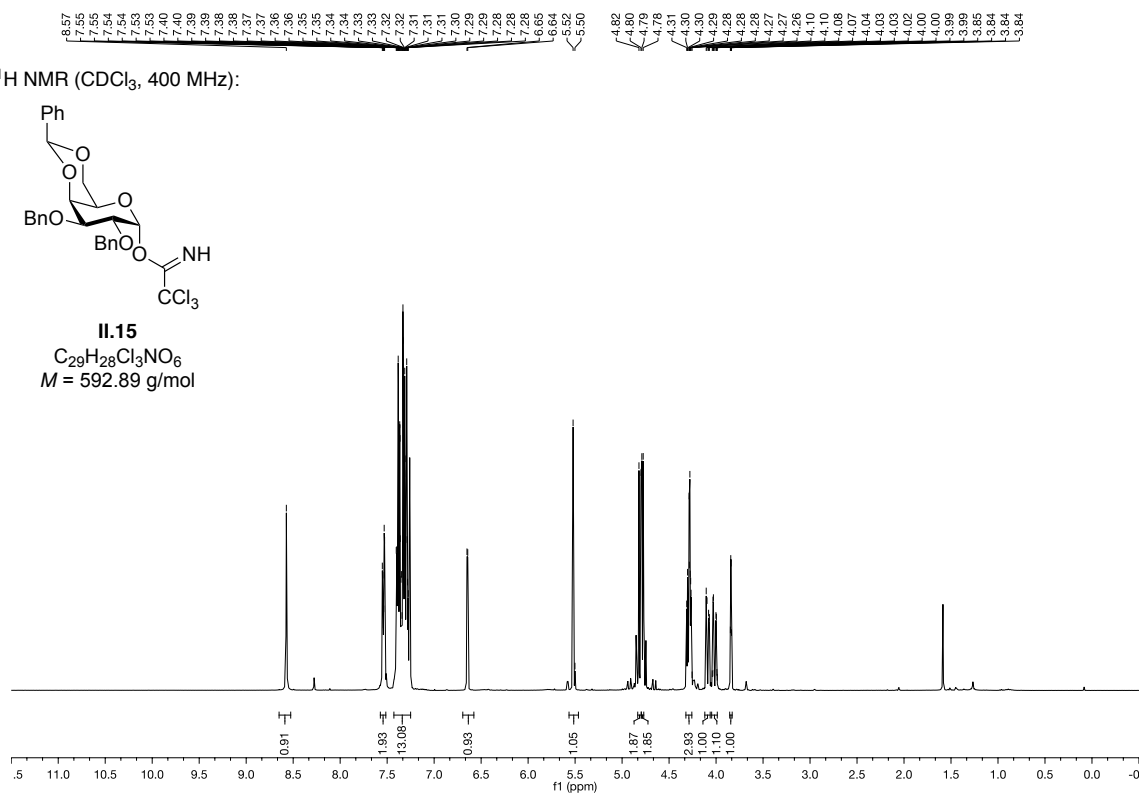
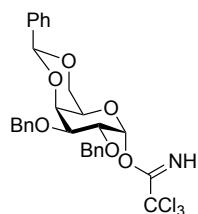
II.20
 $\text{C}_{33}\text{H}_{32}\text{O}_5\text{S}$
 $M = 540.67 \text{ g/mol}$



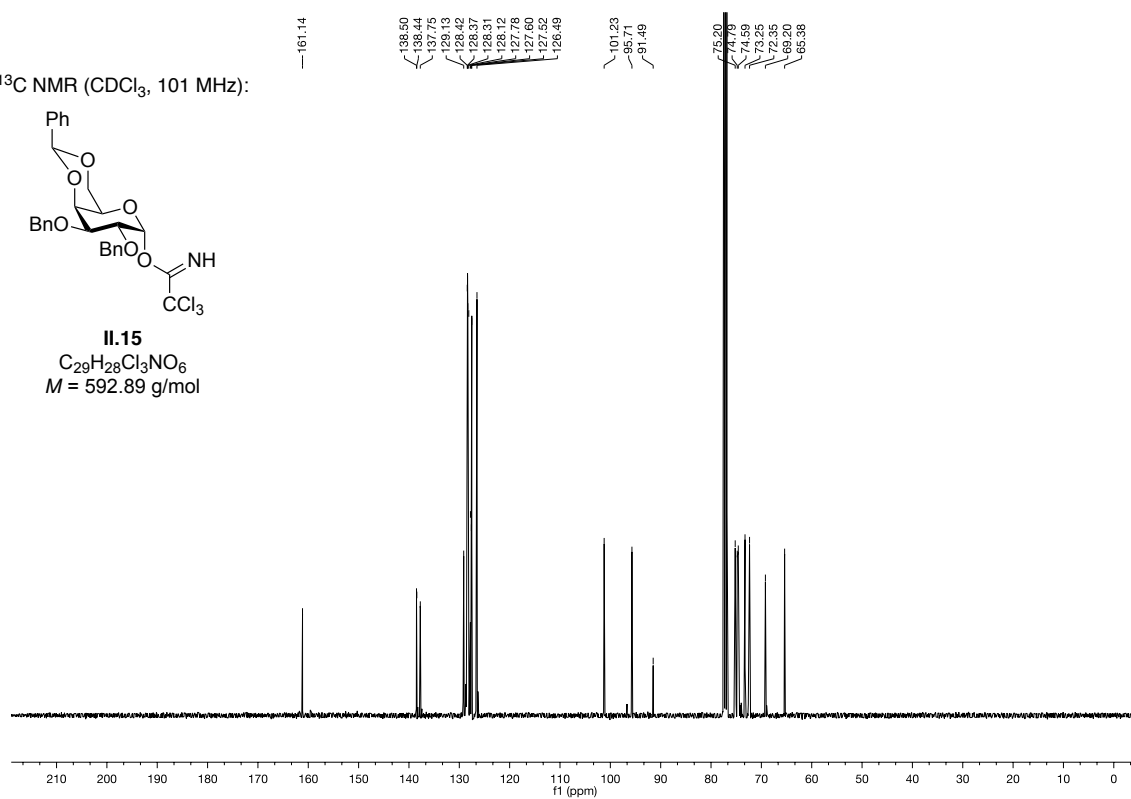


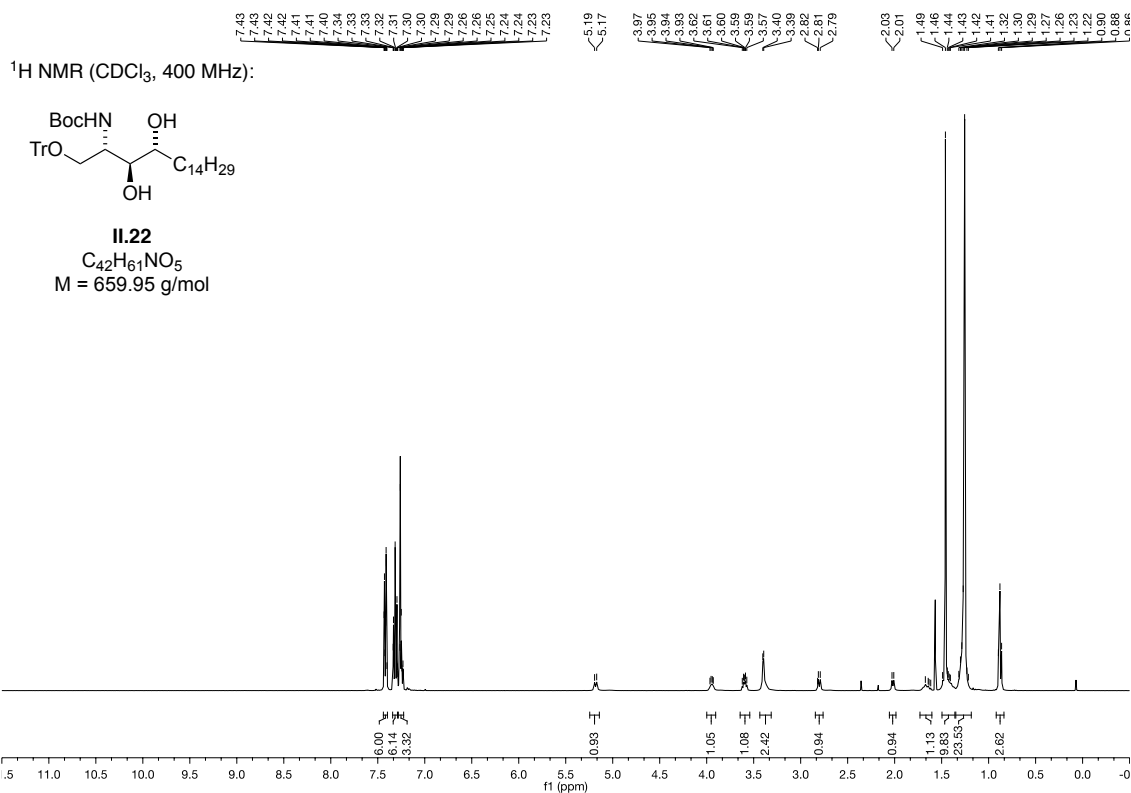
^1H NMR (CDCl_3 , 400 MHz):

II.15
 $\text{C}_{29}\text{H}_{28}\text{Cl}_3\text{NO}_6$
 $M = 592.89$ g/mol

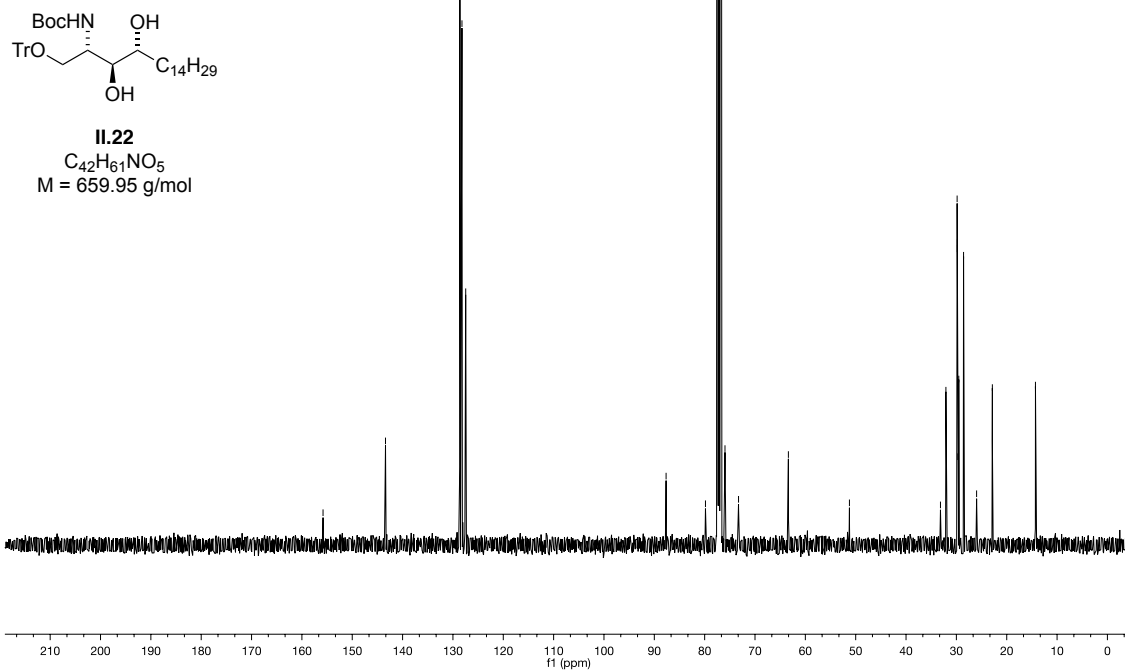
 ^{13}C NMR (CDCl_3 , 101 MHz):

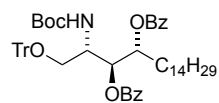
II.15
 $\text{C}_{29}\text{H}_{28}\text{Cl}_3\text{NO}_6$
 $M = 592.89$ g/mol



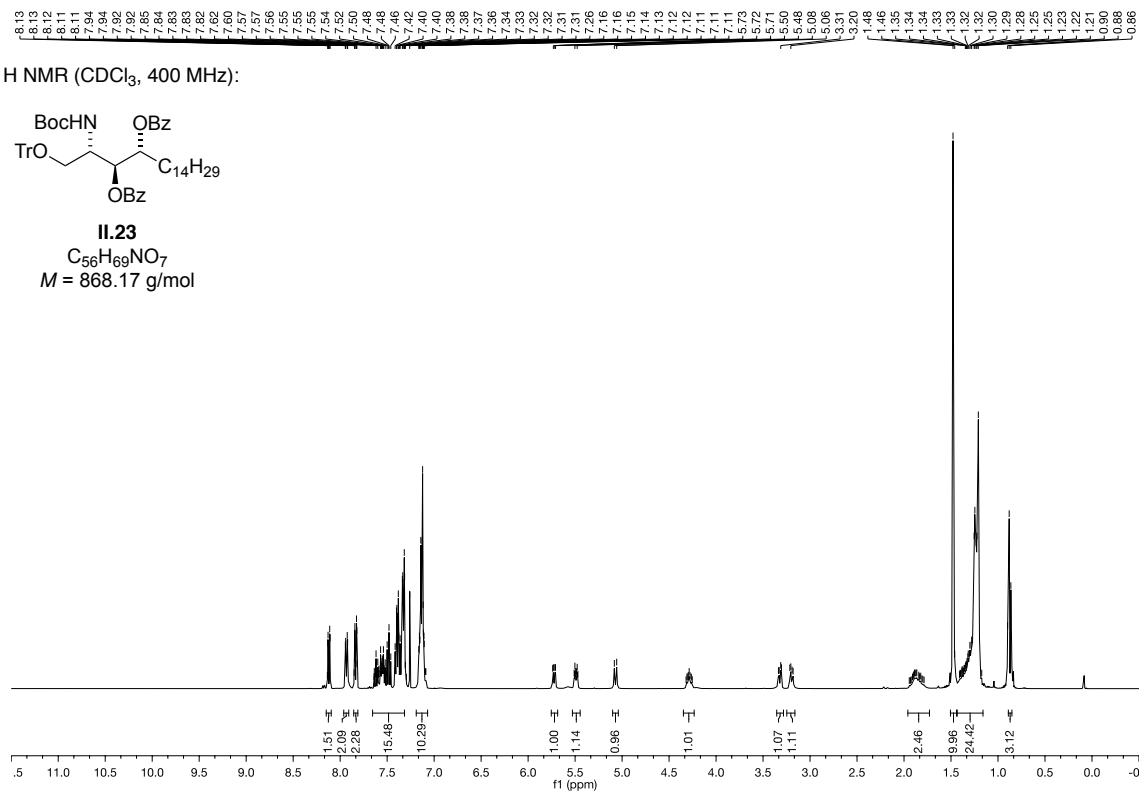
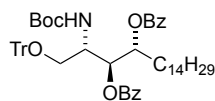


$^{13}\text{C NMR}$ (CDCl_3 , 101 MHz):

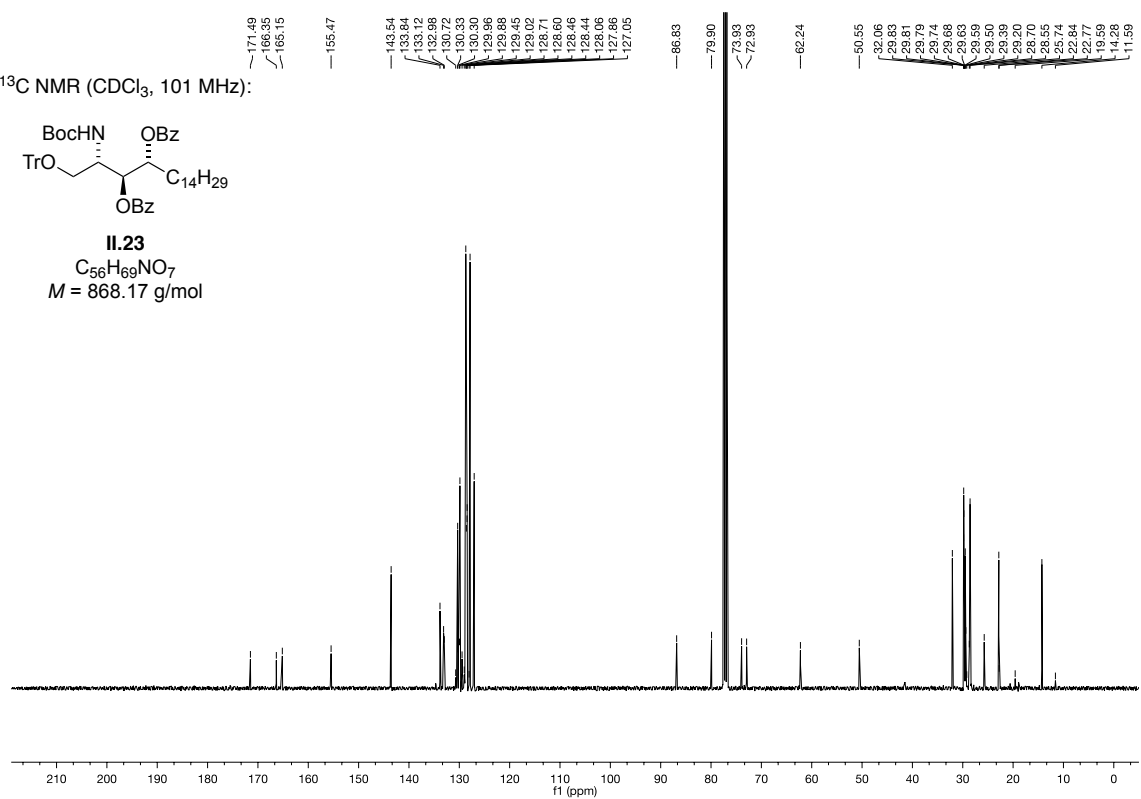


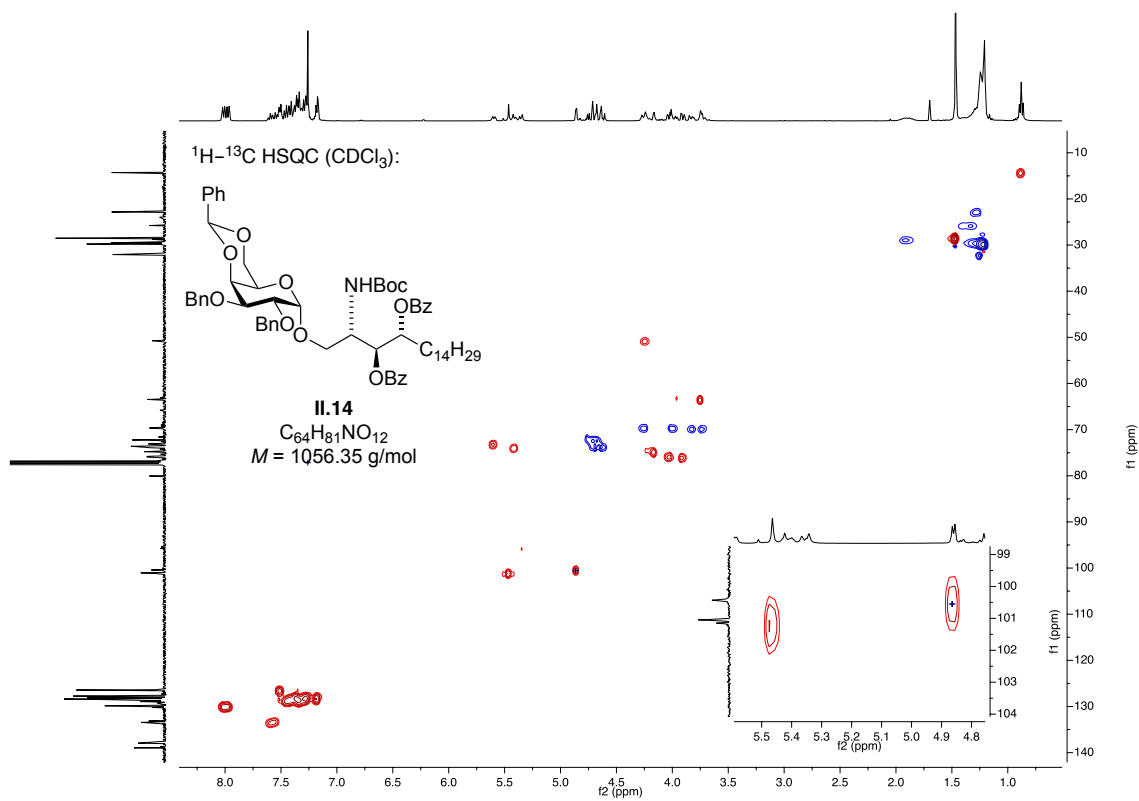
^1H NMR (CDCl_3 , 400 MHz):

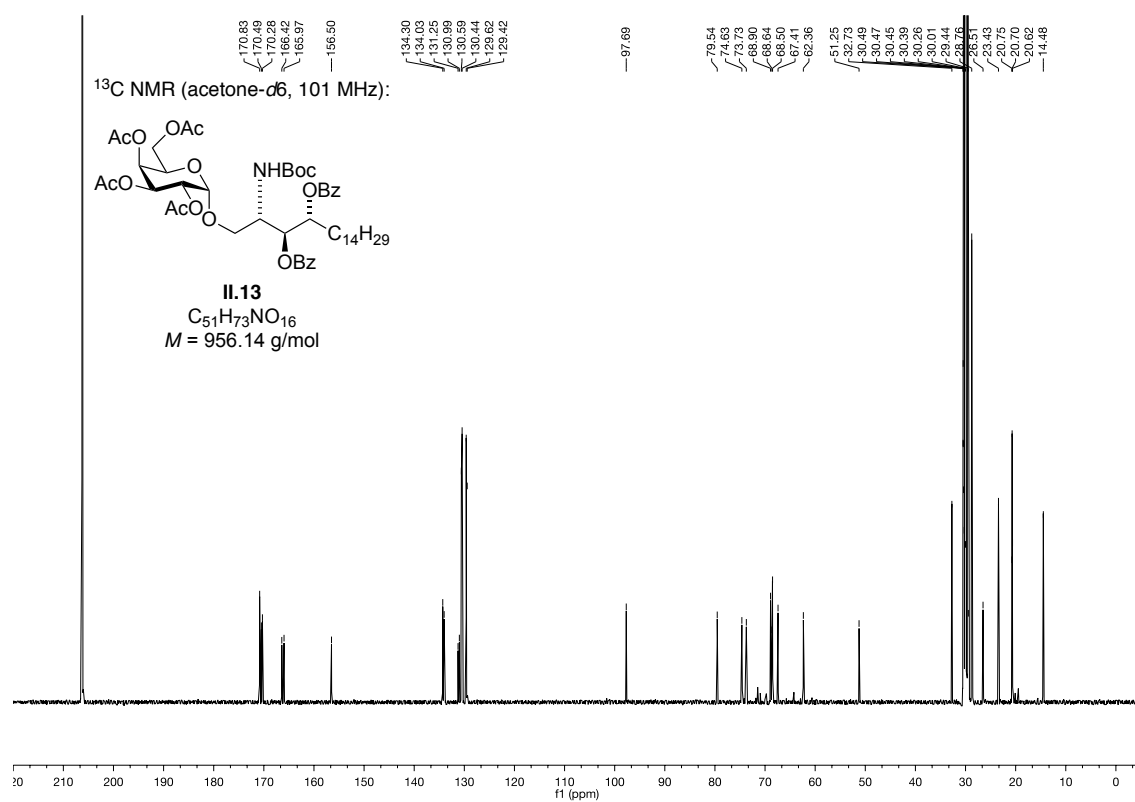
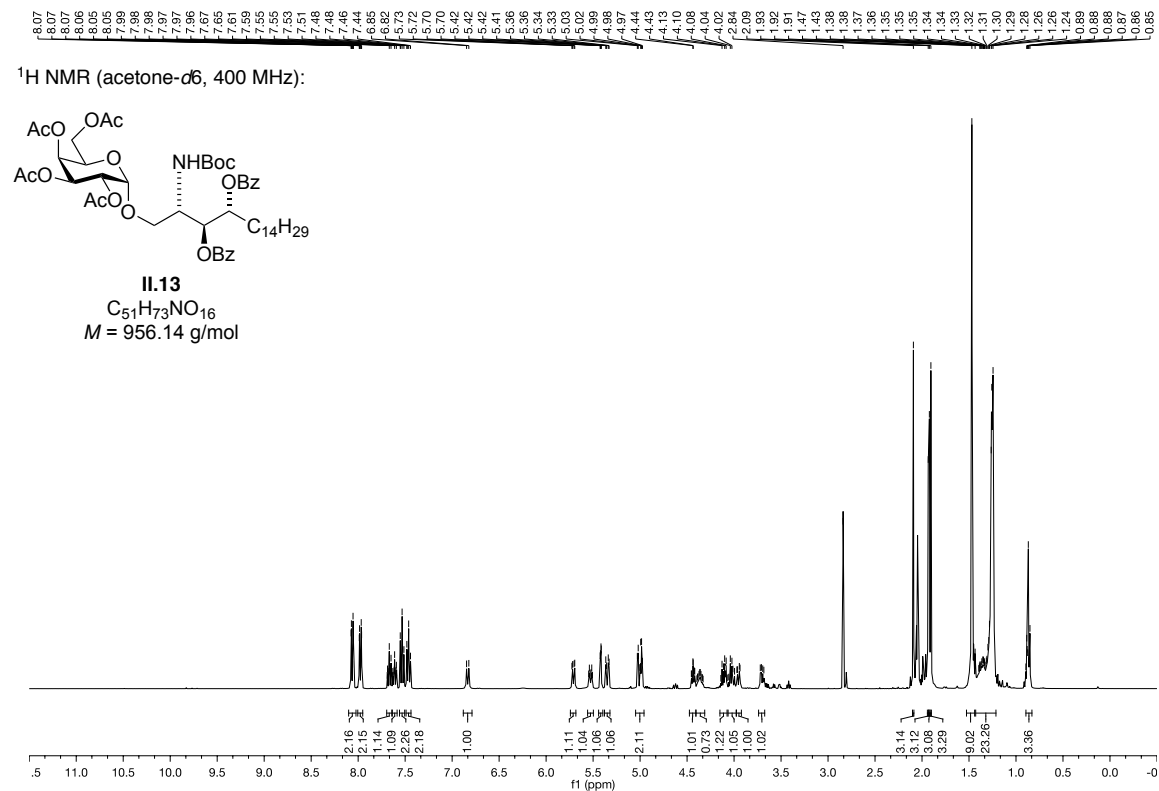
II.23
 $\text{C}_{56}\text{H}_{69}\text{NO}_7$
 $M = 868.17$ g/mol

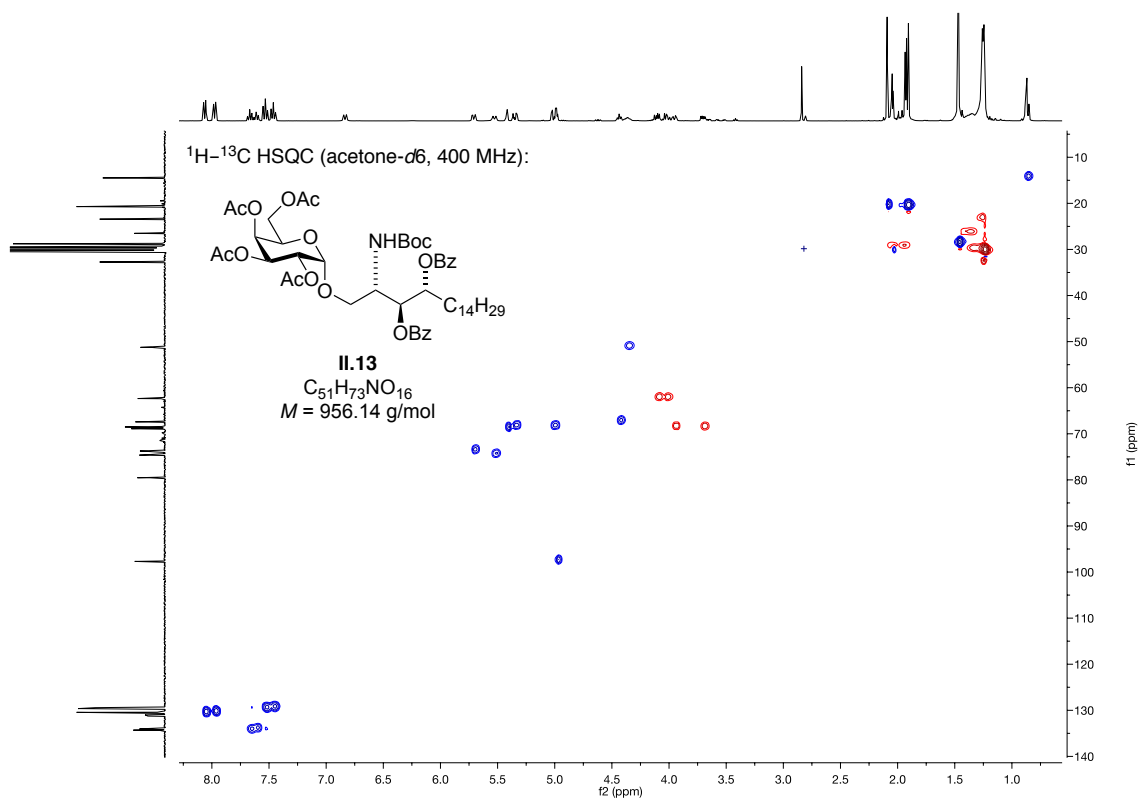
 ^{13}C NMR (CDCl_3 , 101 MHz):

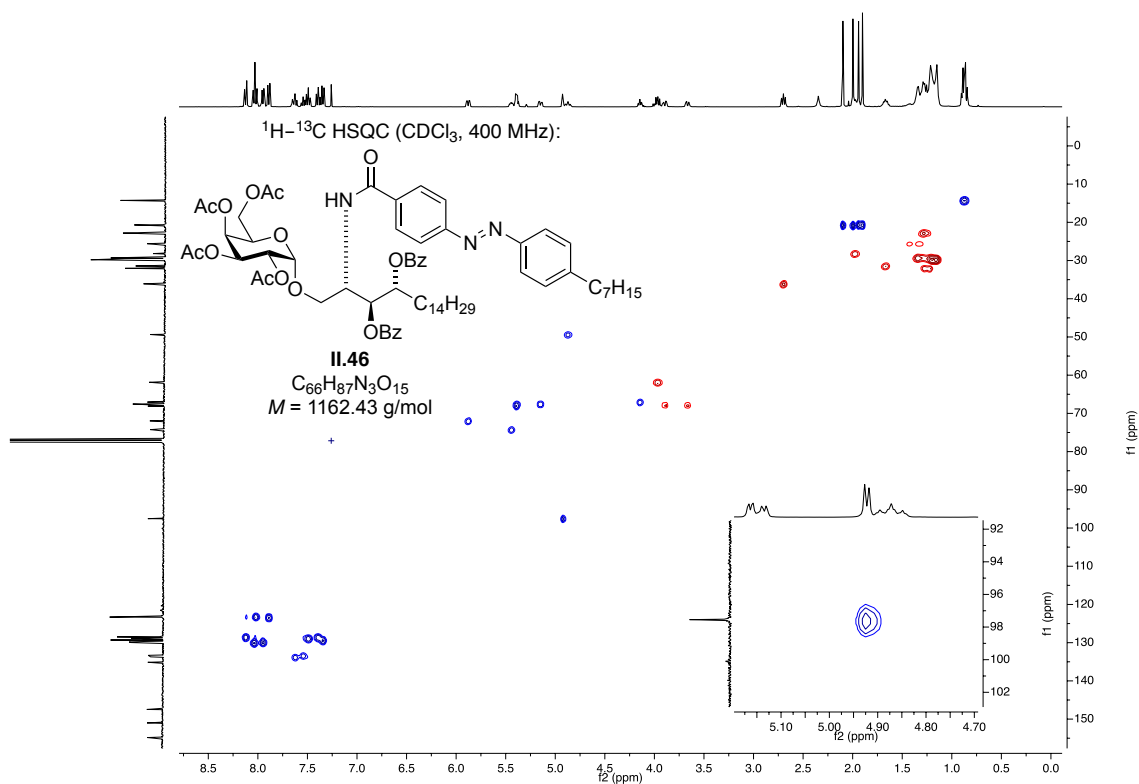
II.23
 $\text{C}_{56}\text{H}_{69}\text{NO}_7$
 $M = 868.17$ g/mol

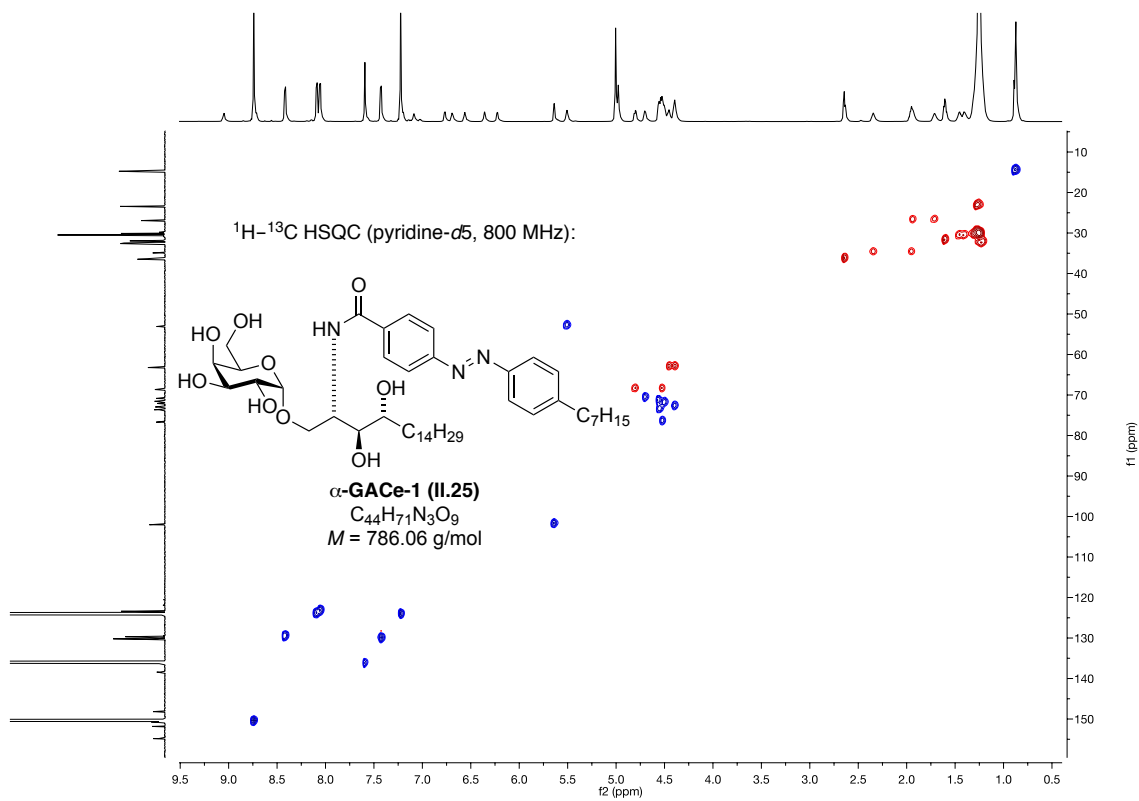


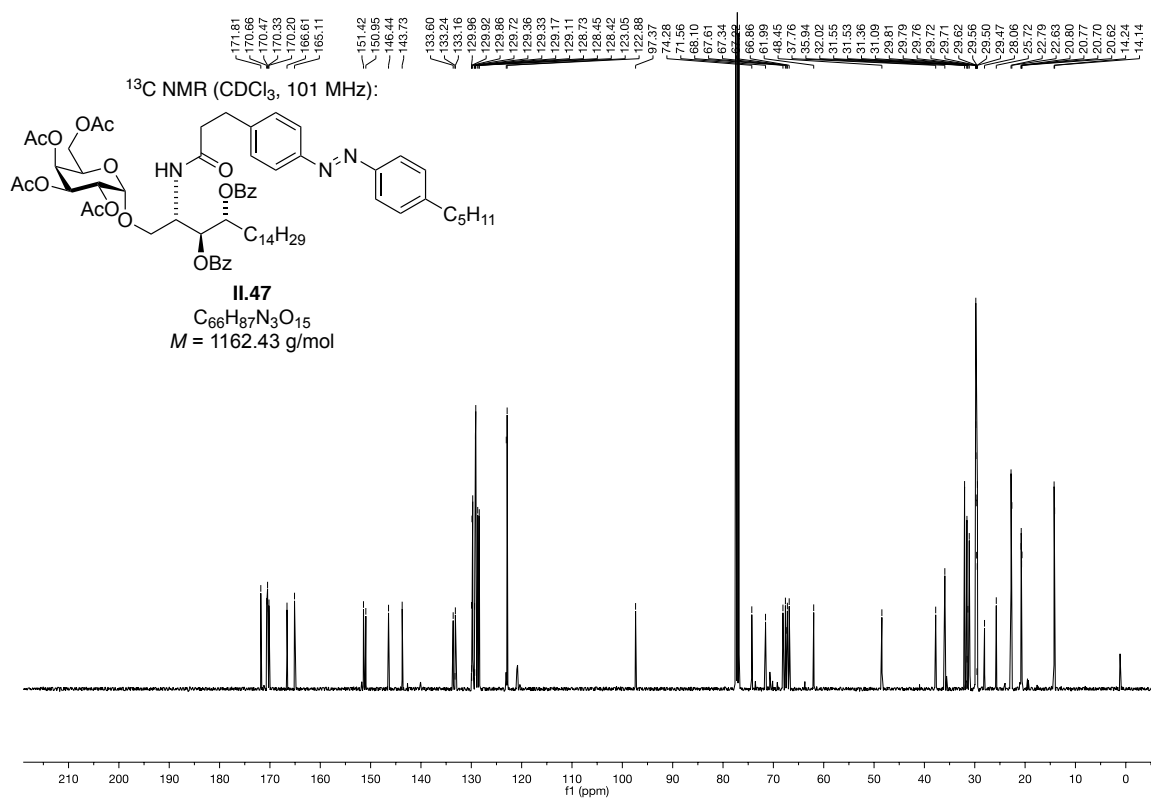
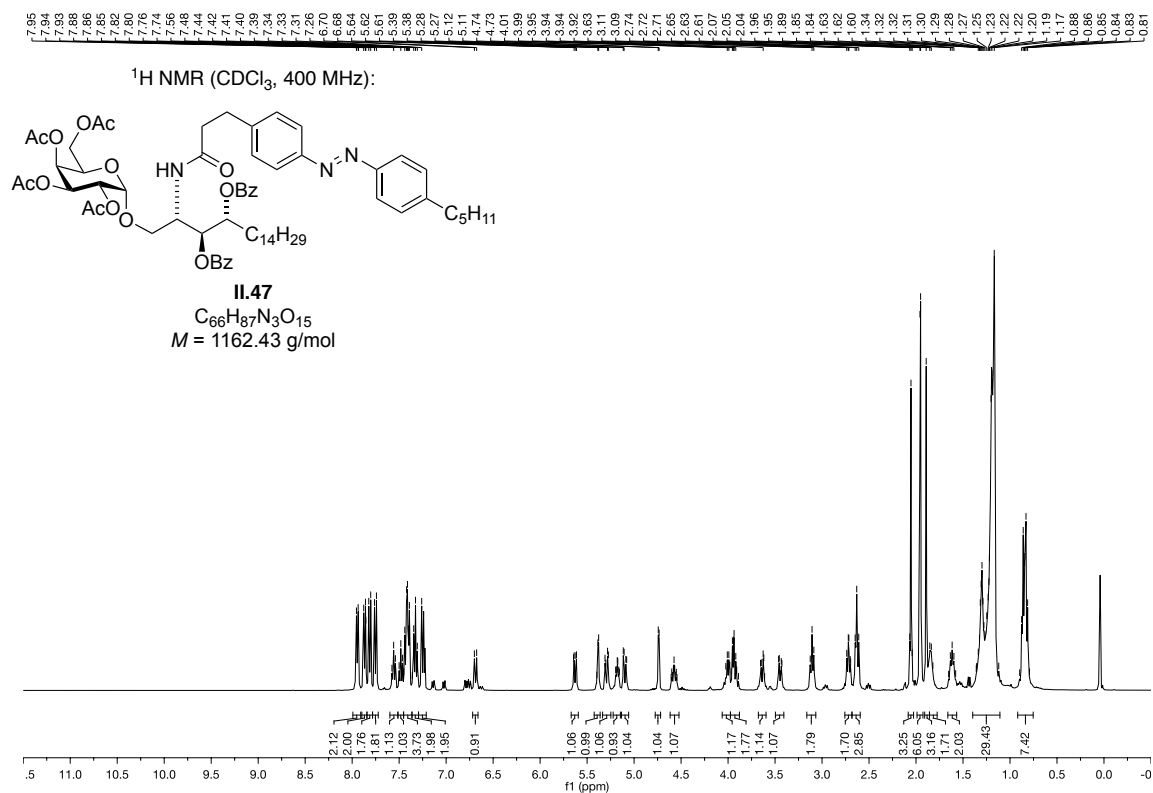


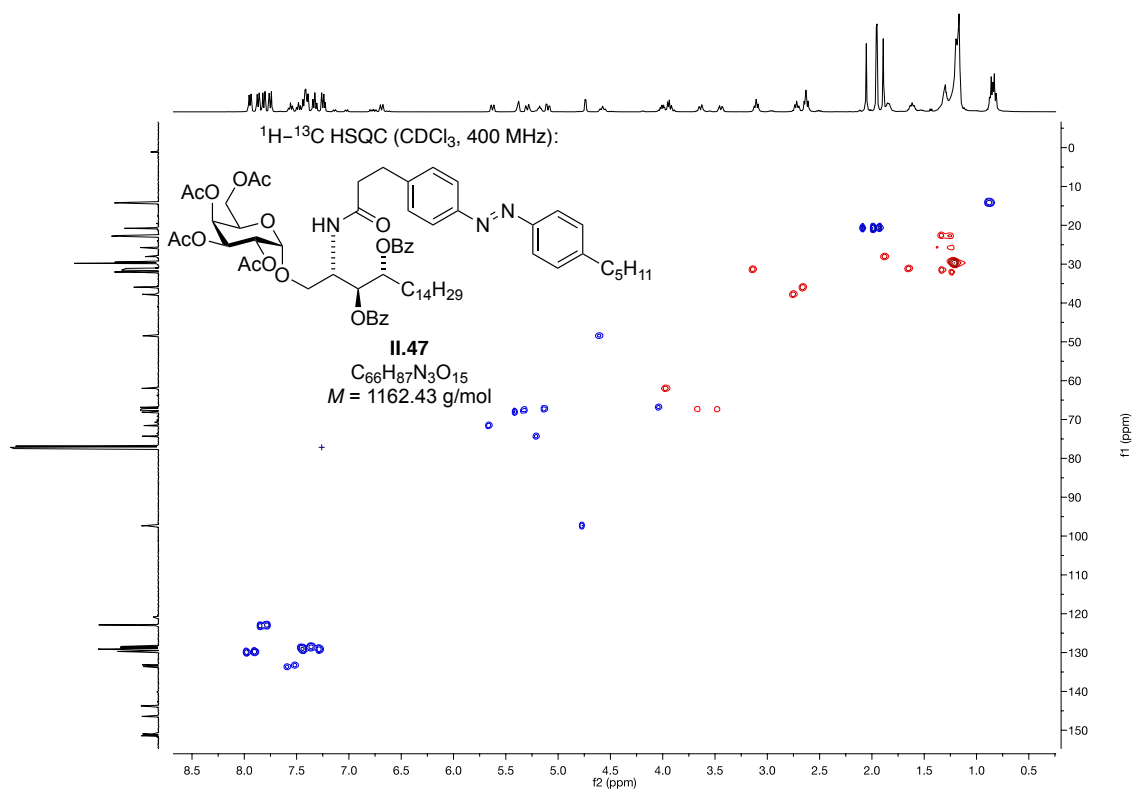


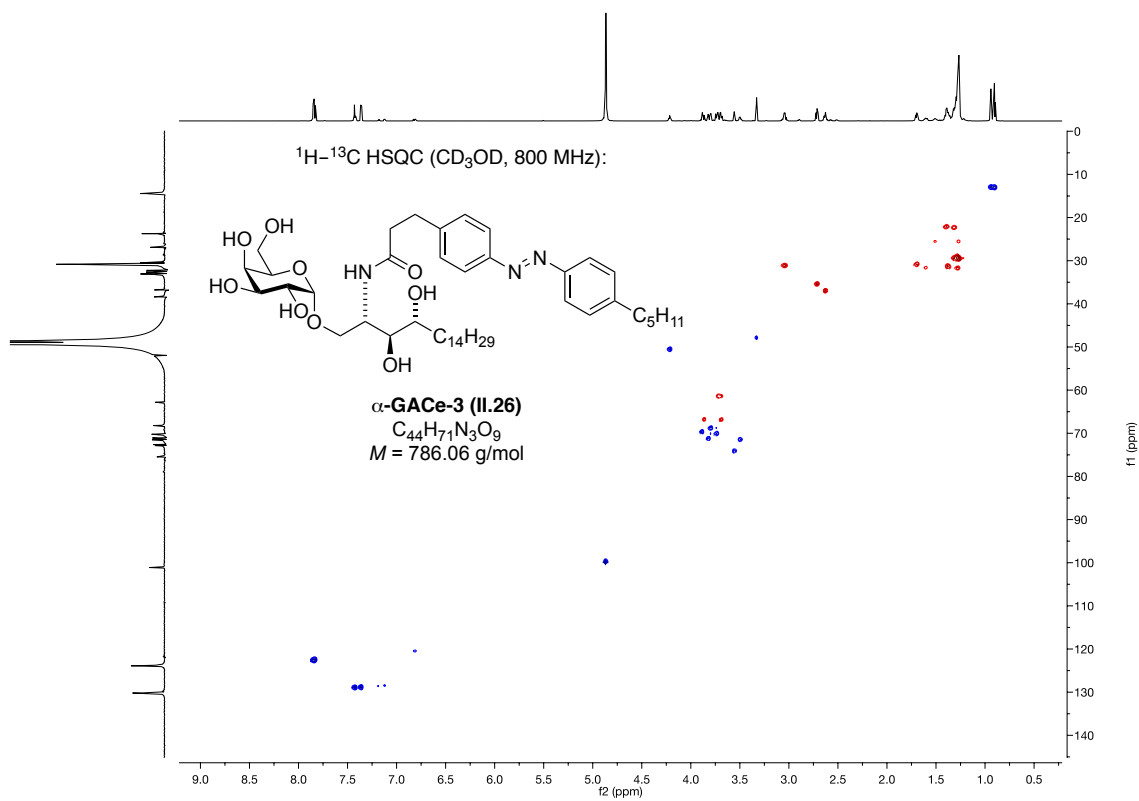


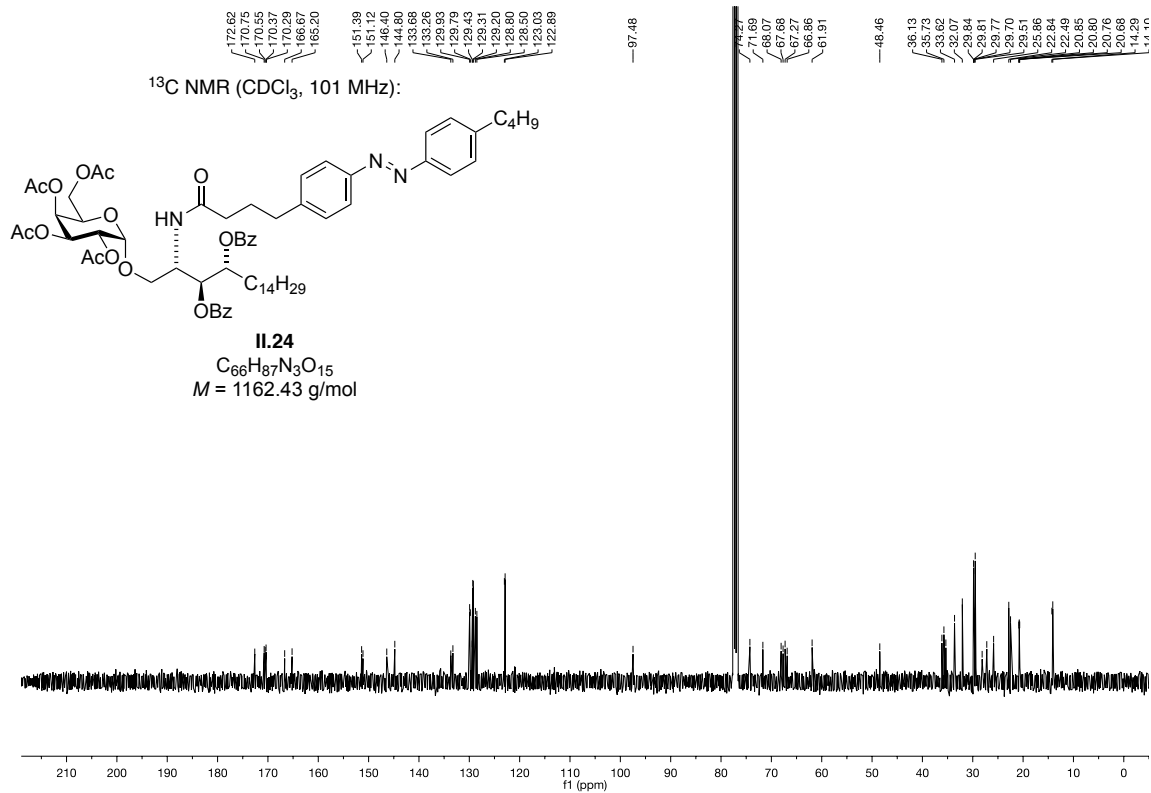
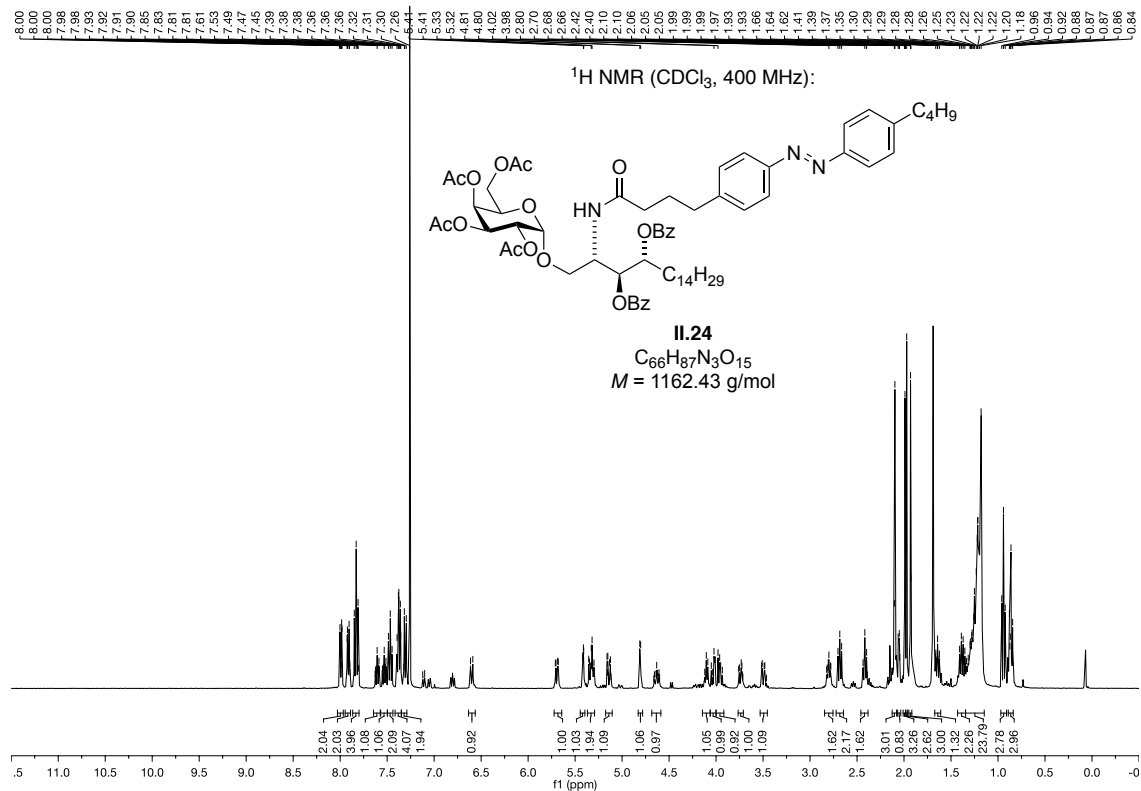


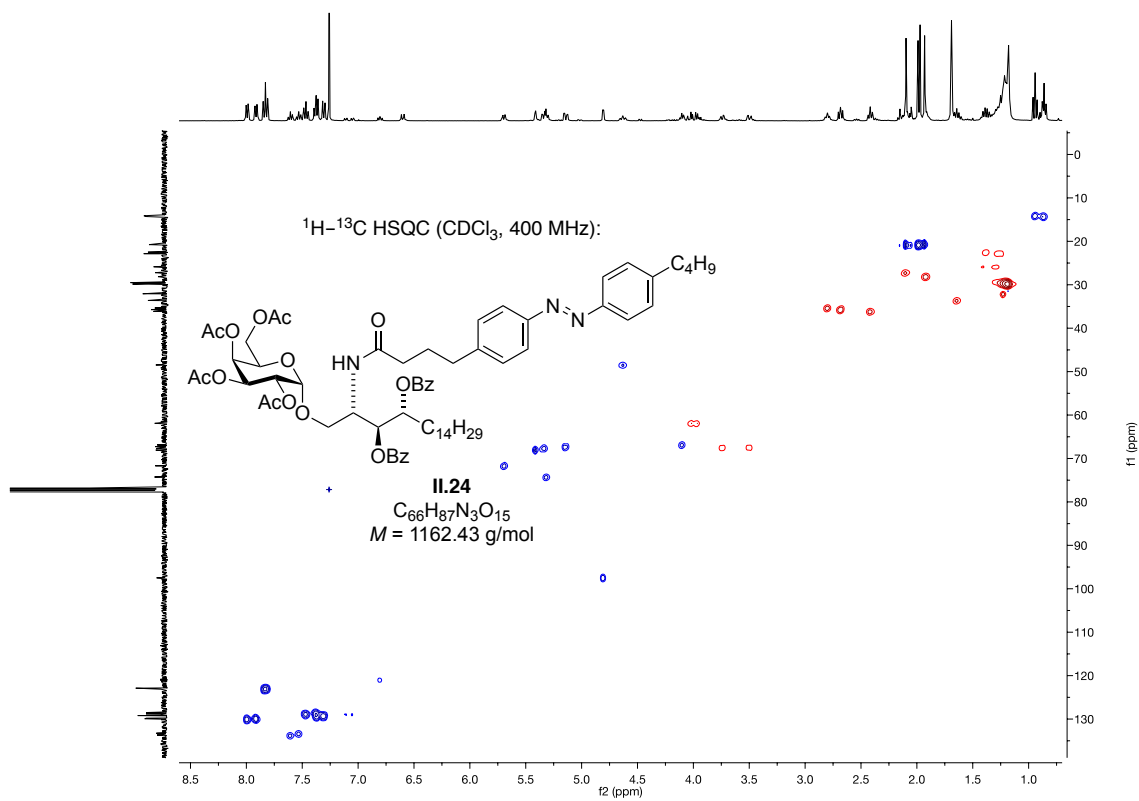


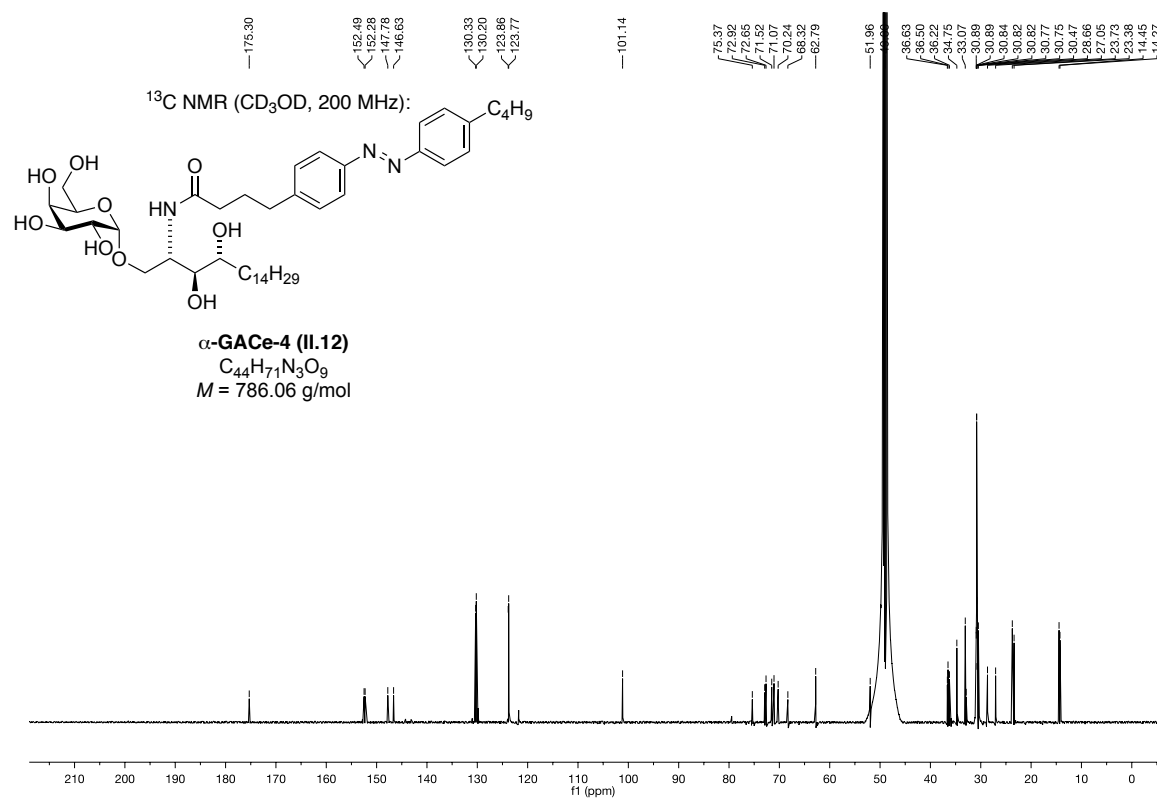
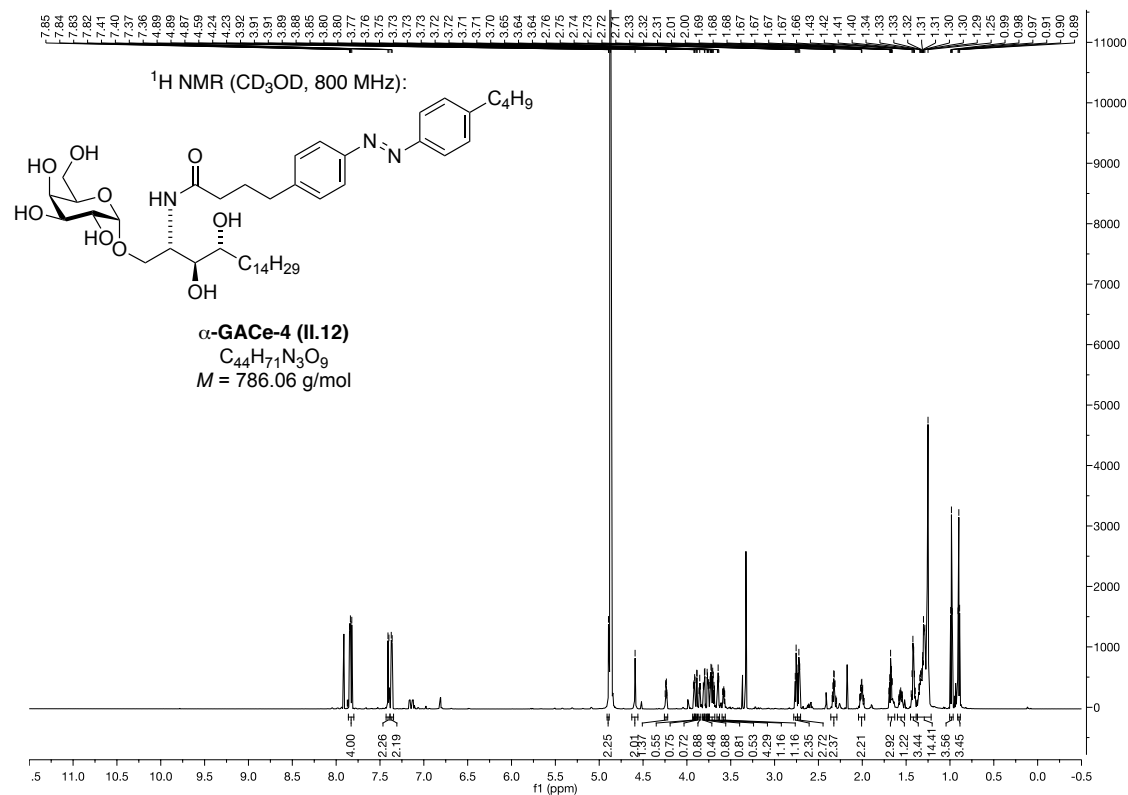


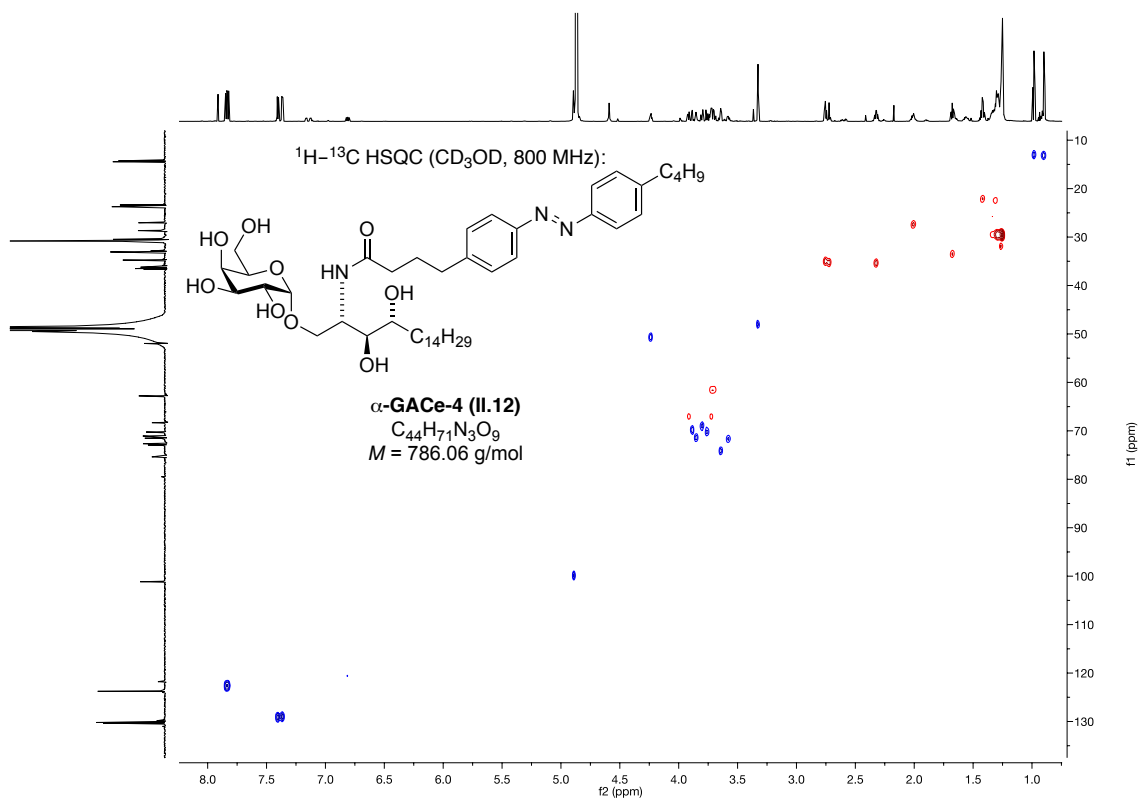


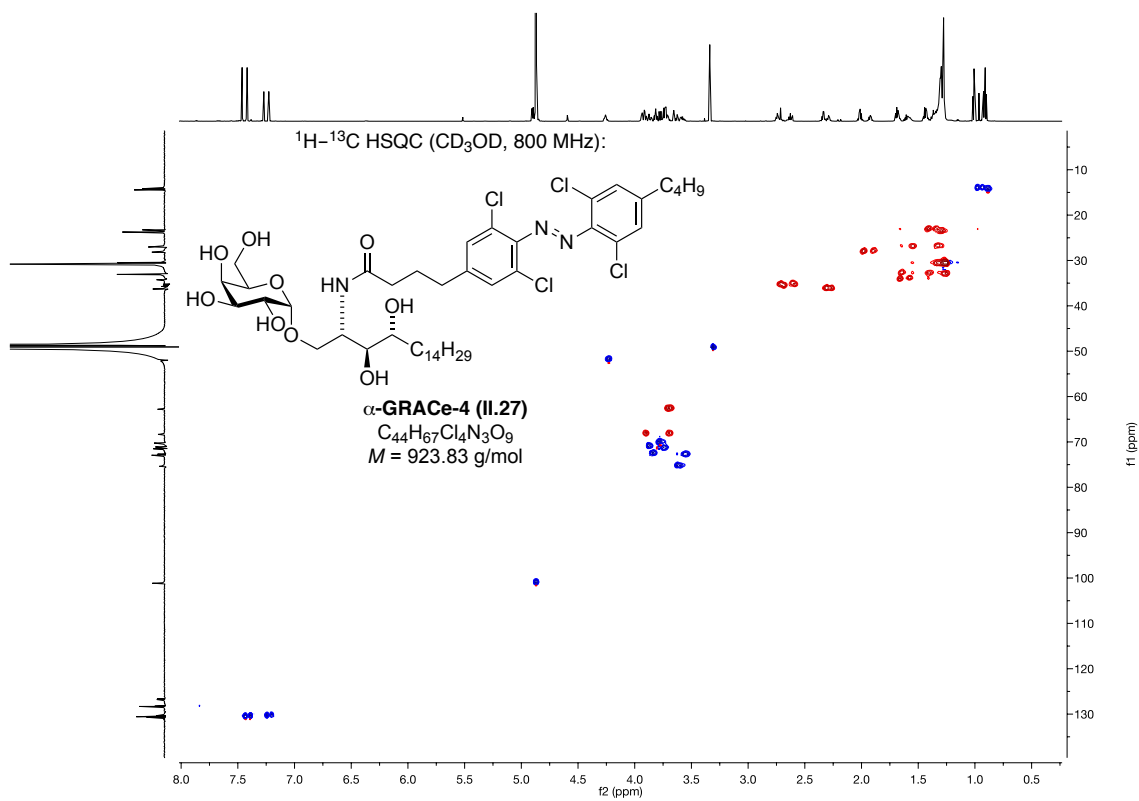




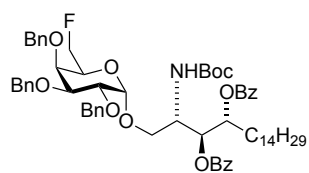






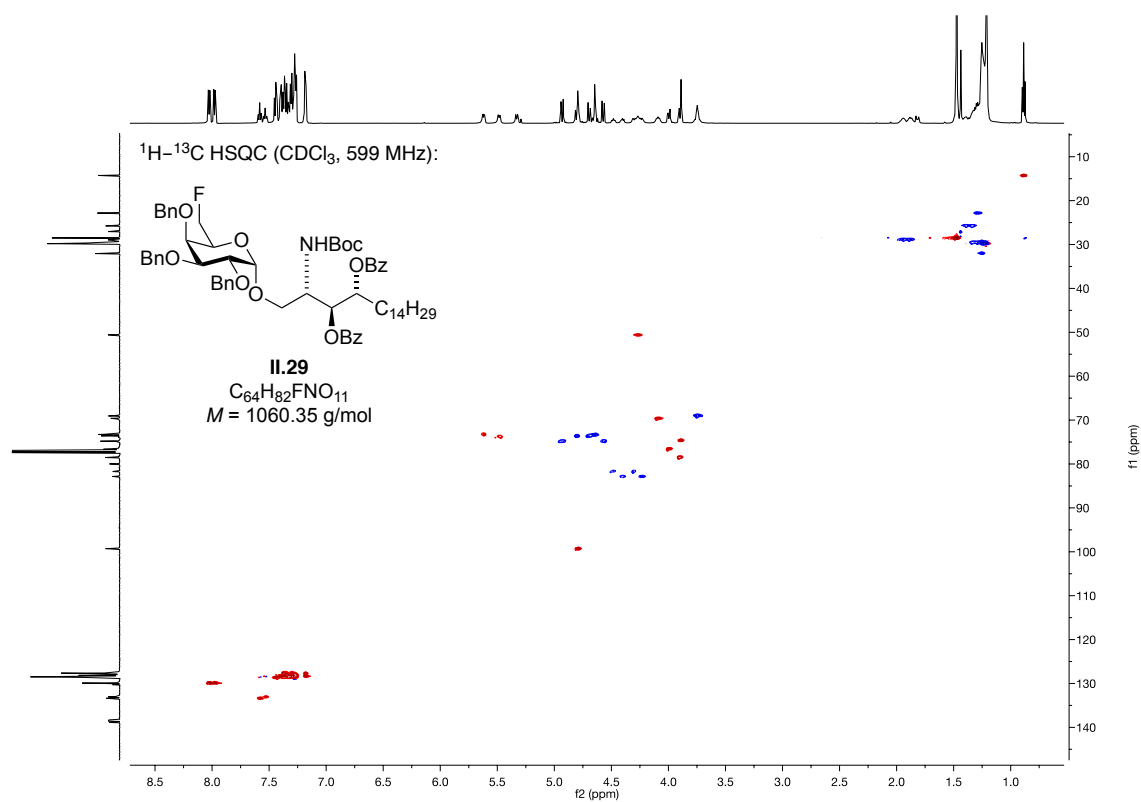
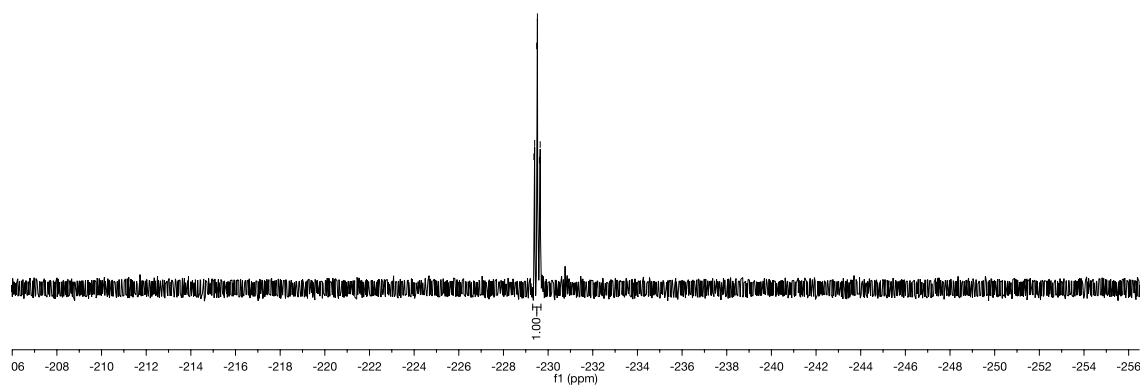


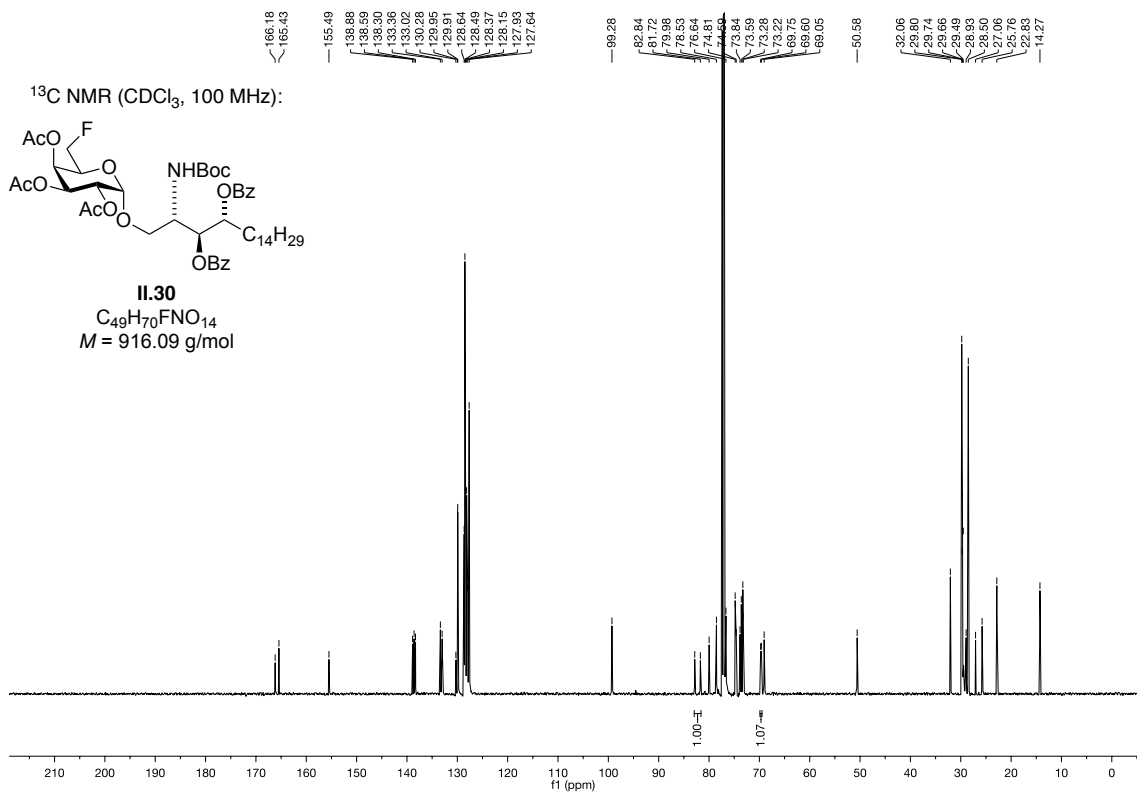
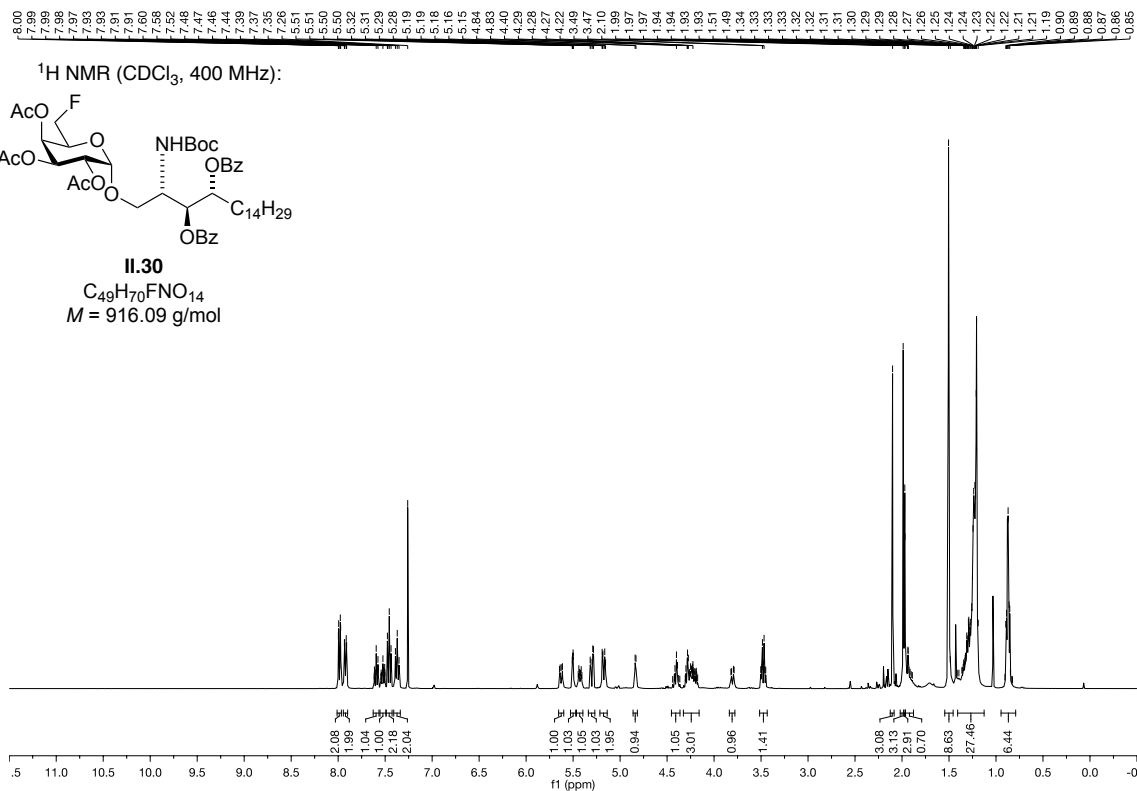
^{19}F NMR (CDCl_3 , 377 MHz):

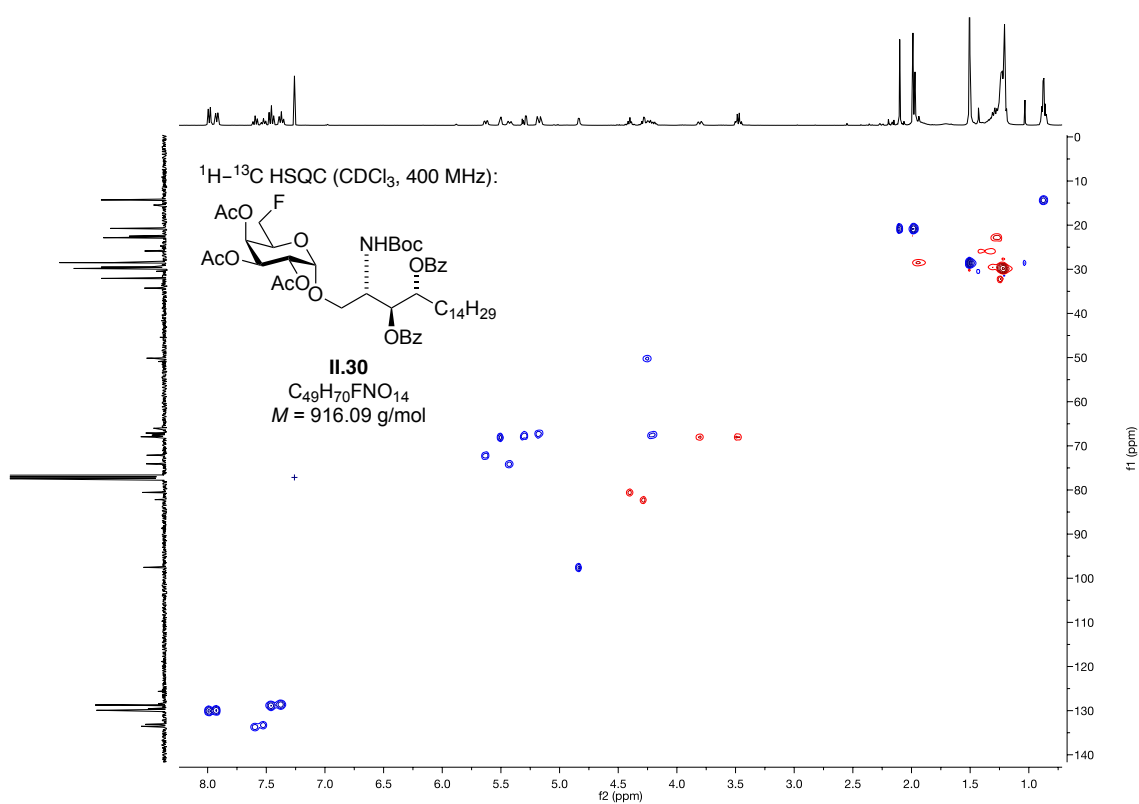
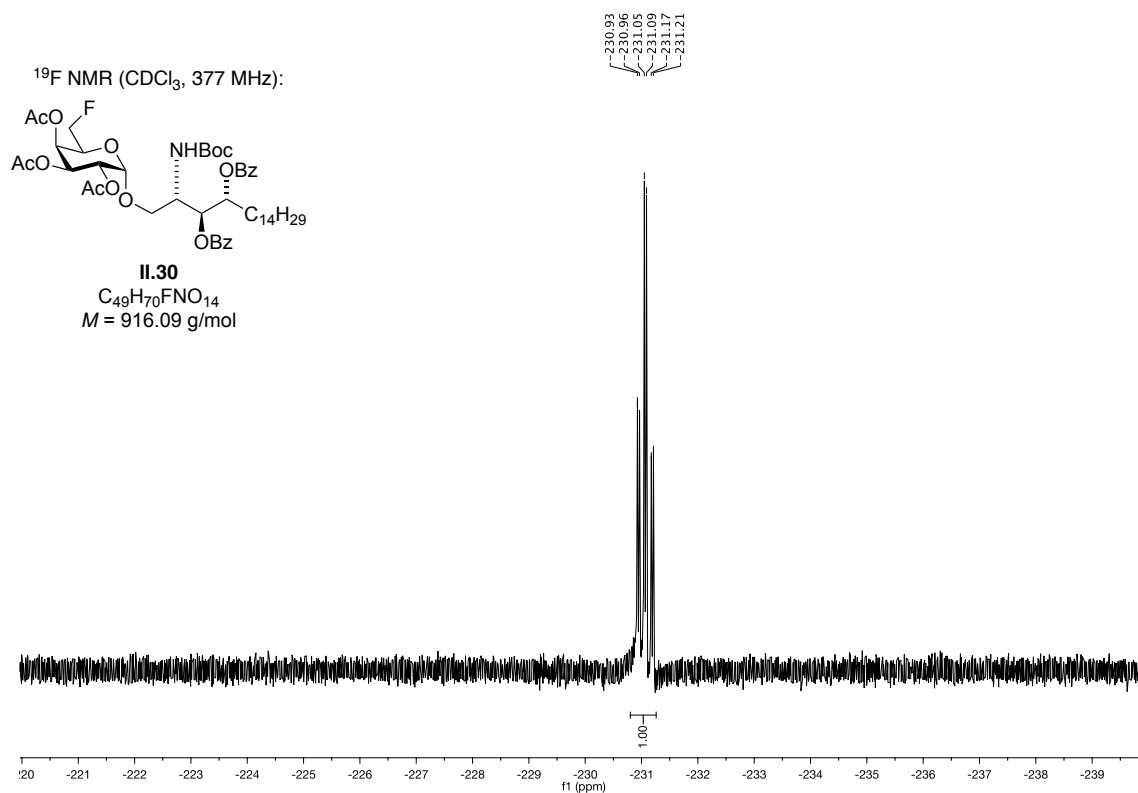


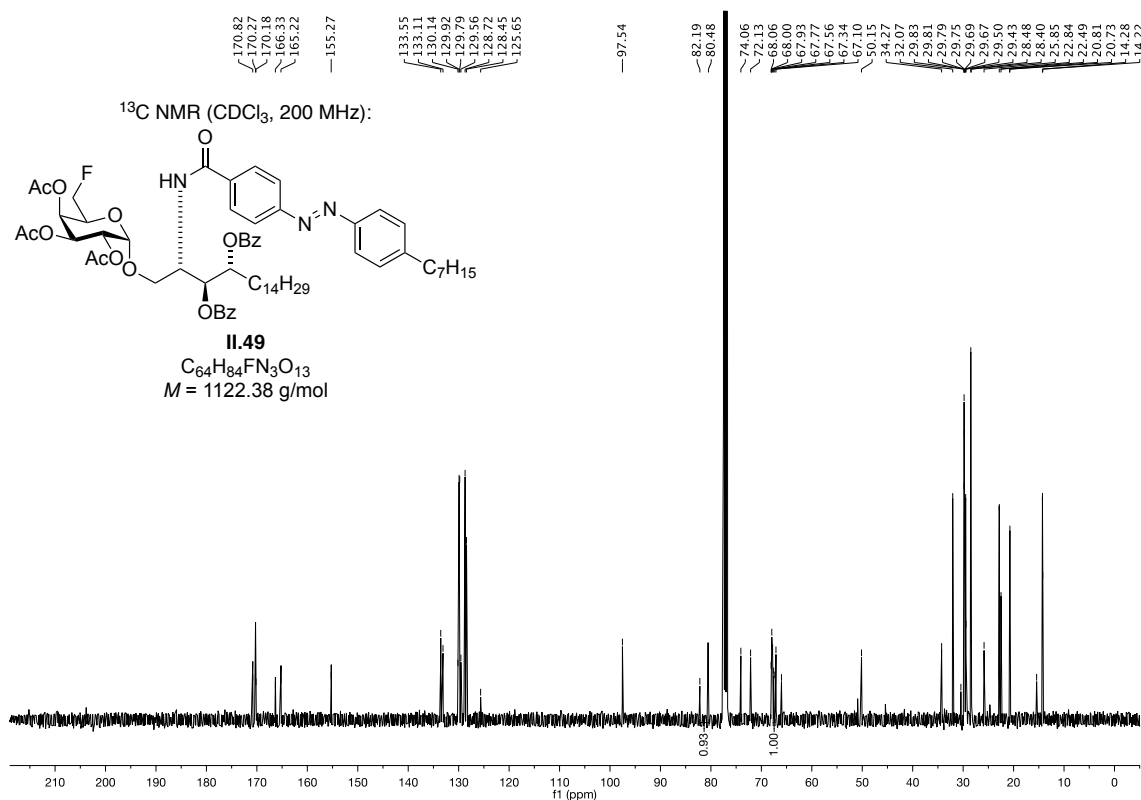
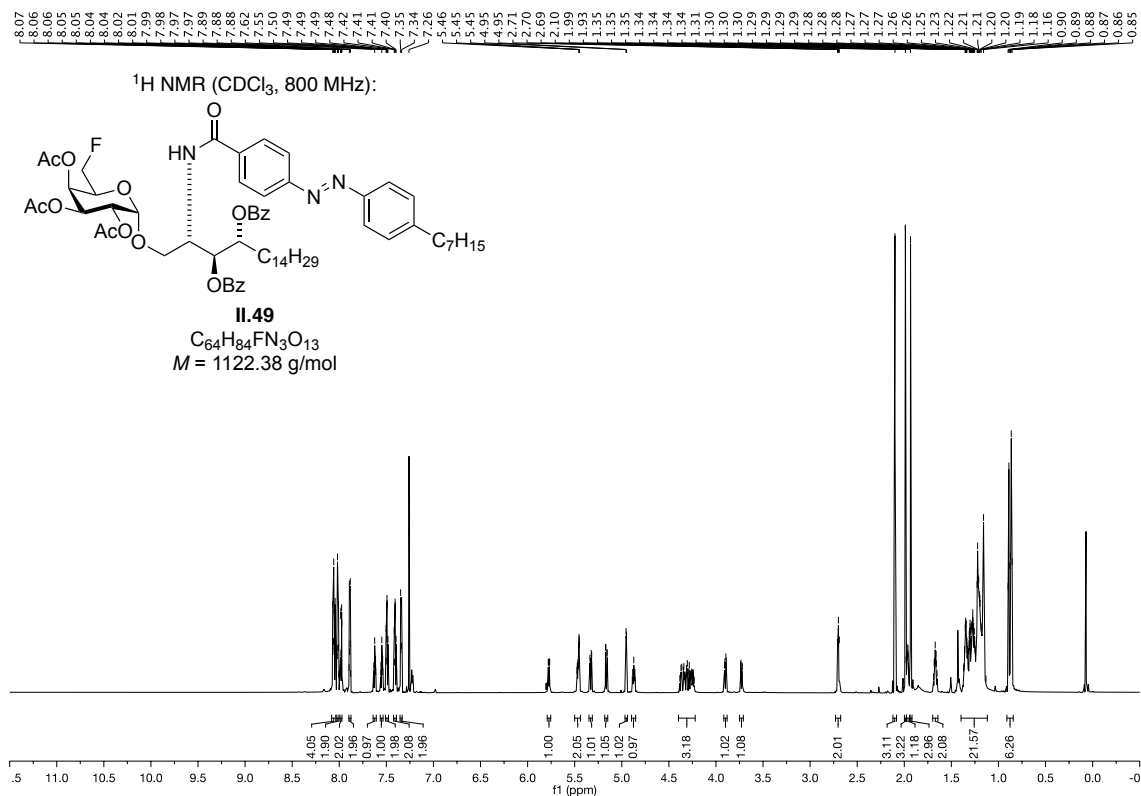
II.29
 $\text{C}_{64}\text{H}_{82}\text{FNO}_{11}$
 $M = 1060.35 \text{ g/mol}$

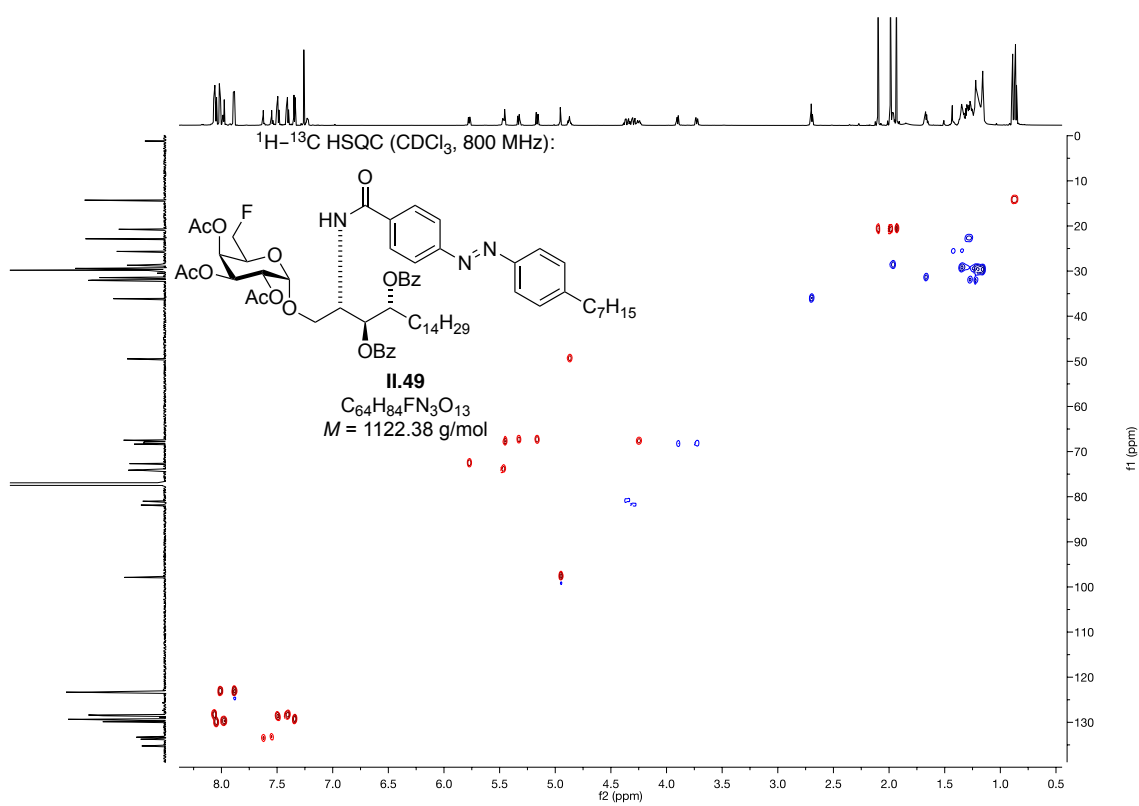
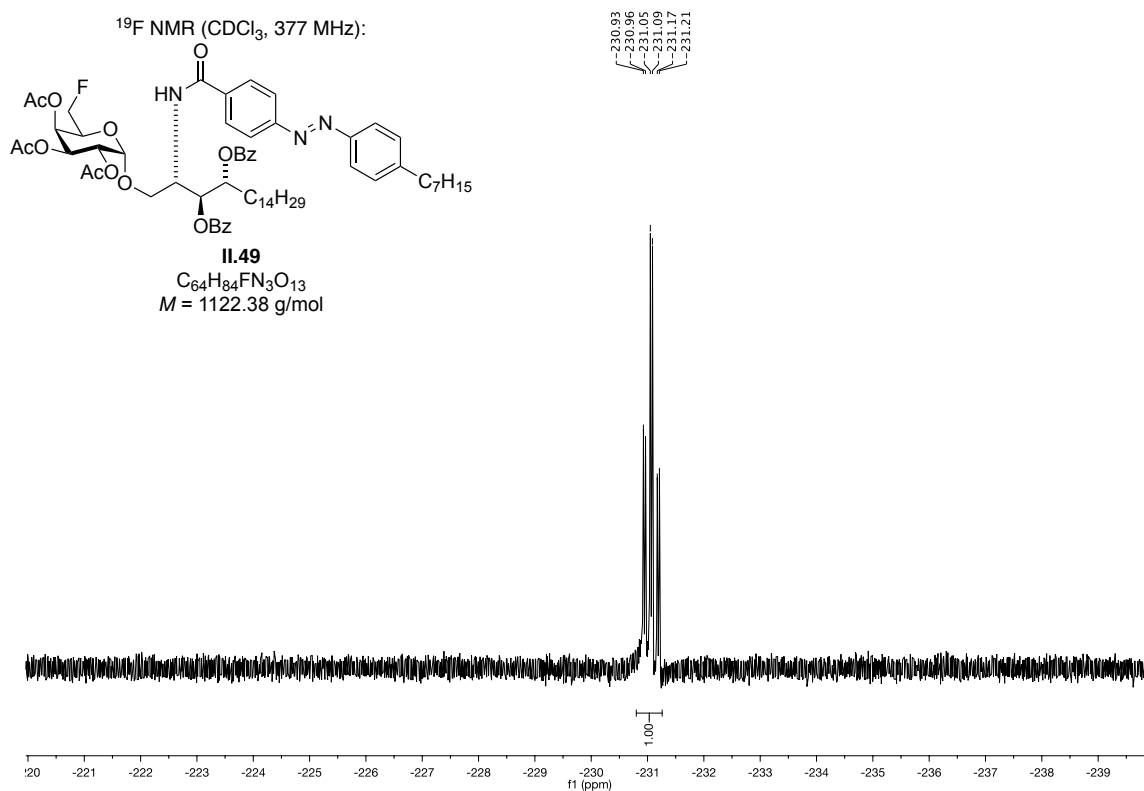
228.36
228.40
228.48
228.52
228.61
228.65

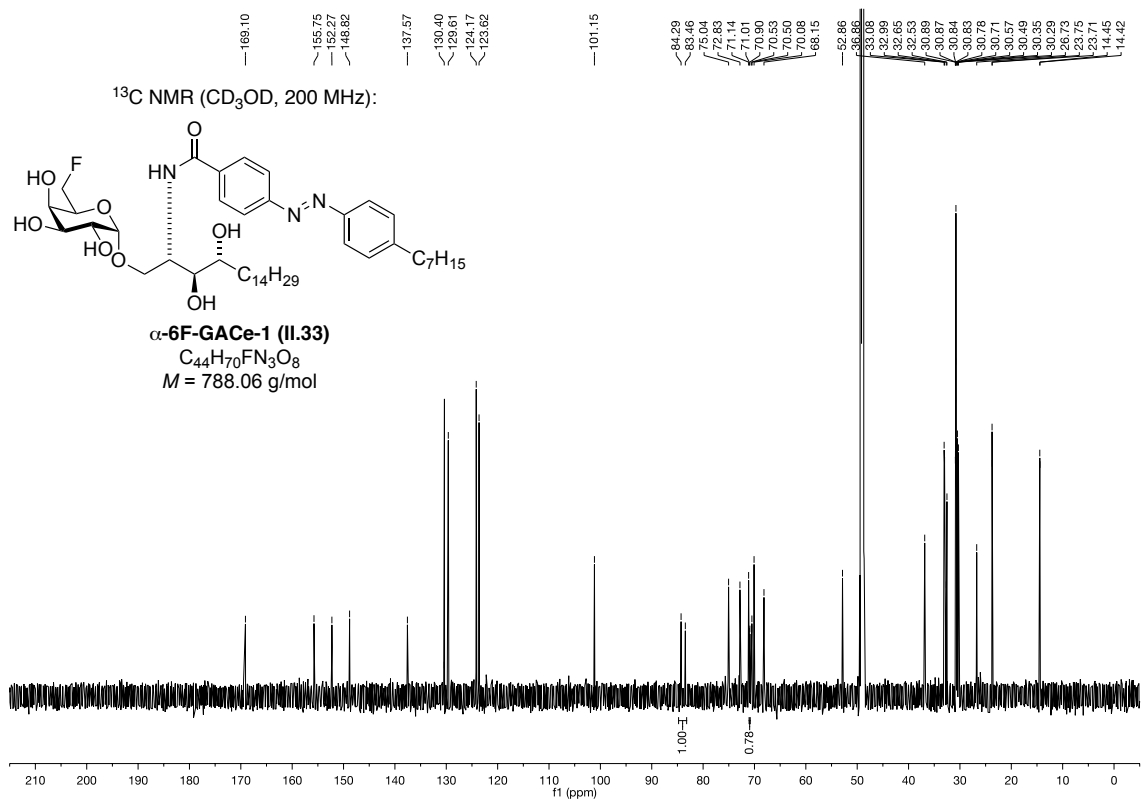
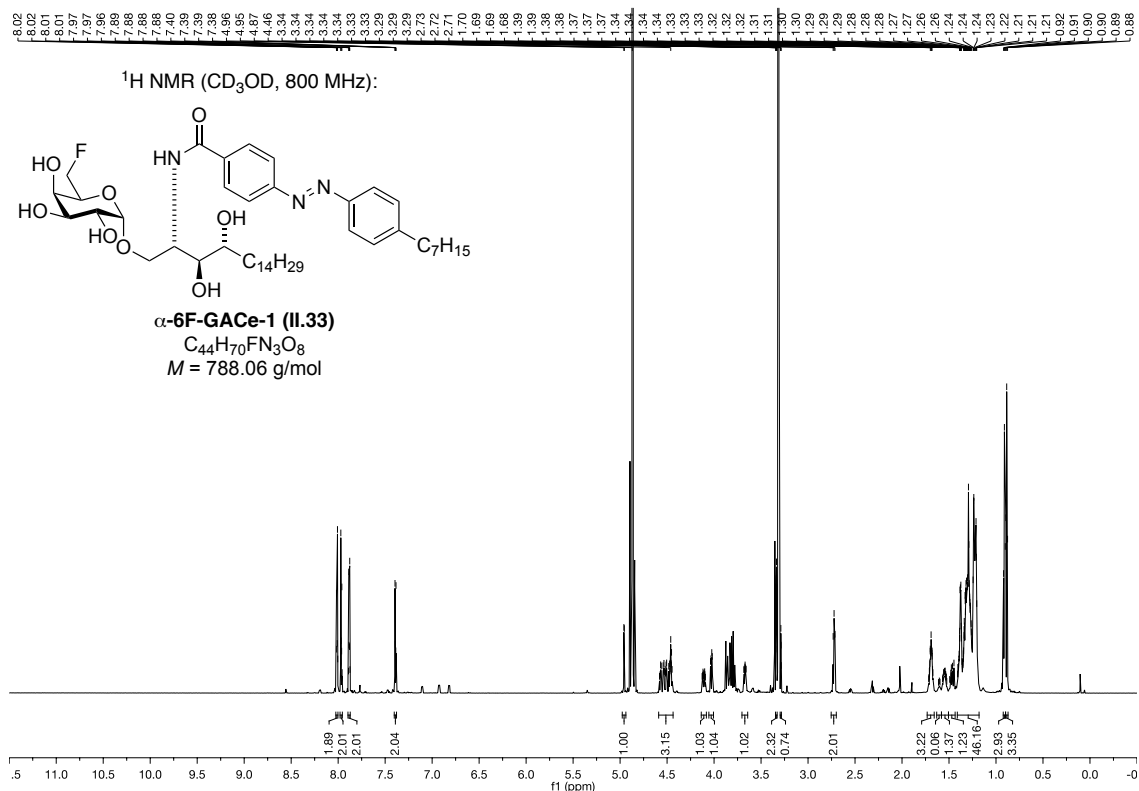


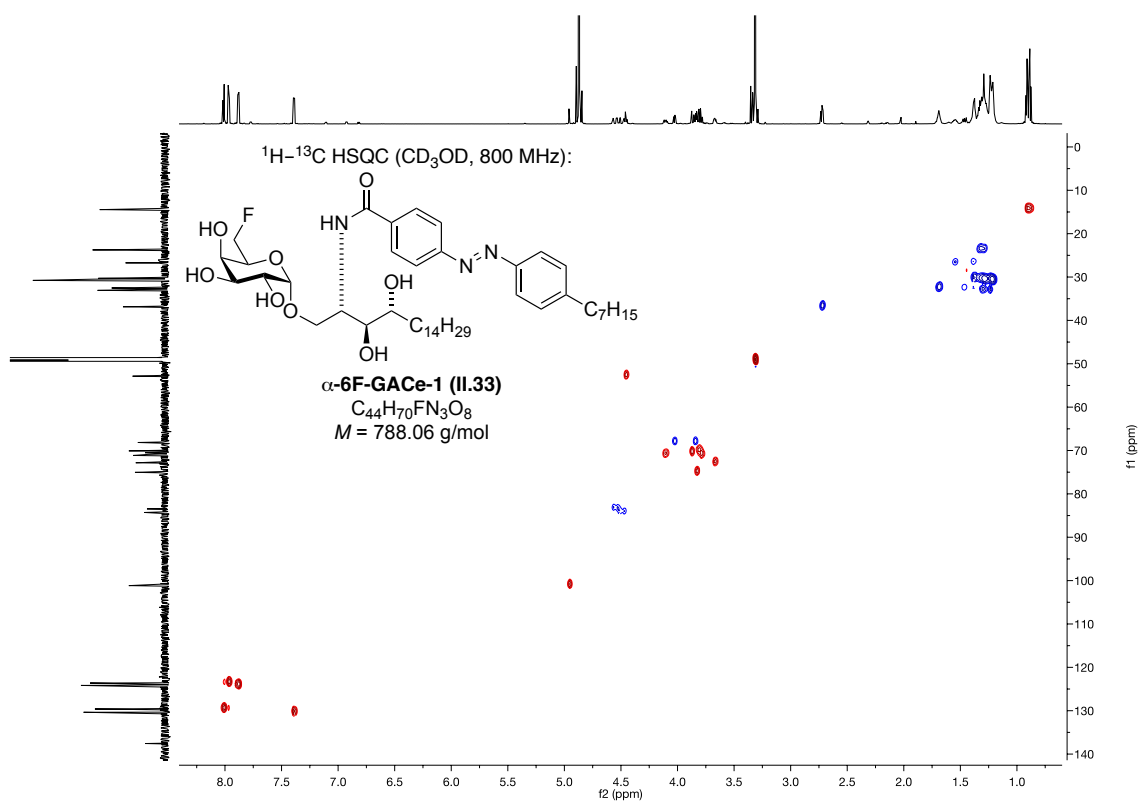
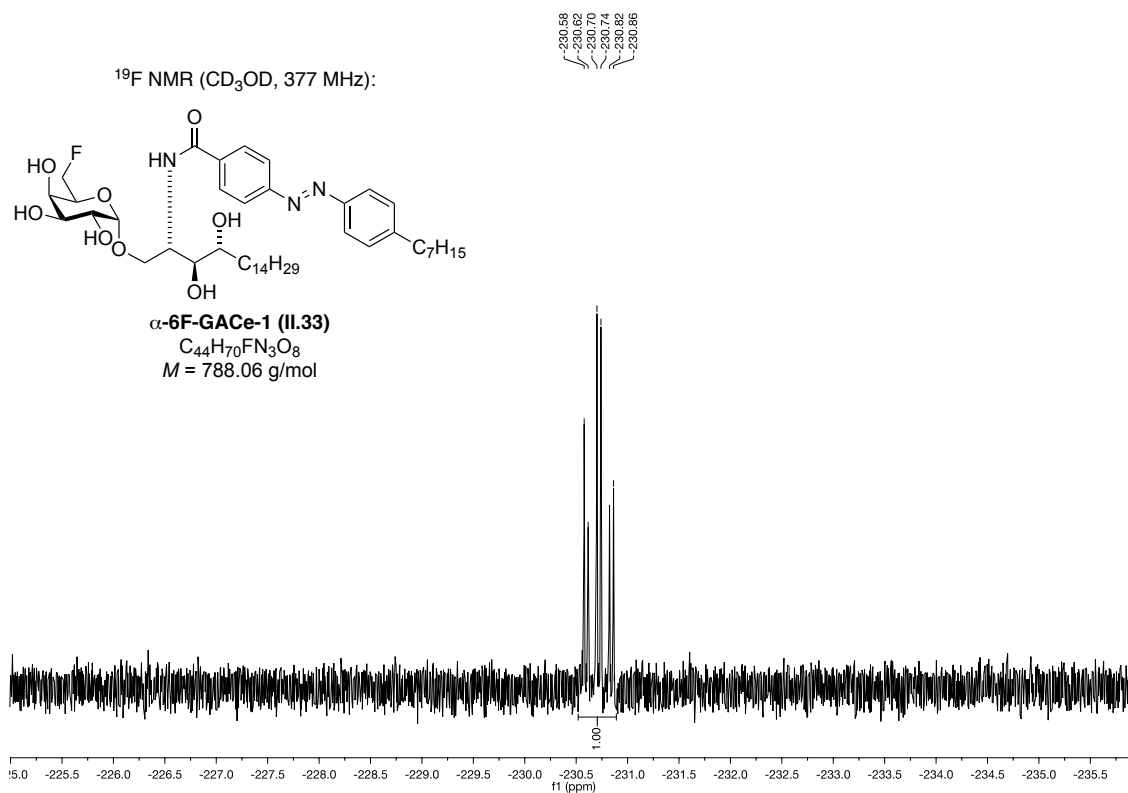


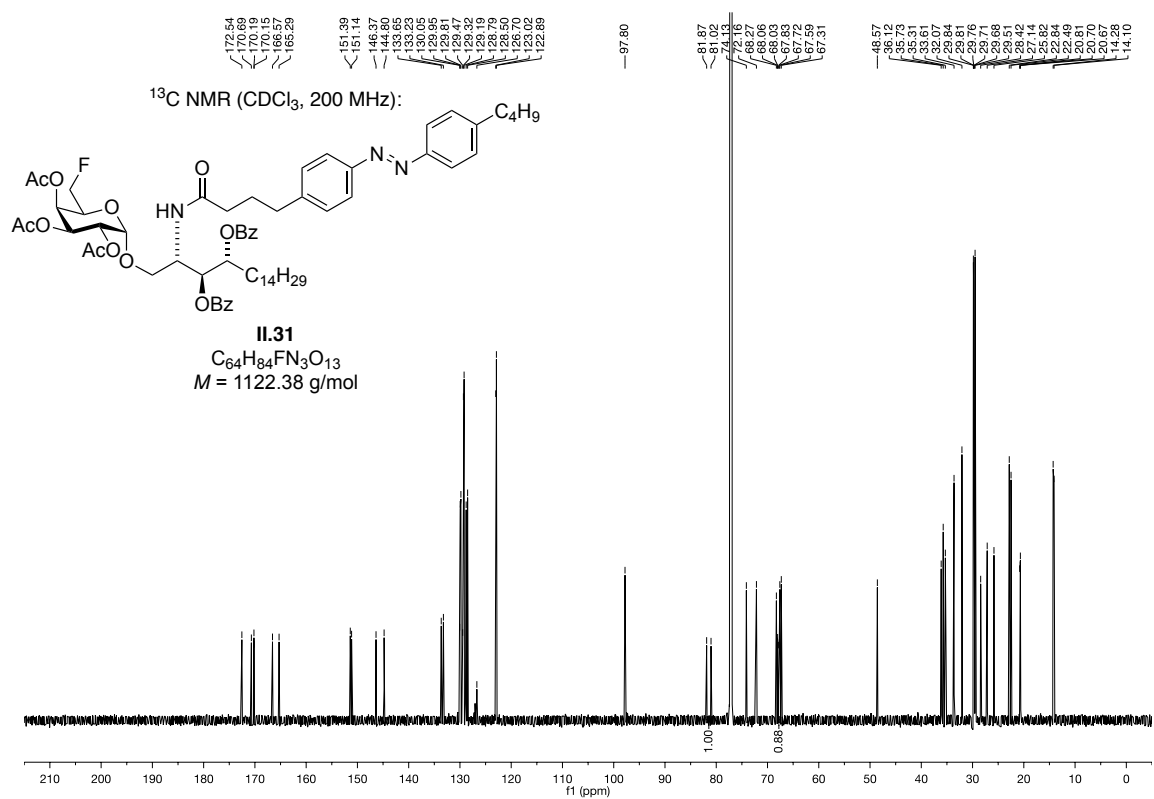
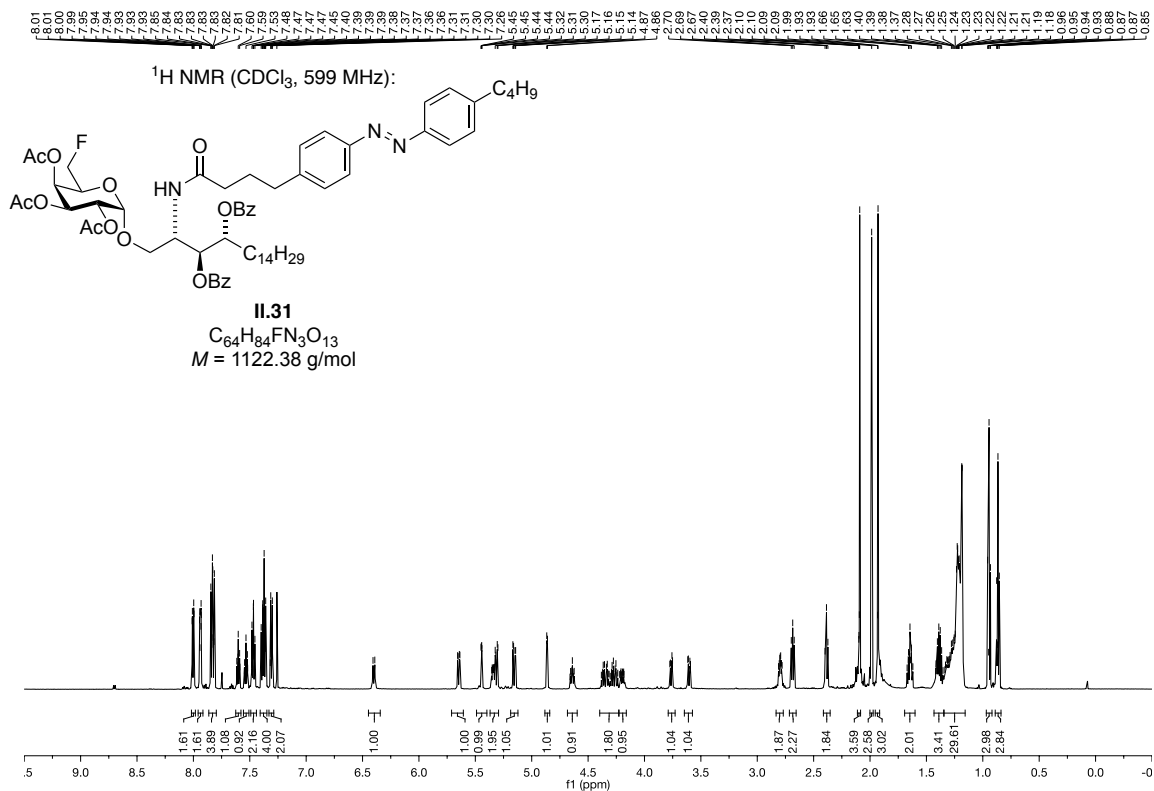


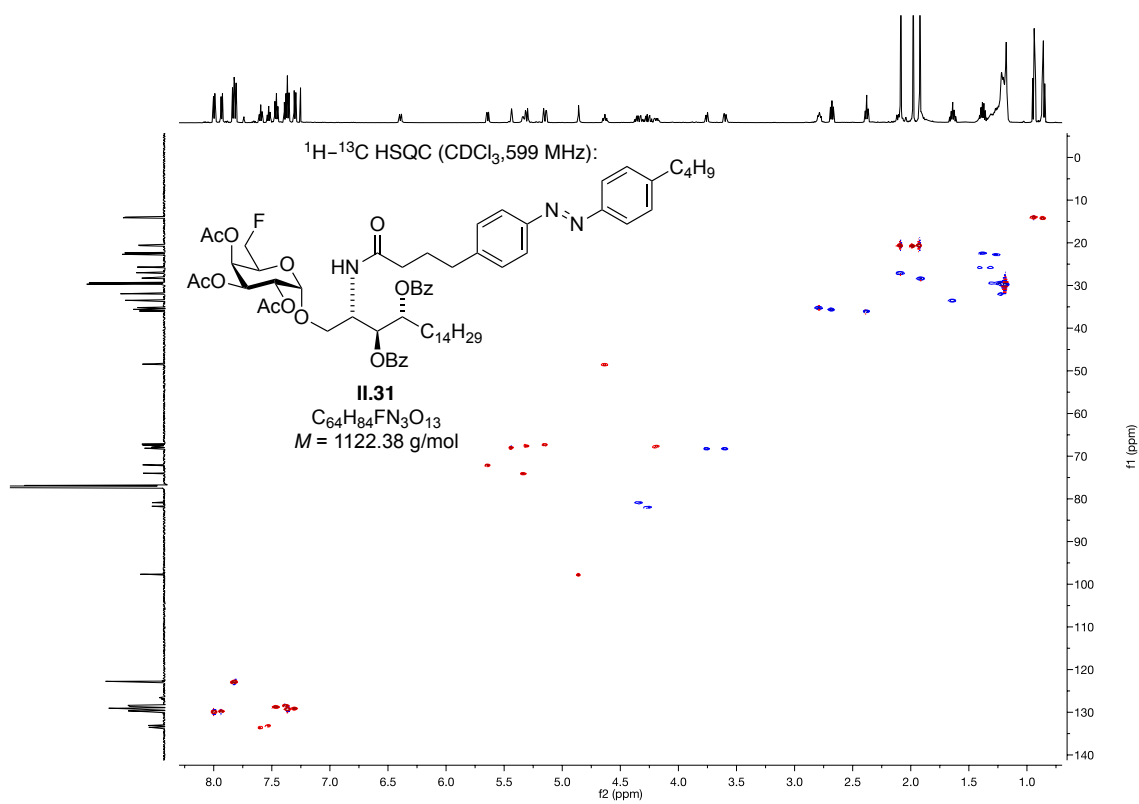
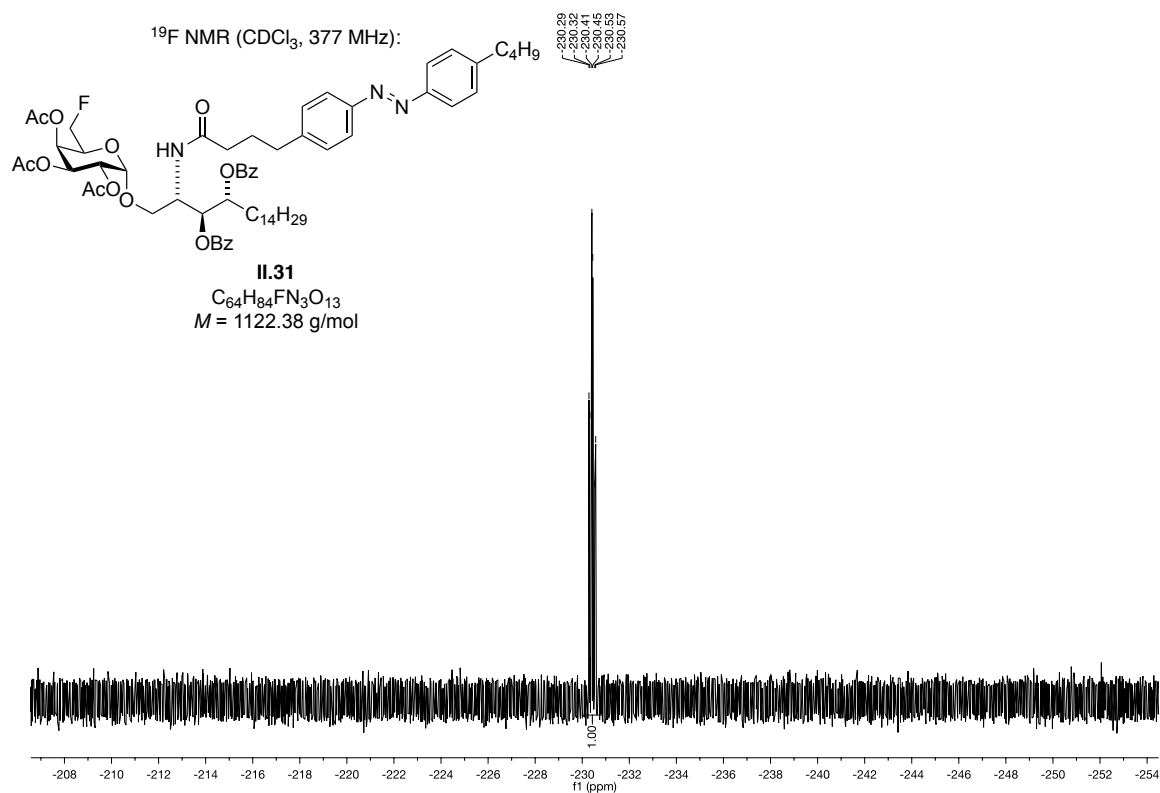


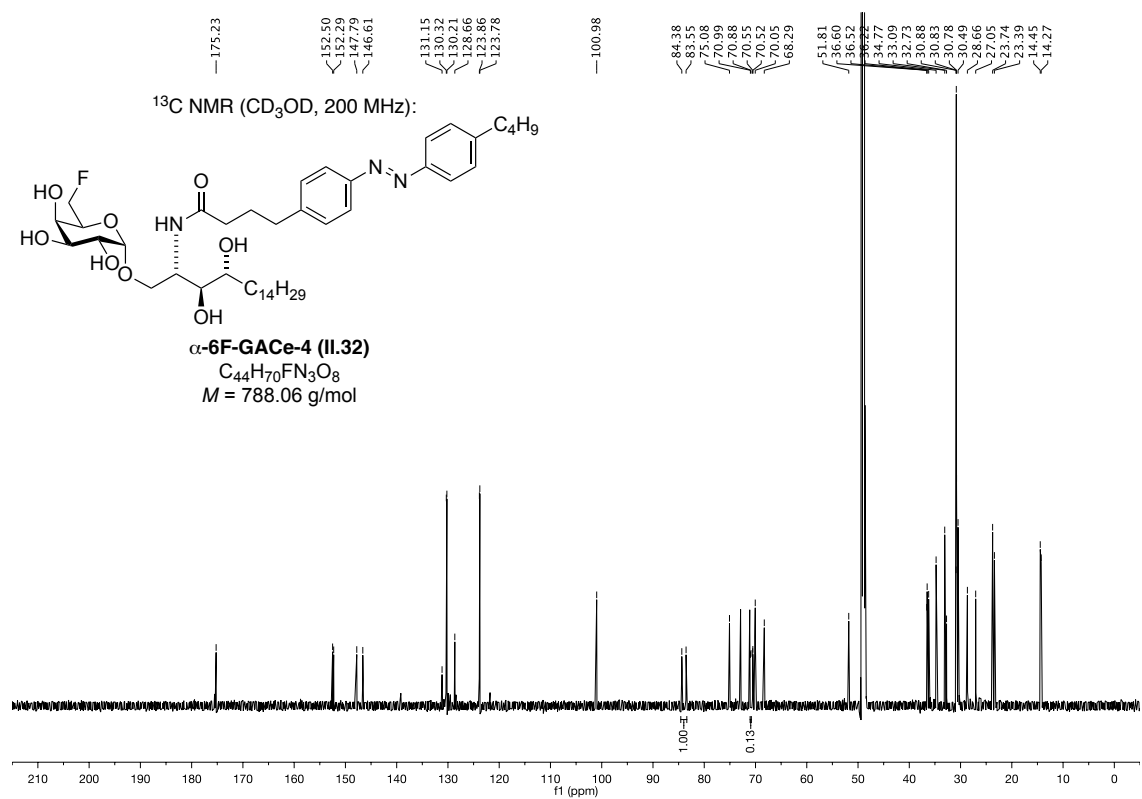
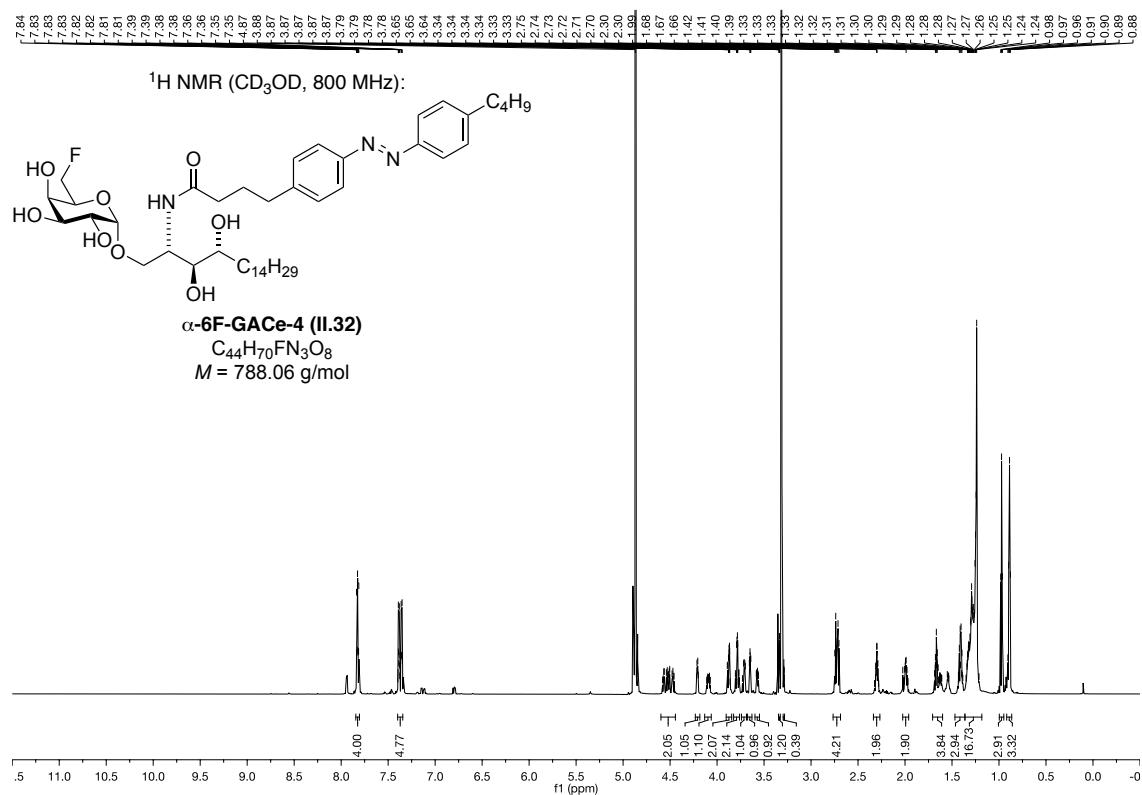


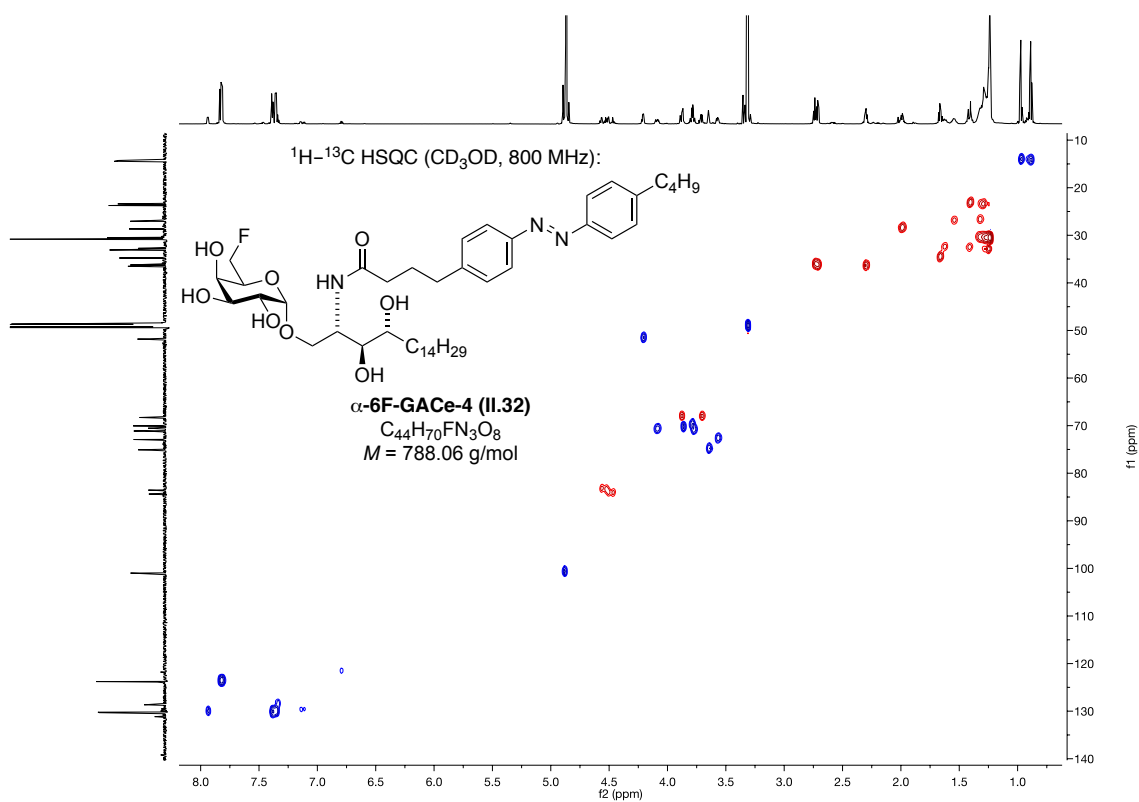
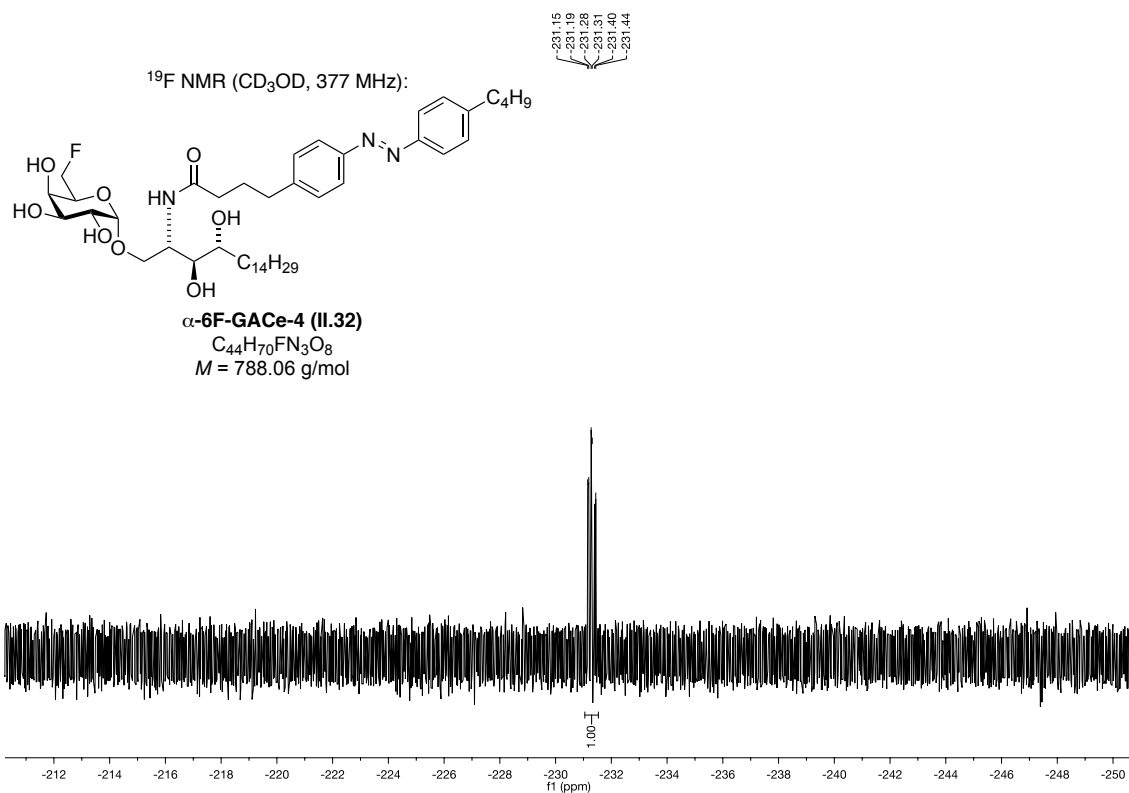


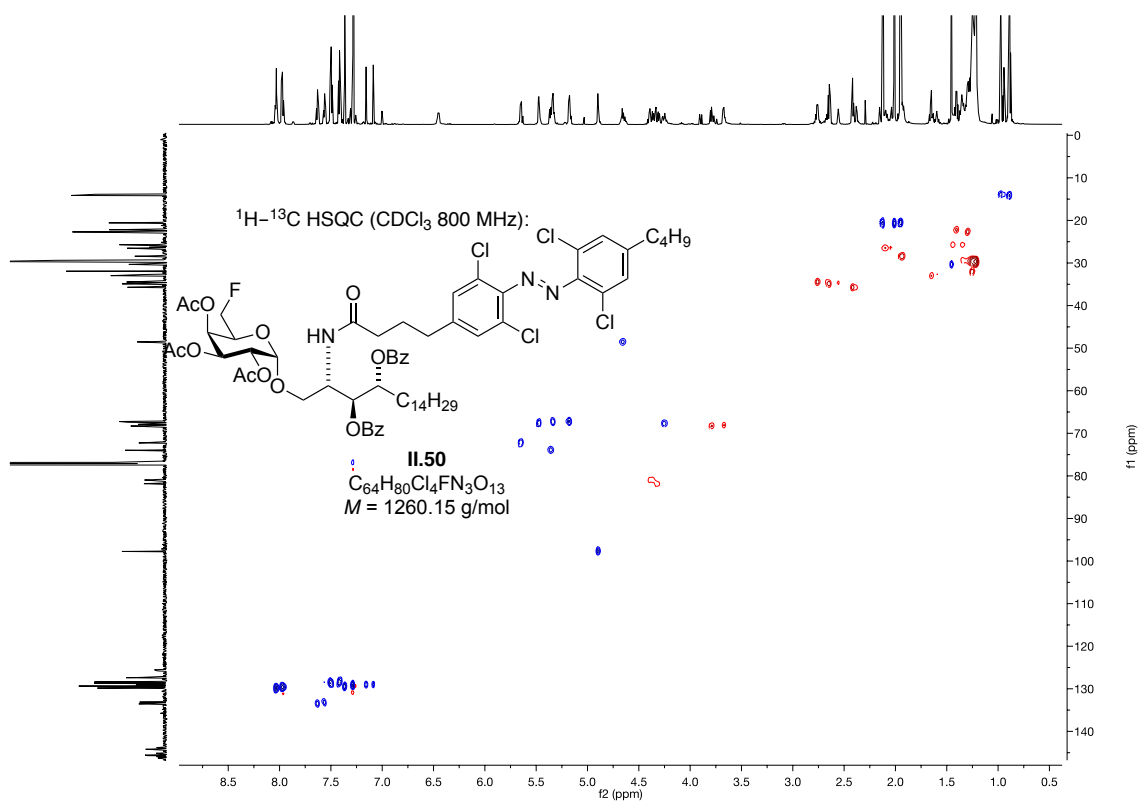
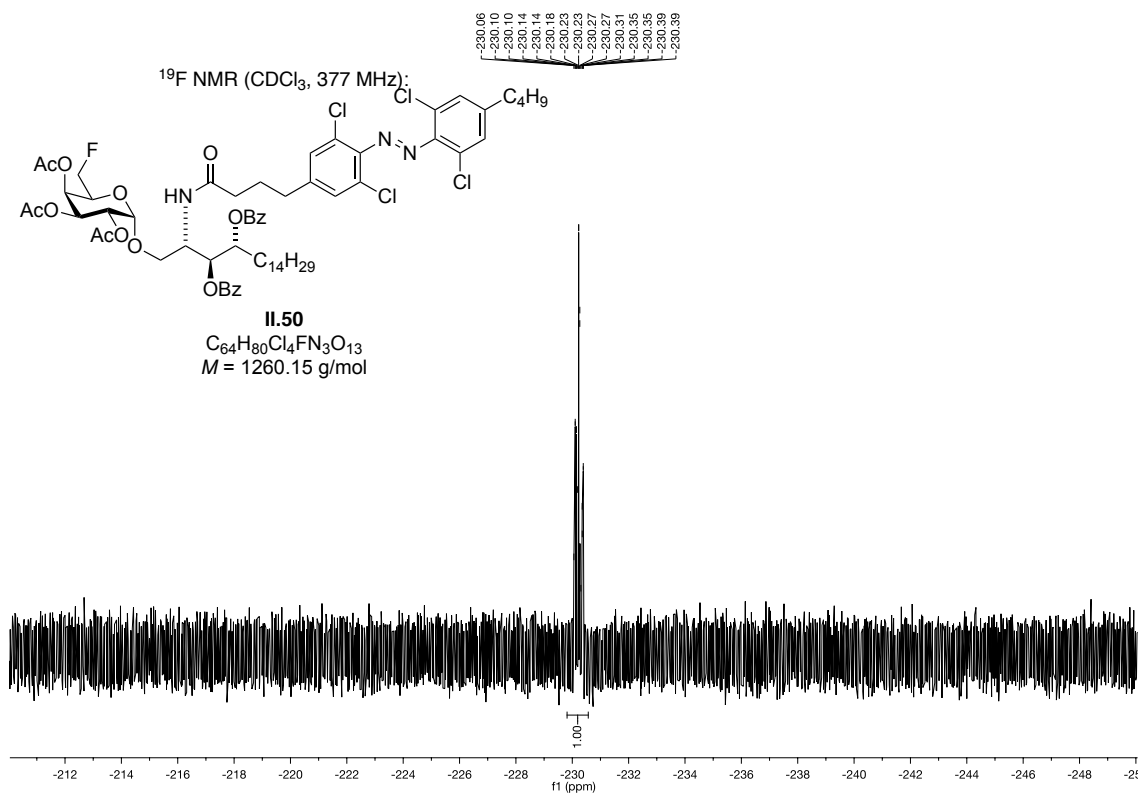


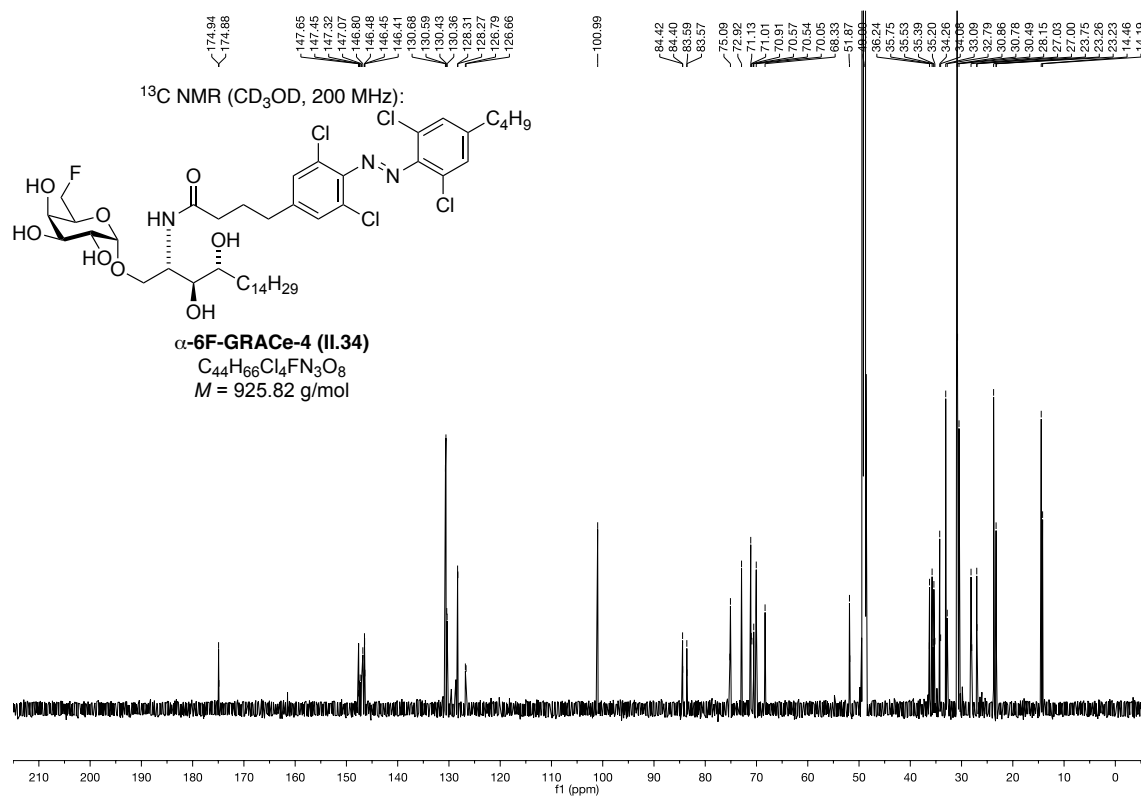
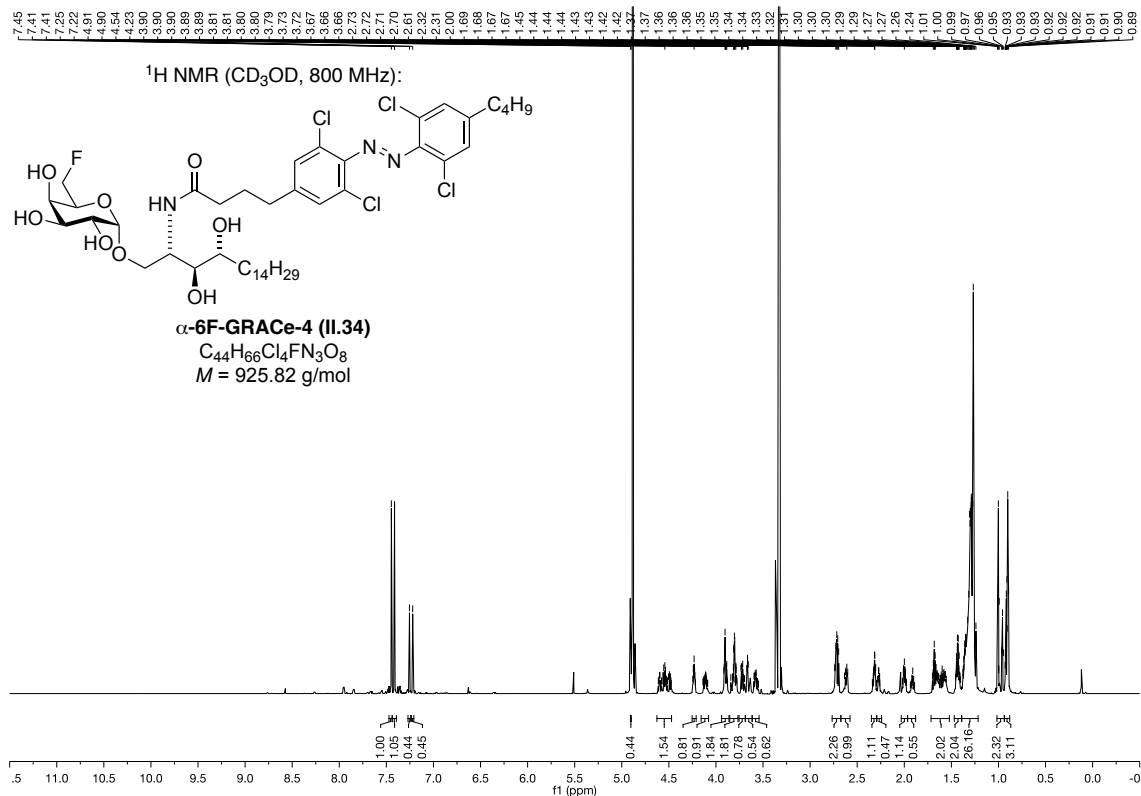


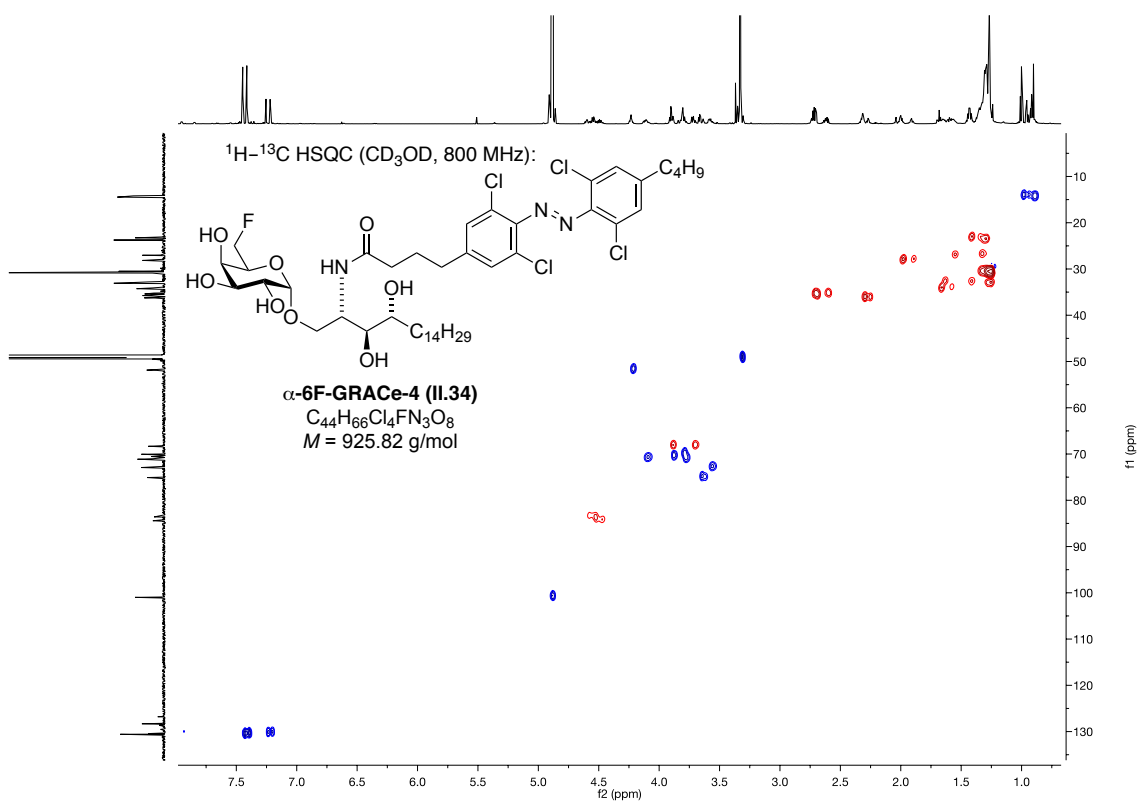
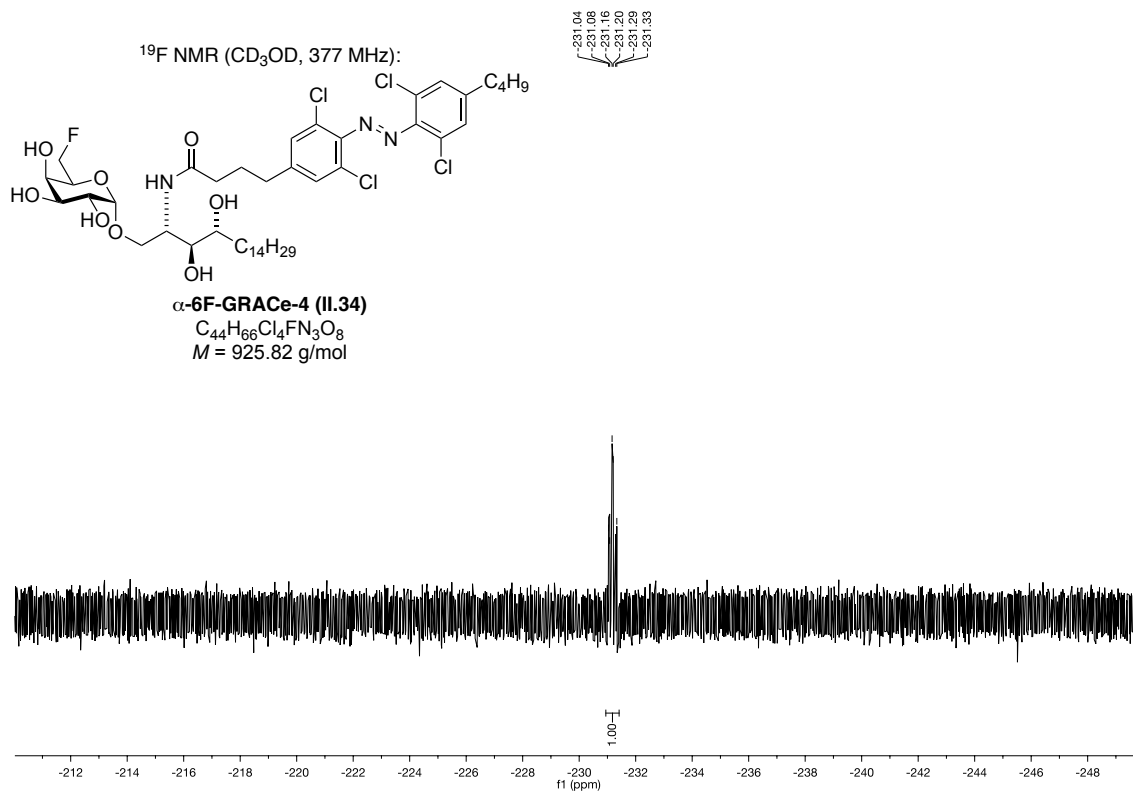


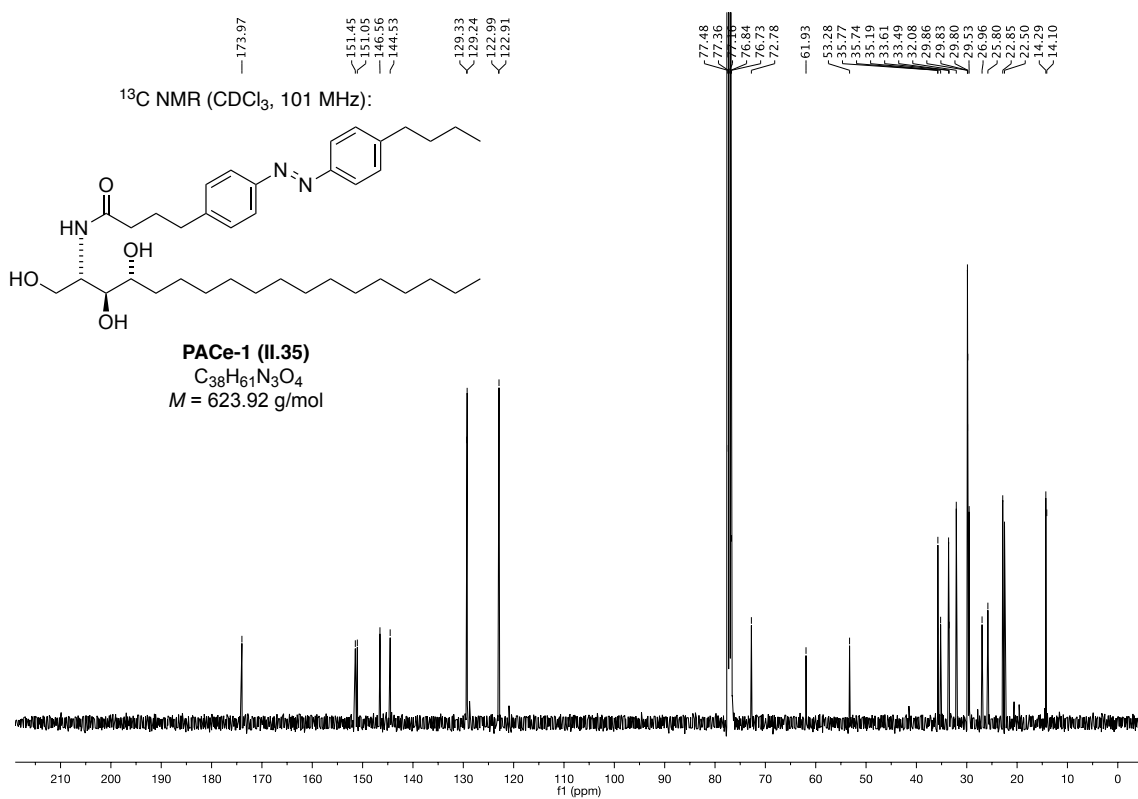
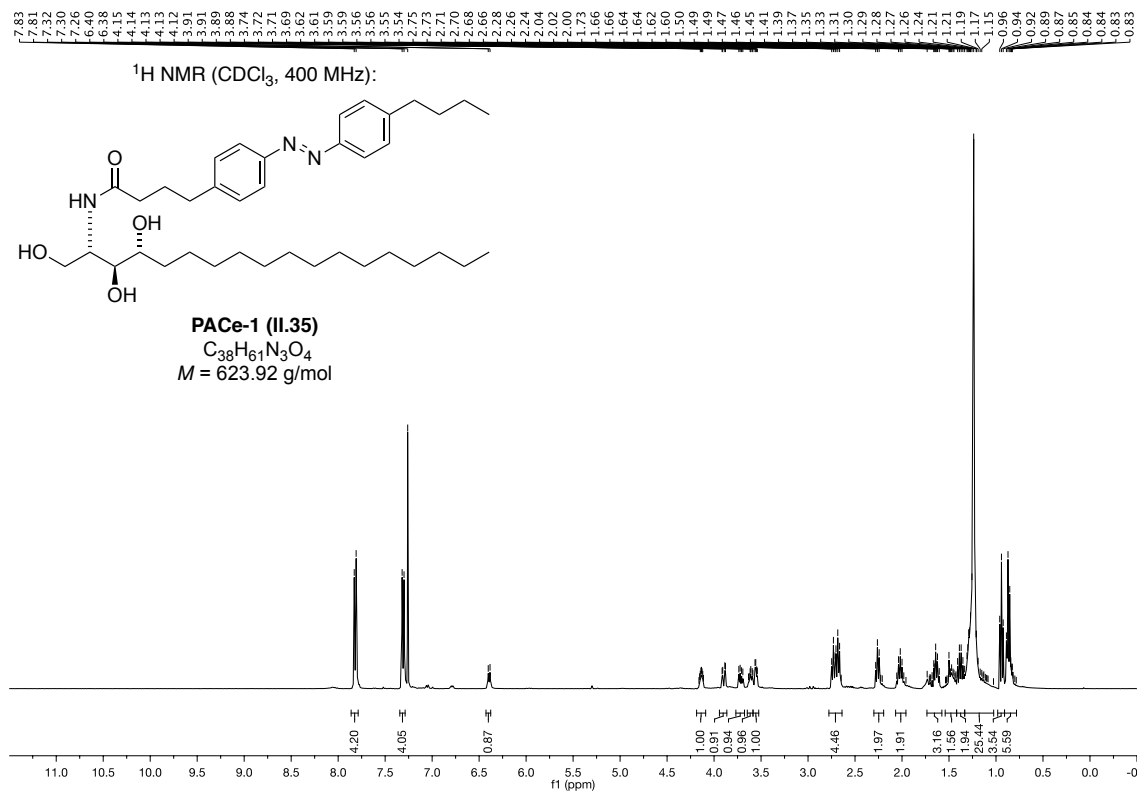


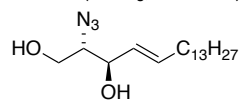
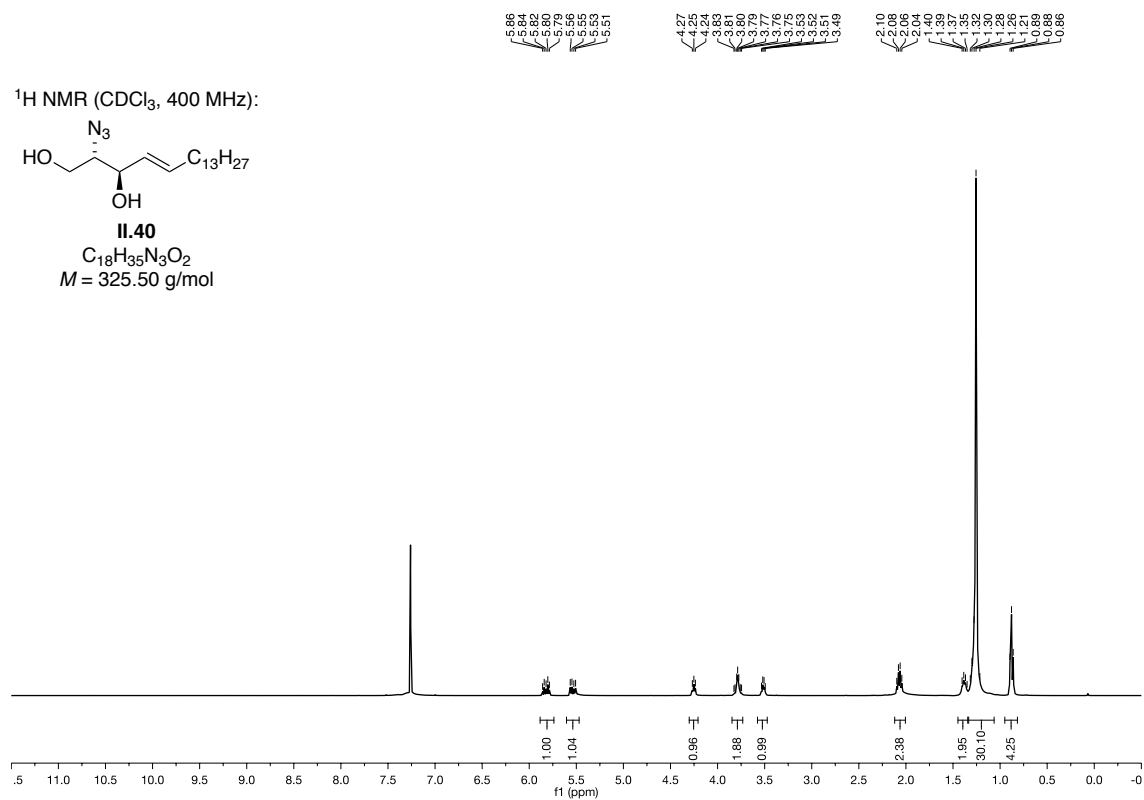
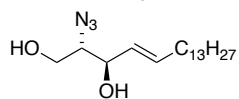
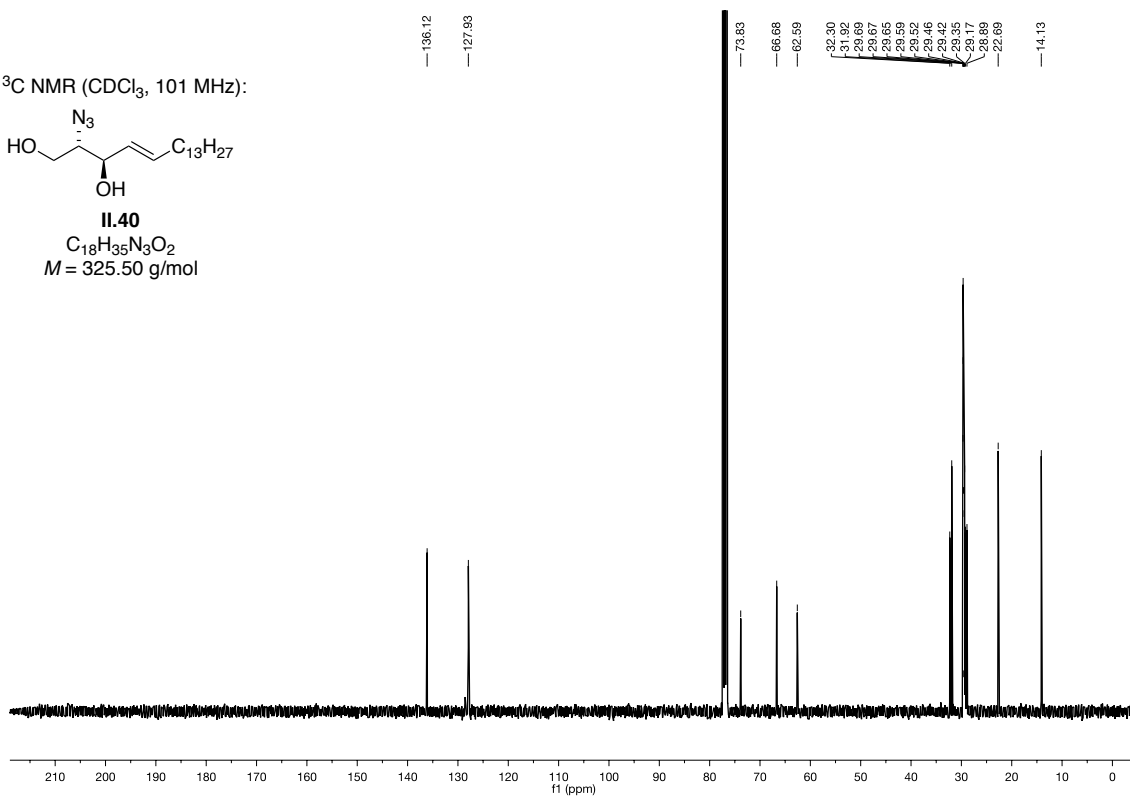


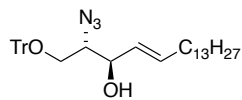




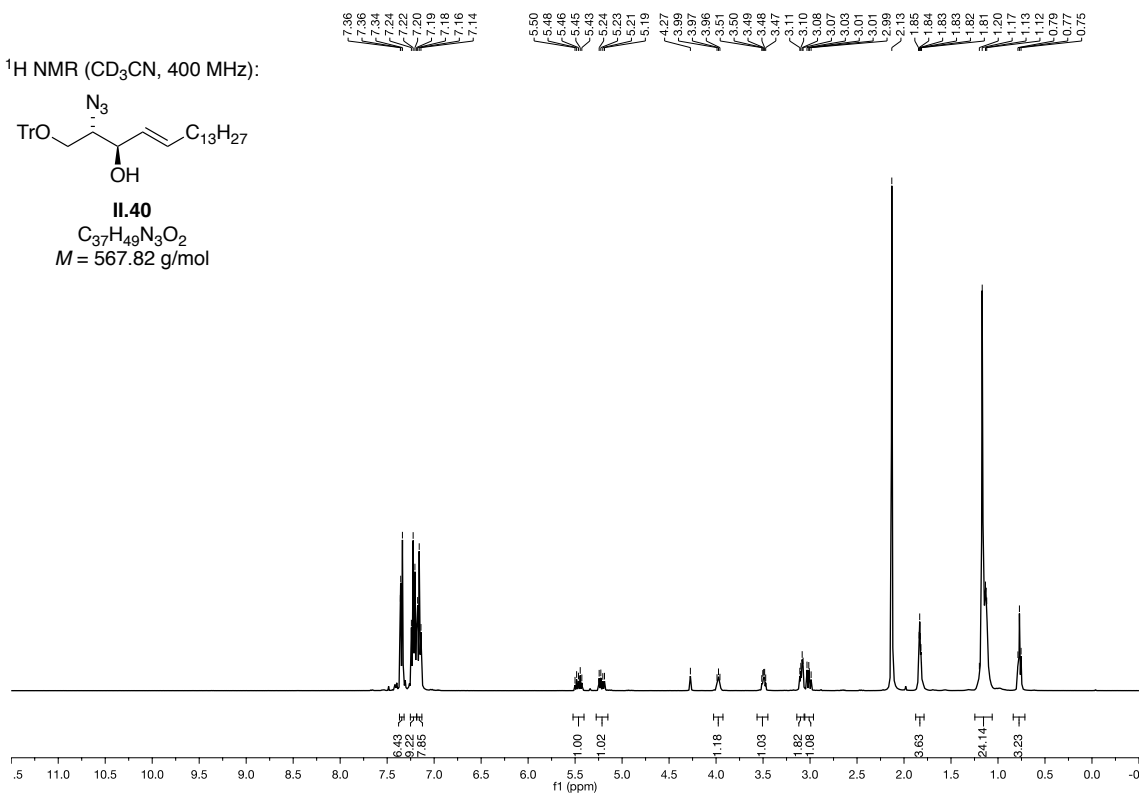
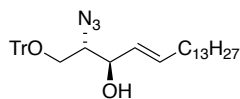




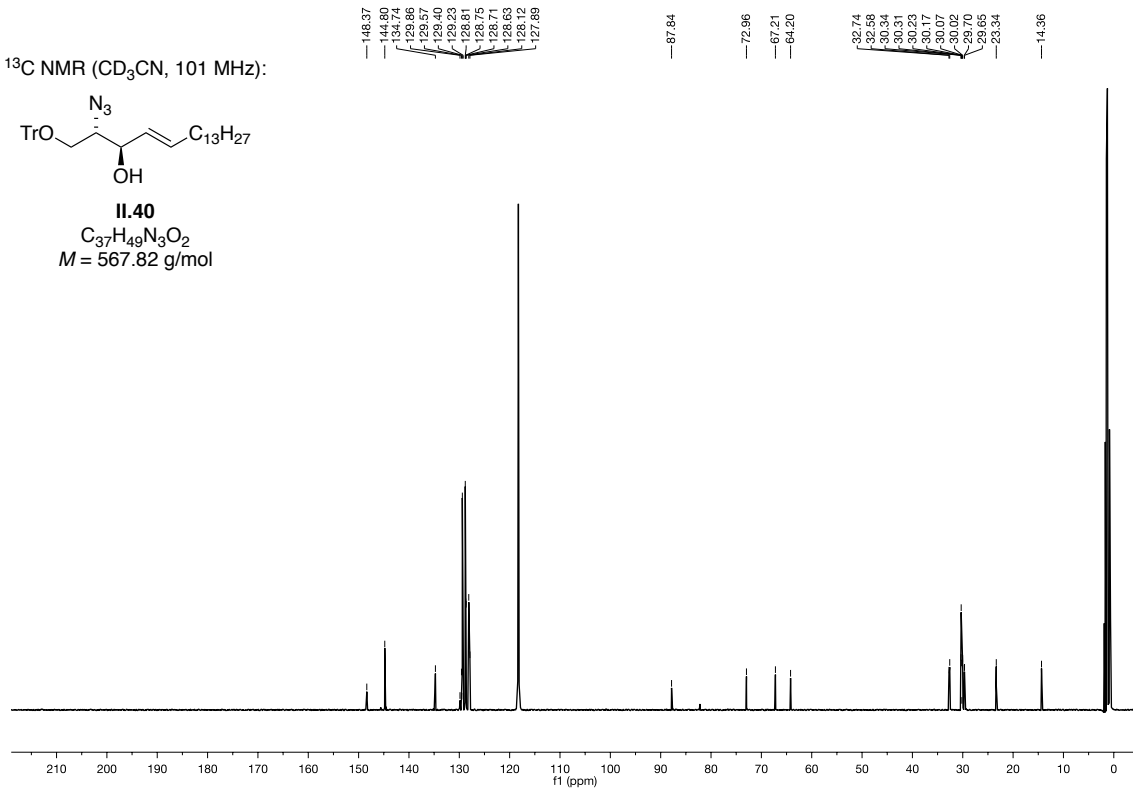
^1H NMR (CDCl_3 , 400 MHz):**II.40** $\text{C}_{18}\text{H}_{35}\text{N}_3\text{O}_2$ $M = 325.50 \text{ g/mol}$  ^{13}C NMR (CDCl_3 , 101 MHz):**II.40** $\text{C}_{18}\text{H}_{35}\text{N}_3\text{O}_2$ $M = 325.50 \text{ g/mol}$ 

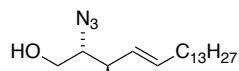
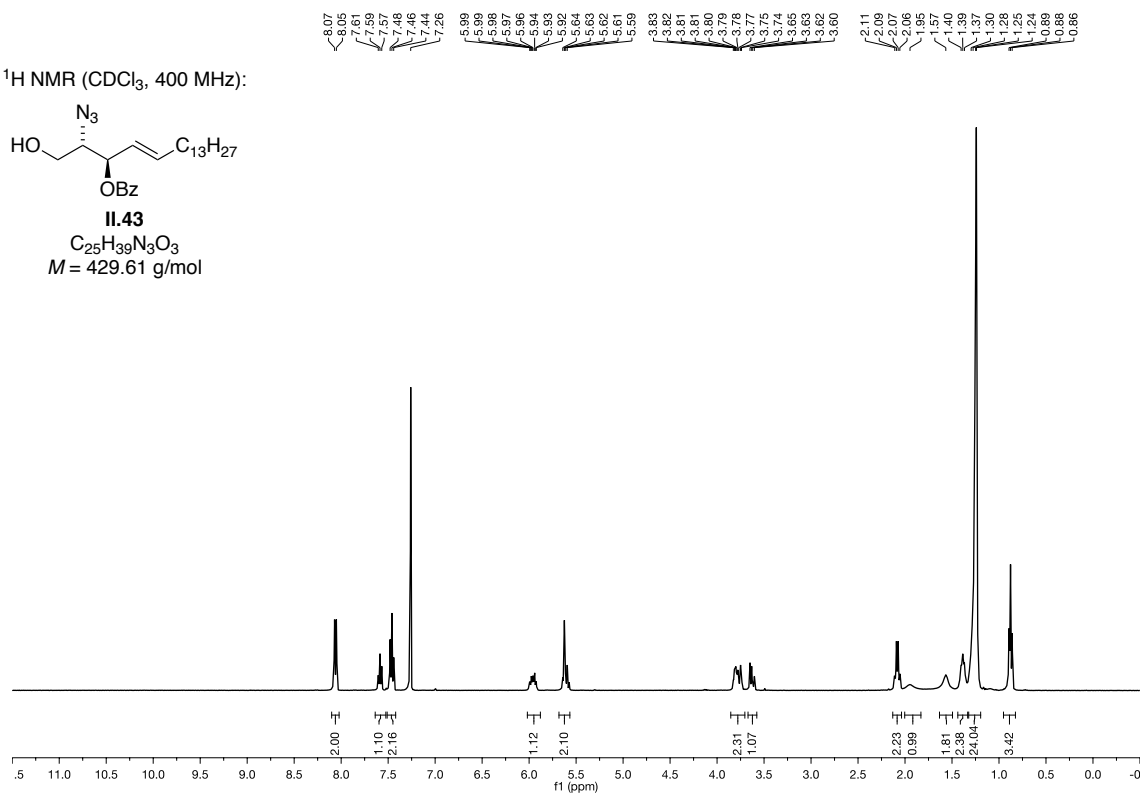
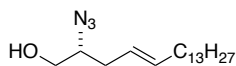
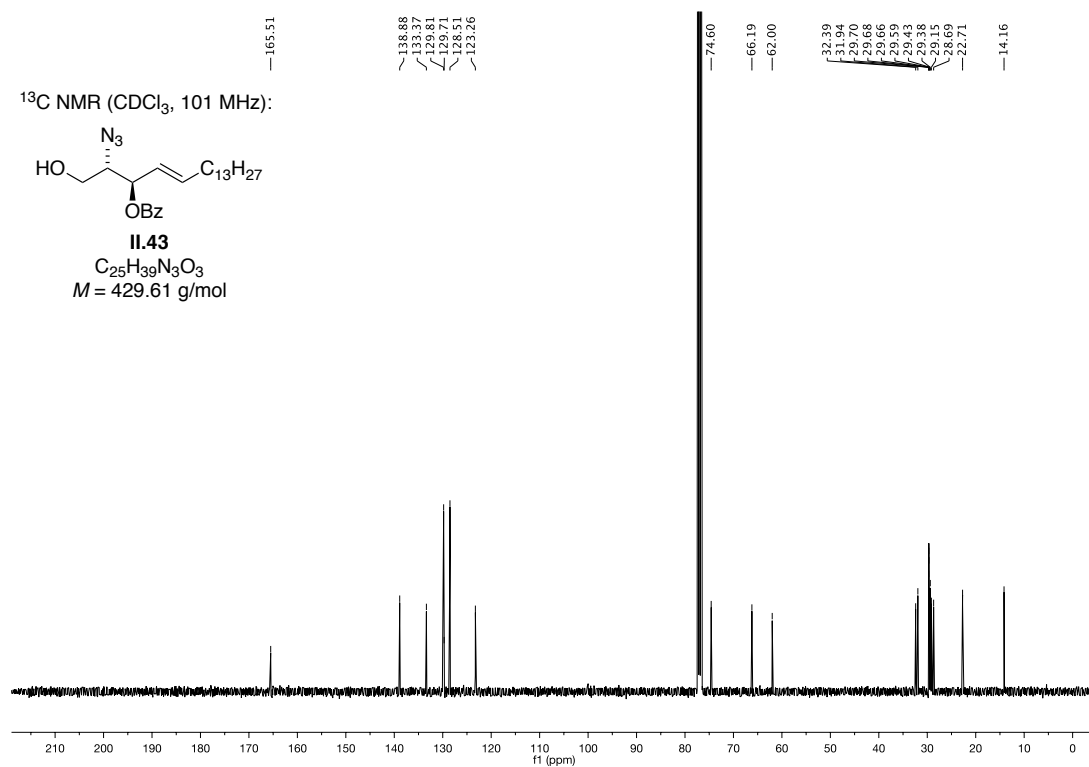
$^1\text{H NMR}$ (CD_3CN , 400 MHz):

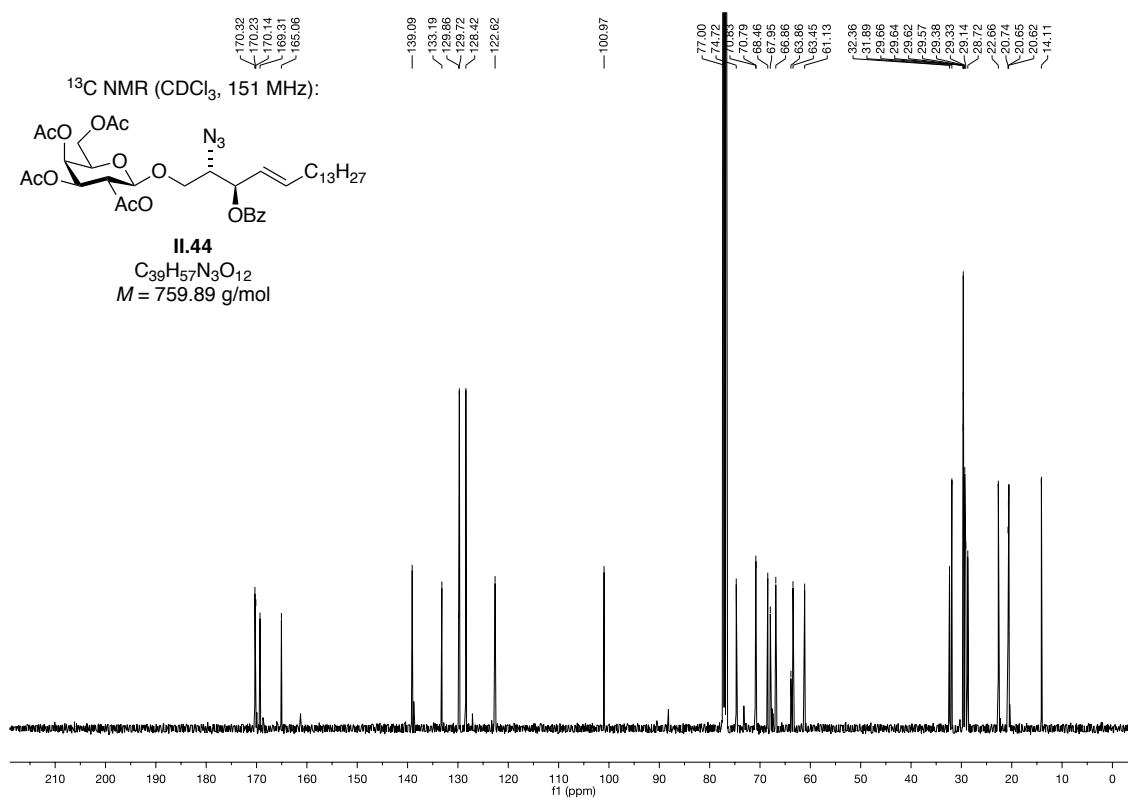
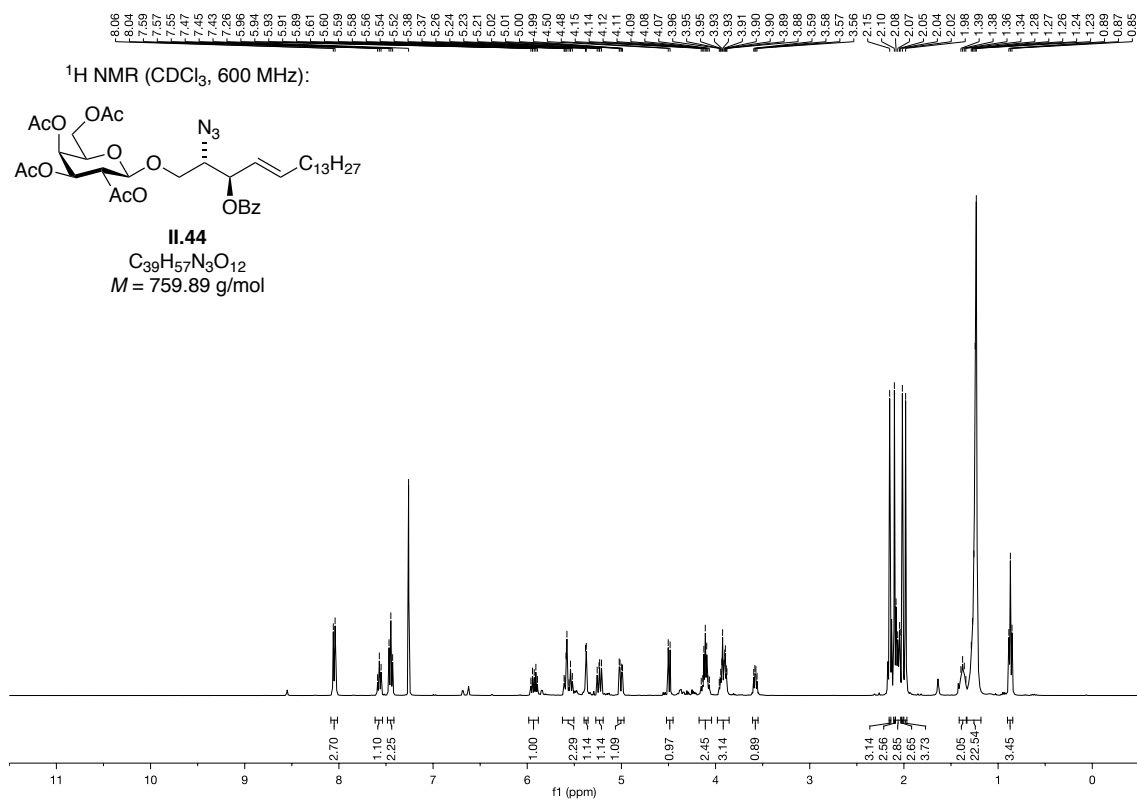
II.40
 $\text{C}_{37}\text{H}_{49}\text{N}_3\text{O}_2$
 $M = 567.82$ g/mol

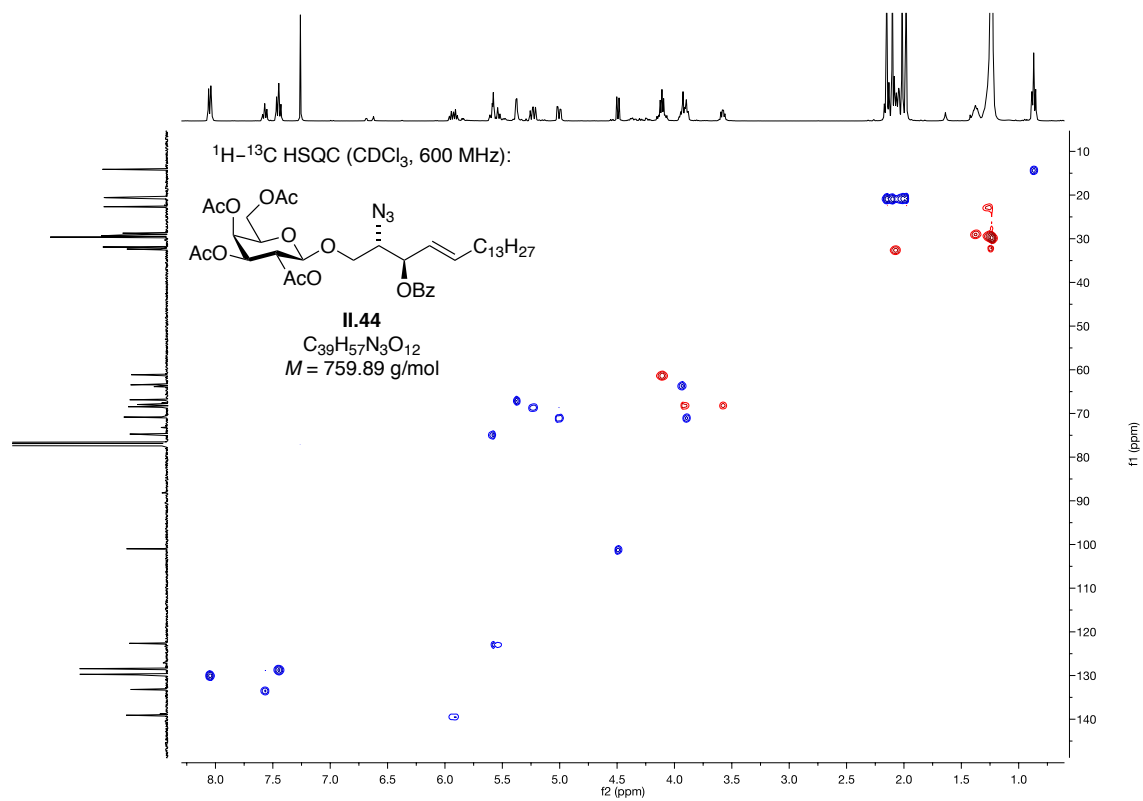
 $^{13}\text{C NMR}$ (CD_3CN , 101 MHz):

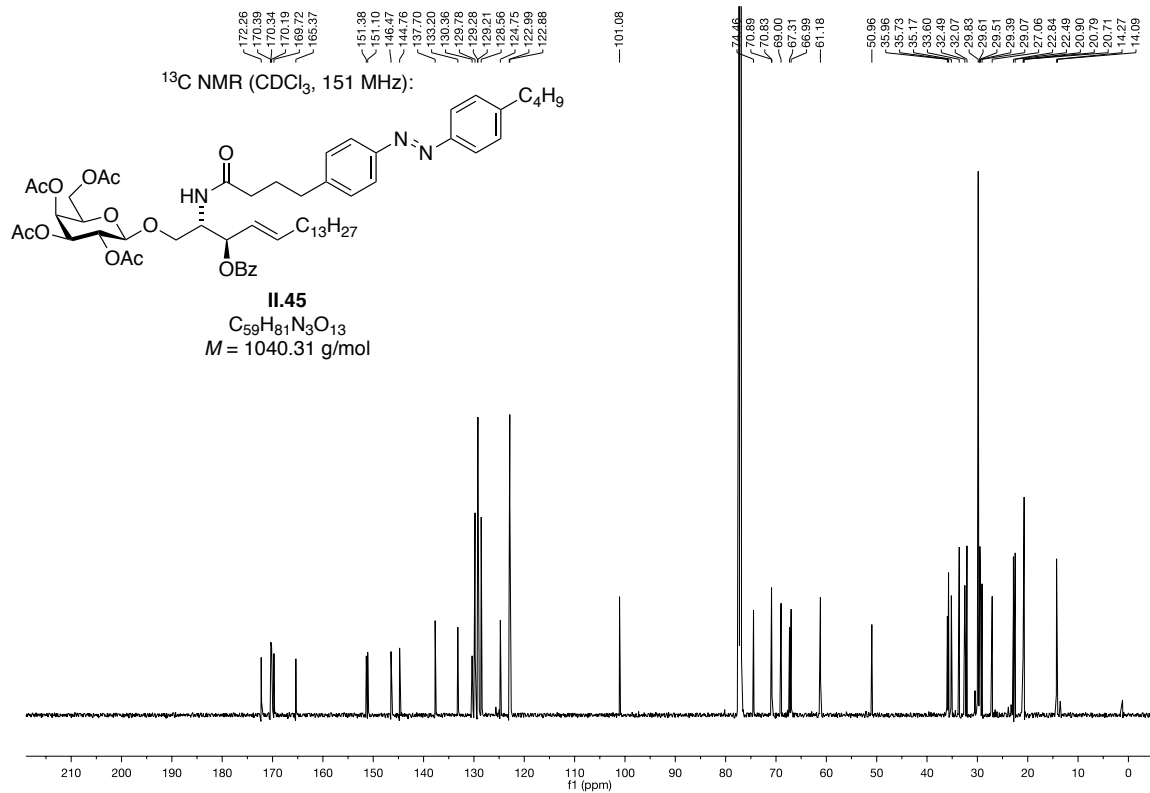
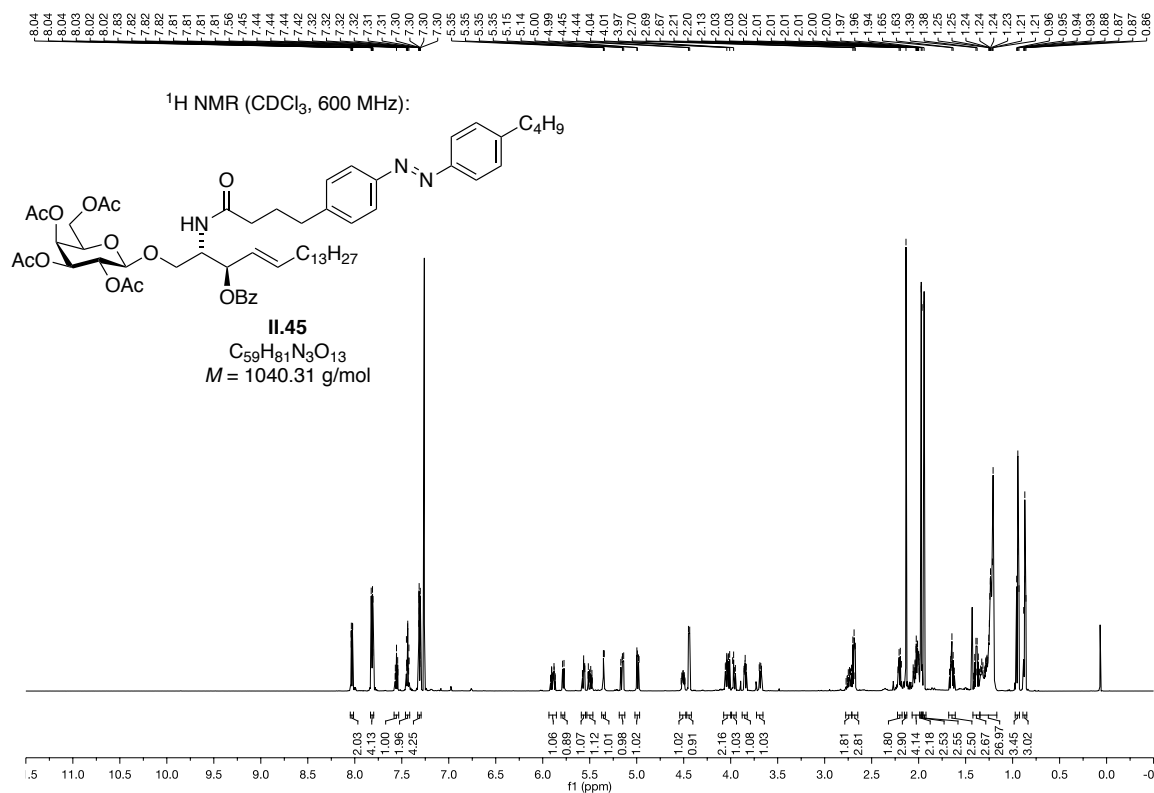
II.40
 $\text{C}_{37}\text{H}_{49}\text{N}_3\text{O}_2$
 $M = 567.82$ g/mol

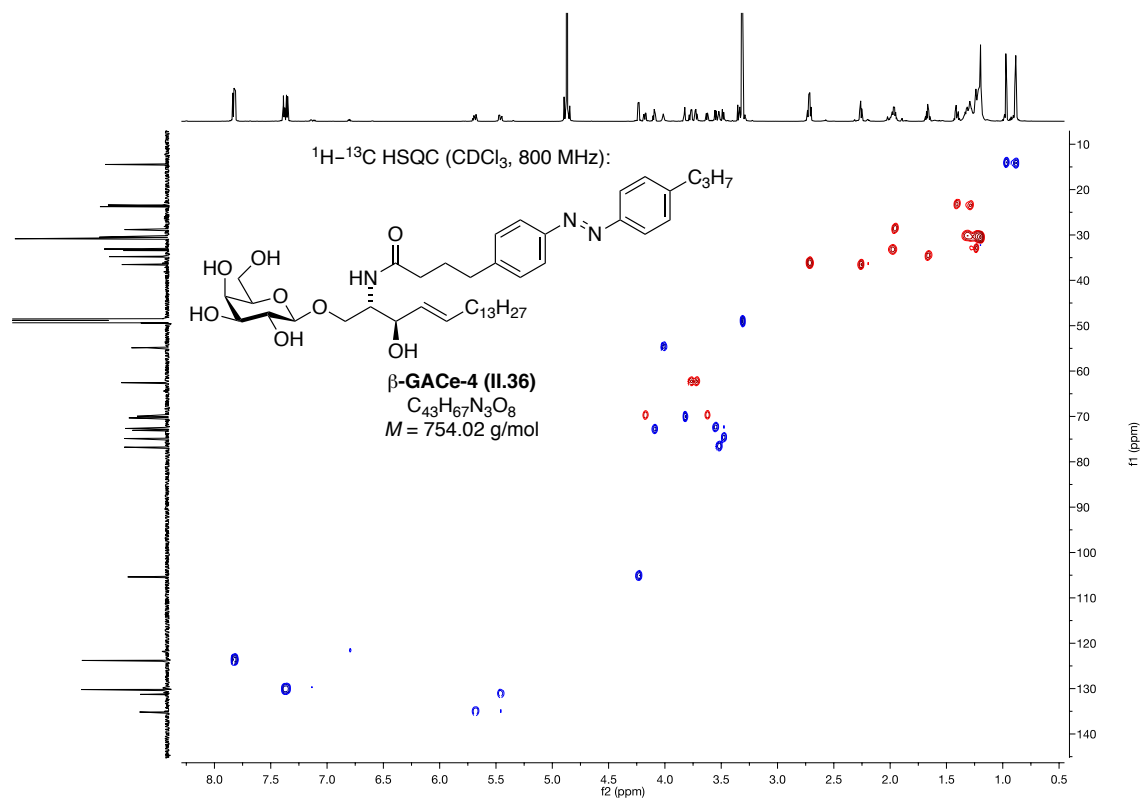


^1H NMR (CDCl_3 , 400 MHz):**II.43** $\text{C}_{25}\text{H}_{39}\text{N}_3\text{O}_3$ $M = 429.61$ g/mol ^{13}C NMR (CDCl_3 , 101 MHz):**II.43** $\text{C}_{25}\text{H}_{39}\text{N}_3\text{O}_3$ $M = 429.61$ g/mol









9.4 Chiral HPLC data

Chiral HPLC of racemic α -allylcyclohexanone I.227

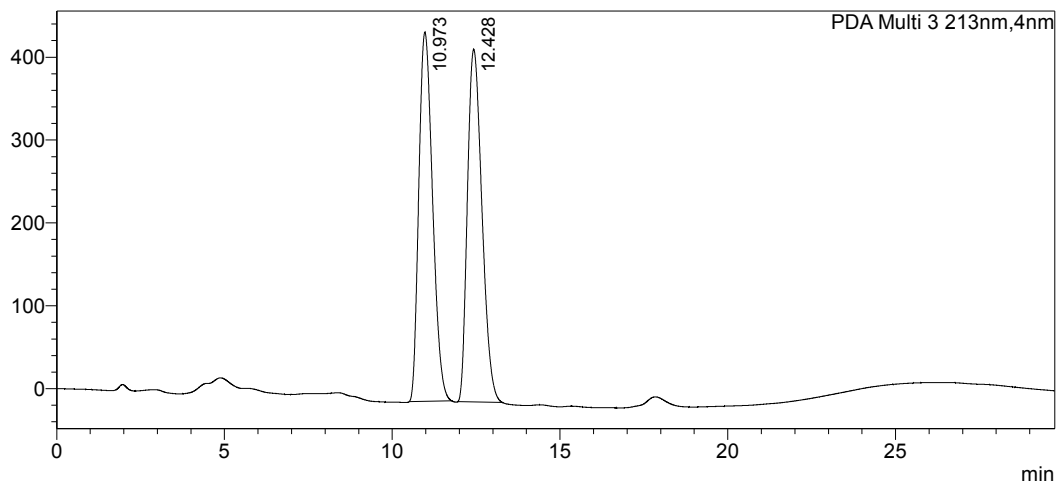
SHIMADZU LabSolutions Analysis Report

<Sample Information>

Sample Name	: NV54-rac_2-5%iPrOH-hept_IB-daicel	Sample Type	: Unknown
Sample ID	: 1		
Data Filename	: NV54-rac_2-5%iPrOH-hept_IB-daicel2.lcd		
Method Filename	: 5%iPrOH-Hept.lcm		
Batch Filename	:		
Vial #	: 1-1		
Injection Volume	: 20 μ L	Acquired by	: System Administrator
Date Acquired	: 11.11.2015 16:01:55	Processed by	: System Administrator
Date Processed	: 11.11.2015 16:31:42		

<Chromatogram>

mAU



<Peak Table>

Detector A Channel 1

Peak#	Ret. Time	Area	Height	Conc.	Unit	Mark	Name
Total							

PDA Ch3 213nm

Peak#	Ret. Time	Area	Height	Conc.	Unit	Mark	Name
1	10.973	12688725	445555	49.805			
2	12.428	12787837	425553	50.195			
Total		25476562	871108				

Example of a chiral HPLC of α -allylcyclohexanone I.227 synthesized with chiral (*S,S*)-DACH-Phenyl Trost ligand (I.235)

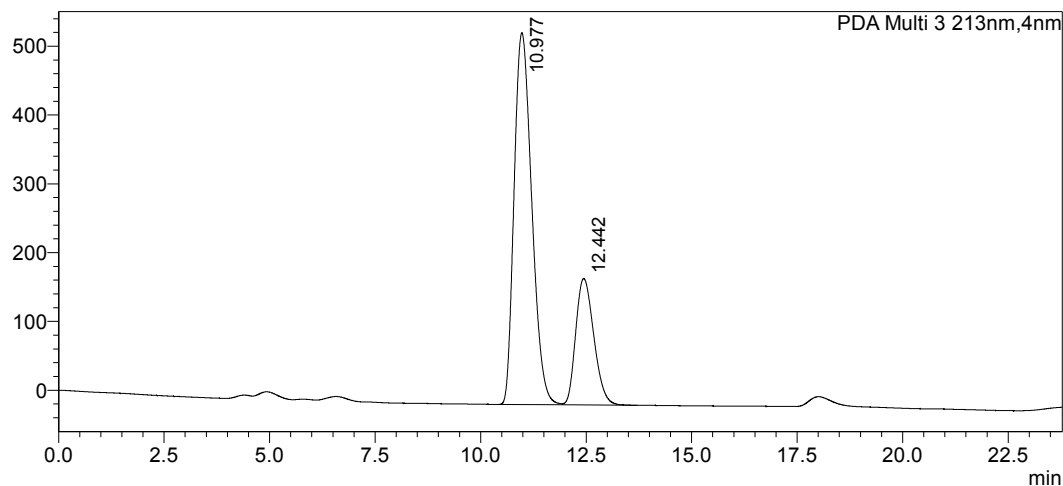
SHIMADZU
LabSolutions Analysis Report

<Sample Information>

Sample Name : NV56A-S-S-DACH_2-5%iPrOH-hept_IB-daicel
Sample ID : 1
Data Filename : NV56A-S-S-DACH_2-5%iPrOH-hept_IB-daicel1.lcd
Method Filename : 5%iPrOH-Hept.lcm
Batch Filename :
Vial # : 1-1
Injection Volume : 20 μ L
Date Acquired : 11.11.2015 16:34:04
Date Processed : 11.11.2015 16:57:53
Sample Type : Unknown
Acquired by : System Administrator
Processed by : System Administrator

<Chromatogram>

mAU



<Peak Table>

Detector A Channel 1

Peak#	Ret. Time	Area	Height	Conc.	Unit	Mark	Name
Total							

PDA Ch3 213nm

Peak#	Ret. Time	Area	Height	Conc.	Unit	Mark	Name
1	10.977	15714567	540261	74.137			
2	12.442	5482158	183836	25.863		V	
Total		21196725	724096				

Chiral HPLC of (R)-I.227 synthesized with chiral (S,S)-DACH-Phenyl Trost ligand (I.235)



Analysis Report

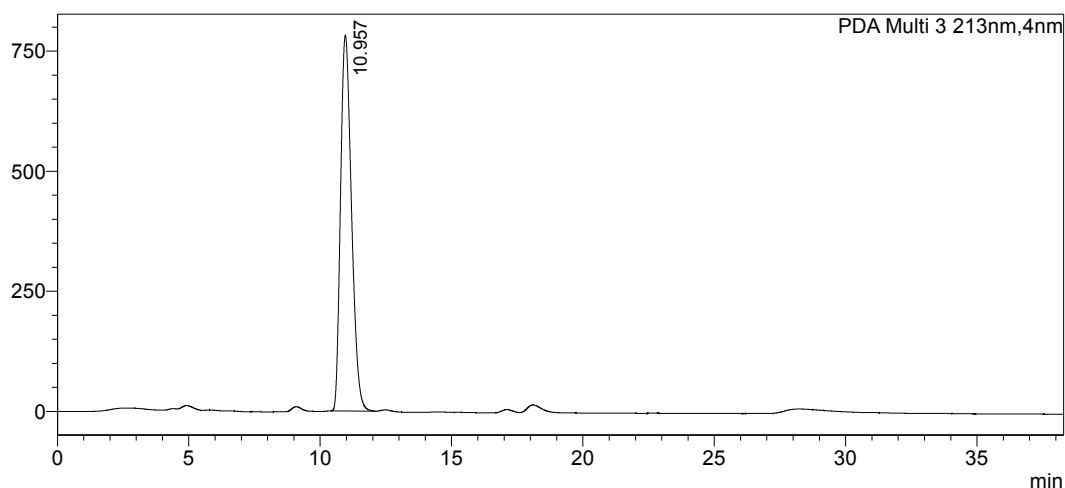
<Sample Information>

Sample Name : NVI-236_E1_2-5%iPrOH-hept_IB-daicel
 Sample ID : 1
 Data Filename : NVI-236_E1_2-5%iPrOH-hept_IB-daicel1.lcd
 Method Filename : 5%iPrOH-Hept.lcm
 Batch Filename :
 Vial # : 1-1
 Injection Volume : 20 uL
 Date Acquired : 11.11.2015 17:27:46
 Date Processed : 11.11.2015 18:06:05

Sample Type : Unknown
 Acquired by : System Administrator
 Processed by : System Administrator

<Chromatogram>

mAU

**<Peak Table>**

Detector A Channel 1

Peak#	Ret. Time	Area	Height	Conc.	Unit	Mark	Name
Total							

PDA Ch3 213nm

Peak#	Ret. Time	Area	Height	Conc.	Unit	Mark	Name
1	10.957	22678366	782145	100.000			
Total		22678366	782145				

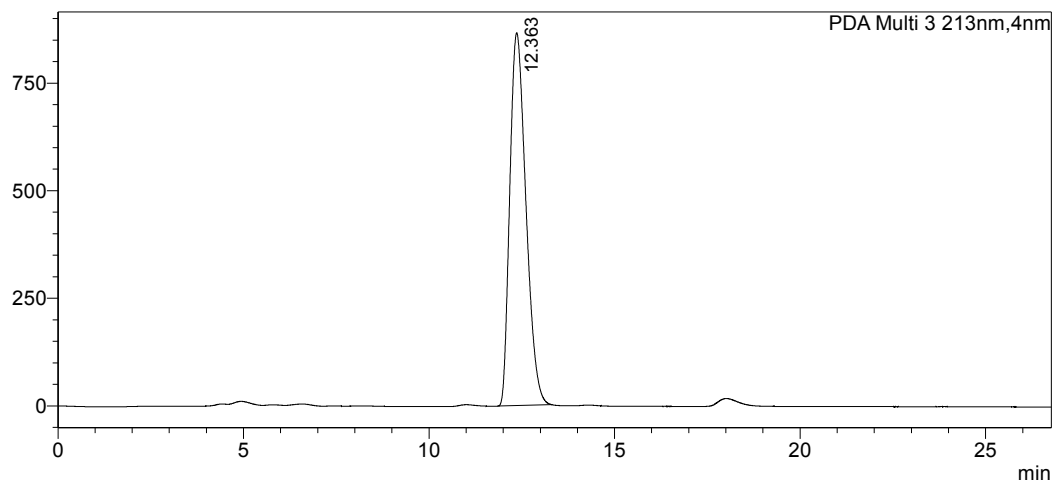
Chiral HPLC of (*S*)-I.227 synthesized with chiral (*R,R*)-DACH-Phenyl Trost ligand (I.235) **Analysis Report****<Sample Information>**

Sample Name : NVI-237_E2_2-5%iPrOH-hept_IB-daicel
Sample ID : 1
Data Filename : NVI-237_E2_2-5%iPrOH-hept_IB-daicel1.lcd
Method Filename : 5%iPrOH-Hept.lcm
Batch Filename :
Vial # : 1-1
Injection Volume : 20 uL
Date Acquired : 11.11.2015 16:59:30
Date Processed : 11.11.2015 17:26:22

Sample Type : Unknown
Acquired by : System Administrator
Processed by : System Administrator

<Chromatogram>

mAU

**<Peak Table>**

Detector A Channel 1

Peak#	Ret. Time	Area	Height	Conc.	Unit	Mark	Name
Total							

PDA Ch3 213nm

Peak#	Ret. Time	Area	Height	Conc.	Unit	Mark	Name
1	12.363	26134792	865580	100.000			
Total		26134792	865580				

10 Literature

- [1] M. Wink, in *Alkaloids: Biochemistry, Ecology, and Medicinal Applications* (Eds.: M. F. Roberts, M. Wink), Springer US, Boston, MA, **1998**, pp. 11–44.
- [2] M. Hesse, *Alkaloids: Nature's Curse Or Blessing?*, Verlag Helvetica Chimica Acta, **2002**.
- [3] E. Fattorusso, O. Tagliatela–Scafati, *Modern Alkaloids : Structure, Isolation, Synthesis and Biology*, 1 ed., Wiley–VCH, Weinheim, **2008**.
- [4] G. A. Cordell, *The Alkaloids, Vol. 52*, Elsevier, London, **1998**.
- [5] M. Wink, in *Studies in Natural Products Chemistry, Vol. 21*, Elsevier, **2000**, pp. 3–122.
- [6] G. A. Cordell, M. L. Quinn–Beattie, N. R. Farnsworth, *Phytotherapy Research* **2001**, *15*, 183–205.
- [7] P. M. Dewick, *Medicinal Natural Products; A Biosynthetic Approach*, third ed., Wiley–VCH, Weinheim, **2009**.
- [8] J. Clayden, M. Donnard, J. Lefranc, D. J. Tetlow, *Chem. Commun.* **2011**, *47*, 4624–4639.
- [9] G. Dake, *Tetrahedron* **2006**, *62*, 3467–3492.
- [10] S. A. A. El Bialy, H. Braun, L. F. Tietze, *Synthesis* **2004**, 2249–2262.
- [11] S. H. Kang, S. Y. Kang, H.-S. Lee, A. J. Buglass, *Chem. Rev.* **2005**, *105*, 4537–4558.
- [12] A. Sharma, J. F. Hartwig, *Nature* **2015**, *517*, 600–604.
- [13] L. Huang, M. Arndt, K. Gooßen, H. Heydt, L. J. Gooßen, *Chem. Rev.* **2015**, *115*, 2596–2697.
- [14] R. Robinson, *Journal of the Chemical Society, Transactions* **1917**, *111*, 762–768.
- [15] B. K. Blount, R. Robinson, *Journal of the Chemical Society* **1933**, 1511–1512.
- [16] C. Schöpf, G. Lehmann, *Liebigs Ann. Chem.* **1935**, *518*, 1–37.
- [17] K. Alder, H. Betzing, R. Kuth, H.-A. Dortmann, *Liebigs Ann. Chem.* **1959**, *620*, 73–87.
- [18] K. Alder, H. A. Dortmann, *Chem. Ber.* **1953**, *86*, 1544–1554.
- [19] K. Alder, H. Wirtz, H. Koppelberg, *Liebigs Ann. Chem.* **1956**, *601*, 138–154.
- [20] D. H. Gnecco Medina, D. S. Grierson, H.-P. Husson, *Tetrahedron Lett.* **1983**, *24*, 2099–2102.
- [21] C. Yue, J. Royer, H.-P. Husson, *J. Org. Chem.* **1992**, *57*, 4211–4214.
- [22] M. F. Mechelke, A. I. Meyers, *Tetrahedron Lett.* **2000**, *41*, 4339–4342.
- [23] F. A. Davis, R. Edupuganti, *Org. Lett.* **2010**, *12*, 848–851.
- [24] M. Brüggemann, A. I. McDonald, L. E. Overman, M. D. Rosen, L. Schwink, J. P. Scott, *J. Am. Chem. Soc.* **2003**, *125*, 15284–15285.
- [25] K. M. Brummond, J. Lu, *Org. Lett.* **2001**, *3*, 1347–1349.
- [26] K. M. Brummond, S.-P. Hong, *J. Org. Chem.* **2005**, *70*, 907–916.
- [27] Y. Shi, B. Yang, S. Cai, S. Gao, *Angew. Chem. Int. Ed.* **2014**, *53*, 9539–9543.

- [28] C. H. Heathcock, E. Kleinman, E. S. Binkley, *J. Am. Chem. Soc.* **1978**, *100*, 8036–8037.
- [29] E. Kleinman, C. H. Heathcock, *Tetrahedron Lett.* **1979**, *20*, 4125–4128.
- [30] C. H. Heathcock, E. F. Kleinman, E. S. Binkley, *J. Am. Chem. Soc.* **1982**, *104*, 1054–1068.
- [31] D. A. Evans, J. R. Scheerer, *Angew. Chem. Int. Ed.* **2005**, *44*, 6038–6042.
- [32] K. Nakahara, K. Hirano, R. Maehata, Y. Kita, H. Fujioka, *Org. Lett.* **2011**, *13*, 2015–2017.
- [33] H. Yang, R. G. Carter, *J. Org. Chem.* **2010**, *75*, 4929–4938.
- [34] H. Yang, R. G. Carter, L. N. Zakharov, *J. Am. Chem. Soc.* **2008**, *130*, 9238–9239.
- [35] D. Schumann, H.-J. Müller, A. Naumann, *Liebigs Ann. Chem.* **1982**, 2057–2061.
- [36] D. Schumann, H. J. Muller, A. Naumann, *Liebigs Ann. Chem.* **1982**, 1700–1705.
- [37] D. Schumann, A. Naumann, *Liebigs Ann. Chem.* **1983**, 220–225.
- [38] D. F. Fischer, R. Sarpong, *J. Am. Chem. Soc.* **2010**, *132*, 5926–5927.
- [39] B. B. Liau, M. D. Shair, *J. Am. Chem. Soc.* **2010**, *132*, 9594–9595.
- [40] A. S. Lee, B. B. Liau, M. D. Shair, *J. Am. Chem. Soc.* **2014**, *136*, 13442–13452.
- [41] M. Azuma, T. Yoshikawa, N. Kogure, M. Kitajima, H. Takayama, *J. Am. Chem. Soc.* **2014**, *136*, 11618–11621.
- [42] E. J. Corey, R. D. Balanson, *J. Am. Chem. Soc.* **1974**, *96*, 6516–6517.
- [43] D. M. Ryckman, R. V. Stevens, *J. Am. Chem. Soc.* **1987**, *109*, 4940–4948.
- [44] N. Fukuda, K. Sasaki, T. V. R. S. Sastry, M. Kanai, M. Shibasaki, *J. Org. Chem.* **2006**, *71*, 1220–1225.
- [45] M. Shibasaki, M. Kanai, N. Fukuda, *Chemistry—an Asian Journal* **2007**, *2*, 20–38.
- [46] K. Namba, T. Shinada, T. Teramoto, Y. Ohfuné, *J. Am. Chem. Soc.* **2000**, *122*, 10708–10709.
- [47] S. B. Herzon, A. G. Myers, *J. Am. Chem. Soc.* **2005**, *127*, 5342–5344.
- [48] A. X. Gao, T. Hamada, S. A. Snyder, *Angew. Chem. Int. Ed.* **2016**, *55*, 10301–10306.
- [49] W. A. Ayer, W. R. Bowman, G. A. Cooke, A. C. Soper, *Tetrahedron Lett.* **1966**, *7*, 2021–2026.
- [50] W. A. Ayer, W. R. Bowman, T. C. Joseph, P. Smith, *J. Am. Chem. Soc.* **1968**, *90*, 1648–1650.
- [51] S. Jin, J. Gong, Y. Qin, *Angew. Chem. Int. Ed.* **2015**, *54*, 2228–2231.
- [52] S. Diethelm, E. M. Carreira, *J. Am. Chem. Soc.* **2013**, *135*, 8500–8503.
- [53] Y. Koseki, H. Sato, Y. Watanabe, T. Nagasaka, *Org. Lett.* **2002**, *4*, 885–888.
- [54] W. N. Speckamp, H. Hiemstra, *Tetrahedron* **1985**, *41*, 4367–4416.
- [55] D. Trauner, J. B. Schwarz, S. J. Danishefsky, *Angew. Chem. Int. Ed.* **1999**, *38*, 3542–3545.
- [56] M. W. Carson, G. Kim, S. J. Danishefsky, *Angew. Chem. Int. Ed.* **2001**, *40*, 4453–4456.
- [57] M. W. Carson, G. Kim, M. F. Hentemann, D. Trauner, S. J. Danishefsky, *Angew. Chem. Int. Ed.* **2001**, *40*, 4450–4452.
- [58] G. Stork, R. A. Kretchmer, R. H. Schlessinger, *J. Am. Chem. Soc.* **1968**, *90*, 1647–1648.

- [59] H. Ishibashi, T. Sato, M. Takahashi, M. Hayashi, K. Ishikawa, M. Ikeda, *Chem. Pharm. Bull.* **1990**, *38*, 907–911.
- [60] H. Fukumoto, T. Esumi, J. Ishihara, S. Hatakeyama, *Tetrahedron Lett.* **2003**, *44*, 8047–8049.
- [61] Q. Wang, A. Padwa, *Org. Lett.* **2006**, *8*, 601–604.
- [62] F. Zhang, N. S. Simpkins, A. J. Blake, *Org. Biomol. Chem.* **2009**, *7*, 1963–1979.
- [63] C. Tsukano, L. Zhao, Y. Takemoto, M. Hirama, *Eur. J. Org. Chem.* **2010**, 4198–4200.
- [64] R. Ding, B.-F. Sun, G.-Q. Lin, *Org. Lett.* **2012**, *14*, 4446–4449.
- [65] J. Liu, R. P. Hsung, S. D. Peters, *Org. Lett.* **2004**, *6*, 3989–3992.
- [66] J. Liu, J. J. Swidorski, S. D. Peters, R. P. Hsung, *J. Org. Chem.* **2005**, *70*, 3898–3902.
- [67] E. J. Corey, G. A. Reichard, *J. Am. Chem. Soc.* **1992**, *114*, 10677–10678.
- [68] E. J. Corey, S. Choi, *Tetrahedron Lett.* **1993**, *34*, 6969–6972.
- [69] E. J. Corey, G. A. Reichard, *Tetrahedron Lett.* **1993**, *34*, 6973–6976.
- [70] T. Sunazuka, T. Nagamitsu, K. Matsuzaki, H. Tanaka, S. Omura, A. B. Smith, *J. Am. Chem. Soc.* **1993**, *115*, 5302–5302.
- [71] H. Uno, J. E. Baldwin, A. T. Russell, *J. Am. Chem. Soc.* **1994**, *116*, 2139–2140.
- [72] T. Nagamitsu, T. Sunazuka, H. Tanaka, S. Ōmura, P. A. Sprengeler, A. B. Smith, *J. Am. Chem. Soc.* **1996**, *118*, 3584–3590.
- [73] E. J. Corey, W. Li, T. Nagamitsu, *Angew. Chem. Int. Ed.* **1998**, *37*, 1676–1679.
- [74] E. J. Corey, W. Li, G. A. Reichard, *J. Am. Chem. Soc.* **1998**, *120*, 2330–2336.
- [75] J. S. Panek, C. E. Masse, *Angew. Chem. Int. Ed.* **1999**, *38*, 1093–1095.
- [76] D. Seebach, M. Boes, R. Naef, W. B. Schweizer, *J. Am. Chem. Soc.* **1983**, *105*, 5390–5398.
- [77] P. S. Baran, C. A. Guerrero, N. B. Ambhaikar, B. D. Hafensteiner, *Angew. Chem. Int. Ed.* **2005**, *44*, 606–609.
- [78] C. C. Hughes, D. Trauner, *Angew. Chem. Int. Ed.* **2002**, *41*, 4556–4559.
- [79] A. Hameed, A. J. Blake, C. J. Hayes, *J. Org. Chem.* **2008**, *73*, 8045–8048.
- [80] C. J. Hayes, A. E. Sherlock, M. P. Green, C. Wilson, A. J. Blake, M. D. Selby, J. C. Prodder, *J. Org. Chem.* **2008**, *73*, 2041–2051.
- [81] A. R. Battersby, H. Gregory, *Journal of the Chemical Society* **1963**, 22–32.
- [82] M. Greshoff, *Ber.* **1890**, *23*, 3537–3550.
- [83] C. Djerassi, H. Schmid, W. G. Kump, A. R. Battersby, J. M. Wilson, R. J. Owellen, D. J. Lecount, H. Budzikiewicz, *Helv. Chim. Acta* **1963**, *46*, 742–751.
- [84] B. W. Bycroft, D. Schumann, M. B. Patel, H. Schmid, *Helv. Chim. Acta* **1964**, *47*, 1147–1152.
- [85] D. Schumann, B. W. Bycroft, H. Schmid, *Experientia* **1964**, *20*, 202–203.
- [86] H. Achenbach, K. Biemann, *J. Am. Chem. Soc.* **1965**, *87*, 4944–4950.
- [87] J. M. F. Filho, B. Gilbert, M. Kitagawa, L. A. P. Leme, L. J. Durham, *Journal of the Chemical society C: Organic* **1966**, 1260–1266.

- [88] B. M. Craven, B. Gilbert, L. A. P. Leme, *Chem. Commun.* **1968**, 955–956.
- [89] B. Craven, *Acta Crystallogr., Sect. B: Struct. Sci.* **1969**, *25*, 2131–2139.
- [90] Y. Ban, Y. Honma, T. Oishi, *Tetrahedron Lett.* **1976**, *17*, 1111–1114.
- [91] M. E. Kuehne, P. J. Seaton, *J. Org. Chem.* **1985**, *50*, 4790–4796.
- [92] E. Wenkert, S. Liu, *J. Org. Chem.* **1994**, *59*, 7677–7682.
- [93] D. Gagnon, C. Spino, *J. Org. Chem.* **2009**, *74*, 6035–6041.
- [94] T. Gallagher, P. Magnus, *J. Am. Chem. Soc.* **1983**, *105*, 2086–2087.
- [95] P. Magnus, T. Gallagher, P. Brown, J. C. Huffman, *J. Am. Chem. Soc.* **1984**, *106*, 2105–2114.
- [96] P. Magnus, P. Brown, *J. Chem. Soc., Chem. Commun.* **1985**, 184–186.
- [97] P. Magnus, I. R. Matthews, J. Schultz, R. Waditschatka, J. C. Huffman, *J. Org. Chem.* **1988**, *53*, 5772–5776.
- [98] P. Magnus, T. Katoh, I. R. Matthews, J. C. Huffman, *J. Am. Chem. Soc.* **1989**, *111*, 6707–6711.
- [99] T. P. Burkholder, P. L. Fuchs, *J. Am. Chem. Soc.* **1988**, *110*, 2341–2342.
- [100] T. J. Greshock, A. W. Grubbs, S. Tsukamoto, R. M. Williams, *Angew. Chem. Int. Ed.* **2007**, *46*, 2262–2265.
- [101] J. D. Eckelbarger, J. T. Wilmot, D. Y. Gin, *J. Am. Chem. Soc.* **2006**, *128*, 10370–10371.
- [102] J. D. Eckelbarger, J. T. Wilmot, M. T. Epperson, C. S. Thakur, D. Shum, C. Antczak, L. Tarassishin, H. Djaballah, D. Y. Gin, *Chemistry—A European Journal* **2008**, *14*, 4293–4306.
- [103] R. A. Altman, B. L. Nilsson, L. E. Overman, J. R. de Alaniz, J. M. Rohde, V. Taupin, *J. Org. Chem.* **2010**, *75*, 7519–7534.
- [104] C. Fang, C. S. Shanahan, D. H. Paull, S. F. Martin, *Angew. Chem. Int. Ed.* **2012**, *51*, 10596–10599.
- [105] T. Kano, T. Hashimoto, K. Maruoka, *J. Am. Chem. Soc.* **2006**, *128*, 2174–2175.
- [106] M. P. Sibi, L. M. Stanley, T. Soeta, *Org. Lett.* **2007**, *9*, 1553–1556.
- [107] E. C. Davison, A. B. Holmes, I. T. Forbes, *Tetrahedron Lett.* **1995**, *36*, 9047–9050.
- [108] K. Wiesner, L. Poon, *Tetrahedron Lett.* **1967**, *8*, 4937–4940.
- [109] H. Dugas, M. E. Hazenberg, Z. Valenta, K. Wiesner, *Tetrahedron Lett.* **1967**, *8*, 4931–4936.
- [110] K. Wiesner, V. Musil, K. J. Wesner, *Tetrahedron Lett.* **1968**, *9*, 5643–5646.
- [111] K. Wiesner, L. Poon, I. Jirkovský, M. Fishman, *Can. J. Chem.* **1969**, *47*, 433–444.
- [112] J. D. Winkler, P. M. Hershberger, *J. Am. Chem. Soc.* **1989**, *111*, 4852–4856.
- [113] T. Sano, J. Toda, T. Ohshima, Y. Tsuda, *Chem. Pharm. Bull.* **1992**, *40*, 873–878.
- [114] D. L. Comins, Y.-M. Zhang, X. Zheng, *Chem. Commun.* **1998**, 2509–2510.
- [115] P.-Q. Huang, S.-Y. Huang, L.-H. Gao, Z.-Y. Mao, Z. Chang, A.-E. Wang, *Chem. Commun.* **2015**, *51*, 4576–4578.
- [116] J. Xie, A. L. Wolfe, D. L. Boger, *Org. Lett.* **2013**, *15*, 868–870.
- [117] T. Taniguchi, G. Tanabe, O. Muraoka, H. Ishibashi, *Org. Lett.* **2008**, *10*, 197–199.

- [118] T. Taniguchi, H. Ishibashi, *Tetrahedron* **2008**, *64*, 8773–8779.
- [119] R. Huisgen, W. Mack, E. Anneser, *Angew. Chem.* **1961**, *73*, 656–657.
- [120] K. Jae Nyoung, E. K. Ryu, *Tetrahedron Lett.* **1993**, *34*, 8283–8284.
- [121] J. N. Kim, K. S. Jung, H. J. Lee, J. S. Son, *Tetrahedron Lett.* **1997**, *38*, 1597–1598.
- [122] Y. Xia, A. P. Kozikowski, *J. Am. Chem. Soc.* **1989**, *111*, 4116–4117.
- [123] Y. Hirasawa, J. Kobayashi, H. Morita, *Heterocycles* **2009**, *77*, 679–729.
- [124] G. T. Ha, R. K. Wong, Y. Zhang, *Chemistry & Biodiversity* **2011**, *8*, 1189–1204.
- [125] L. Qian, R. Ji, *Tetrahedron Lett.* **1989**, *30*, 2089–2090.
- [126] A. P. Kozikowski, Y. Xia, E. R. Reddy, W. Tuckmantel, I. Hanin, X. C. Tang, *J. Org. Chem.* **1991**, *56*, 4636–4645.
- [127] A. P. Kozikowski, G. Campiani, P. Aagaard, M. McKinney, *J. Chem. Soc., Chem. Commun.* **1993**, 860–862.
- [128] I. Y. C. Lee, M. H. Jung, H. W. Lee, J. Y. Yang, *Tetrahedron Lett.* **2002**, *43*, 2407–2409.
- [129] T. Koshiba, S. Yokoshima, T. Fukuyama, *Org. Lett.* **2009**, *11*, 5354–5356.
- [130] M. K. M. Tun, D.-J. Wüstmann, S. B. Herzon, *Chemical Science* **2011**, *2*, 2251–2253.
- [131] S. M. A. Sohel, T. Opatz, *Arxiv* **2014**, *i*, 92–108.
- [132] S. R. Tudhope, J. A. Bellamy, A. Ball, D. Rajasekar, M. Azadi-Ardakani, H. S. Meera, J. M. Gnanadeepam, R. Saiganesh, F. Gibson, L. He, C. H. Behrens, G. Underiner, J. Marfurt, N. Favre, *Org. Process Res. Dev.* **2012**, *16*, 635–642.
- [133] Y. Adachi, N. Kamei, S. Yokoshima, T. Fukuyama, *Org. Lett.* **2011**, *13*, 4446–4449.
- [134] Y. Adachi, N. Kamei, S. Yokoshima, T. Fukuyama, *Org. Lett.* **2014**, *16*, 1273–1273.
- [135] M. Hoshi, O. Kaneko, M. Nakajima, S. Arai, A. Nishida, *Org. Lett.* **2014**, *16*, 768–771.
- [136] K. Chiyoda, J. Shimokawa, T. Fukuyama, *Angew. Chem. Int. Ed.* **2012**, *51*, 2505–2508.
- [137] Z.-H. Chen, Z.-M. Chen, Y.-Q. Zhang, Y.-Q. Tu, F.-M. Zhang, *J. Org. Chem.* **2011**, *76*, 10173–10186.
- [138] G. Stork, K. Zhao, *J. Am. Chem. Soc.* **1990**, *112*, 5875–5876.
- [139] Y. Kishi, F. Nakatsubo, M. Aratani, T. Goto, S. Inoue, H. Kakoi, *Tetrahedron Lett.* **1970**, *11*, 5129–5132.
- [140] Y. Kishi, F. Nakatsubo, M. Aratani, T. Goto, S. Inoue, H. Kakoi, S. Sugiura, *Tetrahedron Lett.* **1970**, *11*, 5127–5128.
- [141] Y. Kishi, M. Aratani, T. Fukuyama, Nakatsub.F, T. Goto, S. Inoue, H. Tanino, S. Sugiura, H. Kakoi, *J. Am. Chem. Soc.* **1972**, *94*, 9217–9219.
- [142] Y. Kishi, T. Fukuyama, M. Aratani, Nakatsub.F, T. Goto, S. Inoue, H. Tanino, S. Sugiura, H. Kakoi, *J. Am. Chem. Soc.* **1972**, *94*, 9219–9221.
- [143] P. A. Grieco, Y. Dai, *J. Am. Chem. Soc.* **1998**, *120*, 5128–5129.
- [144] J. A. MacKay, R. L. Bishop, V. H. Rawal, *Org. Lett.* **2005**, *7*, 3421–3424.
- [145] V. Bhat, K. M. Allan, V. H. Rawal, *J. Am. Chem. Soc.* **2011**, *133*, 5798–5801.

- [146] K. M. Allan, K. Kobayashi, V. H. Rawal, *J. Am. Chem. Soc.* **2012**, *134*, 1392–1395.
- [147] P. M. Wehn, J. Du Bois, *J. Am. Chem. Soc.* **2002**, *124*, 12950–12951.
- [148] A. Hinman, J. Du Bois, *J. Am. Chem. Soc.* **2003**, *125*, 11510–11511.
- [149] R. K. Hill, L. A. Renbaum, *Tetrahedron* **1982**, *38*, 1959–1963.
- [150] T. C. Coombs, Y. Zhang, E. C. Garnier-Amblard, L. S. Liebeskind, *J. Am. Chem. Soc.* **2009**, *131*, 876–877.
- [151] T. Fukuyama, L. V. Dunkerton, M. Aratani, Y. Kishi, *J. Org. Chem.* **1975**, *40*, 2011–2012.
- [152] M. Aratani, L. V. Dunkerton, T. Fukuyama, Y. Kishi, H. Kakoi, S. Sugiura, S. Inoue, *J. Org. Chem.* **1975**, *40*, 2009–2011.
- [153] S. C. Carey, M. Aratani, Y. Kishi, *Tetrahedron Lett.* **1985**, *26*, 5887–5890.
- [154] Y. Inubushi, T. Ibuka, M. Kitano, *Tetrahedron Lett.* **1969**, *10*, 1611–1614.
- [155] Y. Inubushi, M. Kitano, T. Ibuka, *Chem. Pharm. Bull.* **1971**, *19*, 1820–1841.
- [156] T. Ibuka, K. Tanaka, Y. Inubushi, *Tetrahedron Lett.* **1970**, *11*, 4811–4814.
- [157] T. Ibuka, K. Tanaka, Y. Inubushi, *Chem. Pharm. Bull.* **1974**, *22*, 782–798.
- [158] T. Ibuka, K. Tanaka, Y. Inubushi, *Tetrahedron Lett.* **1972**, *13*, 1393–1396.
- [159] T. Ibuka, K. Tanaka, Y. Inubushi, *Chem. Pharm. Bull.* **1974**, *22*, 907–921.
- [160] B. M. Trost, D. A. Bringley, T. Zhang, N. Cramer, *J. Am. Chem. Soc.* **2013**, *135*, 16720–16735.
- [161] E. V. Mercado-Marin, P. Garcia-Reynaga, S. Romminger, E. F. Pimenta, D. K. Romney, M. W. Lodewyk, D. E. Williams, R. J. Andersen, S. J. Miller, D. J. Tantillo, R. G. S. Berlinck, R. Sarpong, *Nature* **2014**, *509*, 318–324.
- [162] B. M. Trost, N. Cramer, H. Bernsmann, *J. Am. Chem. Soc.* **2007**, *129*, 3086–3087.
- [163] H. Ishibashi, M. Okano, H. Tamaki, K. Maruyama, T. Yakura, M. Ikeda, *J. Chem. Soc., Chem. Commun.* **1990**, 1436–1437.
- [164] L. F. Tietze, H. Braun, P. L. Steck, S. A. A. El Bialy, N. Tölle, A. Düfert, *Tetrahedron* **2007**, *63*, 6437–6445.
- [165] K. Shimizu, M. Takimoto, Y. Sato, M. Mori, *J. Organomet. Chem.* **2006**, *691*, 5466–5475.
- [166] M. Movassaghi, M. Tjandra, J. Qi, *J. Am. Chem. Soc.* **2009**, *131*, 9648–9650.
- [167] S. Ieda, T. Kan, T. Fukuyama, *Tetrahedron Lett.* **2010**, *51*, 4027–4029.
- [168] A. C. Flick, M. J. A. Caballero, A. Padwa, *Org. Lett.* **2008**, *10*, 1871–1874.
- [169] B. B. Snider, T. Liu, *J. Org. Chem.* **1997**, *62*, 5630–5633.
- [170] D. A. Evans, D. J. Adams, E. E. Kwan, *J. Am. Chem. Soc.* **2012**, *134*, 8162–8170.
- [171] U. Shah, S. Chackalamannil, A. K. Ganguly, M. Chelliah, S. Kolotuchin, A. Buevich, A. McPhail, *J. Am. Chem. Soc.* **2006**, *128*, 12654–12655.
- [172] P. N. Carlsen, T. J. Mann, A. H. Hoveyda, A. J. Frontier, *Angew. Chem.* **2014**, *126*, 9488–9492.
- [173] H. Li, X. Wang, X. Lei, *Angew. Chem. Int. Ed.* **2012**, *51*, 491–495.

- [174] N. A. Braun, M. Ousmer, J. D. Bray, D. Bouchu, K. Peters, E.-M. Peters, M. A. Ciufolini, *J. Org. Chem.* **2000**, *65*, 4397–4408.
- [175] M. Paladino, J. Zaifman, M. A. Ciufolini, *Org. Lett.* **2015**, *17*, 3422–3425.
- [176] Y. Kaiya, J.-I. Hasegawa, T. Momose, T. Sato, N. Chida, *Chemistry—an Asian Journal* **2011**, *6*, 209–219.
- [177] Y. Ichikawa, K. Okumura, Y. Matsuda, T. Hasegawa, M. Nakamura, A. Fujimoto, T. Masuda, K. Nakano, H. Kotsuki, *Org. Biomol. Chem.* **2012**, *10*, 614–622.
- [178] A. S. Kende, T. L. Smalley, H. Huang, *J. Am. Chem. Soc.* **1999**, *121*, 7431–7432.
- [179] K. C. Nicolaou, D. J. Edmonds, P. G. Bulger, *Angew. Chem. Int. Ed.* **2006**, *45*, 7134–7186.
- [180] K. C. Nicolaou, J. S. Chen, *Chem. Soc. Rev.* **2009**, *38*, 2993–3009.
- [181] A. Padwa, S. K. Bur, *Tetrahedron* **2007**, *63*, 5341–5378.
- [182] H. Pellissier, *Tetrahedron* **2006**, *62*, 1619–1665.
- [183] H. Pellissier, *Tetrahedron* **2006**, *62*, 2143–2173.
- [184] L. J. Sebren, J. J. Devery, C. R. J. Stephenson, *ACS Catalysis* **2014**, *4*, 703–716.
- [185] L. F. Tietze, *Chem. Rev.* **1996**, *96*, 115–136.
- [186] L. F. Tietze, U. Beifuss, *Angew. Chem. Int. Ed.* **1993**, *32*, 131–163.
- [187] J.-C. Wasilke, S. J. Obrey, R. T. Baker, G. C. Bazan, *Chem. Rev.* **2005**, *105*, 1001–1020.
- [188] J. C. Braekman, R. N. Gupta, D. B. MacLean, I. D. Spenser, *Can. J. Chem.* **1972**, *50*, 2591–2602.
- [189] M. Castillo, R. N. Gupta, Y. K. Ho, D. B. MacLean, I. D. Spenser, *Can. J. Chem.* **1970**, *48*, 2911–2918.
- [190] M. Castillo, R. N. Gupta, Y. K. Ho, D. B. MacLean, I. D. Spenser, *J. Am. Chem. Soc.* **1970**, *92*, 1074–1075.
- [191] R. N. Gupta, M. Castillo, D. B. MacLean, I. D. Spenser, J. T. Wrobel, *J. Am. Chem. Soc.* **1968**, *90*, 1360–1361.
- [192] T. Hemscheidt, I. D. Spenser, *J. Am. Chem. Soc.* **1993**, *115*, 3020–3021.
- [193] T. C. Sherwood, A. H. Trotta, S. A. Snyder, *J. Am. Chem. Soc.* **2014**, *136*, 9743–9753.
- [194] K. M. Brummond, J. L. Lu, *Org. Lett.* **2001**, *3*, 1347–1349.
- [195] S. D. Knight, L. E. Overman, G. Pairaudeau, *J. Am. Chem. Soc.* **1993**, *115*, 9293–9294.
- [196] L. E. Overman, M. Sworin, R. M. Burk, *J. Org. Chem.* **1983**, *48*, 2685–2690.
- [197] J. D. White, Y. Li, J. Kim, M. Terinek, *Org. Lett.* **2013**, *15*, 882–885.
- [198] M. S. Karatholuvhu, A. Sinclair, A. F. Newton, M.-L. Alcaraz, R. A. Stockman, P. L. Fuchs, *J. Am. Chem. Soc.* **2006**, *128*, 12656–12657.
- [199] G. M. Williams, S. D. Roughley, J. E. Davies, A. B. Holmes, J. P. Adams, *J. Am. Chem. Soc.* **1999**, *121*, 4900–4901.

- [200] E. C. Davison, M. E. Fox, A. B. Holmes, S. D. Roughley, C. J. Smith, G. M. Williams, J. E. Davies, P. R. Raithby, J. P. Adams, I. T. Forbes, N. J. Press, M. J. Thompson, *J. Chem. Soc., Perkin Trans. 1* **2002**, 1494–1514.
- [201] K. C. Nicolaou, M. Nevalainen, B. S. Safina, M. Zak, S. Bulat, *Angew. Chem. Int. Ed.* **2002**, *41*, 1941–1945.
- [202] K. C. Nicolaou, B. S. Safina, M. Zak, A. A. Estrada, S. H. Lee, *Angew. Chem. Int. Ed.* **2004**, *43*, 5087–5092.
- [203] K. C. Nicolaou, B. S. Safina, M. Zak, S. H. Lee, M. Nevalainen, M. Bella, A. A. Estrada, C. Funke, F. J. Zécari, S. Bulat, *J. Am. Chem. Soc.* **2005**, *127*, 11159–11175.
- [204] K. C. Nicolaou, M. Zak, B. S. Safina, A. A. Estrada, S. H. Lee, M. Nevalainen, *J. Am. Chem. Soc.* **2005**, *127*, 11176–11183.
- [205] K. C. Nicolaou, M. Zak, B. S. Safina, S. H. Lee, A. A. Estrada, *Angew. Chem. Int. Ed.* **2004**, *43*, 5092–5097.
- [206] Y.-M. Zhao, P. Gu, Y.-Q. Tu, C.-A. Fan, Q. Zhang, *Org. Lett.* **2008**, *10*, 1763–1766.
- [207] Z.-H. Chen, Y.-Q. Zhang, Z.-M. Chen, Y.-Q. Tu, F.-M. Zhang, *Chem. Commun.* **2011**, *47*, 1836–1838.
- [208] P. S. Baran, R. A. Shenvi, C. A. Mitsos, *Angew. Chem. Int. Ed.* **2005**, *44*, 3714–3717.
- [209] P. S. Baran, R. A. Shenvi, *J. Am. Chem. Soc.* **2006**, *128*, 14028–14029.
- [210] J. Cassayre, F. Gagosz, S. Z. Zard, *Angew. Chem. Int. Ed.* **2002**, *41*, 1783–1785.
- [211] D. A. Evans, C. A. Bryan, G. M. Wahl, *J. Org. Chem.* **1970**, *35*, 4122–4127.
- [212] A. G. Schultz, A. Wang, *J. Am. Chem. Soc.* **1998**, *120*, 8259–8260.
- [213] S. B. Jones, L. He, S. L. Castle, *Org. Lett.* **2006**, *8*, 3757–3760.
- [214] F. Li, S. S. Tartakoff, S. L. Castle, *J. Am. Chem. Soc.* **2009**, *131*, 6674–6675.
- [215] F. Li, S. S. Tartakoff, S. L. Castle, *J. Org. Chem.* **2009**, *74*, 9082–9093.
- [216] S. B. Herzon, N. A. Calandra, S. M. King, *Angew. Chem. Int. Ed.* **2011**, *50*, 8863–8866.
- [217] K. V. Chuang, R. Navarro, S. E. Reisman, *Angew. Chem. Int. Ed.* **2011**, *50*, 9447–9451.
- [218] S. M. King, N. A. Calandra, S. B. Herzon, *Angew. Chem. Int. Ed.* **2013**, *52*, 3642–3645.
- [219] N. A. Calandra, S. M. King, S. B. Herzon, *J. Org. Chem.* **2013**, *78*, 10031–10057.
- [220] M. Tomita, M. Kitano, T. Ibuka, *Tetrahedron Lett.* **1968**, *9*, 3391–3393.
- [221] S. B. Jones, L. He, S. L. Castle, *Org. Lett.* **2006**, *8*, 3757–3760.
- [222] D. K. Nielsen, L. L. Nielsen, S. B. Jones, L. Toll, M. C. Asplund, S. L. Castle, *J. Org. Chem.* **2008**, *74*, 1187–1199.
- [223] D. K. Semwal, R. Badoni, R. Semwal, S. K. Kothiyal, G. J. P. Singh, U. Rawat, *J. Ethnopharmacol.* **2010**, *132*, 369–383.
- [224] T. Taga, N. Akimoto, T. Ibuka, *Chem. Pharm. Bull.* **1984**, *32*, 4223–4225.
- [225] L. He, Y.-H. Zhang, H.-Y. Guan, J.-X. Zhang, Q.-Y. Sun, X.-J. Hao, *J. Nat. Prod.* **2011**, *74*, 181–184.

- [226] United States Department of Agriculture, U.S. National Plant Germplasm System, "Taxon: *Stephania japonica* (Thunb.) Miers", <http://www.ars-grin.gov/cgi-bin/npgs/html/taxon.pl?417571> (last opened on 30th May 2017)
- [227] Y. X. F. Bingyi, C. Anmin, M. Yingfu, S. Fang, Q. Jinlin, G. Yuan, G. , L. Q. Zhemin, W. Shu, *Encyclopedic Reference of Traditional Chinese Medicine*, Springer, Berlin Heidelberg, **2013**.
- [228] M. Matsui, T. Kabashima, K. Ishida, T. Takebayashi, Y. Watanabe, *J. Nat. Prod.* **1982**, *45*, 497–500.
- [229] G. E. W. Tang, *Chinese Drugs of Plant Origin: Chemistry, Pharmacology, and Use in Traditional and Modern Medicine* Springer, Berlin Heidelberg, **2013**.
- [230] W.-Y. Wu, J.-J. Hou, H.-L. Long, W.-Z. Yang, J. Liang, D.-A. Guo, *Chinese Journal of Natural Medicines* **2014**, *12*, 241–250.
- [231] H. Huang, G. Hu, C. Wang, H. Xu, X. Chen, A. Qian, *Inflammation* **2014**, *37*, 235–246.
- [232] B. Fugmann, S. Lang-Fugmann, W. Steglich, *RÖMPP Encyclopedia Natural Products*, 1 ed., Georg Thieme Verlag KG, Stuttgart, **2000**.
- [233] A. R. Carroll, T. Arumugan, J. Redburn, A. Ngo, G. P. Guymer, P. I. Forster, R. J. Quinn, *J. Nat. Prod.* **2010**, *73*, 988–991.
- [234] X. Peng, B. I. Knapp, J. M. Bidlack, J. L. Neumeyer, *J. Med. Chem.* **2006**, *49*, 256–262.
- [235] A. J. Pihko, A. M. P. Koskinen, *Tetrahedron* **2005**, *61*, 8769–8807.
- [236] P. M. Dewick, *Medicinal Natural Products : A Biosynthetic Approach*, 3 ed., Wiley, Chichester, **2009**.
- [237] A. R. Battersby, R. C. F. Jones, R. Kazlauskas, C. Poupat, C. W. Thornber, S. Ruchirawat, J. Staunton, *J. Chem. Soc., Chem. Commun.* **1974**, *0*, 773–775.
- [238] A. R. Battersby, R. C. F. Jones, R. Kazlauskas, A. P. Ottridge, C. Poupat, J. Staunton, *Journal of the Chemical Society, Perkin Transactions 1* **1981**, *0*, 2010–2015.
- [239] A. R. Battersby, R. C. F. Jones, R. Kazlauskas, C. W. Thornber, S. Ruchirawat, J. Staunton, *Journal of the Chemical Society, Perkin Transactions 1* **1981**, *0*, 2016–2029.
- [240] A. R. Battersby, R. C. F. Jones, A. Minta, A. P. Ottridge, J. Staunton, *Journal of the Chemical Society, Perkin Transactions 1* **1981**, *0*, 2030–2039.
- [241] D. Hager, Ludwig-Maximilians-Universität (München), **2012**.
- [242] A. Hager, Ludwig-Maximilians-Universität (München), **2012**.
- [243] M. Tomita, T. Ibuka, Y. Inubua, K. Takeda, *Tetrahedron Lett.* **1964**, *5*, 3605–3616.
- [244] T. Taga, N. Akimoto, T. Ibuka, *Chemical and Pharmaceutical Bulletin* **1984**, *32*, 4223–4225.
- [245] D.-H. Wang, K. M. Engle, B.-F. Shi, J.-Q. Yu, *Science* **2010**, *327*, 315–319.
- [246] R. Detterbeck, M. Hesse, *Helv. Chim. Acta* **2003**, *86*, 343–360.
- [247] D. C. Behenna, B. M. Stoltz, *J. Am. Chem. Soc.* **2004**, *126*, 15044–15045.
- [248] J. Tsuji, I. Shimizu, I. Minami, Y. Ohashi, *Tetrahedron Lett.* **1982**, *23*, 4809–4812.
- [249] B. M. Trost, J. Xu, *J. Am. Chem. Soc.* **2005**, *127*, 2846–2847.

- [250] D. A. Evans, C. A. Bryan, C. L. Sims, *J. Am. Chem. Soc.* **1972**, *94*, 2891–2892.
- [251] D. Trauner, *Synthesis* **1998**, *1998*, 653–664.
- [252] J. Mulzer, G. Dürner, D. Trauner, *Angew. Chem. Int. Ed.* **1996**, *35*, 2830–2832.
- [253] J. D. White, P. Hrcniar, F. Stappenbeck, *J. Org. Chem.* **1999**, *64*, 7871–7884.
- [254] T. X. Nguyen, Y. Kobayashi, *J. Org. Chem.* **2008**, *73*, 5536–5541.
- [255] M. D. Soffer, R. A. Stewart, J. C. Cavagnol, H. E. Gellerson, E. A. Bowler, *J. Am. Chem. Soc.* **1950**, *72*, 3704–3709.
- [256] G. B. Diamond, M. D. Soffer, *J. Am. Chem. Soc.* **1952**, *74*, 4126–4127.
- [257] M. A. McKervey, S. M. Tuladhar, M. F. Twohig, *J. Chem. Soc., Chem. Commun.* **1984**, *0*, 129–130.
- [258] Á. Gorka, B. Czuczai, P. Szoleczky, L. Hazai, C. Szántay, V. Háda, C. Szántay, *Synth. Commun.* **2005**, *35*, 2371–2378.
- [259] E. V. Cabrera, J. L. Sanchez, A. K. Banerjee, *Org. Prep. Proced. Int.* **2011**, *43*, 364–367.
- [260] I. Moritanl, Y. Fujiwara, *Tetrahedron Lett.* **1967**, *8*, 1119–1122.
- [261] Y. Fujiwara, I. Moritani, M. Matsuda, S. Teranishi, *Tetrahedron Lett.* **1968**, *9*, 633–636.
- [262] Y. Fujiwara, I. Moritani, S. Danno, R. Asano, S. Teranishi, *J. Am. Chem. Soc.* **1969**, *91*, 7166–7169.
- [263] G. Stork, A. Brizzolara, H. Landesman, J. Szmuszkowicz, R. Terrell, *J. Am. Chem. Soc.* **1963**, *85*, 207–222.
- [264] S. F. Martin, *Tetrahedron* **1980**, *36*, 419–460.
- [265] K. Fuji, *Chem. Rev.* **1993**, *93*, 2037–2066.
- [266] E. J. Corey, A. Guzman-Perez, *Angew. Chem.* **1998**, *110*, 402–415.
- [267] J. Christoffers, A. Mann, *Angew. Chem.* **2001**, *113*, 4725–4732.
- [268] I. Denissova, L. Barriault, *Tetrahedron* **2003**, *59*, 10105–10146.
- [269] C. J. Douglas, L. E. Overman, *Proc. Natl. Acad. Sci. U. S. A.* **2004**, *101*, 5363–5367.
- [270] J. Christoffers, A. Baro, *Adv. Synth. Catal.* **2005**, *347*, 1473–1482.
- [271] B. M. Trost, C. Jiang, *Synthesis* **2006**, *2006*, 369–396.
- [272] P. G. Cozzi, R. Hilgraf, N. Zimmermann, *Eur. J. Org. Chem.* **2007**, *2007*, 5969–5994.
- [273] V. Bhat, E. R. Welin, X. Guo, B. M. Stoltz, *Chem. Rev.* **2017**, *117*, 4528–4561.
- [274] B. M. Trost, D. L. Van Vranken, *Chem. Rev.* **1996**, *96*, 395–422.
- [275] B. M. Trost, J. Xu, T. Schmidt, *J. Am. Chem. Soc.* **2009**, *131*, 18343–18357.
- [276] D. C. Behenna, J. T. Mohr, N. H. Sherden, S. C. Marinescu, A. M. Harned, K. Tani, M. Seto, S. Ma, Z. Novák, M. R. Krout, R. M. McFadden, J. L. Roizen, J. A. Enquist, D. E. White, S. R. Levine, K. V. Petrova, A. Iwashita, S. C. Virgil, B. M. Stoltz, *Chem. Eur. J* **2011**, *17*, 14199–14223.
- [277] J. D. Weaver, A. Recio, A. J. Grenning, J. A. Tunge, *Chem. Rev.* **2011**, *111*, 1846–1913.
- [278] J. T. Mohr, B. M. Stoltz, *Chemistry – An Asian Journal* **2007**, *2*, 1476–1491.

- [279] J. A. Keith, D. C. Behenna, N. Sherden, J. T. Mohr, S. Ma, S. C. Marinescu, R. J. Nielsen, J. Oxgaard, B. M. Stoltz, W. A. Goddard, *J. Am. Chem. Soc.* **2012**, *134*, 19050–19060.
- [280] H. Kurosawa, *J. Organomet. Chem.* **1987**, *334*, 243–253.
- [281] J. A. Keith, D. C. Behenna, J. T. Mohr, S. Ma, S. C. Marinescu, J. Oxgaard, B. M. Stoltz, W. A. Goddard, *J. Am. Chem. Soc.* **2007**, *129*, 11876–11877.
- [282] H. Mukherjee, N. T. McDougal, S. C. Virgil, B. M. Stoltz, *Org. Lett.* **2011**, *13*, 825–827.
- [283] R. M. McFadden, B. M. Stoltz, *J. Am. Chem. Soc.* **2006**, *128*, 7738–7739.
- [284] J. A. Enquist, S. C. Virgil, B. M. Stoltz, *Chem. Eur. J* **2011**, *17*, 9957–9969.
- [285] J. J. Day, R. M. McFadden, S. C. Virgil, H. Kolding, J. L. Alleva, B. M. Stoltz, *Angew. Chem. Int. Ed.* **2011**, *50*, 6814–6818.
- [286] N. T. McDougal, S. C. Virgil, B. M. Stoltz, *Synlett* **2010**, *2010*, 1712–1716.
- [287] N. Vrielink, Ludwig–Maximilians–Universität München (Munich), **2013**.
- [288] N. T. McDougal, J. Streuff, H. Mukherjee, S. C. Virgil, B. M. Stoltz, *Tetrahedron Lett.* **2010**, *51*, 5550–5554.
- [289] M. G. Beaver, K. A. Woerpel, *J. Org. Chem.* **2010**, *75*, 1107–1118.
- [290] H. Mayr, B. Kempf, A. R. Ofial, *Acc. Chem. Res.* **2003**, *36*, 66–77.
- [291] F. Corral-Bautista, R. Appel, J. S. Frickel, H. Mayr, *Chem. Eur. J* **2015**, *21*, 875–884.
- [292] H. Mayr, M. Breugst, A. R. Ofial, *Angew. Chem. Int. Ed.* **2011**, *50*, 6470–6505.
- [293] H. Mayr, A. R. Ofial, *Angew. Chem. Int. Ed.* **2006**, *45*, 1844–1854.
- [294] B. M. Trost, F. D. Toste, *J. Am. Chem. Soc.* **1999**, *121*, 4545–4554.
- [295] W.-B. Liu, C. M. Reeves, B. M. Stoltz, *J. Am. Chem. Soc.* **2013**, *135*, 17298–17301.
- [296] M. Pfau, G. Revial, A. Guingant, J. d'Angelo, *J. Am. Chem. Soc.* **1985**, *107*, 273–274.
- [297] S. Giroux, E. J. Corey, *Org. Lett.* **2008**, *10*, 5617–5619.
- [298] Y. Okamoto, T. Ikai, *Chem. Soc. Rev.* **2008**, *37*, 2593–2608.
- [299] G. Pupo, R. Properzi, B. List, *Angew. Chem. Int. Ed.* **2016**, *55*, 6099–6102.
- [300] M. Mahlau, B. List, *Angew. Chem. Int. Ed.* **2013**, *52*, 518–533.
- [301] G. A. Bailey, D. E. Fogg, *J. Am. Chem. Soc.* **2015**, *137*, 7318–7321.
- [302] H. Nishiyama, T. Shiomi, in *Metal Catalyzed Reductive C–C Bond Formation: A Departure from Preformed Organometallic Reagents* (Ed.: M. J. Krische), Springer Berlin Heidelberg, Berlin, Heidelberg, **2007**, pp. 105–137.
- [303] H. W. Lam, P. M. Joensuu, *Org. Lett.* **2005**, *7*, 4225–4228.
- [304] A. J. Catino, A. Sherlock, P. Shieh, J. S. Wzorek, D. A. Evans, *Org. Lett.* **2013**, *15*, 3330–3333.
- [305] P. Nuhant, C. Allais, W. R. Roush, *Angew. Chem. Int. Ed.* **2013**, *52*, 8703–8707.
- [306] T. Shiomi, H. Nishiyama, *Org. Lett.* **2007**, *9*, 1651–1654.

- [307] T. R. Elworthy, E. R. Brill, S.-S. Chiou, F. Chu, J. R. Harris, R. T. Hendricks, J. Huang, W. Kim, L. K. Lach, T. Mirzadegan, C. Yee, K. A. M. Walker, *J. Med. Chem.* **2004**, *47*, 6124–6127.
- [308] A. C. Pinto, R. d. A. Epifanio, W. Camargo, *Tetrahedron* **1993**, *49*, 5039–5046.
- [309] K. S. Feldman, R. F. Campbell, T. R. West, A. D. Aloise, D. M. Giampetro, *J. Org. Chem.* **1999**, *64*, 7612–7617.
- [310] M. S. Bultman, J. Ma, D. Y. Gin, *Angew. Chem. Int. Ed.* **2008**, *47*, 6821–6824.
- [311] S. Das, D. Addis, S. Zhou, K. Junge, M. Beller, *J. Am. Chem. Soc.* **2010**, *132*, 1770–1771.
- [312] J. T. Reeves, Z. Tan, M. A. Marsini, Z. S. Han, Y. Xu, D. C. Reeves, H. Lee, B. Z. Lu, C. H. Senanayake, *Adv. Synth. Catal.* **2013**, *355*, 47–52.
- [313] H. Ishikawa, G. I. Elliott, J. Velcicky, Y. Choi, D. L. Boger, *J. Am. Chem. Soc.* **2006**, *128*, 10596–10612.
- [314] H. Yi, Q. Liu, J. Liu, Z. Zeng, Y. Yang, A. Lei, *ChemSusChem* **2012**, *5*, 2143–2146.
- [315] S. W. M. Crossley, C. Obradors, R. M. Martinez, R. A. Shenvi, *Chem. Rev.* **2016**, *116*, 8912–9000.
- [316] L. F. Tietze, L. Ma, J. R. Reiner, S. Jackenkroll, S. Heidemann, *Chem. Eur. J* **2013**, *19*, 8610–8614.
- [317] M. Zahel, P. Metz, *Beilstein J. Org. Chem.* **2013**, *9*, 2028–2032.
- [318] B. Morandi, Z. K. Wickens, R. H. Grubbs, *Angew. Chem. Int. Ed.* **2013**, *52*, 2944–2948.
- [319] P. K. Koech, M. J. Krische, *Org. Lett.* **2004**, *6*, 691–694.
- [320] J. T. Suri, D. D. Steiner, C. F. Barbas, *Org. Lett.* **2005**, *7*, 3885–3888.
- [321] B. List, *J. Am. Chem. Soc.* **2002**, *124*, 5656–5657.
- [322] H. Vogt, S. Vanderheiden, S. Brase, *Chem. Commun.* **2003**, 2448–2449.
- [323] T. Patra, S. Manna, D. Maiti, *Angew. Chem. Int. Ed.* **2011**, *50*, 12140–12142.
- [324] J. N. Payette, H. Yamamoto, *J. Am. Chem. Soc.* **2008**, *130*, 12276–12278.
- [325] P. D. Pohlhaus, R. K. Bowman, J. S. Johnson, *J. Am. Chem. Soc.* **2004**, *126*, 2294–2295.
- [326] B. Tiwari, J. Zhang, Y. R. Chi, *Angew. Chem. Int. Ed.* **2012**, *51*, 1911–1914.
- [327] V. Van Rheenen, *Tetrahedron Lett.* **1969**, *10*, 985–988.
- [328] N. Issei, H. Toshio, F. Shinichiro, I. Shinya, U. Hiroaki, *Bull. Chem. Soc. Jpn.* **1985**, *58*, 1081–1082.
- [329] K. V. Chuang, R. Navarro, S. E. Reisman, *Chemical Science* **2011**, *2*, 1086–1089.
- [330] A. W. Schammel, G. Chiou, N. K. Garg, *Org. Lett.* **2012**, *14*, 4556–4559.
- [331] J. Yu, X. Z. Wearing, J. M. Cook, *J. Org. Chem.* **2005**, *70*, 3963–3979.
- [332] W. Yin, M. S. Kabir, Z. Wang, S. K. Rallapalli, J. Ma, J. M. Cook, *J. Org. Chem.* **2010**, *75*, 3339–3349.
- [333] C. Zheng, I. Dubovyk, K. E. Lazarski, R. J. Thomson, *J. Am. Chem. Soc.* **2014**, *136*, 17750–17756.

- [334] Y. Shen, L. Li, Z. Pan, Y. Wang, J. Li, K. Wang, X. Wang, Y. Zhang, T. Hu, Y. Zhang, *Org. Lett.* **2015**, *17*, 5480–5483.
- [335] H.-D. Hao, Y. Li, W.-B. Han, Y. Wu, *Org. Lett.* **2011**, *13*, 4212–4215.
- [336] H. Salim, O. Piva, *J. Org. Chem.* **2009**, *74*, 2257–2260.
- [337] P. C. Roosen, C. D. Vanderwal, *Angew. Chem. Int. Ed.* **2016**, *55*, 7180–7183.
- [338] R. M. Coates, J. W. Muskopf, P. A. Senter, *J. Org. Chem.* **1985**, *50*, 3541–3557.
- [339] J. M. Howell, K. Feng, J. R. Clark, L. J. Trzepakowski, M. C. White, *J. Am. Chem. Soc.* **2015**.
- [340] T. J. Osberger, D. C. Rogness, J. T. Kohrt, A. F. Stepan, M. C. White, *Nature* **2016**, *537*, 214–219.
- [341] H.-D. Hao, Shanghai Institute of Organic Chemistry (Shanghai), **2011**.
- [342] P. E. Gormisky, M. C. White, *J. Am. Chem. Soc.* **2013**, *135*, 14052–14055.
- [343] S. A. Weissman, D. Zewge, *Tetrahedron* **2005**, *61*, 7833–7863.
- [344] A. T. Placzek, T. S. Scanlan, *Tetrahedron* **2015**, *71*, 5946–5951.
- [345] H. Zhou, X. Liao, W. Yin, J. Ma, J. M. Cook, *J. Org. Chem.* **2006**, *71*, 251–259.
- [346] S. Yamada, D. Morizono, K. Yamamoto, *Tetrahedron Lett.* **1992**, *33*, 4329–4332.
- [347] V. L. Rendina, S. A. Goetz, A. E. Neitzel, H. Z. Kaplan, J. S. Kingsbury, *Tetrahedron Lett.* **2012**, *53*, 15–18.
- [348] S. Caddick, D. B. Judd, A. K. d. K. Lewis, M. T. Reich, M. R. V. Williams, *Tetrahedron* **2003**, *59*, 5417–5423.
- [349] W.-H. Meng, T.-J. Wu, H.-K. Zhang, P.-Q. Huang, *Tetrahedron: Asymmetry* **2004**, *15*, 3899–3910.
- [350] J.-X. Du, H.-Y. Huang, P.-Q. Huang, *Tetrahedron: Asymmetry* **2004**, *15*, 3461–3466.
- [351] M. Robba, D. Maume, *Tetrahedron Lett.* **1972**, *13*, 2333–2335.
- [352] Y. Nakayama, Y. Maeda, M. Kotatsu, R. Sekiya, M. Ichiki, T. Sato, N. Chida, *Chem. Eur. J.* **2016**, *22*, 3300–3303.
- [353] A. D. Gammack Yamagata, D. J. Dixon, *Org. Lett.* **2017**, *19*, 1894–1897.
- [354] S.-H. Ueng, L. Fensterbank, E. Lacote, M. Malacria, D. P. Curran, *Org. Biomol. Chem.* **2011**, *9*, 3415–3420.
- [355] J. J. Devery, J. D. Nguyen, C. Dai, C. R. J. Stephenson, *ACS Catalysis* **2016**, *6*, 5962–5967.
- [356] T. Miyazawa, K. Minami, M. Ito, M. Anada, S. Matsunaga, S. Hashimoto, *Tetrahedron* **2016**, *72*, 3939–3947.
- [357] D. C. Harrowven, D. P. Curran, S. L. Kostiuk, I. L. Wallis-Guy, S. Whiting, K. J. Stenning, B. Tang, E. Packard, L. Nanson, *Chem. Commun.* **2010**, *46*, 6335–6337.
- [358] C. R. Gault, L. M. Obeid, Y. A. Hannun, *Adv. Exp. Med. Biol.* **2010**, *688*, 1–23.
- [359] S. Degroote, J. Wolthoorn, G. van Meer, in *Seminars in cell & developmental biology, Vol. 15*, Elsevier, **2004**, pp. 375–387.
- [360] R. X. Tan, J. H. Chen, *Nat. Prod. Rep.* **2003**, *20*, 509–534.

- [361] T. Natori, Y. Koezuka, T. Higa, *Tetrahedron Lett.* **1993**, *34*, 5591–5592.
- [362] A. Banchet-Cadeddu, E. Henon, M. Dauchez, J.-H. Renault, F. Monneaux, A. Haudrechy, *Org. Biomol. Chem.* **2011**, *9*, 3080–3104.
- [363] S. Motohashi, K. Nagato, N. Kunii, H. Yamamoto, K. Yamasaki, K. Okita, H. Hanaoka, N. Shimizu, M. Suzuki, I. Yoshino, M. Taniguchi, T. Fujisawa, T. Nakayama, *The Journal of Immunology* **2009**, *182*, 2492–2501.
- [364] G. Giaccone, C. J. A. Punt, Y. Ando, R. Ruijter, N. Nishi, M. Peters, B. M. E. von Blomberg, R. J. Scheper, H. J. J. van der Vliet, A. J. M. van den Eertwegh, M. Roelvink, J. Beijnen, H. Zwierzina, H. M. Pinedo, *Clinical Cancer Research* **2002**, *8*, 3702–3709.
- [365] M. Fujio, D. Wu, R. Garcia-Navarro, D. D. Ho, M. Tsuji, C.-H. Wong, *J. Am. Chem. Soc.* **2006**, *128*, 9022–9023.
- [366] K. O. A. Yu, J. S. Im, A. Molano, Y. Dutronc, P. A. Illarionov, C. Forestier, N. Fujiwara, I. Arias, S. Miyake, T. Yamamura, Y.-T. Chang, G. S. Besra, S. A. Porcelli, *Proc. Natl. Acad. Sci. U. S. A.* **2005**, *102*, 3383–3388.
- [367] J. Schmiege, G. Yang, R. W. Franck, M. Tsuji, *The Journal of Experimental Medicine* **2003**, *198*, 1631–1641.
- [368] J. Broichhagen, J. A. Frank, D. Trauner, *Acc. Chem. Res.* **2015**, *48*, 1947–1960.
- [369] J. Harouse, S. Bhat, S. Spitalnik, M. Laughlin, K. Stefano, D. Silberberg, F. Gonzalez-Scarano, *Science* **1991**, *253*, 320–323.
- [370] J. Fantini, D. G. Cook, N. Nathanson, S. L. Spitalnik, F. Gonzalez-Scarano, *Proceedings of the National Academy of Sciences* **1993**, *90*, 2700–2704.
- [371] K. D. McReynolds, J. Gervay-Hague, *Chem. Rev.* **2007**, *107*, 1533–1552.
- [372] J. C. Conboy, K. D. McReynolds, J. Gervay-Hague, S. S. Saavedra, *J. Am. Chem. Soc.* **2002**, *124*, 968–977.
- [373] D. Smith, R. Byrn, S. Marsters, T. Gregory, J. Groopman, D. Capon, *Science* **1987**, *238*, 1704–1707.
- [374] T. Fehrentz, M. Schönberger, D. Trauner, *Angew. Chem. Int. Ed.* **2011**, *50*, 12156–12182.
- [375] W. A. Velema, W. Szymanski, B. L. Feringa, *J. Am. Chem. Soc.* **2014**, *136*, 2178–2191.
- [376] R. H. Kramer, A. Mourot, H. Adesnik, *Nat. Neurosci.* **2013**, *16*, 816–823.
- [377] D. B. Konrad, J. A. Frank, D. Trauner, *Chem. Eur. J.* **2016**, *22*, 4364–4368.
- [378] A. Damijonaitis, J. Broichhagen, T. Urushima, K. Hüll, J. Nagpal, L. Laprell, M. Schönberger, D. H. Woodmansee, A. Rafiq, M. P. Sumser, W. Kummer, A. Gottschalk, D. Trauner, *ACS Chemical Neuroscience* **2015**, *6*, 701–707.
- [379] J. Broichhagen, M. Schönberger, S. C. Cork, J. A. Frank, P. Marchetti, M. Bugliani, A. M. J. Shapiro, S. Trapp, G. A. Rutter, D. J. Hodson, D. Trauner, *Nature Communications* **2014**, *5*, 5116.

- [380] M. Stein, S. J. Middendorp, V. Carta, E. Pejo, D. E. Raines, S. A. Forman, E. Sigel, D. Trauner, *Angew. Chem. Int. Ed.* **2012**, *51*, 10500–10504.
- [381] M. Stein, A. Breit, T. Fehrentz, T. Gudermann, D. Trauner, *Angew. Chem. Int. Ed.* **2013**, *52*, 9845–9848.
- [382] J. A. Frank, M. Moroni, R. Moshourab, M. Sumser, G. R. Lewin, D. Trauner, *Nature Communications* **2015**, *6*, 7118.
- [383] J. A. Frank, D. A. Yushchenko, D. J. Hodson, N. Lipstein, J. Nagpal, G. A. Rutter, J.-S. Rhee, A. Gottschalk, N. Brose, C. Schultz, D. Trauner, *Nat. Chem. Biol.* **2016**, *12*, 755–762.
- [384] J. A. Frank, H. G. Franquelim, P. Schwille, D. Trauner, *J. Am. Chem. Soc.* **2016**, *138*, 12981–12986.
- [385] J. A. Morales-Serna, O. Boutureira, Y. Díaz, M. I. Matheu, S. Castellón, *Carbohydr. Res.* **2007**, *342*, 1595–1612.
- [386] A. J. Janczuk, W. Zhang, P. R. Andreana, J. Warrick, P. G. Wang, *Carbohydr. Res.* **2002**, *337*, 1247–1259.
- [387] J. Bi, J. Wang, K. Zhou, Y. Wang, M. Fang, Y. Du, *ACS Medicinal Chemistry Letters* **2015**, *6*, 476–480.
- [388] G. Zemplén, A. Kunz, *Berichte der deutschen chemischen Gesellschaft (A and B Series)* **1923**, *56*, 1705–1710.
- [389] T. Tashiro, R. Nakagawa, T. Shigeura, H. Watarai, M. Taniguchi, K. Mori, *Bioorg. Med. Chem.* **2013**, *21*, 3066–3079.
- [390] A. Hoffmann-Röder, E. Schweizer, J. Egger, P. Seiler, U. Obst-Sander, B. Wagner, M. Kansy, D. W. Banner, F. Diederich, *ChemMedChem* **2006**, *1*, 1205–1215.
- [391] E. Schweizer, A. Hoffmann-Röder, K. Schärer, J. A. Olsen, C. Fäh, P. Seiler, U. Obst-Sander, B. Wagner, M. Kansy, F. Diederich, *ChemMedChem* **2006**, *1*, 611–621.
- [392] R. R. Schmidt, P. Zimmermann, *Angew. Chem. Int. Ed.* **1986**, *25*, 725–726.
- [393] A. J. García-Sáez, S. Chiantia, P. Schwille, *J. Biol. Chem.* **2007**, *282*, 33537–33544.
- [394] C. F. Snook, J. A. Jones, Y. A. Hannun, *Biochimica et Biophysica Acta (BBA) – Molecular and Cell Biology of Lipids* **2006**, *1761*, 927–946.
- [395] F. Lafont, L. Abrami, F. G. van der Goot, *Current Opinion in Microbiology* **2004**, *7*, 4–10.
- [396] S. Manes, G. del Real, C. Martinez-A, *Nat. Rev. Immunol.* **2003**, *3*, 557–568.
- [397] H. E. Gottlieb, V. Kotlyar, A. Nudelman, *J. Org. Chem.* **1997**, *62*, 7512–7515.
- [398] K. Hatada, K. Ute, K.-I. Oka, S. P. Pappas, *Journal of Polymer Science Part A: Polymer Chemistry* **1990**, *28*, 3019–3027.
- [399] Z. Li, J. C. Gildersleeve, *J. Am. Chem. Soc.* **2006**, *128*, 11612–11619.
- [400] M. Rommel, A. Ernst, U. Koert, *Eur. J. Org. Chem.* **2007**, *2007*, 4408–4430.
- [401] F. A. W. Koeman, J. P. Kamerling, J. F. G. Vliegthart, *Tetrahedron* **1993**, *49*, 5291–5304.

- [402] V. R. Krishnamurthy, A. Dougherty, M. Kamat, X. Song, R. D. Cummings, E. L. Chaikof, *Carbohydr. Res.* **2010**, *345*, 1541–1547.
- [403] A. Titz, Z. Radic, O. Schwardt, B. Ernst, *Tetrahedron Lett.* **2006**, *47*, 2383–2385.